NASA CR-66324

LUNAR ORBITER I FINAL REPORT

MISSION OPERATIONAL PERFORMANCE

VOLUME III

Boeing Document D2-100727-3

February 3, 1967

THE BOEING COMPANY

Aerospace Group - Space Division

Seattle, Washington

Distribution of this report is provided in the interest of information exchange. Responsibility for the contents resides in the author or organization that prepared it.

FACILITY FORM 602

N67-27419 (ACCESSION NUMBER)

(THRU)

443 (PAGES)

1 (CODE)

CR-66324 (NASA CR OR TMX OR AD NUMBER)

31 (CATEGORY)

GPO PRICE $

CFSTI PRICE(S) $

Hard copy (HC) 3.00

Microfiche (MF) .65

ff 653 July 65

VOLUME III

LUNAR ORBITER I

MISSION OPERATIONAL PERFORMANCE

FINAL REPORT

February 3, 1967

Prepared for the

National Aeronautics and Space Administration

Langley Research Center

By

Aerospace Group - Space Division

THE BOEING COMPANY

Seattle, Washington

FOREWORD

The Lunar Orbiter Mission I Final Report is divided into five volumes as follows:

Volume I	Photographic Mission Summary
Volume II	Lunar Photograph
Volume III	Mission Operational Performance
Volume IV	Extended Mission
Volume V	Appendix

Volume I summarizes the mission and briefly describes the equipment used in its fulfillment. Volume II describes the photographic results obtained on the mission and describes the photo subsystem to provide a basis for understanding limitations and constraints on the photography. Volume III contains a functional description and performance analysis of the spacecraft subsystems as well as description and performance of equipment during launch operations and flight operations. Volume IV summarizes the extended-mission performance. Volume V provides an appendix presenting supporting data for the other volumes.

In each case the Volume I summary provides introductory material for use with the other volumes and should be read first.

CONTENTS

	Page
3.0 MISSION OPERATIONAL PERFORMANCE	1
3.1 SPACECRAFT GENERAL	1
3.1.1 Photo Subsystem	13
3.1.1.1 Photo Subsystem Performance Summary	14
3.1.2 Power Subsystem	14
3.1.2.1 Functional Description	14
3.1.2.2 Performance	17
3.1.3 Communications Subsystem	29
3.1.3.1 Functional Description	29
3.1.3.2 Performance	44
3.1.4 Attitude Control Subsystem (ACS)	49
3.1.4.1 Functional Description	49
3.1.4.2 Performance	75
3.1.5 Velocity Control Subsystem	130
3.1.5.1 Functional Description	130
3.1.5.2 Performance	150
3.1.6 Structures and Mechanisms Subsystem	163
3.1.6.1 Functional Description	163
3.1.6.2 Performance	164
3.2 LAUNCH VEHICLE PERFORMANCE	179
3.2.1 Atlas Performance	179
3.2.1.1 Airframe	179
3.2.1.2 Propulsion	179
3.2.1.3 Guidance and Flight Control	184
3.2.1.4 Pneumatics	188
3.2.1.5 Electrical Power	189
3.2.1.6 Hydraulics	189
3.2.1.7 Propellant-Utilization System	190
3.2.1.8 Range Safety Command System	191
3.2.1.9 Launch Complex and Ground Equipment	191
3.2.2 Agena Performance	193
3.2.2.1 Airframe	196
3.2.2.2 Propulsion	197
3.2.2.3 Electrical Power	200
3.2.2.4 Communications and Control	202
3.2.2.5 Guidance and Control	202

	Page
3.3 LAUNCH OPERATIONS	208
3.3.1 Launch Operation Plan	208
3.3.1.1 Prelaunch Operation Organization	208
3.3.1.2 Launch Operation Organization	211
3.3.2 Launch Base Facilities (General)	215
3.3.2.1 ETR Instrumentation and Communication Facilities	215
3.3.2.2 Atlas Guidance-Ground Equipment	224
3.3.3 Spacecraft Processing	224
3.3.3.1 Hangar "S" (Industrial Area)	224
3.3.3.2 Explosive-Safe Area (ESA 5/6)	229
3.3.3.3 Launch Complex 13	233
3.3.4 Countdown and Launch	235
3.3.4.1 Launch Criteria and Constraints	235
3.3.4.2 Countdown	237
3.3.4.3 Weather	241
3.3.4.4 Tracking Coverage	241
3.3.4.5 Telemetry Coverage	249
3.4 FLIGHT OPERATIONS	251
3.4.1 Mission Control	251
3.4.2 Operational Organization	253
3.4.2.1 SFOF Personnel	253
3.4.2.2 DSIF Personnel	256
3.4.3 Deep Space Network (DSN)	257
3.4.3.1 Space Flight Operations Facility (SFOF)	257
3.4.3.2 Deep Space Instrumentation Facility (DSIF)	266
3.4.4 Mission Conduct	271
3.4.4.1 Operational Control Procedure	271
3.4.4.2 Flight Path Control	281

LIST OF ILLUSTRATIONS

Figure		Page
3.1-1	Spacecraft in Flight Configuration	2
3.1-2	Interface between Subsystems — LO Block Diagram	3
3.1-3	Photo Subsystem Schematic	13
3.1-4	Block Diagram — Power Subsystem	15
3.1-5	Solar Array	16
3.1-6	Power Subsystem Current Profile Initial Orbit 9-10 (Prefault)	19
3.1-7	Battery Characteristics, Initial Orbit 9-10	21
3.1-8	Battery Characteristics, Initial Orbit 31-32	22
3.1-9	End of Discharge — Battery Voltage Mission I	23
3.1-10	Battery Depth of Discharge Mission I	24
3.1-11	Load Profile During Processing — Final Orbit 62F	25
3.1-12	Power Subsystem Current Profile — Final Orbit 159-160 Readout Mode	26
3.1-13	Battery Characteristics — Final Orbit 159-160	28
3.1-14	Average Lunar Orbiter Solar Array Ouput I - V Characteristics	30
3.1-15	Mission I Output Current and Temperature of Solar Panel 1 During Initial Orbit 8	31
3.1-16	Communications Subsystem Block Diagram	33
3.1-17	Telemetry Data Flow Diagram	35
3.1-18	Telemetry Data Format	36
3.1-19	Video Data Flow	38
3.1-20	Command Data Flow	40
3.1-21	Command Transmission Timing Diagram	41
3.1-22	Command Data Format	43
3.1-23	Attitude Control Subsystem Components and Axial Orientation	50
3.1-24	ACS Functional Block Diagram	52
3.1-25	Attitude Control Subsystem Signal Interface	55
3.1-26	Sun Sensor Fields of View	68
3.1-27	Sun Acquisition	69
3.1-28	Canopus Acquisition	70
3.1-29	Inertial Reference Unit—Gyros (Equivalent Circuit)	72
3.1-30	Thrust Vector Control—First Midcourse	115
3.1-31	Pitch Thrust Vector Control — Orbit Injection	116
3.1-32	Yaw Thrust Vector Control — Orbit Injection	117
3.1-33	Thrust Vector Control — Orbit Transfer	119
3.1-34	Thrust Vector Control — Orbit Adjust	120
3.1-35	Roll Transients during Engine Burn	121
3.1-36	Roll Attitude during Orbit Injection Maneuver	122
3.1-37	Nitrogen Usage — Attitude Control Subsystem	124

Figure		Page
3.1-38	Nitrogen Usage — Velocity and Reaction Control	126
3.1-39	Spacecraft Motion — Initial Orbit 22	128
3.1-40	Disturbance Torque in Pitch Axis — Initial Orbit 22	131
3.1-41	Spacecraft Rates — Final Orbit 2	132
3.1-42	Spacecraft Disturbances — Acceleration — Final Orbit 2	133
3.1-43	Pitch Axis Disturbance Due to a -179.7-Degree Roll Maneuver	134
3.1-44	Yaw Axis Disturbance Due to a -179.7-Degree Roll Maneuver	135
3.1-45	Disturbances in Roll and Yaw Axes due to a Pitch Maneuver and in Roll and Pitch Axes due to a Yaw Maneuver	136
3.1-46	Pitch Axis Disturbance due to Antenna Rotation	137
3.1-47	Roll and Yaw Axis Disturbance due to Antenna Rotation	138
3.1-48	Roll Axis Disturbance due to a 30-Degree Antenna Rotation	139
3.1-49	Pitch Axis Disturbance due to a 30-Degree Antenna Rotation	140
3.1-50	Yaw Axis Disturbance due to a 30-Degree Antenna Rotation	141
3.1-51	Camera Motion Disturbance on Roll and Pitch	142
3.1-52	Camera Motion Disturbance on Yaw Axis	143
3.1-53	Velocity and Reaction Control Subsystem	145
3.1-54	Velocity Control Subsystem — Available Nitrogen History	152
3.1-55	Velocity Control Subsystem — Pressure-Time Histories	153
3.1-56	Velocity Control Subsystem — Temperature-Time Histories	155
3.1-57	Velocity Control Subsystem Temperature During Typical Orbit	156
3.1-58	Velocity Control Subsystem Orbit Injection Maneuver — System Pressures and Temperatures	160
3.1-59	Velocity Control Subsystem Orbit Injection Maneuver System Dynamics	161
3.1-60	Deck Locations	165
3.1-61	Transient and Quasi-sine Components of EMD Accelerations — Atlas Phase	171
3.1-62	Transient and Quasi-sine Components of EMD Accelerations — Agena Phase	172
3.1-63	EMD Launch Vibration at BECO Compared to Spacecraft 1 Torsion Test Response	173
3.1-64	EMD Launch Vibrations Compared with Spacecraft Sonic Test and Random FAT	174
3.1-65	EMD Vibrations During Agena First Burn	175
3.1-66	Apparent Degradation of Lunar Orbiter 1 Thermal Coating that Occured during Mission I	176
3.1-67	Change in EMD Temperature (Average) versus Solar Vector — Nominal Sun	177

Figure		Page
3.2-1	Combined Space Vehicle Configuration	180
3.2-2	Atlas SLV Configuration	181
3.2-3	Atlas Booster Engine System Schematic	182
3.2-4	Atlas Vernier and Sustainer Engines System Schematic	183
3.2-5	Guidance and Flight Control Block Diagram	185
3.2-6	Atlas Range Safety and Termination System	192
3.2-7	Agena Basic Configuration	194
3.2-8	Agena Profile	195
3.2-9	Agena Propulsion System Schematic	198
3.2-10	Agena Pressurization System Schematic	199
3.2-11	Agena Power Distribution System	201
3.2-12	Agena Telemetry System Block Diagram	203
3.2-13.	Agena Guidance and Control System	204
3.3-1	Prelaunch Operations Organization	209
3.3-2	Launch Operations Organization	212
3.3-3	ETR Launch Complex 13 — Plan View	216
3.3-4	ETR Launch Complex 13 — Blockhouse Equipment Location	217
3.3-5	ETR Launch Complex 13	218
3.3-6	ETR Tracking Data Handling System	222
3.3-7	ETR Launch Data Transmission Network	223
3.3-8	Hangar "S" (Industrial Area) Layout	225
3.3-9	Hangar "S" (Industrial Area)	226
3.3-10	Three-Axis Test Stand	227
3.3-11	Fueling Operations at ESA	230
3.3-12	Explosive Safe Area (ESA 5/6)	231
3.3-13	Site Plan — Explosive Safe Area (ESA 5/6)	232
3.3-14	Spacecraft Transporter	234
3.3-15	Matchmate	236
3.3-16	Spacecraft Countdown	238
3.3-17	Lunar Orbiter I Countdown 8/10/66 — Second Launch Opportunity	242
3.3-18	Lunar Orbiter Near-Earth Class I Tracking and Data Acquisition	244
3.3-19	Lunar Orbiter Injection Loci for August 1966 Launch Period	245
3.3-20	Lunar Orbiter Uprange Radar Coverage	246
3.3-21	AFETR T/M and Radar Coverage, Spacecraft Injection Phase	247
3.4-1	Typical Mission Operations	252
3.4-2	Operational Organization	254
3.4-3	DSN Computer Configuration	262
3.4-4	Simplified Software Structure	264
3.4-5	Ground Communications Net Configuration	270
3.4-6	Command Preparation Sequence	275
3.4-7	DSS Command Transmission Mode Requirements	279
3.4-8	Lunar Orbiter I Early Orbit Determination Results	290

Figure		Page
3.4-9	Pre-midcourse Aiming Point Dispersions	299
3.4-10	Post-midcourse Aiming Point Dispersions	300
3.4-11	Midcourse Maneuver Doppler Plot	301
3.4-12	Deboost Maneuver Doppler Plot	303
3.4-13	Celestial References — Pre-midcourse	305
3.4-14	Aim Points Before and After Midcourse Correction	307
3.4-15	Lunar Injection Geometry — Day 226	310
3.4-16	Orbit Geometry	314
3.4-17	Real-Time Plot to Estimate J-30	330
3.4-18	Real-Time Plot to Estimate J-40	331
3.4-19	Effect of Moon Model on Final-Ellipse Perilune for Transfer Based on ODPL Moon Model	334
3.4-20	Lunar Orbiter Mission I Perilune Radius History	338
3.4-21	Lunar Orbiter Mission I Apolune Radius History	339
3.4-22	Lunar Orbiter Mission I Orbit Inclination History	340
3.4-23	Lunar Orbiter Mission I Argument of Perilune History	341
3.4-24	Lunar Orbiter Mission I Longitude of Ascending Node History	342
3.4-25	First-Ellipse Perilune Altitude Predictions	343
3.4-26	Geometry Photography Using 180-Degree Roll	345
3.4-27	Perilune Trace	347
3.4-28	Perilune Altitude versus Longitude of Descending Node	349
3.4-29	Targeted Perilune Trace	350
3.4-30	Site Photo Altitude and Lighting Angles	351
3.4-31	Flight Transfer Orbit Geometry Initial: Orbit 44 Final: Orbit 1 233:09:50:58.09	352
3.4-32	Final Orbit Lifetime	353
3.4-33	Mission Phase Second-Ellipse Work Sheet OD No. 5212	357
3.4-34	Mission Phase Second-Ellipse Work Sheet OD No. 5118	358
3.4-35	Mission Phase Second-Ellipse Work Sheet OD No. 5122	359
3.4-36	Mission Phase Second-Ellipse Work Sheet OD No. 5128	360
3.4-37	Perilune Altitude Prediction (Post First-Transfer Ellipse)	361
3.4-38	Photo Quality — Incidence Angle	364
3.4-39	Accuracy in Predicting "I" Site Coverage	365
3.4-40	Geometry and Orientation of Second-Ellipse Orbit 30	367
3.4-41	Orbit Ground Tracks	369
3.4-42	Site Photo Altitude and Lighting Angle	370
3.4-43	Mission Phase Third-Ellipse Work Sheet OD No. 6106	373
3.4-44	Mission Phase Third-Ellipse Work Sheet OD No. 6114	374
3.4-45	Third-Ellipse Perilune History	376

TABLES

		Page
3.1-1	Mission I Key Events	4
3.1-2	Time-Bit Equivalence	61
3.1-3	Maneuver Magnitude Bit-Angle Equivalence	63
3.1-4	Velocity-Bit Equivalence	64
3.1-5	Velocity and Reaction Control Nitrogen Gas Budget	73
3.1-6	Spacecraft Attitudes During Primary-Site Photos	74
3.1-7	Spacecraft Attitudes During Secondary-Site Photos	77
3.1-8	Spacecraft Maneuvers	79
3.1-9	Star Mapping Data	110
3.1-10	Spacecraft Residual and Transient Roll Rates	114
3.1-11	Mission I Daily Maneuver-Acquisition-N_2 Usage	125
3.1-12	Usable-Propellant Summary	147
3.1-13	Upper Module Telemetry Parameters	150
3.1-14	Propellant Heater Activation Summary	163
3.3-1	ETR Instrumentation Summary	219
3.3-2	ETR Station Coordinates	221
3.4-1	Time Synchronization Experiment Results	269
3.4-2	Primary Command Transmission and Verification Modes	278
3.4-3	FPAC Software System	282
3.4-4	Performance of FPAC Software	284
3.4-5	FPAC Organization	285
3.4-6	Trajectory Sequence of Events	287
3.4-7	Powered Flight Trajectory Events	289
3.4-8	Midcourse Maneuver Orbit (OD 1300)	296
3.4-9	Deboost Maneuver Orbit (OD 2104)	297
3.4-10	Pre-Midcourse Encounter Dispersions	298
3.4-11	Post-Midcourse Encounter Dispersions	298
3.4-12	Postinjection Conditions (Selenographic)	308
3.4-13	Solve-For Lists	315
3.4-14	ODPL Solutions from 1300- through 1735-Minute Data Arcs	317
3.4-15	ODPL Solutions from 1995- through 2430-Minute Data Arcs	318
3.4-16	Lunar Models Determined by ODPL and LHDL from 2400-Minute Data Arc	319
3.4-17	Lunar Model Determined by LHDL over 2600-Minute Data Arc	320
3.4-18	ODPL Solution over 2600-Minute Data Arc (Solving for Only State Vector)	321
3.4-19	ODPL Solution over 2600-Minute Data Arc (Solving for State Vector and Harmonics)	322
3.4-20	ODPL Solution over 2800-Minute Data Arc (Solving for State Vector and Harmonics)	323
3.4-21	Converged 2800-Minute State and Harmonics	324

		Page
3.4-22	ODPL Solutions over 2800- through 3500-Minute Data Arcs (Only State Vector Solved for)	325
3.4-23	ODPL Solutions over 4000-Minute Data Arc	327
3.4-24	ODPL 4138 Lunar Model	328
3.4-25	Moon Model Summary	333
3.4-26	Transfer Maneuver Orbit (OD 4150)	335
3.4-27	For Mission Phase First Ellipse	337
3.4-28	Photos Exposed During Second Ellipse	362

LUNAR ORBITER I FINAL REPORT

3.0 MISSION OPERATIONAL PERFORMANCE

The Lunar Orbiter I provided a stable and controllable platform from which to take the pictures discussed in detail in Section 2.0 of this report. It also provided the means of obtaining additional data to extend scientific lunar knowledge. The spacecraft contained instrumentation to sample certain lunar environmental conditions and to determine the performance of the spacecraft subsystems while operating in the cislunar and lunar environments. Information required to further define the exact size and shape of the Moon and the lunar gravitational field are to be derived from the tracking data obtained.

This section of the report contains a functional description and performance analysis of the systems employed to command and control the mission and recover the desired data.

3.1 SPACECRAFT GENERAL

Configuration

The 380-kilogram (853 pound) Lunar Orbiter spacecraft was 1.68 meters (5.5 feet) high, spanned 5.61 meters (18.5 feet) from the tip of the rotatable high-gain dish antenna to the tip of the low-gain antenna, and measured 3.96 meters (12 feet) across the solar panels. Figure 3.1-1 shows the spacecraft in the flight configuration with all elements fully deployed. The mylar thermal barrier is not shown in this illustration. Major components were attached to the largest of three deck structures which were connected by a tubular truss network. Thermal control was maintained by controlling emitted internal energy and absorbed solar energy through the use of a silicone paint covering the bottom side of the deck structure. The entire spacecraft periphery above the large equipment mounting deck was covered with a highly reflective aluminum-coated mylar shroud, which provided an adiabatic thermal barrier. Three-axis stabilization was provided by using the Sun and Canopus for primary angular reference and a three-axis inertial reference system when the vehicle was required to operate off the celestial references during maneuvers or when the Sun and Canopus were occulted by the Moon. Interface between the spacecraft subsystem functions is shown in Figure 3.1-2.

Performance

Achievement of the objectives of the Lunar Orbiter Mission I was not impaired by the performance of the spacecraft, or its subsystems with the exception of the photo subsystem shutter anomaly. Refer to Volume II and Appendix D of this document for discussion of this occurrence.

Performance Summary—Key Events

The key events that occurred during Mission I are shown in Table 3.1-1. For the complete listing of Mission I sequence of events, refer to Appendix C.

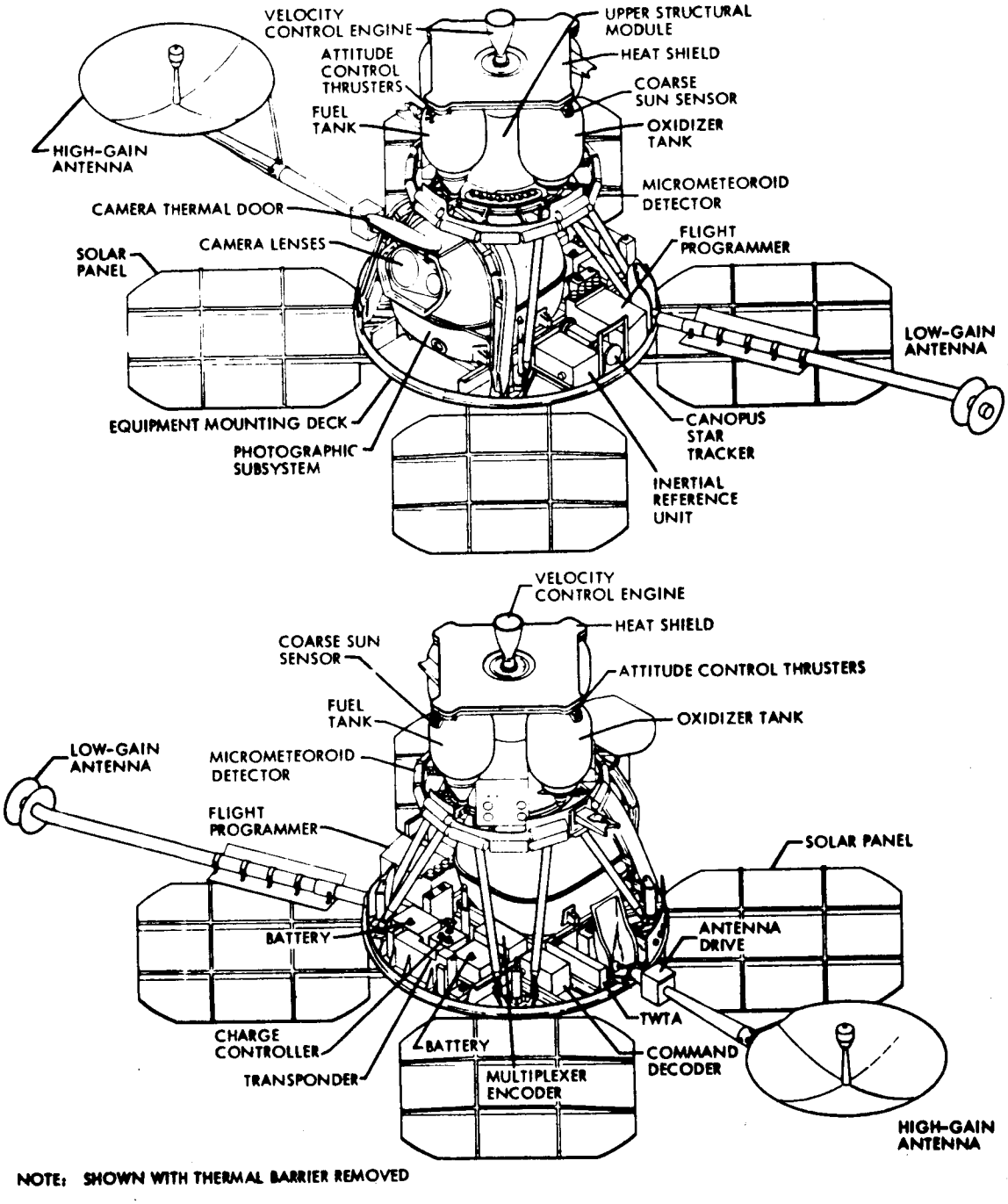

FIGURE 3.1-1: SPACECRAFT IN FLIGHT CONFIGURATION

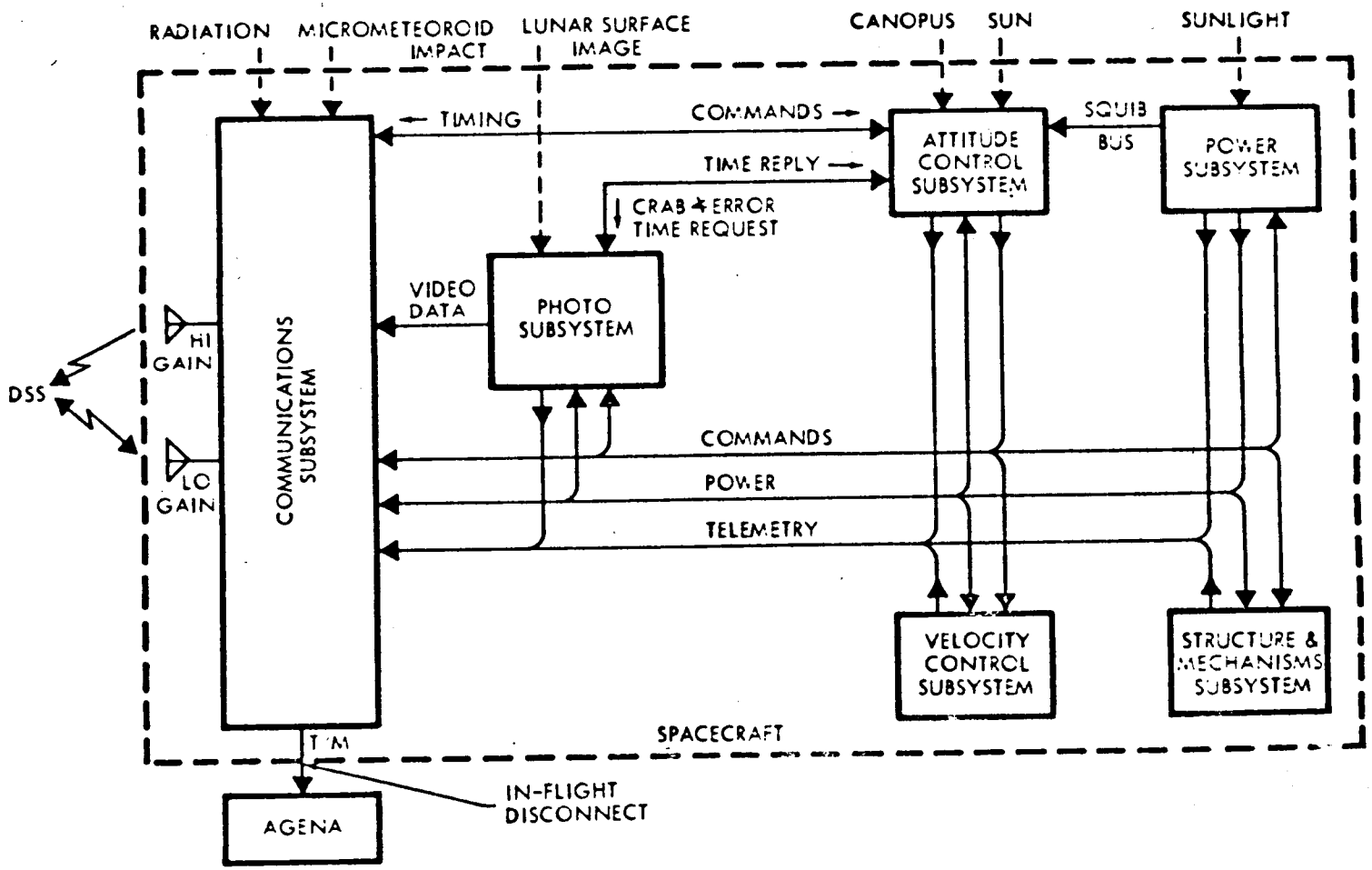

Figure 3.1-2: LUNAR ORBITER BLOCK DIAGRAM

Table 3.1-1: Mission I Key Events

DAY	TIME	EVENT
221	18:30	1st Countdown Scrubbed
222	19:23:00	Spacecraft Clock Start
222	19:26:00.76	Lift Off
222	20:06:48	Spacecraft and Agena Separation
222	20:13	DSS-41 Rise
222	20:13:38	DSS-41 One-Way Lock (SAA) - Signal Strength (at Antenna Output) - 122 dbm
222	20:15:08	High-Gain Antenna Deployed
222	20:15:54	Solar Panel and Low-Gain Antenna Deployed
222	20:21	Sun Presence Signal
222	20:24:26	DSS-41 Two-Way Lock (SCM) - Signal Strength (at Antenna Output) - 96 dbm
222	20:22:03	Sun Acquisition in Pitch (Already Acquired in Yaw at Station Rise)
222	20:43:30	Spacecraft in Communications Mode 3
223	02:21:52	First Star Map - Canopus Acquisition Unsuccessful
223	16:15:32	Moon Reference Established by Canopus Star Tracker
223	19:06:48	Propellant Line Bleed
224	00:00	Ignition, 1st Midcourse Maneuver ΔV = 37.8 mps, 32.1-Second Burn
225	13:50	Canopus Lock Achieved
226	15:34:03.7	Ignition, Lunar Orbit Injection ΔV = 790.0 mps, 578.7-Second Burn
230	14:42:49.9	1st Exposure, Site I-O, First Ellipse (Orbit 26)
230	19:49	Beginning of Readout, First Actual Moon Photo (High-Resolution Frame 7, Site I-O) Orbit 27
233	09:49:58.7	Ignition, First Transfer Maneuver ΔV = 40.2 mps, 22.4-Second Burn

Table 3.1-1: (Cont'd.)

DAY	TIME	EVENT
234	15:22:58.6	First Exposure (of 16) Site I-1, Second Ellipse (Orbit 9)
235	16:36:23.6	First Earth-Moon Photo, Second Ellipse (Orbit 16)
237	16:01:29	Ignition, Second Orbit Transfer Maneuver, ΔV = 5.4 mps, 3.0-Second Burn
239	05:45	Nitrogen Isolation Valve (Velocity Control System) Squib Fired
241	13:23:30.5	First Exposure (of 20) Site 9.2B, Third Ellipse (Orbit 57*) Final Photo Site (*Number Referred to Second Ellipse Beginning).
242	18:14	Bimat Cut (Orbit 65)
242	20:42	First Sequence of Final Readout Initiated (Orbit 66)
257	21:18	End of Final Readout - End of Mission (Orbit 171)

Performance Summary—Resume

Launch Phase

Liftoff and injection into cislunar trajectory by the launch vehicle were well within nominal limits and caused no problems. DSS-71 (Cape Kennedy) traced the spacecraft manually in one-way lock for 3 minutes and twenty seconds.

Cislunar Transit

DSS-41 (Woomera) initial acquisition was completed within 11 minutes (to achieve two-way lock with the SCM antenna) after station rise. The spacecraft communications mode was switched from the acquisition-modulation mode (Mode 4—video modulation mode in the modulation selector, but without any video signal, using the low-gain antenna to achieve higher effective carrier power) to standard operating mode (Mode 3—normal telemetry) about 19 minutes later. When telemetry data became available, solar panels and antennas had already deployed and the Sun had been acquired in yaw. The first Sun acquisition (of 250 during the flight) was completed (by acquisition in pitch) within 56 minutes after launch, well within the battery power constraint of 1.5 hours. DSS-72 (Ascension Island) and DSS-51 (Johannesburg) acquired and tracked the spacecraft for brief periods, the former for training purposes only. DSS-51 was unable to record telemetry data due to high spacecraft angular rates that made it difficult to maintain lock. First acquisition and handover to DSS-61 (Madrid) required an excessive time (58 minutes) due to an incorrect initial transmitter setting and a spacecraft transponder frequency that differed considerably from the predicted value. Succeeding acquisitions by all stations were normally smooth and rapid.

Until the time of attempted initial Canopus acquisition, the mission proceeded precisely by the preflight plan. The Canopus sensor was turned on at 02:14:57 (Day 223), at which time the roll error signal immediately showed a negative saturation level and the map signal voltage was approximately 1.5 times the preflight calculated Canopus signal voltage. The preliminary estimate of the situation was that the sensor was apparently responding to excess reflected light from the spacecraft structure, the most likely candidate being the low-gain antenna. The first star map was executed (roll plus 360 degrees) at 02:21:52 August 11 (Day 223). The roll error switched to plus saturation level on passing the Moon and remained at that level. The star map signal saturated on passing the Moon and subsequently stabilized at a background level approximately equal to the expected Canopus signal.

A number of experiments and tests were devised and carried out during the flight from which evolved operational techniques that successfully circumvented the Canopus acquisition anomaly and permitted effective spacecraft orientation and control. Canopus lock was achieved at 13:50 on August 13. Lock was subsequently lost apparently due to "glint" (light reflection). The final technique adopted was use of the Canopus sensor during periods of solar occultation to verify and/or correct spacecraft orientation.

This Canopus sensor difficulty was one of the two major instances of anomalous performance that were solved for mission control purposes by real-time modifications of operations techniques, resulting in major reorientation of preflight mission planning. The Canopus

sensor was turned on and off 133 times and operated for a total of 68 hours. Nine star maps were made during Lunar Orbiter Mission I. The experiments and attitude updates required by the Canopus sensor anomaly (and the thermal problems discussed below) contributed significantly to the difference between number of planned maneuvers (94) and those actually executed (374).

Roll reference for the midcourse maneuver was established by using the Moon instead of Canopus. The Moon was acquired about 45 minutes prior to engine ignition and maneuvers were performed using it as a reference to properly align the spacecraft thrust vector. Ignition time was 00:00:12.8 on August 12, 1966. Programmed ΔV was 37.8 mps, burn time was 32.7 ± 1 second. Velocity change achieved was exactly as programmed; actual burn time was 32.1 seconds. Attitude-maneuver, holding and thrust-vector-control accuracies were within specification limits. No second midcourse maneuver was required.

About 1.5 hours after the midcourse maneuver, the first thermal relief maneuver (of five during the cislunar phase) was performed, orienting the spacecraft 36 degrees off the Sunline for approximately 8.5 hours. This procedure had been planned, as the spacecraft equipment mounting deck temperature was expected to rise during continual Sun orientation in cislunar flight. The first maneuver was not required as early as had been expected. During this portion of the flight, the EMD thermal protective coating was degrading at approximately the expected initial rate.

The communications subsystem functioning was nominal in all respects during this mission phase. Incident to the Canopus sensor problems, the high-gain antenna (HGA) was rotated 2 degrees left and the traveling-wave-tube amplifier (TWTA) was turned on August 12 (at 09:43 and 09:51 respectively) for a signal-strength map during a 360 degree roll. It had not been planned to use the TWTA or HGA during cislunar flight. During the entire mission, the TWTA was operated 148 times for a total operating time of 211.1 hours during which operation was satisfactory. The HGA was rotated (in 1-degree increments) 907 times during the mission, in all cases responding properly. Ranging was conducted after the midcourse maneuver and interstation time synchronization was achieved.

Photo subsystem environmental conditions during cislunar transit were nominal in all respects.

No unexpected thermal problems arose during the transit phase, and all mechanical operations (antenna and solar-panel deployment) were properly performed. Propellant tank temperatures were 10 to 15 degrees lower than anticipated, but remained within limits.

The support provided by the Deep Space Network (DSN) and the flexibility and real-time response capability displayed by the mission operational personnel were in all respects equal to the occasion. Frequent spacecraft maneuvers caused discontinuities in doppler tracking data; however, this difficulty was successfully handled throughout the mission. Data acquisition, transmission, and processing gaps were minimal.

Lunar Orbit Injection and First Ellipse

The lunar-orbit-injection maneuver was performed during the first solar occultation, which began at 15:22:56 GMT on August 14. Canopus had been acquired at 00:49:43.0 the same day and, about an hour later, the spacecraft was commanded to the inertial-hold mode in roll (by a roll + 0.011-degree command). A roll correction maneuver, performed about 2 hours prior to the maneuver, was based on drift rates established earlier during a 4-hour drift test begun at 21:45 on August 10. During this inertial hold, the fifth thermal relief maneuver was performed (7.5 hours off-Sun 36 degrees) to establish optimum temperature conditions for the critical injection maneuver. The maneuver sequence was initiated with attitude control deadband closure at 15:27:03.2 on August 14. Engine ignition occurred at 15:34:03.6 of the same day. Programmed velocity change and burn time were 790.0 mps and 588.3 ± 10 seconds. Actual performance figures were 789.7 mps and 578.7 seconds respectively.

The difference between planned and actual burn times does not indicate a performance anomaly in that engine cutoff was commanded by the flight programmer after integration of the accelerometer output pulses. The accelerometer/programmer engine burn termination effected cutoff on all four velocity maneuvers to an extremely high order or accuracy. Attitude orientation and holding, and thrust vector stabilization accuracies are amply attested to by the achievement of an injection maneuver very closely approaching design values. This confirmation applies to total system performance, verifying the tracking, trajectory computation and prediction, and spacecraft command techniques employed.

The Canopus sensor indicated clear and positive Canopus presence immediately after first Sun occulation (prior to injection maneuver). For the remainder of the flight, operational practice was to turn the sensor on only during selected Sun occultation periods for Canopus reference verification and/or update. Regular plotting of roll drift rates and frequent updating of the reference directions resulted in successful mission control and accurate orientation for photo sequences.

During the first ellipse (and thereafter), spacecraft events and conditions, as well as new requirements stated on short notice, continued to require variations from planned procedures and development of operational techniques to meet changing circumstances.

The Goldstone test film loaded in the photo subsystem prior to launch was successfully read out during Orbit 6, August 15, at 15:20 GMT. At about this same time, it began to be apparent that the thermal protective coating on the spacecraft equipment mounting deck was degrading (temperature rising) at a considerably greater rate than had been predicted. The rate of absorption of solar energy continued to increase after it had been expected to level off. This caused the spacecraft equipment mounting deck temperatures to creep steadily higher with each successive orbit.

As nearly as can be determined, the coefficient of emissivity in the infrared region (by which the spacecraft radiated excess heat during solar occultation periods) was approximately as predicted. However, total heat content gradually increased. This condition became acute during the second and third ellipses.

Variation in indicated downlink signal strengths during the first ellipse appeared to correlate with the spacecraft mechanical operations, particularly rotation of the high-gain antenna. Programmed antenna rotations during Orbits 19 and 20 were deleted in an attempt to localize the anomaly. While some correlation was developed between power variations and high-gain-antenna rotations and orientation, no positive relationship has been evident between DSS reports and spacecraft telemetry. Throughout the mission, transponder output varied within a normal range according to temperature (between 596 mw at 60°F and 540 mw at 85°F). Occasional fluctuations of 5 to 10 mw were evidenced, but the net effect was small, and downlink signal was adequate. Isolated instances of difficulty in acquisition or downlink degradation (e.g., -145 dbm on August 19, 1966) occurred. It is suspected that most (if not all) of these conditions resulted from improper pointing of the DSS antennas.

Planning included turning on the propellant tank heaters every orbit to ensure maintenance of proper fuel and oxidizer temperatures. This was found to be unnecessary early in the first ellipse, and the last use of the heaters for this purpose ended early on August 17.

About 30 hours after injection, the first evidence of a leak in the nitrogen gas regulator appeared in the form of a continuing pressure buildup in the fuel and oxidizer tanks. The leaking gas (at a rate of about 0.1 lb/day) was lost to the attitude control system but this did not seriously affect the mission. The relief valve cracked at 20:00 on August 22, (Day 234) permitting gas to vent overboard. Isolation squibs were fired on Day 239 at 04:45, after the second transfer maneuver, preventing further gas loss.

On August 18 at 16:25 (Orbit 20), one of the power transistors in the shunt regulator array failed (either a collector-to-emitter or a collector-to-base short would produce the effect observed). The net result was a constant additional load of 1.2 to 1.5 amperes on the power subsystem. This had two partially compensating effects: First, it increased the depth of battery discharge during Sun occultation thereby delaying the time in succeeding Sunlight periods at which battery temperatures began to rise due to overcharging. Second, and more important, the additional load reduced the maximum off-Sun angle at which sufficient array power was available to support readout power demands, which was the time when temperature problems became most acute. Minor anomalies occured in solar panel temperature sensor performance; however, power performance proved to be adequate throughout the mission.

First photo subsystem operation (subsequent to Goldstone test film readout) took place on August 18 at 12:12:13.06 (Orbit 25), when 11 frames were advanced and processed to put active film in position for the first photo sequence on the following orbit. This sequence was for 20 exposures of Site I-O, and the first shutter operation occurred at 14:42:49.9. The entire maneuver and photo sequence was apparently nominal in all respects; however, when the first readout was conducted about 5 hours later (19:50:42 GTM), the major technical anomaly of the flight was evidenced. While the moderate-resolution frame was of excellent quality, the high-resolution frame 5 was degraded. A number of tests were devised, and the second transfer maneuver was eventually executed (to lower perilune altitude) in attempts to correct the problem, but no noticeable success was achieved. The malfunction has subsequently been diagnosed as operation of the 610-mm shutter trip at incorrect times by

electrical transients generated within the photo subsystem. Different frames indicate that the shutter was fired variously during film advance (smear parallel to long dimension of photo frame) or during shutter reset (smear perpendicular to long dimension of frame) or at a time when both effects appeared.

The first of a number of "short notice" changes in planned photographic sequences occurred with the taking of a photograph of the far side of the Moon on Orbit 33 at 17:05:21.0 on August 19. Two roll maneuvers were performed to obtain a picture of the Moon's surface in what was planned as a film-set advance. Similarly, nearly all film-set frames were used for Moon photographs. Despite the heavy additonal load in reprogramming and commanding the spacecraft, nearly all requests were satisfied. Other changes in planned operations were required by tests on the high-resolution camera shutter and evidence of Bimat dryout and sticking (detected in Orbits 40 and 42).

Second and Third Ellipses

The first transfer maneuver to the photographic orbit occurred at the end of Orbit 44 of the first ellipse. The two-axis maneuver (roll + 43.3 degrees, pitch + 25.31 degrees) began at 09:41:58.0 GMT on August 21. Engine ignition occurred at 09:49:58.7. Actual velocity change was again very nearly the design value and the desired orbit was achieved to a high degree of accuracy.

A second orbit transfer (or orbit adjustment) maneuver was performed on August 25, the maneuver sequence being initiated in roll at 15:45:20.6 GMT. Ignition occurred at 16:01:29. The principal reason for this orbit adjustment was to achieve a lower perilune altitude, thereby raising the V/H sensor ratio in an attempt to achieve better results from the high-resolution camera. No noticeable improvement was achieved.

System performance during this portion of the mission, with the exception of the erratic operation of the 610-mm focal length camera shutter, met all mission requirements.

Photographic operations were completed essentially according to preflight planning except for addition of maneuvers required to utilize film-set frames for secondary photography. These included the Earth photos, which required two-axis maneuvers. At times, the preparation and transmission of commands to the spacecraft approached the saturation level. Thermal conditions and spacecraft orientation problems required frequent maneuvers. Some readout periods were cancelled to allow spacecraft cooling, and roll updates were necessary in darkness when the Canopus sensor could be used. Attitude accuracies within ± 0.2 degree were achieved for all scheduled photo sites except Site I-7, when a roll error of -1.75 degrees resulted due to lack of time to perform a roll update. One photo was taken with the spacecraft pitched 36 degrees for cooling.

Spacecraft pitchoff angles for cooling were progessively increased as deck temperatures continued to mount, even though successively higher limits were set for acceptable deck temperatures. These limits were essentially set by spacecraft performance, the principal guide being satisfactory performance of the inertial reference unit (IRU). The maximum temperature indicated by the deck sensor nearest the IRU was 102.9°F, above the preflight qualification test level of 100°F. An attempt was made

to use deeper discharge of the battery during Sun occultation (by turning on propellant tank heaters) to alleviate the deck temperature problem; however, no success was achieved. A preprogrammed sequence to ptich on and off the Sun was used for several orbits, followed by real-time commands to varying angles depending on circumstances. Eventually the spacecraft was kept pitched off the Sun, using Sun sensors and solar array parameters for angle determination and gyro drift and updates for control. Virtually all of final readout was conducted with the spacecraft pitched off the Sun. Final readout periods were lengthened from the preflight planning figure of 86 minutes to 102 minutes (and longer—maximum readout period was 128.93 minutes) as power availability to support longer readouts (even when pitched off the Sun and with the constant drain imposed by the shunt regulator failure) was demonstrated. The maximum pitchoff angle during readout was 33 degrees.

The gas regulator failure and the unexpectedly large number of maneuvers required for attitude updating and thermal relief resulted in a high nitrogen usage rate. From August 23 to 31, during photo maneuvers and with a programmed pitch off and on every orbit, gas usage was 0.375 pound per day. Adaption of more economical procedures resulted in a noticeable saving. Optimization procedures adopted were to remain off in pitch, update in pitch and yaw with the coarse Sun sensors, and in roll with theCanopus sensor. Gas usage from September 1 to 14 was 0.09 pound per day.

The constant off-Sun orientation of the spacecraft and the lengthening of readout periods required new communications and command techniques. The antenna pointing routine in user program SGNL would not handle the coordinate transformation required by the high pitch angles. A number of small antenna-signal-strength maps, usually using combined antenna rotations and spacecraft yaw maneuvers, were required to attain satisfactory power levels for readout. Eventually a coordinate transformation routine was included in user program CORL, after which antenna orientation became more of a science and less of an art. Revised procedures were also adopted for the command sequence to expedite initiation of readout. The SLOE at the receiving station executed the succeeding commands based on specified signal-strength readings and video optimization requirements. The DSS's acquired in two-way lock and achieved rapid command readiness. The antenna pointing system used at the DSS during readout functioned well; in only one instance was the antenna driven off point, resulting in a brief loss of data. TWTA power output was from 10.5 to 12.2 watts, and video link performance was adequate to meet all requirements.

Summation

Programmer and command flow have been only touched on in the foregoing synopsis. The command decoder, flight programmer, and telemetry readout responded correctly to all commands during the flight. There were 4,510 commands executed; i.e., stored in the programmer memory (2,522) or executed as real-time commands (1,988). A small but unknown number of additional commands were processed by the command decoder and programmer arising from aborted or retransmitted commands. Due to repetitive execution of stored routines, it is estimated that the programmer executed approximately 15,000 commands. The flight programmer clock drifted a total of +1.6 seconds in approximately 30,000,000 incrementations. Clock switchover was never required, nor was the multiplexer/encoder ever required to switch to its internal clock. Command preparation on occasion

became a frantic process, due to late definition of exact inputs or requirements, late changes, or requirements for programmer core storage in excess of an efficient level, thus necessitating programming workarounds. While all requirements were met, there were some cases of spacecraft core maps being stored at the very last minute. Effective use was made of the programmer breadboard in the SFOF for diagnosing problems and verifying command sequences.

During the mission, ground transmitter power was reduced from 10 kw to a final level of 2.5 kw to maintain indicated spacecraft AGC level at approximately -90 dbm. Command capability was not lost until a much lower power level was reached in a special test after the completion of the mission. It appears more likely that the spacecraft transducer was exhibiting deterioration than that sensitivity was increased by 6 db.

Attitude maneuver rates in the narrow deadband were all within specification (0.5 ± 0.05 degree), for open (2 degrees) deadband, roll rates were within the range 0.047 to 0.051 degree per second, and pitch varied from 0.036 to 0.059 degree per second. No verification of open deadband rates in yaw was achieved.

The radiation dosage measurement system performed properly. A 1.0-rad increase upon the cassette dosimeter indicated passage through the Van Allen belt as expected. Dosage indications built up gradually—a small solar proton-event on August 29 was not significant. After Bimat cut, a large proton event on September 2 caused a rapid buildup; however, no film damage resulted because all film had been exposed and processed by this time.

Spacecraft environmental conditions were maintained within the functional limits of all equipment, albeit by constant operational scrambling. The power system was adequate to the demands made upon it.

The photo subsystem performed quite well overall, again excepting the high-resolution camera shutter. Environmental control was maintained within design limits during the flight. The V/H sensor tracking rate apparently averaged about 8% lower than predicted. The V/H sensor was operated for 50 minutes 45 seconds, with an average on time of 3 minutes, 37 seconds. The sensor was operated beyond the standard 6-minute limit for Site I-O with NASA cognizance. Film transport operated within limits, although lengthwise scratches on the film indicate the possibility of foreign material in the mechanism. Some deterioration was evident in the anode of the line scan tube of the optical mechanical scanner. Some Bimat stick and dryout occurred and some evidence exists of uneven pressure during processing.

Support provided by the ground system was very good. There were occasional data transmission or processing losses, some equipment failures, and some difficulty in acquisition or tracking, but in no case was accomplishment of the mission jeopardized.

The completion of the mission as flown is ample testiment to the flexibility and capacity of the spacecraft to operate and perform under other than nominal conditions. The mission also demonstrated the flexibility and responsiveness of the operational control personnel in reacting to conditions and devising modified procedures to meet the requirements imposed by conditions.

3.1.1 PHOTO SUBSYSTEM

The photographic subsystem (shown schematically in Figure 3.1-3) was a highly versatile photo laboratory which contained two cameras, a film supply, film processor, processing web (Bimat) supply, an optical electronic readout system, a velocity-over-altitude detection device to preclude image smear induced by spacecraft velocity, and the control electronics necessary to program the photographic sequences within the photo subsystem. Operational flexibility has been emphasized by providing operations personnel with controls to adjust key system parameters (e.g., time interval between frames, shutter speed, line-scan tube focus).

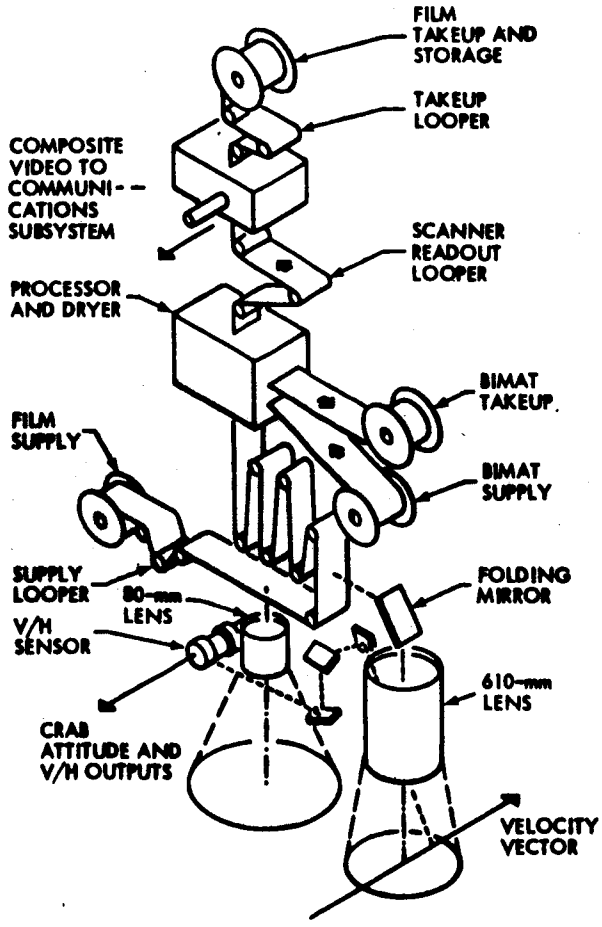

FIGURE 3.1-3: PHOTO SUBSYSTEM SCHEMATIC

3.1.1.1 PHOTO SUBSYSTEM PERFORMANCE SUMMARY

The basic photo subsystem operation was excellent throughout the mission. The processing and readout of the pictures was according to design. The photos taken with the 80-mm medium-resolution lens were of excellent quality. The photos of the sites taken with the 610-mm high-resolution lens with the V/H operating generally suffered from smear as discussed in Volume II. Despite attempts to improve these photos, the smear continued to a greater or lesser extent.

Functional description and details of the photo subsystem performance are covered in Volume II of this report.

3.1.2 POWER SUBSYSTEM

3.1.2.1 FUNCTIONAL DESCRIPTION

The power subsystem was the sole source of electrical power used by the spacecraft during all phases of the mission. A simplified block diagram of the power subsystem is shown in Figure 3.1-4. The subsystem was comprised of (1) the solar array, (2) storage battery, (3) charge controller, and (4) shunt regulator. The solar array collected radiant solar energy and converted it into electrical energy. This electrical energy supplied spacecraft loads and recharged the battery as necessary. Prior to Sun acquisition and during Sun occultation, spacecraft loads were supplied by the battery. The shunt regulator served to maintain a constant spacecraft bus-voltage during lunar days by dissipating excessive solar array power. The charge controller provided proper charging current to the battery.

Solar Array

The solar array consisted of four identical panel structures, each with an area of 13.1 square feet, upon which were mounted 2714 N-on-P silicon solar cells, each 2 by 2 cm, which collected radiant solar energy and converted it to electrical energy. The cells were arranged in five diode isolated circuits as follows:

1) Three circuits consisting of 104 six-cell modules connected in series. Cells within a module were connected in parallel.

2) One circuit consisting of 104 eight-cell modules connected in series. The cells within each module were connected in parallel.

3) One circuit, the auxiliary solar cell patch, consisting of 10 cells connected in series.

Four circuits (1, 2) on each panel were connected in parallel, through isolation diodes, to a bus common to all panels; the resultant spacecraft array consisted of 10,816 solar cells. The auxiliary solar-cell circuit (40 cells) provided base voltage and current necessary to saturate the main pass transistor of the charge controller. (Refer to Figure 3.1-5).

Solar panel deployment was initiated by a stored program command. Panel cooling was accomplished through radiation into space from the off-Sun side. Performance telemetry instrumentation monitored solar array voltage, current, and temperature.

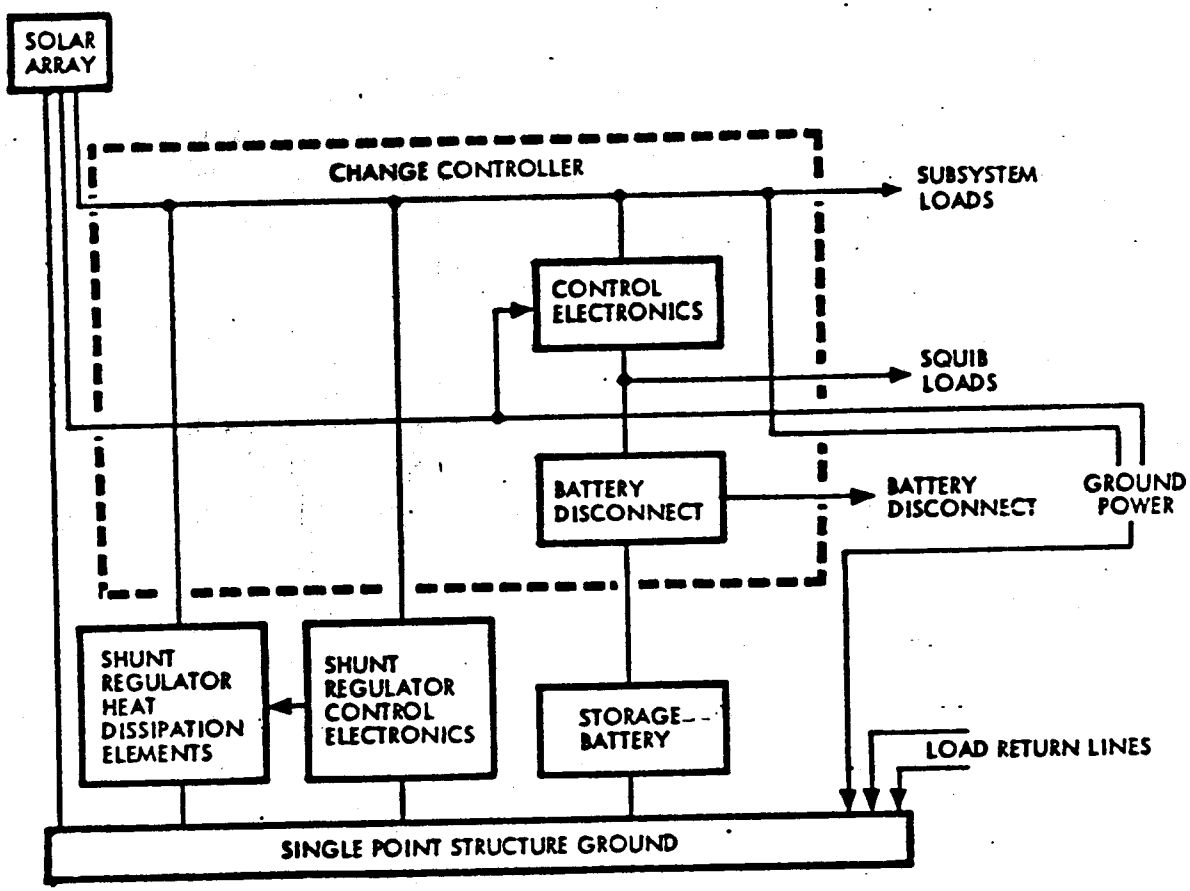

FIGURE 3.1-4: POWER SUBSYSTEM BLOCK DIAGRAM

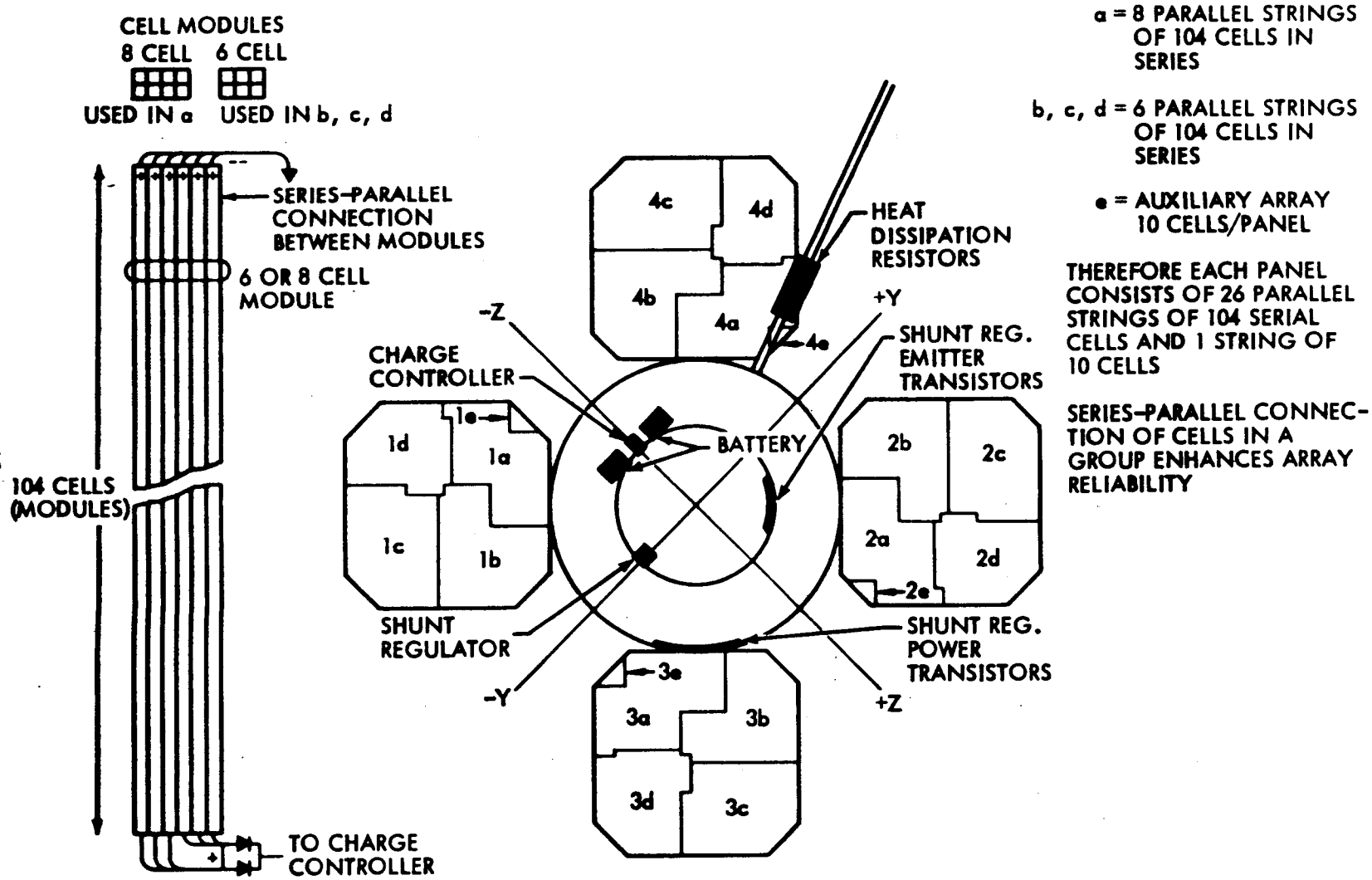

FIGURE 3.1-5: SOLAR ARRAY

Storage Battery

Electrical energy from the solar array was stored in two 10-cell nickel-cadmium batteries with a total nominal capacity of 12 ampere hours. The storage batteries provided all electrical energy from T-6 minutes prior to launch until Sun acquisition and during periods of Sun occultation. The batteries and solar array shared the load whenever the solar array output was insufficient to meet spacecraft load demands. The battery was charged at the nominal constant voltage until battery cell temperatures reached approximately 125°F, when protection circuitry switched the charge current to a trickle-charge rate. Current, voltage, and temperature of the battery were monitored by the telemetry system.

Charge Controller

The battery-charge controller regulated the battery charging rate to protect the battery from overvoltage and overtemperature conditions while charging in a minimum time. Under normal conditions, the maximum charging current was 2.85 amperes. When on trickle charge, the maximum charging current was 0.3 ampere.

Shunt Regulator

The shunt regulator operated only when the solar array provided more electrical energy than was required to satisfy the electrical loads and battery charging requirements. It limited the solar-array bus to a level of 30.56 volts, bypassing the excess current to heat-dissipation elements outside the heat shield. Closely regulated 20-volt, direct-current outputs provided a telemetry and spacecraft bus voltage reference.

3.1.2.2 PERFORMANCE

Boost and Acquisition Phase

From 6 minutes prior to liftoff until Sun acquisition, spacecraft power was supplied by the battery. It was fully charged at launch with a terminal voltage of 30.0 volts. Twenty minutes after liftoff, while discharging at 3.83 amperes, the terminal voltage was 25.28 volts. The spacecraft load during this phase was made up of the subsystem loads in approximately the following proportions:

Communications	26%
Attitude Control	55%
Velocity Control	7%
Photographic	5%
Power Subsystem Losses	7%

Just prior to Sun acquisition, the battery voltage was 24.96 volts. At this time, the battery had been discharged to a depth of approximately 30%.

Cislunar Phase

After Sun acquisition, the current supplied to the spacecraft was 3.43 amperes at 30.56 volts. This was lower than the estimate of 3.94 amperes at the same voltage. Battery charging current was 2.85 amperes as predicted, and the internal power subsystem loss was 0.49 ampere at 30.56 volts on the buss. Array current stabilized at 12.67 amperes, giving a power output of 387 watts with a mean panel temperature of 90°F. Solar power was more than sufficient to supply the load demand during cislunar flight; therefore, the shunt regulator dissipated the excess energy and kept the bus voltage stabilized at 30.56 volts. Maximum shunt regulator dissipation was 260 watts, occurring while the charge controller was in the trickle charge mode with battery charge rate at 0.28 ampere.

The array current was reduced to 11.47 amperes during the midcourse maneuver, when the spacecraft was pitched 25.2 degrees from the Sunline, resulting only in decreased shunt regulator dissipation by a corresponding amount. Subsequently, the spacecraft was pitched 36 degrees from the Sunline to reduce the temperature of the equipment mounting deck. The array current under this condition was 10.33 amperes with a mean panel temperature of 69°F. All spacecraft power loads during this phase of the mission were supplied from the solar array and bus voltage was maintained at 30.56 volts.

Charge controller operation during this period was as anticipated. The normal charge current of 2.85 amperes was maintained until the battery approached the fully charged state, then the charge current was reduced in accordance with the battery voltage and module temperatures sensed by the charge controller for the constant-voltage mode of operation. The charge controller changed to the trickle charge mode when battery temperature reached 125°F and returned to the constant-voltage mode when the temperature fell to 119°F. While the spacecraft was held at 36 degrees off-Sun, the battery temperature was approximately 96°F. Battery charge in the constant-voltage mode during most of the cislunar phase was limited between 1.0 and 2.0 amperes. Typical limiting range of voltage-temperature combinations were between 27.8 volts at 118°F and 28.6 volts at 94°F.

On August 14, the spacecraft entered the Moon's shadow for the first time, and the spacecraft went onto battery power. The deboost maneuver was performed during Sun occultation and all spacecraft loads during this time were supplied satisfactorily. Drain on the battery during engine burn was 7.78 amperes, and the energy taken from the battery during this first occultation period was approximately 3.27 ampere hours.

Ellipse Phase

Figure 3.1-6 shows the relationship between array current, load current, shunt regulator current, and battery current for Orbit 9-10 in the first ellipse. Array current at 30.56 volts is seen to be 12.73 amperes for an average panel temperature of 92°F; thus, there was no apparent array degradation up to that time. Load currents in the lunar orbit cruise mode of operation averaged about 4.0 amperes during the daylight period and 3.6 amperes at night. Both values were less than expected; this may have been due to the spacecraft being somewhat hotter than estimated, and the demand from the spacecraft heaters was less. The charge controller continued to operate satisfactorily, limiting the charge rate to a constant 2.85 amperes until battery temperature and voltage caused a changeover to

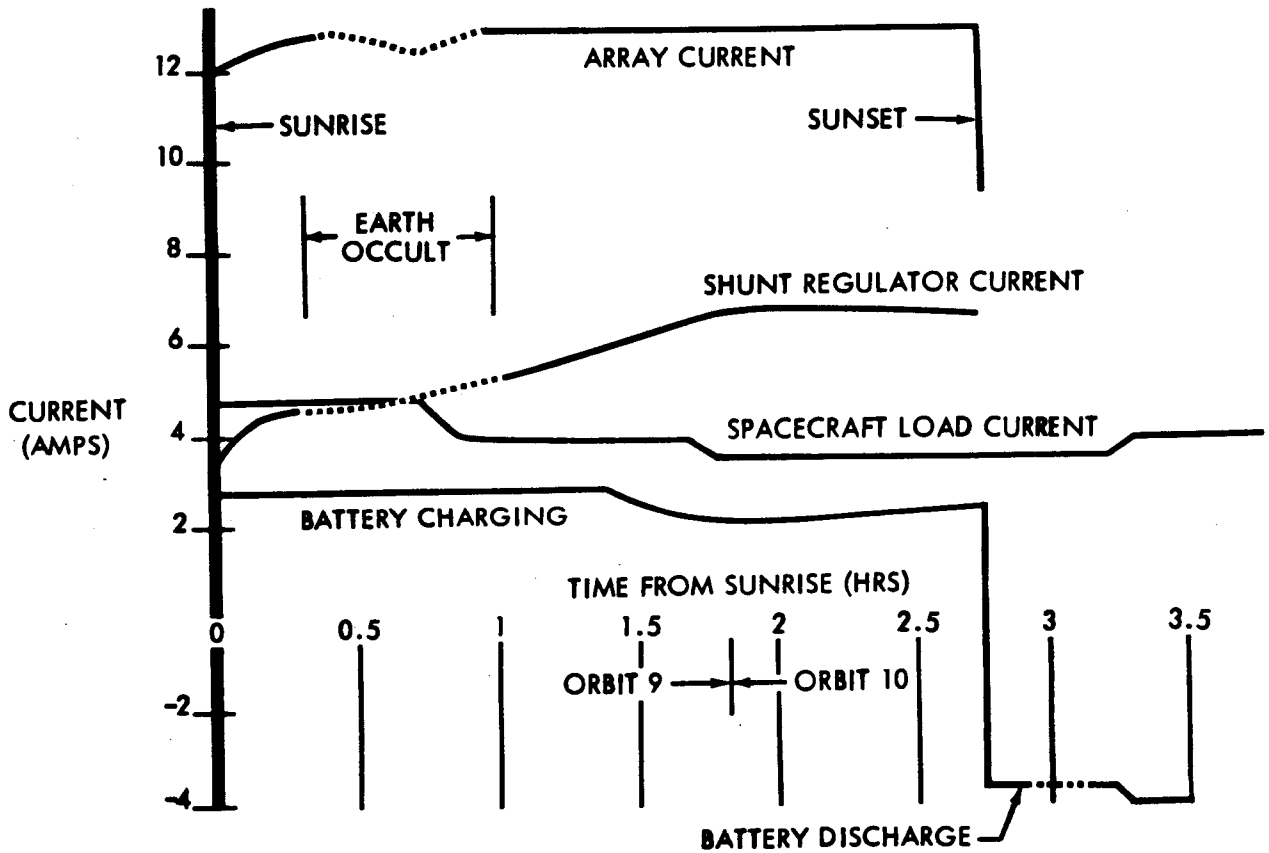

FIGURE 3.1-6: POWER SUBSYSTEM CURRENT PROFILE — INITIAL ORBIT 9-10 (PREFAULT)

the constant-voltage mode with an attendant tapering off in charge rate. Shunt regulator performance was satisfactory through Orbit 19 of the first ellipse. During Sun occultation in Orbit 20, the shunt regulator drew excessive current, and it was concluded that a transistor had shorted in one of the dissipative networks. (See Appendix D). Typical battery performance during the first ellipse is illustrated by Figures 3.1-7 and 3.1-8 showing curves of current, temperature, and voltage during the charge-discharge cycles of Orbits 9-10 and 31-32. These curves show the limiting action of the charge controller as it changes from the constant-current mode to the constant-voltage mode of operation. Battery voltage decreased under overcharge (constant-voltage mode) because of the increasing battery temperature at that time. The battery-temperature curves show: (1) how the heat output increases as the battery approaches the fully charged condition and (2) overcharge is a low-efficiency operation as indicated by the steep temperature increase. The higher discharge rate indicated in Figure 3.1-8 for Orbit 31 was representative of the discharge rates occurring in each orbit after Orbit 20 and was due to the power transistor failure in the shunt regulator circuit (refer to Appendix D). Based upon a nominal battery capacity rounded to 13 ampere-hours, the depth of discharge during Orbit 10 Sun occultation was 26.7%. The depth of discharge for Orbit 31 was 35.7%. The overcharge ratio calculated for Orbits 9-10 and 31-32, respectively, was 2.02 and 1.43. This ratio provides an index of battery and charge-controller operation associated with energy balance. Within the range of battery temperatures encountered, an overcharge ratio of 1.35 is considered reasonable for energy balance. Higher values calulated from telemetry indicate the margin of safety within each cycle.

The power transistor failure, which became apparent at Sunset of Orbit 20, increased the nighttime discharge by an average of 1.26 amperes for the rest of the mission. Resultant battery end-of-discharge voltage was decreased from 24.50 to 24.35 as shown in Figure 3.1-9 and the depth of discharge was increased from 26.5 to 34.0% as shown in Figure 3.1-10. However, this greater depth of discharge did not degrade the battery enough to threaten its capability to support the photographic mission.

After injection into the final lunar orbit, the power subsystem continued to perform satisfactorily although there was still a continuous drain on the system of approximately 1.1 to 1.5 amperes due to the shunt regulator fault. This additional load on the system did not affect the picture-taking, processing, or readout phases of the mission. However, for thermal reasons, it was necessary to pitch the spacecraft off the Sunline, thus reducing the output from the solar array. The fault then became a factor in determining how far the spacecraft could be pitched and still maintain the desired bus voltage and energy balance. Referring to Figures 3.1-11 through 3.1-12 it is seen that photographic readout imposed the greatest load demands on the system. Hence readout was not started until at least 10 minutes after Sunrise. This delay allowed time for the array to warm up, providing nominal power output. When the spacecraft was pitched off the Sun line to reduce the temperature of the equipment mounting deck, it was determined that with a pitch angle of 16 degrees, the bus voltage would remain at 30.56 volts during readout even when the array was at its maximum temperature. By delaying readout until after the spacecraft had passed over the subsolar point, it was found that this angle could be increased to 22 degrees.

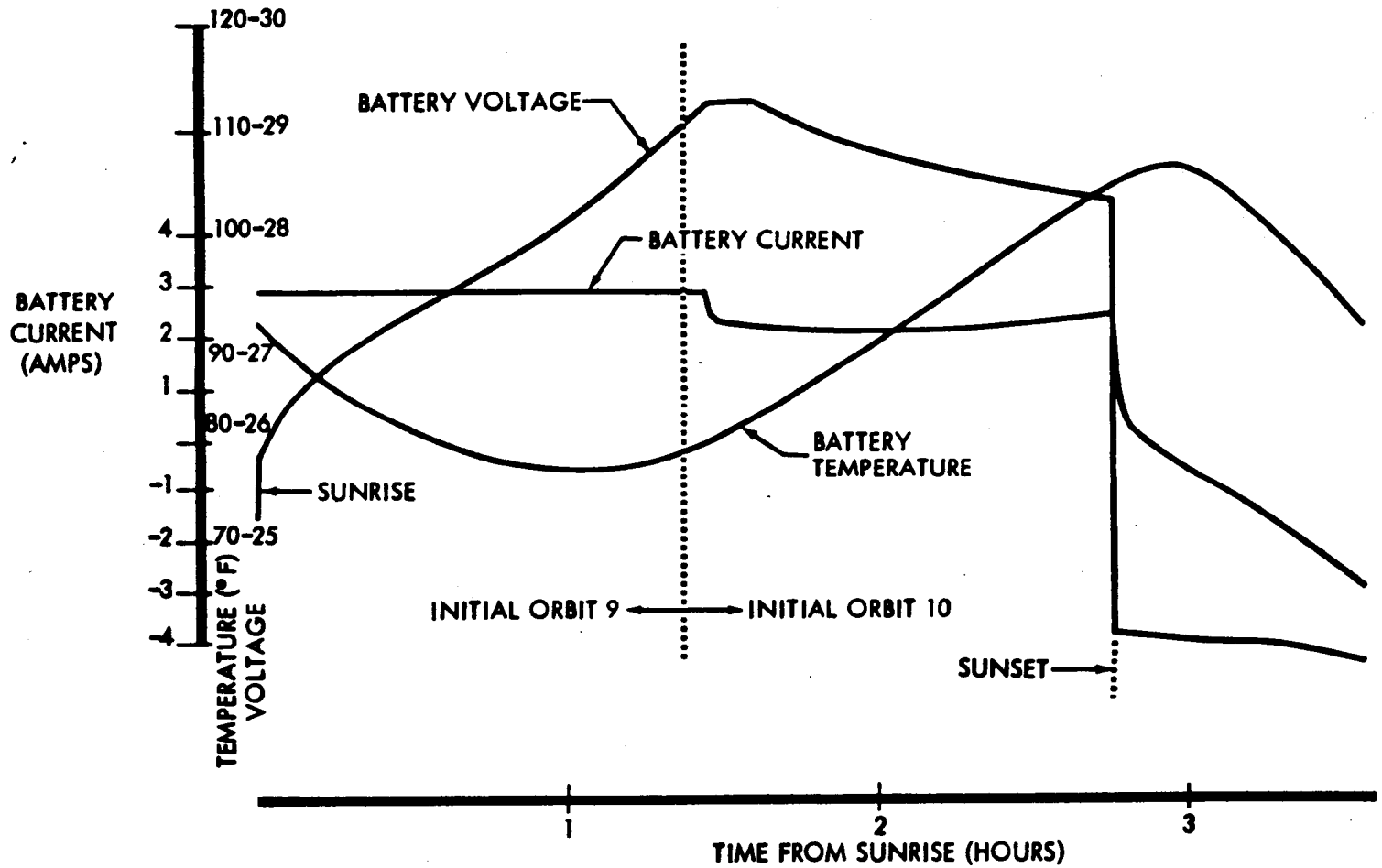

FIGURE 3.1-7: BATTERY CHARACTERISTICS — INITIAL ORBIT 9-10

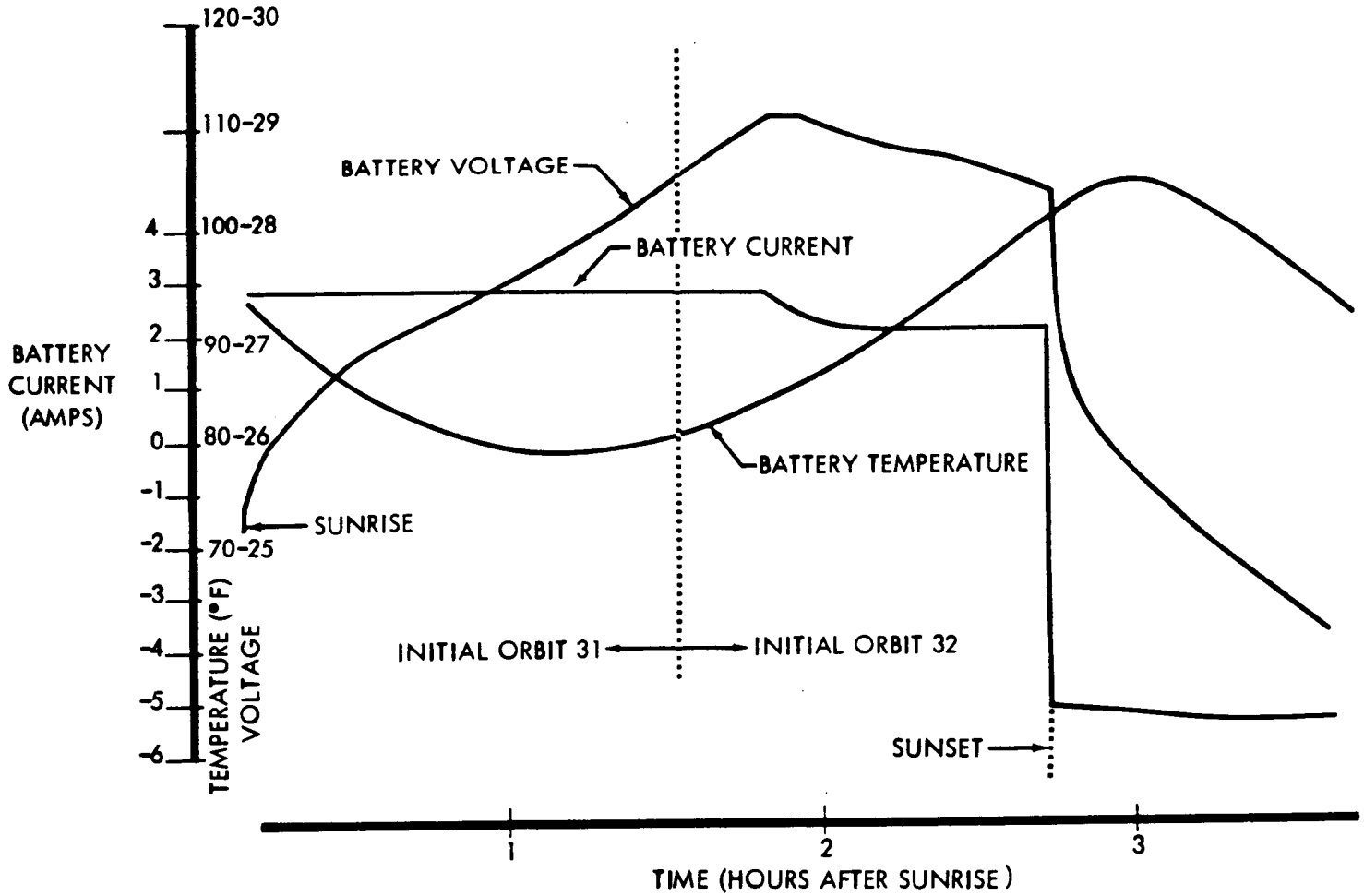

FIGURE 3.1-8: BATTERY CHARACTERISTICS — INITIAL ORBITS 31-32

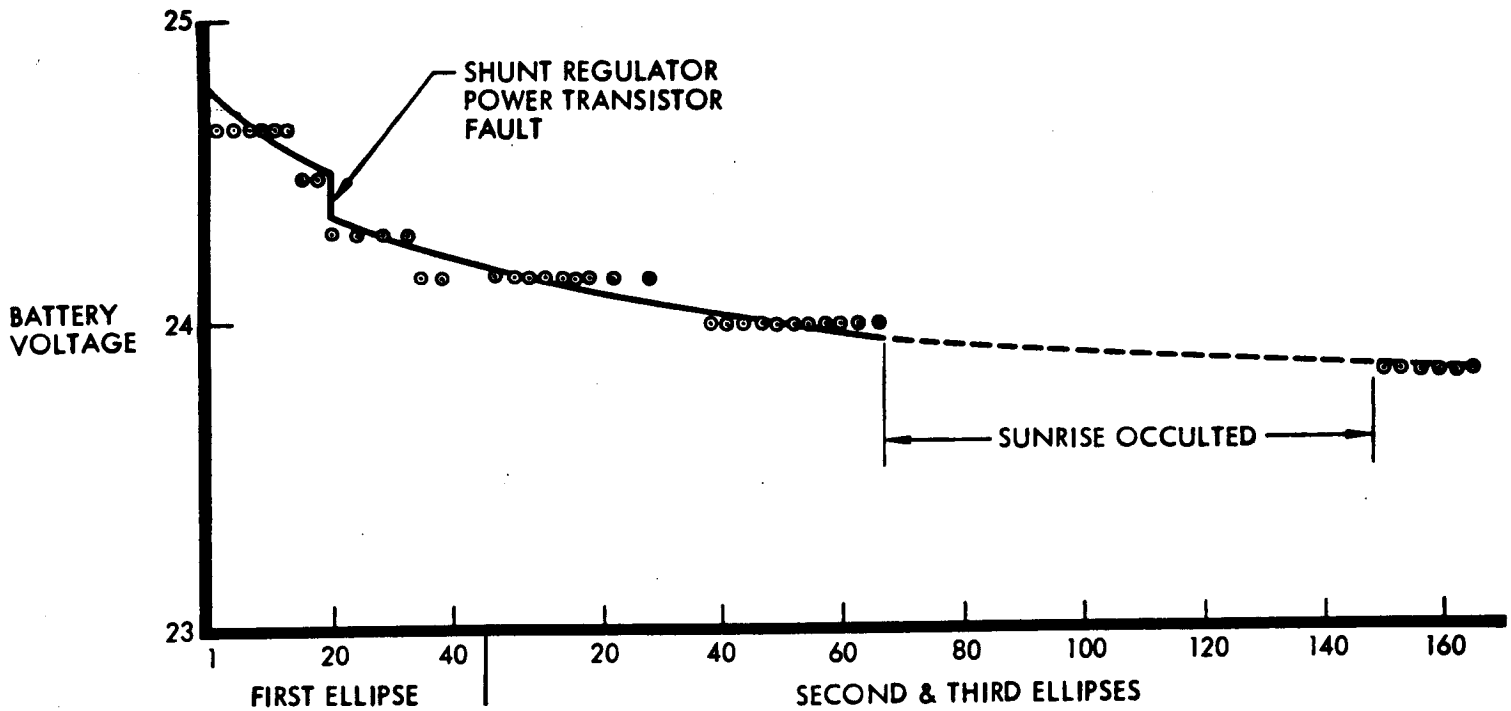

FIGURE 3.1-9: END-OF-DISCHARGE BATTERY VOLTAGE—MISSION I

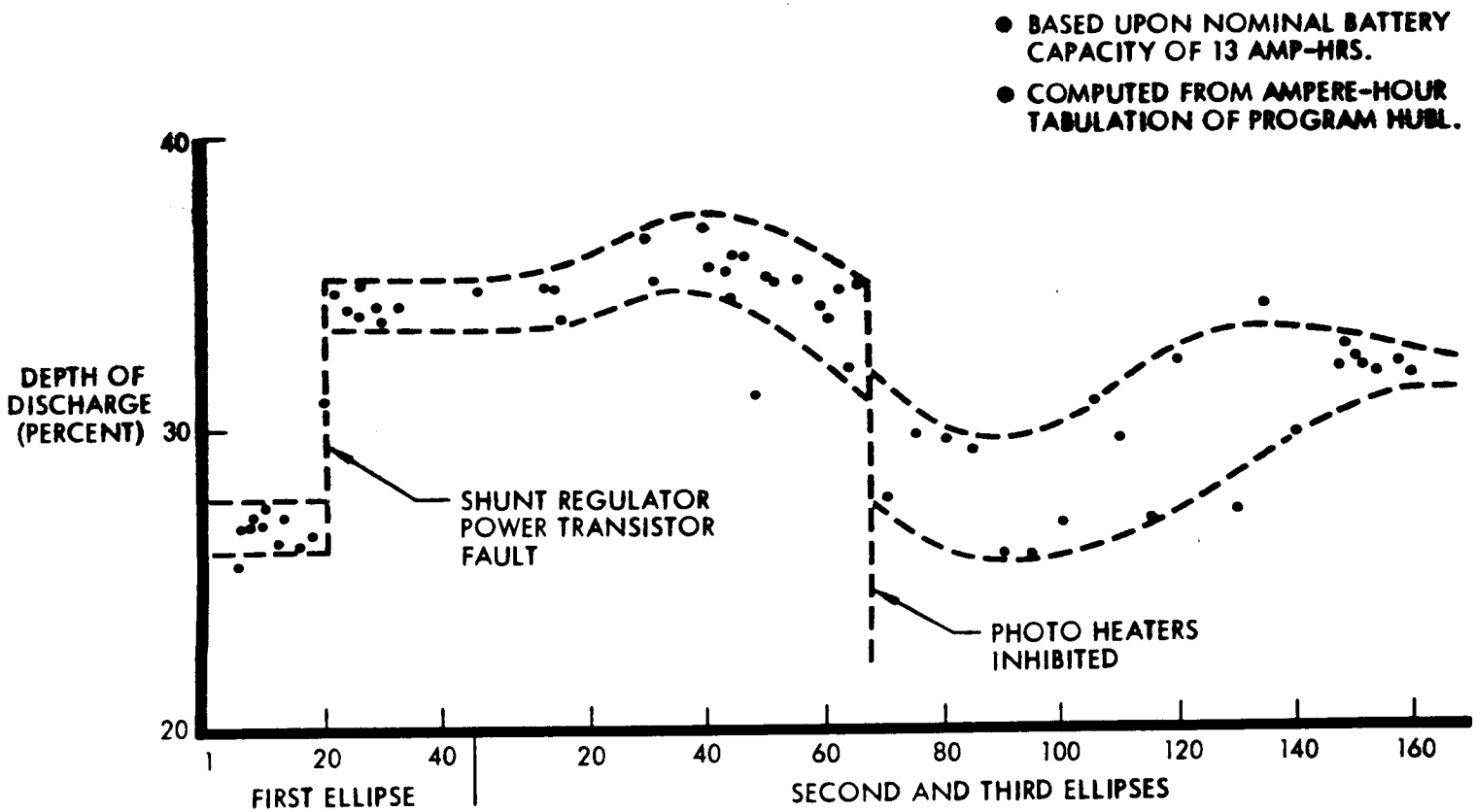

FIGURE 3.1-10: BATTERY DEPTH OF DISCHARGE—MISSION I

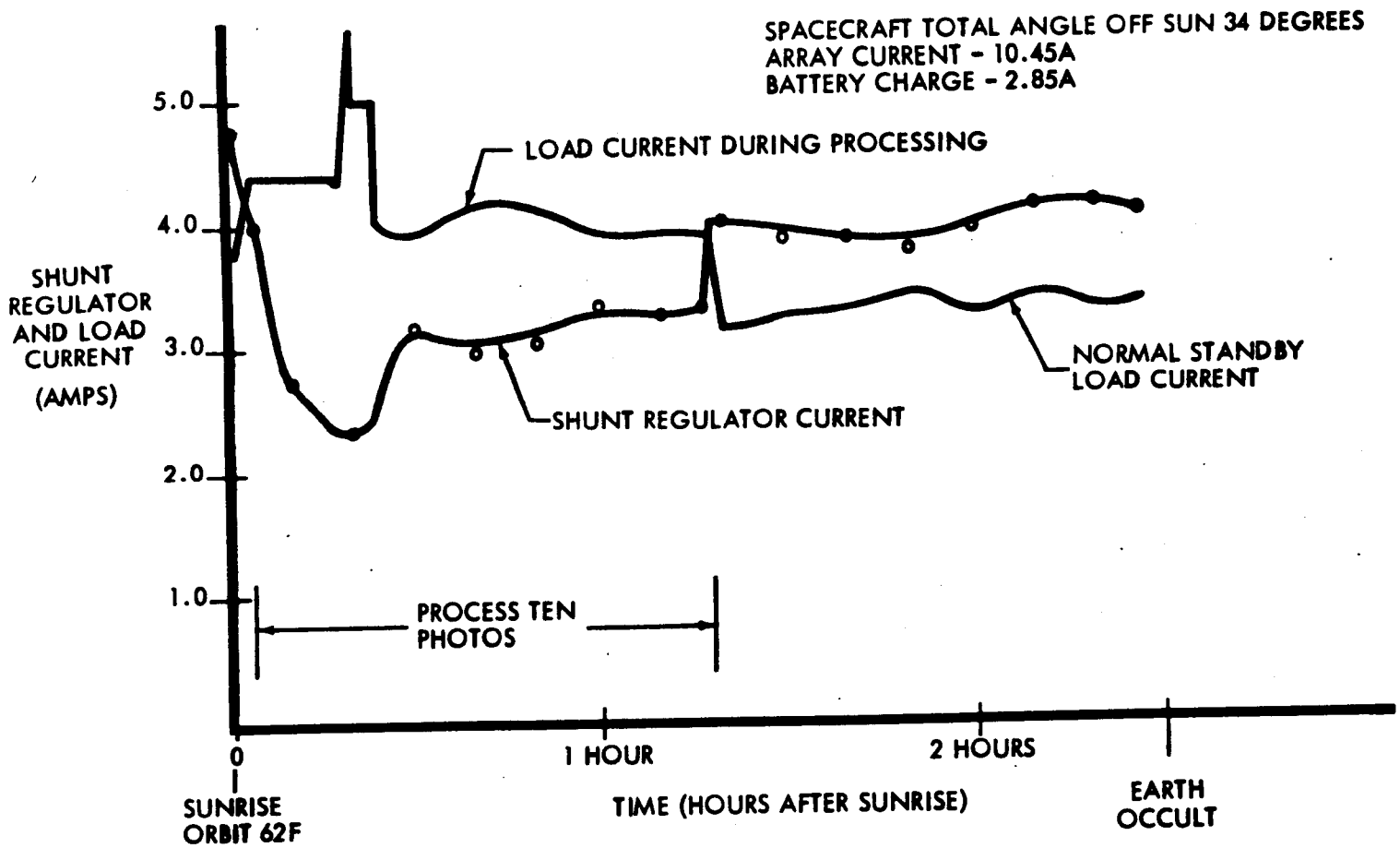

FIGURE 3.1-11: LOAD PROFILE DURING PROCESSING — FINAL ORBIT 62F

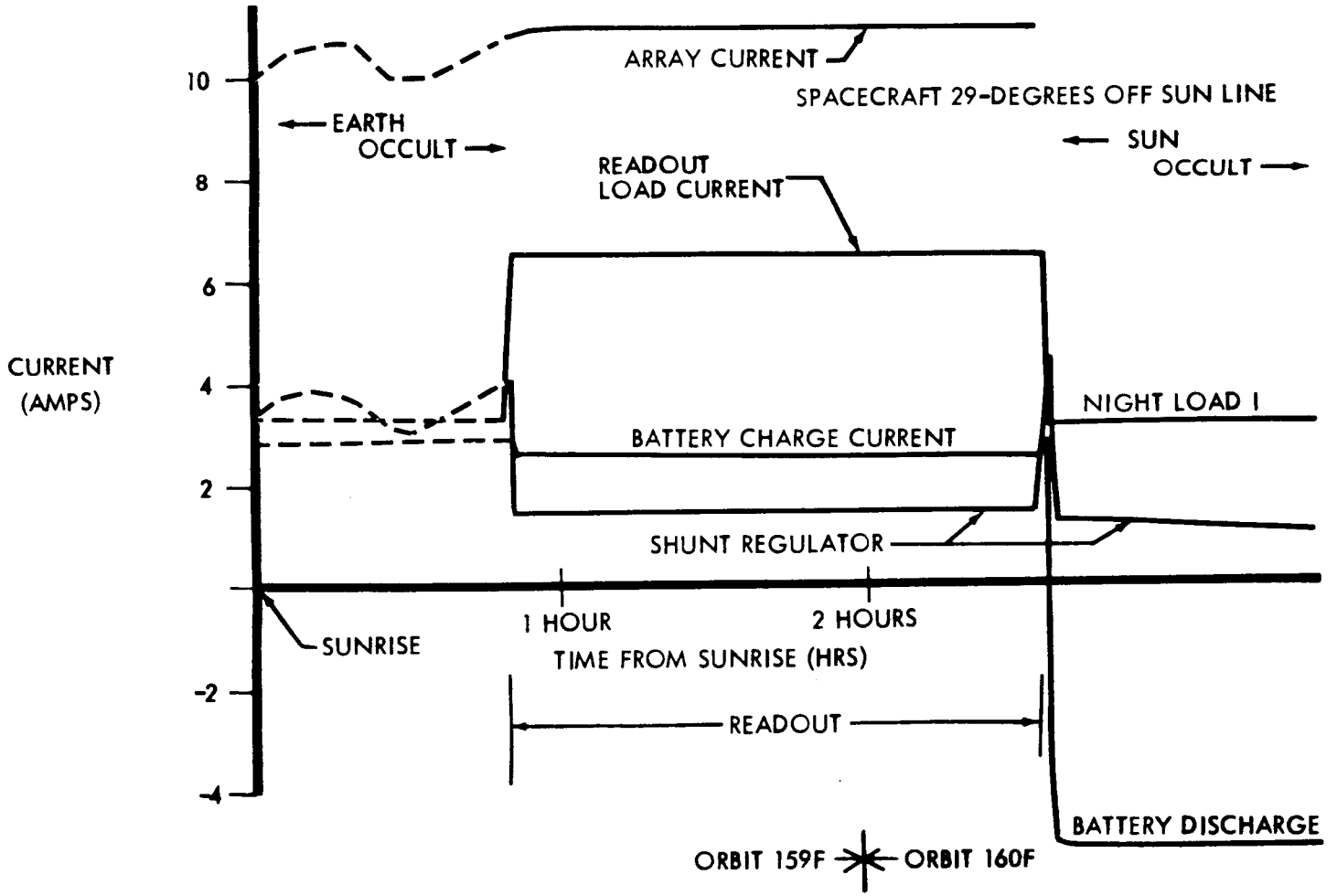

FIGURE 3.1-12: POWER SUBSYSTEM CURRENT PROFILE — FINAL ORBIT 159-160 READOUT MODE

For non-readout periods, a pitch angle of 36 to 37 degrees was used to give even greater cooling. At this pitch angle, no surplus power was available from the solar array, causing the shunt regulator to turn off and the buss voltage to drop to the battery charging voltage of 28.0 volts. This allowed the spacecraft to be cooled by turning off the Sunline and still have sufficient battery charging current during Sunlight to maintain energy balance.

Typical battery performance during the final readout orbits is illustrated by Figure 3.1-13 which shows curves of battery current, temperature, and voltage during the charge-discharge cycle of Orbits 159-160. It was typical operating procedure during this mission phase to operate with the solar array misaligned from the Sun by 25 to 33 degrees during readout. This resulted in a cooler battery and a lower charge rate as illustrated in Figure 3.1-13, which shows a charge rate of 2.5 amperes at 29.5 degrees off Sun. This value would have been 2.85 amperes if array current were not limited by spacecraft attitude. Depth of discharge for this orbit was 31.8% and overcharge ratio was 1.51. During Sun occultation in Orbits 107 and 108, the propellant heaters were left on in an effort to increase the depth of discharge, thus decreasing the battery heat output during the succeeding charge period. Depth of discharge was increased by approximately 1.3 ampere-hours (10% of total capacity), and peak temperature of the battery during the next charge period was 7°F below the preceding orbit. However, the cooling effect on the equipment mounting deck was negligible.

The criteria for battery performance degradation over the mission period is the end-of-discharge voltage. This is plotted in Figure 3.1-9 and shows that after 200 cycles battery voltage at end of discharge was 23.8 volts. Specification requires the battery voltage to be over 22.7 volts. A good safety margin is indicated for battery life during the photographic mission.

During Orbit 67, the photo subsystem heaters were inhibited and left off. This shows as an incremental step in the battery depth of discharge in Figure 3.1-10. This figure represents depth of discharge as an envelope that widens during the central portion of the final orbits. The scattering of points is due to the method used by the HUBL program for inserting predicted values where no telemetry is available. In the portion of the mission where night-time was totally or partically obscured by Earth occultation, predicted values of battery current were used, thus scattering ampere-hour calculated values.

An evaluation of telemetry data over the period from solar panel deployment to the completion of photo readout on September 14, 1966 (2:57 GMT) revealed that the solar array performance degraded very little. The evaluation of array degradation was limited by the fact that it should have been made by comparison of the array output during an early orbit with that obtained during a late orbit at a time when the array was oriented normal to the Sun for the entire orbital day. This would ensure observation of array performance over its entire temperature range, which is required for a definitive array-degradation evaluation. By the middle of Mission I, it became evident that long periods of spacecraft orientation directly on-Sun would result in excessive spacecraft temperatures possibly causing a subsystem malfunction. Accordingly, in the latter part of the primary mission there was little data obtained with the array oriented normal to the Sun.

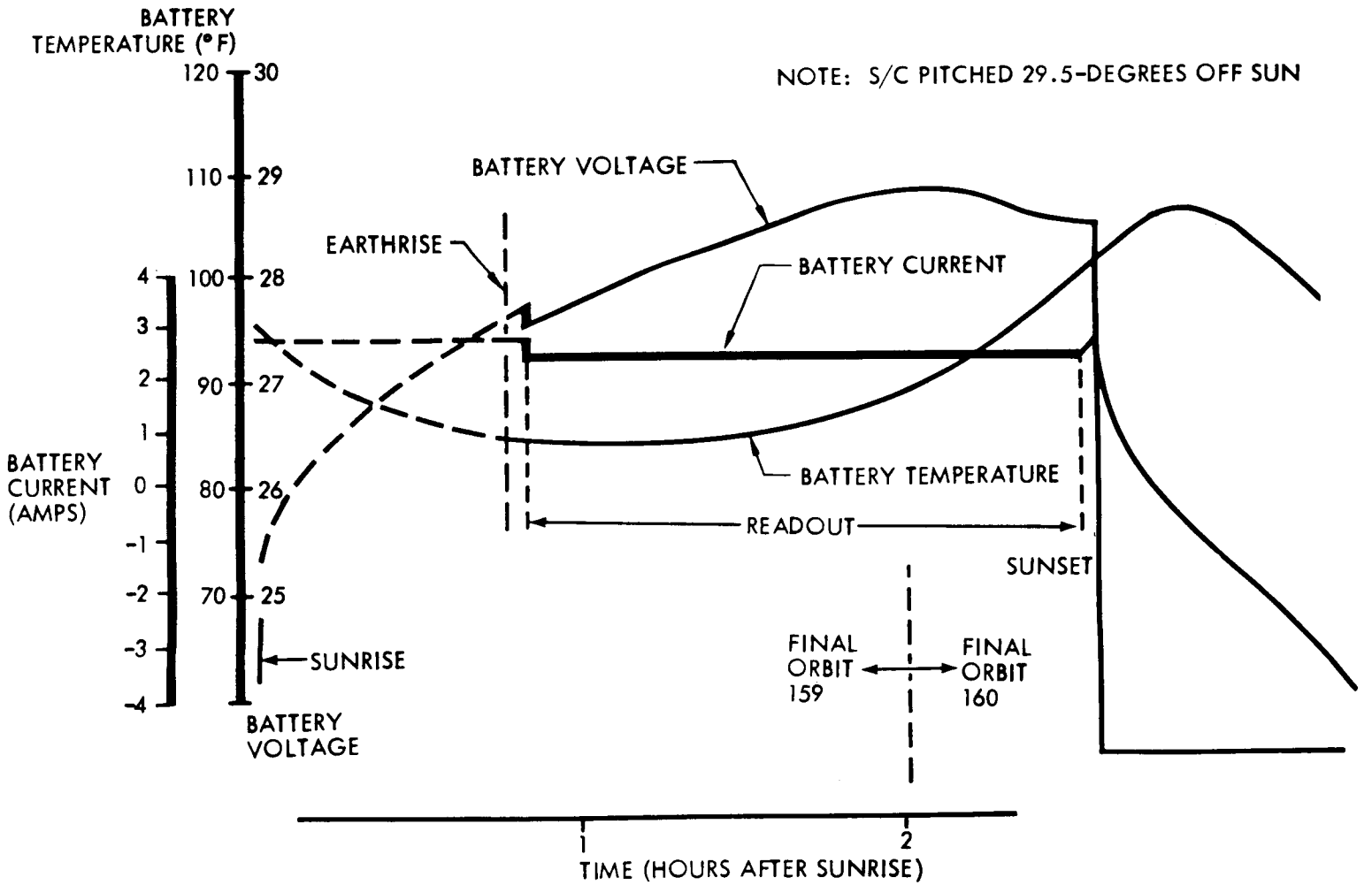

FIGURE 3.1-13: BATTERY CHARACTERISTICS — FINAL ORBIT 159-160

It should also be noted that the degradation effects are somewhat concealed because the operating point design of the array was deliberately chosen away from the maximum power point of the array (approximately 40.9 volts) to minimize the effects of solar array degradation on power system performance.

The extreme observed panel temperatures approximated those predicted: High 210.1°F (99°C), Low -189.9°F (-123.5°C). Temperature sensors on panels in Positions 1 and 2 tracked well throughout the mission; Panel 4 sensor also tracked well but at temperatures 10 to 20°F higher than average during the day. It is likely that the higher temperature readings on Panel 4 result from the proximity of the shunt-regulator emitter resistor assembly mounted on the low-gain antenna.

The temperature sensor of Panel 3 tracked with Panels 1 and 2 only during small temperature fluctuations. Rapid temperature changes occurring during Sunrise and Sunset caused this sensor to differ from the others; such an anomaly suggests sensor delamination from the panel surface.

Within the limits of telemetry error, the array output was approximately 1% higher than specified, and near the output expected when compared to solar array test data obtained from the calibrated Lunar Orbiter artificial light test stand and high-altitude Sunlight tests.

Figure 3.1-14 is an average of Lunar Orbiter array performance based upon calibrated Lunar Orbiter artificial light illuminators. Figure 3.1-15 is typical array performance during early orbits of Mission I.

On completion of readout on September 14, 1966, the spacecraft was put into the extended mission cruise mode configuration, at which time all nonessential loads were turned off, leaving an average daytime load of 3.25 ampers and a nighttime load of 3.35 amperes.

3.1.3 COMMUNICATIONS SUBSYSTEM

3.1.3.1 FUNCTIONAL DESCRIPTION

3.1.3.1.1 Summary

The Lunar Orbiter I communications subsystem was an S-band system capable of transmitting telemetry and receiving commands over the Moon-Earth distance. The tracking, telemetry, and command communications were conducted via DSIF sites at Goldstone, California (DSS-12), Madrid, Spain (DSS-61), and Woomera, Australia (DSS-41). The checkout station at Cape Kennedy (DSS-71) was active during the checkout, launch, and boost phases. The spacecraft equipment design was compatible with the 85-foot antenna grid at the three prime stations. Each site had a nominal view period for communications of about 12 hours each day, interrupted periodically by the occultation in each lunar orbit.

*AVERAGE LUNAR ORBITER SOLAR ARRAY OUTPUT I-V CHARACTERISTICS

ILLUMINATING SOURCE: L/O ILLUMINATOR AT RCA-AED CALIBRATED TO 139.6 MW/CM^2

ANGLE OF INCIDENCE: NORMAL

TEMPERATURE LEVEL FOR DATA REDUCTION: 50°C (122°F)

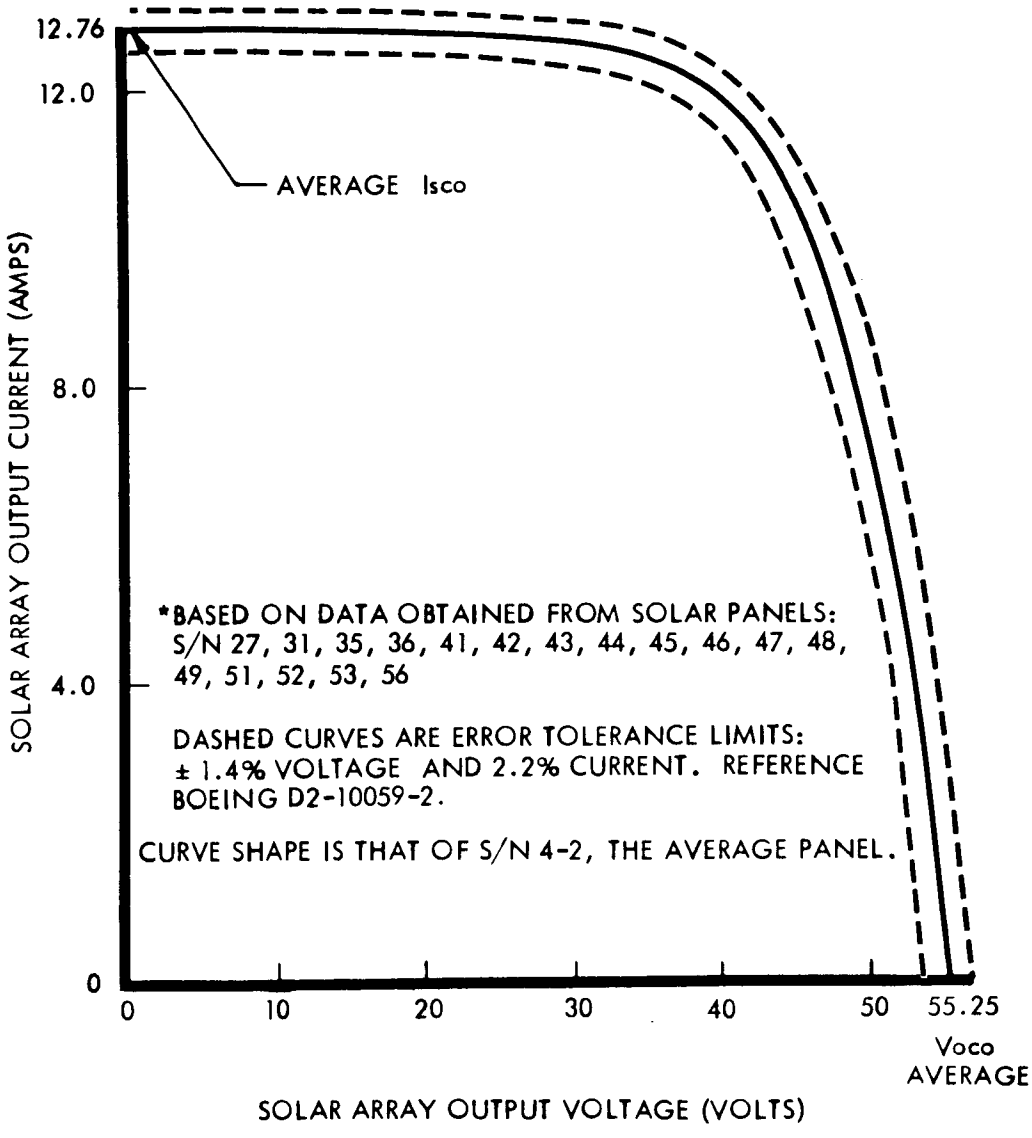

FIGURE 3.1-14: AVERAGE* LUNAR ORBITER SOLAR ARRAY OUTPUT I-V CHARACTERISTICS

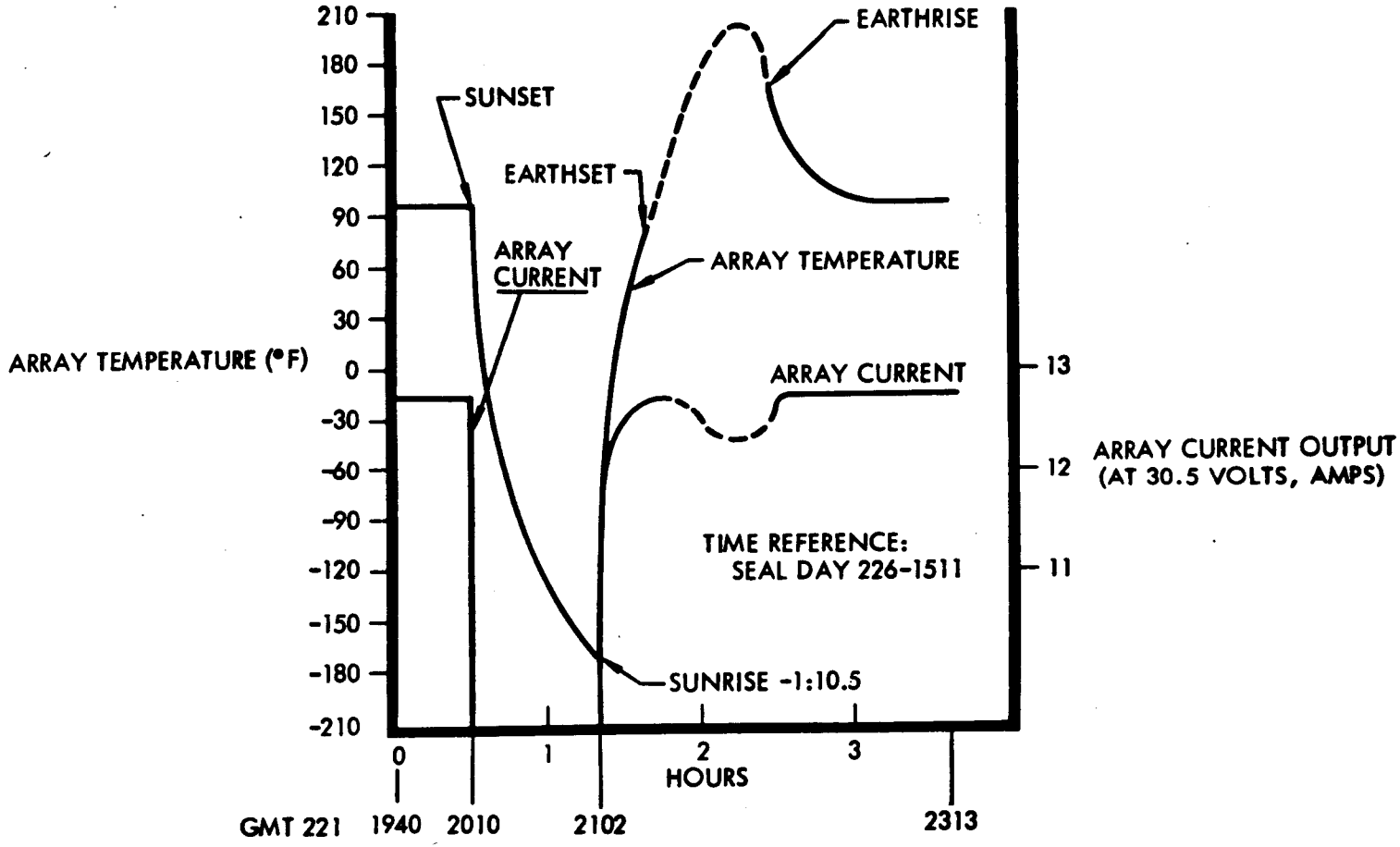

FIGURE 3.1-15: MISSION I OUTPUT CURRENT AND TEMPERATURE OF SOLAR PANEL 1 DURING INITIAL ORBIT 8

The communications subsystem provided the following capability:

1) Received, decoded, and verified command messages.

2) Transmitted spacecraft performance data, lunar environmental data, and video data (photographic data).

3) Operated in two transmitting power modes:

   a) Low power during acquisition, tracking, ranging, and telemetry data transmission.

   b) High power during transmission of photo video data.

4) Received and retransmitted turnaround ranging signals.

5) Slave transmitted carrier frequency to received carrier frequency for two-way doppler tracking and provided an auxiliary precision frequency oscillator for one-way doppler tracking.

6) The necessary controls for operating the subsystem in its various modes and turning it on or off in response to programmer or ground-supplied commands.

A block diagram of the subsystem is shown in Figure 3.1-16.

Subsystem functions could be performed in four operating modes:

Mode 1 (ranging and performance telemetry) provided a turnaround lunar ranging loop for range tracking of the spacecraft. Range-tracking data and performance telemetry data were transmitted simultaneously.

Mode 2 (photo video and performance telemetry) provided the capability to transmit photo video data and performance telemetry data simultaneously.

Mode 3 (performance telemetry) provided the capability to transmit performance telemetry data only.

Mode 4 (initial acquisition aid) was implemented by selecting Mode 2 modulation with no video input data.

Two-way doppler tracking of the spacecraft was provided during Modes 1, 3, and 4. A capability existed to change initial acquisition for future missions through additional mode switching. Mode 4 substantially increased the amount of carrier power in the down-link, thereby increasing the range at which initial acquisition could be accomplished.

3.1.3.1.2 Functional Details

Spacecraft transmission was initiated by real-time command during prelaunch and remained operational throughout the mission. The capability for command reception was demonstrated in each of the modes listed in Section 3.1.3.1.1. Particular modulation modes were selected and controlled in response to discrete commands issued by the flight programmer.

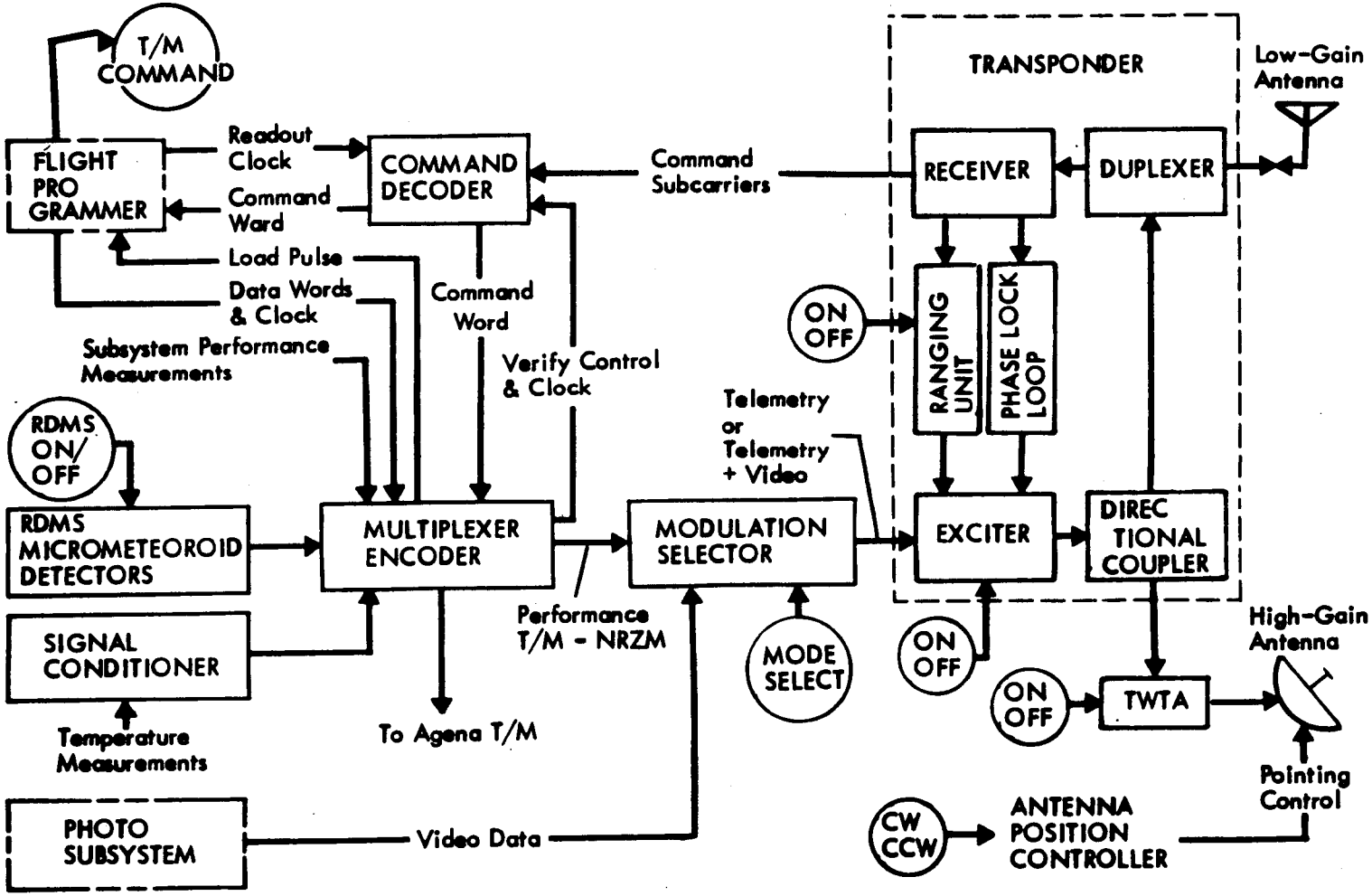

FIGURE 3.1-16: COMMUNICATIONS SUBSYSTEM BLOCK DIAGRAM (POWER CONNECTIONS NET SHOWN)

Performance Telemetry

Spacecraft and subsystem performance data, radiation data, micrometeoroid data, and command verification were classified as performance telemetry. Detailed listing of these measurements was provided in Boeing Document D2-100187-2, "Lunar Orbiter Spacecraft Performance Telemetry List." Briefly, the signals were:

1) Sixty-four digital measurements at one sample per frame, including two signals transmitted as analogs and 53 1-bit discrete signals; 102 bits per frame were required (excluding the two analog channels).

2) Seventy-five analog measurements, including one channel at eight samples per frame; 83 8-bit words per telemetry frame were required (including the two digital measurements).

3) Eight 20-bit digital words from the flight programmer, including one vehicle time word, at one sample per frame (required 160 bits per frame).

4) One 26-bit digital command word (verification) at one sample per frame.

5) One 43-bit word per frame for telemetry frame synchronization.

Telemetry data flow within the spacecraft is shown in Figure 3.1-17.

Performance data signals were generated by digital and analog transducers associated with each subsystem. Except for a few temperature measurements, all analog signals were conditioned to a standard voltage level by the individual subsystems. The temperature signals from thermistor transducers were conditioned to the required signal level by a communications subsystem signal conditioner prior to multiplexing. Nominal input range for analog signals was 0 to 5 v.d.c. Each signal was connected to the appropriate input to the 78 analog gates (including three spares). The instantaneous amplitude of each analog signal was sampled by the sequential operation of these gates. The sequencing provided 85 samples per telemetry frame maximum. Each sample was converted to an 8-bit straight binary word with the most significant digit first. Digital transducer signals, whose characteristics were -2 to -2.5 v.d.c. for a logic zero and 4.0 to 8.5 v.d.c. for a logic one, and from 1 to 9 bits per signal, were routed through digital gates at the rate of one sample per frame for each signal (maximum of 133 1-bit samples per frame). The output of the radiation and micrometeoroid detectors was included in the digital signals.

Data words from the flight programmer were serially entered into a 20-bit shift register at 2.4-kc shift rate, controlled by the flight programmer; eight load pulses were provided to the flight programmer to control the input of these words. The 26-bit command word was entered into the telemetry raster through separate circuitry. When no command verification was in process, alternate 0's and 1's were placed in this word position.

All samples and words and a 43-bit frame-synchronization code work were assembled into a 1152-bit frame. The format for this frame is shown in Figure 3.1-18, which corresponded to 128 9-bit words. The 9th bit, in the case of the analog data and certain multidigit words, was the complement of the 8th bit. These and the other "complement bits" in the frame

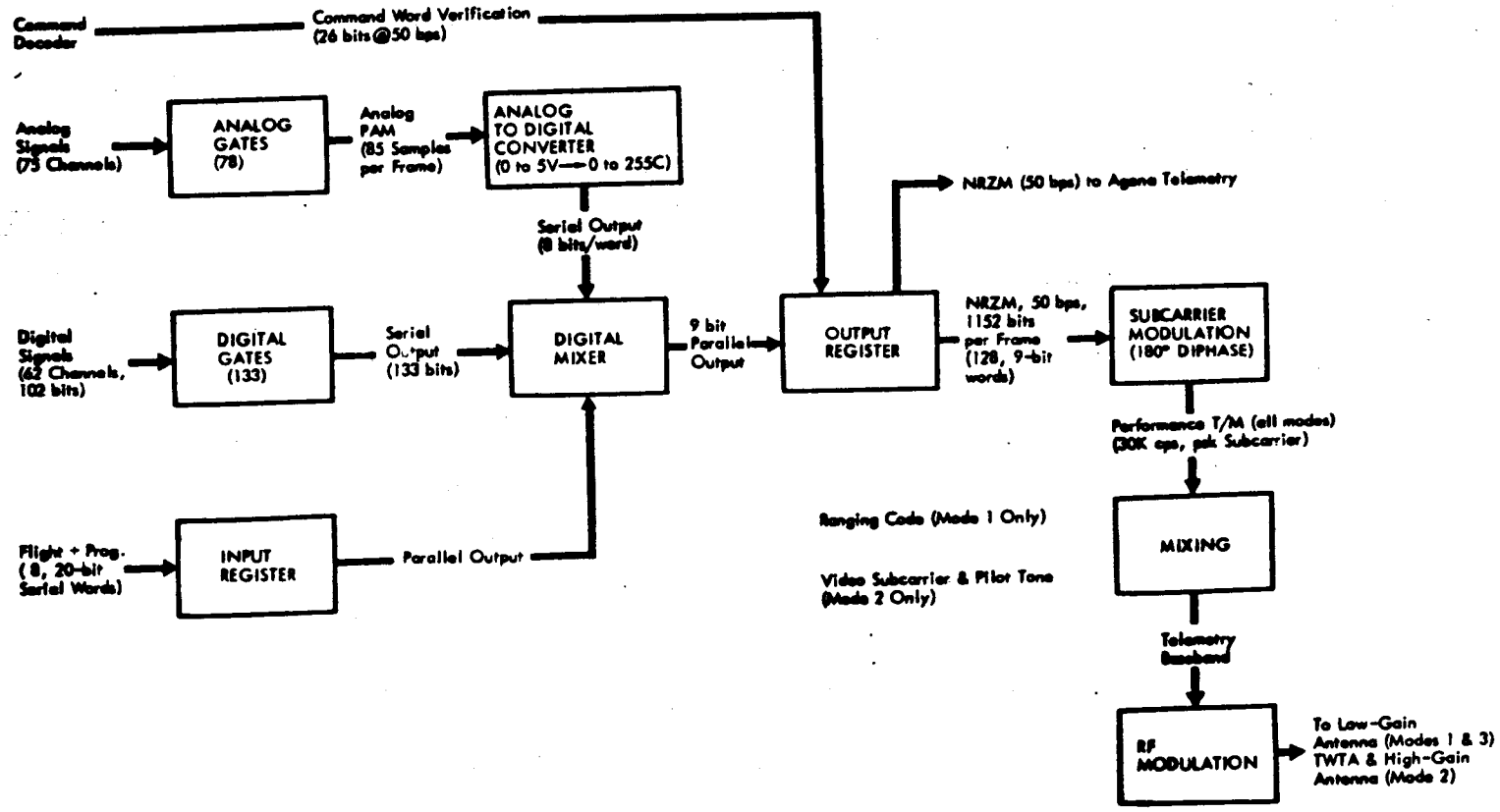

FIGURE 3.1-17: PERFORMANCE TELEMETRY DATA FLOW

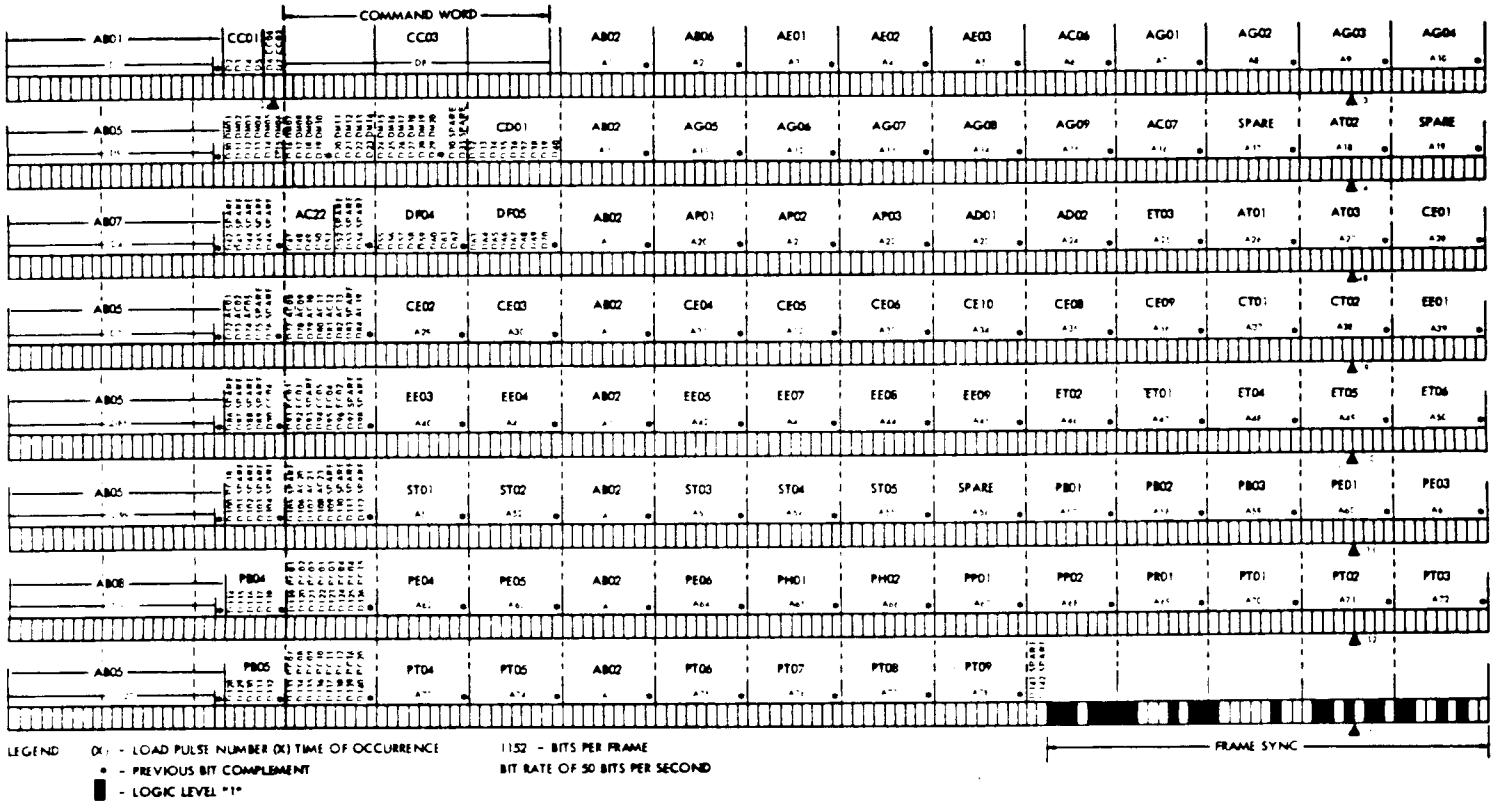

FIGURE 3.1-18: TELEMETRY DATA FORMAT

enhanced telemetry bit synchronization in ground equipment. The telemetry bit stream was serially coded to make a level shift for each bit valued at "1" (NRZ-M-1), at 50 bits per second (bps).

The telemetry Mode 1 NRZ-M-1 signal was diphase modulated (180 degrees, PSK) on a 30-kHz subcarrier, mixed with the ranging code, phase modulated on the S-band return frequency, and transmitted from the low-gain antenna. Mode 2 was similar except: (1) the modulation index was reduced; and (2) the telemetry subcarrier was multiplexed with the photographic subsystem video data and pilot tone to modulate the S-band transmitter (vestigial sideband), amplified by the TWTA, and transmitted over the high-gain antenna. Mode 3 was identical to Mode 1 except only performance telemetry was transmitted.

Prior to booster separation, a signal-isolation device connected the NRZ-M pulse train to the Agena telemetry; the pulse train was then frequency modulated on IRIG Channel F of Agena FM/FM telemetry.

Photo Subsystem Video Data

The data output of the photo subsystem was a 0- to 230-kc analog signal, produced by line scanning the processed film through a photomultiplier tube. This signal was supplied to the communications subsystem for processing through the telemetry link. The data flow and modulation spectra are shown in Figure 3.1-19.

Upon receipt of the video signal and a Mode 2 (video and performance telemetry) control signal from the flight programmer, the input video signal (0 to 230 kc) was amplitude modulated on a 310-kc crystal-controlled video subcarrier. Both the video subcarrier modulation frequency and the upper sideband of the mixture were then suppressed, producing a vestigial sideband (VSB-AM) modulation signal. Also, a 38.75-kc pilot tone was derived by dividing the 310-kc video subcarrier by eight. The pilot tone was used to re-establish the video subcarrier at the DSS. The vestigial sideband signal, the pilot tone, and the 30-kc telemetry subcarrier were summed in a wideband amplifier to form a composite signal. The composite signal was modulated onto the S-band carrier, amplified by the TWTA, and transmitted from the high-gain antenna.

Tracking Data

Doppler—Both one-way and two-way doppler tracking of the spacecraft was accomplished at each DSS. If no up-carrier was present at the input to the spacecraft transponder receiver, the transponder automatically switched to a crystal oscillator for control of the downlink carrier frequency. When the DSS receiver was phase locked to this carrier, one-way doppler tracking was accomplished at the DSS. One-way doppler tracking consisted of comparing the frequency of the received carrier at the DSS with the known frequency of the carrier transmitted from the spacecraft. The difference represented velocity-dependent frequency shift (range rate).

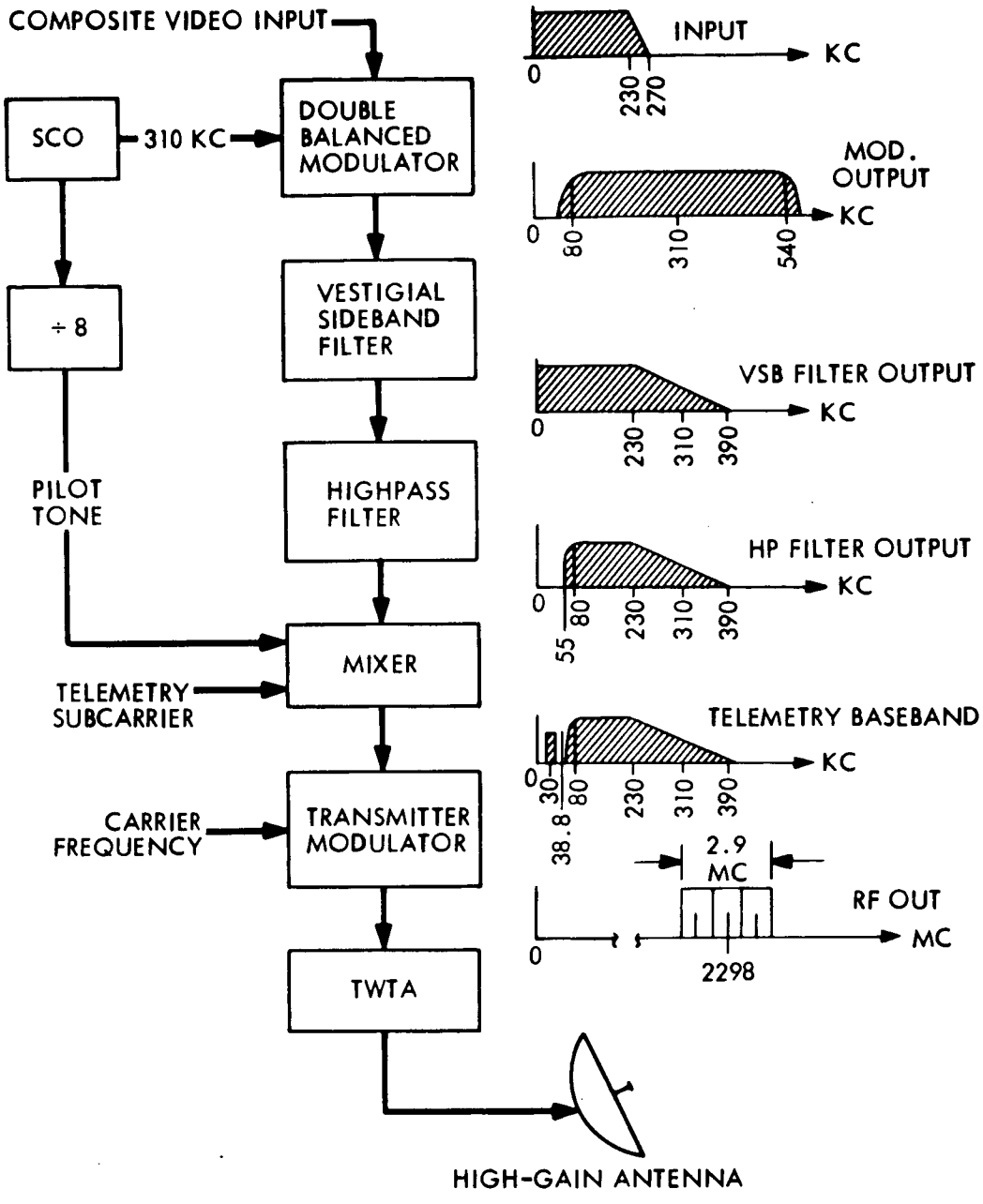

FIGURE 3.1-19: VIDEO DATA FLOW

Two-way doppler tracking was accomplished whenever an up-link carrier had transmitted frequency and power consistent with spacecraft requirements, and whenever a downlink carrier had transmitted frequency and power consistent with DSS requirements. When the up-link carrier was received by the spacecraft, the receiver tracked the incoming frequency (in this condition it was said to be phase locked). This tracking was accomplished by generating an intermediate frequency, which was a function of the phase error between the received and generated intermediate frequencies (ϕ = zero locked-tracking) and subsequently used it to detect and demodulate the incoming signal. The internally generated frequency, through a set of frequency multipliers, was used for the transmission frequency. By this means, transmitter frequency (down-link) was controlled to a precise, phase-coherent, 240 to 221 ratio with the received carrier frequency. At the DSS, the DSIF receiver was phase locked to the down-link carrier and the range rate was determined from the doppler shift with respect to the DSIF-transmitted frequency.

Ranging—For determining spacecraft range, a pseudo-random-noise code was phase modulated directly on the up-link carrier at the DSS. At the spacecraft, the code was detected and remodulated on the spacecraft down-link carrier. On the ground, the code was detected from the down-link carrier and compared in phase with the previously transmitted code. The phase difference (time) was then converted into a spacecraft range.

Command Data

The command data flow within the spacecraft is shown in Figure 3.1-20. The functions of this system were:

1) To accept properly enabled and transmitted command data;

2) To demodulate and temporarily store the transmitted command word;

3) To provide the received command word to the telemetry (to permit ground verification);

4) To supply the command word to the flight programmer (following initiation by ground control);

5) To provide a means for switching flight programmer timing to a redundant clock.

The tone frequencies and the sequence of frequencies were classified confidential (refer to Boeing Document D2-100264, "Lunar Orbiter Command Data," September 15, 1964). Functional sequence timing of the command data flow is illustrated in Figure 3.1-21.

Note that two tones were always transmitted in this sequence.

Enable sequence—To initiate transmission of commands to the spacecraft, one of two enable tones and the command subcarrier tone were modulated on the S-band rf carrier at the DSS. When received by the spacecraft via the low-gain antenna, the tones were removed from the carrier and demodulated. The enable signal gated operating power into the selected temporary storage register (demodulator power was on at all times). The registers were also reset and cleared of any previous command data during this sequence. The enable signal was transmitted continuously during the entire command, verify, and execute sequence.

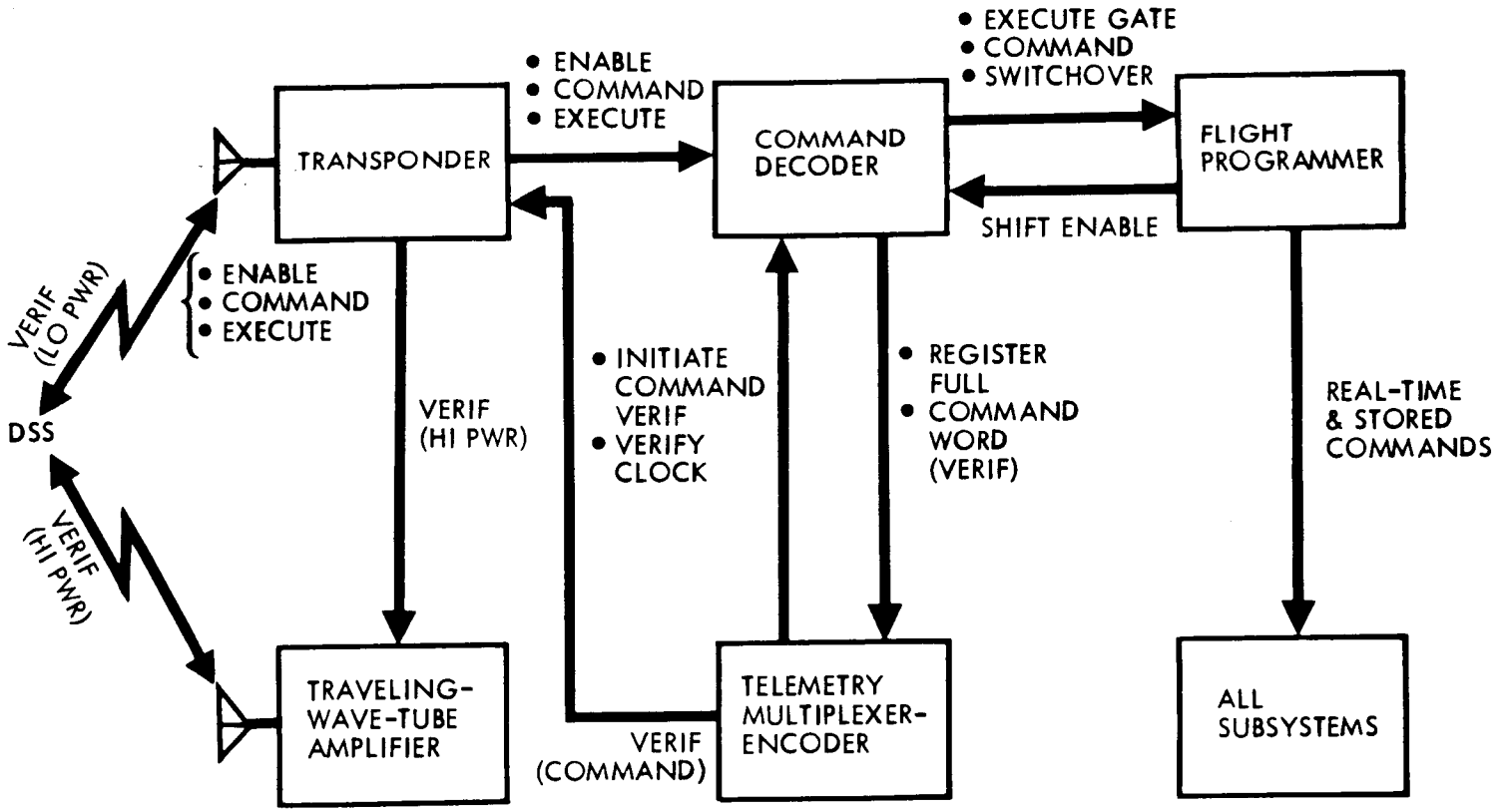

FIGURE 3.1-20: COMMAND DATA FLOW

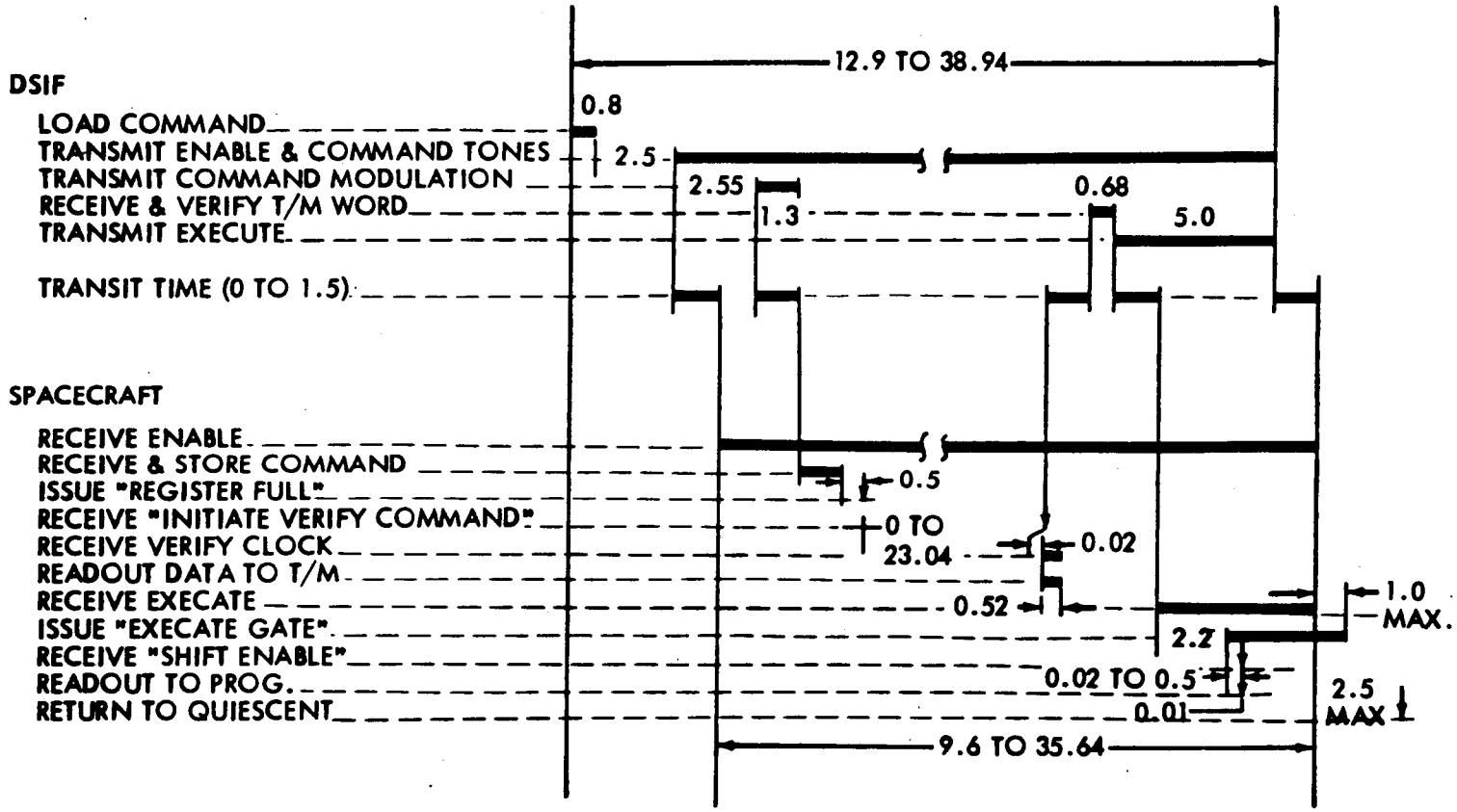

NOTE: TIMING IS FOR ONE VERIFICATION ONLY — ADD 23.04 SECONDS FOR EACH ADDITIONAL WORD.

FIGURE 3.1-21: COMMAND TRANSMISSION TIMING DIAGRAM

Command word sequence—After the enable tone had been processed (about 2 seconds), the 26-bit command word was phase modulated on the S-band rf carrier at the DSS. The 26-bit command word was detected from the rf carrier, demodulated, and held in temporary storage in the previously enabled register. Once the command word was stored in the register, additional command inputs were inhibited until the removal of the enable signal. The structure of the command word is shown in Figure 3.1-22.

Address verification sequence—The first four bits of the 26-bit command word comprised the spacecraft identification address code. Each spacecraft was assigned a unique code. After the complete command word was entered in the register, the address bits were non-destructively sampled through a patching arrangement. (If the pattern of the address bits did not match the code patching for the particular vehicle, the following sequences were inhibited).

Command word verification sequence—When the correct address had been verified, a "register full" signal was generated. This signal was transmitted over the telemetry as a 1-bit digital measurement. Within 23.04 seconds (the telemetry frame period) after "register full," the telemetry initiated command verification (ICV). The ICV signal set the readout commutator to nondestructively gate the register contents to the telemetry. A verify clock signal, 26-pulse duration at 50 pulses per second from the telemetry, caused the register data to be serially gated to the telemetry. The first clock pulse controlled readout of the first stored data bit and continued until all 26 bits had been read out. The command word was then formatted in the telemetry digital data stream. At the DSS, the command word was separated from the rest of the telemetry frame and compared with the originally transmitted command word. The readout and verification sequence continued until the execute sequence was initiated or the enable tone was removed. This depended upon the number of correct or incorrect comparisons required at the DSS.

Execute sequence—After the command word had been verified at the DSS, an execute tone was added to the S-band rf signal modulation. The execute tone was removed from the S-band carrier in the rf section and demodulated to produce an execute gate. This gate caused the flight programmer to issue a "shift enable" signal which, together with the programmer 2.4-kc clock pulses, enabled readout of the command word. The stored command word, excluding the 4-bit address, was read out of the register to the flight programmer in serial form.

Switchover sequence—There were two separate redundant clocks in the flight programmer. Had it become necessary to switch to the redundant clock, the following procedure would have been used. A command containing the correct spacecraft address would have been read into one of the registers. This would have supplied a signal to the switchover gate associated with that register, after the address had been verified. Transmission of an enable tone for the opposite register would then have caused the decoder to issue a switchover signal to the flight programmer. The command transmission sequence would have terminated by removal of the enable tone, which returned the system to a quiescent state.

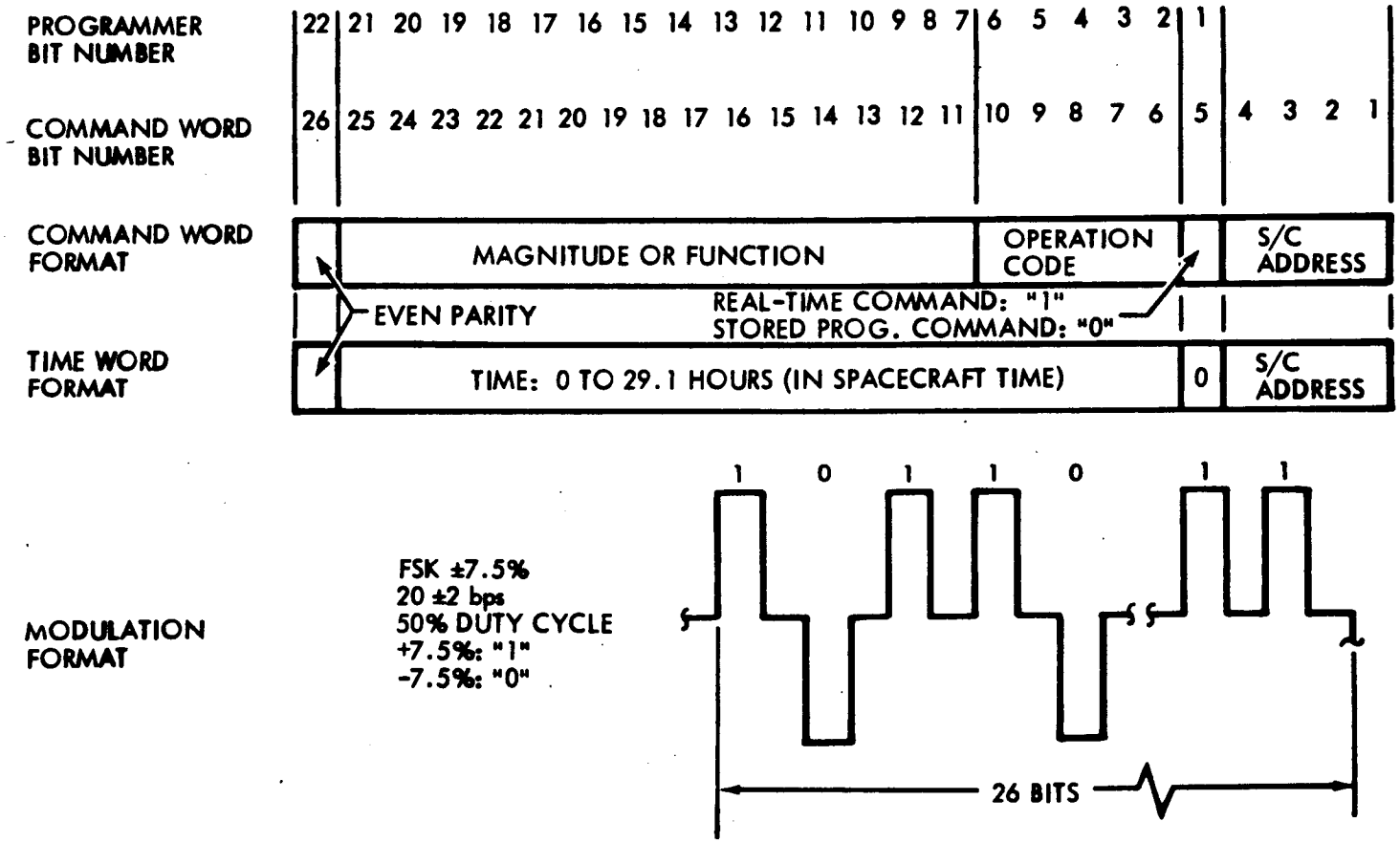

FIGURE 3.1-22: COMMAND DATA FORMAT

3.1.3.2 PERFORMANCE

3.1.3.2.1 Summary

The spacecraft received and executed approximately 4500 commands and read out 211 frame pairs of film without incident. Only in two instances were early handovers between ground stations necessary: once when DSS-41 had trouble acquiring the spacecraft and could not hold a lock (subsequently, the transmitter frequency was reduced and the lock was held; upon handover to DSS-61 the problem disappeared); the other early handover was due to a power-supply failure at DSS-41.

The high-power telemetry mode performed perfectly using the traveling-wave-tube-amplifier (TWTA) and high-gain antenna for transmitting the video and telemetry signals. An occasional decrease in signal margin for the low-gain antenna in low-power telemetry mode was observed; however, the signal level remained well above the required threshold for continual data integrity.

Timing correlations between stations were successfully accomplished. This was the first time that any timing correlations between DSS stations had been accomplished using spacecraft ranging data.

Readout of the test film while in initial orbit showed no degradation in quality since the prelaunch checks; photographic film was read out satisfactorily.

Telemetry Link

Down-link telemetry operation was approximately 5 db above the nominal link design throughout most of the mission. At times there were occasional unexpected down-link power decreases of as much as 10 db; however, no problems were encountered with telemetry error rates or resultant demodulator synchronization.

Command Link

In general, up-link operation was excellent. During lunar orbit, DSIF transmitter power levels of 5 kw produced spacecraft automatic gain control (AGC) levels that were between 4 and 7.5 db above nominal design, and during the total mission no known erroneous commands were received at the spacecraft due to low signal to noise ratios on the communications link. Spacecraft AGC closely followed ground-transmitted power levels, as expected, and was noticeably susceptible to ground-antenna pointing errors. Spacecraft AGC telemetry levels varied inversely with spacecraft temperatures. AGC excursions due to temperature extremes normally were 2 to 4 db during the orbit.

Video Link

The video link was the signal path linking the spacecraft photo scanner output (picture data) to the DSS station GRE equipment. The link was considered established when the high-gain antenna was aligned with the DSIF, the modulation selector was in Mode 2, and the TWTA was on. To satisfy mission requirements, the video link performance could not degrade the photographic data signal in either signal-to-noise ratio or bandwidth. These requirements

were met if the total power at the DSS station receiver was greater than -104 dbm, and if the video analyst at the DSS station could resolve the 80-line subsets of each tribar pattern in the pre-exposed edge data.

During Mission I, the video link performance was more than sufficient to satisfy this requirement over the entire 10,852 minutes programmed for video readout. The reported total power at the DSS receiver never fell below the threshold value of -104 dbm during a readout period. The video analyst at the station was able to resolve the 80-line subsets of each tribar pattern for each readout period. An examination of the DSS station receiver total power readings revealed no evidence of potential problems.

Ranging Link

The ranging link was the signal path linking the transponder ranging loop input and output to ranging equipment at the DSS. The link was established when the ranging loop modules were activated by the "ranging on" command. To satisfy the ranging subsystem objectives, the link must preserve the ranging code, provide a carrier power in excess of -137.3 dbm at the transponder, and a carrier power above -159.6 dbm at the DSS station receiver.

The minimum carrier power at the spacecraft and DSS station receivers during each ranging period exceeded these requirements. Results do not suggest that ranging was degraded by the link.

3.1.3.2.2 Performance Details

Boost and Acquisition Phase

Spacecraft telemetry data were received and recorded by both "F" band (VHF) and "S" band (UHF) from the launch vehicle and the spacecraft, respectively, in the near-Earth portion of the mission phase prior to spacecraft/Agena separation. After separation, antenna deployment was confirmed by telemetry at 60 minutes after liftoff, the spacecraft was acquired by Woomera (DSS-41) without difficulty, and two-way lock was rapidly accomplished. At 75 minutes and 50 seconds after liftoff, the real-time command 32 (Video Modulation Mode Off) was transmitted and executed by DSS-41. The communication subsystem appeared to be operating normally with a received signal approximately 5 db better than predicted.

Cislunar Phase

The TWTA was turned on during roll and yaw maneuvers to assist in the determination of spacecraft attitude after pointing the antenna to 38 degrees in spacecraft coordinates, which made the beam intercept the Earth when correct roll orientation was achieved.

The first principal event of the cislunar phase was the first midcourse maneuver. The sequence of commands for this event was transmitted to the spacecraft by DSS-41 following the acquisition of the Moon (see discussion elsewhere for this substitution of Canopus reference). The transmission and execution of commands and performance of the midcourse maneuver were very satisfactory and no second midcourse maneuver was required.

Extensive Mode 1 ranging operations were performed during the cislunar phase with no problems in the communication subsystem.

A problem of rising deck temperatures early in cislunar cruise, which caused the spacecraft to be flown 36 degrees off the Sun, together with the inability of the star tracker to acquire Canopus, created a new problem in pointing the high-gain antenna. The Signal Margin Prediction Program computed the high-gain antenna pointing based on a Sun-Canopus reference; but when the spacecraft was pitched for cooling, the Sun-Canopus reference was lost, and the computed high-gain antenna pointing was of no value. Therefore, to effectively use the Signal Margin Prediction Program, a method for relating the actual spacecraft attitude to a Sun-Canopus reference was determined. The user program, CORL, was rewritten so that the output consisted of trajectory data transformed in accordance with the attitude that the spacecraft had assumed. CORL was programmed to operate on the INTL/LIFL trajectory data, which was expressed in the Sun-Canopus reference. This was accomplished by keeping the "X" and "Z" axes in the inertial hold mode and rotating the high-gain antenna. This change in CORL compensated for spacecraft attitude and eliminated the high-gain antenna pointing problem entirely. The high-gain antenna was also used during 360-degree roll maneuvers in an effort to substantiate and refine the spacecraft attitude reference. The communication subsystem contributed to the successful spacecraft insertion into initial lunar orbit by performing flawlessly throughout.

During cislunar flight, the transponder automatic gain control (AGC) reflected the effect of increasing range on the up-link signal strength, as well as the discrete increases in ground transmitter power. In most cases, telemetry tracked the reported discrete changes in ground transmitter power within 1 db, although a reported 6-db decrease followed by a 6-db increase were shown as -4.6 dbm and +4.4 dbm in transponder AGC. AGC indication was also found to vary inversely with temperature (a typical orbital temperature cycle of 25° F caused a 2- to 4-db cycle in AGC measurement). The change in vehicle-Earth range through an orbit was insufficient to affect transponder AGC. There was as much as 2-db difference from one Deep Space Station to the next.

During the cislunar phase, the communications subsystem performance may best be described in terms of its components or principal elements as follows.

Signal conditioner/multiplexer—The multiplexer/encoder zero reference was constant at 0 millivolt throughout the countdown and mission. The temperature reference was within +1% at all times, the variation being 4.68 to 4.76 volts. This variation was attributed to variation in power-supply voltage, temperature of the signal conditioner, and variation of load by the thermal sensors. There was no evidence of any multiplexer variation as evidenced by the constant values of the zero reference and supply voltage measurements.

Calibration changes in TWTA rf power output telemetry measurement—Vendor calibration curves were not directly applicable since the high-gain antenna and cable configuration effected the values used. A final high-gain antenna calibration based on a revised VSWR was prepared after the SFOF calibration tapes were complete. (Reference Boeing Document D2-100197-4.) Since the new entry exceeded the available space for calibration, a substitute second-order curve was prepared. This calibration was entered by card and was used from

225:19:21 to 241:15:50 GMT. The "off" condition value of 0 watt was prepared and used through the end of the mission. The final calibration was a third-order fit in the areas of interest (0.1% difference between 10 and 13 watts, 2% between 9 and 14 watts). The value was: $(-1.7935E-1) + (9.1252E-2)\ x - (7.9225E-4)\ x^2 + (2.83756E-6)x^3$.

Traveling-wave-tube amplifier (TWTA)—Although the thermal environment was somewhat more severe than expected, the performance of the TWTA throughout the mission was nominal or better. The total operating time after launch was 211.1 hours. It was operated 148 times. The helix and collector current were probably the best indicators of tube performance change. During the mission, the turn-on values increased by 1.5 to 2.0 ma in the helix current and decreased from 4 to 5 ma in the collector current. The steady-state values were higher by about 0.5 ma in the helix and lower by about 2 ma in the collector. It appeared that the TWTA was affected by temperature stresses, probably in terms of its geometry.

Discrete functions performance indications—All discrete functions were performed properly as shown by telemetered information and verified by other available data:

1) The proper multiplexer/encoder serial number was continuously indicated.

2) Antenna deployment was confirmed by telemetry and the value remained unchanged thereafter.

3) Multiplexer/encoder on external clock (flight programmer) was continuously displayed.

4) Command word pressure (register full) and command word verification telemetry operated properly. This included 4510 commands actually stored in or executed by the programmer, plus aborted commands and additional words required where incorrect spacecraft identification occurred in stored program command sequences that were rejected by the command decoder, requiring retransmission of the sequence.

Ellipse Phases

During the first two of the three elliptical orbit phases, communications subsystem performance contributed significantly to the success of the photo and readout functions of Mission I by continuing its excellent performance. In addition to continuing the performance described in the cislunar phase, there were 907 1-degree antenna rotations commanded and confirmation received by telemetry that the antenna had been rotated 1 degree in the proper direction without error. The commands to turn the TWTA on and off gave similar accurate performance.

During each orbit, the transponder static phase error (SPE) displayed a sinusoidlike cyclic variation with average total excursions of about 4.5 degrees. This variation was a direct result of the doppler shift in the spacecraft-received frequency, and was dependent on the orbit. The total excursion was slightly greater in the early orbits and near the end of the primary mission; slightly less in the middle orbits. The amplitude was generally centered about 0 degree with equal positive and negative swings; this verified the transmission frequency predictions. In later orbits, the negative amplitude became somewhat greater than the positive (including doppler effect). For Lunar Orbiter I, the correlation between up-link

rf frequency and SPE was approximately -5.1 kc per degree. The average peak doppler, therefore, was about ±11.5 kc.

The telemetered transponder output power indication varied inversely with temperature; typical values were 595 mw at 60° F and 540 mw at 85° F. It was not possible to determine the effect of temperature on actual down-link transmitted power. Another phenomenon of transmitter power output was an abrupt change in value, up or down, ranging in magnitude from 5 mw to as high as 85 mw (about 7% of full scale). The net effect of a series of up and down changes was very small. Nearly all were concurrent with some spacecraft physical activity, such as a high-gain antenna rotation or a spacecraft attitude or velocity maneuver. Since the changes were unpredictable and generally small (about 0.2 db), no conclusive data could be obtained on the corresponding actual down-link signal level. There was no correlation between these abrupt changes in transponder power and the much greater abrupt changes in ground AGC. The last significant discontinuity occurred midway through the mission (on GMT Day 238), after which the peak values of transponder power during an orbital thermal cycle were 25 to 35 mw less than in the early portion of the mission. There were numerous instances where the transponder rf power output telemetry deviated from its nominal profile. These unpredictable deviations occurred in the interval of a telemetry frame, and their magnitudes ranged up to 85 milliwatts. Refer to the Transponder Telemetry Power Change anomaly in Appendix D.

The average length of TWTA on time during the final readout phase of the mission was 106.5 minutes. Power output was normally between 10.5 and 12.2 watts with very little change apparent through the end of readout. This measurement indicated no change in the performance of the TWTA tube with time. However, some variations in output power were noticeable at higher operating temperatures; slightly larger variations were observed following tube turnon. When the rate of temperature increase was lower for the first few minutes, tube power output frequently decreased from the turn-on value (e.g., at 243:10:05 the power dropped to 9.68 watts, 0.32 watt below link margin requirement). The maximum temperature indicated during the mission was 187.5° F. Also, during the final readout, discrete shifts occurred in the helix accompanied by 1- or 2-count changes in collector current and an occasional 1-count change in TWT power. These shifts occurred in both directions, but the trend was to generally higher helix voltage or any particular temperature relationship was observed.

Maintaining transponder AGC below -90 dbm throughout the mission (a command transmission constraint placed on the Deep Space Stations) required a progressive decrease in ground transmitter power from +40 dbw to +37, +35, and finally +33 dbw. Since no factor could be found that would tend to gradually increase the signal level received by the transponder, it is concluded that the transducer that monitors the transponder AGC was changing calibration through the mission, perhaps as a result of higher-than-expected temperatures. Since a true -90 dbm resulted in a signal margin of more than 35 db above the measured command threshold, the apparent change in this telemetry channel caused little concern.

Command modulation on the up-link was clearly evident; one tone caused a decrease in received carrier of about 2 db; two simultaneous tones, 3 to 4 db. Ranging modulation caused the up-link carrier to drop by approximately 10 db. Both effects were consistent.

During a drop in the down-link ground-received rf power from -135 dbm to -147 dbm, the transponder AGC indicated a drop of about 4 db in the spacecraft-received power from 230:15:30 to 231:16:00 GMT. Lesser drops occurred on Days 234 and 237. The received power at the DSS receiver remained above threshold during these periods. Telemetered rf power output (CE10) from the spacecraft did not indicate a loss during these periods. Refer to the RF Signal Level Drop anomaly in Appendix D.

3.1.4 ATTITUDE CONTROL SUBSYSTEM (ACS)

3.1.4.1 FUNCTIONAL DESCRIPTION

3.1.4.1.1 General Summary

Major elements of the ACS are:

1) Flight electronics control assembly (CLE and Programmer);
2) Switching assembly;
3) Sun sensors;
4) Star tracker
5) Inertial reference unit;
6) Thrust vector control assembly;
7) Reaction control assembly.

Figure 3.1-23 shows the ACS component locations.

Major functions of the ACS include:

1) Acquire and maintain an inertially fixed reference attitude during the coast and picture readout phases of the mission as dictated by thermal control, solar power, and high-gain-antenna radiation requirements. The inertial reference during the 30-day photographic mission was established by a line to the Sun and a line to Canopus.
2) Perform attitude maneuvers to acquire and maintain attitude required for velocity control adjustments for midcourse correction, orbit injection, and orbit transfer; reacquire previous reference attitude subsequent to velocity adjustment.
3) Perform attitude maneuvers to acquire and maintain attitude required for photography, including attitude adjustment for image motion compensation; reacquire previous reference attitude subsequent to photography.
4) Compute spacecraft velocity changes from the measurement of acceleration during engine firing (flight programmer).
5) Initiate all spacecraft events either by stored program commands or earth generated commands received via the communication subsystem (flight programmer).
6) Provide spacecraft time to the photo subsystem, and timing reference for the communication subsystem (flight programmer).

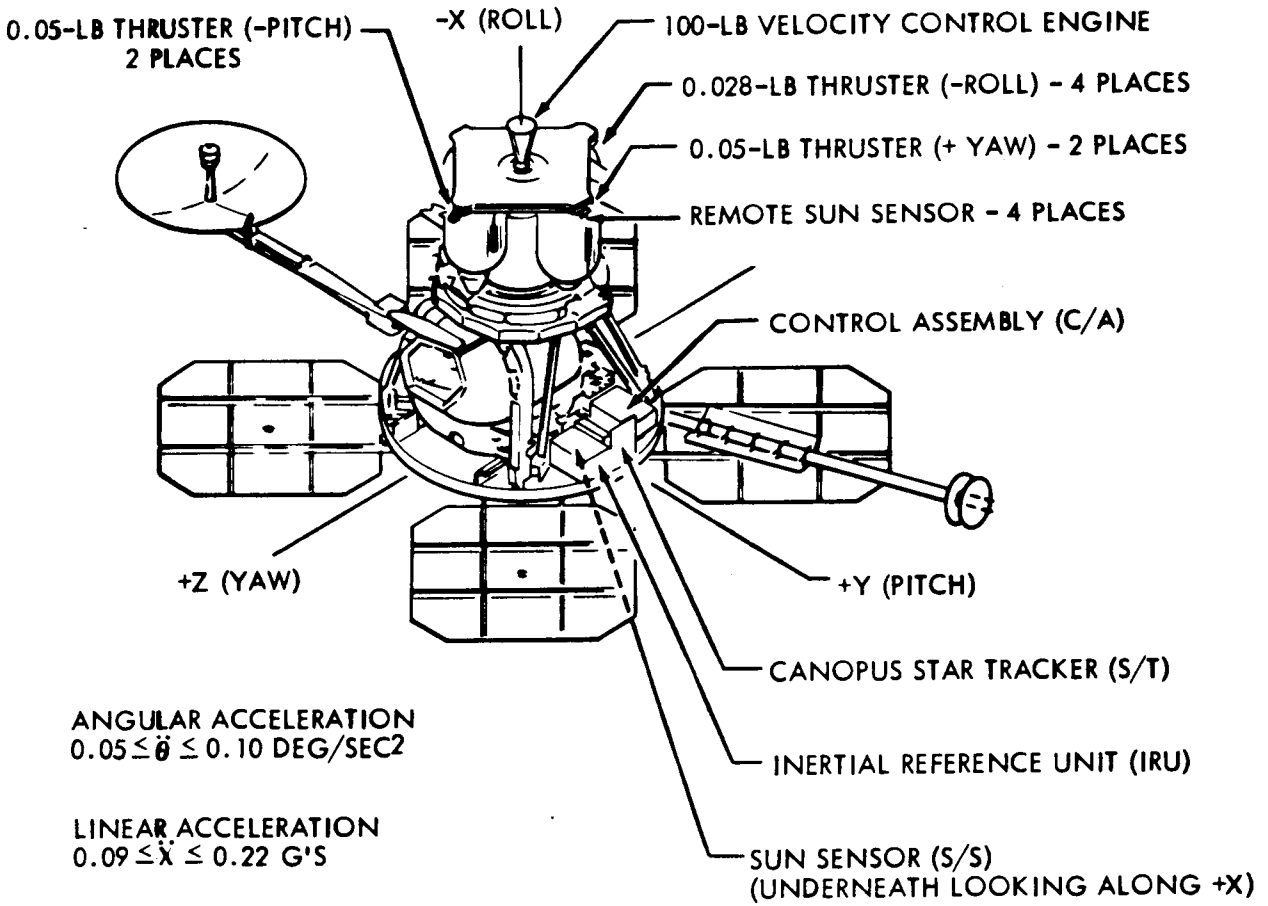

FIGURE 3.1-23: ATTITUDE CONTROL SUBSYSTEM COMPONENTS AND AXIAL ORIENTATION

7) Provide telemetry data to identify spacecraft attitude, velocity, time, and stored program status.

The system was basically a rate-limited conventional on-off gas reaction control system. The rate damping signal was provided by a rate gyro for each axis during normal operation with the Sun sensor (pitch and yaw reference) or star tracker (roll reference) not occulted. The deadband (limit cycle) could be either 0.2 or 2.0 degrees according to command. Figure 3.1-24 shows the functional relationship of ACS Components.

An onboard programmer was employed to control the spacecraft activities as directed by real-time commands or by commands stored in its memory. The programmer performed arithmetic and logic functions as required by the ACS to properly execute its commands and provide spacecraft control. The storage capability of the programmer memory was equivalent to at least 16 hours of spacecraft operation. The closed loop electronics (CLE) for the operation of the ACS and the flight programmer were integral parts of the flight electronics control assembly (FECA), providing a common power supply and availability of common inputs. This common location for these two electronic portions of the ACS simplified operations and increased reliability.

The commands for deployment of the solar panels and antennas were issued at the appropriate times by the flight programmer based on stored instructions.

The ACS (flight programmer) provided spacecraft time and square-wave trains at several frequencies for controlling and synchronizing spacecraft operations.

Orientation of the spacecraft in space was to the Sun for the pitch and yaw axes and to the star Canopus for the roll axis. The orientation to the Sun also controlled power to the solar panels. Canopus is the brightest star in the southern hemisphere and one of the brightest stars in the heavens, which simplifies acquisition. Its location in the southern hemisphere is always within 14.2 degrees of the normal to the Sun-Moon ecliptic plane, which provided a reference not subject to extreme angular excursions during the motion of the Moon about the Sun.

Reaction-control torques for attitude maneuvers, and stabilization were provided by cold gas (nitrogen) thrusters (see Figure 3.1-23 for location). The N_2 gas supply was common to the ACS and the VCS. The cold-gas thrusters were controlled so that the minimum "on" time was 11 milliseconds to minimize the effects of noise on the operating life of the thruster and to improve the limit cycle performance. An additional input connection was provided for the yaw axis to permit crab angle input from the photo subsystem. This connection provided an operating mode to reduce smear during photo sequences. (This mode was not used during Mission I).

In the absence of Canopus-Sun references, attitude stabilization was maintained by the inertial reference unit with the spacecraft operating in the inertial hold mode (damped by a passive lead-lag network in the CLE).

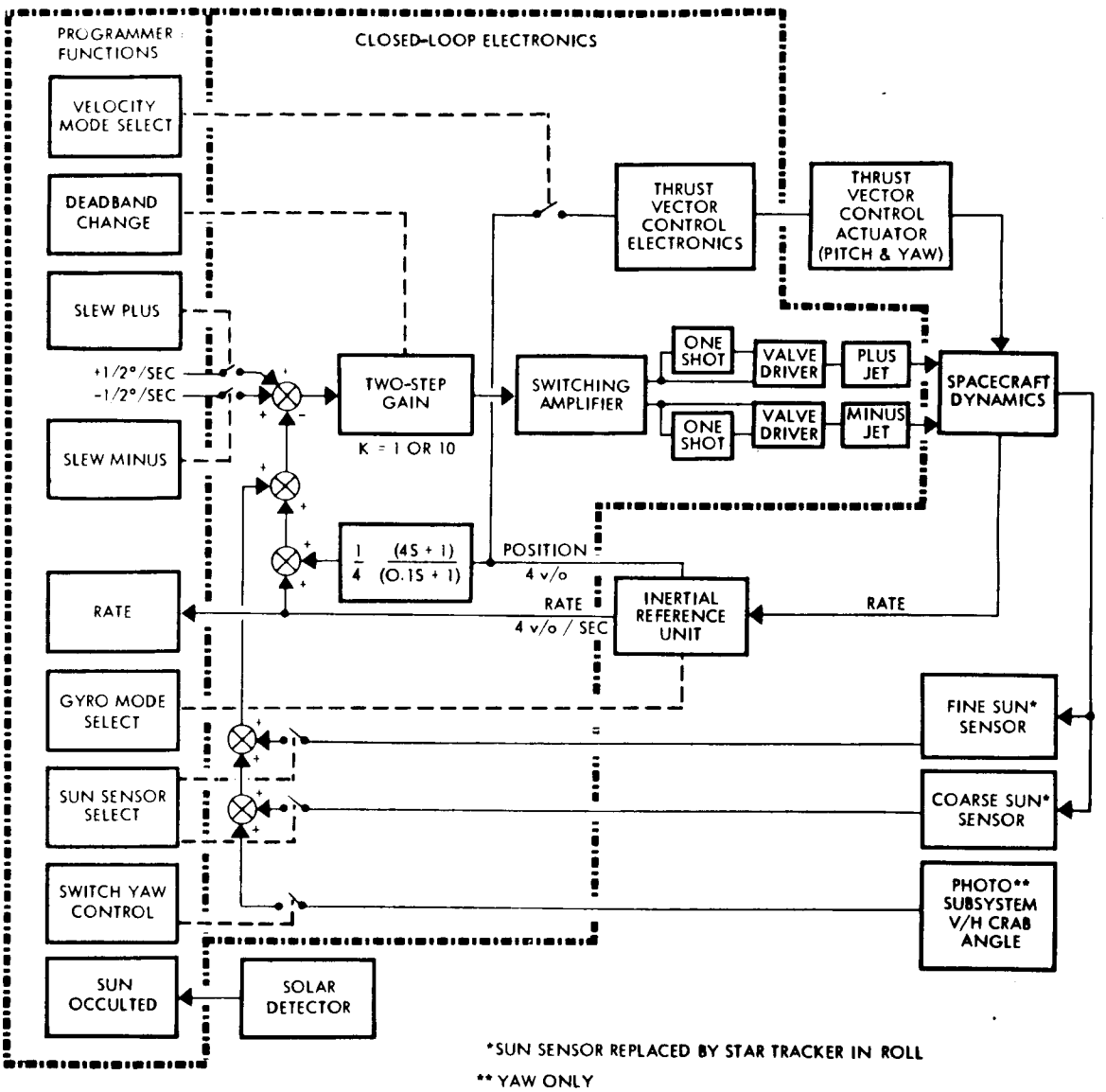

FIGURE 3.1-24: ACS FUNCTIONAL BLOCK DIAGRAM

During the main engine firing, the control torques about the pitch and yaw axes were provided by an electric motor servo-driven thrust vector control (TVC) system used in conjunction with the main engine. The ΔV that was imparted to the spacecraft was controlled by the digital integration of the spacecraft acceleration as measured by a pulse rebalance accelerometer.

3.1.4.1.2 Detailed Functional Description

Flight Electronics Control Assembly

Closed-loop electronics (CLE)—The closed-loop electronics included the reaction jet valve drivers, signal summing amplifiers and limiters, Sun sensor amplifiers and limiters, thrust vector control signal amplifiers and compensation networks, reaction control compensation networks, slew signal generators, switching functions, and signal conditioning for certain telemetry channels. Its prime function was that of closing the loop between the vehicle dynamics and sensor outputs. More specifically, functions of the CLE were to:

1) Close rate and attitude loops with inputs from IRU, Sun sensor, and Canopus star tracker;
2) Provide lead/lag compensation on IRU attitude signals for reaction control and TVC;
3) Amplify and limit Sun sensor outputs;
4) Accept mode switch commands from the programmer to
   a) ± slew about three axes at 0.5 deg sec. each,
   b) Limit cycle deadzone change of 10 to 1 ratio (±2 or ±0.2 degrees)
   c) Connect and disconnect fine and coarse Sun sensors,
   d) Connect and disconnect star tracker;
5) Provide on-off commands to valve drivers for all three axes;
6) Provide "one-shot" limits (11 ms) on thrusters for minimum impulse bit operation;
7) Provide telemetry inputs;
8) Provide test signal inputs to the ACS.

Flight programmer—The flight programmer, a low-speed digital computer, was the primary center for storing, routing, and controlling execution of spacecraft commands. It interfaced with all major spacecraft subsystems and provided control of the spacecraft in accordance with commands received from the command decoder (real-time commands) and commands stored in the memory (stored-program commands). The flight programmer was capable of executing spacecraft system control from memory for prolonged periods of time without ground intervention. The programmer was operated primarily in the stored-program mode supplemented by real-time commands as necessary.

In the stored-program mode, the commands were stored in memory and executed in a sequential routine according to program instructions. This included the capability of selecting any stored program command as a function of program instructions.

In the real-time mode, the transmitted commands were executed immediately (within 150 milliseconds) after being received by the programmer. This mode also permitted ground selection of the next memory command to be executed.

The programmer was provided with an initial stored program before launch. Instructions were stored in memory word address locations and were executed sequentially by incrementing the next memory address to be performed each time a command was executed. The initial stored program was organized to execute a repetitive stored address routine. Values employed for attitude maneuvers and time comparisons were sequentially stored in blocks of memory locations. The programmer cycled through these blocks, using these values during a set period of time. At the conclusion of this period a new set of time and magnitude values were stored in these blocks, and the programmer recycled through these blocks executing the new values at a new designated time. This procedure was repeated many times throughout the mission, enabling the repetitive main routine to obtain different time and maneuver values for each period from a very few memory words. This type of programming greatly reduced the size of the memory required.

Subsystem interfaces—The major subsystems controlled by the programmer are listed below. Under each subsystem heading are listed the major functions of that subsystem controlled or performed by the programmer. Figure 3.1-25 further identifies interfaces within the attitude control subsystem.

1) Attitude control subsystem
   The programmer issued discrete signals by command to perform the following functions.

   a) Select the deadband mode, ±2.0 or ±0.2 degrees, for the closed-loop electronics.

   b) Turn on or off both coarse and fine Sun sensors for both yaw and pitch axes to provide different spacecraft control modes.

   c) Connect the Sun sensor into the pitch and yaw axes controllers for spatial referenced attitude control of the spacecraft.

   d) Connect the Canopus tracker into the roll axis controller for spatial referenced attitude control of the spacecraft.

   e) Issue slewing commands to roll, pitch, and yaw controllers.

   f) Select the roll, pitch, and yaw rate gyro modes (rate or rate integrating).

   g) Switch the yaw controller between two controlling signals: the yaw rate gyro and the image motion compensation.

   h) Initialize the attitude control subsystem until Agena separation.

   i) Control power application to the inertial reference unit gyros, the inertial reference unit accelerometer, and the Canopus star tracker.

   j) Issue discrete signals by command to fire the nitrogen squib valves to arm the reaction control subsystem.

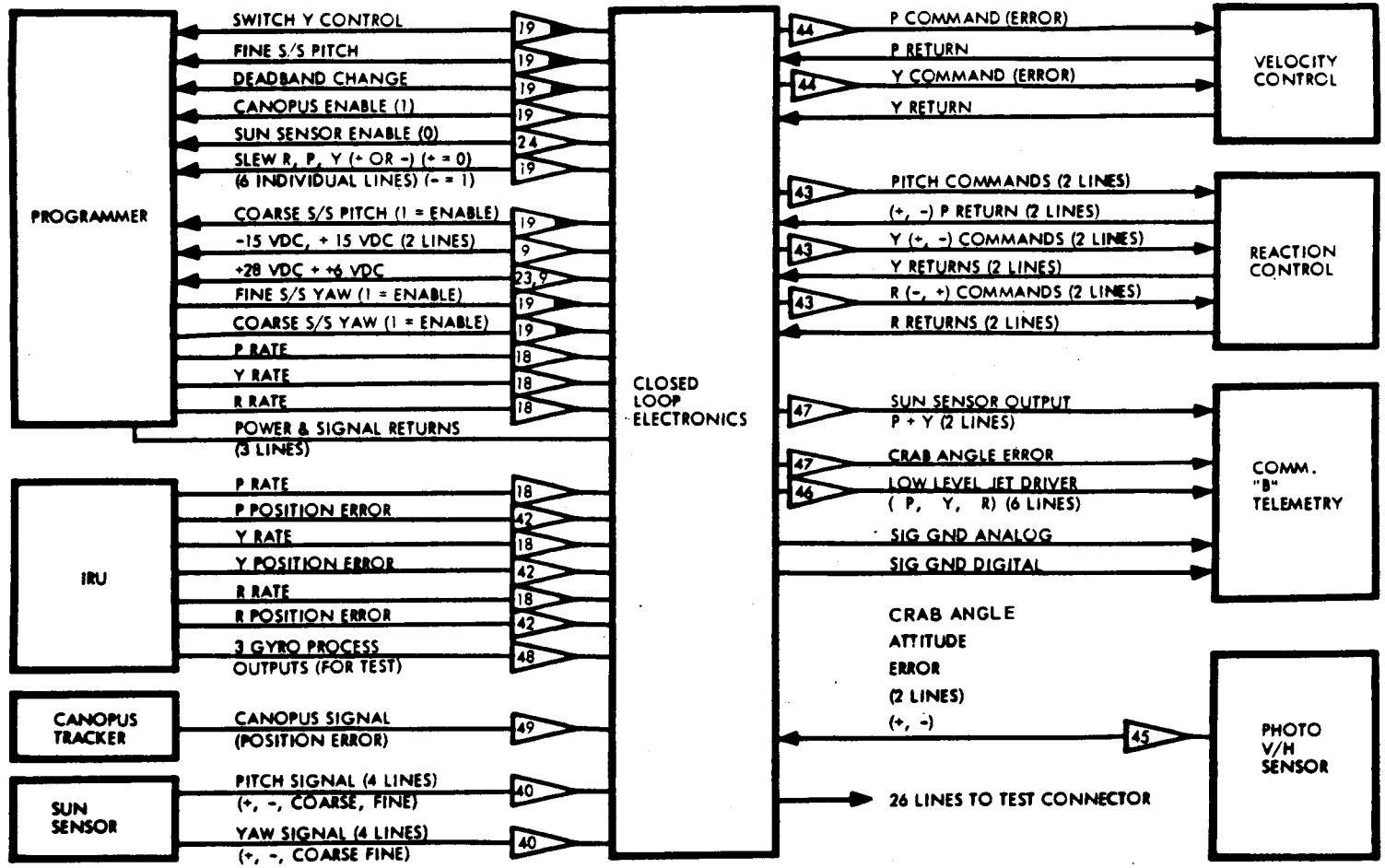

FIGURE 3.1-25: ATTITUDE CONTROL SUBSYSTEM SIGNAL INTERFACE

The programmer received signals from the attitude control subsystem to perform the following functions:

k) At the occurrence of Sun or Canopus occultation, perform the switching of the attitude control system to inertial reference and record time of occurrence. Time of occultation will be telemetered.

l) On receipt of a rate gyro signal, perform an analog to digital conversion and integrate the results to determine the positional change during a roll, pitch, or yaw maneuver.

m) On receipt of an acceleration signal from the inertial reference unit, perform an integration to determine the velocity change caused by a velocity maneuver.

2) Velocity control subsystem—

a) The programmer issued discrete signals through the switching assembly to the velocity control system to arm the system prior to velocity maneuvers.

b) The programmer issued a discrete signal to the velocity control system to fire the main engine. The cessation of this signal stopped the firing of the main engine.

c) The programmer issued discrete commands to activate the thrust vector actuators in pitch and yaw to stabilize the craft during main engine firing.

3) Spacecraft photographic subsystem—

a) The programmer issued all discrete signals by command to sequence the taking of pictures, picture readout, and camera adjustment.

b) The flight programmer issued spacecraft time to the camera on request after each picture frame.

4) Communications subsystems—

a) The programmer provided two 2.4-kc clock signals to the command decoder.

b) The programmer issued, on command, one or two enable pulses to shift data from the command decoder register to the programmer.

c) The programmer selected one of two alternate modes of rf modulation by command. These were video modulation or ranging modulation.

d) The programmer controlled the emission of rf by turning the transponder exciter on or off.

e) The programmer turned the traveling-wave-tube amplifier on and off by command. The on signal was automatically turned off when the Sun was occulted and automatically re-established when the Sun was required, via logic controlled by a Sun present signal.

f) The programmer provided programmer performance data to the telemetry encoder.

g) The programmer provided shift pulses at a 2.4-kc rate to the telemetry register and a 50-cps square-wave train to serve as a basic telemetry timing signal.

h) The programmer issued discrete signals in 1-degree increments to rotate the high-gain antenna. These signals maintained the high-gain antenna in the proper position orientation for transmission to Earth. These commands were issued throughout the spacecraft's mission by both real-time and stored program commands.

i) The programmer issued a signal to turn on or off the radiation dosage measurement system.

The programmer received the following commands from the communications subsystem:

j) The programmer received serial data from either one of two command decoder registers.

k) The programmer received a signal from the command decoder indicating that the data stored in the command decoder register was valid and ready for readout.

l) The programmer received signals from the multiplexer encoder controlling readout of programmer data initiating the issuance of programmer telemetry information.

5) Structural and mechanical subsystem—

a) The programmer issued discrete commands through the switching assembly to deploy the solar panels.

b) The programmer issued discrete commands through the switching assembly to deploy the low- and high-gain antennas.

c) The programmer issued discrete commands through the switching assembly to turn on and off the tank deck heaters.

d) The programmer issued discrete commands through the switching assembly to open and close the camera thermal door.

Five states of the flight programmer—The flight programmer had five states of operation during which all programmer functions were performed. These five states are listed and discussed below:

1) FSA state—The normal execution of all stored program commands except the comparison phase of compare time, wait time, and maneuver commands was performed.

2) FSB state—The execution of the comparison phase of compare time, wait time, and stored program maneuver commands was performed.

3) FSC state—The programmer was in the halt condition. Under this condition, no stored program or real-time commands were executed. Time incrementation and output to telemetry continued as usual. A real-time jump command was normally used to get the programmer out of halt mode. It could enter the halt mode in flight due to a parity error out of memory or a commanded clock switchover.

4) FSD state—The complete execution of all real-time commands except magnitudes was performed. Also, initial execution of real-time magnitude commands, storage of stored program commands transmitted from the ground, storage of Sun and Canopus occultation times, and the first part of time delivery to the photo system are functions that were performed during FSD state.

5) FSE state—The execution of the comparison phase of real-time magnitude commands and the last part of time delivery to the photo subsystem was performed.

Memory loading and readout—

1) Storing commands in the programmer memory—When a command word or a time word was to be stored in a specified memory location, a command was transmitted to the spacecraft designating this desired location. This command was a store program address (SPA) instruction. After transmitting the real-time SPA instruction, the word for storage could then be sent.

   If words were to be stored in successive memory locations, the SPA instruction was required for the memory address designation of the first word in the sequence only. If, however, it was desired to store words out of sequence, two commands had to be transmitted for each instruction to be stored. For example, if 10 words were to be stored in sequence, 11 instructions must have been transmitted (one SPA instruction and the 10 words for storage); whereas, if 10 words were to be stored out of sequence, 20 instructions must have been transmitted (one SPA instruction for each word that was stored plus the 10 instructions for storage). The storage procedures discussed above were followed when the spacecraft was on the ground or in flight.

2) Readout of stored commands—There were two methods of reading out stored memory words. In the first, the programmer received a hard line signal (prelaunch only), named "spacecraft clock reset," that enabled the stored words to be read out of the memory after each word was stored during preflight storage operations. During flight the procedure for reading words out of memory was to transmit a telemeter memory command (TEM) containing the memory address of the word to be telemetered to ground. The requested word was telemetered within 23.04 seconds after the TEM command had been executed. A separate TEM command had to be given for each word that was to be telemetered by this second method. Any one of the 128 memory words could be read by use of the TEM command.

Fixed memory address assignment—The programmer memory was composed of 128 words, eight of which contained special data and were designated as fixed memory addresses (FMA0 through FMA7). The remainder were used for storing spacecraft commands and program instructions. The contents of these fixed memory locations follows:

FMA0 - This word contained the value of the spacecraft time.

FMA1 - This word contained the memory address of the next stored program command to be executed.

FMA2 - This word contained: (1) The contents of a memory location requested by programmer command for telemetry to ground; or (2) The integrated value of an attitude or velocity magnitude during the execution of a maneuver command. The integrated value would also appear in TM time slot FMA3, FMA4, FMA5 and FMA6 during maneuvers.

FMA3 - This word contained the operation code and memory address of a stored program command that was interrupted by the execution of a real-time command. At the conclusion of the RTC, the contents of FMA3 were replaced into the logic circuitry of the programmer.

FMA4 - This word contained the memory address of the word into which the next transmitted stored program command had to be inserted.

FMA5 - This word contained Canopus occultation time.

FMA6 - This word contained Sun occultation time.

FMA7 - This word contained the value of the spacecraft clock that determined the time at which the execution of a WAT command was concluded.

Word format—The programmer used two types of words; a command word that contained an instruction to be executed, and a time word that contained a time value to be compared to, thereby controlling the time of execution of commands.

A ground-transmitted word received by the command decoder contained 26 bits. Four of these bits were used for spacecraft address only. The programmer received 22 bits from the command decoder. The breakdown of the 22 bits of a command word follows: One bit designated the command to be a stored program command (SPC) or a real-time command (RTC). Five bits determined the type of command (for example, a maneuver command). Fifteen bits contained either the function or magnitude of the command, whichever was applicable depending upon the type of command. ("Function" referes to either a memory address or a particular discrete command, while "magnitude" pertains to the required amount of an attitude or velocity maneuver). The final bit of the command word was used for even-parity generation. A transmitted command (RTC or SPC) must have contained an even number of "ones" (even parity) before it was executed.

The breakdown of the 22 bits of a time word follows: One bit designated the command to be an SPC or an RTC. Twenty bits determined a time value and the last bit was used for even parity generation.

Commands transmitted from the ground were sent while the programmer was executing a wait-time (WAT), compare-time (COT), or infinite-jump command. The sequence of transmission follows.

A tone signal was transmitted to the spacecraft to switch the command decoder to the OPERATE mode. The 26-bit word was then transmitted to the spacecraft and stored in the command decoder. Next, the spacecraft transmitted a replica of the word to the ground, where it was verified. Upon verification, a signal was transmitted to the spacecraft releasing 22 bits of the word to the programmer. Finally, the tone signal was terminated and the command decoder returned to the STANDBY mode.

After receiving the transmitted word, the programmer recognized it to be a stored program command or real-time command, storing it if the former type and executing it if the latter.

Description of programmer commands

a) SPA - Store Program Address: A SPA command was a word containing a five-bit operation code and a seven-bit function address. The seven-bit address designated the word in memory in which the next transmitted stored program command was to be stored. A SPA command was always a real-time command.

b) WAT - Wait Time: A WAT command was a word containing a five-bit operation code and 15 function bits for a time value. The time value chosen added to the spacecraft clock value and the sum was then compared with the spacecraft clock value. The programmer issued no stored program commands until the designated amount of time had been waited. At the conclusion of the WAT command, the programmer continued to sequentially execute the stored program. Fifteen different wait times from 3.2 seconds to 29 hours, 7 minutes, and 37.6 seconds were possible. A WAT command was always a stored program command.

c) COT - Compare Time: A COT command was a word containing a five-bit operation code and a seven-bit function address. The address specified a location in memory that contained a time value that was to be compared with the spacecraft clock. When executing a COT command the programmer compared this time value to the continuously updating spacecraft clock and issued no stored program commands until a comparison occurred. When time comparison did occur, the programmer continued to sequentially execute the stored program. Table 3.1-2 shows a time-bit equivalence within the programmer.

d) EMP - Execute Magnitude Plus: This command was a word containing a five-bit operation code and a seven-bit function address. The EMP instruction was used to command velocity and attitude maneuvers performed in the stored program mode. The seven-bit function address specified a location in memory that contained the type and amount of magnitude to be performed. There are seven types of maneuvers that the programmer could execute: roll plus (ROP), roll minus (ROM), pitch plus (PIP), pitch minus (PIM), yaw plus (YAP), yaw minus (YAM), and a change of velocity (VEL). Each type of maneuver is a 20-bit word containing a five-bit operation code to specify the type and

Table 3.1-2: Time-Bit Equivalence

WORD BIT NO.	BIT TIME VALUE IN SECONDS	HOURS	MIN.	SEC.	COMMENTS
2	0.1	0	0	0.1	The execution of a WAIT TIME (WAT) and a COMPARE TIME (COT) always imposes an additional 0.1 second delay in the execution of the following instruction. Therefore, the execution of a command following a 3.2-second WAIT TIME will occur 3.3 seconds later.
3	0.2	0	0	0.2	
4	0.4	0	0	0.4	
5	0.8	0	0	0.8	
6	1.6	0	0	1.6	
7	3.2	0	0	3.2	
8	6.4	0	0	6.4	
9	12.8	0	0	12.8	
10	25.6	0	0	25.6	
11	51.2	0	0	51.2	NOTE: With bits 2 through 21 equal to zero in a TIME word, a time comparison will occur 29 hours, 7 minutes and 37.6 seconds later.
12	102.4	0	1	42.4	
13	204.8	0	3	24.8	
14	409.6	0	6	49.6	
15	819.2	0	13	39.2	
16	1,638.4	0	27	18.4	
17	3,276.8	0	54	36.8	
18	6,553.6	1	49	13.6	
19	13,107.2	3	38	27.2	
20	26,214.4	7	16	54.4	
21	52,428.8	14	33	48.8	
Maximum	Value	29	7	37.5	
Cycle	Time	29	7	37.6	

15 bits to determine the angular magnitude or velocity change. Table 3.1-3 contains the angular magnitude represented by each bit and Table 3.1-4 contains the velocity change designated by each bit.

When the EMP command was executed, the function address was incremented by 1. Therefore, if this EMP instruction was again executed, the programmer performed a different maneuver, namely the one contained in the memory location designated by the incremented function address. An EMP command was a stored program command only.

e) EMM - Execute Magnitude Minus: This is similar to EMP except the EMM command changed the direction (from plus to minus and minus to plus) of the maneuver referenced by the function address of the EMM command. For example, if a pitch plus magnitude was referenced by an EMM command the maneuver performed was a pitch minus. An EMM command was a stored program command only.

f) TEM - Telemeter Memory: A TEM command was a word containing a five-bit operation code and a seven-bit function address. The address specified a word in memory that was to be shifted to telemetry and transmitted to Earth. A TEM command was a real-time command only.

g) TER - Terminate: A TER command was a word containing a five-bit operation code. This command caused termination of any current command being executed. A TER command was a real-time command only. At the issuance of this command, the command currently being executed was terminated and the programmer proceeded to execute the next stored instruction.

h) JMP - Jump: A JMP command was a word containing a five-bit operation code and a seven-bit function address. This command caused the programmer to go to the instruction stored in the memory location addressed by the function address. After executing this command, the programmer continued from this point to sequentially execute the stored program. A JMP command could be performed either as a stored program or real-time command.

i) JPM - Jump Modified: A JPM command was a word containing a five-bit operation code and a seven-bit function address. This command caused the programmer to go to the instruction stored in the memory location addressed by the function address. After executing this command, the programmer continued from this point to sequentially execute the stored program.

When a JPM command was executed, the function address was incremented by 1. Therefore, if this JPM command was again executed, the programmer would have jumped to a different memory location, namely the one designated by the incremented function address.

A JPM command could be performed either as a stored program or real-time command.

j) CTP - Camera Take Picture: A CTP command was a word containing a five-bit operation code and 15 function bits to control camera action in the picture taking sequence. There were 15 CTP commands, all of which could be performed as either real-time or stored program commands.

Table 3.1-3: Maneuver Magnitude Bit-Angle Equivalence

BIT NUMBER	ANGLE EQUIVALENCE			ANGLE EQUIVALENCE (SECONDS)	BIT NUMBER
	DEGREES	MINUTES	SECONDS		
7	0	0	39.6	39.6	7
8	0	1	19.2	79.2	8
9	0	2	38.4	158.4	9
10	0	5	16.8	316.8	10
11	0	10	33.6	633.6	11
12	0	21	7.2	1,267.2	12
13	0	42	14.4	2,534.4	13
14	1	24	28.8	5,068.8	14
15	2	48	57.6	10,137.6	15
16	5	37	55.2	20,275.2	16
17	11	15	50.4	40,550.4	17
18	22	31	40.8	81,100.8	18
19	45	3	21.6	162,201.6	19
20	90	6	43.2	324,403.2	20
21	180	13	26.4	648,806.4	21
Maxim. Value	360	26	52.8		
		Bits 7 - 21 - All Zero			

Table 3.1-4: Velocity - Bit Equivalence

WORD BIT NO.	VELOCITY CHANGE 0.1 FT/SEC INCREMENT	VELOCITY CHANGE IN M/SEC 0.03048 0061 M/S = 0.1 FT/SEC
7	0.1	0.030480061
8	0.2	0.060960122
9	0.4	0.12920244
10	0.8	0.243840488
11	1.6	0.487680976
12	3.2	0.975361952
13	6.4	1.950723904
14	12.8	3.901447808
15	25.6	7.802895616
16	51.2	15.605791232
17	102.4	31.211582464
18	204.8	62.423164928
19	409.6	124.846329856
20	819.2	249.692659712
21	1638.4	499.385319424
MAX. VALUE	3276.7	998.740158787
MAX. MANEV. (ALL ZEROS)	3276.8	998.770638848

k) ROC - Readout Camera: An ROC command was a word containing a five-bit operation code and 15 function bits to command the camera in the readout mode. There were ROC commands, all of which could be performed as either real-time or stored program commands.

l) COM - Communications: The COM command was a word containing a five-bit operation code and 15 function bits to command the communication electronics. There were 12 COM commands, all of which could be performed as either real-time or stored program commands.

m) DEP - Deployment and Arming: The DEP command was a word containing a five-bit operation code and 15 function bits to command deployment and arming operations. There were nine DEP commands, all of which could be performed as either real-time or stored program commands.

n) ACF - Attitude Control Functions: The ACF command was a word containing a five-bit operation code and 15 function bits to perform operations in the attitude control system. There were 15 ACF commands, all of which could be performed as either real-time or stored program commands.

o) ACS - Attitude Control System: The ACS command was a word containing a five-bit operation code and 15 function bits to control equipment in the attitude control system. There were 12 ACS commands, all of which could be performed as either real-time or stored program commands.

p) ROP - Roll Plus: The ROP command was a word containing a five-bit operation code and a 15-bit angular magnitude. When executed by the programmer, the command caused the spacecraft to roll the angle designated by the 15-bit-magnitude value and remain in that position. The ROP command could be performed as either a stored program or real-time command. If performed as a stored program command, ROP was used in conjunction with EMP or EMM.

If ROP was used with EMP, the resultant roll was in the positive direction; whereas if it was used with EMM, the roll was in the minus direction. If ROP was performed as a real-time command, the maneuver was positive.

q) ROM - Roll Minus: Same as ROP except opposite in direction.

r) PIP - Pitch Plus: The PIP command was a word containing a five-bit operation code and a 15-bit angular magnitude. When executed by the programmer, the command caused the spacecraft to pitch the angle designated by the 15-bit magnitude value and remain in that position. The PIP command could be performed as either a stored program or real-time command. If performed as a stored program command, PIP was used in conjunction with EMP or EMM. If PIP was used with EMP, the resultant maneuver was a pitch in the positive direction; whereas, if it was used with EMM, the pitch was in the negative direction. If PIP was performed as a real-time command, the maneuver was in the positive direction.

s) PIM - Pitch Minus: Same as PIP except opposite in direction.

t) YAP - Yaw Plus: The YAP command was a word containing a five-bit operation code and a 15-bit angular magnitude. When executed by the programmer, the command caused the spacecraft to yaw the angle designated by the 15-bit-magnitude value and remain in that position. The YAP command could be performed as either a stored program command, or real-time command. If performed as a stored program command, YAP was used in conjunction with EMP or EMM. If YAP was used with EMP, the resultant maneuver was a yaw in the positive direction; whereas, if it was used with EMM, the yaw was in the negative direction. If YAP was performed as a real-time command, the maneuver was in the positive direction.

u) YAM - Yaw Minus: Same as YAP except opposite in direction.

v) VEL - Velocity: The VEL command was a word containing a five-bit operation code and a 15-bit velocity change magnitude. When executed by the programmer, the command caused the spacecraft to change its velocity by the amount of the 15-bit magnitude value. The VEL command could be performed as either a stored program or a real-time command. If performed as a stored program command, VEL was used in conjunction with EMP. If performed as a real-time command, VEL will operate by itself.

Maneuver command magnitude bit-angle equivalence—The method by which Table 3.1-3 was determined is presented below.

The voltage-to-frequency converter in the programmer was designed to present an output train of 50 pps with an input voltage (from the gyro) of 2.2 volts. With this same gyro output voltage the spacecraft would maneuver at a rate of 0.55 degree per second. Therefore, one pulse represents an angular magnitude of 39.6 seconds of arc.

$$(1 \text{ pulse} = \frac{0.55 \text{ deg}}{50} = 0.011 \text{ degree} = 39.6 \text{ seconds}).$$

Since bit 7 is the least significant bit of a magnitude word, it represents 39.6 sec. The value of each higher numbered bit is that of the previous bit doubled. It is required to know the value of time involved in an attitude maneuver command. The nominal rate of maneuver is 0.55 deg./sec. Therefore, if a 30-degree maneuver is commanded it should take 54.5 seconds (30/0.55 = 54.5) to complete. Of course, if the spacecraft maneuver rate were to deviate from the above-mentioned nominal value, a new conversion factor would be used in calculating the maneuver duration time.

Velocity-bit equivalence—Table 3.1-4 contains the velocity magnitude representation of each bit in a magnitude word.

The accelerometer contained two output lines. One line contained $+\Delta V$ pulses and the other line contained $-\Delta V$ pulses. The algebraic sum of the pulses on these lines is proportional to the change in velocity. With no acceleration, the pulse repetition rate on each line is 100 pps. With the maximum plus acceleration (20 ft/sec^2 , 0.62 g) the pulse repetition rate on the $+\Delta V$ line is 200 pps and on the $-\Delta V$ line is 0. Since 200 pulses/sec corresponds to

20 ft/sec^2, 1 pulse represents 0.10 ft/sec = 0.0031 g-sec. Since bit 7 is the least significant bit of a magnitude word, it represents 0.10 ft/sec change in velocity. The value (ft/sec) represented by each higher numbered bit is that of the previous bit doubled.

Switching Assembly

The switching assembly provided on/off control of actuating power to valve drivers and other control elements in the ACS. It responded to commands from the Flight Control Assembly as if it contained relays.

Sun Sensors

The Sun sensors provided a celestial reference for the pitch and yaw axes by providing an output signal to the closed-loop electronics indicative of the angular deviation of the line to the Sun from the sensor reference line, which was parallel to the roll axis.

The Sun sensors were photocell pickups, oriented physically to provide quick Sun acquisition. The main sensor, mounted on the exposed side of the EMD, provided coarse (hemispheric) and fine (± 15-degree) pickup. The four remote sensors, located near the thruster assemblies on the upper deck (± Y and ± Z axes) periphery, overlapped in all directions in coverage to account for the other hemisphere. The fine sensor cell quadrature arrangement provided accurate position control capability. Figures 3.1-26 and 3.1-27 show the field of view for both coarse and fine Sun sensors.

Canopus Star Tracker (CST)

The star tracker provides a celestial reference for the roll axis by locking onto and tracking the star Canopus. The tracker location is shown in Figure 3.1-28. Design of the Canopus tracker provides that, approximately 6 hours after launch, it is turned on and the Canopus acquisition sequence is started. Until this time, the roll axis in the rate limit mode. A 360-degree maneuver is commanded while a star map is telemetered to the ground and compared against an overlay of the predicted star map signal. This comparison defines the roll angle of the craft relative to Canopus at the end of the 360-degree maneuver. A second maneuver is commanded to orient the spacecraft to Canopus with a negative roll error. The third maneuver in the sequence is an "acquire Canopus plus" command which rolls the spacecraft in a positive direction until Canopus recognition is received by the control assembly from the tracker. Upon receipt of the recognition signal, the maneuver plan is terminated and the tracker acquires the star. The roll axis is then in the Canopus-referenced limit cycle mode and continues that way until subsequent maneuvers.

Inertial Reference Unit

The TRU senses attitude rates about the three control axes by means of three "strapped down", floated, rate integrating gyros. The operating mode for each gyro is completely independent, but the pitch gyro is in inertial hold during a yaw maneuver, and the yaw gyro in the inertial hold mode during a pitch maneuver. The inertial hold mode is used whenever off-Sunline attitude is required, such as during velocity-change and photo-taking maneuvers (inertial hold mode is synonymous with rate integrate mode where position error is

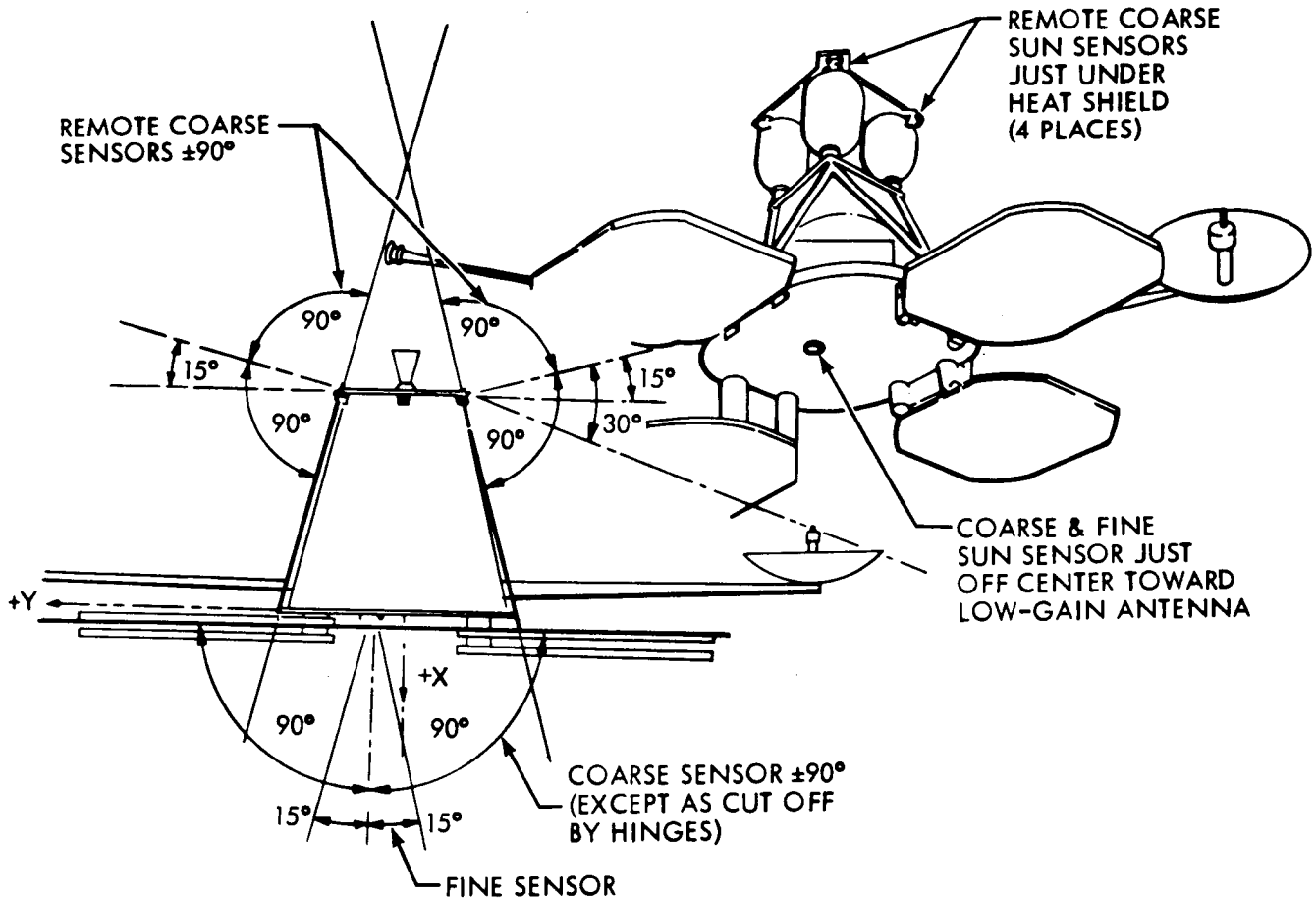

FIGURE 3.1-26: SUN SENSOR FIELDS OF VIEW

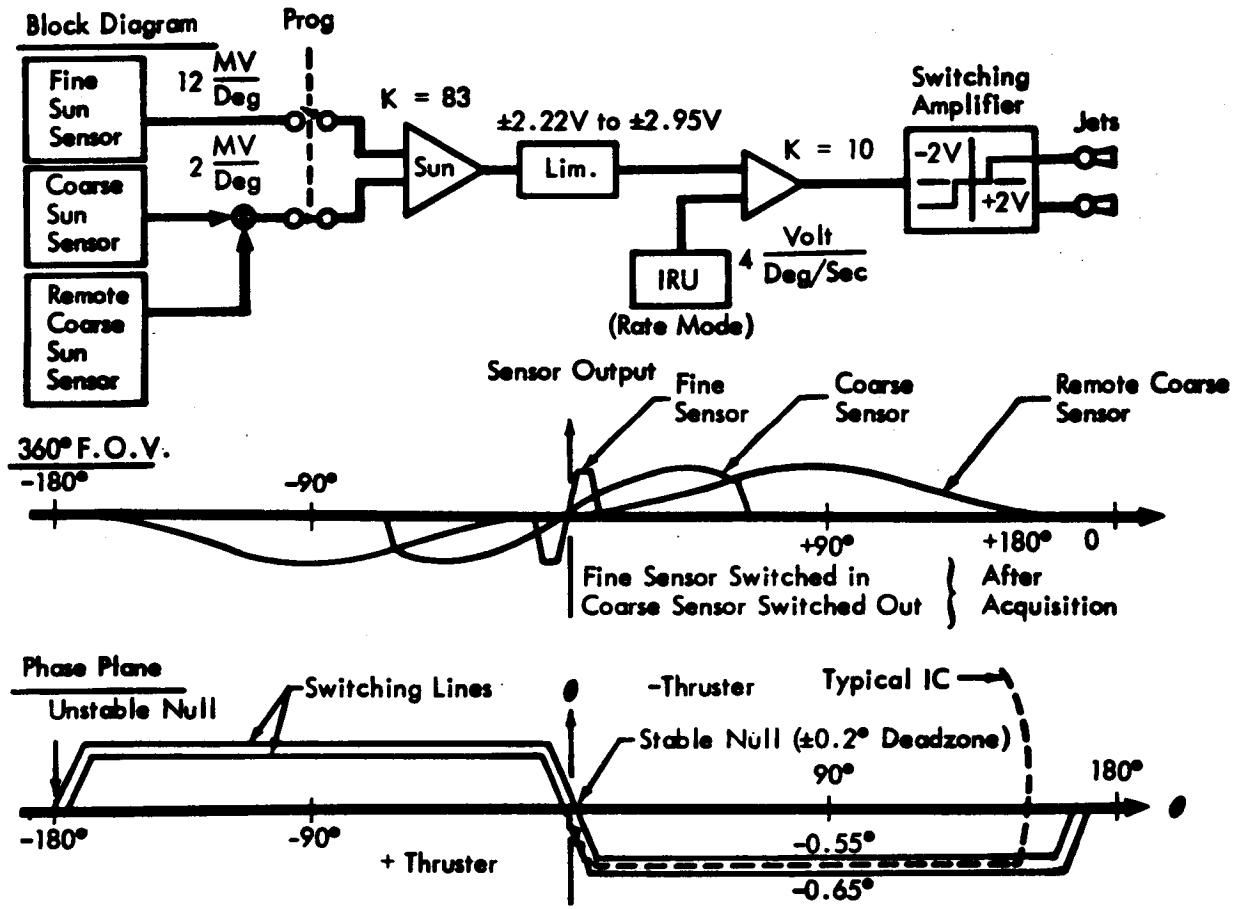

FIGURE 3.1-27: SUN ACQUISITION

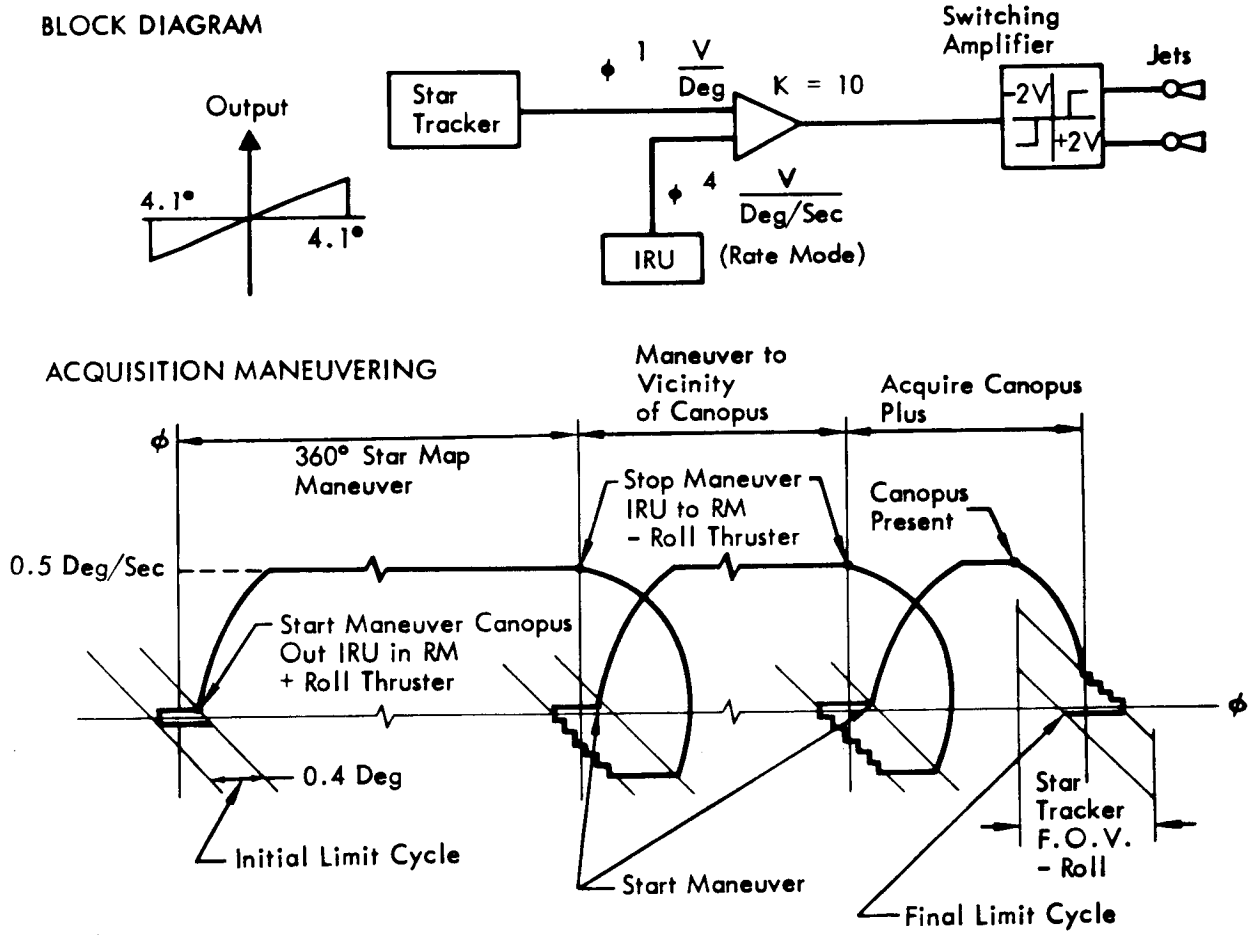

FIGURE 3.1-28: CANOPUS ACQUISITION

resultant). The rate mode is used, primarily, during attitude change maneuvers for traversed angle control. Also, during optical sensor stabilized cruise, the gyros are in the rate mode to prevent excessive precession (to the stops). A simplified equivalent diagram of the inertial reference unit is shown in Figure 3.1-29.

The IRU also provided accurate acceleration information to control burn times of the rocket motor during midcourse, orbit-injection, and orbit-transfer maneuvers. To accomplish this, a linear accelerometer was mounted parallel to the rocket thrust line. The output of the accelerometer was integrated in the CLE and presented to the programmer for comparison with the commanded velocity change. When the command ΔV was reached, the programmer reacted to stop fuel and oxidizer flow, thus terminating velocity change. The accelerometer was the pulse-integrating, pendulum type, functionally illustrated in Figure 3.1-29.

Thrust Vector Control (TVC)

Control of pitch and yaw during firing of the spacecraft velocity engine was provided by swivelling the engine using electronically controlled servo actuators. These actuators were energized simultaneously with the engine control valves. Roll control during velocity engine firing was by the conventional method of roll thrusters as used during normal flight.

Reaction Control Assembly

The control torques in roll, pitch, and yaw were provided by reaction control thrusters. The N_2 gas was stored in a supply tank and distributed by a system of tubing and regulators to the attitude control velocity control and system. Thrusters provided are:

Two 0.05-lb thrusters	- Yaw (+ and -, fired singly)
Two 0.05-lb thrusters	- Pitch (+ and -, fired singly)
Four 0.028-lb thrusters	- Roll (+ and -, fired in pairs)

Minimum thruster-on time is 11 milliseconds. Table 3.1-5 shows the nitrogen budget for this flight for the velocity- and reaction-control subsystems.

3.1.4.1.3 Operational Modes

The ACS operated in different modes of control in consonance with the requirements existing during the several mission phases and the particular spacecraft operations that were performed.

The Celestial Hold mode used outputs of the Sun sensor and star tracker to maintain a reference orientation. The rate integrating gyros operating in the rate mode provided damping. This was a limit cycle operation of the reaction control system.

The Inertial Hold mode used the rate integrating mode of the gyro to obtain position information. A lead-lag network was used to develop rate information for stabilization of the vehicle using reaction control thrusters. This was a limit cycle operation of the system.

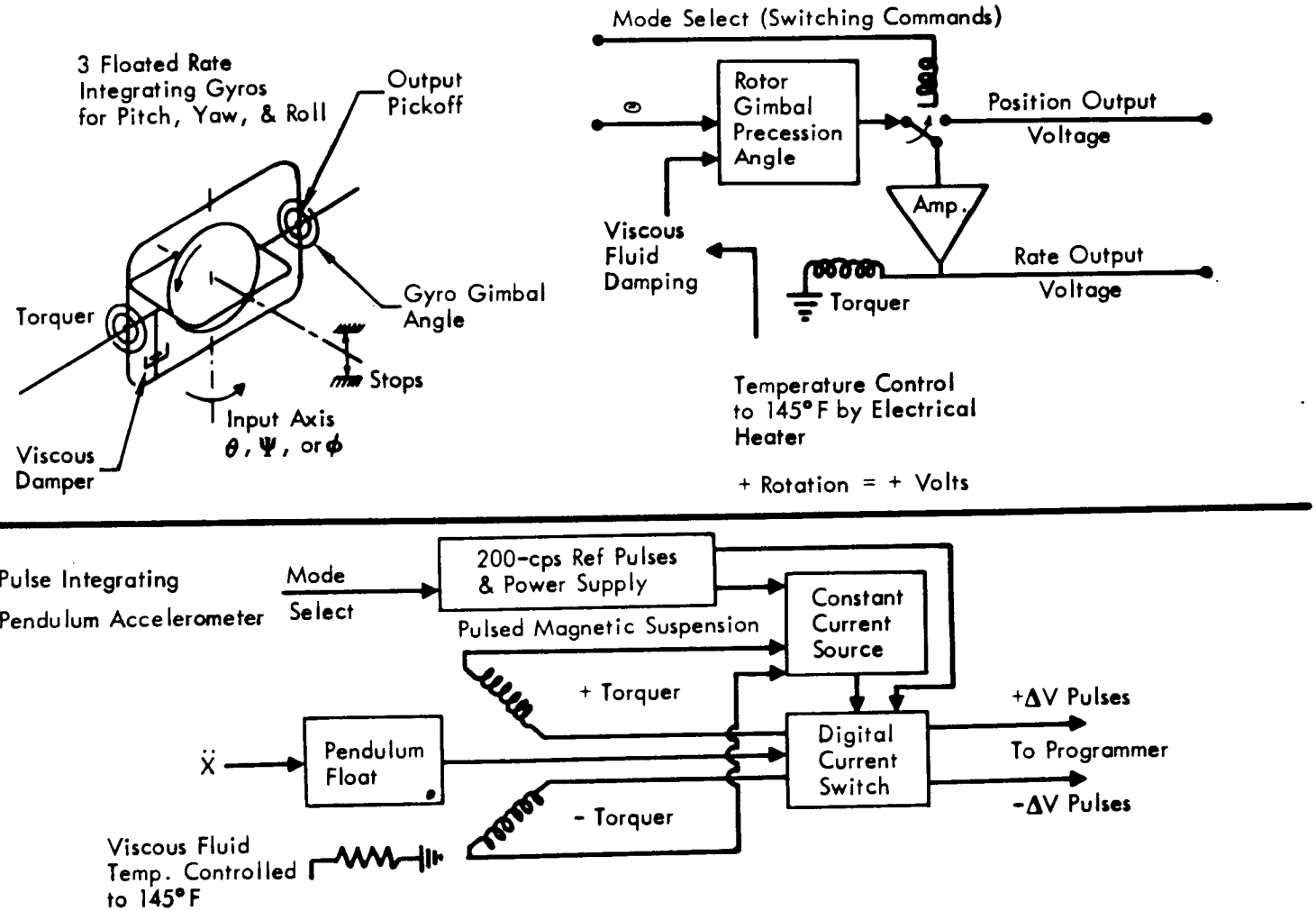

FIGURE 3.1-29: INERTIAL REFERENCE UNIT- GYROS (EQUIVELENT CIRCUIT)

Table 3.1-5: Velocity and Reaction Control Nitrogen Gas Budget

MISSION PHASE	NITROGEN WEIGHT	
	ITEM	TOTAL
Photographic Mission		
Initial Mission	0.22	
Cislunar Coast	0.06	
Midcourse Maneuvers		
1st Midcourse	0.14	
2nd Midcourse	0.18	
Initial Orbit Injection	0.14	
Final Orbit Transfer	0.09	
Photo Maneuvers (12)	1.19	
Photo Transmission (10 days)	0.68	
Lunar Orbit Coast (17 days)	0.12	
Celestial Reacquisition	0.84	
Disturbances	0.14	
R/C Cross Coupling	0.20	
Photo Mission Total		4.00
Extended Mission		
Lunar Orbit Coast	1.79	
Celestial Reacquisition	0.56	
Disturbances	1.48	
R/C Cross Coupling	0.19	
Extended Mission Total		4.02
Reserve		1.98
Total Nitrogen Budget, Reaction System		10.00
Velocity Control Subsystem		
Propellant Expulsion	3.84	
Reserve	0.16	
Velocity Control Total		4.00
Combined Systems		
Leakage	0.49	
Residual	0.09	
Total Nitrogen for Combined Reaction and Velocity Control		14.58

PHOTO SITE & FRAME	TIME (DAY - HR - MIN.)	ATTITUDE MANEUVER (DEG)				ATTITUDE ACCURACY DURING PHOTO TIME (DEG				ATTITUDE RATE DURING PHOTO TIME (DEG/SEC		
		ROLL	YAW	PITCH	ERROR	ROLL	YAW	PITCH	CRAB ANGLE	ROLL	YAW	PITCH
1-0 (5 - 24)	230 - 14 - 43	+3.6	+12.45	-8.10	+0.25	0.04 to 0.13	0 to 0.13	-0.13 to 0.14	0 to 0.9	-0.003	-0.0018	[illegible]
1-1 (52 - 67)	234 - 15 - 23	+5.36	+12.46	-9.60	+0.07							
1-2 (68 - 83)	234 - 18 - 51	+5.43	+12.48	-4.98	0	-0.10 to -0.15	0.10 to 0.14	-0.06 to -0.12	0.2 to 0.5	+0.0083	-0.0035	+0.0015
1-3 (85 - 100)	235 - 08 - 46	+5.70	+12.60	-1.60	+0.25	-0.06 to -0.12	0.05 to 0.10	-0.02 to 0.04	0.15 to 0.17	-0.0015	-0.0025	+0.0015
1-4 (105 - 112)	236 - 09 - 10	+5.90	+12.50	-2.40	+0.04	-0.07 to -0.11	0.05 to 0.14	-0.09 to 0.03	0.10 to 0.3	+0.0010	-0.0024	+0.0019
1-5 (118 - 133)	237 - 13 - 02	+6.50	+12.60	-2.30	0	-0.06 to -0.10	0.16 to 0.11	-0.05 to -0.09	0.10 to 0.15	+0.0011	-0.0033	-0.0012
1-6 (141 - 148)	238 - 23 - 33	+6.90	+12.90	-16.70	+0.28	0.12 to 0.14	-0.03 to 0.07	0.06 to 0.12	0.10 to 0.20	-0.0020	-0.0017	-0.0020
1-7 (157 - 172)	240 - 06 - 28	+7.60	+12.80	-12.90	-1.75	0 to -0.06	0.01 to -0.08	0 to 0.09	1.00	+0.0013	-0.0018	+0.0020
1-8.1 (176 - 183)	241 - 06 - 32	+8.04	+12.81	-11.33	+0.45	0.02 to 0.15	+0.03 to -0.18	-0.06 to -0.15	0 to 0.15	+0.0021	+0.0024	+0.0008
1-9.2a (184 - 199)	241 - 09 - 57	+8.11	+12.81	-6.86	+0.02	0.12 to 0.14	0.05 to 0.08	-0.03 to 0.05	0.15	0	-0.0010	+0.0012
1-9.2b (200 - 215)	241 - 13 - 24	+8.20	+12.80	-8.30	-0.05	0.07 to 0.13	0.16	0.05 to 0.15	0.15 to 0.50	+0.0017	0	+0.0022

TABLE 3.1-6: SPACECRAFT ATTITUDES DURING PRIMARY SITE PHOTOS

Additional lead-lag networks were used for stabilization during powered flight when pitch and yaw signals were applied to the thrust vector control (TVC) actuators.

The Constant Rate maneuver mode used the integrating gyro in its rate mode to obtain rate information for control through the reaction control thrusters. When a maneuver was desired, a slew signal was issued and the spacecraft was rotated one axis at a time at a constant rate by the reaction thrusters. The rate signal was integrated by the programmer and compared with the commanded final value to obtain a specified change in attitude. The rate mode could be selected without a slew command and spacecraft rates controlled to less than an amount determined by the deadband selection.

The Velocity Correction mode was used to perform velocity corrections required for mid-course, injection, and transfer maneuvers. The attitude control system was operated in the inertial hold mode, with pitch and yaw stabilization provided by TVC actuators, and roll control provided by the roll thrusters of the reaction control system.

The Photographic Hold mode was used during photography. The spacecraft was operated in the inertial hold mode with the yaw axis at zero yaw. Zero yaw axis was verified by the crab angle sensor output.

3.1.4.2 PERFORMANCE

3.1.4.2.1 Performance Summary

All spacecraft events and maneuvers in Lunar Orbiter Mission I were accurately controlled by the attitude control subsystem (ACS).

The primary site photos required three-axis maneuvering from the normal Canopus-Sun reference to a reference that aligned the camera axis to predetermined positions computed for each site. A roll, yaw, pitch rotation sequence was followed for each primary site photo. It was necessary to consider several sources of attitude error that could affect successful photography. These were attitude maneuver angle error, holding error, and high attitude rates.

The attitude maneuver angle error consisted primarily of the roll angle deviation from Canopus prior to starting the maneuver sequence. This error would not exist if the spacecraft had been operating with the star tracker locked on Canopus. Since the tracker operation was hampered by high glint (from reflected light) the roll axis was placed in an inertial hold mode that had an inherent drift rate of approximately +0.51 degree per hour. Canopus acquisition and tracking was possible during Sunset periods, and an accurate roll reference was established during the Sunset prior to each photo maneuver. Table 3.1-6 contains a list of attitude maneuver errors for each photo site. An accuracy tolerance of ± 0.2 degree was satisfied in all cases except for Site I-7, which had an error of -1.75 degree. Canopus reference had been lost on the orbit previous to Site I-7 photography. Updating maneuvers were considered but were not executed because of the close proximity of the Site I-7 photo activity. The roll error was also considered to be within an acceptable tolerance for a successful photograph.

A detailed description of the Canopus tracker anomaly will be found in Appendix D.

Attitude holding accuracy and attitude rates during the interval for which the shutter was opened are also listed in Table 3.1-6. Attitude positions and attitude rates were well within design tolerances of ± 0.2 degree and ± 0.01 degree per second respectively.

Film-set photos generally did not require maneuvers and were taken by merely opening the camera door and shutter. A few farside photos were made by rotating the spacecraft about the roll axis. Only the two Earth photos required two axis maneuvers. Table 3.1-7 contains attitude angles at the time the shutter was open. Attitude accuracy and rates were within the tolerance of ± 0.2 degree and ± 0.01 degree per second, respectively.

The off-nominal operation caused by the Canopus tracker glint problem, high-gain-antenna pointing constraints, power constraints, thermal constraints, and gyro drift required continuous calculation and planning for future attitude reference updating and maneuvers. The criteria for the total angle (combination of pitch and yaw) off the Sun for thermal control were changed periodically as new data were obtained and a maximum angle of 37 degrees was finally established. Power and thermal constraints generally determined the pitch attitude while antenna pointing and Canopus tracker constraints determined the yaw (± 10 degrees) and roll (± 4 degrees) attitude. The gyro drift rates determined the signs of the update maneuvers so that each axis drifted back through or into the field of view of the respective sensor. The true drift rates for the roll, pitch, and yaw axes were approximately + 0.51 degree per hour, + 0.33 degree per hour, and + 1.33 degree per hour, respectively.

The Canopus tracker and Sun sensor were the primary devices used to determine attitude position but other methods had to be used when these sensors were saturated or not effective. The coarse Sun sensors were saturated at ± 24 degrees (true) while the Canopus tracker was generally turned on during Sunset periods. When Sunset and Earthset occurred in close proximity Canopus viewing time was severely limited or nonexistent. The tracker could be turned on in Sunlight and an error signal would be generated if Canopus were within the field of view of the tracker. Solar panel current was used to determine total angle of the Sun when the pitch Sun sensors were saturated. Pitch angle could therefore be determined from total off-Sun angle and yaw angle. The high-gain-antenna sweep pattern was also used as a backup pitch attitude source when roll and yaw were known (i.e., during readout). The antenna was rotated to a predicted value prior to the attitude update maneuver and the antenna signal strength was observed as the maneuver was performed. The "correctness" of the maneuvers were determined from the signal strength. The variety of alternative and backup maneuvers employed on this mission demonstrated the outstanding versatility of the ACS.

Table 3.1-8 is a detailed history of attitude control events as they occurred during Mission I.

TIME DAY:HR:MIN:SEC	FRAME	SITE	ATTITUDE ANGLE (DEG) ROLL	PITCH	YAW
230:21:56:25.0	25	FS	-2.87	0.0	0.0
231:05:11:16.2	26	FS	+0.31	0.0	0.0
231:08:48:44.6	27	FS	+0.38	0.0	0.0
231:17:05:21.0	28	BS	-179.65	0.0	0.0
231:23:18:31.8	29	FS	+0.8	0.0	0.0
232:07:35:00.8	30	BS	-179.65	0.0	0.0
232:13:46:59.3	31	FA	+0.5	0.0	0.0
232:13:47:33.2	32	FA	+0.5	0.0	0.0
232:13:49:31.8	33	FA	+0.5	0.0	0.0
232:13:49:57.0	34	FA	+0.5	0.0	0.0
232:14:52:01.0	35	BS	-180.0	0.0	0.0
232:14:52:14.2	36	BS	-180.0	0.0	0.0
232:14:54:09.9	37	BS	-180.0	0.0	0.0
232:14:54:23.1	38	BS	-180.0	0.0	0.0
232:14:58:01.1	39	BS	-180.0	0.0	0.0
232:14:58:09.5	40	BS	-180.0	0.0	0.0
232:21:00:36.9	41	FS	-0.8	0.0	0.0
233:04:14:40.8	42	FS	+2.4	0.0	0.0
---	43	FS	---	---	---
233:11:28:00.3	44	FS	+1.3	0.0	0.0
---	45	FS	---	---	---
233:18:23:02.7	46	FS	-2.6	0.0	0.0
233:18:23:09.6	47	FS	-2.6	0.0	0.0
234:01:22:50.9	48	B-2	-0.9	0.0	0.0
234:01:23:04.0	49	B-2	-0.9	0.0	0.0
234:08:24:13.1	50	FS	-195.0	0.0	0.0
234:08:24:19.8	51	FS	-195.0	0.0	0.0
235:01:44:26.3	84	FS	-2.95	0.0	0.0

Table 3.1-7: SPACECRAFT ATTITUDE DURING SECONDARY-SITE PHOTOS

TIME DAY:HR:MIN:SEC	FRAME	SITE	ATTITUDE ANGLE (DEG) ROLL	PITCH	YAW
---	101	FS	---	---	---
235:16:36:23.6	102	EARTH	+188.8	+25.6	0.0
235:22:39:56.8	103	B-5	-1.5	0.0	0.0
---	104	TEST	---	---	---
235:16:04:03.1	113	B-7	-0.1	0.0	0.0
236:16:04:09.8	114	B-7	-0.1	0.0	0.0
---	115	B-5	---	---	---
237:00:09:40.9	116	B-5	+180.0	0.0	0.0
237:07:15:00.9	117	EARTH	+187.2	+45.4	0.0
237:19:55:00.8	134	B-8	+1.95	0.0	0.0
237:23:21:38.8	135	B-8	-2.1	0.0	0.0
238:03:48:35.7	136	BS	+181.9	0.0	0.0
238:06:14:30.9	137	-36° PITCH	+0.4	-35.7	+1.5
238:09:41:35.9	138	FS	-0.9	0.0	0.0
238:16:34:39.0	139	FS	-1.6	0.0	0.0
238:20:01:11.5	140	FS	-1.5	0.0	0.0
239:02:53:37.1	149	B-9	+1.9	0.0	0.0
239:06:18:38.3	150	B-10	+1.3	0.0	0.0
239:09:47:24.9	151	B-10	+29.0	0.0	0.0
---	152	FS	---	---	---
239:23:30:54.7	153	B-11	+14.0	0.0	0.0
239:23:31:04.7	154	B-11	+14.0	0.0	0.0
239:23:31:14.6	155	B-11	+14.0	0.0	0.0
239:23:31:24.6	156	B-11	+14.0	0.0	0.0
240:13:21:58.6	173	FS	-3.2	0.0	0.0
240:20:06:00.8	174	FS	-1.8	0.0	0.0
241:03:05:35.9	175	FS	-2.5	0.0	0.0

Table 3.1-7: CONTINUED

GMT				ANGLE		EVENT		
222	20	10	33.2	1	0.	$ DBC	1C	
222	20	26	30.1	7	360. Deg	$ 360 DEG. ROLL - SUN ACQ.	2C	
222	20	53	1.2	2	0.	$ DBO	3C	
222	21	41	55.7	1	0.	$ DBC	4C	
222	21	45	46.1	13	0.	$ SUNSET (DRIFT TEST)	5C	
223	01	46	10.4	1	0.	$ DBC (ACQUIRE SUN)	6C	
223	01	46	10.5	12	0.	$ SUNRISE (END DRIFT TEST)	7C	
223	02	19	1.4	1	0.	$ DBC	8C	
223	02	21	52.1	7	360.	$ STAR MAP ROLL 1	9C	Begin Canopus Acquisition
				9	95.		10C	
223	**06**	**01**	**46.0**	9	95.	**Roll +360 Degs**	11C	
223	08	10	36.7	12	0.	$ ACQUIRE SUN	12C	
223	10	17	30.0	7	360.0	$ EMP-ROP STAR MAP	13C	
223	10	48	22.0	9	95.0	$ EMP-YAP TRACKER TEST (+95 DEG)	14C	
223	10	54	53.0	9	95.0	$ EMM-YAP RETURN TO SUN(-95 DEG)	15C	
223	11	00	55.0	12	0.0	$ ACQUIRE SUN	16C	
223	14	26	28.0	7	27.4	$ ROLL TO MOON (+27.4 DEG)	17C	First Acquisition of the Moon
223	14	42	36.0	7	2.0	$ ROLL SEARCH (-2.0 DEG)	18C	
223	14	53	0.0	7	1.0	$ ROLL SEARCH (-1.0 DEG)	19C	
223	16	15	9.0	10	0.0	$ ACQUIRE MOON	20C	
223	16	44	20.0	7	93.0	$ RETURN TO CANOPUS (+93.0 DEG)	21C	
223	23	0	30.4	7	95.0	$ ROLL	22C	First Midcourse Maneuver
223	23	20	0.1	1	0.	$ DBC	23C	
223	23	23	18.8	7	73.35	$ ROLL EMP ROP	24C	
223	23	49	25.6	8	25.24	$ PITCH EMP PIM	25C	
223	23	59	59.7	2	0.	$ DBO	26C	
224	00	00	1.3	3	(32.2 Sec)	$ BURN EMP 124 Ft/Sec	27C	
224	00	01	49.1	1	0.	$ DBC	28C	
224	00	02	45.4	8	25.24	$ PITCH EMM PIM	29C	
224	00	04	32.6	7	73.35	$ ROLL EMM ROP	30C	
224	00	07	16.9	12	0.	$ ACQUIRE SUN	31C	

Time in Seconds

TABLE 3.1-8: SPACECRAFT MANUEVERS

GMT				ANGLE		EVENT		
224	00	14	0.1	7	35.0 Deg	$ ROLL	32C	
224	01	33	52.5	8	36.0	$ PITCH NEG 36 DEG	33C	First Thermal Maneuver
224	09	46	9.0	8	36.0	$ PITCH POS 36 DEG	34C	
224	09	52	41.0	12	0.	$ ASU AND LOCK	35C	
224	14	51	49.0	8	36.0	$ PITCH NEG 36 DEG	36C	
225	02	34	33.0	8	36.0	$ PITCH POS 36 DEG	37C	
225	02	40	18.0	8	0.	$ ASU AND LOCK	38C	Begin Canopus Tracker Diagnostic Tests
225	03	03	35.4	7	90.0	$ ROLL POS 90 DEG	39C	
225	03	12	34.0	7	360.0	$ ROLL POS 360 DEG	40C	
225	03	34	38.0	7	104.0	$ ROLL NEG 104.0 DEG	41C	
225	05	54	0.0	2	0.	$ OPEN DEADBAND	42C	
225	05	55	20.0	7	40.0	$ ROLL POS 40.0 0.05 RATE	43C	
225	07	16	1.4	1	0.	$ CLOSE DEADBAND	44C	
225	07	35	59.8	9	38.	$ YAW MINUS	45C	
225	10	43	23.0	9	38.	$ YAW PLUS	46C	
225	10	51	03.	12	0.	$ ASU	47C	
225	11	07	34.	7	20.1	$ ROM	48C	Canopus First Acquired by the Spacecraft
225	11	27	32.	7	4.2	$ ROP	49C	
225	11	47	30.	7	8.4	$ ROM	50C	
225	12	37	25.	7	4.2	$ ROM	51C	
225	13	47	42.	10	0.	$ ACA	52C	
225	14	46	27.	11	0.	$ CANOPUS SET(LEROLLPLACED ON IH	53C	
225	14	51	48.0	8	36.0	$ EMP PIM THERMAL RELIEF(-36DEG)	54C	
225	20	00	0.0	10	0.0	$ ACQUIRE CANOPUS	55C	
225	20	12	51.0	11	0.0	$ INERTIAL HOLD-ROLL AXIS	56C	
225	20	23	24.4	9	11.2	$ EMP-YAW-TRACKER TEST(-11.2 DEG	57C	
225	20	49	20.0	8	36.0	$ EMP-PIM-THERMAL RELIEF(-36 DEG	58C	
225	23	42	31.0	8	36.0	$ EMP-PIM-RETURN (+36 DEG)	59C	
225	23	55	34.0	9	11.2	$ EMP-ROM-RETURN (+11.2 DEG	60C	
226	00	13	37.0	12	0.0	$ ACQUIRE SUN	61C	
226	00	49	43.0	10	0.0	$ ACQUIRE CANOPUS	62C	
226	02	18	45.0	8	36.0	$ PITCH -36.0	63C	

TABLE 3.1-8: CONTINUED

GMT				ANGLE		EVENT			
226	09	35	9.0	8	36.0 Deg	$ PITCH + 36.0		64C	
226	09	37	20.0	12	0.	$ ASU		65C	
226	13	22	24.	7	2.3	$ROLL MINUS		66C	
226	15	22	56.	13	0.	$SUNSET		67C	First Sunset
226	15	27	3.2	1	0.	$ DBC		68C	Lunar Orbit Injection Maneuver
226	15	27	55.0	7	19.16	$ EMP-ROP ROLL		69C	
226	15	29	24.8	8	108.72	$ EMP-PIM PITCH		70C	
226	15	34	3.4	2	0.	$ DBO		71C	
226	15	34	3.6	3	(588. Sec)	$ BURN	2591 Ft/Sec	72C	
226	15	45	17.0	8	108.72	$ PITCH EMM-PIM		73C	
226	15	49	45.9	7	19.16	$ ROLL EMM-ROP		74C	
226	15	51	15.6	12	0.	$ ACQUIRE SUN		75C	
226	16	02	06.	12	0.	$SUNRISE		76C	
226	22	24	57.0	13	0.0	$ SUNSET 2		77C	
226	23	17	10.0	12	0.0	$ SUNRISE 2		78C	
227	02	02	40.0	13	0.0	$ SENSET 3		79C	
227	02	55	17.3	12	0.0	$ SUNRISE 3		80C	
227	05	40	01.4	13	0.0	$ SUNSET 4		81C	
227	06	32	14.0	12	0.0	$ SUNRISE 4		82C	
227	09	17	45.0	13	0.0	$ SUNSET 5		83C	
227	10	09	58.	12	0.0	$ SUNRISE 5		84C	
227	12	55	05.	13	0.0	$ SUNSET 6		85C	
227	13	47	19.	12	0.0	$ SUNRISE 6		86C	
227	16	32	49.	13	0.	$ SUNSET 7		87C	Roll to Negative Side of Canopus
227	16	35	30.	7	39.2	$ ROLL-39.2		88C	
227	16	37	36.0	2	0.	$ OPEN DB		89C	Wide Deadband (2.0 Deg)
227	17	25	52.	12	0.	$ SUNRISE 7		90C	
227	19	56	43.	1	0.	$ DB.CLOSURE		91C	
227	20	10	33.	13	0.	$ SUNSET 8		92C	
227	20	29	25.	7	27.82	$ ROLL PLUS 27.82		93C	Return to Tracker Field of View
227	21	02	23.	12	0.	$ SUNRISE 8		94C	

TABLE 3.1-8: CONTINUED

	GMT			ANGLE		EVENT		
227	23	47	53.	13	0. Deg	$ SUNSET 9	95C	— Begin Continuous Roll Updates
228	0	0	31.	7	5.15	$ ROLL POS 5.15	96C	
228	00	40	07.0	12	0.	$ SUNRISE 9	97C	
228	03	25	37.0	13	0.	$ SUNSET 10	98C	
228	04	17	27.0	12	0.	$ SUNRISE 10	99C	
228	07	02	58.0	13	0.0	$ SUNSET 11	100C	
228	07	55	11.0	12	0.0	$ SUNRISE 11	101C	
228	10	40	41.0	13	0.0	$ SUNSET 12	102C	
228	11	32	32.0	12	0.0	$ SUNRISE 12	103C	
228	14	21	06.6	13	0.0	$ SUNSET 13	104C	
228	14	47	59.0	7	6.4	$ ROM (-6.4 DEG)	105C	
228	15	10	15.0	12	0.0	$ SUNRISE 13	106C	
228	17	55	46.0	13	0.0	$ SUNSET 14	107C	
228	18	47	36.0	12	0.0	$ SUNRISE 14	108C	
228	21	33	29.0	13	0.0	$ SUNSET 15	109C	
228	22	25	20.0	12	0.0	$ SUNRISE 15	110C	
229	01	10	50.0	13	0.0	$ SUNSET 16	111C	
229	02	02	40.0	12	0.0	$ SUNRISE 16	112C	
229	04	48	34.0	13	0.0	$ SUNSET 17	113C	
229	05	00	28.0	7	353.7	$ ROP 353.7 DEG	114C	— Star Map in Moon's Shadow
229	05	40	29.0	12	0.0	$ SUNRISE 17	115C	
229	08	25	54.0	13	0.0	$ SUNSET 18	116C	
229	09	17	45.0	12	0.0	$ SUNRISE 18	117C	
229	12	03	38.0	13	0.0	$ SUNSET 19	118C	
229	12	55	28.0	12	0.0	$ SUNRISE 19	119C	
229	15	41	45.0	13	0.0	$ SUNSET 20	120C	
229	16	32	49.0	12	0.0	$ SUNRISE 20	121C	
229	19	18	42.0	13	0.0	$ SUNSET 21	122C	
229	19	44	49.0	7	6.2	$ ROLL (-6.2)	123C	
229	20	10	33.0	12	0.0	$ SUNRISE 21	124C	
229	22	56	26.0	13	0.0	$ SUNSET 22	125C	
229	23	47	53.0	12	0.0	$ SUNRISE 22	126C	
230	02	34	9.0	13	0.0	$ SUNSET 23	127C	

TABLE 3.1-8: CONTINUED

GMT				ANGLE		EVENT		
230	03	25	37.0	12	0.0 Deg	$ SUNRISE 23	128C	
230	06	11	30.0	13	0.0	$ SUNSET 24	129C	
230	07	02	57.0	12	0.0	$ SUNRISE 24	130C	
230	09	49	14.0	13	0.0	$ SUNSET 25 ◁1	131C	
230	10	40	41.0	12	0.0	$ SUNRISE 25	132C	
230	13	26	34.0	13	0.0	$ SUNSET 26	133C	
230	14	18	02.0	12	0.0	$ SUNRISE 26	134C	
230	14	37	40.0	7	3.6	$ ROLL +3.6	135C	Sight A-0 Photo Maneuver
230	14	38	44.0	9	12.5	$ YAW +12.45	136C	
230	14	40	02.0	8	8.1	$ PITCH -8.1	137C	
230	14	48	05.0	8	8.1	$ PITCH +8.1	138C	
230	14	49	13.0	9	12.5	$ YAW -12.5	139C	
230	14	50	34.0	7	3.6	$ ROLL -3.6	140C	
230	14	51	49.0	12	0.0	$ ACQUIRE SUN	141C	
230	14	51	50.	1	0.	$ DBC(TO PICKUP YAW ACQUISITION)	142C	
230	17	04	18.	13	0.	$ SUNSET 27	143C	
230	17	55	45.	12	0.	$ SUNRISE 27	144C	
230	20	42	02.	13	0.	$ SUNSET 28	145C	
230	21	00	34.	7	6.0	$ ROLL-6.0 DEG.	146C	
230	21	33	29.0	12	0.	$ SUNRISE 28	147C	
231	00	14	23.0	13	0.0	$ SUNSET 29	148C	
231	01	10	50.0	12	0.0	$ SUNRISE 29	149C	
231	03	59	07.0	13	0.0	$ SUNSET 30	150C	
231	04	48	33.0	12	0.0	$ SUNRISE 30	151C	
231	07	34	50.0	13	0.0	$ SUNSET 31	152C	
231	08	25	54.0	12	0.0	$ SUNRISE 31	153C	
231	11	12	20.0	13	0.0	$ SUNSET 32	154C	
231	11	34	37.0	7	5.5	$ ROLL MINUS 5.5	155C	
231	12	03	38.0	12	0.0	$ SUNRISE 32	156C	
231	14	49	54.0	13	0.0	$ SUNSET 33	157C	
231	15	41	21.0	12	0.0	$ SUNRISE 33	158C	
231	15	50	31.0	7	179.7	$ ROM	159C	First Backside Photo Maneuver Frame 28
231	17	40	31.0	7	176.0	$ ROM	160C	

◁1 Roll - 4.6 Deg

TABLE 3.1-8: CONTINUED

GMT				ANGLE		EVENT		
231	18	27	38.0	13	0.0 Deg	$ SUNSET 34	161C	
231	19	18	42.0	12	0.0	$ SUNRISE 34	162C	
231	22	04	35.0	13	0.0	$ SUNSET 35	163C	
231	22	14	11.0	7	7.0	$ ROLL (-7.0 DEG)	164C	
231	22	56	26.0	12	0.0	$ SUNRISE 35	165C	
232	01	42	42.0	13	0.0	$ SUNSET 36	166C	
232	02	33	46.0	12	0.0	$ SUNRISE 36	167C	
232	05	20	26.0	13	0.0	$ SUNSET 37	168C	
232	06	10	44.0	12	0.0	$ SUNRISE 37	169C	
232	06	20	22.0	7	183.5	$ ROLL -183.5 DEG	170C	Frame 30 Photo Maneuver
232	08	13	34.0	7	182.89	$ ROLL -182.89 DEG	171C	
232	08	58	09.0	13	0.0	$ SUNSET 38	172C	
232	09	49	14.0	12	0.0	$ SUNRISE 38	173C	
232	12	35	30.0	13	0.0	$ SUNSET 39	174C	
232	13	26	34.0	12	0.0	$ SUNRISE 39	175C	
232	14	03	29.0	7	181.0	$ ROLL -181.0 DEG PHOTO 175A	C	Frames 35 through 40 Photo Maneuver
232	15	20	11.0	7	183.7	$ ROLL -183.7 DEG	176C	
232	16	13	14.0	13	0.0	$ SUNSET 40	177C	
232	17	04	18.0	12	0.0	$ SUNRISE 90	178C	
232	19	50	57.0	13	0.0	$ SUNSET 41	179C	
232	20	42	02.0	12	0.0	$ SUNRISE 41	180C	
232	23	28	18.0	13	0.0	$ SUNSET 42	181C	
233	00	19	22.0	12	0.0	$ SUNRISE 42	182C	
233	03	06	02.0	13	0.0	$ SUNSET 43	183C	
233	03	57	06.0	12	0.0	$ SUNRISE 43	184C	
233	06	43	45.0	13	00	$ SUNSET 44	185C	
233	07	06	25.0	7	4.82	$ ROLL -4.82 DEG	186C	
233	07	34	27.0	12	0.0	$ SUNRISE 44	187C	
233	09	41	58.0	7	43.4	$ ROLL +43.4 DEG ORBIT TRANSFER	188C	Orbit Transfer Maneuver
233	09	44	16.0	8	25.3	$ PITCH +25.31 DEG	189C	
233	09	49	58.2	2	0.0	$ OPEN DEADBAND	190C	
233	09	50	0.80	[illegible]	(22.7 Sec)	$ BURN ORBIT TRANSFER 131.9 FPS	191C	
233	09	52	19.0	1	0.0	$ CLOSE DEADBAND	192C	

Time in Sec

TABLE 3.1-8: CONTINUED

GMT					ANGLE	EVENT		
233	09	53	10.0	8	25.3 Deg	$ PITCH -25.3 DEG	193C	Orbit Transfer Maneuver
233	09	54	52.0	7	43.4	$ ROLL -43.4 DEG	194C	
233	09	57	10.9	12	0.0	$ ACQUIRE SUN	195C	
233	10	20	43.0	13	0.0	$ SUNSET 1	196C	
233	11	12	10.0	12	0.0	$ SUNRISE 1	197C	
233	13	49	37.0	13	0.0	$ SUNSET 2	198C	
233	14	41	04.0	12	0.0	$ SUNRISE 2	199C	
233	17	18	54.0	13	0.0	$ SUNSET 3	200C	
233	17	47	28.0	7	7.04	$ ROLL-7.04 DEG	201C	
233	18	10	21.0	12	0.0	$ SUNRISE	202C	
233	20	48	10.0	13	0.0	$ SUNSET 4	203C	
233	21	39	15.0	12	0.0	$ SUNRISE 4	204C	
233	21	42	43.0	8	30.0	$ PITCH -30	205C	
234	00	17	04.0	13	0.0	$ SUNSET 5	206C	
234	00	18	48.0	8	30.0	$ PITCH +30	207C	
234	01	08	08.0	12	0.0	$ SUNRISE 5	208C	
234	03	46	21.0	13	0.0	$ SUNSET 6	209C	
234	04	01	45.0	7	3.8	$ ROLL (-3.83 DEG)	210C	
234	04	37	48.0	12	0.0	$ SUNRISE 6	211C	
234	06	40	03.3	8	30.0	$ PITCH 30 SUNSET 7 07 15 15	212C	
234	07	31	30.0	8	30.0	$ PITCH (-30 DEG) THERMAL	213C	
234	08	15	32.0	12	0.0	$ SUNRISE 7 ASU COMMAND NOT ON	214C	
234	10	44	31.0	13	0.0	$ SUNSET 8	215C	
234	11	36	22.3	12	0.0	$ SUNRISE 8	216C	
234	14	13	48.0	13	0.0	$ SUNSET 9	217C	
234	14	53	44.0	7	1.11	$ ROLL NEG 1.111 DEG	218C	
234	15	04	53.0	12	0.0	$ SUNRISE 9	219C	
234	15	15	41.0	7	5.36	$ ROLL +5.36 SIGHT A1 PHOTO	220C	Sight A-1 Photo Maneuver
234	15	16	47.0	9	12.46	$ YAW +12.46 SIGHT A1 PHOTO	221C	
234	15	18	08.0	8	9.60	$ PITCH -9.60 SIGHT A1 PHOTO	222C	
234	15	24	25.0	8	9.60	$ PITCH +9.60 SIGHT A1 PHOTO	223C	
234	15	25	34.0	9	12.46	$ YAW -12.46 SIGHT A1 PHOTO	224C	

TABLE 3.1-8: CONTINUED

GMT				ANGLE		EVENT			
234	15	26	43.0	7	5.36 Deg	$ ROLL -5.36 SIGHT A1 PHOTO		225C	Sight A-1 Photo Maneuvers
234	15	27	55.0	12	0.0	$ AGC COMMAND USE SUNRISE		226C	
234	17	42	42.0	13	0.0	$ SUNSET 10		227C	
234	18	13	28.0	7	1.56	$ ROLL -1.56 ROLL UPDATE		228C	
234	15	34	09.0	12	0.0	$ SUNRISE 10		229C	
234	18	45	41.0	7	5.43	$ ROLL +5.43 SIGHT A2 PHOTO		230C	Sight A-2 Photo Maneuvers
234	18	46	30.0	9	12.48	$ YAW +12.48 SIGHT A2 PHOTO		231C	
234	18	48	00.0	8	4.98	$ PITCH -4.98 SIGHT A2 PHOTO		232C	
234	18	52	09.0	8	4.98	$ PITCH +4.98 SIGHT A2 PHOTO		233C	
234	18	53	10.0	9	12.48	$ YAW -12.48 SIGHT A2 PHOTO		234C	
234	18	54	30.0	7	5.43	$ ROLL -5.43 SIGHT A2 PHOTO		235C	
234	18	55	40.0	12	0.0	$ AGC COMMAND USE SUNRISE		236C	
234	21	11	59.0	13	0.0	$ SUNSET 11		237C	
234	22	03	03.0	12	0.0	$ SUNRISE 11		238C	
235	00	40	33.0	13	0.0	$ SUNSET 12		239C	
235	01	07	07.0	7	5.95	$ ROLL MINUS 5.95		240C	
235	01	32	20.0	12	0.0	$ SUNRISE 12		241C	
235	04	10	09.0	13	0.0	$ SUNSET 13	242	C	
235	05	01	14.0	12	0.0	$ SUNRISE 13	243	C	
235	07	39	26.0	13	0.0	$ SUNSET 14	244	C	
235	08	30	30.0	12	0.0	$ SUNRISE 14	245	C	
235	08	41	53.0	7	5.7	$ ROLL PLUS 5.7	246	C	Sight A-3 Photo Maneuvers
235	08	42	15.0	9	12.6	$ YAW PLUS 12.6	247	C	
235	08	43	11.0	8	1.6	$ PITCH MINUS 1.6	248	C	
235	08	47	47.0	8	1.6	$ PITCH PLUS 1.6	249	C	
235	08	48	41.0	9	12.6	$ YAW MINUS 12.6	250	C	
235	08	50	05.0	7	5.7	$ ROLL MINUS 5.7	251	C	
235	08	51	15.0	12	0.0	$ ACQUIRE SUN	252	C	
235	11	08	20.0	13	0.0	$ SUNSET 15	253	C	
235	11	59	24.0	12	0.0	$ SUNRISE 15	254	C	
235	14	37	37.0	13	0.0	$ SUNSET 16		255C	
235	14	59	30.0	7	3.5	$ ROLL MINUS 3.5		256C	
235	15	23	41.0	12	0.0	$ SUNRISE 16		257C	

TABLE 3.1-8: CONTINUED

GMT				ANGLE		EVENT			
236	12	23	13.0	12	0.0 Deg	$ SUNRISE 22		290C	
236	15	01	25.0	13	0.0	$ SUNSET 23		291C	
236	15	34	26.0	7	3.1	$ ROLL -3.1		292C	
236	15	52	29.0	12	0.0	$ SUNRISE 23		293C	
236	18	30	19.0	13	0.0	$ SUNSET 24		294C	
236	19	21	33.0	12	0.0	$ SUNRISE 24		295C	
236	21	59	59.0	13	0.0	$ SUNSET 25		296C	
236	22	50	40.0	12	0.0	$ SUNRISE 25		297C	
236	23	30	25.0	7	176.35	$ ROP		298C	Frame 106 Film Set
237	01	28	52.0	13	0.0	$ SUNSET 26		299C	
237	02	19	34.0	12	0.0	$ SUNRISE 26		300C	
237	02	30	26.0	7	176.74	$ ROP		301C	
237	04	57	46.0	13	0.0	$ SUNSET 27		302C	
237	05	48	51.0	12	0.0	$ SUNRISE 27		303C	
237	07	04	51.0	7	187.0	$ ROLL 187		304C	Earth Photo Maneuver No. 2
237	07	11	47.0	8	45.4	$ PITCH 45.4		305C	
237	07	16	24.0	8	45.4	$ PITCH -45.4		306C	
237	07	18	45.0	7	187.0	$ ROLL -187		307C	
237	07	25	15.0	12	0.0	$	ACQUIRE SUN	308C	
237	08	25	26.0	13	0.0	$ SUNSET 28		309C	
237	08	51	29.0	7	3.0	$ ROLL -3		310C	
237	09	18	59.0	12	0.0	$ SUNRISE 28		311C	
237	11	55	57.0	13	0.0	$ SUNSET 29		312C	
237	12	47	1.0	12	0.0	$ SUNRISE 29		313C	
237	12	57	05	7	6.5	$ ROLL +6.5		314C	Sight A-5 Photo Maneuver
237	12	58	11.0	9	12.6	$ YAW +12.6		315C	
237	12	59	29	8	2.3	$ PITCH -2.3		316C	
237	13	03	28	8	2.3	$ PITCH +2.3		317C	
237	13	04	26	9	12.6	$ YAW -12.6		318C	
237	13	05	48	7	6.5	$ ROLL -6.5		319C	
237	13	06	59	12	0.0	$ ACQUIRE SUN		320C	
237	13	57	47	7	1.3	$ ROLL -1.3		321C	
237	15	20	0.0	13	0.0	$ SUNSET 30		322C	

TABLE 3.1-8: CONTINUED

GMT				ANGLE		EVENT		
235	16	25	23.8	7	188.7 Deg	$ ROLL PLUS 188.7	258C	Earth Photo Maneuvers
235	16	32	32.6	8	25.6	$ PITCH PLUS 25.6	259C	
235	16	37	43.0	8	25.6	$ PITCH MINUS 25.6	260C	
235	16	39	04.6	7	188.7	$ ROLL MINUS 188.7	261C	
235	16	46	36.4	12	0.0	$ ASU	262C	
235	18	06	30.0	13	0.0	$ SUNSET 17	263C	
235	18	57	35.0	12	0.0	$ SUNRISE 17	264C	
235	21	35	47.0	13	0.0	$ SUNSET 18	265C	
235	22	13	25.0	7	5.02	$ ROLL -5.016	266C	
235	22	26	52.0	12	0.0	$ SUNRISE 18	267C	
236	01	05	04.0	13	0.0	$ SUNSET 19	268C	
236	01	56	08.0	12	0.0	$ SUNRISE 19	269C	
236	02	10	41.1	7	6.13	$ ROLL +6.13	270C	Maneuver for V/H Sensor and Camera Test
236	02	11	50.0	9	12.75	$ YAW +12.75	271C	
236	02	13	05.0	8	5.47	$ PITCH -5.47	272C	
236	02	17	06.4	8	5.47	$ PITCH +5.47	273C	
236	02	18	13.2	9	12.75	$ YAW -12.75	274C	
236	02	19	34.0	7	6.13	$ ROLL -6.13	275C	
236	02	20	43.0	12	0.0	$ SUNRISE ASU	276C	
236	04	33	58.0	13	0.0	$ SUNSET 20	277C	
236	05	25	02.0	12	0.0	$ SUNRISE 20	278C	
236	08	03	15.0	13	0.0	$ SUNSET 21	279C	
236	08	35	57.6	7	3.16	$ ROLL -3.16	280C	
236	08	54	19.0	12	0.0	$ SUNRISE 21	281C	
236	09	04	28.1	7	5.9	$ ROLL +5.9	282C	Sight A-4 Photo Maneuver
236	09	05	31.4	9	12.5	$ YAW +12.5	283C	
236	09	06	47.9	8	2.4	$ PITCH -2.4	284C	
236	09	11	44.1	8	2.4	$ PITCH +2.4	285C	
236	09	12	40.4	9	12.5	$ YAW -12.5	286C	
236	09	13	56.8	7	5.9	$ ROLL -5.9	287C	
236	09	15	26.0	12	0.0	$ SUNRISE ASU	288C	
236	11	32	8.0	13	00.	$ SUNSET 22	289C	

TABLE 3.1-8: CONTINUED

GMT					ANGLE	EVENT		
237	15	44	29.3	7	0.01 Deg	$ ROLL +.01	323C	Orbit Adjust Maneuver
237	15	45	20.5	7	34.2	$ ROLL +34.2	324C	
237	15	47	23.6	8	129.7	$ PITCH -129.7	325C	
237	16	1	29.0	2	0.0	$ DBO	326C	
237	16	1	43.0		(2.8 Sec)	$ BURN 17.7 FT/S	327C	
237	16	2	24.5	1	0.0	$ DBC	328C	
237	16	2	51.9	8	129.7	$ PITCH +129.7	329C	
237	16	07	59.2	7	34.2	$ ROLL -34.2	330C	
237	16	9	58.6	7	0.1	$ ROLL +0.01	331C	
237	16	16	18.0	12	0.0	$ SUNRISE 30	332C	
237	18	52	0.0	13	0.0	$ SUNSET 31	333C	
237	19	42	30.0	12	0.0	$ SUNRISE 31	334C	
237	22	20	00.0	13	0.0	$ SUNSET 32	335C	
237	22	46	29.6	7	5.6	$ ROLL -5.64	336C	
237	23	08	20.0	12	0.0	$ SUNRISE	337C	
238	01	46	55.0	13	0.0	$ SUNSET 33	338C	
238	02	34	55.0	12	0.0	$ SUNRISE 33	339C	
238	03	39	57.0	7	182.0	$ ROLL+181.995	340C	Frame 136 Photo
238	04	07	27.0	7	183.13	$ ROLL-183.128	341C	
238	05	13	30.0	13	0.0	$ SUNSET 34	342C	
238	05	32	27.0	8	36.0	$ PITCH-36.0	343C	
238	09	12	24.0	8	36.0	$ PITCH +36.0	344C	
238	09	35	47.0	12	0.0	$ ASU SUNRISE	345C	
238	12	03	0.0	13	0.0	$ SUNSET 36	346C	
238	12	37	39.0	7	4.0	$ ROLL -4.0 DEG	347C	
238	12	54	0.0	12	0.0	$ SUNRISE 36	348C	
238	14	24	33.0	8	0.011	$ INERTIAL HOLD MANVR	349C	Pitch and Yaw Drift Test
238	16	33	35.0	12	0.0	$ SUN ACQUISITION	350C	
238	19	03	0.0	13	0.0	$ SUNSET 38	351C	
238	19	32	38.0	7	1.7	$ ROLL - 1.7 DEG	352C	
238	19	46	44.0	12	0.0	$ SUNRISE 38	353C	
238	20	34	08.0	8	28.16	$ PITCH MINUS 28.160 DEG	354C	
238	21	16	42.0	8	16.90	$ PITCH MINUS 16.896 DEG	355C	

Time in Seconds

TABLE 3.1-8: CONTINUED

GMT				ANGLE		EVENT		
238	22	43	54.0	8	45.1 Deg	$ PITCH PLUS 45.1	356C	
238	22	58	51.0	7	1.8	$ ROLL PLUS 1.8	357C	
238	23	12	56.0	12	0.0	$ SUNRISE 39	358C	
238	23	26	42.0	7	6.9	$ ROLL PLUS 6.9	359C	
238	23	27	51.0	9	12.9	$ YAW PLUS 12.9	360C	
238	23	29	09.0	8	16.7	$ PITCH MINUS 16.7	361C	Sight A-6 Photo Maneuvers
238	23	34	37.0	8	16.7	$ PITCH PLUS 16.7	362C	
238	23	36	07.0	9	12.9	$ YAW MINUS 12.9	363C	
238	23	37	08.0	7	6.9	$ ROLL MINUS 6.9	364C	
238	23	38	40.0	12	0.0	$ ASU SUNRISE	365C	
239	00	14	26.0	8	16.0	$ PITCH PLUS 16.0 THERMAL	366C	
239	02	45	54.0	8	16.0	$ PITCH MINUS 16.0 TO SUN	367C	
239	02	48	45.0	12	0.0	$ ASU SUNRISE	368C	
239	03	07	31.0	8	16.0	$ PITCH PLUS 16.0 THERMAL	369C	Fire N_2 Squib 239-05-48
239	06	14	33.0	7	4.5	$ ROLL MINUS 4.5 UPDATE	370C	
239	07	42	30.0	8	16.0	$ PITCH MINUS 16.0 TO SUN	371C	
239	07	46	44.0	12	0.0	$ ASU SUNRISE	372C	
239	08	40	18.0	13	0.0	$ SUNSET 42	373C	
239	09	31	57.0	12	0.0	$ SUNRISE 42	374C	
239	09	39	43.0	7	25.1	$ ROLL PLUS 25.1	375C	
239	09	51	35.0	7	28.0	$ ROLL MINUS 28.0	376C	
239	09	54	01.0	8	16.0	$ PITCH PLUS 16.0 DEG	377C	
239	14	26	39.0	8	11.3	$ PITCH PLUS 11.3 DEG	378C	
239	16	09	24.0	8	28.2	$ PITCH MINUS 28.2 DEG	379C	
239	16	24	45.0	12	0.0	$ SUNRISE	380C	Begin Stored Program Pitch Maneuvers for Thermal
239	16	30	55.0	8	16.0	$ PITCH PLUS 16.0 DEG	381C	
239	16	35	32.0	8	12.0	$ PITCH PLUS 12.0 DEG	382C	
239	18	53	0.7	8	16.0	$ PITCH -16	383C	
239	18	54	57	12	0.0	$ SUNRISE ASV ORBIT 44	384C	
239	19	00	0.0	13	0.0	$ SUNSET 44	385C	
239	19	50	57.0	12	0.0	$ SUNRISE ASV ORBIT 45	386C	
239	19	59	26.3	8	16	$ PITCH +16	387C	
239	22	19	40.2	8	16	$ PITCH -16	388C	

TABLE 3.1-8: CONTINUED

GMT				ANGLE		EVENT		
239	22	21	3.6	12	0.0 Deg	$ SUNRISE ASV ORBIT 46	389C	
239	22	24	23.0	13	0.0	$ SUNSET 46	390C	
239	23	17	33.0	12	0.0	$ SUNRISE 46	391C	
239	23	18	27.6	7	5.0	$ ROLL +5.0	392C	
239	23	33	4.5	8	16.0	$ PITCH +16.0	393C	
240	01	45	46.4	8	16.0	$ PITCH -16.0	394C	
240	01	47	19.9	12	0.0	$ SUNRISE ASV	395C	
240	02	32	14.0	7	5.0	$ ROLL +5.0	396C	
240	02	41	35.6	7	5.0	$ ROLL -5.0	397C	
240	02	42	21.6	7	5.0	$ ROLL -5.0	398C	
240	02	43	45.0	12	0.0	$ SUNRISE 47	399C	
240	02	45	2.6	7	5.0	$ ROLL -5.0	400C	Lost Canopus and Canopus Search
240	02	48	56.4	8	16.0	$ PITCH +16.0	401C	
240	03	50	13.8	8	16.0	$ PITCH -16.0	402C	
240	04	22	26.0	12	0.0	$ SUNRISE ASV	403C	
240	04	26	11.0	7	360.0	$ ROLL +360.0	404C	
240	04	42	53.6	8	16.0	$ PITCH +16	405C	
240	05	11	39.7	8	16.0	$ PITCH - 16 DEG.	406C	
240	05	13	3.9	12	0.0	$ ASU - SUNRISE	407C	
240	05	18	41.0	13	0.0	$ SUNSET	408C	
240	05	52	0.0	7	12.0	$ ROLL NEG 12.0	409C	
240	06	10	21.0	12	0.0	$ SUNRISE	410C	
240	06	22	26.0	7	7.6	$ ROLL POS 7.6 A7	411C	
240	06	23	35.0	9	12.8	$ YAW POS 12.8 A7	412C	
240	06	24	53.0	8	12.9	$ PITCH NEG 12.9 A7	413C	
240	06	30	39.0	8	12.9	$ PITCH POS 12.9 A7	414C	Sight A-7 Photo Maneuvers
240	06	31	51.0	9	12.8	$ YAW NEG 12.8 A7	415C	
240	06	33	11.0	7	7.6	$ ROLL NEG 7.6 A7	416C	
240	06	34	32.0	12	0.0	$ ASU SUNRISE	417C	
240	06	36	57.0	8	16.0	$ PITCH POS 16.0 THERMAL	418C	
240	08	38	6.5	8	16.0	$ PITCH NEG 16.0 TO SUN	419C	
240	08	39	29.6	12	0.0	$ ASU - SUNRISE	420C	
240	08	45	0.0	13	0.0	$ SUNSET 49	421C	

TABLE 3.1-8: CONTINUED

GMT				ANGLE		EVENT	
240	09	36	33.0	12	0.0 Deg	$ SUNRISE 49	422C
240	09	41	41.0	8	16.0	$ PITCH POS 16.0 THERMAL	423C
240	12	05	48.9	8	16.0	$ PITCH NEG 16.0 TO SUN	424C
240	12	07	11.5	12	0.0	$ ASU - SUNRISE	425C
240	12	11	18.0	13	0.0	$ SUNSET 50	426C
240	13	03	09.0	12	0.0	$ SUNRISE 50	427C
240	13	10	23.0	7	5.70	$ ROLL NEG 5.70 UPDATE	428C
240	13	24	13.0	8	16.0	$ PITCH POS 16.0 THERMAL	429C
240	15	31	7.2	8	16.0	$ PITCH MINUS 16.0	430C
240	15	32	30.6	12	0.0	$ ASU	431C
240	15	37	36.0	13	0.0	$ SUNSET 51	432C
240	16	28	47.0	12	0.0	$ SUNRISE 51	433C
240	16	36	43.9	8	28	$ PITCH PLUS 28 - THERMAL	434C
240	18	57	25.9	8	28	$ PITCH MINUS 28	435C
240	18	59	13.3	12	0.0	$ ASU	436C
240	19	03	55.0	13	0.0	$ SUNSET 52	437C
240	19	55	9.8	12	0.0	$ SUNRISE 52	438C
240	19	55	37.0	7	3.5	$ ROLL -3.5 DEG.	439C
240	20	18	57.0	8	34.0	$ PITCH +34 DEG	440C
240	22	23	0.0	8	34.0	$ PITCH -34 DEG	441C
240	22	30	0.0	13	0.0	$ SUNSET -ASU	442C
240	23	21	46.0	12	0.0	$ SUNRISE 53	443C
240	23	29	29.0	8	37.0	$ PITCH +37 DEG	444C
241	01	50	30.7	8	37.0	$ PITCH -37 DEG	445C
241	01	51	54.2	12	0.0	$ ACQUIRE SUN	446C
241	01	56	28.3	13	0.0	$ SUNSET 54	447C
241	02	45	8.4	7	7.0	$ ROLL -7.0 DEG	448C
241	02	47	59.0	12	0.0	$ SUNRISE 54. ACQ SUN	449C
241	03	19	36.7	8	37.0	$ PITCH +37.0 DEG	450C
241	05	16	39.2	8	37.0	$ PITCH -37.0 DEG	451C
241	05	19	0.7	12	0.0	$ ACUQIRE SUN	452C
241	05	22	45.0	13	0.0	$ SUNSET 55	453C

TABLE 3.1-8: CONTINUED

GMT				ANGLE		EVENT		
241	06	26	30.6	7	8.0 Deg	$ ROLLU+8.04 DEG SITE 8.1	454C	Sight A-8.1 Photo Maneuvers
241	06	27	39.7	9	12.8	$ YAW +12.81 DEG	455C	
241	06	23	35.8	8	11.3	$ PITCH -11.33 DEG	456C	
241	06	34	11.9	8	11.3	$ PITCH +11.33 DEG	457C	
241	06	35	29.4	9	12.8	$ YAW -12.81 DEG	458C	
241	06	36	52.4	7	8.0	$ROLL - 8.04 DEG	459C	
241	06	38	0.0	12	0.0	$ ACQUIRE SUN	460C	
241	07	34	34.7	7	1.9	$ ROLL - 1.87	461C	
241	08	49	2.2	13	0.0	$ SUNSET 56	462C	
241	09	40	47.0	12	0.0	$ SUNRISE SUN LOUC 56	463C	
241	09	51	17.6	7	8.1	$ ROLL +8.11 DEG SITE 9.2A	464C	Sight A-9.2a Photo Maneuvers
241	09	52	29.4	9	12.8	$ YAW +12.81 DEG	465C	
241	09	53	52.2	8	6.9	$ PITCH -6.86 DEG	466C	
241	09	58	57.6	8	6.9	$ PITCH +6.86 DEG	467C	
241	10	00	10.2	9	12.8	$ YAW -12.81 DEG	468C	
241	10	01	33.2	7	8.1	$ ROLL -8.11 DEG	469C	
241	10	02	40.0	12	0.0	$ ACQUIRE SUN	470C	
241	11	10	17.8	7	1.6	$ ROLL -1.59 DEG UPDATE	471C	
241	12	15	17.0	13	0.0	$ SUNSET 57	472C	
241	13	06	59.0	12	0.0	$ SUNRISE 57	473C	
241	13	17	56.0	7	8.2	$ ROLL +8.2 PHOTO	474C	Sight A-9.2b Photo Maneuvers
241	13	19	12.0	9	12.8	$ YAW +12.8	475C	
241	13	20	26.0	8	8.3	$ PITCH -8.3	476C	
241	13	25	44.0	8	8.3	$ PITCH +8.3	477C	
241	13	26	53.0	9	12.8	$ YAW -12.8	478C	
241	13	28	41.0	7	8.2	$ ROLL -8.2	479C	
241	13	30	12.0	8	33.8	$ PITCH +33.8	480C	
241	15	33	35.0	8	33.8	$ PITCH -33.8	481C	
241	15	40	20.0	13	0.0	$ SUNSET 58	482C	
241	16	33	11.0	12	0.0	$ SUNRISE 58	483C	
241	16	43	54.0	8	34.0	$ PITCH MINUS	484C	
241	19	01	55.0	8	34.0	$ PITCH PLUS	485C	

TABLE 3.1-8: CONTINUED

GMT				ANGLE		EVENT		
241	19	09	02.0	13	0.0 Deg	$ SUNSET 59	486C	
241	20	00	10.0	12	0.0	$ SUNRISE 59	487C	
241	20	10	11.0	8	15.0	$ PITCH MINUS	488C	
241	22	28	0.0	8	15.0	$ PITCH PLUS	489C	
241	22	28	40.0	12	0.0	$ ACQUIRE SUN	490C	
241	22	34	0.0	13	0.0	$ SUNSET 60	491C	
241	23	25	00	12	0.0	$ SUNRISE 60	492C	
241	23	36	24.3	8	15.0	$ PITCH-15	493C	
242	01	55	4.1	8	15.0	$ PITCH +15	494C	
242	01	56	25.5	12	0.0	$ SUNRISE ASU	495C	
242	02	1	10.5	13	0.0	$ SUNSET 61	496C	
242	02	52	17	12	0.0	$ SUNRISE 61	497C	
242	02	57	41.6	8	15.0	$ PITCH-15	498C	
242	05	21	25.0	8	15.0	$ PITCH +15	499C	
242	05	22	44.0	12	0.0	$ SUNRISE ASU	500C	
242	05	27	31.0	13	0.0	$ SUNSET 62	501C	
242	06	18	47.0	12	0.0	$ SUNRISE 62	502C	
242	06	24	18.2	8	34.0	$ PITCH-34	503C	
242	08	47	49.8	8	34.0	$ PITCH+34	504C	
242	08	49	45.7	12	0.0	$ SUNRISE ASU	505C	
242	09	44	22.0	7	6.1	$ ROLL NEG 6.1 UPDATE	506C	
242	09	45	0.0	12	0.0	$ SUNRISE	507C	
242	09	50	57.0	8	15.0	$ PITCH NEG 15 OFF SUN	508C	Coarse Sun Sensors On 242:12:10:55
242	12	14	07.0	8	15.0	$ PITCH POS 15 TO SUN	509C	
242	13	11	12.0	12	0.0	$ SUNRISE	510C	
242	13	16	35.0	8	15.0	$ PITCH NEG 15 OFF SUN	511C	Fine Sun Sensors Off 242:14:17:38
242	15	40	32.0	8	15.0	$ PITCH POS 15 TO SUN	512C	
242	16	37	25.0	12	0.0	$ SUNRISE	513C	
242	16	43	13.0	8	15.0	$ PITCH NEG 15 OFF SUN	514C	
242	19	08	20.0	8	15.0	$ PITCH POS 15 TO SUN	515C	
242	19	55	0.0	12	0.0	$ ASU SUNRISE PRE PROGRAM	516C	
242	20	09	35.0	8	15.0	$ PITCH MINUS 15 DEG THERMAL	517C	
242	22	34	35.0	8	15.0	$ PITCH PLUS 15	518C	

TABLE 3.1-8: CONTINUED

GMT				ANGLE		EVENT		
242	23	30	36.0	12	0.0 Deg	$ ACQUIRE SUN	519C	Begin Continuous Off Sun Operation
242	23	35	45.0	8	15.0	$ PITCH MINUS 15 THERMAL	520C	
243	01	56	05.0	7	6.0	$ ROLL MINUS 6 CANOPUS UPDATE	521C	
243	03	21	34.0	8	7.0	$ PITCH MINUS 7 THERMAL	522C	
243	04	08	42.0	9	6.0	$ YAW MINUS 6 ANTENNA POINTING	523C	
243	10	00	0.0	7	7.0	$ ROLL MINUS	524C	
243	11	59	59.8	9	9.0	$ YAW MINUS	525C	
243	17	00	02.0	8	4.0	$ PITCH NEG 4.0	526C	
243	20	57	20.0	9	7.0	$ YAW NEG 7.0	527C	
244	01	54	33.0	7	7.0	$ ROLL NEG 7.0	528C	
244	03	34	22.5	9	8.0	$ YAW -8.0 DEG	529C	
244	06	53	29.3	9	7.5	$YAW -7.5 DEG.	530C	
244	08	53	46.3	8	4.0	$ PITCH -4.0 DEG.	531C	
244	13	49	01.0	9	8.0	$ YAW -8.0 DEG	532C	
244	15	46	28.0	7	7.7	$ ROLL MINUS 7.7 DEG	533C	
244	20	36	30.0	8	3.0	$ PITCH - 3.0 DEG	534C	
244	20	59	26.0	9	4.5	$ YAW -4.5 DEG	535C	
245	05	20	49.0	7	6.0	$ ROLL-6DEG UPDATE ANTENNA TEST	536C	
245	05	23	33.0	9	10.0	$ YAW-10DEG UPDATE ANTENNA TEST	537C	
245	12	22	14.3	8	4.0	$ PITCH -4.0 DEG	538C	
245	15	49	33.6	8	6.5	$ PTICH -6.5 WRONG COMMAND	539C	
245	15	54	49.6	9	10.1	$ YAW -10.1 DEG	540C	
245	17	08	59.8	8	6.4	$ PITCH 6.4 DEG	541C	
245	17	12	0.6	7	5.0	$ ROLL 5.0 DEG	542C	
246	00	08	28.0	9	8.0	$ YAW -8.0 DEG	543C	
246	02	12	30.0	8	3.0	$ PITCH -3.0 DEG	544C	
246	02	16	29.0	7	7.7	$ ROLL -7.7 DEG	545C	
246	05	38	28.0	9	10.0	$ YAW -10.0 DEG	546C	
246	14	38	30.0	7	6.5	$ ROLL -6.5 DEGREES UPDATE	547C	
246	14	41	29.0	8	4.0	$ PITCH -4.0 DEGREES UPDATE	548C	
246	14	44	50.0	9	8.5	$ YAW -8.5 DEGREES UPDATE	549C	
247	02	14	31.0	7	8.0	$ ROLL NEG 8.0 UPDATE	550C	
247	02	17	29.0	8	3.0	$ PITCH NEG 3.0 UPDATE	551C	

TABLE 3.1-8: CONTINUED

GMT				ANGLE		EVENT	
247	02	20	27.0	9	[illegible] Deg.	$ YAW NEG 8.8 UPDATE	552C
247	07	23	21.0	9	6.0	$ YAW NEG 6.0 UPDATE	553C
247	12	35	29.0	9	10.5	$ YAW NEG 10.5 UPDATE	554C
247	15	54	01.0	8	4.0	$ PITCH -4.0 DEG	555C
247	17	22	17.0	8	3.0	$ PITCH +3.0 DEG	556C
247	19	40	46.7	7	7.5	$ ROLL -7.5 DEG	557C
[illegible]	00	36	22.0	9	8.0	$ YAW-8.0 NEG UPDATE	558C
[illegible]	02	20	30.0	8	3.5	$ PITCH NEG 3.5 UPDATE	559C
248	09	13	27.0	7	6.7	$ ROLL NEG 6.7 UPDATE	560C
248	09	17	29.0	9	10.6	$ YAW NEG 10.6 UPDATE	561C
248	10	42	16.0	8	3.0	$ PITCH NEG 3.0 THERMAL	562C
248	14	19	12.0	9	6.0	$ YAW NEG 6.0	563C
248	19	56	10.0	7	5.5	$ ROLL -5.5 DEG	564C
248	19	57	49.0	9	6.3	$ YAW -6.3 DEG	565C
[illegible]	19	59	23.0	8	2.0	$ PITCH -2.0 DEG	566C
249	02	23	21.6	9	7.3	$ YAW -7.3 DEG	567C
249	05	48	29.9	8	2.8	$ PITCH -2.8 DEG	568C
249	09	14	27.0	7	8.5	$ ROLL NEG 8.5	569C
249	09	34	28.0	9	8.3	$ YAW NEG 8.3	570C
249	16	04	43.0	8	2.1	$ PITCH NEG 2.1	571C
249	22	55	24.6	8	1.3	$ PITCH -1.3 DEG	572C
249	23	01	3.9	9	15.8	$ YAW -15.8 DEG	573C
249	23	22	57.9	7	4.7	$ ROLL -4.7 DEG	574C
250	05	56	28.0	8	3.10	$ PITCH -3.10 DEG	575C
250	07	40	29.0	8	5.85	$ PITCH -5.85 DEG	576C
250	09	22	28.0	9	10.00	$ YAW -10.00 DEG	577C
250	09	44	27.0	7	7.75	$ ROLL -7.75 DEG	578C
250	23	07	30.0	8	2.7	$ PITCH NEG 2.7	5579C
250	23	11	25.0	7	5.8	$ ROLL NEG 5.8	580C
250	23	19	29.0	9	11.7	$ YAW NEG 11.7	581C
251	09	44	44.0	7	6.80	$ ROLL NEG 6.8	582C
251	09	54	46.0	9	10.20	$ YAW NEG 10.2	583C
251	12	56	27.0	8	8.60	$ PITCH NEG 8.6	584C

TABLE 3.1-8: CONTINUED

GMT					ANGLE	EVENT		
251	16	12	27.0	7	3.75 Deg	$ ROLL NEG 3.75	585C	
251	16	16	31.0	9	7.0	$ YAW NEG 7.0	586C	
252	06	00	23.9	7	7.2	$ ROLL NEG 7.2	587C	
252	06	06	38.6	9	12.8	$ YAW NEG 12.8	588C	
252	06	19	35.9	8	6.2	$ PITCH NEG 6.2	589C	
252	16	50	31.0	9	13.0	$ YAW NEG 13.0	590C	
252	19	47	31.0	7	7.9	$ ROLL MINUS 7.9 DEGREES	591C	
253	06	10	22.9	7	5.3	$ ROLL -5.3 DEG	592C	
253	06	13	3.9	9	11.0	$ YAW -11.0 DEG	593C	
253	07	42	32.9	8	4.6	$ PITCH -4.6 DEG	594C	
253	16	50	28.0	9	18.0	$ YAW NEG 18.0	595C	
253	20	06	29.0	7	8.3	$ ROLL NEG 8.3	596C	
254	03	31	23.0	8	7.0	$PITCH NEG 7.0DEG	597C	
254	06	30	29.0	7	353.8	$ROLL PLUS 353.8DEG	598C	Star Map Roll Update
254	13	45	30.0	9	13.8	$ YAW NEG 13.8	599C	
254	16	36	38.0	12	0.0	$ SUNRISE ASU	600C	Star Map
254	16	38	56.0	13	0.0	$ SUNSET REAL SUNSET	601C	Star Map
254	16	44	27.0	7	360.0	$ ROLL PLUS 360.0	602C	Star Map
254	16	59	14.0	8	30.0	$ PITCH NEG 30.0	603C	Star Map
254	17	12	32.0	7	5.0	$ ROLL NEG 5.0	604C	Star Map
254	20	11	55.0	9	8.55	$ YAW NEG 8.55	605C	
255	00	02	05.0	7	5.2	$ ROLL NEG 5.2	606C	
255	03	10	28.0	8	3.4	$ PITCH NEG 3.4	607C	
255	06	40	30.0	9	14.5	$ YAW NEG 14.5 DEG	608C	
255	09	48	11.0	8	3.6	$ PITCH NEG 3.6 DEG	609C	
255	13	14	59.0	7	6.4	$ ROLL NEG 6.4 DEG	610C	
255	16	41	39.0	9	7.0	$ YAW NEG 7.0	611C	
255	20	20	27.0	7	5.0	$ ROLL NEG 5.0	612C	
256	00	00	29.0	9	7.2	$ YAW NEG 7.2	613C	
256	00	04	26.0	8	4.3	$ PITCH NEG 4.3	614C	
256	03	20	27.0	9	4.1	$ YAW NEG 4.1	615C	
256	06	45	27.0	9	10.0	$ YAW NEG 10.0	616C	
256	13	25	25.0	7	8.5	$ ROLL NEG 8.5	617C	

TABLE 3.1-8: CONTINUED

	GMT				ANGLE	EVENT		
256	16	44	50.0	8	5.0 Deg	$ PITCH -5.0 DEG	618C	
256	16	59	42.0	9	8.0	$ YAW -8.0 DEG	619C	
257	00	00	29.0	7	6.3	$ ROLL -6.3 DEG	620C	
257	05	53	11.0	8	10.0	$ PITCH -10.0	621C	
257	10	20	0.0	9	7.5	$ YAW MINUS 7.5 DEGREES	622C	
257	12	13	26.0	7	1.75	$ ROLL MINUS 1.75 DEGREES	623C	
257	13	35	46.0	7	167.8	$ ROLL PLUS 167.8 DEGREES	624C	
257	13	45	24.0	9	14.0	$ YAW PLUS 14.0 DEGREES	625C	
257	13	48	28.0	7	360.0	$ ROLL PLUS 360.0 DEGREES	626C	
257	14	03	25.0	9	14.0	$ YAW MINUS 14.0 DEGREES	627C	
257	14	05	30.0	7	193.17	$ ROLL PLUS 193.17 DEGREES	628C	
257	14	17	25.0	8	30.0	$ PITCH MINUS 30 DEGREES	629C	
257	16	43	32.8	9	8.2	$ YAW -8.2 DEG	360C	
257	17	04	42.9	7	6.0	$ ROLL -6.0 DEG	631C	
257	20	23	35.0	3	4.5	$ PITCH -4.5 DEG	632C	
257	20	26	36.2	7	10.4	$ ROLL -10.4 DEG	633C	
257	20	29	31.5	9	10.5	$ YAW -10.5 DEG	634C	
258	16	30	27.0	9	7.0	$ YAW -7.0 DEG	635C	
258	16	42	47.0	12	0.0	$ ACQUIRE SUN	636C	
258	16	55	27.0	13	0.0	$ SUNSET	637C	
258	17	44	13.0	12	0.0	$ ACQUIRE SUN	638C	
258	17	47	0.0	2	0.0	$ OPEN DEADBAND	639C	
258	17	48	26.0	7	360.0	$ ROLL +360 DEG	640C	1ST BOS Test
258	19	50	30.0	8	40.0	$ PITCH -40 DEG	641C	
258	20	14	22.0	8	40.0	$ PITCH +40 DEG	642C	
258	20	17	26.0	12	0.0	$ ACQUIRE SUN	643C	
258	21	21	10.0	7	360.0	$ ROLL +360 DEG	644C	2nd BOS Test
258	20	21	39.0	13	0.0	$ SUNSET	645C	
258	22	22	28.0	8	40.0	$ PITCH -40.0 DEG	646C	Set Up for Overnight Drift
258	22	25	29.0	7	11.0	$ ROLL -11.0 DEG	647C	

TABLE 3.1-8: CONTINUED

GMT				ANGLE		EVENT		
258	22	28	24.0	9	17.4 Deg	S YAW -17.4 DEG	648C	Setup for Overnight Drift
259	16	30	28.0	8	95.0	$ PITCH -95 DEG GLINT TEST	649C	Glint Test
259	16	36	34.0	7	360.0	S ROLL +360.0 DEG	650C	
259	16	50	27.0	8	80.0	S PITCH +80.0 DEG	651C	
259	17	05	29.0	7	100.0	S ROLL -100 DEG	652C	
259	17	50	22.0	7	100.0	S ROLL +100 DEG	653C	
259	18	00	0.0	8	30.0	S PITCH -30 DEG	654C	
259	19	21	21.0	9	8.0	$ YAW -8 DEG	655C	

000656

TABLE 3.1-8: CONTINUED

3.1.4.2.2 Detailed Performance Description

Major Attitude Maneuvers

A description of major attitude maneuvers as they occurred throughout the cislunar and lunar phases of the mission follows:

EVENT	GMT
Launch During the launch and boost phases of flight the ACS had power applied to components but, in general, the subsystem remained dormant until after injection into the cislunar phase.	222:19:26:00
Fired N2 system squibs This energized the reaction control system.	222:20:10:07.4
Sun acquisition complete Sun acquisition was first completed in yaw and then in pitch. The Sun was completely acquired before the backup roll maneuver was started.	222:20:22:03
Roll + 360 degrees This roll is part of the Sun acquisition sequence.	222:20:26:53
Fine Sun sensors turned on and open deadband	222:20:53:22
Coarse Sun sensors turned off	222:20:54:13
GYRO DRIFT TEST	
Pitch + 0.011 degree Switched pitch and yaw gyros to inertial hold for a drift test.	222:21:45:56
Acquire Sun End of pitch and yaw drift test.	223:01:49:24
CANOPUS ACQUISITION	
Canopus tracker on	223:02:14:57
Roll 360 degrees First star map maneuver. Could not locate Canopus due to glint problem. Refer to Appendix D for a complete analysis of this problem.	223:02:21:52
Roll 360 degrees	223:06:01:46
SECOND STAR MAP MANEUVER	
Roll + 360 degrees Star map maneuver number two. An antenna signal strength map was made during this maneuver also.	223:10:17:49.8

EVENT	GMT
Yaw + 95 degrees This maneuver was performed to put the low-gain antenna in the shadow of the spacecraft to determine if reflections off the antenna were the cause of the glint problem. The maneuver was unsuccessful because the antenna was not shaded by the spacecraft without an additional roll maneuver. Consequently the results of this test were inconclusive.	223:10:48:22
Yaw - 95 degrees Return to the Sun	223:10:54:53
Acquire the Sun	223:10:59:07
MOON ACQUISITION	
Roll + 27.4 degrees to vicinity of the Moon Try to acquire the Moon to use as a reference for the first midcourse.	223:14:26:28
Roll - 2 degrees	223:14:42:24.2
Roll - 1 degree Above maneuvers performed to reduce the Canopus tracker roll error (AG09) below telemetry saturation.	223:14:52:09.2
"Canopus recognition simulator" and "acquire Canopus plus" commands sent. The "acquire Canopus" command was requested but the "acquire Canopus plus" command was erroneously transmitted and executed. With the Canopus recognition simulator turned on, the programmer logic will not execute the slew command or gyro switching command as a result of the acquire Canopus command. Therefore, nothing happened. The correct sequence was then transmitted and proper acquisition was accomplished.	223:15:09:00
Acquire Canopus	223:15:09:00
Canopus recognition simulator on	223:15:15:00
Acquire the Moon Both acquire Canopus (ACA) and Canopus recognition simulator on (CRS) were required to acquire the Moon. Brightness of the Moon was above the Canopus upper tracker gate so that the tracker did not execute the Canopus presence signal.	223:16:15:32.2
Roll + 93.0 degrees to vicinity of Canopus Maneuver away from the Moon of the vicinity of Canopus so the tracker would not be permanently degraded due to looking at the bright Moon.	223:16:48:05.7

EVENT	GMT
FIRST MIDCOURSE	
Roll - 95.0 degrees to vicinity of Moon	223:23:00:30.4
Acquire the Moon	223:23:15:38
Roll + 73.35 degrees for first midcourse	223:23:23:18
Pitch - 25.24 degrees for first midcourse	223:23:49:25
Velocity burn of 124.0 feet/second	224:00:00:18.3
Pitch + 25.24 degrees from first midcourse	224:00:02:45.4
Roll - 73.35 degrees from first midcourse	224:00:04:32.6
Reacquire Sun The above eight maneuvers were done for first midcourse. At the completion of the sequence, the Canopus tracker was looking at the Moon again. To minimize the time the tracker was looking at the Moon, a roll maneuver to the vicinity of Canopus was made.	224:00:07:16.1
Roll + 85.9 degrees to vicinity of Canopus	224:00:14:00
FIRST THERMAL MANEUVER	
Pitch - 36.0 degrees from the Sun Thermal constraint	224:01:33:52.5
Pitch + 36.0 degrees to the Sun	224:09:46:09
Acquire Sun	224:09:52:46
Pitch - 36.0 degrees from the Sun Thermal constraint	224:14:51:48
Pitch + 36.0 degrees to the Sun	225:02:34:33
Acquire Sun	225:02:40:18
CANOPUS TRACKER DIAGNOSTIC	
Roll + 90 degrees Set up spacecraft for a roll of 360 degrees by Canopus.	225:03:03:29.5
Roll + 360 degrees for antenna map. This maneuver was made to make an antenna signal strength map to locate Canopus. The Moon was still within view of tracker and the antenna signal strength agreed with Moon reference within 1 degree. The star map remained undefined due to the glint problem.	225:03:12:34
Roll - 104 degrees to approximately - 20 degrees from Canopus.	225:05:34:38

EVENT	GMT
Open the deadband	225:05:48:23
Roll + 40.0 degrees The above three maneuvers were performed so the spacecraft would roll by Canopus at a low rate (0.05 degree per second) to determine if the tracker would lock on Canopus at the low angular rate. The Canopus tracker failed to lock on as the spacecraft maneuvered at 0.051 degree per second by Canopus.	225:05:55:20
Close deadband	225:07:16:01
Yaw - 38 degrees to close the tracker Sun shutter. This maneuver was made to close the bright-object sensor on the Canopus tracker to determine if glint was the reason for the problem or whether the tracker electronics had failed. The test gave conclusive results that the tracker was performing normally and the problem was caused by glint.	225:07:35:59
Yaw + 38 degrees to the Sun	225:10:43:23
Acquire the Sun	225:10:51:03
Roll + 20 degrees to vicinity of Canopus	225:11:07:34
Canopus tracker off	225:11:12:29
Canopus tracker on	225:11:22:33
Roll + 4.2 degrees	225:11:27:32
Canopus tracker off	225:11:32:29
Canopus tracker on	225:11:42:31
Roll - 8.4 degrees	225:11:47:07
Canopus tracker off	225:11:52:07
Canopus tracker on	225:12:02:29
Roll - 4.2 degrees	225:12:37:25
Canopus tracker off	225:13:14:40
Canopus tracker on The above twelve commands were performed to search for Canopus. The tracker was turned off, then on again to determine if it would lock on and track Canopus if the star was within the field of view of the tracker when it was turned on. The method was successful and the tracker did lock onto Canopus with the last command.	225:13:19:40
Acquired Canopus	225:13:47:42.2

EVENT	GMT
Roll + 0.011 degree Put roll axis in inertial hold.	225:14:45:45
Acquired Canopus	225:20:00:34
Roll + 0.011 degree Put roll axis in inertial hold.	225:20:12:51
Yaw - 11.2 degrees	225:20:23:24
Pitch - 36.0 degrees The spacecraft was yawed -11 degrees to align the +y axis of the spacecraft with Canopus. The maneuver was performed so the spacecraft could be pitched away from the Sun without pulling Canopus from the field of view of the tracker. The scheme failed, however, because the tracker bright-object sensor closed.	225:20:49:20
Pitch + 36 degrees to the Sun	225:23:42:31
Yaw + 11.2 degrees to the Sun	225:23:55:34
Acquire the Sun	226:00:13:37
Tracker off	226:00:25:31
Tracker on	226:00:30:31
Acquire Canopus	226:00:49:43
Roll + 0.011 degree Put roll axis in inertial hold.	226:01:10:50
Pitch - 36.0 degrees	226:02:18:45
Pitch + 36.0 degrees	226:09:35:09
Acquire the Sun	226:09:37:20
Roll - 2.3 degrees This was a roll update maneuver.	226:13:22:28
First Sunset	226:15:22:56
LUNAR ORBITER INJECTION	
Roll + 19.2 degrees for injection	226:15:28:18
Pitch - 108 degrees for injection	226:15:29:50
Velocity change of 2591 feet per second	226:15:44:03
Pitch + 108.0 degrees	226:15:46:12
Roll - 19.2 degrees	226:15:50:35

EVENT	GMT
ROLL UPDATE SEQUENCES	
Roll - 39.2	227:16:35:30
Roll + 27.8	227:20:29:25
Roll + 5.2	228:00:00:31
Roll - 6.4	228:14:47:59
After injection, roll attitude was obtained by turning on the star tracker during Sunset to determine spacecraft roll error. The first maneuver was made to roll the spacecraft to the negative side of Canopus so the roll error would be within the tracker field of view just prior to the next required maneuver sequence.	
Subsequently, it was decided that the roll error would be updated such that Canopus remained within the ± 4.1-degree field of view. Gyro drift was very predictable throughout the flight, making this procedure operable. Because of predictable gyro drift, the spacecraft attitude could be predicted hours into the future.	
Roll + 353.7 degrees	229:05:00:28
A star map maneuver was made during a roll update. A check of maneuver accuracy was also made. Refer to the section on closed-loop electronics for analysis of maneuver accuracy.	
HIGH-ORBIT SITE I-0 PHOTO MANEUVERS*	
Roll + 3.6 degrees	230:14:37:40
Yaw + 12.4 degrees	230:14:38:44
Pitch - 8.1 degrees	230:14:40:02
Pitch + 8.1 degrees	230:14:48:05
Yaw - 12.5 degrees	230:14:49:13
Roll - 3.6 degrees	230:14:50:34
*This is a typical maneuver sequence for photo maneuvers. See the sequence of events for the other photo maneuvers.	
ORBIT TRANSFER	
Roll + 43.4 degrees	233:09:41:58
Pitch + 25.3 degrees	233:09:44:16
Open deadband	233:09:49:58
Velocity change of 131.9 feet per second	233:09:50:01
Close deadband	233:09:52:19

EVENT	GMT
Pitch - 25.3 degrees	233:09:53:10
Roll - 43.4 degrees	233:09:54:52
Acquire the Sun	233:09:57:11

The above maneuver sequence was used to change the orbit of the orbiter to an orbit low enough for the photographic mission.

PHOTO SEQUENCE

For the next several days maneuvers were made for photography. See Table 3.1-8 for a complete listing of these maneuvers.

ORBIT ADJUST

Roll + 0.011 degree	237:15:44:29.3
Roll + 34.2 degrees	237:15:45:20.5
Pitch - 129.7 degrees	237:15:47:23
Deadband opened	237:16:02:04.5
Engine burn for a velocity change of 17.7 feet per second	237:16:02:04.7
Deadband closed	237:16:02:06.9
Pitch + 129.7 degrees	237:16:03:59.2
Roll - 34.2 degrees	237:16:07:59.2
Roll + 0.011 degree	237:16:09:58.6

The above maneuvers were performed to execute an adjustment to the orbit. The +0.011-degree maneuvers were done before and after the orbit-adjust sequence because the flight programmer was programmed for a three-axis maneuver for Site I-5 photos and this was the easiest way of using the stored sequence. There was not enough time to change the map or enough room in the programmer to store both a three-axis maneuver and a two-axis maneuver.

During the burn sequence, a 51.2-second wait period was removed following the closure of deadbands after the burn to allow enough time to power down the spacecraft before Sunset.

PITCH AND YAW GYRO DRIFT TEST

Pitch 0.011 degree	238:14:24:33
Acquire Sun	238:16:33:35

EVENT	GMT
FIRED THE NITROGEN SQUIB	
Nitrogen squib fired Nitrogen was leaking slowly through the regulator in the velocity control system into the propellant tanks. When the pressure in these tanks exceeded 233 psia the relief valves began venting nitrogen overboard. At the above time the velocity control system was isolated by the squib and the leak disappeared.	239:05:48:00
PITCH OFF THE SUN	
Pitch + 16.0 degrees	239:09:54:01.0
Pitch + 11.3 degrees First a pitch maneuver of 16 degrees was executed and the spacecraft was still too hot so an additional 11.3-degree pitch maneuver was commanded.	239:14:26:39.0
STORED PROGRAM PITCH OFF THE SUN	
Pitch + 16.0 degrees This thermal maneuver was done through a stored program command because Earthset was occurring ahead of Sunset and a stored program command extended the time of pitchoff.	239:16:30:55
Pitch + 12.0 degrees The previous + 16.0-degree thermal maneuver was considered inadequate. A real-time command was transmitted to increase this angle to 28 degrees.	239:16:35:32
CONTINUOUS OFF-SUN OPERATION	
Coarse Sun sensors on	242:12:10:55
Fine Sun sensors off Began tests to devise a method for continuous off-Sun operation to provide thermal relief as well as antenna pointing for photo readout. Final decision was to operate off the Sun continuously with update maneuvers in all three axes when required. The coarse Sun sensors were used to monitor spacecraft orientation in pitch and yaw. The Canopus tracker was turned on during each Sun occultation period to determine roll attitude. As a result of this technique nitrogen consumption was minimized.	242:14:17:38
YAW SUN SENSOR EXPERIMENT	
Turned fine yaw sensors on	243:20:32:25
Fine yaw Sun sensors off	243:21:25:00

EVENT	GMT
Coarse yaw Sun sensors on	243:21:50:00
Fine yaw Sun sensors on	243:22:10:01
Fine yaw Sun sensors off Attempted to use the fine yaw Sun sensors to improve the resolution of yaw position determination while pitched off the Sun. Greater degradation of yaw sensor output with pitch angle than expected was noted and this scheme could not be employed.	244:01:30:24

Equipment Performance

Sun sensor—The Sun sensors for Mission I performed as expected. In addition they provided an accurate celestial reference for a variety of nonstandard situations. The capability of having fine or coarse, or both, sensor modes was invaluable and contributed greatly to the success of the mission.

The initial Sun acquisition took place automatically within 53 minutes after launch and within 10 minutes after separation, reaction control squib firing, and deployment. The maximum allowable time for Sun acquisition due to battery constraints was 1 hour after launch. During initial Sun acquisition, as soon as the telemetry data was good it was observed that the Sun had already been acquired in yaw. The Sun was then acquired in pitch and the telemetry data was good for this acquisition. Reacquisitions of the Sun after Sun occultation or attitude maneuvers were performed approximately 250 times, perfectly. Only one good value was obtainable from the data for the rate limit during acquisition. The rate observed was 0.575 degree per second and the design value was 0.60 ± 0.05 degree per second. An attempt was made to plot a phase plane for both acquisitions; however, due to the sampling once every 23 seconds and rate telemetry saturation at ± 0.01 degree per second, this was not possible.

The Sun sensor indicated deadbands were close to predicted values and to data obtained during air bearing tests. Deviations from symmetrical limit cycles were observed and were due to the following disturbances:

1) Gravity gradient;

2) Solar pressure on the high-gain antenna (caused yaw to move toward the negative switching line);

3) Cross coupling due to thruster misalignment.

These disturbance torques are covered in detail in a later section entitled "Disturbance Torques".

The Sun sensor readings while in the dark (Sun occultation) were determined to be very close to those observed during ground testing. These values were useful to obtain an estimate of the null shift in sensor position readings when viewing the Sun.

The coarse eyes proved to be extremely useful during photo readout as a means of conserving nitrogen since they provided a means by which orientation could be monitored without reacquiring the Sun on every orbit. In fact, by using the coarse eyes the Sun did not have to be acquired at all. By monitoring the coarse Sun sensors the orientation of pitch and yaw was known at all times. Later in the mission, when thermal problems required pitch angles in excess of pitch coarse Sun sensor telemetry saturation, an accurate knowledge of gyro drift, antenna signal strength, and solar array current was used to ascertain pitch orientation.

The reading of the Sun sensor telemetry was not as expected when the spacecraft was pitched and the pitch Sun sensor telemetry was not as expected when the spacecraft was yawed. For example, with the pitch attitude at 30 degrees, yaw Sun sensor indicated angle would be expected to be reduced by cos. 30 degrees or 0.866 because of the change in angle at which the Sun was striking the yaw Sun sensors. However, it was actually observed that yaw was reduced by 0.75. Thus, with a yaw of 10 degrees, the Sun sensor telemetry would indicate 7.5 degrees.

Canopus star tracker—The star tracker performed very well in the face of an extremely serious "glint" problem. The only anomaly in connection with the star tracker was the low map signal voltage sensitivity; this is described in detail in Appendix D of this report. During Sunset phases of the lunar orbit the star tracker operated perfectly.

The accuracy of the roll error signal sensitivity AG09 was within ± 0.05 degree for the 6.0- to 8.0-degree roll update maneuvers. Based on several careful checks during the mission no detectable error was noted within the resolution of the telemetry, which is on the order of ± 0.04 degree. Bias offset could not be evaluated.

The bright-object sensor operated as expected. It actuated at 77.1, 72.9, 76.6, and 77.2 (±0.7) degrees from the Sunline in yaw. During the second glint test the tracker actuated at ± 86.4 degrees from the Sunline in roll.

The tracking mode switch and the Canopus presence signal gates worked as expected. Tracking mode was actuated at about 0.74-volt map signal. The lower Canopus presence gate was at 1.14 volts. The upper Canopus presence gate was actuated at 3.8 volts.

Time and cycle data on the tracker, reconstructed after the mission, showed that the tracker was turned on and off 133 times. The tracker was on for 68 hours.

During the several mapping runs several stars, listed in Table 3.1-9, were observed. Generally speaking, the values indicated in this table show the right relationship to one another, except for the first readings on stars 6 and 8.

Inertial reference unit—The IRU performed satisfactorily throughout the mission, accumulating approximately 820 hours of on-time from launch to the end of readout. The parameters that could be observed or computed from telemetry data were nominal with two exceptions -- yaw gyro drift, and yaw gyro wheel current.

Table 3.1-9: Star Mapping Data

SIDL IDENTIFICATION	NAME	RIGHT ASCENSION (HR:MIN)	DECLINATION (DEG:MIN)	SIDL CANOPUS RATIO	MAP SIGNAL (VOLTS)
1	α Canis Majoris (Sirius)	6:43.0	-16:40	2.33	3.45, 3.70
2	α Carinae (Canopus)	6:22.8	-52:40	1.0	1.5, 1.7, 1.75, 1.75
3	α Lyrae (Vega)	18:35.1	+38:45	0.44	1.15
4	β Orionis (Rigel)	5:12.1	- 8:16	0.41	1.08
6	β Centauri (Hadar)	14:0.3	-60:08	0.45	0.80, 1.30
7	α Centauri (Rigel Kentauris)	14:36.2	-60:37	0.53	1.20
8	α Crucis (Acrux)	12:23.9	-62:50	0.38	0.74, 1.25
10	α Canis Minoris (Procyon)	7:36.7	+ 5:21	0.26	1.00
11	α Aurigae (Capella)	5:12.9	+45:57	0.35	0.93, 1.00 0.95
13	β Crucis (Mimosa)	12:44.8	-59:25	0.16	0.80
17	ε Canis Majoris (Adhara)	6:56.7	-28:54	0.13	0.70
53	α Orionis (Betelgeuse)	5:52.5	+ 7:24	0.21	0.95, 0.90
84	α Scorpii (Antares)	+16:26.3	-26:20	0.13	0.93
502	Jupiter	--	--	1.45	3.80

Rate mode accuracy—Using data on +360-degree-roll maneuvers for which initial and final star tracker position signals were available, it was found that a 360-degree-roll command actually resulted in a maneuver of +360.4 degrees. Of the 0.4-degree error, approximately 0.1 degree was from drift. The remaining 0.3 degree distributed over the total maneuver resulted in a total system roll rate mode flight control error of 0.08%, well within the component tolerances of 0.1% for the gyro and 0.1% for the velocity/frequency converter. Pitch and yaw axes maneuver accuracies were not available from data on this mission.

Gyro rate-integrate mode accuracy—A measure of rate-integrate mode scaling accuracy is not possible from spacecraft telemetry data. One method of generating some confidence in the rate-integrate mode accuracy is by comparing the celestial sensor error to the gyro position error. The gyro and Sun sensor outputs agree within a closer tolerance than the Sun sensor telemetry resolution (0.05 degree).

Gyro drift—Gyro drift calculations were taken from the spacecraft maneuver and position history graphs, except for a few points early in the mission. Because the spacecraft was operated off the Sunline throughout most of the mission, the indicated pitch and yaw attitude differed from the true attitude. The following procedure was used to calculate drifts. The maneuver magnitude was assumed to be correct. The drift interval was taken over two to three orbits. The interval was selected so that no maneuvers were performed during the interval in any axis. A further restriction imposed on the drift interval solution was performed just prior to or just after the interval so that the scale factor based on maneuver magnitude could be used as a correction to the indicated drift. Following is the equation used to determine drift rates.

$$\text{drift} = \left(\frac{\Delta \text{ indicated angle}}{\Delta \text{ time}}\right)\left(\frac{\text{commanded maneuver angle}}{\text{indicated maneuver magnitude}}\right)$$

The design drift tolerance originally was ±0.3 degree per hour, but was relaxed to 0.5 degree per hour. The mission drift tolerance was ±1.0 degree per hour. Both the pitch and roll gyro drift rates were less than the design tolerance. The yaw gyro drift rate exceeded mission and design tolerances but caused no serious operating problems (the selected tolerances were more stringent than required).

A slight drift rate increase -- less than 0.1 degree per hour per 30 days -- occurred in the roll gyro. Near the end of the regular mission the roll drift rate reached the design tolerance of 0.5 degree per hour.

The yaw gyro drift rate increased about 0.4 degree per hour during the mission. The drift rate at the end of the regular mission was between 1.3 and 1.4 degrees per hour.

The pitch gyro drift rate increased during the first part of the mission. There was an apparent decrease in the drift rate after Day 245. Because the Sun sensors were being operated in the coarse mode with the spacecraft off the Sunline at a large angle during the latter part of the mission, the absolute drift rate value or the trend is questionable. Indirect measurements place the mission end drift rates at approximately 0.3 degree per hour.

Gyro wheel currents—There were no long-term changes in the gyro wheel current telemetry output. All three gyro wheel current measurements are affected by IRU temperature; therefore, long-term changes in wheel currents could be obscured by temperature changes and might not be detected.

On one occasion the yaw gyro wheel current jumped from 83.25 to 86.2 m.a. and gradually decreased to the original value. No conclusive explanation was found for this behavior but no serious results were apparent. Sperry has noted similar phenomena infrequently in ground testing and explain it as the result of lubricant motion in the bearings.

Accelerometer—The accelerometer was turned on at 222:12:03:14 GMT and remained on throughout the mission.

In all four velocity maneuvers the commanded and indicated ΔV were equal. Comparison of actual ΔV calculated from tracking data and indicated ΔV for the orbit injection maneuver shows agreement of these values within the resolution of the measurements.

Gyro temperature—The gyro temperature telemetry is a pseudotemperature output signal derived from the addition of error signals from the roll, pitch, and yaw gyro heater control circuits. This measurement is conventionally expressed in percent of full scale with 0 to 100% corresponding to the telemetry output range of 0 to 5 volts. An approximate correlation with temperature equates this to a range of 5° F centered at 145° F.

Behavior of gyro temperature, AT02, was consistent and, within the limits of test experience, predictable. All significant short- or long-term changes in AT02 were correlated with environmental changes as reflected by ST03 deck temperature and/or bus voltage, EE01.

Careful observation of gyro temperature was made as ST03 temperature ranged above 100° F to define the point at which the gyro heaters go full off in an effort to maintain thermal balance. This point is critical because thereafter the gyro temperature would be expected to increase 1:1 with deck temperature. To define with any confidence the points at which one or more gyro heater loops saturated appears too complex for the scope of this report: however, it is probable that at least two heaters lost control before AT02 saturated at 101.2%. Behavior of AT02, at the rates of ST03 increase experienced on this mission, provided warning of temperature problems well in advance of potentially harmful conditions.

Closed-loop electronics—The closed-loop electronics performed within design tolerances throughout the mission. The CLE successfully selected, on command from the programmer, the IRU, Sun sensors, and Canopus star tracker, closing the loop between sensor outputs and vehicle dynamics. The crab angle sensor was not used in conjunction with the ACS during the mission.

Rate limits during attitude maneuvers were well within the design tolerances of 0.5 ± 0.05 degree per second for all axes using the narrow (0.2 degree) deadband. Maneuvers were also performed in the wide (2 degree) deadband for the roll and pitch axes. Rates of approximately 0.047 to 0.051 degree per second were observed in the roll axis while rates of 0.036 to 0.059 degree per second were observed in the pitch axis. Rate fluctuations would be expected during the 0.05-degree-per-second maneuvers due to gravity gradient and torque due to solar pressure effects. These effects are not apparent for the 0.5-degree-per-second maneuvers due to the relatively short time intervals involved.

Observed attitude deadband accuracy was within one telemetry data count for the wide (±2.0 degrees) and narrow (±0.2 degree) deadbands. The data count resolutions for the attitude control sensors follow:

0.24 degree	Gyro Error Resolution
0.044 degree	Fine and Coarse Sun Sensor Resolution
0.050 degree	Fine Sun Sensor Resolution
0.299 degree	Coarse Sun Sensor Resolution
0.033 degree	Star Tracker Resolution

Narrow deadband was used throughout the mission except during a few isolated instances. The attitude control mission history in Table 3.1-8 contains these times.

The minimum pulse widths for the jets based on the "one shot" in the CLE varied between 0.011 and 0.012 second for all three axes. These values were possible in the inertial hold and gyro rate modes for both the 2.0- and 0.2-degree deadband. It appeared that 50% of the rate changes during the attitude hold mode for the mission were in the "single pulse" category. Pulsing refers to the number of times the thrusters open (or "pulse") when the spacecraft reached one edge of the deadband, i.e., single pulse or multiple pulses.

Compensation networks for the thrust vector control system and inertial reference unit appeared to perform correctly. The IRU compensation network (lead-lag) was used to obtain a "pseudo rate" whenever the gyros were in an inertial hold mode. Performance by this network was very similar to that obtained with the gyros in the rate mode. Gains and compensations associated with the TVC system are discussed in the following section.

Thrust vector control system—The thrust vector control system performed perfectly throughout the mission. Four successful engine burns were accomplished with burn times ranging from 3.0 to 579 seconds. (One additional burn occurred after the primary mission was complete). The thrust vector control system maintained stable operation throughout all the burns.

Because of the long telemetry sampling period, very little detail relative to stability and performance of the system is available. All of the available telemetry indicated that the system was stable at the completion of each engine burn. Based upon analog studies,

transient spacecraft rates at the end of burn were lower than predicted maxima. Transients after each burn are shown in Table 3.1-10.

Maximum engine misalignment with the center of gravity (c.g.) was in the pitch axis for first midcourse. The actuator was required to move the engine 0.4 degree to align with the c.g. System response for first midcourse is shown in Figure 3.1-30.

Pitch and yaw responses for the orbit injection burn are shown in Figures 3.1-31 and 3.1-32. Engine alignment with the c.g. after first midcourse was very good. Throughout the burn the average pitch actuator position had to increase another 0.3 degree to maintain c.g. alignment. Yaw actuator deflections were about 0.1 to 0.2 degree. The calculated d.c. actuator command (3.31 degrees actuator per degree gyro) is plotted with the actuator position. The actuator position and command signals agree very closely. The oscillation of actuator position as shown in Figures 3.1-32 and 3.1-33 was expected, since the actuators hunt or limit cycle with a peak-to-peak actuator motion. Residual spacecraft rates of the spacecraft after engine shutdown indicate that the magnitude of this limit cycle was within predictions.

Table 3.1-10: Spacecraft Residual and Transient Roll Rates

SPACECRAFT RESIDUAL RATES AFTER ENGINE BURNS		
MANEUVER	PITCH RATE (DEG/SEC)	YAW RATE (DEG/SEC)
First Midcourse	-0.003	-0.008
Orbit Injection	+0.032	-0.073
Orbit Transfer	-0.041	-0.008
Orbit Adjust	-0.023	-0.018
TRANSIENT ROLL RATES FROM THRUST VECTOR COUPLING		
MANEUVER	START TRANSIENT ROLL RATES (DEG/SEC)	STOP TRANSIENT ROLL RATES (DEG/SEC)
First Midcourse	-0.008	+0.012
Orbit Injection	-0.012	0
Orbit Transfer	-0.013	+0.007
Orbit Adjust	0	0

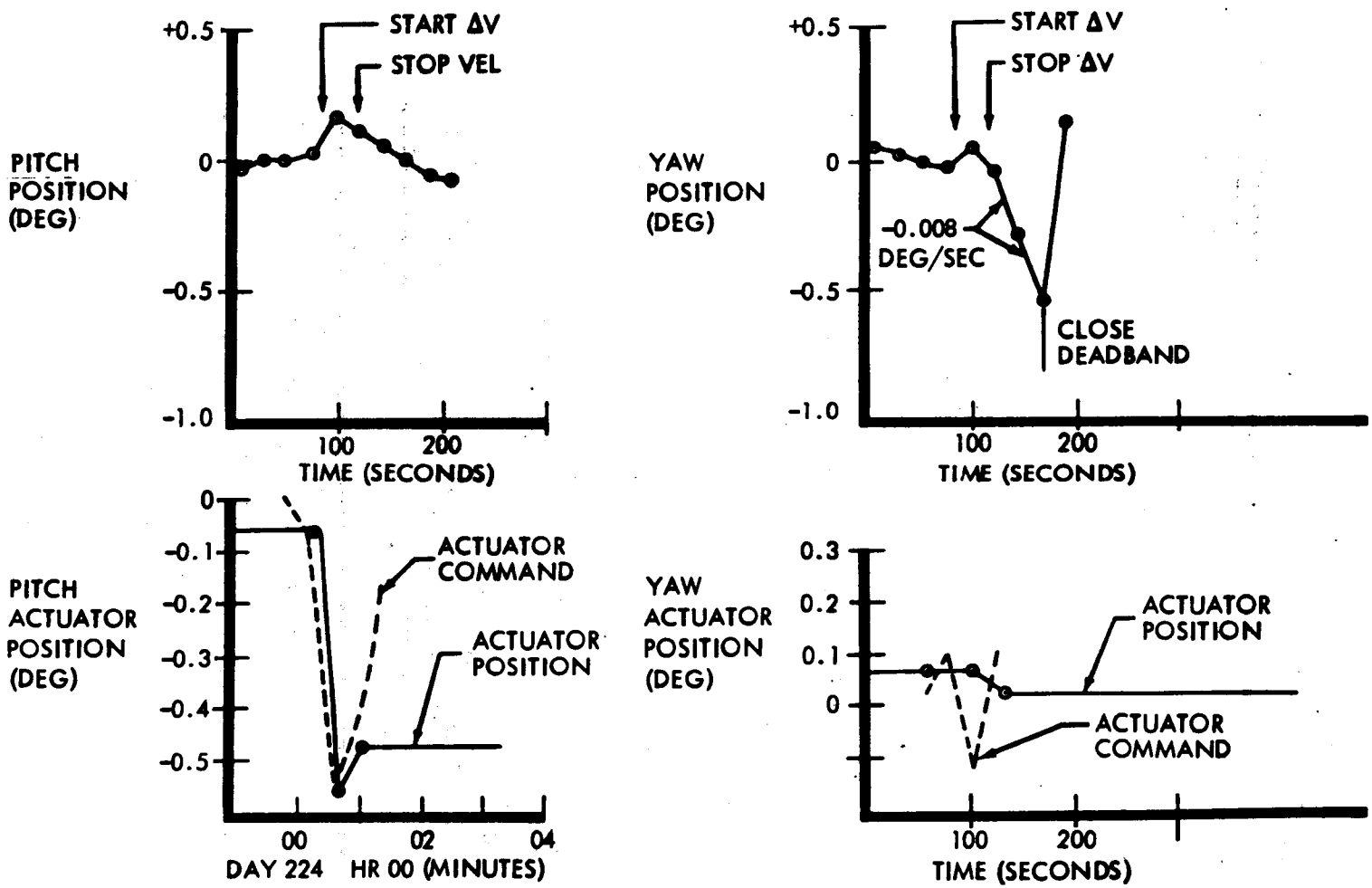

FIGURE 3.1-30: THRUST VECTOR CONTROL — FIRST MIDCOURSE

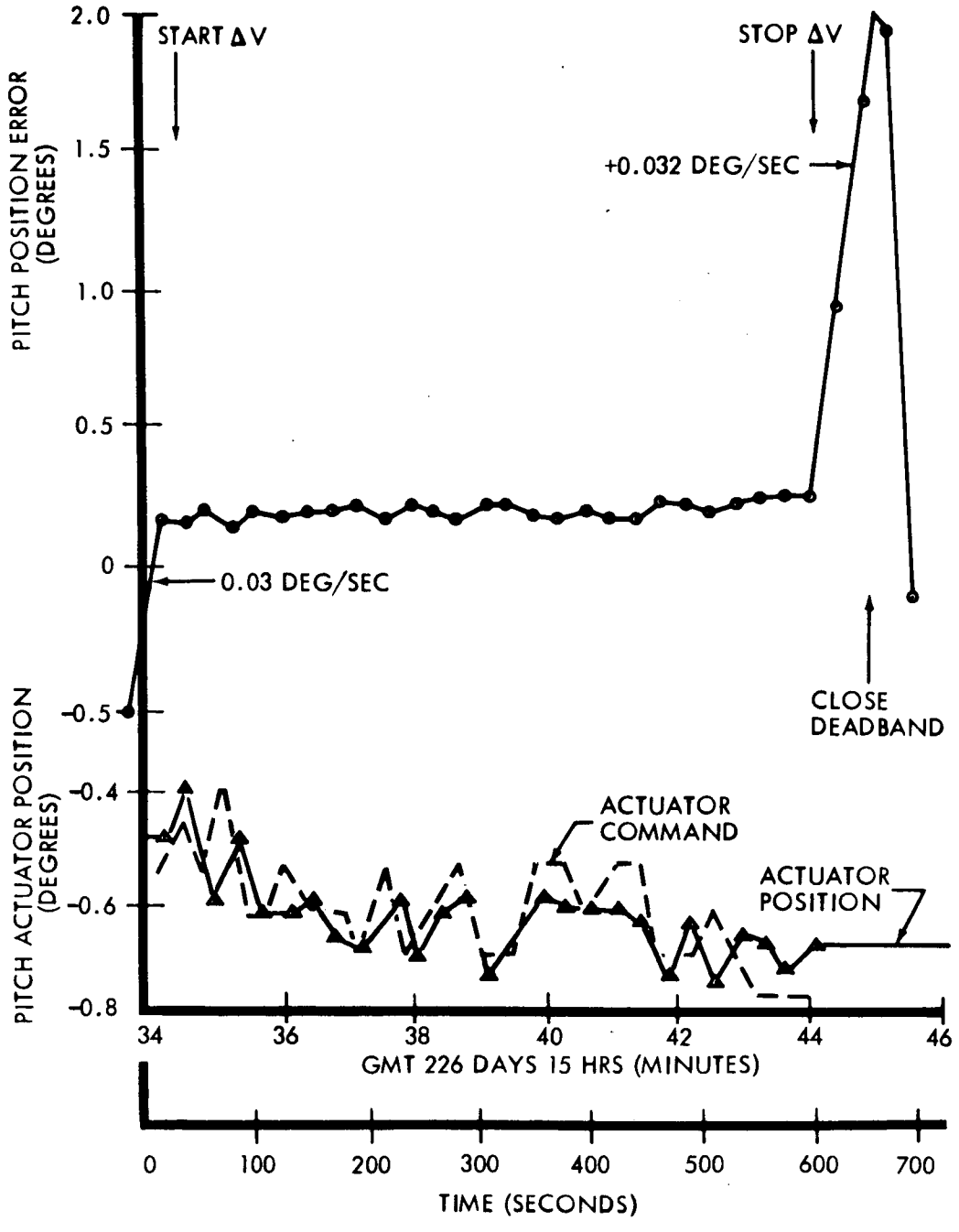

FIGURE 3.1-31: PITCH THRUST VECTOR CONTROL — ORBIT INJECTION

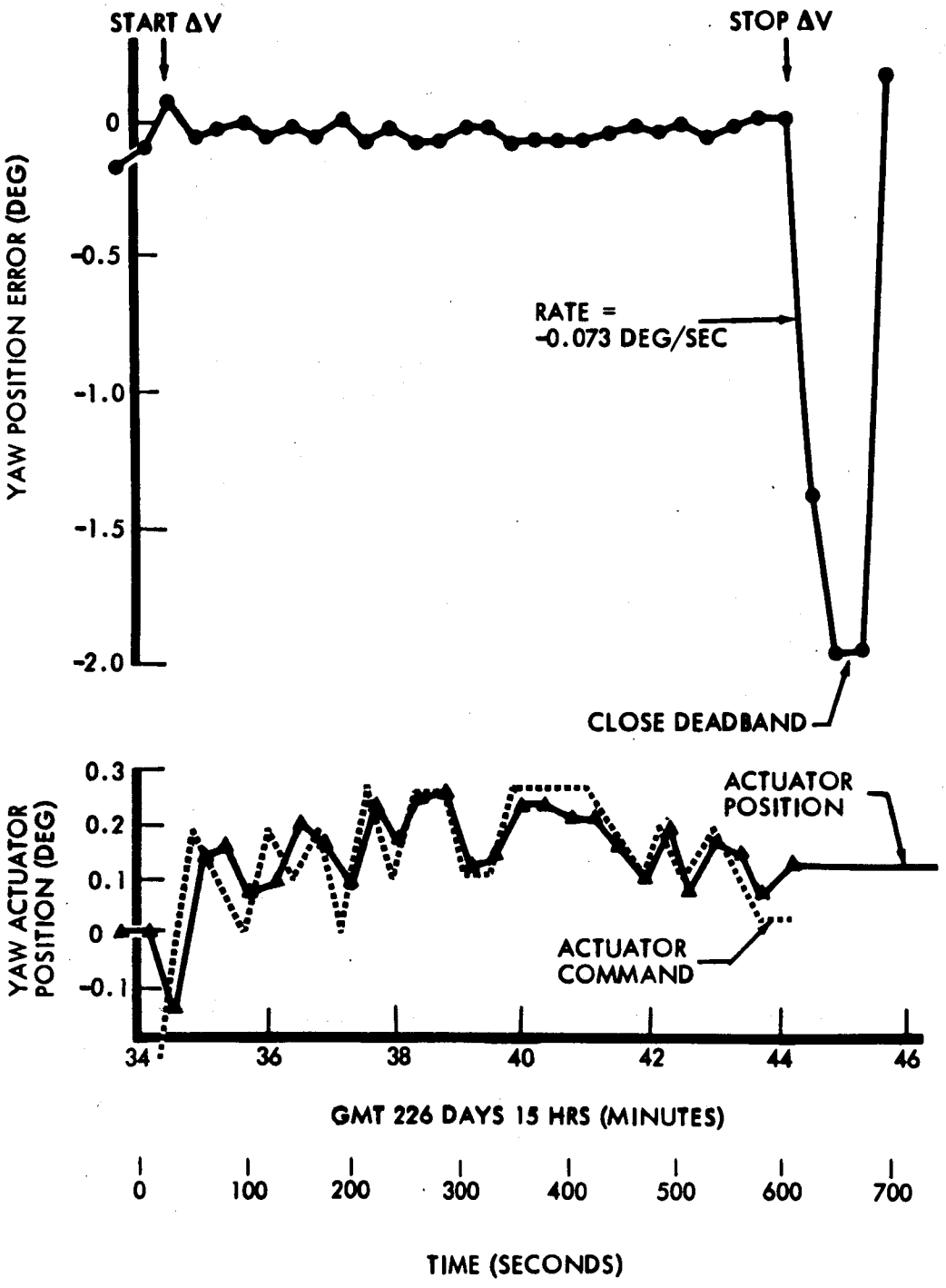

FIGURE 3.1-32: YAW THRUST VECTOR CONTROL — ORBIT INJECTION

The orbit transfer maneuver is shown in Figure 3.1-33. The larger actuator excursion in yaw during the burn may be due to sampling the actuator position during the initial transient. In this burn the shutdown rates of the spacecraft were quite small, indicating that the spacecraft was stabilized before engine shutdown.

Figure 3.1-34 shows the small orbit adjustment burn. This burn was short enough so that the spacecraft and actuators were probably in the startup transient at engine shutdown. Actuator excursions and spacecraft residual rates indicate that this transient was probably very stable. The yaw actuator was stopped in a transient state since it moved about 0.35 degree from its initial position.

Figures 3.1-35 and 3.1-36 show roll position during engine burns. Transient rates coupled into the roll axis due to engine operation were small in all cases. A summary of roll rate transients resulting from the engine operation is shown in Table 3.1-10.

All telemetry indications show that the thrust vector system performed as expected. The spacecraft remained quite stable for all four of the engine burns and the actuators responded as commanded.

Reaction control system—The reaction control system thrusters performed satisfactorily throughout the mission. The number of thruster operations, estimated by reviewing vehicle telemetry data for the primary mission, as tabulated below.

THRUSTER OPERATIONS

MODE	ROLL	PITCH	YAW	TOTAL
Limit Cycle	6,547	9,609	9,926	26,082
Maneuvers	298	294	156	748
Total	6,845	9,903	10,082	26,830

When the spacecraft drifted to the edge of the deadband, the reacting thruster(s) was actuated. A single pulse of the thruster jet or multiple pulses may occur; however, the estimate above is based upon one thruster operation each time the spacecraft drifted to the edge of a deadband.

Individual thruster performance was evaluated for a number of spacecraft maneuvers. The actual and predicted thrust values for each axis are tabulated below.

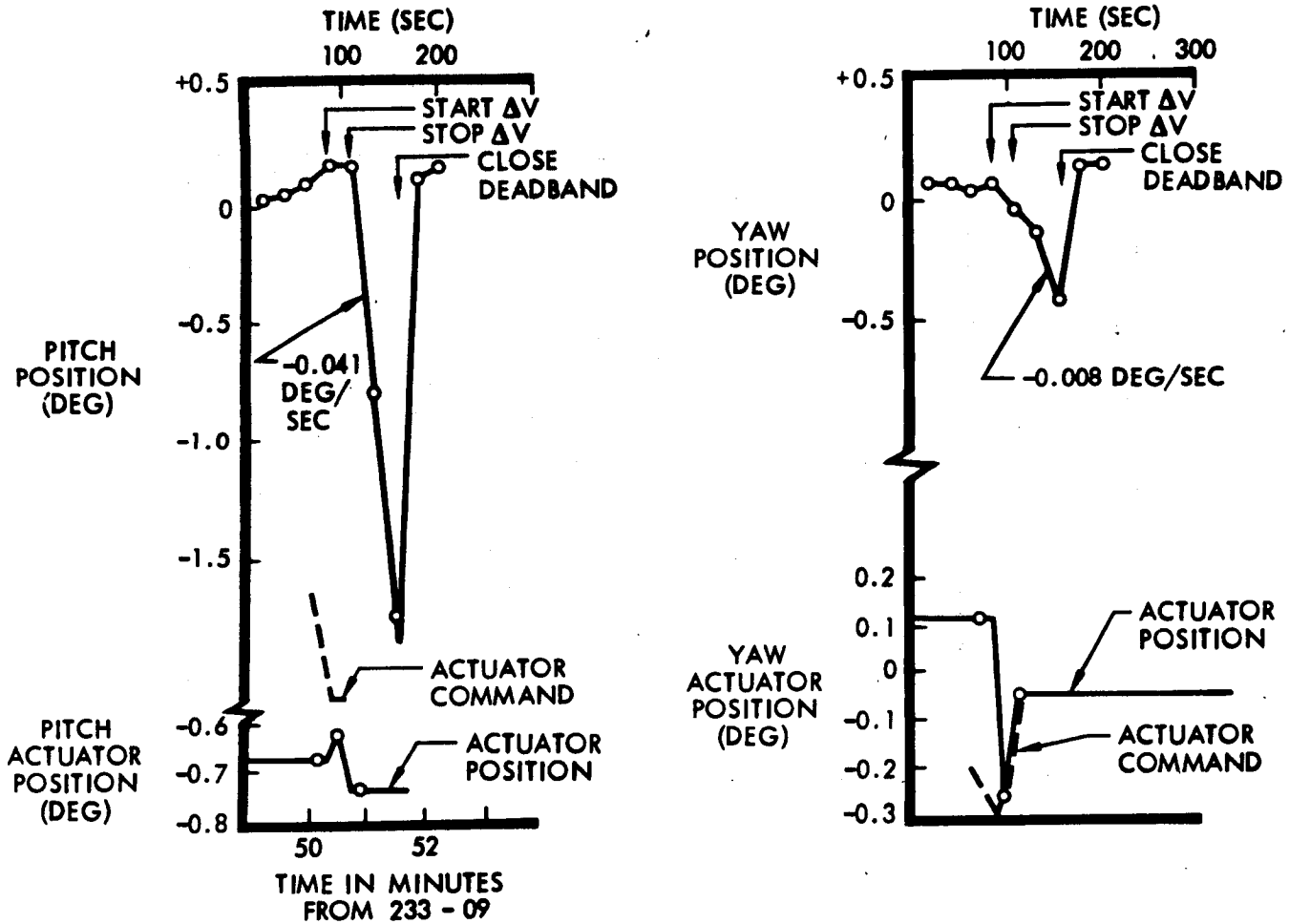

FIGURE 3.1-33: THRUST VECTOR CONTROL — ORBIT TRANSFER

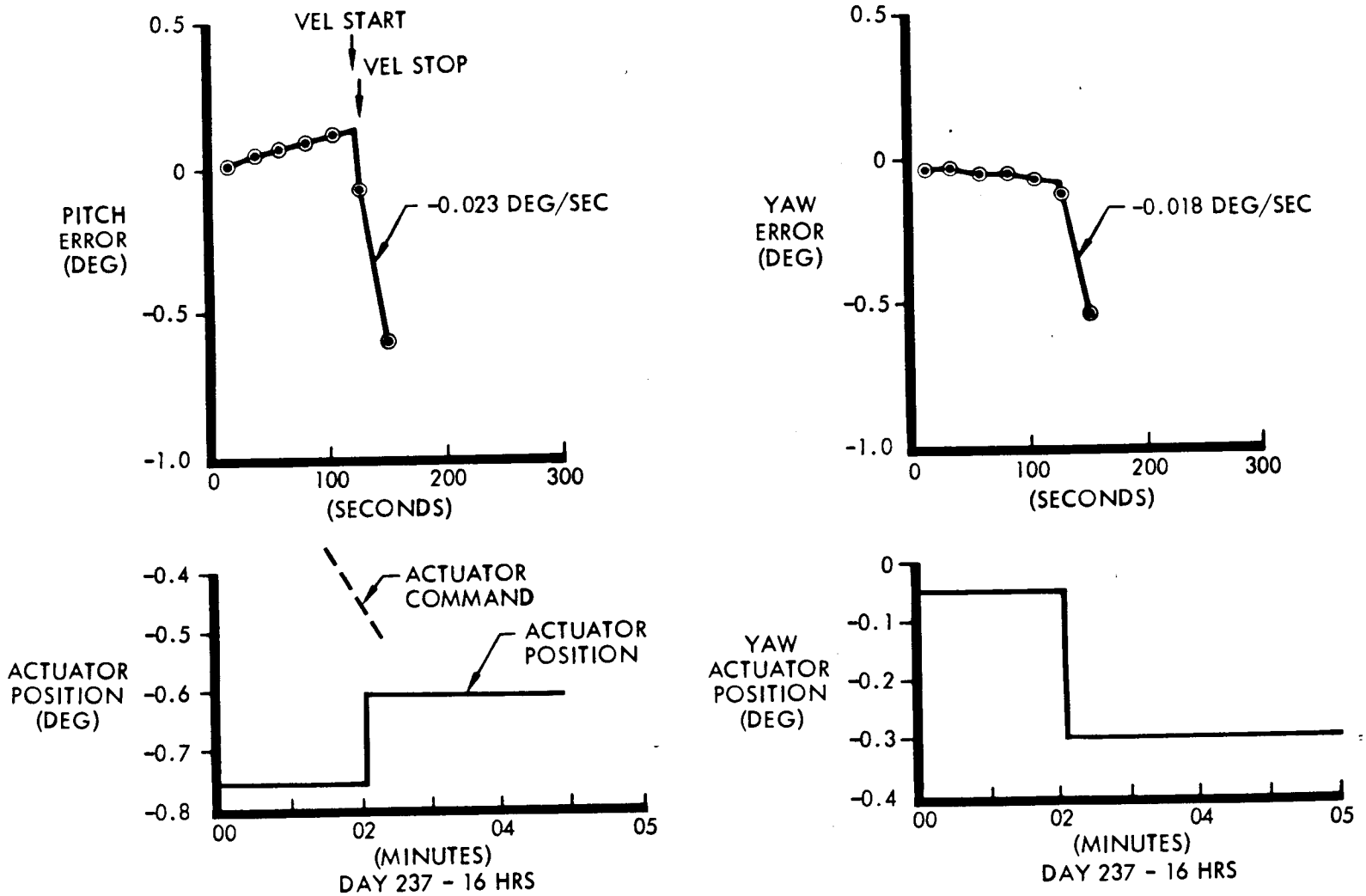

FIGURE 3.1-34: THRUST VECTOR CONTROL — ORBIT ADJUST

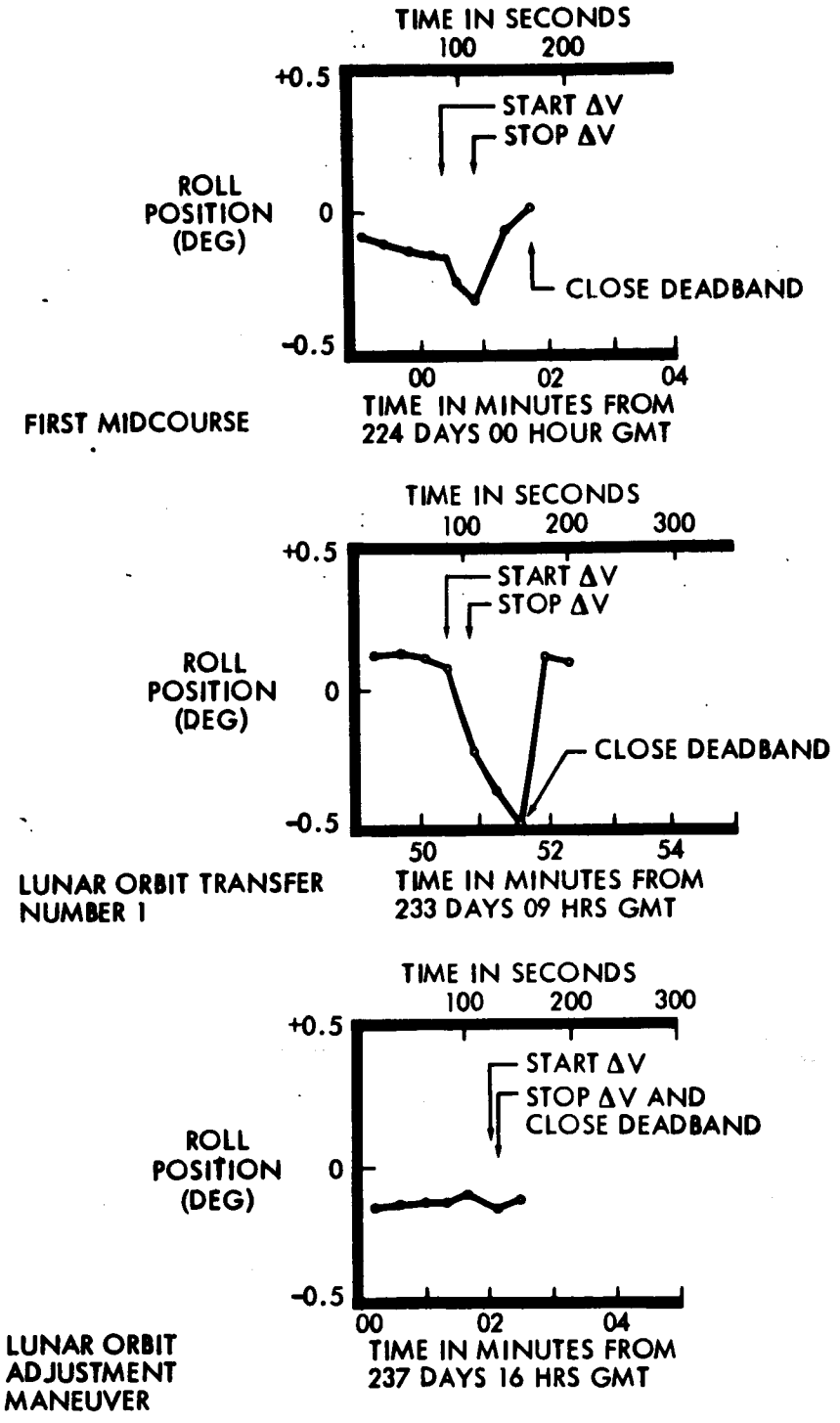

FIGURE 3.1-35: ROLL TRANSIENTS DURING ENGINE BURNS

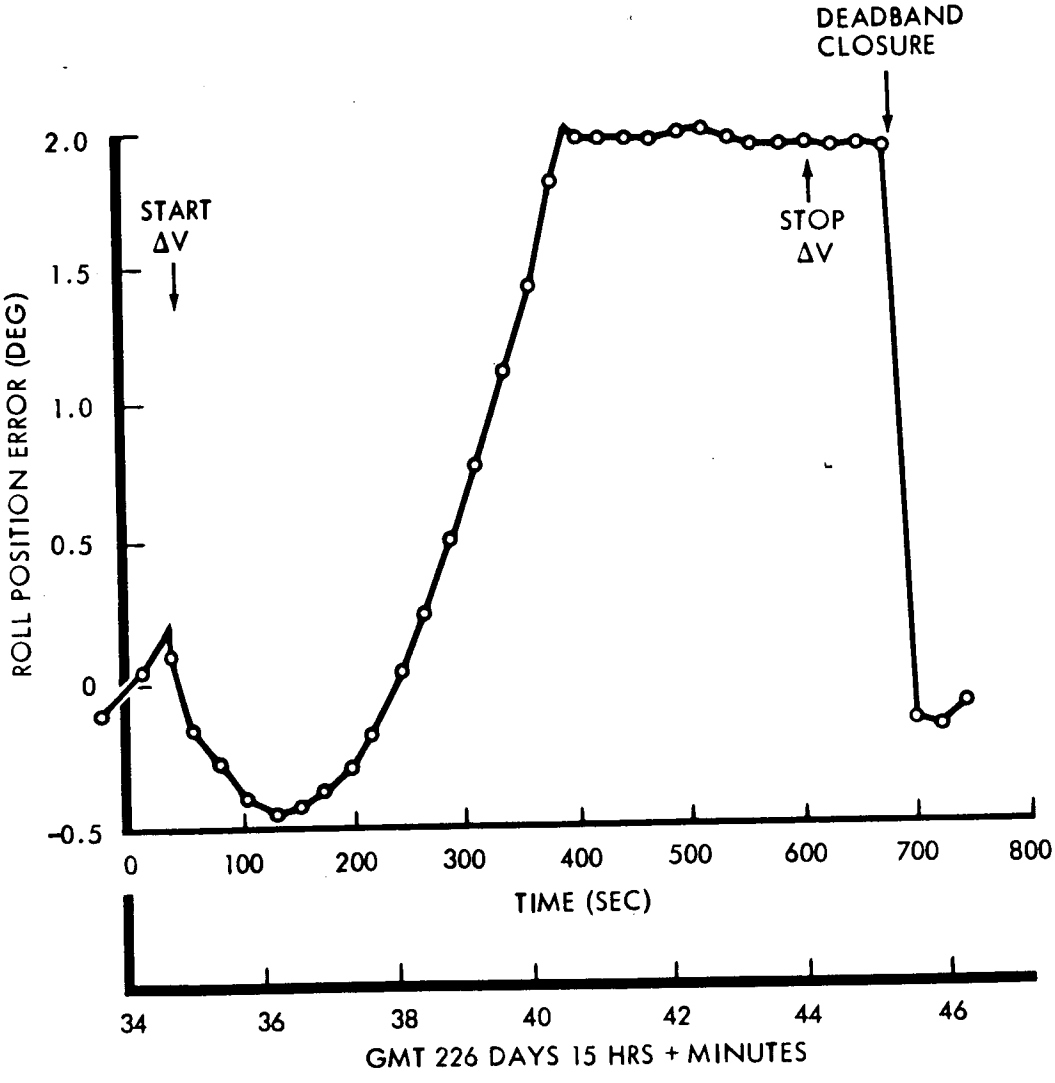

FIGURE 3.1-36: ROLL ATTITUDE DURING LUNAR ORBIT INJECTION MANEUVER

THRUSTER PERFORMANCE

AXIS	PREDICTED THRUST (LB)	ACTUAL THRUST (LB)
Roll (2)	0.072 ± 0.002	0.071
Yaw	0.060 ± 0.003	0.057
Pitch	0.063 ± 0.003	0.066

The thrust values are within the tolerance of the predicted values for all three axes. The specific impulse of the nitrogen for steady-state maneuvers was confirmed to be 71 lb-sec/lb., as predicted.

Nitrogen Consumption

Nitrogen consumption by the ACS for Mission I is presented in Figure 3.1-37. Estimated usage based on actual Mission I events is presented for a comparison between predicted values and actual values. Refer to Table 3.1-5 for a budget estimate of nitrogen consumption.

For a complete listing of the Mission I sequence of events pertaining to nitrogen consumption, refer to Table 3.1-8. This sequence of events, along with Table 3.1-11, will clarify the major slope changes in Figure 3.1-38.

The actual consumption exceeded the predicted usage by a substantial amount because of the unusually large number of maneuvers that were performed. Preflight estimates were based on a total of 94 maneuvers being performed; however, 374 maneuvers were actually performed. It is of importance to note that even after performing this large number of maneuvers, sufficient nitrogen was left to achieve a predicted 6-month extended mission. This is with an extended mission mode of reacquiring the Sun every day with control of the attitude in roll, pitch, and yaw.

In Figure 3.1-37, there are two actual nitrogen consumption curves. One is labeled "Pressure-Temperature-Volume Calculation," the other, "Dynamic Calculation." These two curves represent independent calculations of the nitrogen used during the mission. The PVT curve is calculated using pressure and temperature data for the nitrogen storage bottle. The dynamic curve is calculated by the program GASL, which calculates nitrogen consumption by analyzing the rate, position, etc., from telemetry data and using nitrogen consumption equations based on these dynamic parameters. The two curves are in good agreement in slope for the latter phases of the mission. The main reasons for the difference between the curves in early phases of the mission are uncertainty in the leakage rate of nitrogen and the low limit cycle consumption values.

The estimated curves that are presented consist of two parts: a minimum baseline and a conservative baseline. The minimum baseline assumes a nominal one-pulse operation

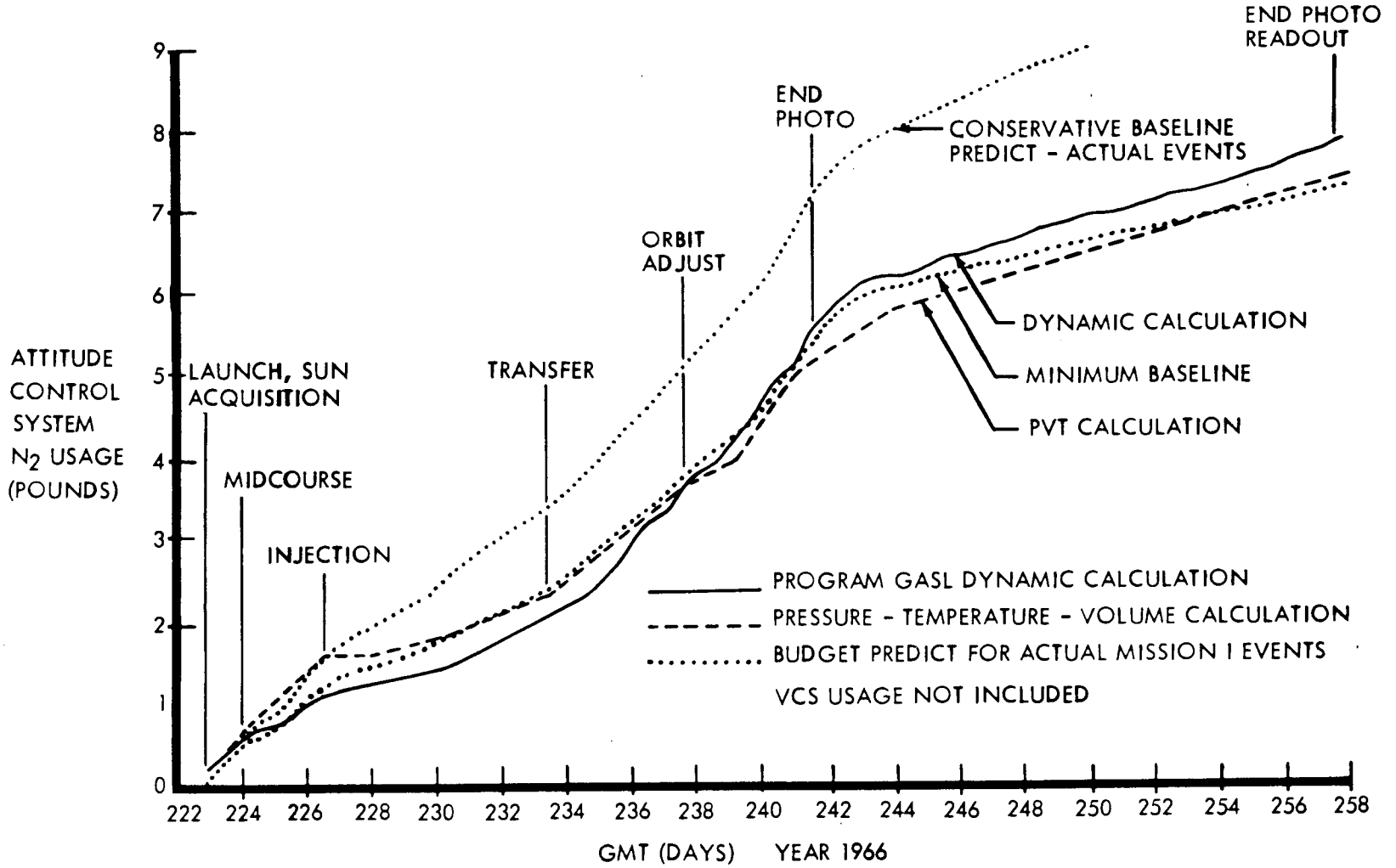

FIGURE 3.1-37: NITROGEN USAGE — ATTITUDE CONTROL SUBSYSTEM

Table 3.1-11: Mission I Daily Maneuver - Acquisition - N_2 Usage

DAY	ROLL MANEUVERS	PITCH MANEUVERS	YAW MANEUVERS	SUN ACQUISITION	DAILY* N_2 USAGE-POUNDS
222	1	0	0	1	0.164**
223	10	1	2	2	0.326
224	2	4	0	2	0.148
225	10	4	3	2	0.400
226	4	4	0	6	0.252
227	2	0	0	6	0.124
228	2	0	0	7	0.138
229	2	0	0	7	0.138
230	4	2	3	7	0.228
231	4	0	0	7	0.178
232	4	0	0	6	0.164
233	4	3	0	8	0.222
234	7	7	4	7	0.341
235	7	4	2	7	0.294
236	7	4	4	9	0.342
237	10	6	2	8	0.386
238	7	7	2	7	0.321
239	4	13	0	8	0.309
240	10	18	2	13	0.564
241	9	16	6	11	0.538
242	1	14	0	10	0.286
243	2	2	3	0	0.088
244	2	2	4	0	0.098
245	2	3	2	0	0.087
246	2	2	3	0	0.088
247	2	3	3	0	0.097
248	2	3	4	0	0.107
249	2	3	3	0	0.097
250	2	3	2	0	0.087
251	2	1	2	0	0.069
252	2	1	2	0	0.069
253	2	1	2	0	0.069
254	3	2	2	1	0.112
255	3	2	2	0	0.098
256	1	2	4	0	0.078

* Does not include limit cycle N_2 usage

** Day 222 also includes rate reduction after separation.

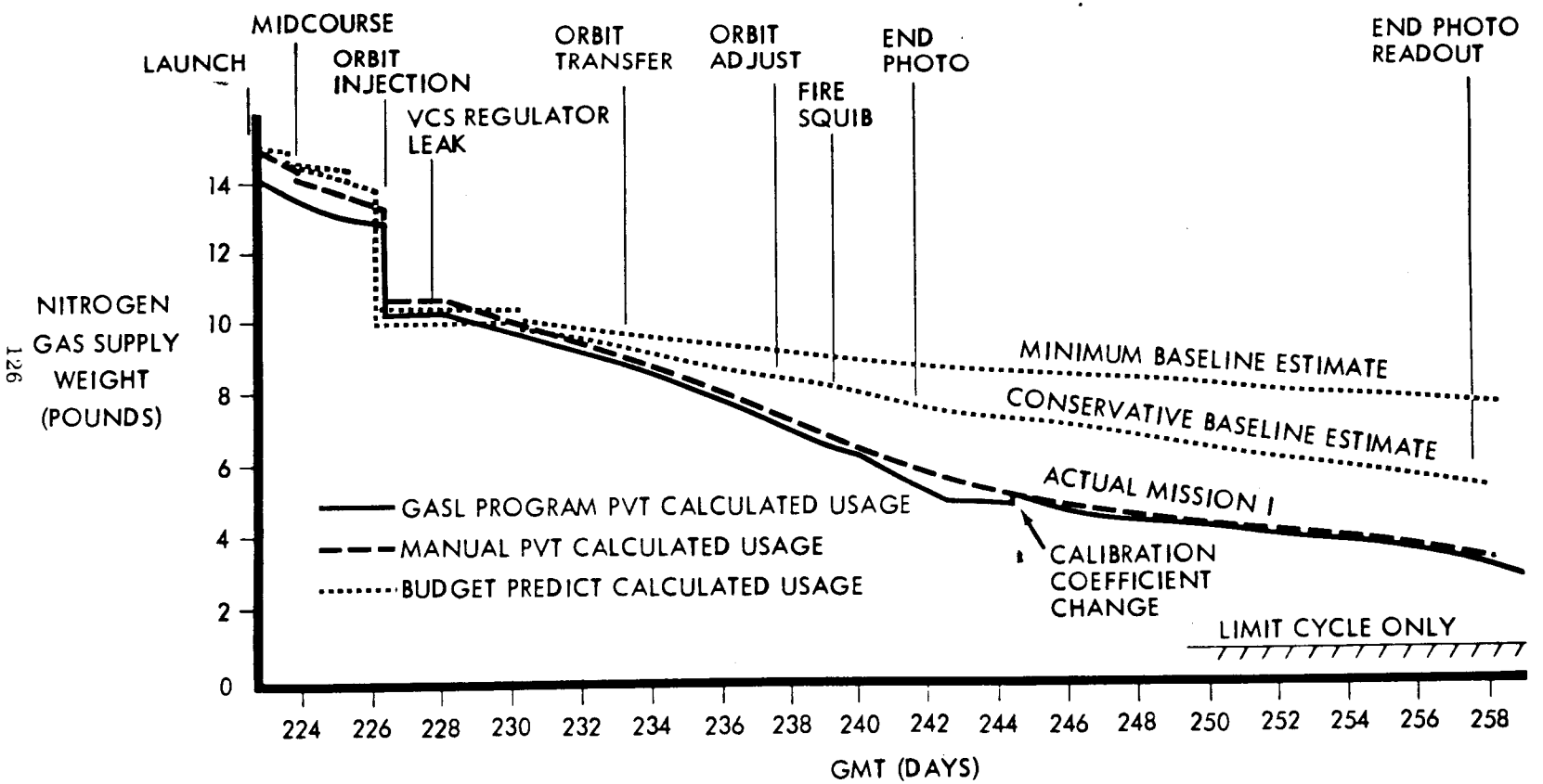

FIGURE 3.1-38: NITROGEN USAGE — VELOCITY AND REACTION CONTROL

during limit cycle, whereas the conservative baseline assumes a multiple-pulse operation during limit cycle; the minimum baseline predicts approximately 0.004 pound of nitrogen per day for limit cycle, whereas the conservative baseline predicts approximately 0.10 pound per day.

Figure 3.1-38 shows that the actual usage follows the minimum baseline. During orbit limit cycle, data was analyzed and showed the system to be 50-50 single and double pulsing. However, the nitrogen consumption is approximately the same as for pure single-pulse operation due to the disturbance torques.

A representative data sample of typical orbital limit cycling is described in the following section, "Disturbance Torque Summary." It will be noted that, due to the disturbance torques, the gas usage would be approximately the same for limit cycle regardless of the deadband. Being in wide deadband during a maneuver does save approximately 10 times as much nitrogen as being in narrow deadband.

Figure 3.1-39 presents the total nitrogen used by the combined velocity control system, leakage, and the attitude control system. The two "actual" curves are pressure-volume-temperature calculated curves. The manually calculated curve is obtained by calculating many points over a period of time and then averaging over these points. The GASL PVT curve is obtained from that portion of the GASL program that calculates nitrogen remaining at a single point in time based on pressure, volume, and temperature of the nitrogen storage bottle at that time. The difference in the two curves during the early part of the mission stems from incorrect bottle volume and pressure coefficients being used by program GASL. In the later parts of the mission, program GASL PVT values agree very closely with manual PVT values, as they should. The graph clearly shows the time at which calibration coefficients were changed for the program GASL.

The nitrogen consumption rate for maneuvers agrees very closely with prediction values as shown by comparison in the table below.

	PREINJECTION		INJECTION TO TRANSFER		TRANSFER ON	
	Predict	Actual*	Predict	Actual*	Predict	Actual*
Roll	0.0240	0.0243	0.0211	0.0215	0.0210	0.0211
Pitch	0.0184	0.0188	0.0093	0.0094	0.0088	0.0089
Yaw	0.0209	0.0210	0.0108	0.0110	0.0102	0.0103

The above numbers are pounds of nitrogen per maneuver.
*Average of several data points.

The most interesting aspect of the nitrogen consumption for Mission I is the sequence of events that took place during photo readout between Days 244 and 257. From Day 235 to Day 243, the average nitrogen used for attitude control was 0.375 pound per day. This

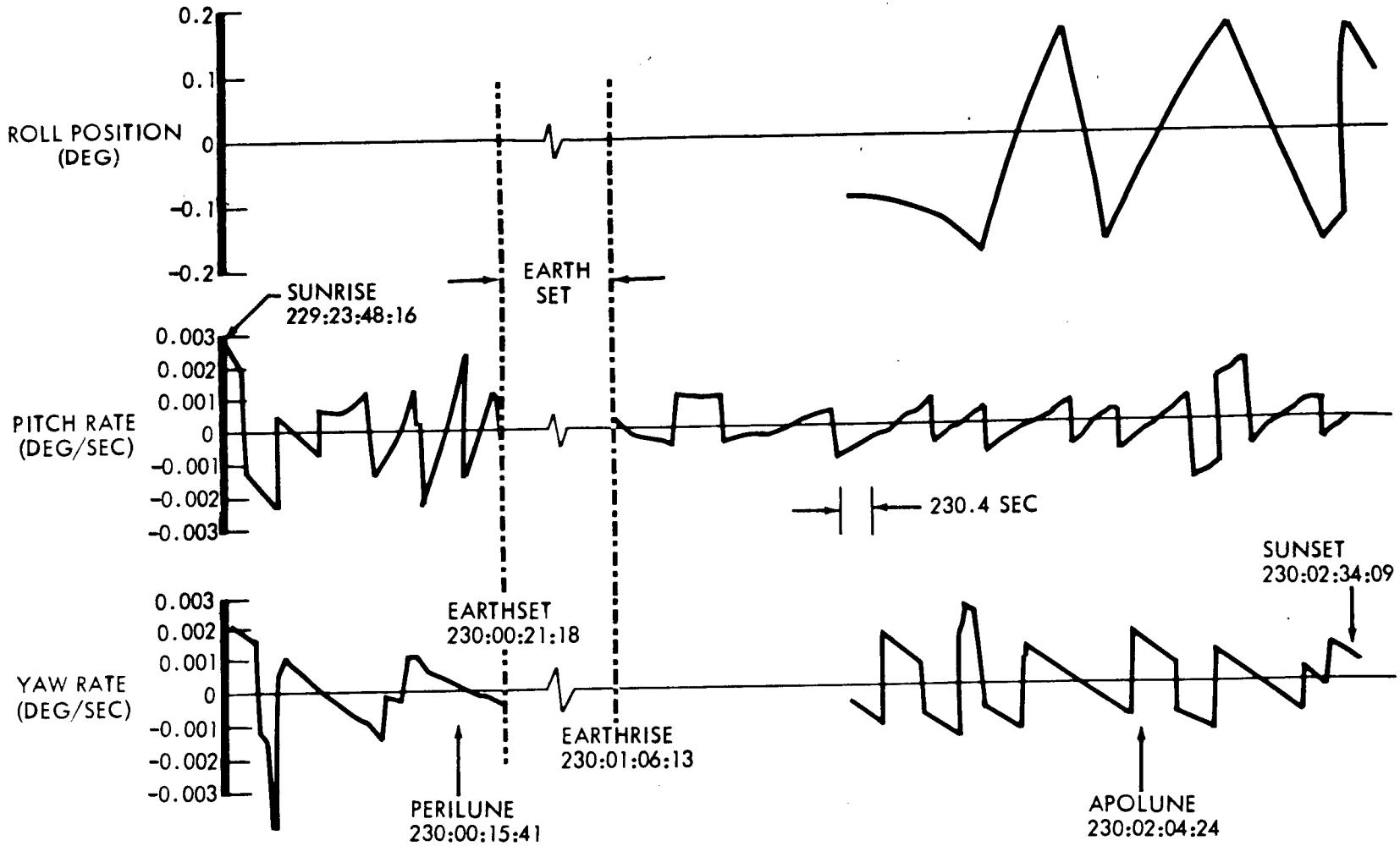

FIGURE 3.1-39: SPACECRAFT MOTION — INITIAL ORBIT 22

high usage rate was due to photo maneuvers, and pitching off the Sun and reacquisition every orbit. Gas optimization studies were then performed, and it was decided that the following procedure would be used:

1) Stay off the Sunline at a constant angle in pitch;

2) Update the pitch angle as often as required by using the coarse Sun sensors;

3) Update the yaw angle as often as required by using the coarse Sun sensors;

4) Update the roll angle as often as required by viewing Canopus every Sun occultation.

This procedure was followed all during photo readout. From Day 244 to Day 257, the average nitrogen used for attitude control was approximately 0.09 pound per day.

A certain portion of the nitrogen was vented overboard due to a leak in the regulator to the velocity control system. This leak was estimated to be 0.10 pound of nitrogen per day from the nitrogen supply tank. The leak occurred over a time period from Day 228 to Day 238. At 0549 on Day 238 (238:05:49 GMT), the nitrogen shutoff squib was fired to isolate the leaking regulator from the nitrogen supply tank.

Disturbance Torque Summary

Throughout the flight the spacecraft encountered disturbance torques from several sources. These disturbance torques, which affect the motion of the spacecraft and the nitrogen consumption, can be divided into two categories: (1) external torques that are present almost continuously; and (2) internal torques that are generated by the spacecraft and are transient in nature.

The two primary external disturbance torques encountered were solar pressure and gravity gradient. During cislunar flight, gravity gradient torques were negligible and the solar pressure contribution could be isolated. For a period of a few hours, the disturbance torques remained constant. Listed below is a sample of these torque values together with predicted values. The signs of the torques agree with predictions; however, the pitch and yaw torques are about 60% of the predicted values.

AXIS	PREDICTED*	ACTUAL AT GMT 224:10:00:00
Roll	-0.28×10^{-6} lb-ft	-0.32×10^{-6} lb-ft
Pitch	$+1.4 \times 10^{-6}$ lb-ft	$+0.82 \times 10^{-6}$ lb-ft
Yaw	-7.28×10^{-6} lb-ft	-4.7×10^{-6} lb-ft

*Solar pressure on the high-gain antenna, which was at +32 degrees at this time.

After the spacecraft was in orbit, the gravity gradient torque was pronounced. Figure 3.1-39 is a plot of typical spacecraft motion in high orbit. The yaw torque is about -5.2×10^{-6} foot-pounds, which is almost the same as cislunar torques. However, the pitch axis torques was oscillatory as the spacecraft proceeded through the orbit.

Figure 3.1-40 shows the torque variation in pitch, which was determined by graphically differentiating the pitch rate curve in Figure 3.1-41. The torque is cyclic throughout the orbit as was predicted and the magnitudes of the torques are approximately the same as the predicted values.

Figures 3.1-41 and 3.1-42 are examples of spacecraft rates and disturbance torques, respectively, for the low orbit. The two examples show that the magnitude of the pitch torque does not vary greatly with the two orbits. Predictions would indicate, for an identical situation (i.e., orbital orientation with respect to the Sun and spacecraft inertias), that the low-altitude orbit torques would be about 25% higher. However, the spacecraft inertias did change between examples and the analysis has not been performed to determine precise predictions of the gravity gradient torque effects.

The other major disturbance torques were caused by the spacecraft equipment. The primary disturbance torque in this category was the coupling of a reaction jet of one axis into the other two axes. This disturbance torque was most disturbing during spacecraft maneuvers. Figures 3.1-43, 3.1-44, and 3.1-45 are plots of spacecraft motion in the other axes due to jet operation. The magnitude of the disturbances is difficult to determine due to the long sampling period.

Another disturbance torque on the spacecraft was caused by movement of spacecraft equipment. The prime disturbance contributor in this category was rotation of the high-gain antenna. Figures 3.1-46 and 3.1-47 show the typical effects of high-gain antenna rotation upon spacecraft motion for a rotation of the antenna by 1 degree. Figures 3.1-48, 3.1-49, and 3.1-50 show the large spacecraft disturbance caused by rotating the antenna several degrees in sequence. Nitrogen consumption and actual disturbance rates cannot be determined due to the sampling period of telemetry.

The other significant disturbance torque source was caused by the motion of the camera thermal door and moving parts within the camera. Disturbed spacecraft motion for a typical camera picture sequence is shown in Figures 3.1-51 and 3.1-52. The yaw axis was affected the most, with a small effect in pitch and no noticeable effect in roll.

All of the above disturbances affect limit cycle operation and nitrogen consumption; however, detailed analyses of the exact disturbance levels are difficult due to the long sampling period.

3.1.5 VELOCITY CONTROL SUBSYSTEM

3.1.5.1 FUNCTIONAL DESCRIPTION

3.1.5.1.1 Summary

Midcourse correction, lunar orbit injection, and orbit transfer were provided by the velocity control subsystem.

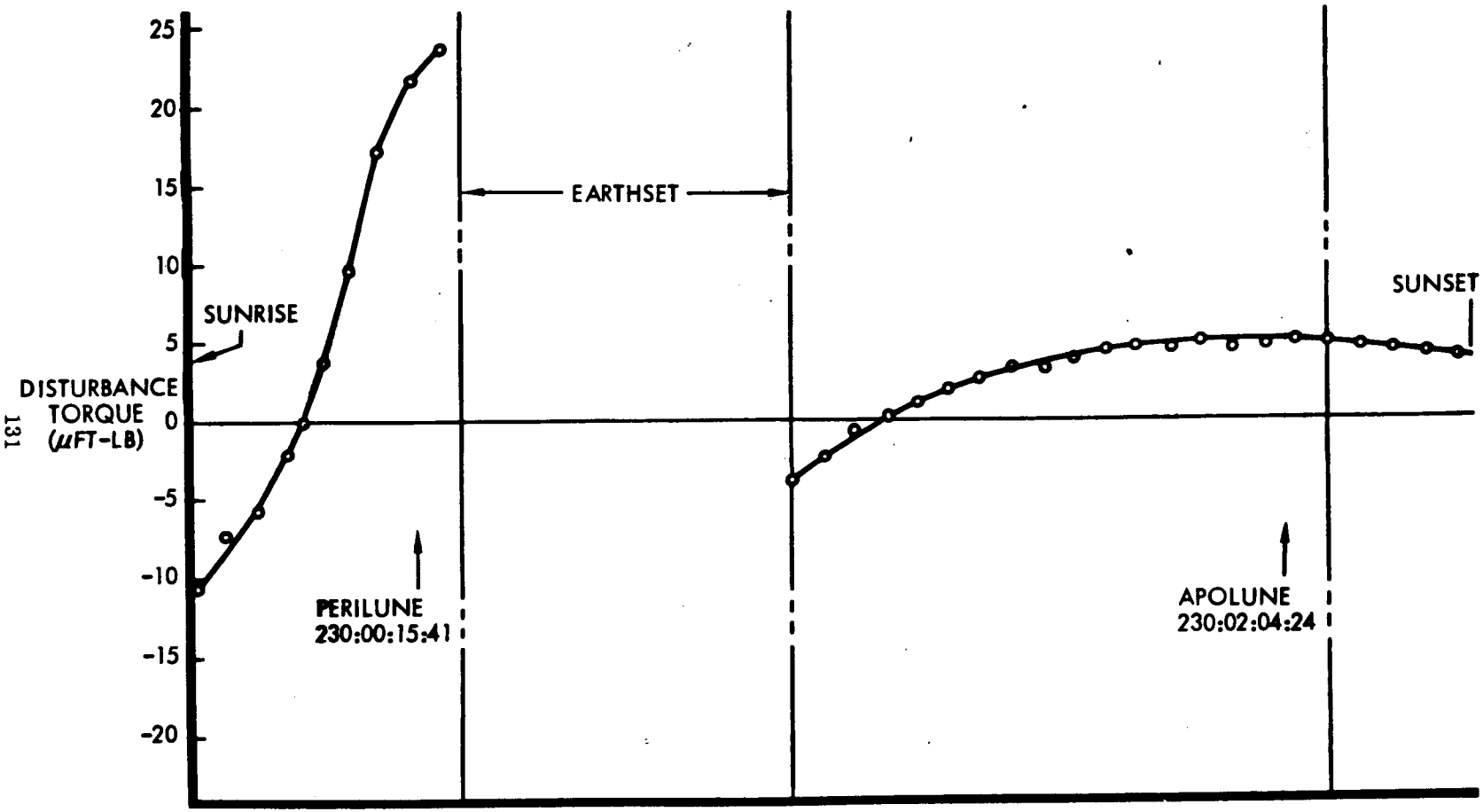

FIGURE 3.1-40: DISTURBANCE TORQUE IN PITCH AXIS — INITIAL ORBIT 22

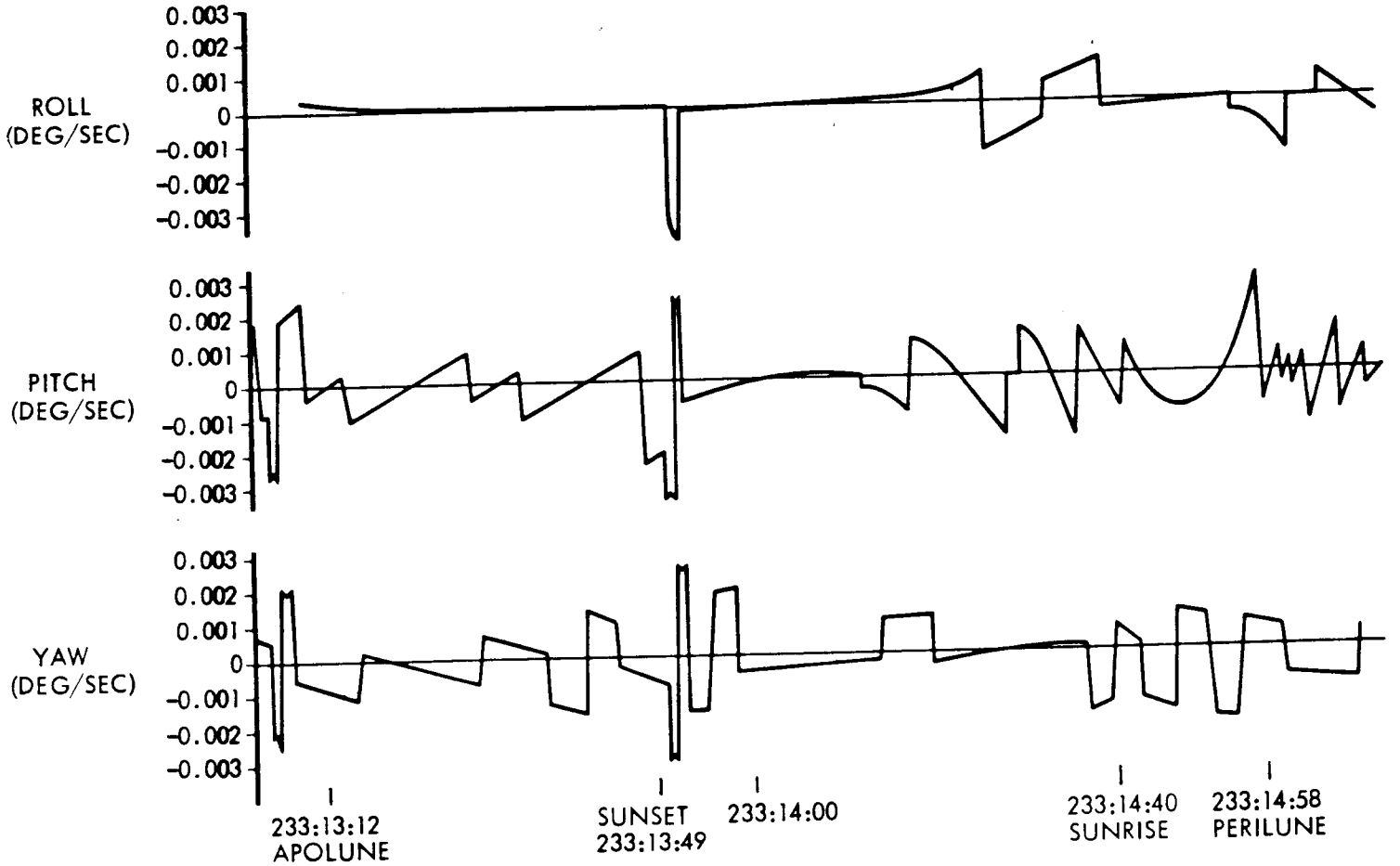

FIGURE 3.1-41: SPACECRAFT RATES — FINAL ORBIT 2

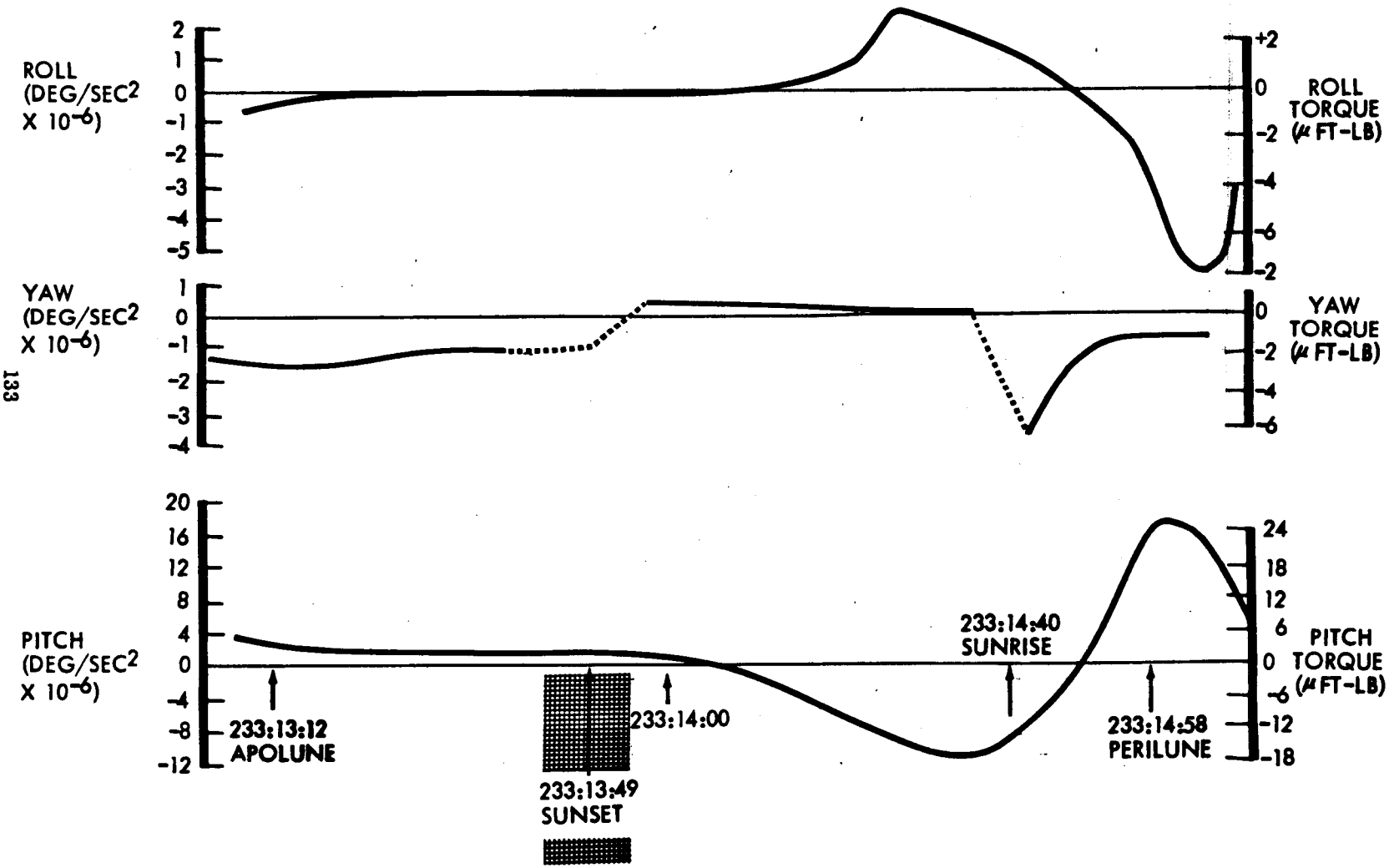

FIGURE 3.1-42: SPACECRAFT DISTURBANCES — ACCELERATION — FINAL ORBIT 2

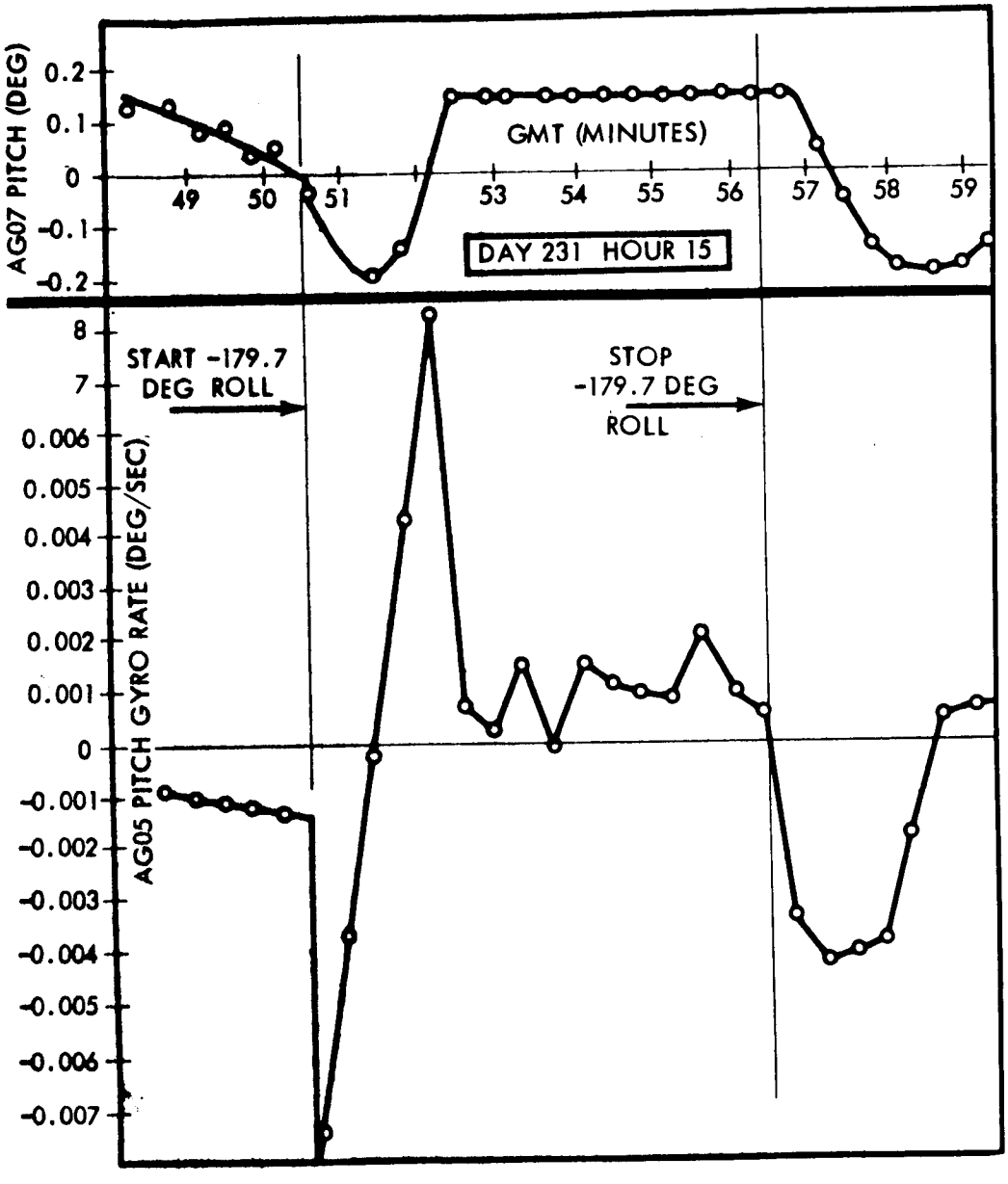

FIGURE 3.1-43: PITCH AXIS DISTURBANCE DUE TO A -179.7-DEGREE ROLL MANEUVER

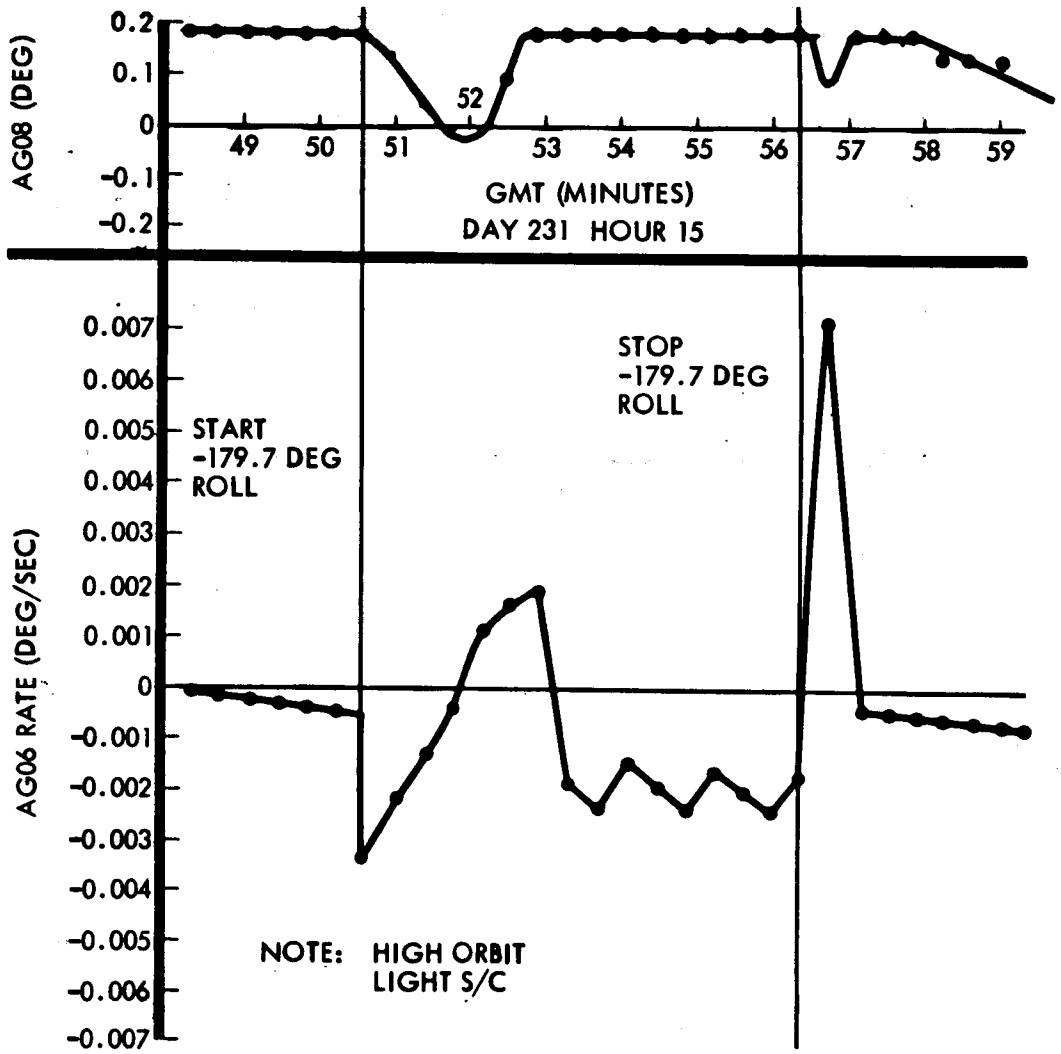

FIGURE 3.1-44: YAW AXIS DISTURBANCE DUE TO A -179.7 DEGREE ROLL MANEUVER

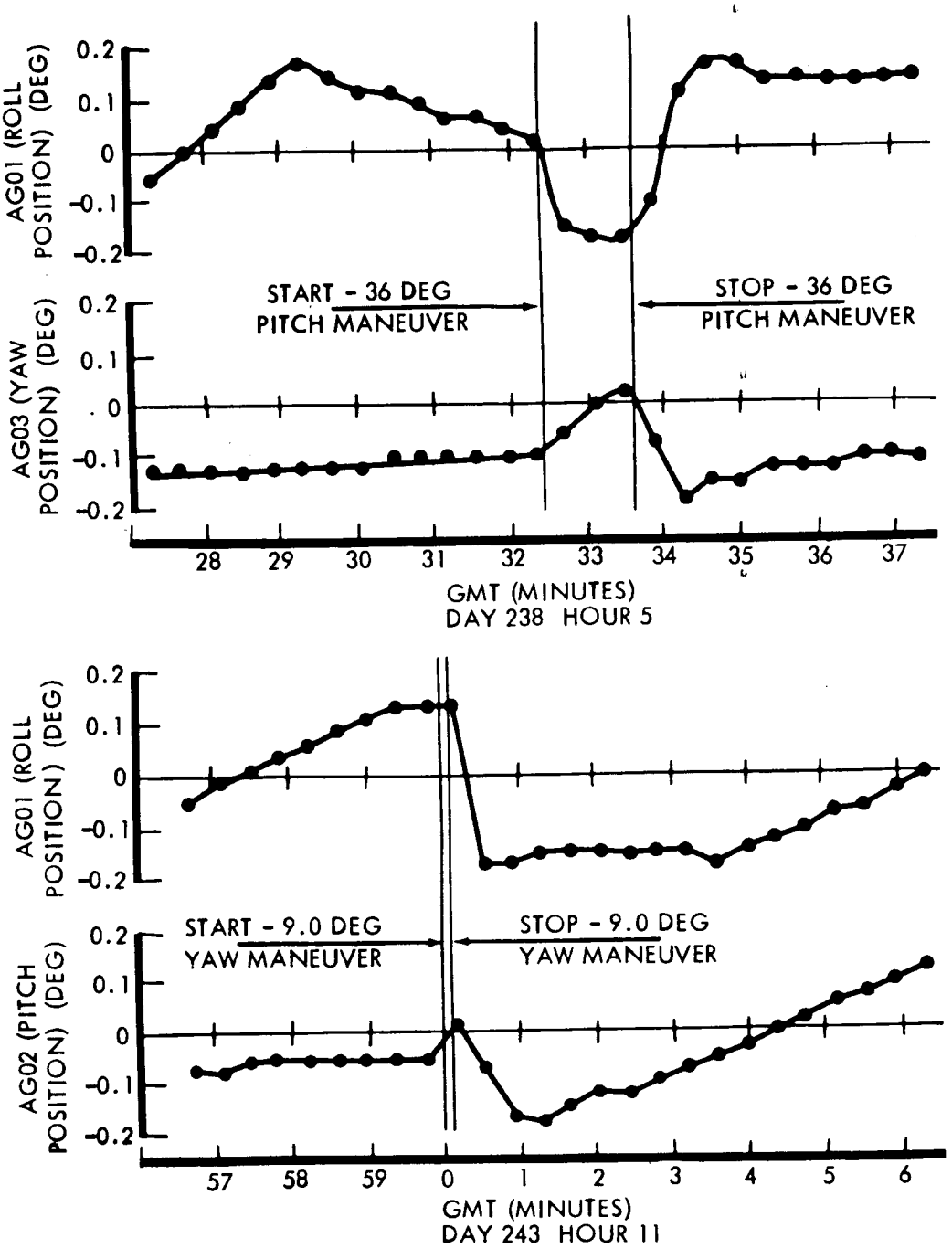

FIGURE 3.1-45: DISTURBANCES IN ROLL AND YAW AXES DUE TO A PITCH MANEUVER AND IN ROLL AND PITCH AXES DUE TO A YAW MANEUVER

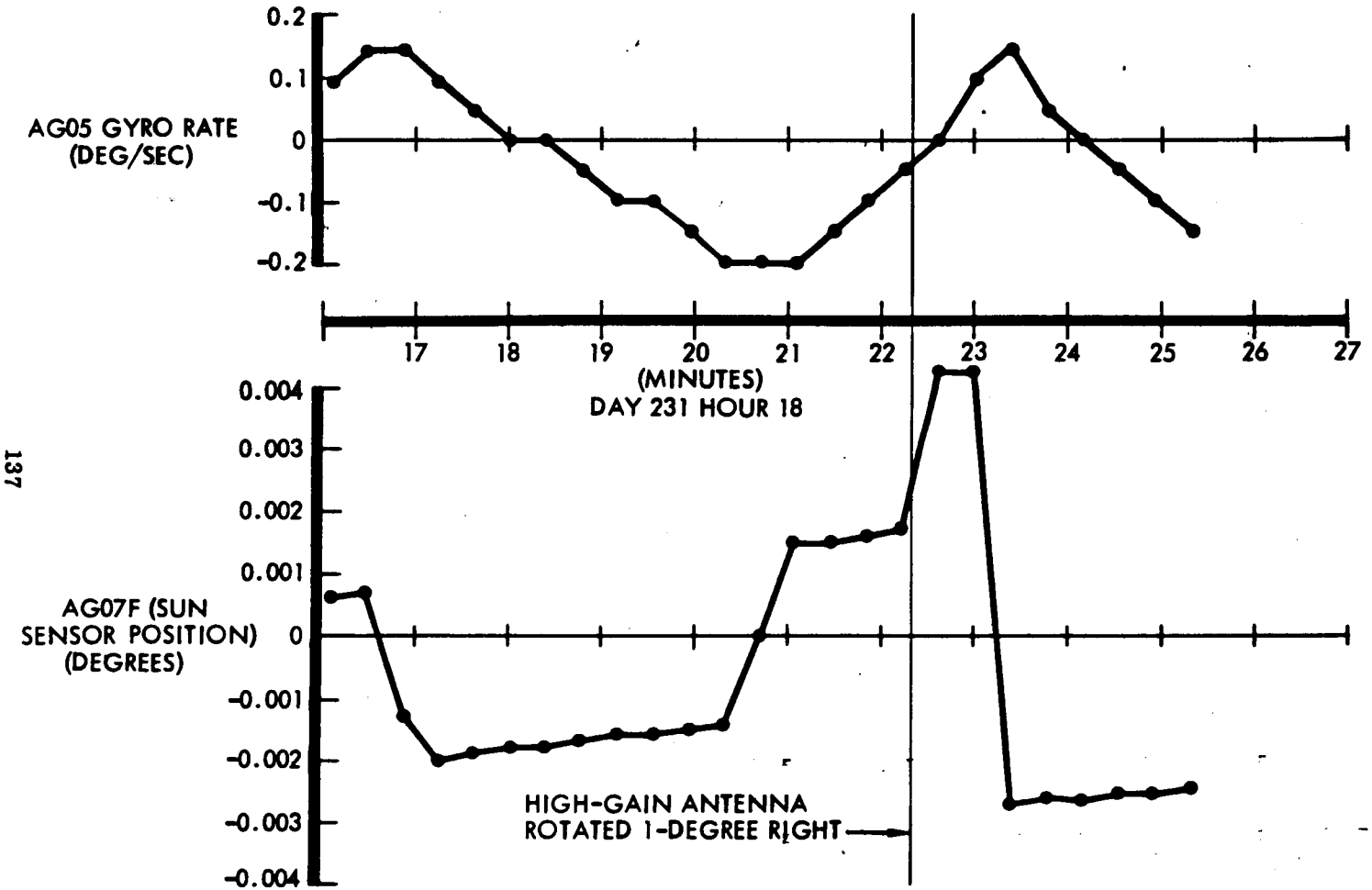

FIGURE 3.1-46: PITCH AXIS DISTURBANCE DUE TO AN ANTENNA ROTATION

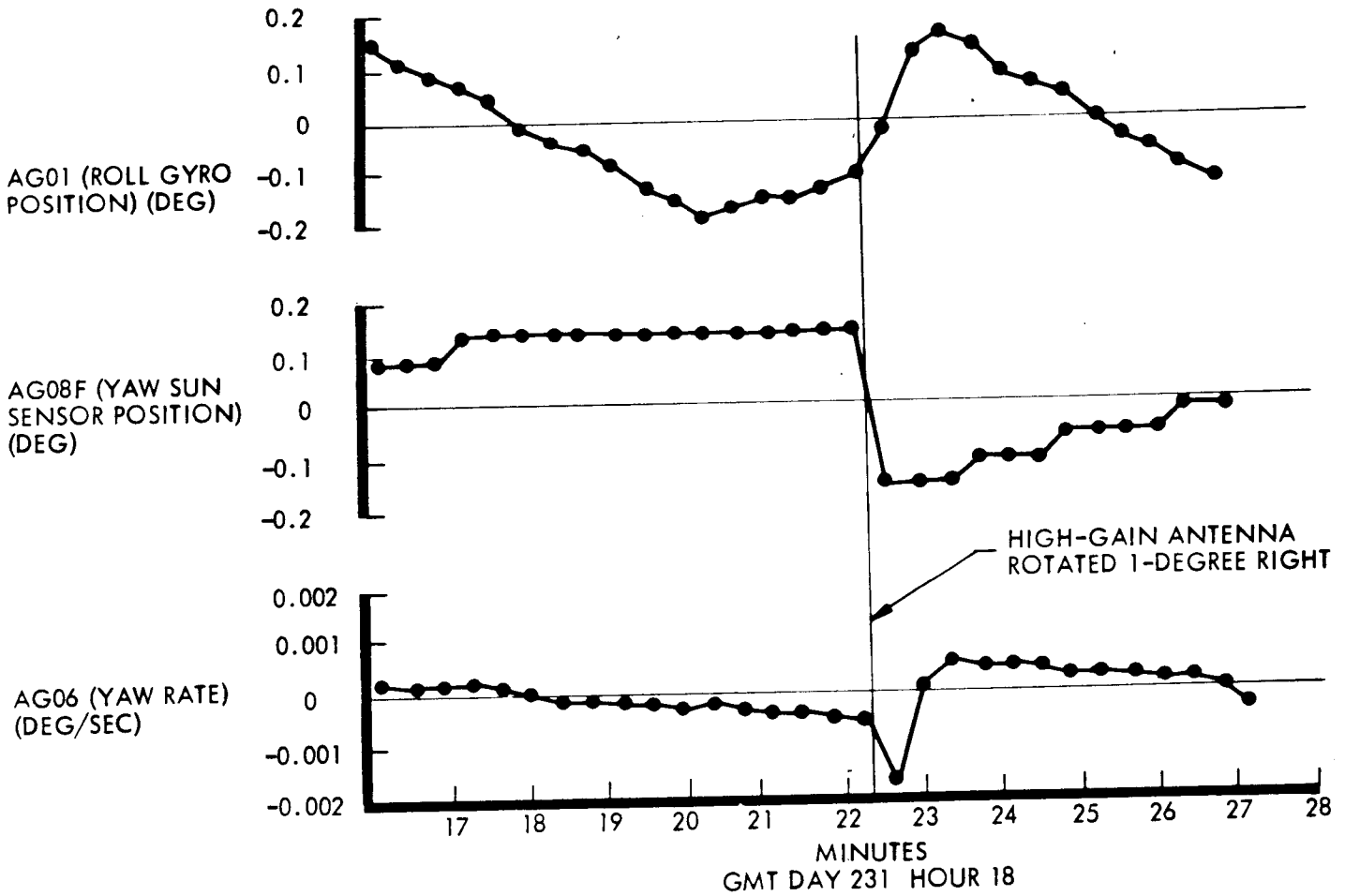

FIGURE 3.1-47: ROLL AND YAW AXIS DISTURBANCE DUE TO ANTENNA ROTATION

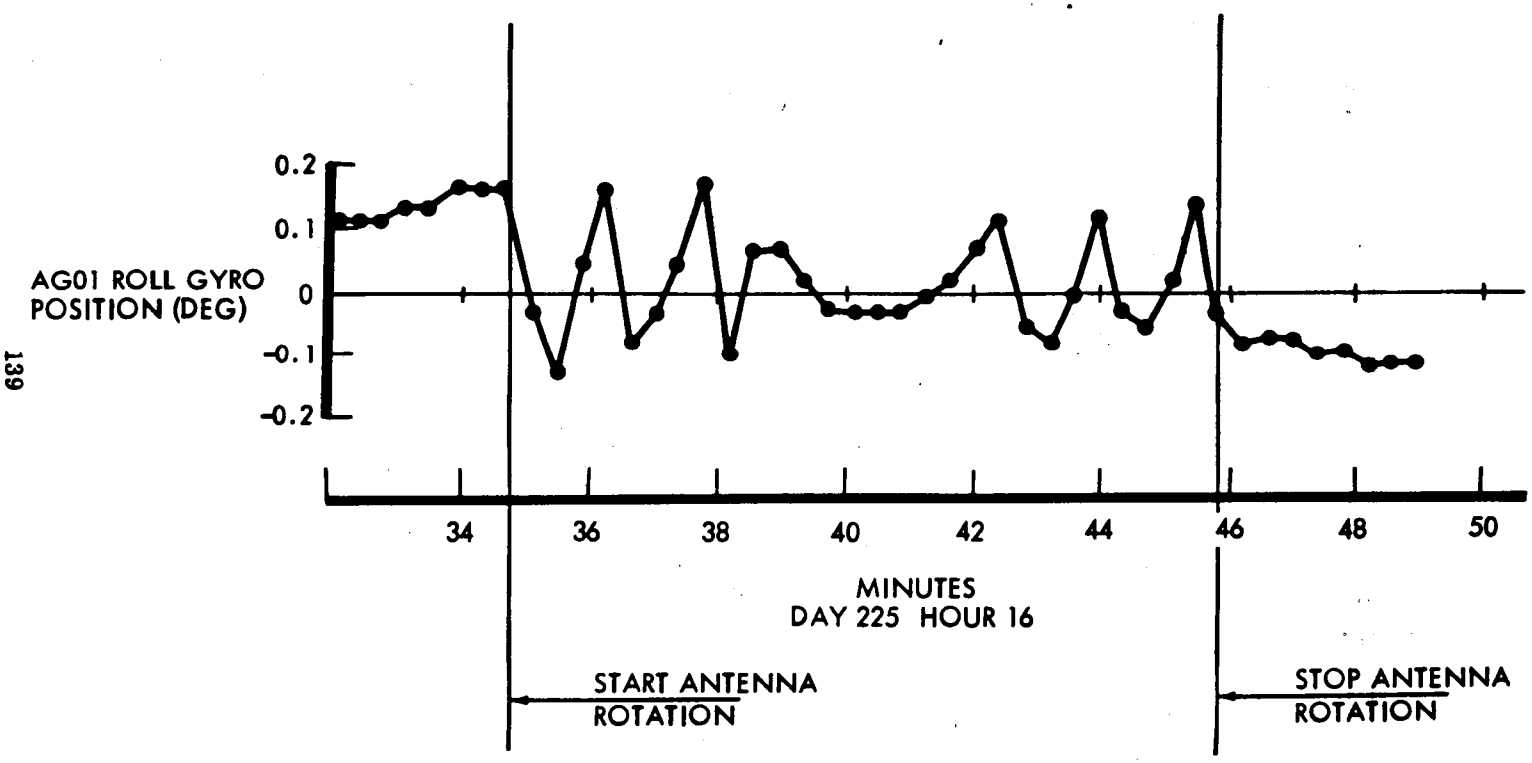

FIGURE 3.1-48: ROLL AXIS DISTURBANCE DUE TO A 30-DEGREE ANTENNA ROTATION

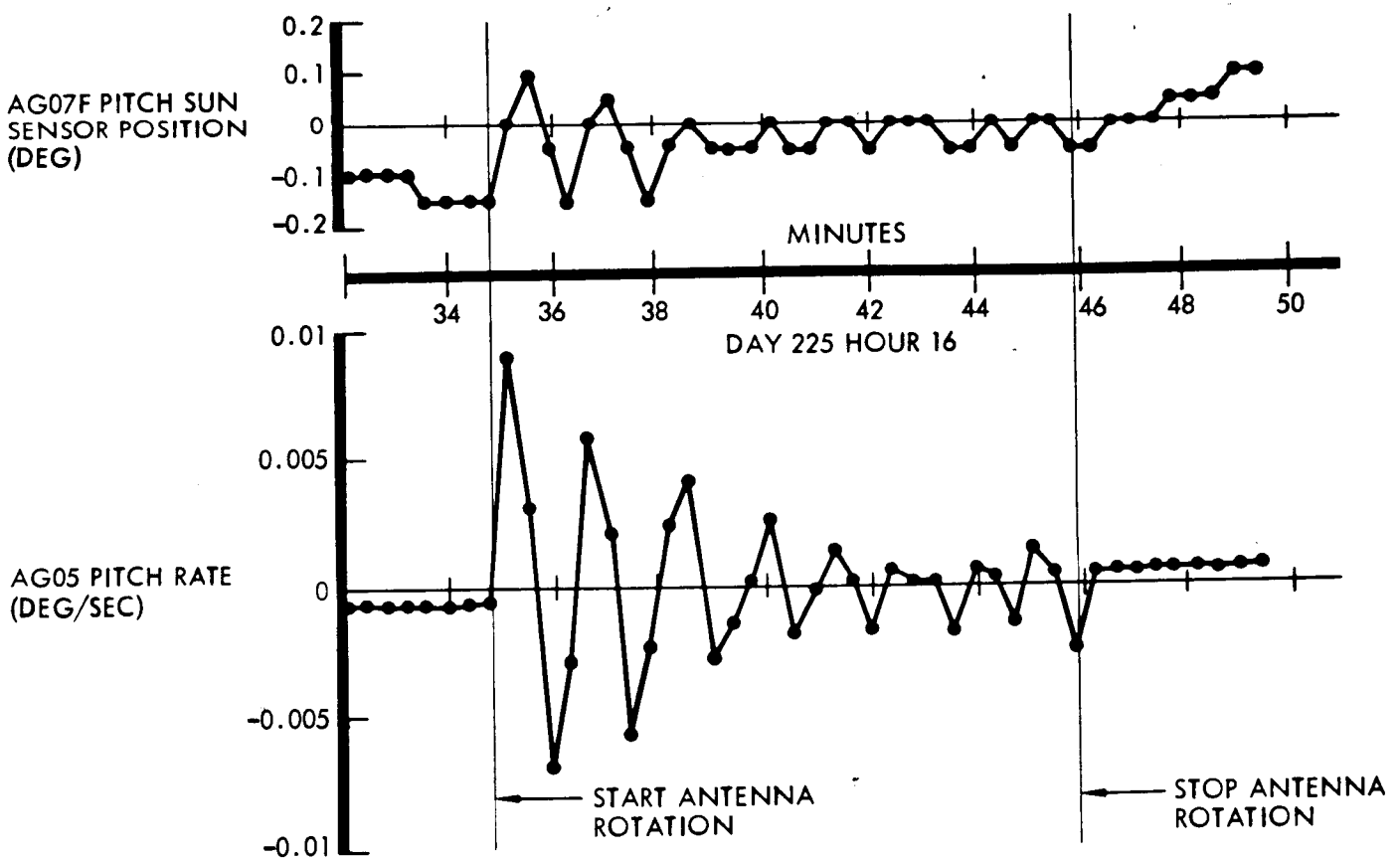

FIGURE 3.1-49: PITCH AXIS DISTURBANCES DUE TO A 30-DEGREE ANTENNA ROTATION

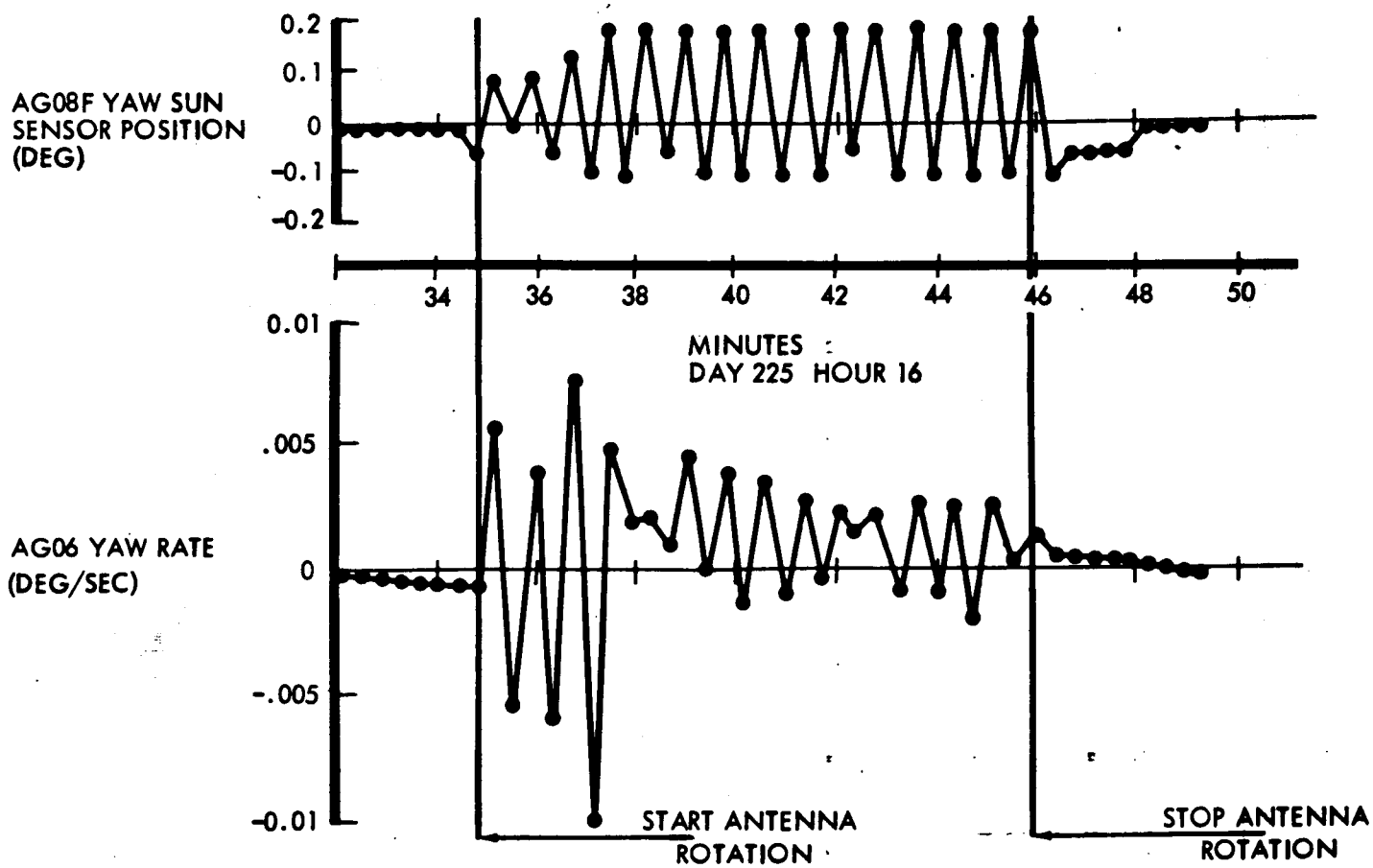

FIGURE 3.1-50: YAW AXIS DISTURBANCES DUE TO A 30-DEGREE ANTENNA ROTATION

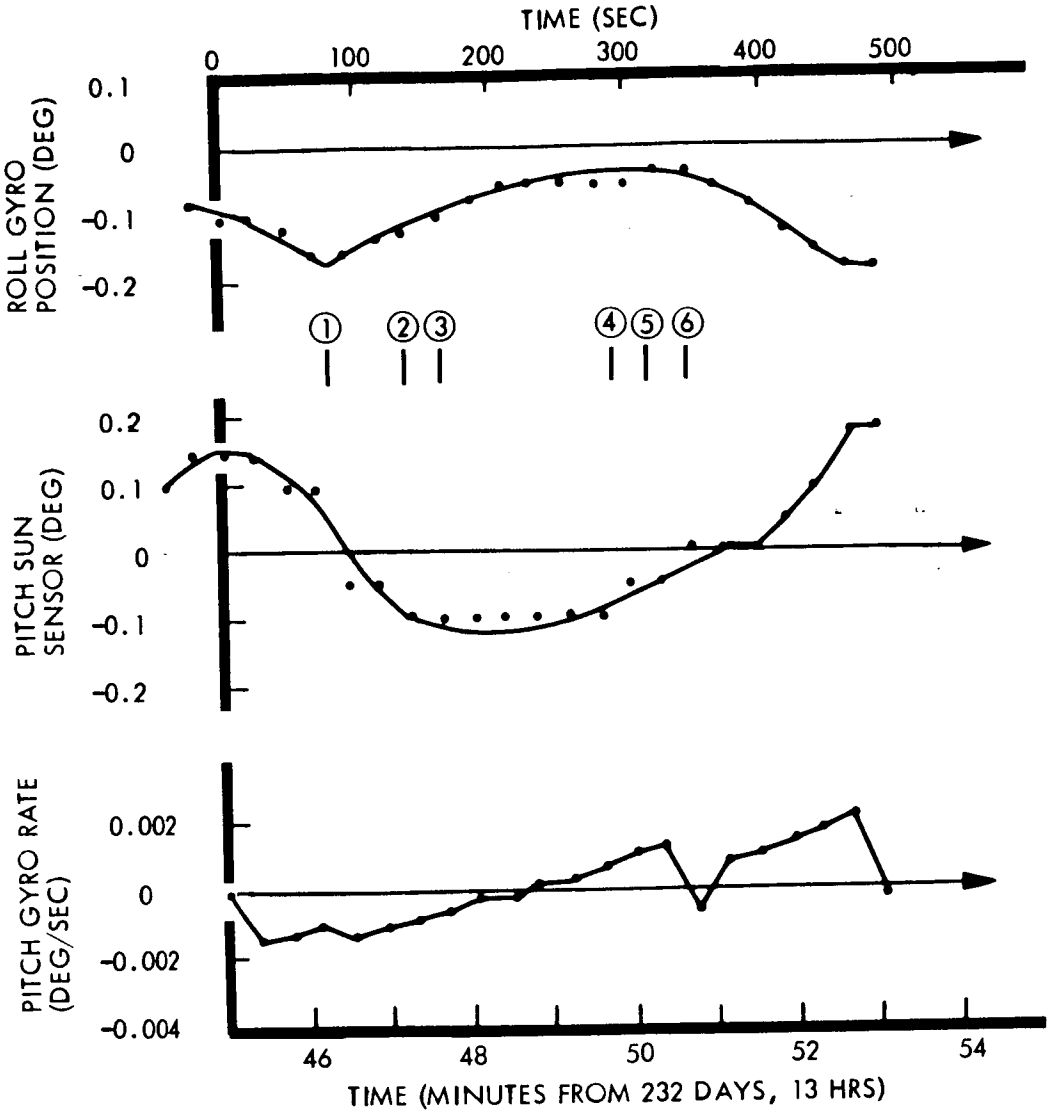

EVENTS	FLAG
CAMERA DOOR OPEN	①
FRAME 21 TAKEN	②
FRAME 32 TAKEN	③
FRAME 33 TAKEN	④
FRAME 34 TAKEN	⑤
CAMERA DOOR CLOSED	⑥

FIGURE 3.1-51: CAMERA MOTION DISTURBANCE ON ROLL AND PITCH

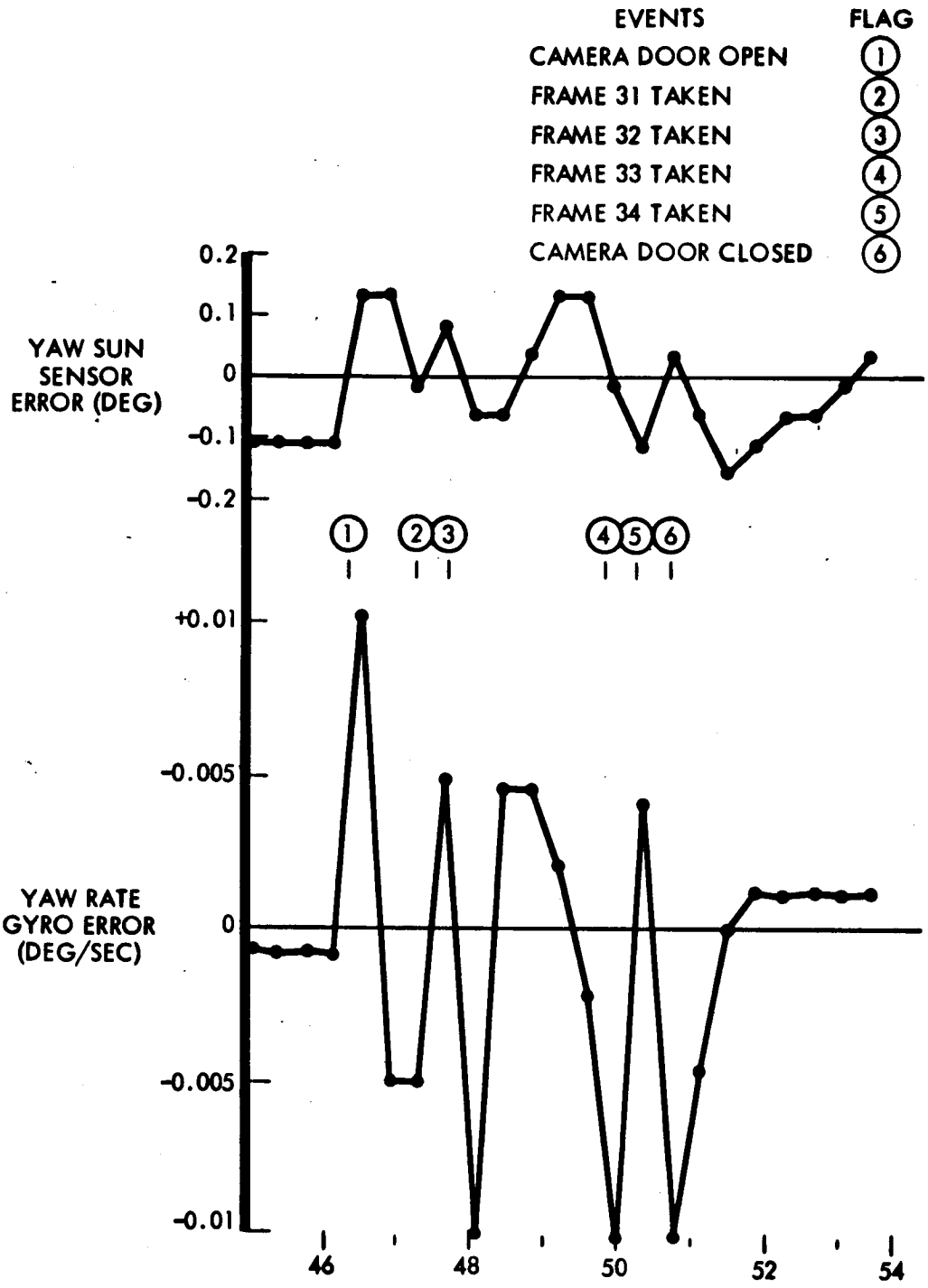

FIGURE 3.1-52: CAMERA MOTION DISTURBANCES ON YAW AXIS

When the velocity-control engine valves were commanded to open, gas pressure acting on propellant tank bladders forced the fuel and oxidizer into the 100-pound-thrust engine. No ignition system was required because the propellants ignited when mixed, and thrust continued until the engine valves were closed. To determine thrust duration, velocity change rate was detected by an accelerometer, integrated, and compared with requirements stored in the flight programmer.

3.1.5.1.2 Detail Description

The VCS was a constant-thrust, liquid bipropellant, pressure-fed propulsion system, completely self-contained except for the electrical and structural interfaces. The principal subsystem components were the rocket engine, fuel and oxidizer tanks, nitrogen storage tank, pressure regulator, and connecting lines. The system is shown schematically in Figure 3.1-53. The principal components are discussed below.

Rocket Engine

The rocket engine was a radiation-cooled Marquardt MA 109 engine that provided a nominal thrust of 100 pounds. The engine was mounted in two-axis gimbals with thrust-vector control provided by electromechanical actuators.

Thrust was produced when the oxidizer (nitrogen tetroxide) and the fuel (Aerozine-50) met in the combustion chamber and ignited. Use of a hypergolic propellant ensured proper engine ignition in the space environment. Aerozine-50 is composed of 50%, by weight, hydrazine and UDMH.

The VC engine has the following performance characteristics:

Vacuum Thrust	100 ± 5 pounds
Nominal Specific Impulse	276 lb-sec/lb
Mixture Ratio	2.00 ± 0.05 o/f

These values are referenced to the nominal propellant pressure of 170 psi at the inlet to the engine valves.

The rocket engine has rapid-response characteristics because of its fast valve times and small manifold volumes. The time interval between the valve command and 90% thrust is approximately 25 milliseconds.

Small electric heaters on the engine propellant valves ensured proper propellant flow by maintaining the valve temperature at 80 to 85°F. During engine operation, thermal soak from the combustion chamber raised the valve temperature to a stable value of approximately 150°F if the duration of operation was 100 seconds or more. After cutoff, propellant flow is no longer available to cool the injector head, and thermal soakback will momentarily increase valve temperature to approximately 230°F. The maximum value occurs 3 to 5 minutes after shutdown.

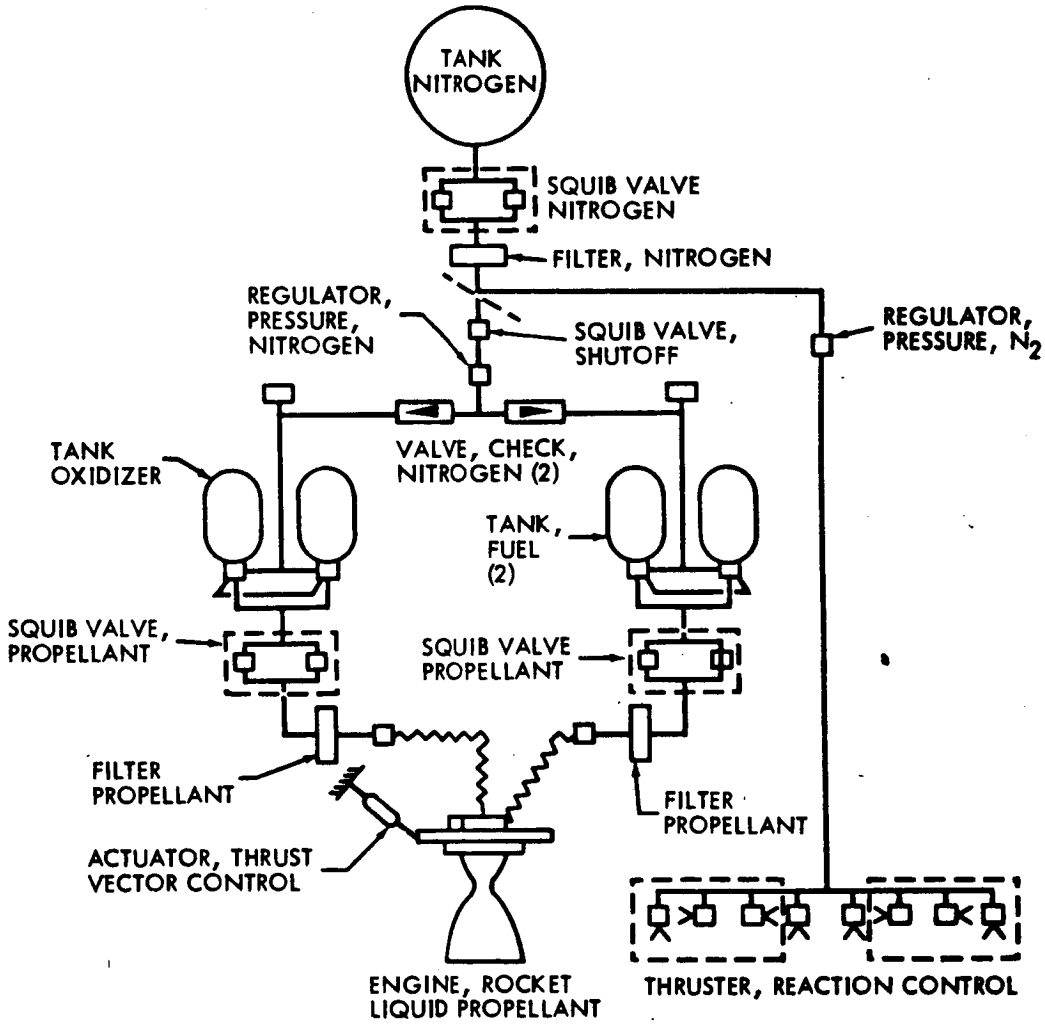

FIGURE 3.1-53: VELOCITY AND REACTION CONTROL SUBSYSTEM

Fuel and Oxidizer Tanks

Two tanks were used for the fuel and two for the oxidizer; the tanks of each pair were placed diametrically opposite each other to minimize center-of-gravity changes. The propellant tanks were forged from a titanium alloy (Ti-6Al-4V; 6% aluminum, 4% vanadium) and had a working pressure limit of 236 psig, a proof pressure of 480 psig, and a burst pressure of 540 psig. The oxidizer tank had a nominal volume of 1.035 cubic feet and the fuel tank 0.851 cubic foot. These tanks were structurally identical to the Apollo Command Module reaction-control-propellant tankage, though they were operated in a different environment.

The tank diffuser and standpipe assembly included a "liquid side vent" line to permit expanding the bladder to the tank wall prior to tank filling. A usable-propellant summary is presented in Table 3.1-12.

Propellant containment and expulsion in a O-g environment was accomplished by a teflon bladder within the propellant tank. In the fuel tanks, the bladder was a 6-mil laminate of TFE and FEP teflon attached to the forward and aft extremities of the standpipe assembly. The oxidizer bladder was attached in the same manner and was nominally a 6.25-mil laminate of TFE, aluminum, and FEP; the aluminum was incorporated to provide a more positive barrier to nitrogen transmission and minimize the amount of nitrogen in solution with the oxidizer. The teflon bladder was capable of expelling 98 to 99% of the propellant before the pressure loss across the unit became excessive.

Heaters on the propellant tanks warmed the tanks when commanded on at propellant temperatures below 40°F. (Fuel temperatures below approximately 35°F would have caused fractional separation of the fuel blend constituents.)

Nitrogen Storage Tank

The nitrogen storage tank was a spherical titanium storage vessel. The stored gas was used to pressurize the VCS propellant tanks and served as a working fluid for the reaction-control-subsystem cold-gas thrusters. No heating other than the natural conduction and radiation from other spacecraft components was provided.

Characteristics of the spacecraft nitrogen storage tank are as follows:

Volume	1597.5 cu. in. (nominal)
Maximum Loading Pressure	3535 psig @61° F
Limit Pressure	3820 psig @85°F
Proof Pressure	5730 psig
Minimum Burst Pressure	7640 psig

Table 3.1-12: Usable-Propellant Summary

	OXIDIZER	FUEL
Maximum System Volume, cu ft	2.0722	1.7078
Minimum System Volume, cu ft	2.0677	1.6997
Propellant Density (95°F), lb/cu ft	88.05 ± 0.15	55.65 ± 0.15
Maximum Capacity, lb	182.77	95.29
Minimum Capacity, lb	181.94	94.35
Minimum Ullage (95°F), cu ft	0	0
AGE Load Tolerance, lb	±0.60	±0.45
AGE Off-Load Tolerance, lb	±0.25	±0.25
Nominal Loaded, lb	181.69	94.10
Minimum Guaranteed, lb	180.49	93.20
Trapped Propellant, lb		
Lines	-0.44	-0.28
Tanks (2% Apollo Load)	-3.62	-1.84
Minimum Available, lb	176.43	91.08
	267.51	
Available Propellant, lb		
MR = 1.98	265.54	
MR = 2.06	262.07	
MR = 1.90	264.13	
Guaranteed Minimum Usable, lb	262.07	
Nominal Usable, lb	266.50	

NOTE: The above listing is somewhat conservative in that tolerances are treated arithmetically, not statistically.

The weight of nitrogen loaded was 15.1 pounds. Of this total, approximately 3.25 pounds of nitrogen were employed in the VCS for propellant expulsion; the remainder was used by the reaction-control subsystem in maneuvering the spacecraft.

Nitrogen Pressure Regulator

The VCS nitrogen-pressure regulator reduced the supply pressure to the desired propellant tank pressure. At a maximum nitrogen flow rate of 7 scfm, the regulated outlet pressure was 191 ± 2 psi; at a no-flow condition, the outlet pressure did not exceed 198 psi.

Connecting Lines and Valves

The connecting lines and valves between the liquid-propellant engine and the pair of oxidizer tanks included the following: an oxidizer fill valve, oxidizer vent valve, a dual squib valve, a tank and fill valve, a propellant filter, a trim orifice, and a hose connecting the oxidizer line to the engine. Corresponding components were used between the engine and the pair of fuel tanks.

Prior to actuation, the propellant squib valves were closed to seal the propellants in the tanks and prevent flow to the engine.

Stainless steel tubing with brazed fittings connected the nitrogen storage tank, pressure regulator, various valves, and the propellant tanks.

A squib-operated nitrogen valve sealed the nitrogen in its tank, preventing pressurization of the propellant tanks and reaction control thrusters until actuated by command.

A squib-operated shutoff valve was located between the VCS regulator and the nitrogen tank to terminate the nitrogen supply when all VCS activities were completed. The propellant tanks remained sufficiently pressurized for the VCS to be used even with the nitrogen supply terminated by the shutoff valve.

Electrical Interface

The VCS was a self-contained propulsion system with the exception of externally generated electrical input functions. The electrical functions are:

1) Nitrogen squib valve actuation plus backup command;
2) Propellant squib valve actuation plus backup command;
3) Engine solenoid valve control;
4) Nitrogen cutoff squib valve actuation plus backup command;
5) Engine valve heater power;
6) Tank deck heater power.

All VCS squib valves were actuated in the same manner. Actuation commands, including backup commands, were programmed in the spacecraft programmer (real-time command capability also existed). To actuate a squib valve, the switching assembly impressed a 6-volt, 50-millisecond pulse on the squib valve initiator, which then fired the main squib valve charge. Nominal squib valve firing current was 5 amperes. The valves had a rated no-fire condition of 1 ampere, 1 watt for 5 minutes.

The VCS rocket engine had individual solenoid valves to control the flow of fuel and oxidizer. In response to programmer commands, the switching assembly impressed a 21- to 31-volt signal on both valves simultaneously. Because of impedance differences, the fuel solenoid valve opened approximately 2 milliseconds ahead of the oxidizer valve. When pressurized, fuel valve opening time was 5.7 to 7.4 milliseconds, and oxidizer valve opening time was 7.8 to 9.5 milliseconds. At an impressed voltage of 28 v.d.c., the nominal power demand was 56 watts per valve. Removal of the command voltage allowed the valves to close under spring pressure. Fuel valve closing time was 4.0 to 7.5 milliseconds, and oxidizer valve closing time was 4.5 to 8.0 milliseconds.

An electrical heater was attached to the rocket engine's injector manifold to prevent the manifold and valves from becoming too cold during exposure to the space environment. The heater maintained this portion of the engine above a minimum temperature of 20°F to prevent propellant freezing. The heater was operative whenever the spacecraft was on internal power; there was no ground command function associated with the engine heater. At a nominal voltage of 28 volts, the heater power demand was 9 to 10 watts. At a minimum power of 6 watts, the heater maintained the engine valves at 44°F; at maximum power (11 watts), the valve temperature was approximately 105°F.

Four electrical heaters were attached to the VCS structure to provide additional heat input. The heaters were activated by ground command whenever temperature telemetry data (ST04) indicated a need for more heat. The heaters provided 60 watts of heat input. The actual on command was the primary propellant squib command; the off command was the squib backup command.

The VCS design and propellant selection imposed a relatively narrow operating temperature range to be provided by the passive thermal balance control. The operating temperature was 40 to 85°F. Temperatures below 35°F approach the freezing point of the fuel and could cause fractional separation of the fuel blend constituents. Temperatures above 85°F could increase tank pressures to above 236 psia, which could actuate the relief valve, thus causing a loss of nitrogen pressurant; the gas budget did not include provision for relief valve operation. The minimum temperature constraint of 20°F on the engine valves was not approached when the engine heaters operated correctly.

The telemetric parameters listed in Table 3.1-13 plus others indirectly associated with the status and condition of the subsystem were used to monitor its operation. The accelerometer output, AB05, was repeated five times in each 23.04-second telemetry frame.

Table 3.1-13: Upper Module Telemetry Parameters

CODE	PARAMETER	RANGE	ACCURACY
AP01	Nitrogen Supply Pressure	0-4000 psi	5 psi
AP02	Fuel Tank Pressure	0-250 psi	5 psi
AP03	Oxidizer Tank Pressure	0-250 psi	5 psi
AT01	Nitrogen Supply Temperature	-58 to 122°F	5°F
AT03	Engine Valve Temperature	0-252°F	5°F
AB05	Accelerometer Output	0-2200 fps	±0.1 fps
AC20	Oxidizer Valve OPEN/CLOSED	On-Off	
AC21	Fuel Valve OPEN/CLOSED	On-Off	
AC23	Tank Deck Heaters	On-Off	
AD01	Pitch Actuator Position	±3 deg	2.5 deg
AD02	Yaw Actuator Position	±3 deg	2.5 deg
ST04	Tank Deck Temperature	-13 to 100°F	5°F
ST05	Heat Shield Temperature	-13 to 100°F	5°F

NOTE: Unless otherwise indicated, telemetry accuracies are in ±% of full scale and represent data accuracy after computer processing.

3.1.5.2 PERFORMANCE

3.1.5.2.1 Summary

Prelaunch propellant and nitrogen servicing operations were conducted without incident. There were 276.79 pounds of propellant and 15.10 pounds of nitrogen loaded; the spacecraft launch weight was 852.84 pounds. Based on these weight data, the initial nominal velocity increment capability of the VCS was determined to be 1027 meters per second with a 3-sigma dispersion of 43 meters per second.

All VCS tests conducted during actual and simulated countdowns were accomplished without incident. Each countdown test consisted of a simulated 240-fps maneuver to deflect the gimbal actuators, followed by a 60-fps maneuver to recenter them.

Operation and performance of the VCS were excellent throughout the mission. The four required propulsive maneuvers were conducted without incident. These maneuvers consisted of a midcourse trajectory refinement, orbit injection, and two orbit transfers. Of the on-board velocity increment capability of 1027 ± 43 mps, 873.4 mps were expended.

One difficulty with the system was a slight internal leakage through the regulator; this developed following the orbit-injection maneuver. This leak allowed propellant-tank pressures to increase to the relief valve settings; the relief valves operated, permitting overboard venting at a rate commensurate with the influx of nitrogen. Additionally, an anomaly in the nitrogen supply pressure was observed on Telemetry Channel AP01 prior to launch. When the spacecraft was on internal (battery) power and bus voltage decayed below approximately 27.6 volts, the transducer output began to decay and fluctuate erratically. This behavior was attributed to malfunction of the voltage regulation circuit within the transducer. Refer to Appendix D for further discussion of these anomalies. Neither of these conditions were injurious to the mission. The former resulted in loss of approximately 1 pound of nitrogen that might otherwise have been available for attitude control, and the latter tended to complicate data analysis.

Figure 3.1-54 presents the quantity of nitrogen gas remaining in the storage tank throughout the primary mission. The gas weight data was calculated on the basis of the storage tank's known volume, pressure, temperature, and compressibility factor. A higher-than-budgeted gas consumption occurred between midcourse and ellipse injection; this resulted from the many spacecraft attitude maneuvers that were performed in establishing the Canopus celestial reference. Following injection, the effects of the regulator leakage on remaining nitrogen are readily apparent. Upon completion of site photography, attitude maneuvers were minimized as much as possible commensurate with requirements for antenna pointing and thermal control. During the readout phase, nitrogen was being consumed at an average rate of approximately 0.125 lb/day.

Figure 3.1-55 shows the variations in subsystem-pressure telemetry measurements during the flight. These data are plotted at 12-hour increments. The increasing propellant-tank pressure as a result of the regulator leakage was readily apparent. The decay in propellant pressure after 25 days was the result of further venting through the relief valves without gas replenishment (the shutoff squib valve had been actuated). Relief valve operation occurred because the tank deck heaters were activated on three successive orbits (during Sun occultation) in an attempt to partially discharge the batteries and reduce their temperature. These operations increased local VCS temperatures to the point where tank pressure increased to 233 to 234 psia, the relief valves allowed the excess pressure to vent overboard, followed by a gradual pressure decay to 223 to 224 psia as the system cooled and the relief valves reseated. Relief valve venting performance is discussed in more detail in Appendix D.

Analysis of flight data indicated that during the midcourse and orbit-injection maneuvers, the rocket engine delivered an average thrust of 101.3 pounds. Engine thrust during the two ellipse-transfer maneuvers was 113.6 pounds; this was higher than nominal because of high propellant-tank pressures and large ullage volume during the two transfer maneuvers. The engine specific impulse was determined to be 276 pound-seconds per pound.

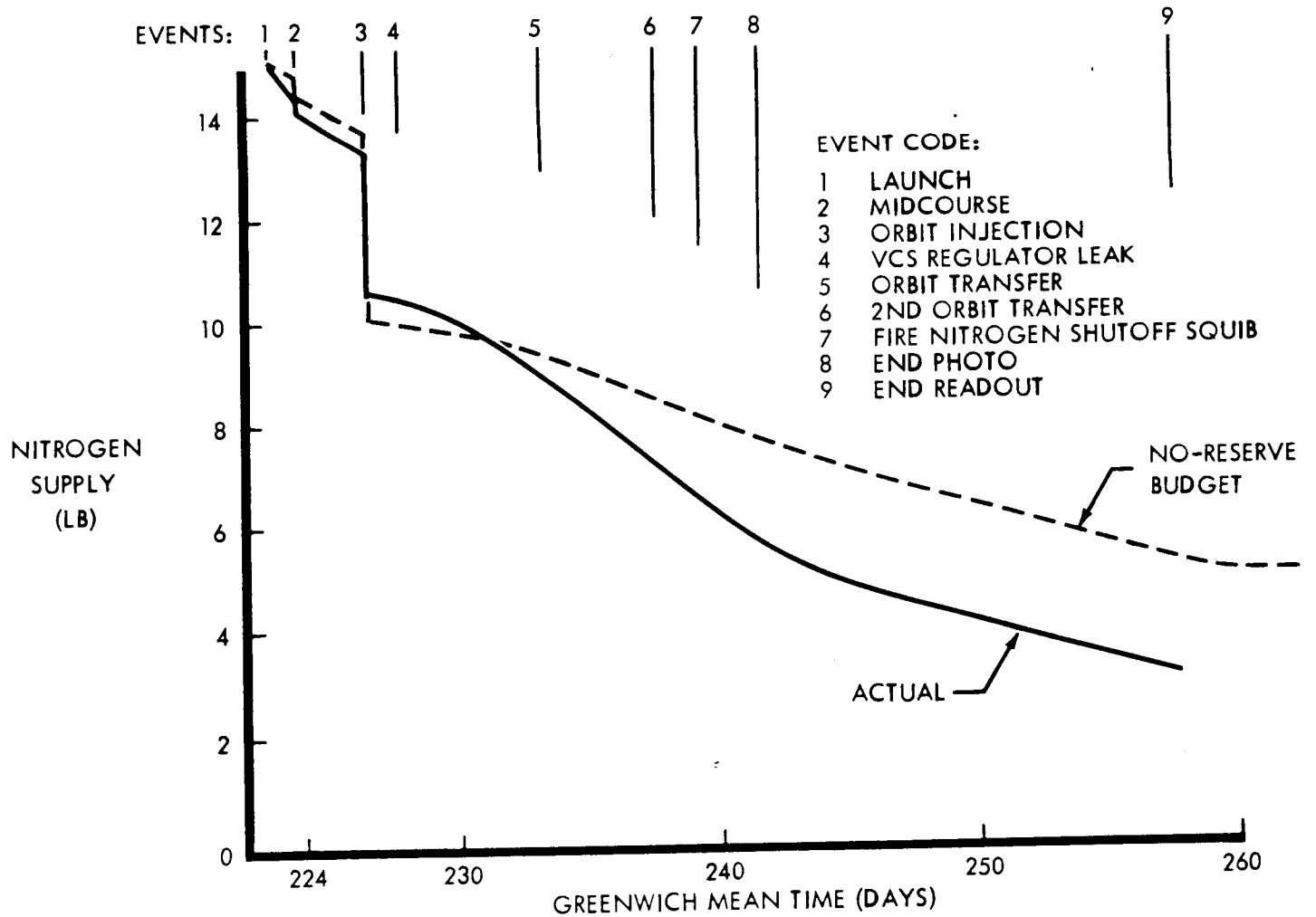

FIGURE 3.1-54: VELOCITY CONTROL SUBSYSTEM AVAILABLE NITROGEN HISTORY

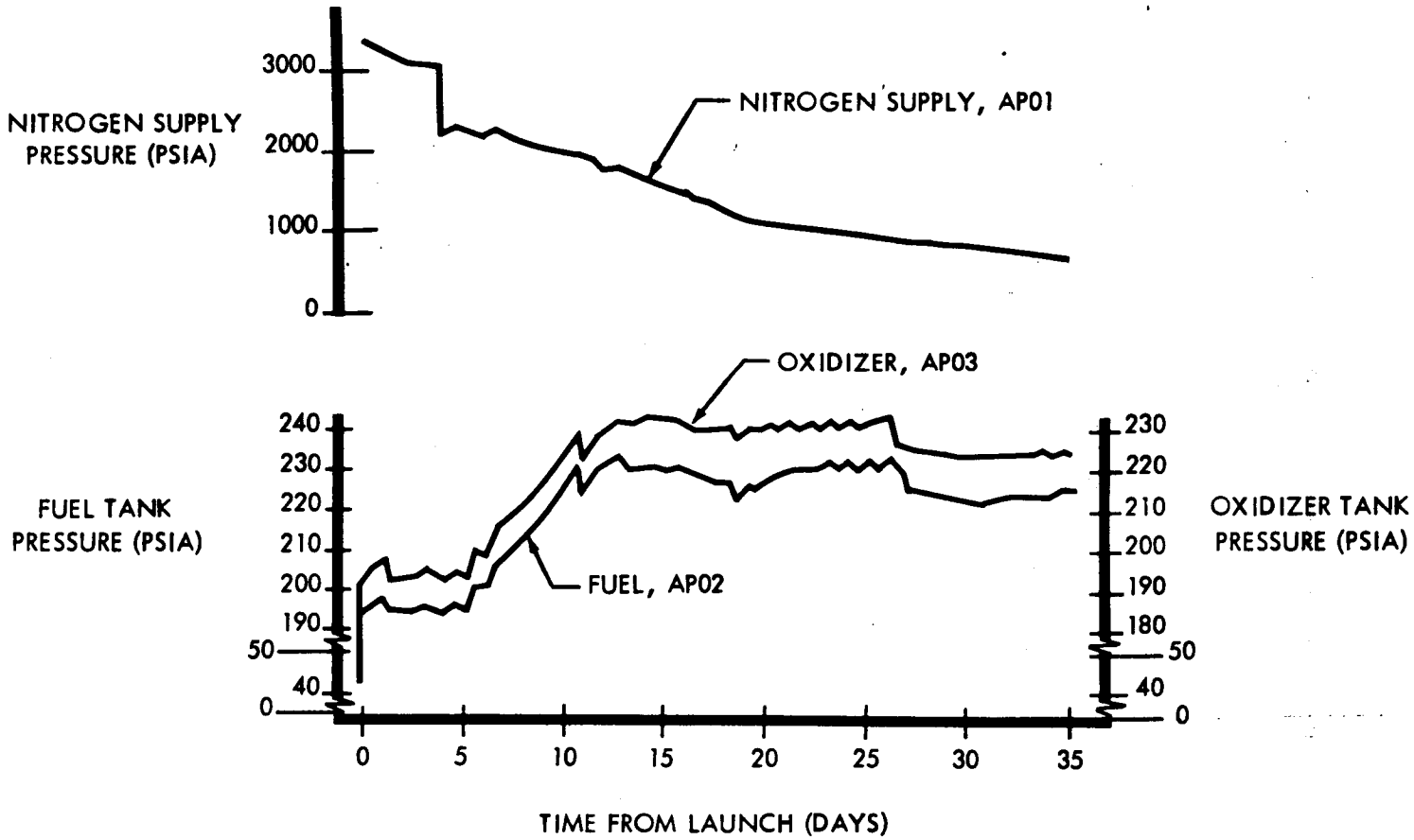

FIGURE 3.1-55: VELOCITY CONTROL SUBSYSTEM PRESSURE-TIME HISTORIES

Subsystem temperatures were somewhat different than predicted by analysis and test. During cislunar cruise, system temperatures were 10 to 15°F colder than predicted, and during lunar orbit the temperatures were 10 to 15°F warmer than predicted. System temperatures were generally in the region of 50 to 75°F throughout the flight—a satisfactory operating regime.

Figure 3.1-56 plots subsystem temperature time histories. Observe that each measurement reflects a gradually increasing thermal environment as the mission progressed, the local VCS temperatures being driven by increases in EMD temperature. Temperatures increased about 5 to 10°F during the mission; all temperatures remained well within acceptable limits. Temperature variations during a typical orbit are shown in Figure 3.1-57 where data is plotted for 10-minute intervals. The minimum temperature observed during Sun occultation condition was about 39°F as recorded by Telemetry Point ST04.

Nitrogen and propellant isolation squib valves and the nitrogen shutoff squib valve were actuated without incident.

Thrust vector control actuator performance is discussed under the attitude control subsystem.

3.1.5.2.2 Detail Description

Launch and Acquisition Phase

The successful launch countdown was initiated on August 10th. The VCS countdown test was successfully conducted at 14:05 GMT; all parameters were normal for launch. A normal launch ensued at 19:26 GMT.

Upon acquisition by DSS-41 at 20:25 GMT, it was verified that the propellant tanks had been pressurized to a nominal value of 194 psia.

Gimbal actuator positions before and after launch are listed below:

PITCH (DEGREES)		YAW (DEGREES)	
BEFORE	AFTER	BEFORE	AFTER
-0.052	-0.052	0.091	0.091

Cislunar Phase

As a result of thermal stabilization, tank pressures gradually increased to a stable value of 196 psia, at approximately 21:00 GMT.

Bleeding the propellant lines between the engine and the then-closed propellant squib valves occurred at 19:06 GMT on August 11th. Engine valves were opened for 30 seconds, thereby increasing valve temperature by 10.5°F as expected.

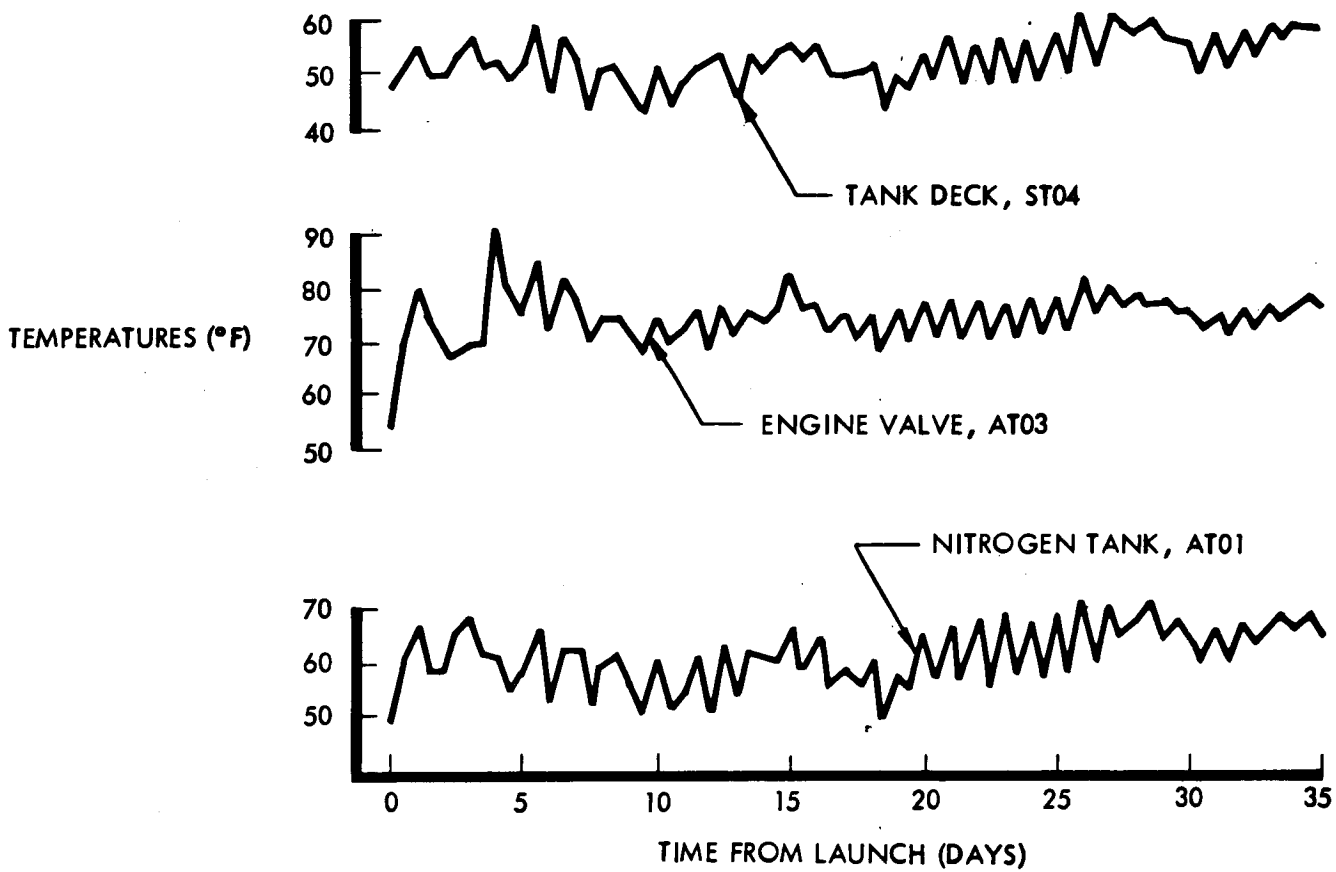

FIGURE 3.1-56: VELOCITY CONTROL SUBSYSTEM TEMPERATURE-TIME HISTORIES

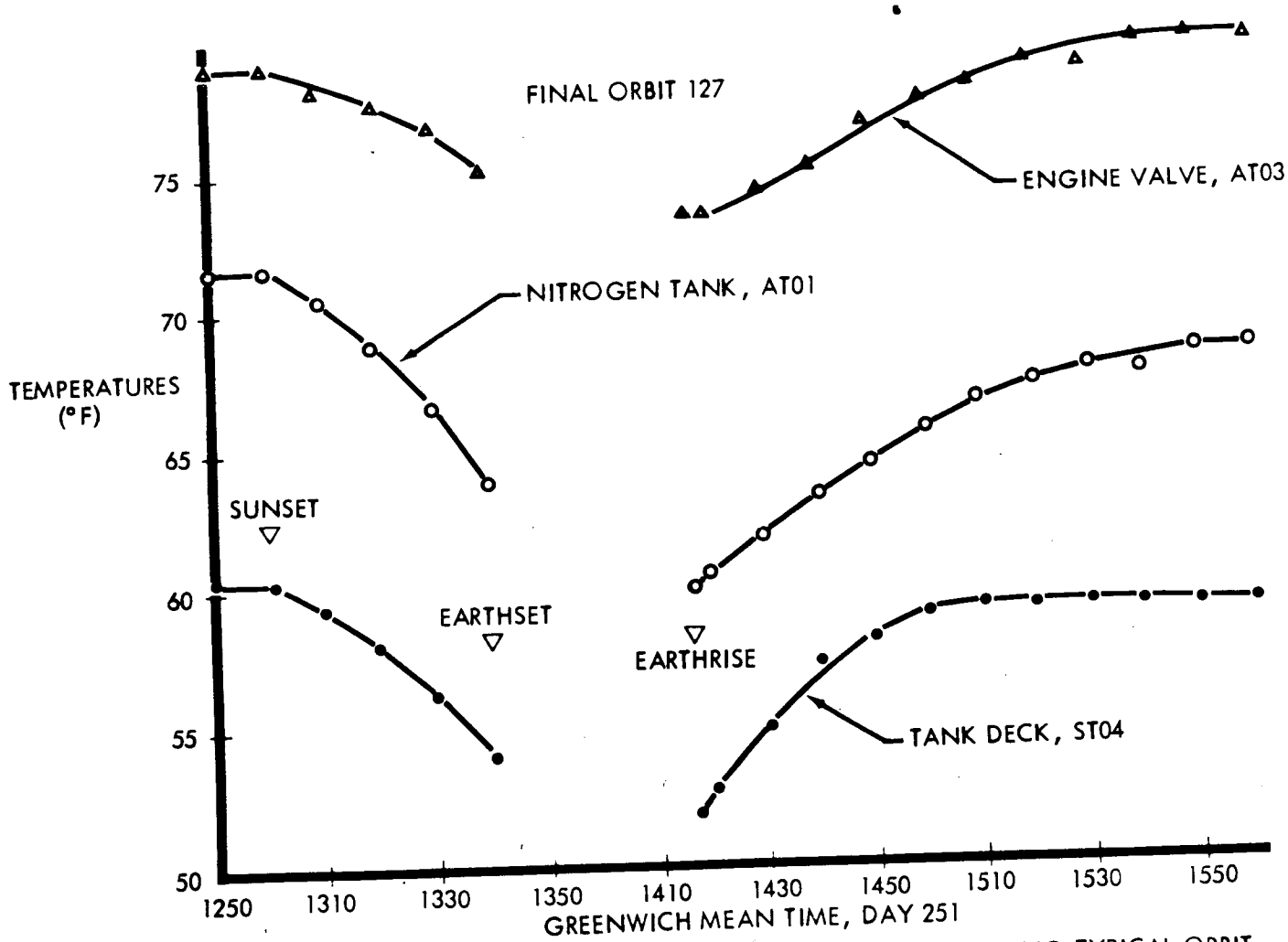

FIGURE 3.1-57: VELOCITY CONTROL SUBSYSTEM TEMPERATURES DURING TYPICAL ORBIT

Preparation for the midcourse maneuver commenced at 23:49 GMT with activation of the propellant isolation squib valves. Positive confirmation of valve actuation was received when propellant tank pressures decayed 4 to 6 psi (the ullage volume increased as propellant filled the downstream lines).

The midcourse maneuver for trajectory adjustment was conducted at 24:00:00 GMT Aug. 11, without incident; actual engine operation parameters compared with predicted values are shown below.

MIDCOURSE	VELOCITY CHANGE (MPS)	BURN TIME (SEC)	THRUST (LB)	SPECIFIC IMPULSE (LB-SEC/LB.)
Prediction	37.8	32.7 ± 1	99.8	275.2
Actual	37.8	32.1	101.6	276

Actual performance data are calculated results. By knowing spacecraft weight and determining engine operating time and final acceleration from telemetry data, the analytical approach was to assume a specific impulse and calculate a final acceleration value. Iterations were performed to converge calculated and actual acceleration, thereby determining average engine thrust level and specific impulse. It is these values that are reflected above.

The engine valve temperature after thermal soak-back reached a maximum of 96°F following the midcourse maneuver.

Gimbal actuator positions before and after the midcourse maneuver are listed below. It should be noted that the trend in actuator position from one maneuver to the next reflects the motion of spacecraft center of gravity.

PITCH (DEGREES)		YAW (DEGREES)	
BEFORE	AFTER	BEFORE	AFTER
-0.052	-0.466	0.068	0.021

Ellipse Phase

The ellipse-injection maneuver performed Aug. 14 at 15:34 GMT was completely successful and in all aspects essentially as programmed. Engine operating time was calculated to be 578.7 seconds; engine valve temperature was 69°F during engine operation, reaching a maximum value of 106°F approximately 1.5 hours following the maneuver. Actual results compared with predictions were as follows:

INJECTION	VELOCITY CHANGE (MPS)	BURN TIME (SEC)	THRUST (LB)	SPECIFIC IMPULSE (LB-SEC/LB)
Prediction	790.0	588.3 ± 10	99.75	274.7
Actual	789.7	578.7	101.3	276

It was possible to infer an average operating mixture ratio; this was accomplished by adjusting flight conditions with the proper influence coefficients, and then comparing the results with engine acceptance test data. From the ellipse-injection maneuver, the estimated operation mixture ratio was found to be 2.01 to 1.98, depending on interpretation of local temperatures.

DSIF tracking data for the orbit-injection maneuver were analyzed to evaluate velocity maneuver accuracy. Spacecraft telemetry data do not verify the accuracy of a velocity maneuver—only that the flight programmer has properly counted a specific number of accelerometer pulses. (The accelerometer could produce a "fast" or "slow" count, and spacecraft telemetry would indicate a proper maneuver whereas tracking data would not.) The tracking data analysis used Orbital Determination Solution 4138. This state vector solution had an epoch about 20 minutes after the predicted end of burn (good tracking data was not available during this 20-minute period). The state vector was integrated backward to the postmaneuver estimate of thrust-termination time.

The resulting comparison of orbital parameters at this point provides an indication of the accuracy of the maneuver:

	OD 4138 INTEGRATED BACKWARD	PREDICTED END OF BURN	DIFFERENCE
Radius (km)	2846.8011	2846.1140	0.6871
Velocity (km/sec)	1.2929086	1.2928321	0.0000765
Azimuth (deg)	64.737171	64.806885	0.069714
Flight Path Angle (deg)	-17.567870	-17.565204	0.002666

The velocity difference tabulated above is less than the ±0.1-meter-per-second uncertainty in velocity determination from tracking data. The uncertainty, therefore, must be regarded as the limit of possible accelerometer error. Thrust-vector pointing error during the maneuver is indicated by the position and direction differences noted.

Figures 3.1-58 and 3.1-59 present VCS telemetry data during the orbit-injection maneuver, Figure 3.1-58 shows pressure and temperature data, and Figure 3.1-59 plots dynamic data in the form of gimbal actuator position and accelerometer output. Gimbal actuator position before and after the injection maneuver were as follows:

PITCH (DEGREES)		YAW (DEGREES)	
BEFORE	AFTER	BEFORE	AFTER
-0.466	-0.695	0.021	0.114

Nitrogen supply pressure is not shown in Figure 3.1-58 because of a transducer anomaly. Rather marked fluctuations in propellant tank pressures were observable during the first 3 minutes of operation. This cyclic behavior was attributed to longitudinal propellant sloshing coupled with the small ullage volume that existed at initiation of the maneuver.

Similar characteristics have been observed during the propellant tank longitudinal vibration test. The periodic 1-psi variations in oxidizer pressure later in the maneuver are the result of telemetry system resolution. Note that the engine valve temperature remained essentially constant throughout the injection maneuver; i.e., 68 to 69°F. This was to be expected on the basis of engine testing with cool (55°F) propellants. The maximum valve temperature following the maneuver and resulting from thermal soak-back was 106°F.

Approximately 30 hours after injection, telemetry data indicated that propellant tank pressures were slowly increasing. It became apparent that the VCS nitrogen regulator had developed an internal leak. This increasing pressure continued (with an interruption caused by the orbit-transfer maneuver) until approximately 20:00 GMT on August 22nd. At that point, the fuel-tank pressure relief valve became unseated, allowing incoming leakage flow to vent overboard. Leakage into the VCS continued until 05:45 GMT on August 27th when the nitrogen shutoff squib valve was actuated. This leakage anomaly is more fully discussed in Appendix D.

The maneuver to transfer to the second ellipse was conducted at 09:49:59.7 GMT on August 21st. The desired velocity change of 40.2 mps was achieved with an engine operating time of 22.4 seconds. Tracking data indicated that the desired perilune altitude was achieved with an error of less than 0.5 km. Actual results compared with predictions were as follows:

TRANSFER	VELOCITY CHANGE (MPS)	BURN TIME (SEC)	THRUST (LB)	SPECIFIC IMPULSE (LB-SEC/LB)
Prediction	40.15	22.7 ± 1.6	112.6	274.5
Actual	40.2	22.4	113.6	276

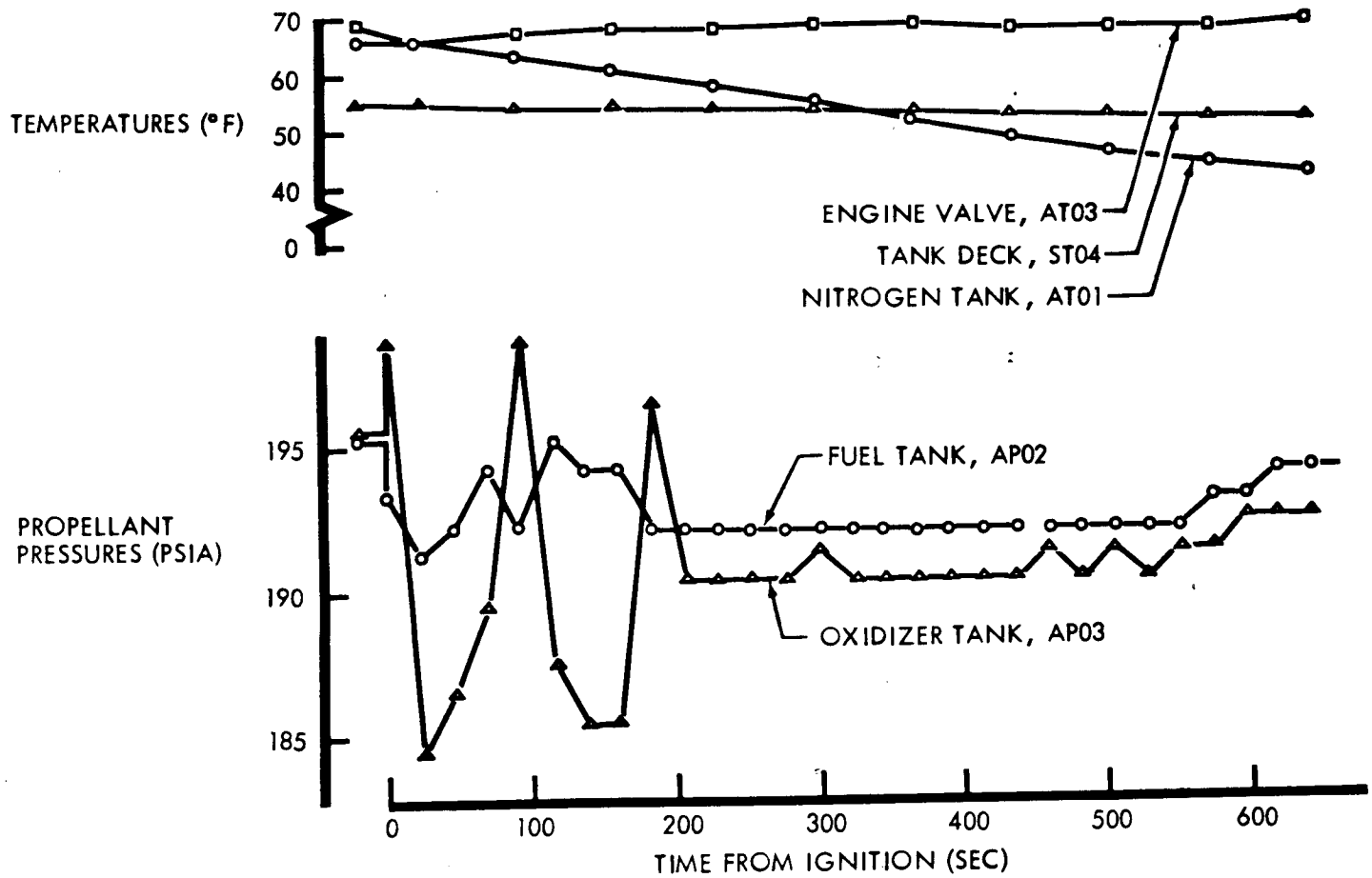

FIGURE 3.1-58: VELOCITY CONTROL SUBSYSTEM ORBIT INJECTION MANEUVER SYSTEM PRESSURES AND TEMPERATURES

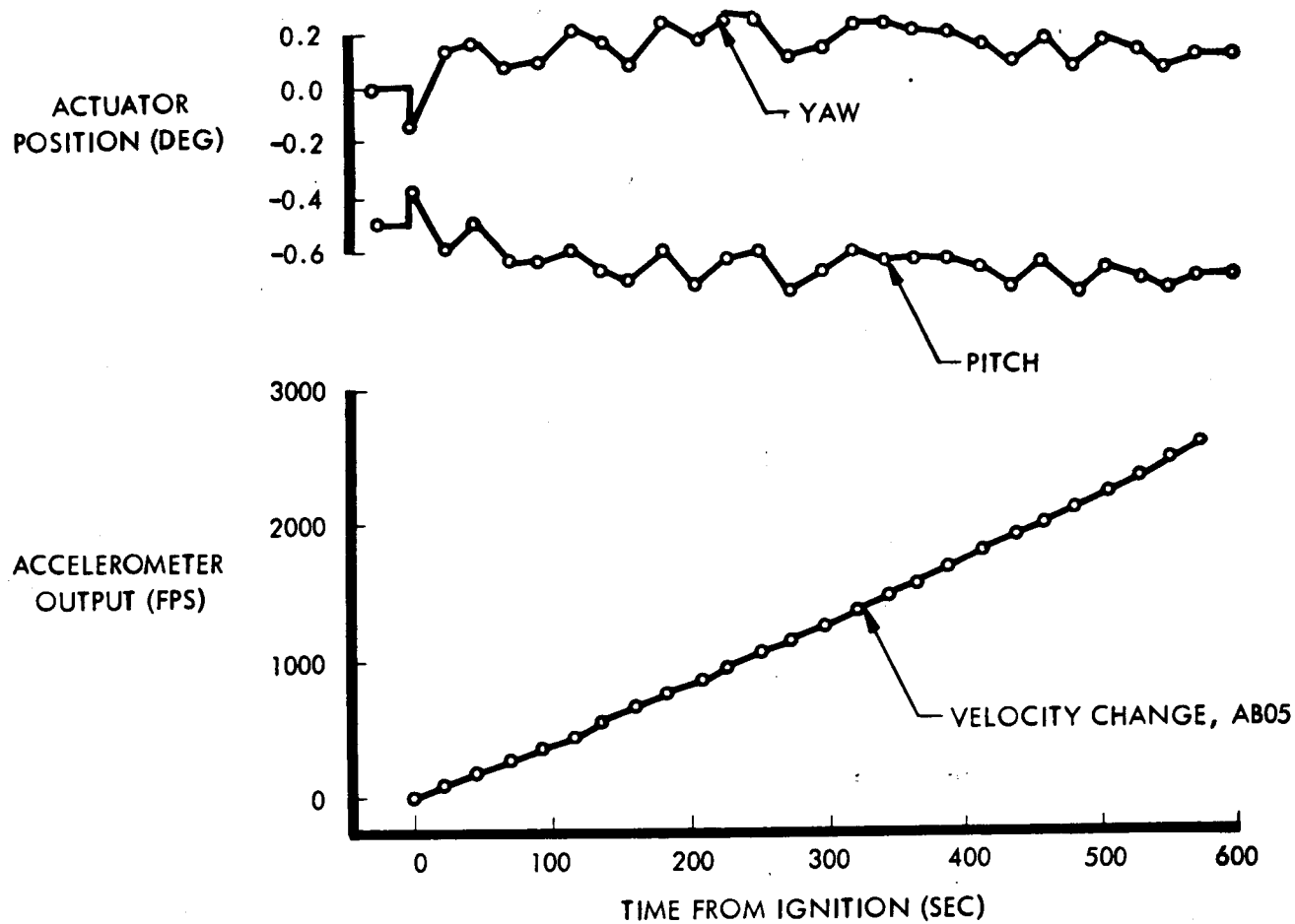

FIGURE 3.1-59 VELOCITY CONTROL SUBSYSTEM ORBIT INJECTION MANEUVER SYSTEM DYNAMICS

The maximum engine valve temperature resulting from soakback may have been reached during Earth occult; however, the highest recorded temperature was 106°F.

Thrust vector control actuator positions before and after the maneuver to transfer to the second ellipse are listed below:

PITCH (DEGREES)		YAW (DEGREES)	
BEFORE	AFTER	BEFORE	AFTER
-0.673	-0.764	0.138	-0.048

An ellipse-adjustment maneuver was performed at 16:01:29 GMT on August 25th to reduce the perilune still further (to approximately 40 km). The programmed velocity change of 5.4 mps was achieved with an engine operating time of 3.0 seconds. Tracking data again indicated an error of less than 0.5 km in the achieved perilune altitude. Actual results compared with predictions were as follows:

ELLIPSE ADJUSTMENT	VELOCITY CHANGE (MPS)	BURN TIME (SEC)	THRUST (LB)
Prediction	5.43	3.0 ± 1	114
Actual	5.4	3.0	113.6

Since this burn was of such short duration, the maximum engine valve temperature following soakback was only 87°F.

Gimbal actuator positions before and after the adjustment maneuver were as follows:

PITCH (DEGREES)		YAW (DEGREES)	
BEFORE	AFTER	BEFORE	AFTER
-0.764	-0.604	-0.048	-0.303

As summarized in Table 3.1-14 propellant tank heaters were activated on seven occasions for a total on time of 698 minutes. The three latter activations were during Sun occultation in an attempt to alleviate high battery temperatures.

These heater activations raised temperatures and propellant pressures sufficiently to cause further propellant tank relief-valve action. With no further heater activations, the local VCS temperatures decayed, and propellant pressures decayed to approximately 223 to 224 psia. The propellant tank pressures stabilized at this value on (approximately) September 8th.

Table 3.1-14: Propellant Heater Activation Summary

ON	OFF	TIME
227/0302	0532	150 min.
227/2248	2342	54
228/0425	0656	151
229/0218	0444	146
248/1626	1731	65
248/1952	2057	65
248/2314	249/0021	67 min.

3.1.6 STRUCTURES AND MECHANISMS SUBSYSTEM

3.1.6.1 FUNCTIONAL DESCRIPTION

3.1.6.1.1 Summary

The basic spacecraft structure was three decks with tubular truss and arch between the lower decks and semi-monocoque cone structure to the upper deck. Equipment items were mounted within the frame. Hinged to the equipment mount deck were four solar panels, a 3-foot-diameter high-gain antenna, and a low-gain antenna that were deployed after injection into the cislunar trajectory.

Mechanisms included fluid-damped spring-operated actuators used to deploy the antennas and solar panels, a step-actuated motor and gears for operation of the camera thermal door, gimbaled support at the engine deck for the velocity control engine, and squib-actuated pin-release devices for the antennas and solar panels.

Thermal control consisted of paints and surfaces designed to provide equipment environmental temperatures by radiant and conductive heat interchange. To reduce radiation to deep space, the spacecraft was enclosed by a thermal barrier from the engine deck to the equipment mount deck (EMD). A heat shield protected the engine deck from high temperatures generated by the engine.

Interface items consisted of accelerometer instrumentation, electrical wiring and breakaway connector, and mating surfaces and clearances for the Agena adapter and shroud.

3.1.6.1.2 Detail Description

Structure

The spacecraft structure consisted of an equipment mounting deck, a tank deck, and heat shield and engine deck and interconnecting support structure. The location of these decks and the associated station designation is shown in Figure 3.1-60.

The equipment mounting deck (EMD) located at STA 237 had a structural ring with a stiffened web and provided:

1) Equipment mounting provisions;
2) An interface with Agena D adapter ring and separation V-band clamping blocks;
3) Support for the antennas and solar panels and the deployment mechanism;
4) Thermal control heat transfer surface;
5) Attachment provisions for thermal barrier.

The tank deck (STA 202.3 - 204.5) had a stiffened integrally machined frame and provided:

1) Mounting provisions for the fuel and oxidizer tanks, the nitrogen gas storage pressure vessel, and subsystem components;
2) Mounting provisions for support and release mechanism for the stowed high-gain antenna;
3) Mounting provisions for twenty micrometeoroid detectors.
4) Attachment provisions for the thermal barrier.
5) Mounting for the camera thermal door mechanism.

The heat shield and engine deck (STA 179) had an insulated, bead-stiffened plate with the engine supported by a gimbal ring and provided:

1) Mounting provisions for the velocity control engine gimbal and components;
2) A heat shield to insulate the spacecraft from the high temperatures generated by the velocity control engine;
3) Mounting provisions for attitude control low-level thrusters;
4) Mounting provisions for the support and release mechanism for the stowed low-gain antenna;
5) Ground handling attachment location;
6) Attachment provisions for thermal barrier;
7) Lateral support for the tops of propellant tanks;
8) Support for Sun sensors.

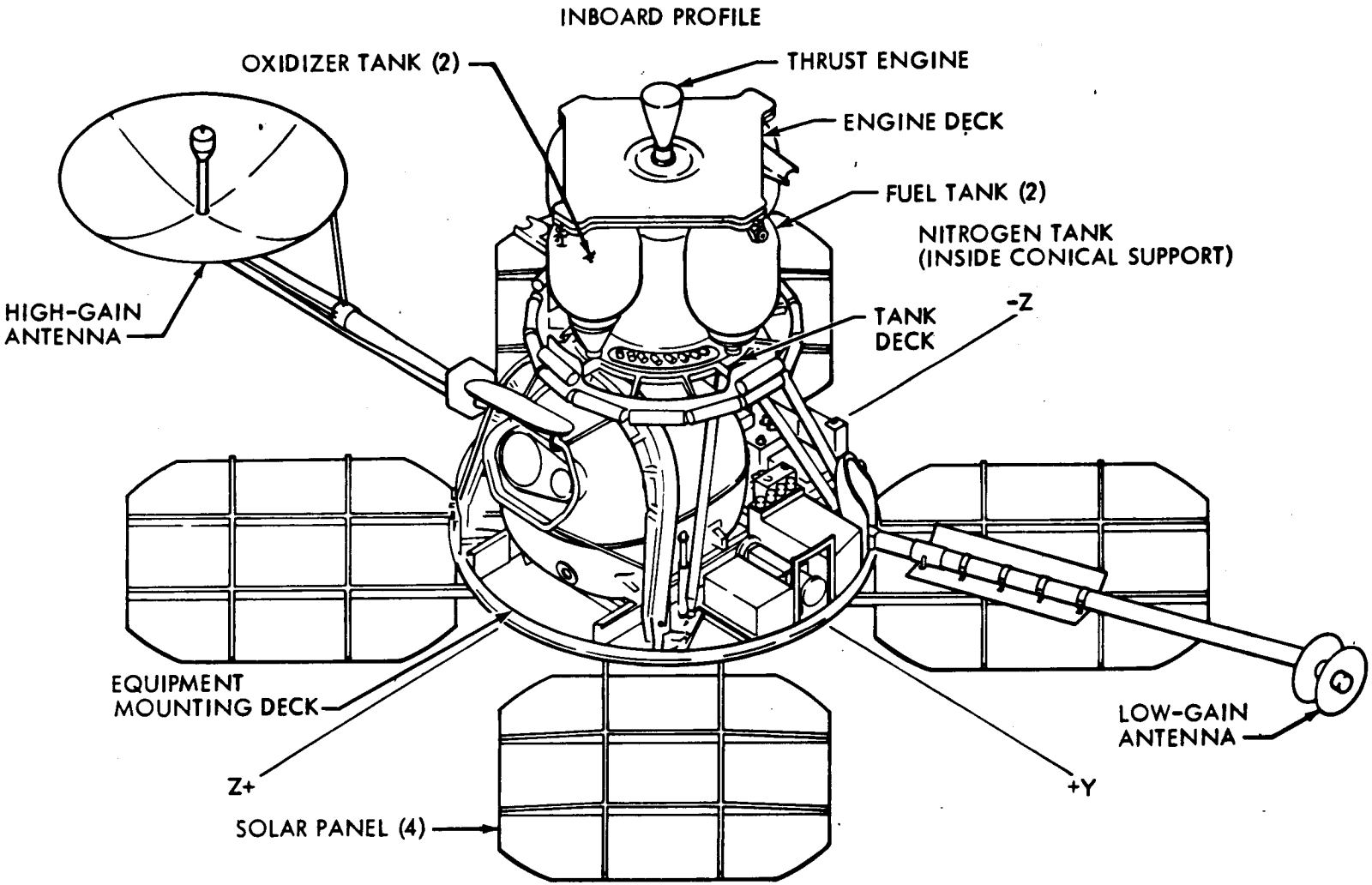

FIGURE 3.1-60: DECK LOCATIONS

The primary truss structure (STA 202 - 237) had a tubular pinned-end truss and arch, for maximum access to the equipment on the equipment mounting deck. The truss and arch provided:

1) The structural attachment between the equipment mounting deck and the tank deck;

2) Support for tubing and wire runs between the decks;

3) A thermal capacitance sink for dampening temperature transients;

4) Support for camera thermal door and frame.

The support structure (STA 179 - 202) consisted of a truncated cone and cylinder with cutouts for access to the velocity control subsystem components. It provided:

1) The structural attachment between the engine deck and tank deck;

2) A thermal capacitance sink for dampening temperature transients;

3) Support for tubing and wire runs between the decks;

4) Support for subsystem components;

5) Support for gimbaled engine actuators.

Instrumentation was provided for measuring temperature.

Mechanisms

Mechanisms included the deployment mechanism for the solar panels, antennas, the movable engine thrust vector control mount, and the camera thermal door.

Solar panels—The solar panels were locked in the stowed position with two electrically initiated ordnance-actuated pin-release mechanisms. Each solar panel was deployed by an internally damped spring actuator and held deployed by latches. Solar panel deployment sequence mechanical interlocks were provided.

High- and low-gain antennas—The antennas were locked in the stowed position with electrically initiated ordnance-actuated pin-release mechanisms. They were deployed and held deployed by separate internally damped spring actuators identical to those used on the solar panels.

Movable engine mount—A gimbaled mount was provided to allow thrust vector control of the rocket engine. The gimbaled mount was permitted motion in two directions with respect to the spacecraft upper structure. The hinge center lines were on the Y and Z axes and were parallel to the Y-Z plane.

Instrumentation—Instrumentation was provided for indicating the deployed position of the solar panels, high- and low-gain antennas, and the camera thermal door "open" position.

Camera thermal door—The camera thermal door provided an opening in the thermal barrier to uncover the camera lenses during picture taking and to protect the camera from thermal exposure when not in use. The door frame was supported from the arch by four tubular struts. The door was hinge-connected to a drive unit composed of a gear train and a d.c. stepper motor.

Tank heaters—Four tank heaters were mounted on the cone structure (STA 179 - 202), one adjacent to each fuel and oxidizer tank. The tank heaters were controlled by the fuel and oxidizer squib valve commands and circuitry after the squibs had been fired. Instrumentation was provided to indicate tank heater power ON or OFF.

Flight vibration accelerometers—One accelerometer was installed on the EMD, sensing in the X-axis, and another on the tank deck, sensing in the Z-axis. The signals from these accelerometers were transmitted via launch vehicle telemetry to ground receivers during the period from launch through spacecraft separation.

Spacecraft Integration Elements

Components and functions of the spacecraft integration elements were:

1) Electrical wiring that provided electrical interconnection of spacecraft subsystems;

2) Ordnance that provided devices for release of antennas, solar panels, and operation of the valves for velocity and attitude control subsystem pressurization;

3) Thermal control that provided controlled environment for spacecraft subsystems.

Electrical wiring—The electrical wiring consisted of the connectors, multiple conductor cables, and coaxial cables used to conduct signals and power between the spacecraft electrical and electronics equipment and to the electrical inflight disconnect receptacle (GFE) at the Agena adapter interface.

Ordnance—The ordnance devices consisted of an ordnance cartridge in combination with a pin release mechanism or in combination with a valve actuation mechanism. These devices were used as follows:

	Mechanism Quantity	Cartridge Quantity	Bridgewire Per Cartridge
1) Pin release mechanism type			
a) To deploy solar panels	2	2	2
b) To deploy low-gain antenna	1	1	2
c) To deploy high-gain antenna	1	1	2

	Mechanism Quantity	Cartridge Quantity	Bridgewire Per Cartridge
2) Valve actuation mechanism type			
a) To open nitrogen squib valves	1	2	1
b) To open oxidizer squib valves	1	2	1
c) To open fuel squib valves	1	2	1
d) To close nitrogen shut-off valve	1	1	2

Each ordnance cartridge contained two bridgewire circuits that provided redundant capability of electrically initiating the charge to allow operation of the mechanism. Each ordnance device that was installed as a single unit in any ordnance-actuated device had redundnat firing circuits and bridge wires. Each ordnance device that was installed as one of a pair of any ordnance-actuated device had one bridge wire connected to a firing circuit.

Thermal Control

Thermal control elements consist of (1) the thermal barrier, (2) the equipment mounting deck (EMD) heat exchange, (3) the heat shield insulation, (4) the thermal coatings, and (5) the protrusions protection or isolation. The thermal control operated by controlling heat transfer to or from the EMD through the thermal barrier and the heat shield and between the parts of the spacecraft. The control was passive, preset, and static. Heat flow was directed through predetermined paths to keep the balance of heat received from the Sun, heat generated in the equipment, and heat lost by radiation into deep space within desirable limits throughout the mission. The net effect of the isolation and single surface thermal coating of low solar absorptivity to infrared emissivity ratio (α_S/ϵ_{IR}) was to produce an average design internal spacecraft temperature and average EMD temperature of 35 to 85° F. (Values are nominal—local areas exceeded these limits under some conditions).

Thermal barrier—The thermal barrier completely enclosed the spacecraft between the heat shield and the equipment mounting deck and provided a nearly adiabatic spacecraft boundary. The barrier was a multilayer, aluminized-mylar membrane with a highly reflective coating on the interior surfaces and a special solar heat protective coating on the exterior.

Equipment mounting deck (EMD) heat exchange—The EMD provided the primary means of heat exchange. The heat transfer across this deck was controlled by applying surface coatings to obtain the required absorptivity-to-emissivity value. Heat-generating electronic equipment boxes were attached to the EMD to ensure the desired thermal connection. Careful design of thermal joints provided suitable joint areas and contact pressures and involved use of indium foil in critical applications.

Heat shield insulation—The engine heat shield protected the spacecraft internal components from radiated heat loads generated by the velocity control engine. It insulated above the deck by means of a multilayered foil-screen laminate. The shield also provided insulation to reduce heat transfer out of the spacecraft when the velocity control engine was not operating.

Thermal coatings—Most metallic parts inside the thermal barrier were coated with a non-reflective black paint to produce near black-body emissivity. The good thermal coupling of all spacecraft major masses maintained even equipment temperatures and precluded fast temperature change.

Protrusions—The protrusions were those parts of the spacecraft that extended through the thermal barrier, the EMD, or the heat shield. These included the high- and low-gain antennas, hinges and support bracket, the velocity control engine, the camera thermal door, micrometeoroid detectors, shunt power transistors, solar panel hinges, actuators, attitude control nozzles, and Sun sensors. Thermal losses from these protrusions were controlled by isolation of the protrusion from prime structure.

3.1.6.2 PERFORMANCE

3.1.6.2.1 Summary

Spacecraft structures performed as planned by producing a stable, rigid platform for the equipment, and for extension of the antennas and solar panels. Actuation of solar panels and antennas, opening and closing of the camera thermal door, and operation of the pin-release ordnances were performed as planned and programmed during all phases of spacecraft operation.

Agena telemetry covering launch through Agena second cutoff indicated that the EMD launch vibrations were substantially lower than the vibration levels recorded during flight acceptance tests (FAT).

Spacecraft temperatures were maintained within functional equipment limits during the mission by orienting the spacecraft off the Sun. The amount of off-Sun operation was programmed by the required balance of EMD temperature and allowed reduction in electrical power input from the solar panels.

There were no micrometeoroid hits recorded during the entire mission.

3.1.6.2.2 Performance Details

Boost and Acquisition Phase

Structures and mechanisms components performed almost as planned. Actuation of pin-release ordnance mechanisms for the deployment of the antennae and the solar panels occurred approximately 45 minutes 17 seconds after liftoff and was verified by telemetry a few minutes later when the spacecraft was acquired by Woomera (DSS-41).

Vibration data recorded from Agena telemetry at liftoff to Agena separation was substantially lower than recorded during flight acceptance level tests. Lateral acceleration data was not obtained on Agena Channel 12 due to malfunction (source unknown) in the instrumentation. The output of the thrust (longitudinal) accelerometer located on the EMD was telemetered satisfactorily via Agena Channel 13. The oscillatory and nonoscillatory components are shown as data points in Figures 3.1-61 and 3.1-62, together with data from the liftoff record and a few data points from filtered records. For comparison, the upper envelope of the response of the same accelerometer to the spacecraft sine FAT vibration is overlaid. Most of the vibration data points fall well below the FAT envelope. The only oscillatory components that exceeded the FAT envelope were from BECO and Agena second cutoff. The 19-H_Z second cutoff data point was a single cycle of oscillation. It represented the EMD fundamental-mode rebound and was obviously highly damped. The 72-H_Z second cutoff data point was the peak value of six cycles of oscillation and represented a higher-mode response of the EMD to the cutoff transient. The 61-H_Z BECO measurement is replotted in Figure 3.1-63 along with the torsion test data at the same location from the qualification test (QT) spacecraft. The flight response was one-tenth the QT pulse response and less than half the torsion sweep test response.

Acceleration power spectra are shown in Figure 3.1-64, liftoff and transonic, and Figure 3.1-65, Agena burn. The power spectra are plotted out to 800 H_Z; however, the calibration is uncertain above 220 H_Z, the nominal limit of the telemetry channel. The response of the same accelerometer to the spacecraft 6-g random test (1/3 of full FAT) is overlaid in Figure 3.1-64, together with Lunar Orbiter I sonic test response at the same location. The flight responses were less than the test curves.

The EMD thermal coating provided a higher temperature heat sink than expected. (See thermal control anomaly discussion, Appendix D). Measured data from paint coupons prepared at the time the EMD was painted gave indication that the ratio of solar absorptivity to infrared emissivity ($\alpha s/\epsilon ir$) would produce an EMD average temperature lower than occurred on Lunar Orbiter I. Figure 3.1-66 shows FAT level temperatures as compared to Lunar Orbiter I flight data. Degradation of the paint that occurred at a high rate during the initial phases of flight appears to be due to space effects not simulated in the laboratory.

Cislunar Phase

The pitch maneuver (minus 25.2 degrees) executed for the midcourse correction reduced both the EMD temperature (as telemetered by ST03) and the tank deck temperature (ST04) by a few degrees. The spacecraft was pitched off the Sun for about 12 minutes.

ST03 was used as the criterion for thermal control of the spacecraft electronics. Orientation of the spacecraft off the Sun effectively controlled the spacecraft temperature levels and resulted in EMD temperature changes as shown in Figure 3.1-67.

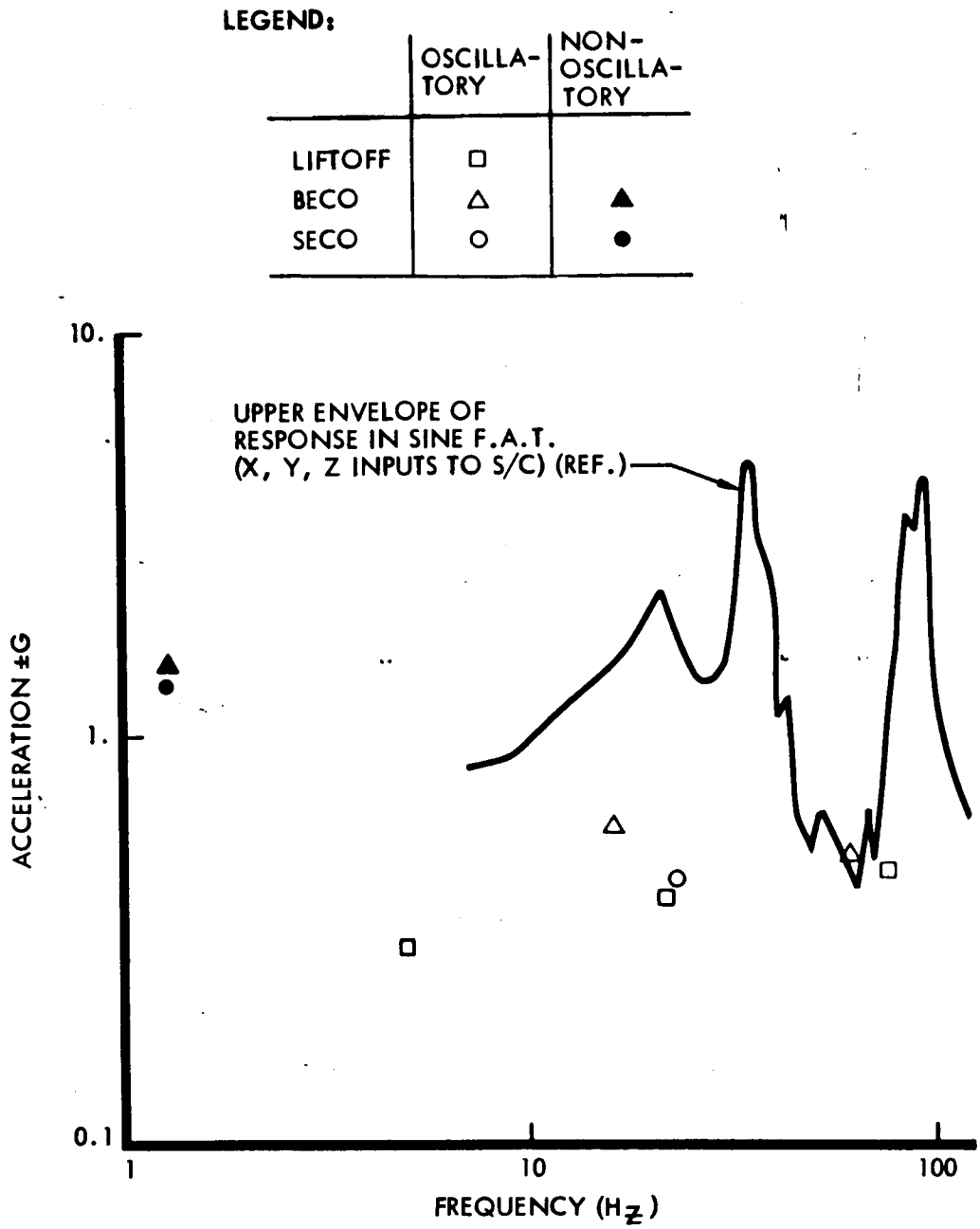

FIGURE 3.1-61: TRANSIENT AND QUASI-SINE COMPONENTS OF EMD ACCELERATIONS — ATLAS PHASE

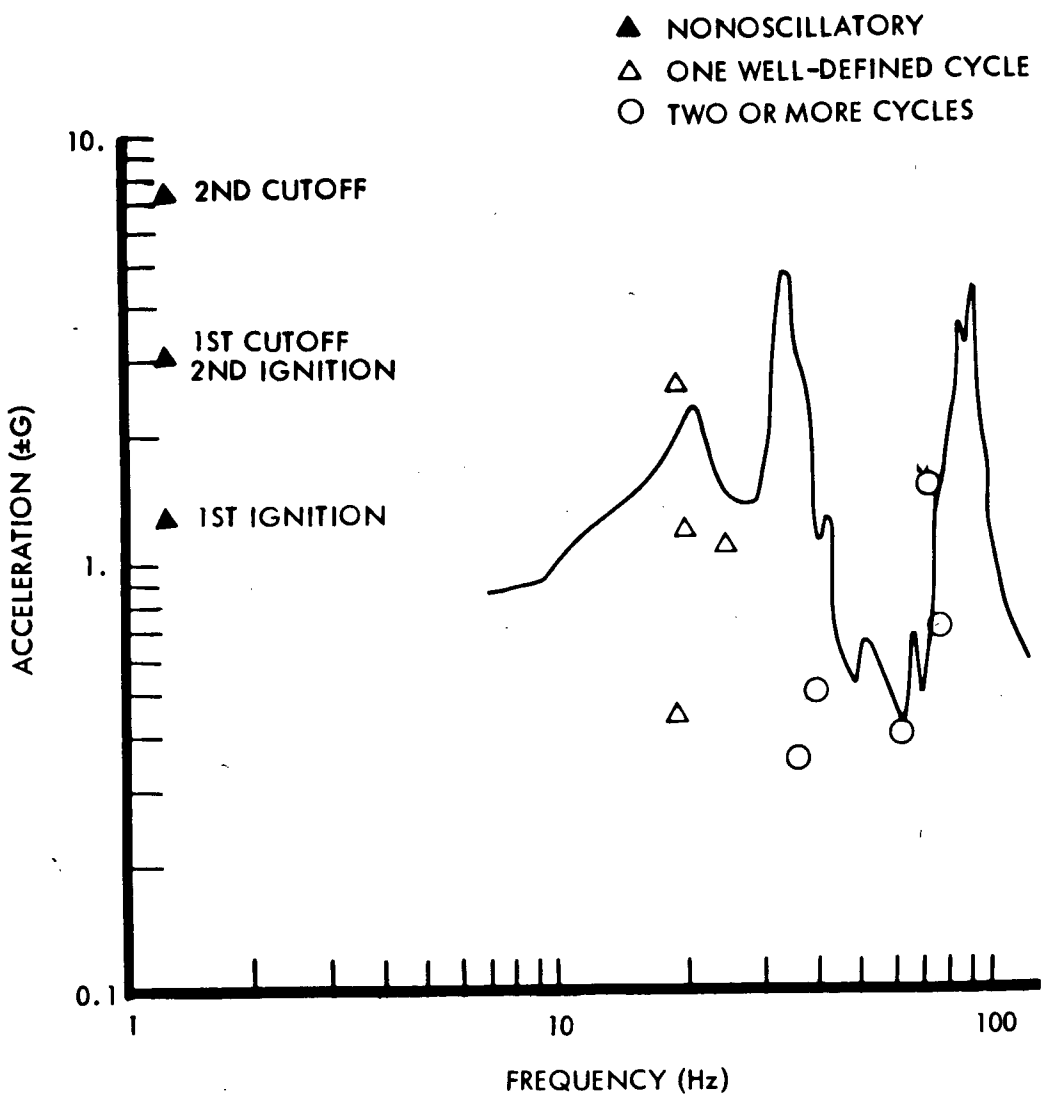

FIGURE 3.1-62: TRANSIENT AND QUASISINE COMPONENTS OF EMD ACCELERATION — AGENA PHASE

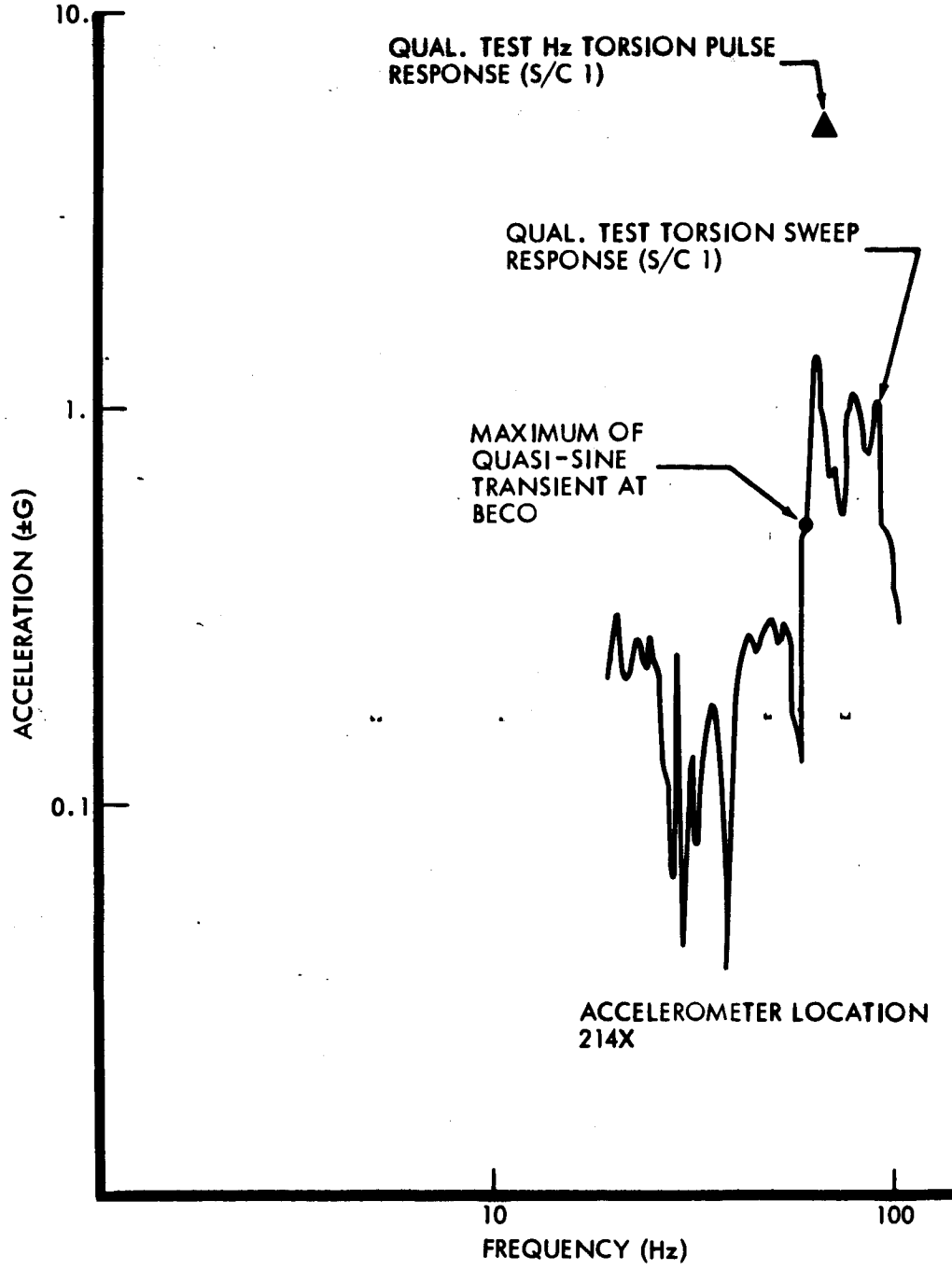

FIGURE 3.1-63: EMD LAUNCH VIBRATION AT BECO, COMPARED TO SPACECRAFT 1 TORSION TEST RESPONSE

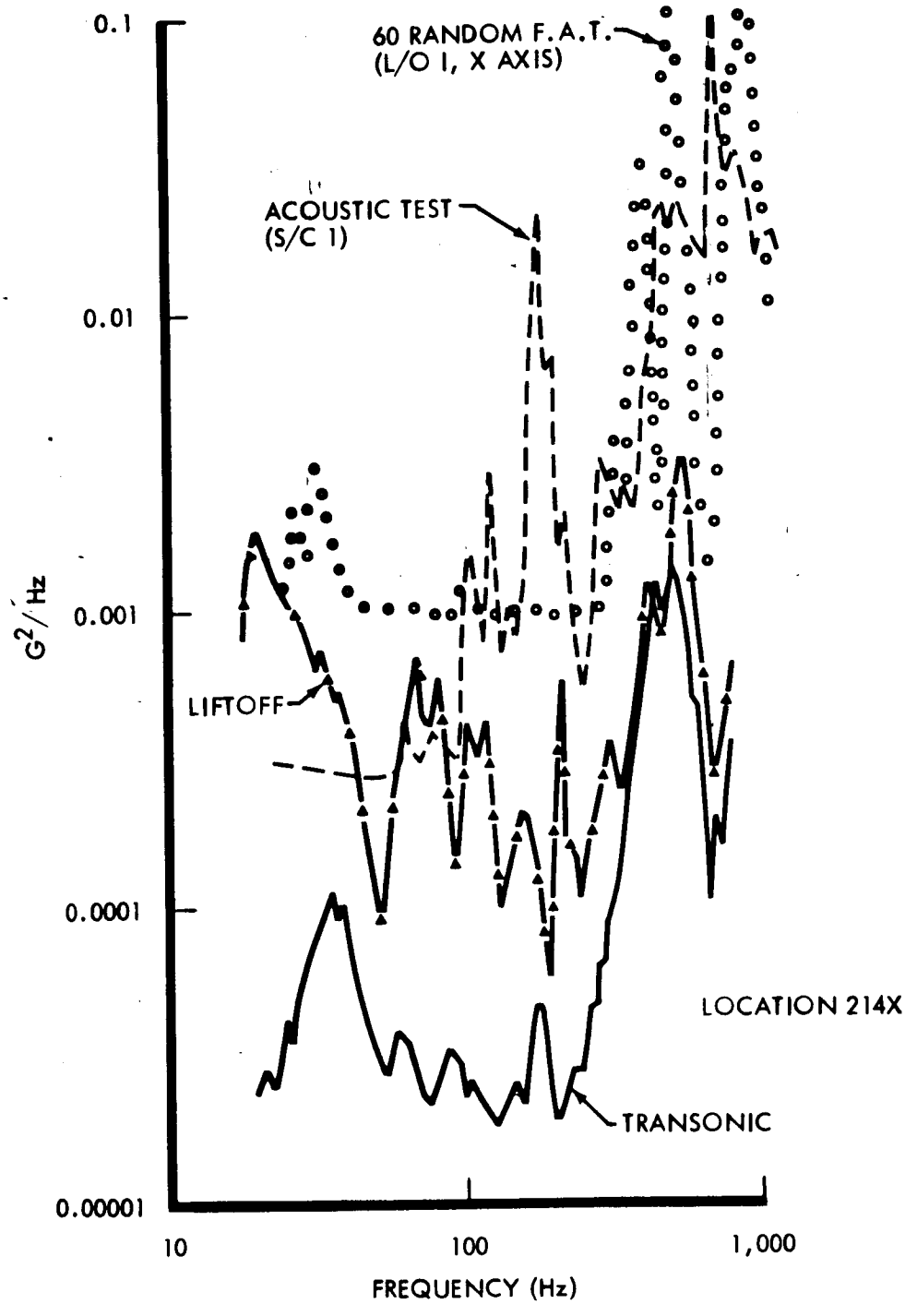

FIGURE 3.1-64: EMD LAUNCH VIBRATIONS COMPARED WITH SPACECRAFT SONIC TEST AND RANDOM FAT

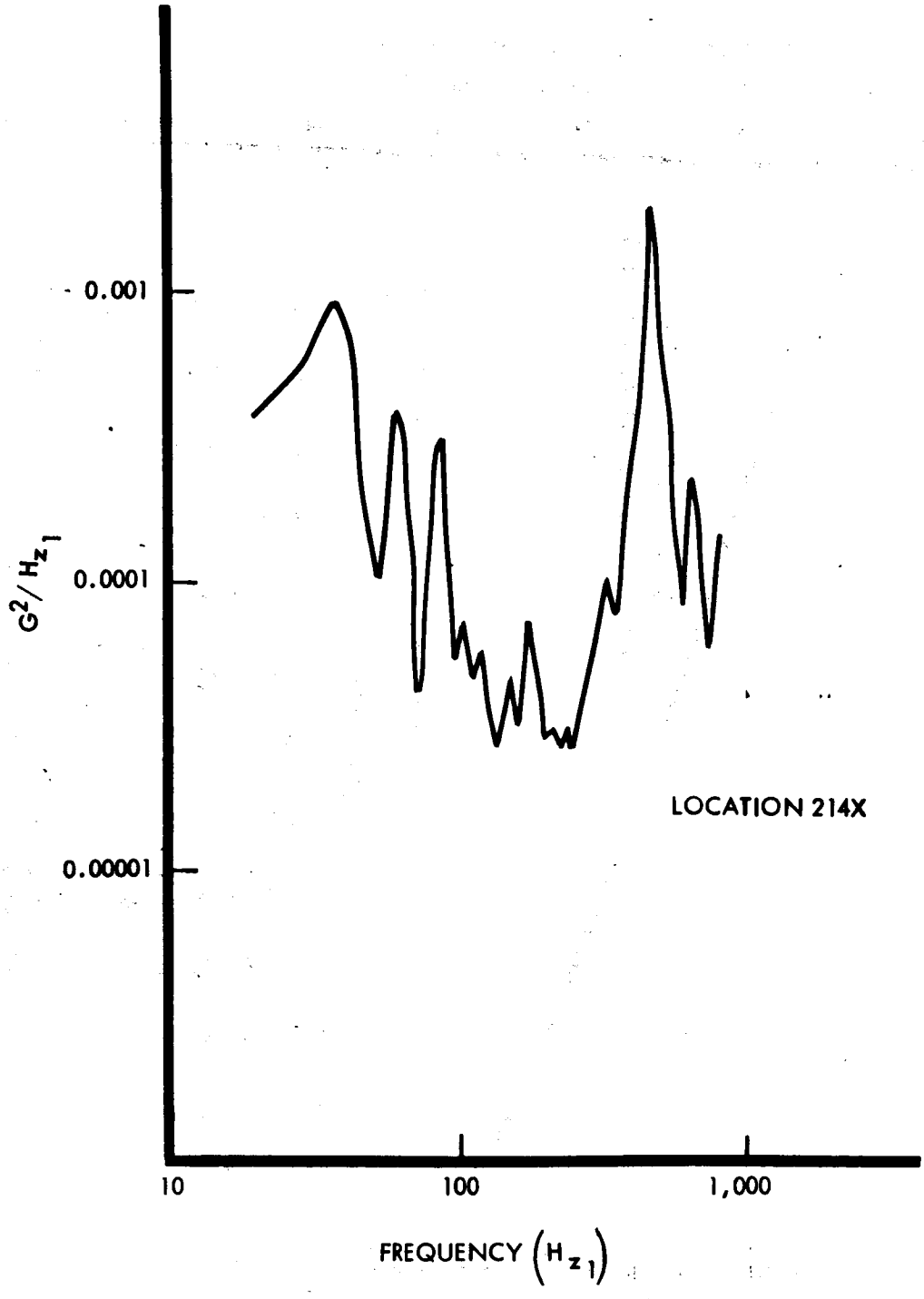

FIGURE 3.1-65: EMD VIBRATIONS DURING AGENA FIRST BURN

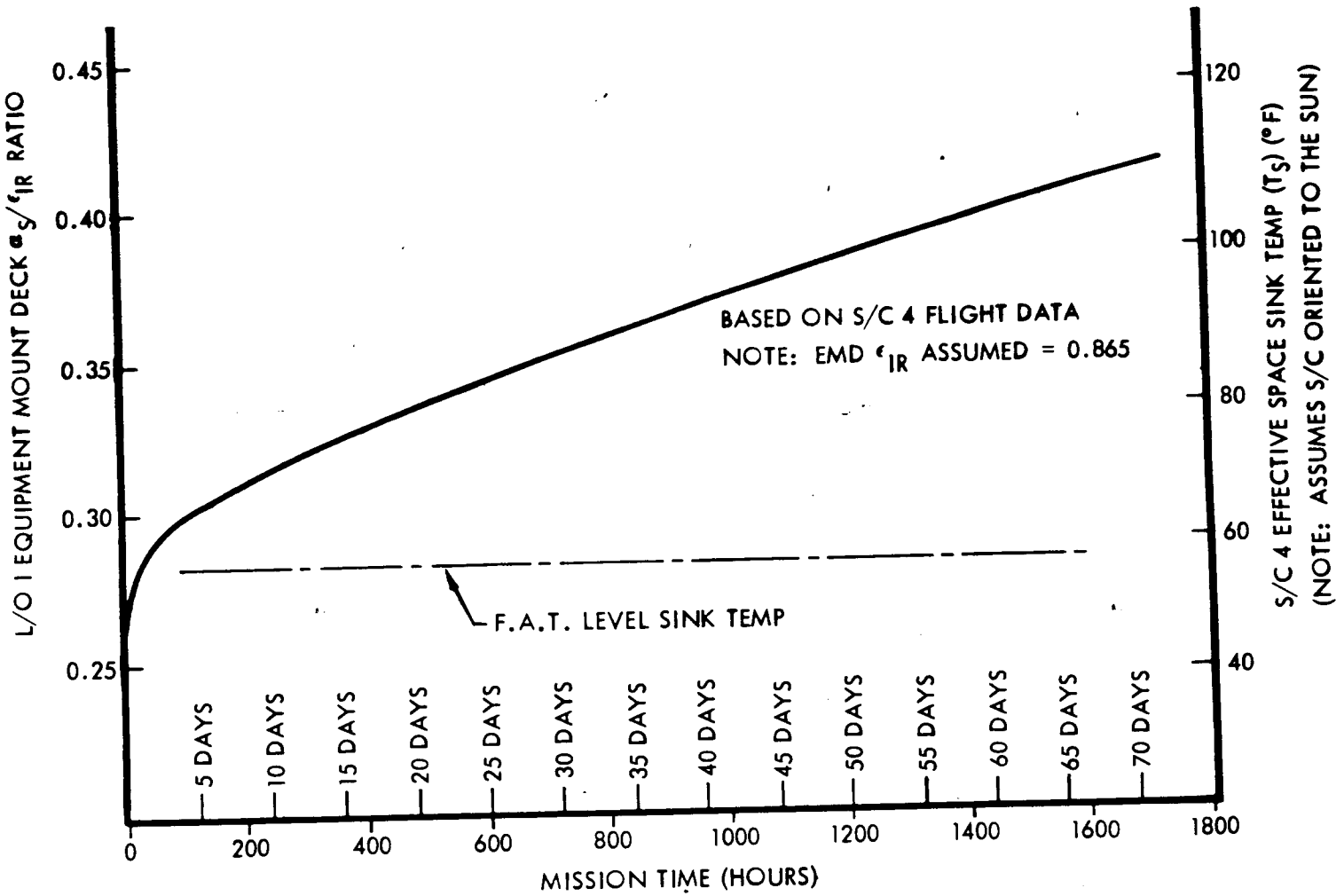

FIGURE 3.1-66: APPARENT DEGRADATION OF LUNAR ORBITER I THERMAL COATING THAT OCCURRED DURING MISSION I

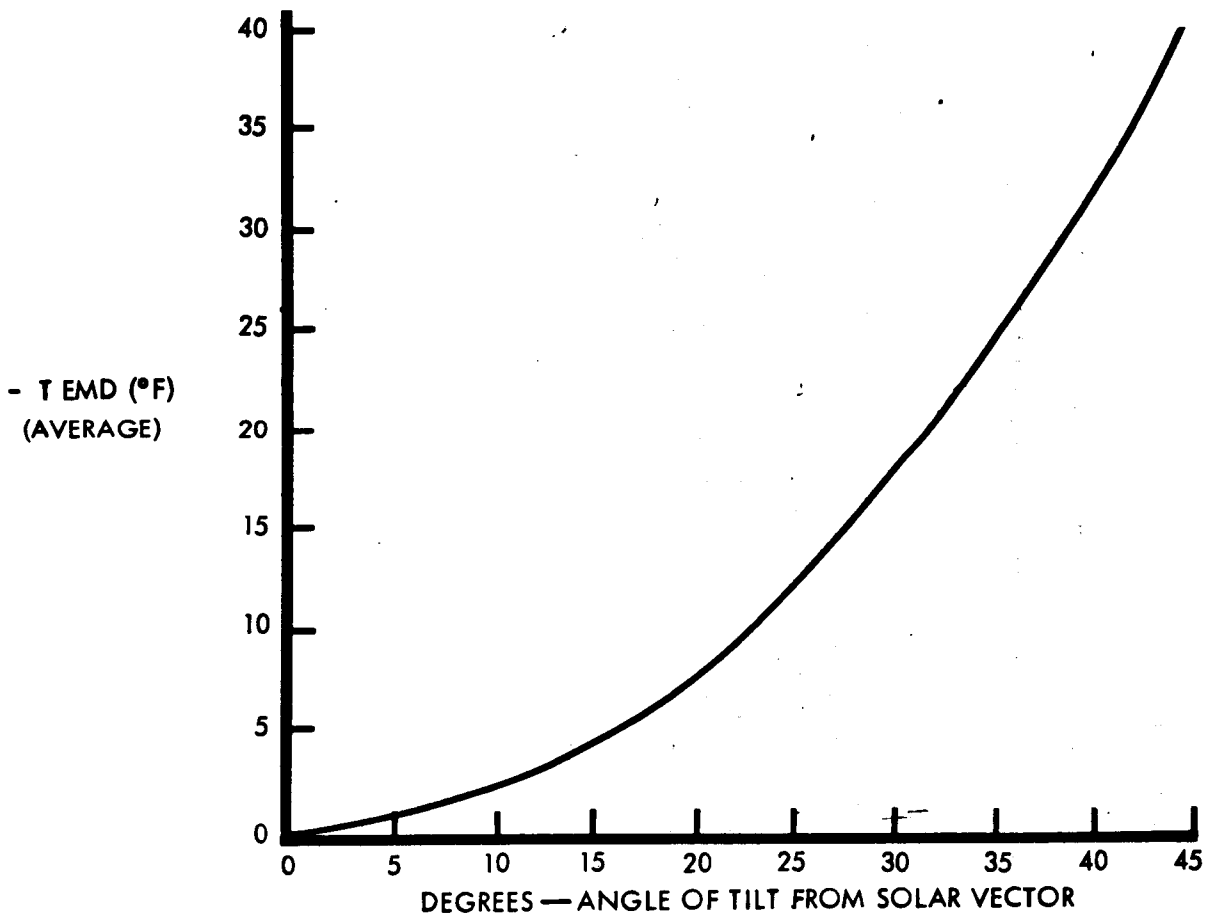

FIGURE 3.1-67: CHANGE IN EMD TEMPERATURE (AVERAGE) VERSUS SOLAR VECTOR — NOMINAL SUN

Primary interaction between the pitch-off maneuver and spacecraft electrical power (EPS), attitude control (ACS), and communications (CS) subsystems required close surveillance for the following reasons:

1) EPS—Because of reduced maximum potential in both available power load and voltage at off-Sun angles;

2) ACS—Because of increased nitrogen usage rates caused by additional spacecraft maneuvers;

3) CS—Because of required high-gain-antenna pointing angles.

The additional commands and maneuvers did not detract from the spacecraft primary mission.

Ellipse Phase

All components of the structures and mechanisms subsystem performed as planned, with the exception of the EMD thermal control, which required continued surveillance. Prior to this phase it was planned to control the frequency of pitch-off maneuver by the TWTA temperature (that is, keeping it below 85° F). However, this was discarded in favor of allowing an uncontrolled linear drift that was accomplished by pitching off the Sun 36.5 degrees and letting the spacecraft drift back. The drift took approximately 25 hours, at which time the spacecraft EMD had reached allowable upper temperature limits and required another pitch-off. This procedure was successfully maintained throughout photo readout. By this plan the spacecraft nitrogen supply, which had been excessively used during spacecraft search for Canopus, was conserved sufficiently to allow the orbit change that took place during the extended mission.

3.2 LAUNCH VEHICLE PERFORMANCE

Lunar Orbiter I was placed in Earth orbit by a launch vehicle consisting of an Atlas SLV-3 (S/N 5801) primary booster, and in the proper cislunar trajectory by an Agena D upper-stage booster (Model 62205 S/N 6630). The combined space vehicle configuration is shown in Figure 3.2-1.

3.2.1 ATLAS PERFORMANCE

The SLV-3 booster profile and general configuration are shown in Figure 3.2-2. Assembled Atlas overall dimensions were 841.8 inches long with a cylindrical section diameter of 120 inches.

3.2.1.1 AIRFRAME

Configuration

The welded stainless-steel sheet metal frame consisted of a tank section and an aft thrust section. The tank section was a monocoque structure that derived most of its rigidity from internal pressure. A thrust ring with a webbed bulkhead at the aft end prevented radial distortion of the tank by stresses created during engine thrust. The liquid-oxygen feed line, tank pressurization lines, cabling, and equipment pods containing electrical and electronic equipment were all attached external to the tank. The aft thrust section, which separates after booster engine cutoff (BECO), housed the booster engine, its thrust chamber, nacelles, and associated equipment.

Performance

Vehicle structural integrity was satisfactorily maintained throughout powered flight and beyond SLV-3/Agena separation. The 5-Hz longitudinal oscillations following liftoff reached a maximum peak-to-peak level of 1.0 g and were damped out by approximately T+19 seconds. Peak accelerations of 6.1 and 3.1 g were indicated at BECO and SECO, respectively. Staging and SLV-3/Agena separation were satisfactory. Adapter pressure and temperature measurements indicated that environmental conditions were satisfactory.

A tabulation of engine compartment temperatures at selected times is presented in Table 4-1 of Lunar Orbiter A Launch Report.

3.2.1.2 PROPULSION

Configuration

The North American Rocketdyne MA-5 liquid-propulsion rocket engine system was comprised of two 165,000-pound booster thrust chambers, a 57,000-pound thrust sustainer engine, and two 670-pound thrust vernier engines. These engines were single start and equipped for hypergolic ignition. Each engine was gimbaled for attitude control. The booster engine system was jettisoned after burn termination (BECO). A simplified schematic of the booster, and sustainer and vernier engine systems, are shown in Figures 3.2-3 and 3.2-4.

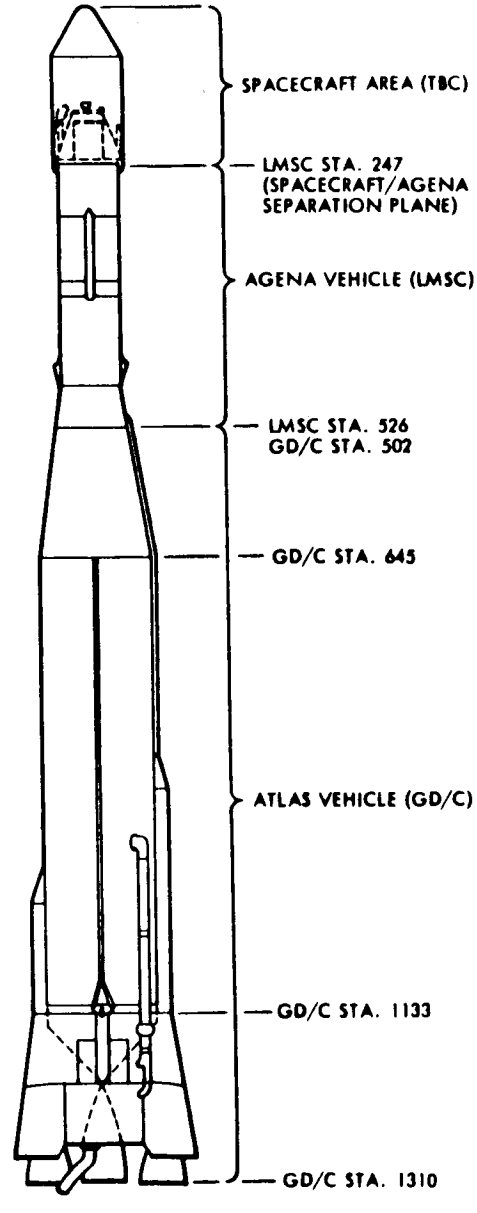

FIGURE 3.2-1: COMBINED SPACE VEHICLE CONFIGURATION

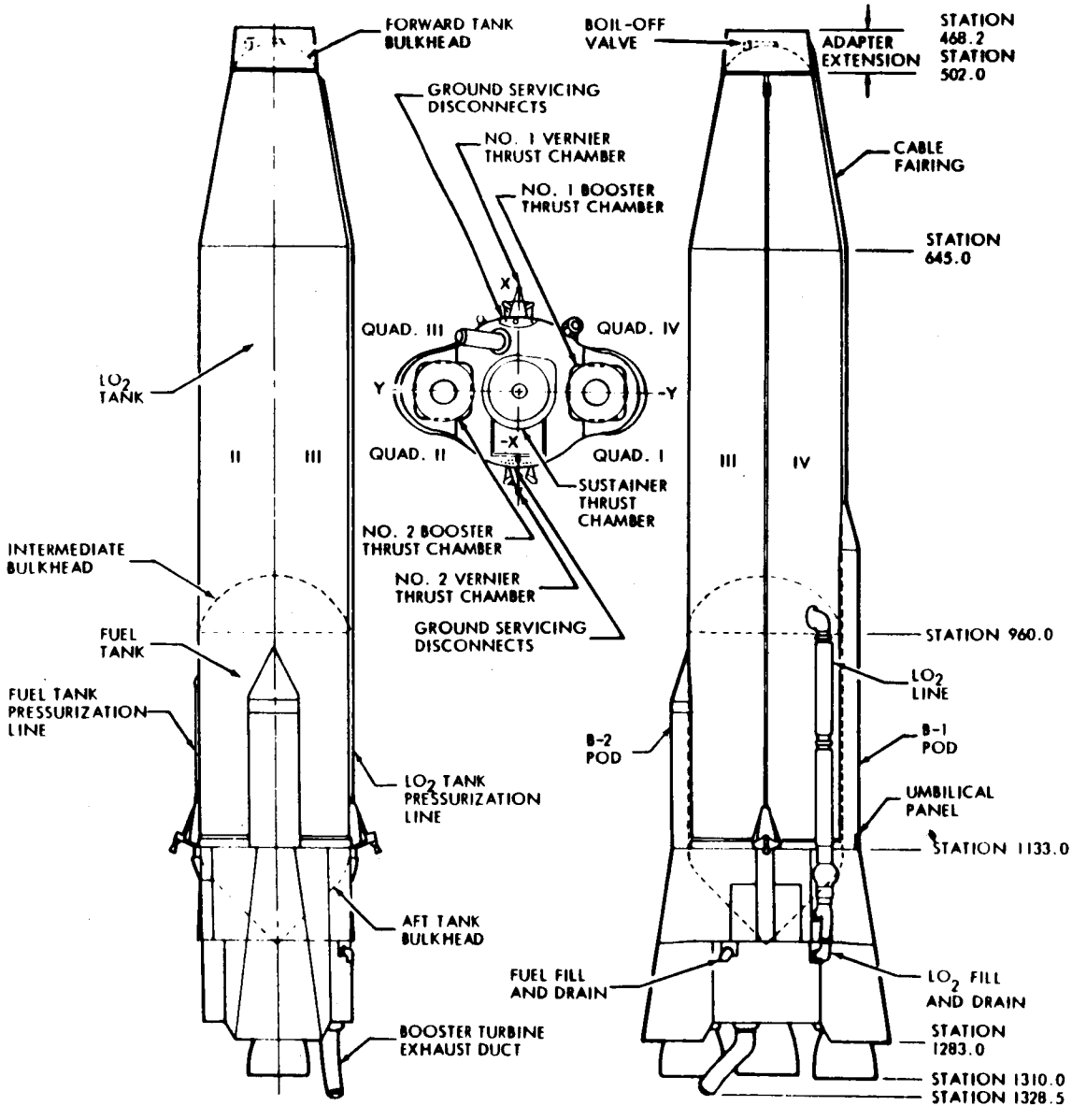

FIGURE 3.2-2: ATLAS SLV CONFIGURATION

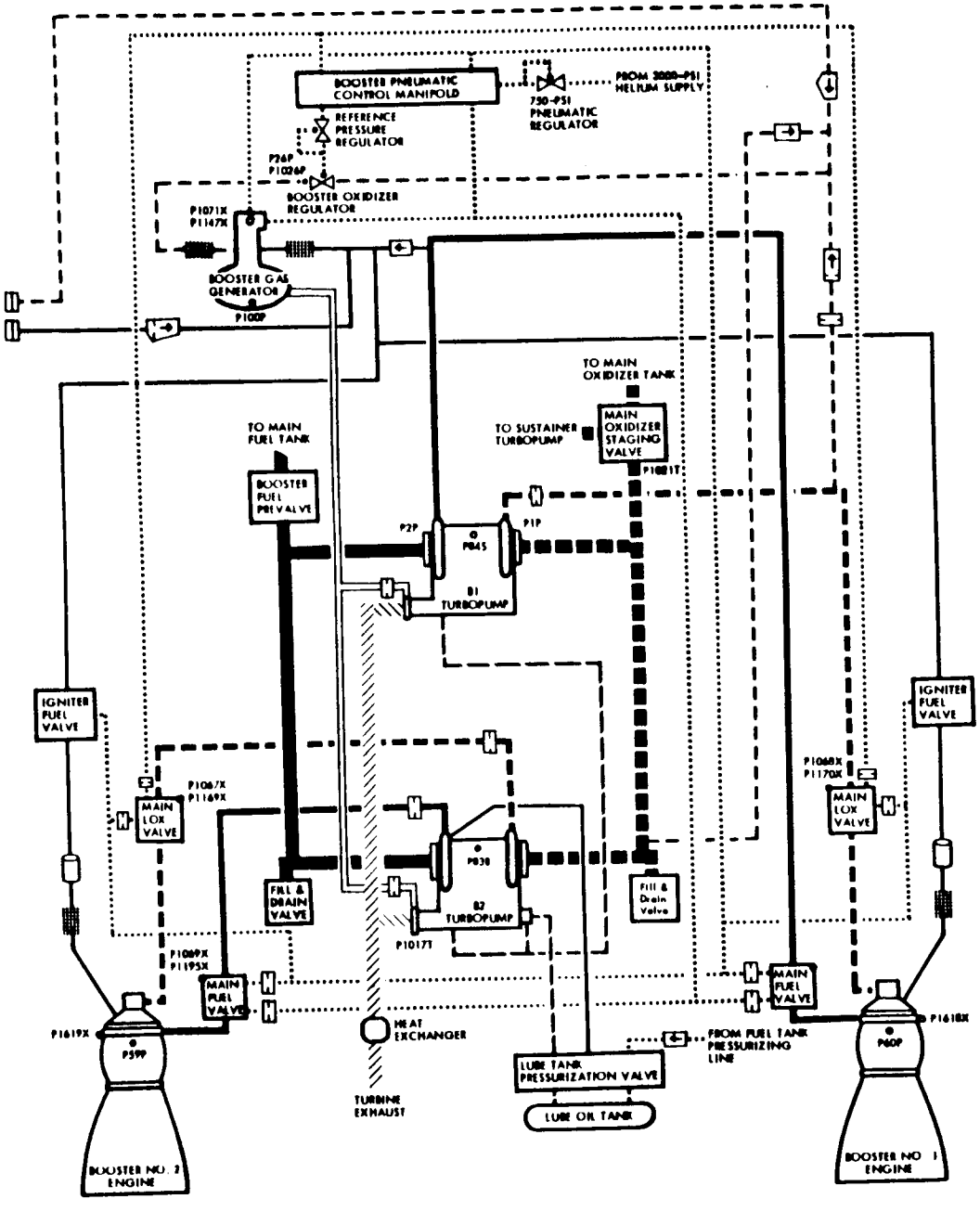

FIGURE 3.2-3: ATLAS BOOSTER ENGINE SYSTEM SCHEMATIC

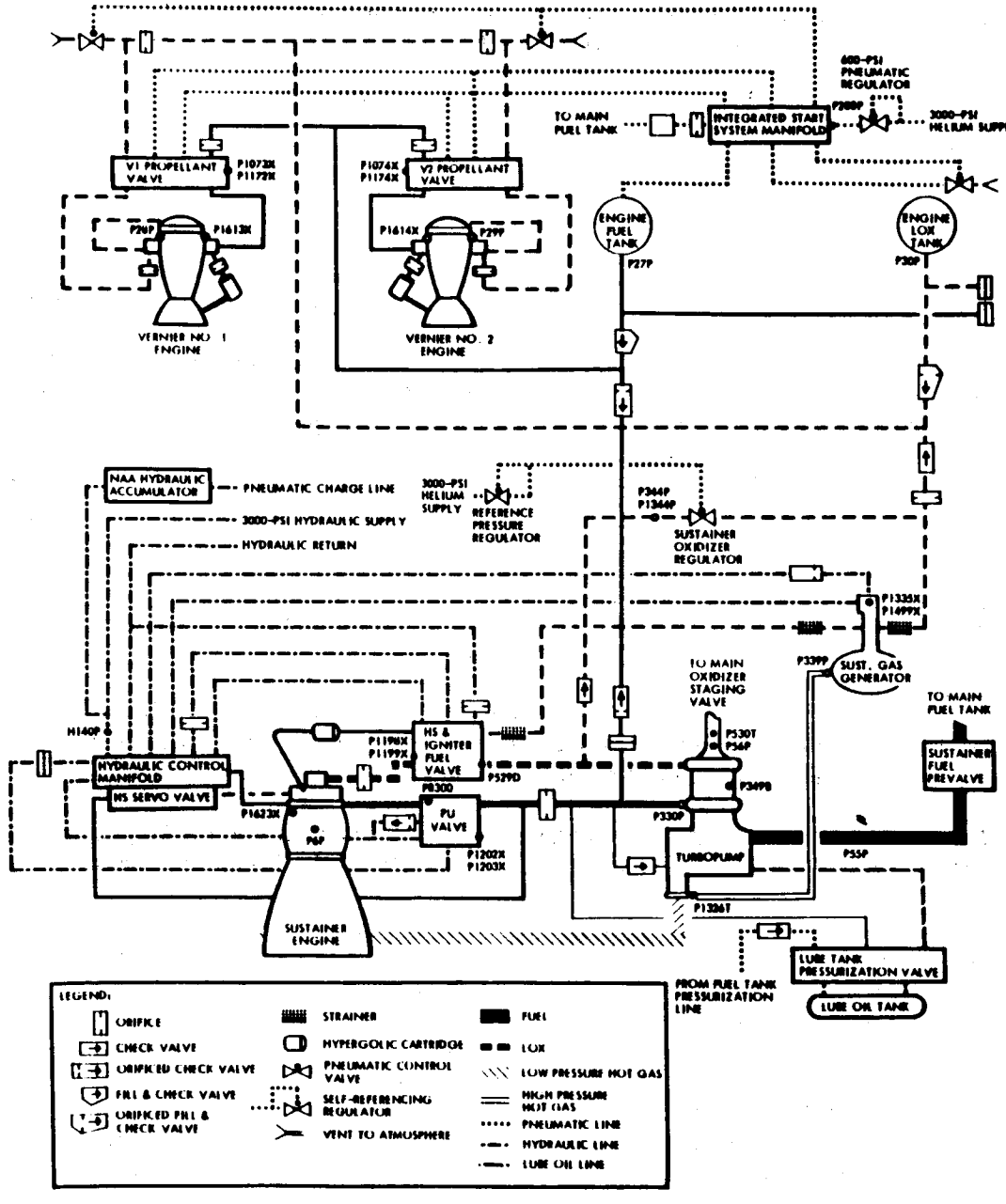

FIGURE 3.2-4: ATLAS VERNIE & SUSTAINER ENGINES SYSTEM SCHEMATIC

Performance

Propulsion-system operation was satisfactory throughout the flight. Engine thrust rises and decays appeared normal. Engine valve and timer operating times were within specifications. Cryogenic leakage was not evident on this flight.

A tabulation of propulsion-system telemetered data is presented in Table 4-2 of the Lunar Orbiter A Launch Report.

3.2.1.3 GUIDANCE AND FLIGHT CONTROL

Configuration

The airborne General Electric Mod III-C guidance package included a rate beacon, pulse command beacon, decoder, three universal canister mounting bases, antenna assembly, associated waveguide, and electrical cabling. The main ground elements of the radio guidance subsystem were monopulse X-band position radar, continuous-wave X-doppler radar (used to measure velocity), and a Burroughs computer.

The basic units of the flight control subsystem were the flight programmer, gyro package, servo control electronics, and hydraulic controllers. A block diagram of this system is shown in Figure 3.2-5.

Performance

Guidance

Evaluation of ground and telemetered airborne data indicated that both the Mod III-A ground station and Mod III-G airborne guidance equipment performed satisfactorily. Insertion and orbital parameters were satisfactory.

All discrete and steering commands were transmitted normally by the ground station, received by the beacon, decoded, and forwarded to the flight-control system.

Guidance steering was enabled within the flight-control system at T+80 seconds; however, booster-phase steering was not transmitted. Sustainer-phase steering was initiated at T+137.7 seconds with a pitch-up command of 100% for two computer cycles followed by a pitch-down command of 25% for two computer cycles at T+142.7 seconds. Yaw steering was 100% left at T+137.7 seconds for two computer cycles followed by 15% yaw right at T+144.2 seconds. Pitch and yaw steering was reduced to within ±15% by T+153 seconds and remained in this state until initiation of vernier attitude steering at T+291.1 seconds. Vernier attitude steering consisted of 95% pitch-down and a 72% yaw-right command for one computer cycle. Both pitch and yaw steering were reduced to zero prior to VECO.

The following guidance system discrete generation times were observed. All indicated times are referenced to an initial spacecraft motion of 2 inches, which occurred at 19:26:00.716 GMT.

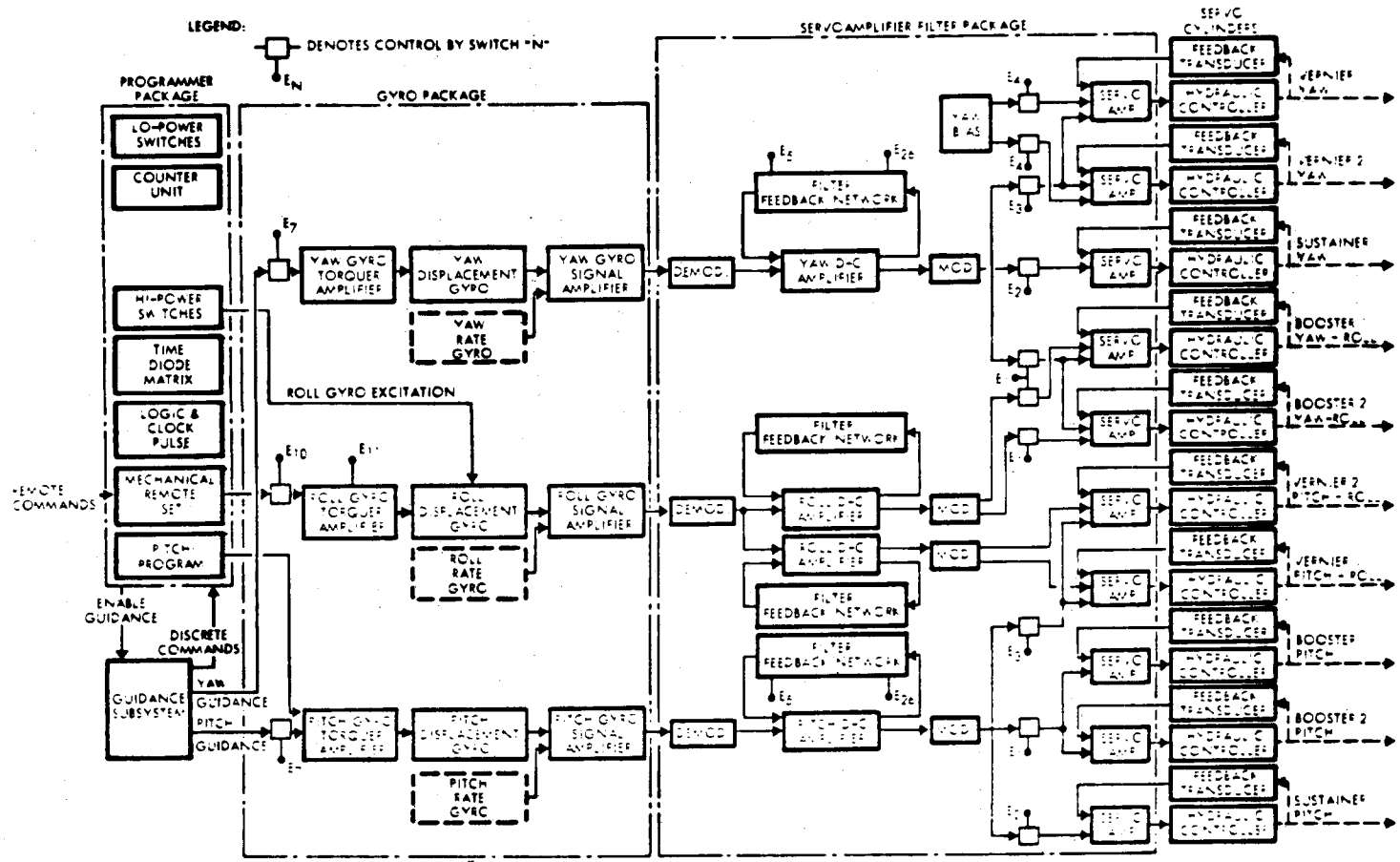

FIGURE 3.2-5: GUIDANCE AND FLIGHT CONTROL BLOCK DIAGRAM

Event	Time (+sec)
BECO	128.717
Start Secondary Timer	271.200
SECO	290.884
Start Primary Timer	294.887
VECO	311.777
Jettison Shroud	314.217
Separation	316.217

The following coarse ellipse parameters and insertion parameters at VECO +2 seconds were obtained from the guidance system data:

Parameter	Value
Semimajor axis	14,512,105 feet
Semiminor axis	12,707,193 feet
Velocity magnitude	18,520 feet per second
Velocity to be gained	+0.40 feet per second
Filtered yaw velocity	-3.12 feet per second
Filtered altitude rate minus Desired altitude rate	+15.25 feet per second

Tracking subsystem—Tracking was first started with the vehicle in conical mode in the first cube at T+60.6 seconds; the mode was switched to automatic monopulse tracking at T+66.4 seconds, with a good flag presented to the computer by T+69.6 seconds.

Angular tracking errors during the sustainer/vernier phase of flight averaged 0.12 mr peak-to-peak. The range servo error averaged 7 feet peak-to-peak. Average signal level during this period was -51 dbm.

Track-lock was continuous from acquisition until T+387.5 seconds. Final loss of vehicle monopulse tracking occurred at T+392.3 seconds at an elevation angle of 3.87 degrees. Signal level at this time was at the noise level.

Rate subsystem—Rate-lock with all good flags was accomplished by T+57.9 seconds and was continuous thereafter until T+380.4 seconds when the signal level had reached the noise level.

The parallax corrector was switched out at approximately T+150 seconds as planned.

During the sustainer/vernier phase of flight, the range rate noise was less than 0.7 feet per second peak-to-peak, and the lateral rate noise averaged 0.02 feet per second peak-to-peak. The central rate-received signal level averaged -72 dbm and by SECO had decreased to -82 dbm. The signal levels at Stations 3 and 4 were within 2 db of central throughout this period.

Computer subsystem—Performance of the computer subsystem was satisfactory throughout the countdown and flight. The guidance program was successfully verified before removal from the computer. A successful simulated rerun of the flight was performed, indicating that no transient computing-system errors occurred during the flight.

The ASCO signal was inhibited throughout the flight, as planned.

Airborne equipment—Performance of the Mod III-G airborne equipment was satisfactory throughout the flight. All values telemetered from the airborne canisters during the flight corresponded satisfactorily with those obtained during the laboratory checkout test.

The pulse beacon was locked solid in the first cube at T+59.2 seconds. From T+49.7 to T+59.2 seconds, the beacon-received signal was intermittent as expected due to look angle. From T+124.0 to T+130.6 seconds, the received signal was again intermittent. Solid lock was then maintained until T+383.6 seconds. The final loss of lock occurred at T+393.6 seconds with the received signal at the noise level.

Solid rate-beacon lock was maintained from T+58.1 to T+380.4 seconds, at which time the recieved signal was at the noise level.

The steering and discrete commands transmitted from the ground station were properly processed by the decoder. Spurious pitch and yaw commands were evident, as expected, during period of intermittent pulse beacon lock, from T+49.8 to T+58.9 seconds, and from T+124.1 to T+130.6 seconds.

Flight control—Operation of the flight-control system was satisfactory. Vehicle stability was maintained throughout powered flight. The programmed roll and pitch maneuvers were generated normally, and satisfactory system response was indicated. All monitored programmer-switch functions occurred correctly, and correct response to guidance steering and discrete commands was indicated. Vehicle angular displacements and rates were negligible at VECO.

At liftoff, the data exhibited a clockwise roll transient of 0.7 degree at a peak rate of 1.9 degrees per second, and a positive pitch transient of 0.3 degree at a peak rate of 1.3 degrees per second. These transients were satisfactorily damped on activation of the autopilot at 42 inches of rise. First-bending-mode oscillations were observed in pitch and yaw until approximately T+2 seconds. Thereafter, second-bending-mode oscillations were observed; these were essentially damped out by approximately T+10 seconds. These latter oscillations are excited by the normal longitudinal mode experienced at liftoff.

Very-low-amplitude, first-mode oscillations were observed in both pitch and yaw throughout most of the booster phase. The first mode was also excited in pitch and yaw at BECO and was satisfactorily damped. First-bending-mode oscillations following BECO have been observed on most SLV-3 vehicles. Other bending modes were not observed.

Rigid-body oscillations occurred throughout the flight from liftoff until SECO, except for a short time from T+30 to T+40 seconds. These oscillations occurred predominantly in yaw during booster phase and predominantly in pitch during sustainer phase. Low-amplitude, rigid-body oscillations were observed in the roll channel at the end of the sustainer phase and during the vernier solo phase.

Engine deflections due to wind shear and aerodynamic loading appeared normal, with maximum booster pitch deflections of -0.7 degree for B1 and -1.2 degrees for B2 at T+59 seconds, and +1.2 degrees for B1 (engine) and +0.7 degree for B2 (engine) at T+74 seconds.

The staging sequence appeared normal with small vehicle movements in pitch and yaw. A roll transient of 0.5 degree at a peak rate of 2.6 degrees per second was observed at BECO. System response resulted in an overshoot of 0.6 degree at a peak rate of 2.1 degrees per second. The transients occurring at BECO and at staging were damped satisfactorily.

Normal SLV-3 propellant-slosh indications were observed during booster phase. Low-amplitude Agena slosh oscillations were indicated during the latter portion of booster phase and during sustainer phase. Previous SLV-3/Agena vehicles have exhibited similar characteristics.

Guidance steering was enabled by the autopilot at T+80 seconds, but no booster-phase guidance commands were transmitted. Some small-amplitude spurious commands were generated by the airborne guidance equipment from T+124 to T+131 seconds. Normal sustainer phase steering was initiated at approximately T+138 seconds, and satisfactory system response was indicated.

The flight-control system satisfactorily responded to all guidance discrete commands, and the appropriate signals were relayed to the upper stage.

3.2.1.4 PNEUMATICS

Configuration

The pneumatic system was comprised of helium storage bottles, pressure regulators, and a liquid oxygen relief valve. Six booster helium storage bottles were provided for main propulsion tank pressurization, one helium storage bottle for controls supply pressure, and one bottle for booster jettison. Other parts of the system included disconnects and relief valves. Regulators are used to control liquid oxygen and fuel tank pressure.

Performance

Pneumatic-system performance was satisfactory. Flight data indicated that propellant-tank pressures were adequately maintained and control pressures were satisfactory. The minimum transient pressure indicated by telemetry measurement F116P, Differential Pressure Across the Bulkhead, during longitudinal oscillation following liftoff, was 8.8 psid at T+3.45 seconds.

During the initial portion of the flight, the usual 2.5- and 5-Hz oxcillations were observed. The 2.5-Hz oscillations were damped out by approximately T+7 seconds, and the 5-Hz oscillations were damped out by approximately T+25 seconds.

Landline and telemetry data indicated no system anomalies. Calculations indicated there were 153.4 pounds of helium in the booster-tank helium bottles at ignition and that 81.8 pounds were consumed during flight.

Pneumatic-system data, taken at selected times, is presented in Table 4-4 of the Lunar Orbiter A Launch Report.

3.2.1.5 ELECTRICAL POWER

Configuration

A silver-zinc 28-volt battery supplied primary power. Secondary power was provided by a rotary Leland converter, which converts 28 v.d.c. to 400-Hz, 3-phase, 115 to 125 v.a.c. for the flight control system. Prior to launch, external power was supplied through the umbilical. A changeover switch was provided for switching from external to internal prior to launch.

Performance

Performance of the electrical system was satisfactory. Telemetered data indicated that electrical power to all user systems was within specifications. Electrical system telemetry data is presented in Table 4-6 of the Lunar Orbiter A Launch Report.

The main battery output during the 30-second battery load check was as follows: open circuit prior to switch to internal power, 34.7 v.d.c.; under load at end of 30 seconds, 28.1 v.d.c.; open circuit after switch to external power, 30.4 v.d.c.

Blockhouse panel meter readings taken at T-10 seconds were: vehicle systems input, 27.61 v.d.c.; 400-Hz a.c. Phase A, 115.2 v.a.c., 399.5 Hz.

3.2.1.6 HYDRAULICS

Configuration

Two independent systems furnished hydraulic pressure in flight. The booster-engine system provided hydraulic pressure to gimbal the booster engines prior to staging. It included a variable-displacement pump, reservoir, four booster engine actuators, associated valves, and plumbing.

The sustainer-vernier engine system included a variable-displacement pump, reservoir, accumulator, two sustainer engine actuators, four vernier engine actuators, pressure manifold, return manifold, head suppression valve, gas-generator bleed valve, propellent-utilization valve, and associated valves and plumbing. This system was used to gimbal the sustainer and vernier engines and to operate the gas generator and propellant utilization valves.

During vernier solo phase, hydraulic pressure was provided for vernier-engine gimbaling from two pressurized accumulators. The vernier hydraulic lines were isolated from the sustainer hydraulic lines by check valves to maintain hydraulic pressure.

Performance

Operation of the hydraulic system was satisfactory. The system furnished adequate pressure to satisfy user system demands. Oil evacuation was properly effected in the booster and sustainer/vernier systems at approximately T-23 seconds.

Steady-state pressures were approximately 3165 psia in the booster and 3190 psia in the sustainer/vernier systems. The vernier solo accumulators bottomed out approximately 63 seconds after SECO at 940 psia.

Hydraulic-system telemetry data, taken at selected times during flight, is presented in Table 4-3 of the Lunar Orbiter A Launch Report.

3.2.1.7 PROPELLANT-UTILIZATION SYSTEM

Configuration

The Acoustica propellant-utilization system was composed of a CA110 computer, stillwells longitudinally centered in each propellant tank, and ground support equipment. The two stillwells housed six sensing probes and provided protection against fuel-sloshing. The sensors were arranged in corresponding pairs (one fuel and one liquid oxygen). If both probes of a pair were uncovered at the same time, the propellant-utilization valve was repositioned to change the feed pattern and ensure that each tank contained the same amount of residuals.

The Model CA110G five-card computer measured time between uncovering of the liquid-oxygen and fuel-sensor pairs and translated it into an error signal; the signal opening or closing the propellant utilization valve. There was a maximum error time at each level of approximately 12 seconds. If the second sensor at any level did not uncover before this time, the computer would reset the propellant-utilization valve to nominal, step to the next pair of sensors, and await uncovering of this pair of sensors.

Performance

Operation of the propellant-utilization system was satisfactory. The propellant-utilization valve responded properly to the error counter output signal. Response of the head suppression valve was correct with reference to propellant-utilization valve position and LO_2 acceleration head.

Calculation of residuals based on differential pressure-port uncovering times indicated there were approximately 1194 pounds of LO_2 and 753 pounds of fuel remaining at SECO. This represents approximately 6.6 seconds of additional burn time before a theoretical LO_2 depletion would have occurred with 234 pounds of fuel remaining.

Table 4-3 of the Lunar Orbiter A Launch Report presents sensor uncovering times and valve positions at each station. Computer S/N 1009 was flown on this vehicle. Propellant-utilization valve calibrations for this flight were as follows:

Lower limit	22.5 degrees
Nominal	28.5 degrees
Upper limit	42.3 degrees

3.2.1.8 RANGE SAFETY COMMAND SYSTEM

Configuration

The range safety command system included a destructor and the destructor control unit. The block diagram of this system is shown in Figure 3.2-6. The destructor control unit consisted of two antenna pairs, an antenna ring coupler, two receiver-decoder units, an arming device, a power and signal control unit, and a battery pack. System electrical power was supplied by two manually activated primary-type batteries. The system provided for vehicle destruct, engine cutoff, or both.

Performance

System performance was satisfactory throughout powered flight.

Telemetry measurement P100P, BGG Combustion Chamber Pressure, was erratic from liftoff until approximately T+40 seconds, then was satisfactory for the remainder of the booster phase of flight. The first 40 seconds of data were characteristic of wiper-arm liftoff within the transducer. Adequate data were recovered for propulsion system performance evaluation.

No other anomalies or failures were observed.

3.2.1.9 LAUNCH COMPLEX AND GROUND EQUIPMENT

Configuration

The major facilities at ETR Launch Complex 13 included the launch service building, launcher, service tower, umbilical mast with boom, propellant storage and transfer equipment, gas storage and loading equipment, shops, storage, and associated plumbing and wiring. It also included bonding meter, simulators, and cooling air supply.

Performance

Aerospace Ground Equipment

Performance of the aerospace ground equipment (AGE) was satisfactory in supporting the launch countdown. A problem was encountered with the hydraulic pumping unit when an overload relay failed. One set of the relay contacts came off when the rivet holding them broke loose. A jumper was placed across the circuit and operation was continued.

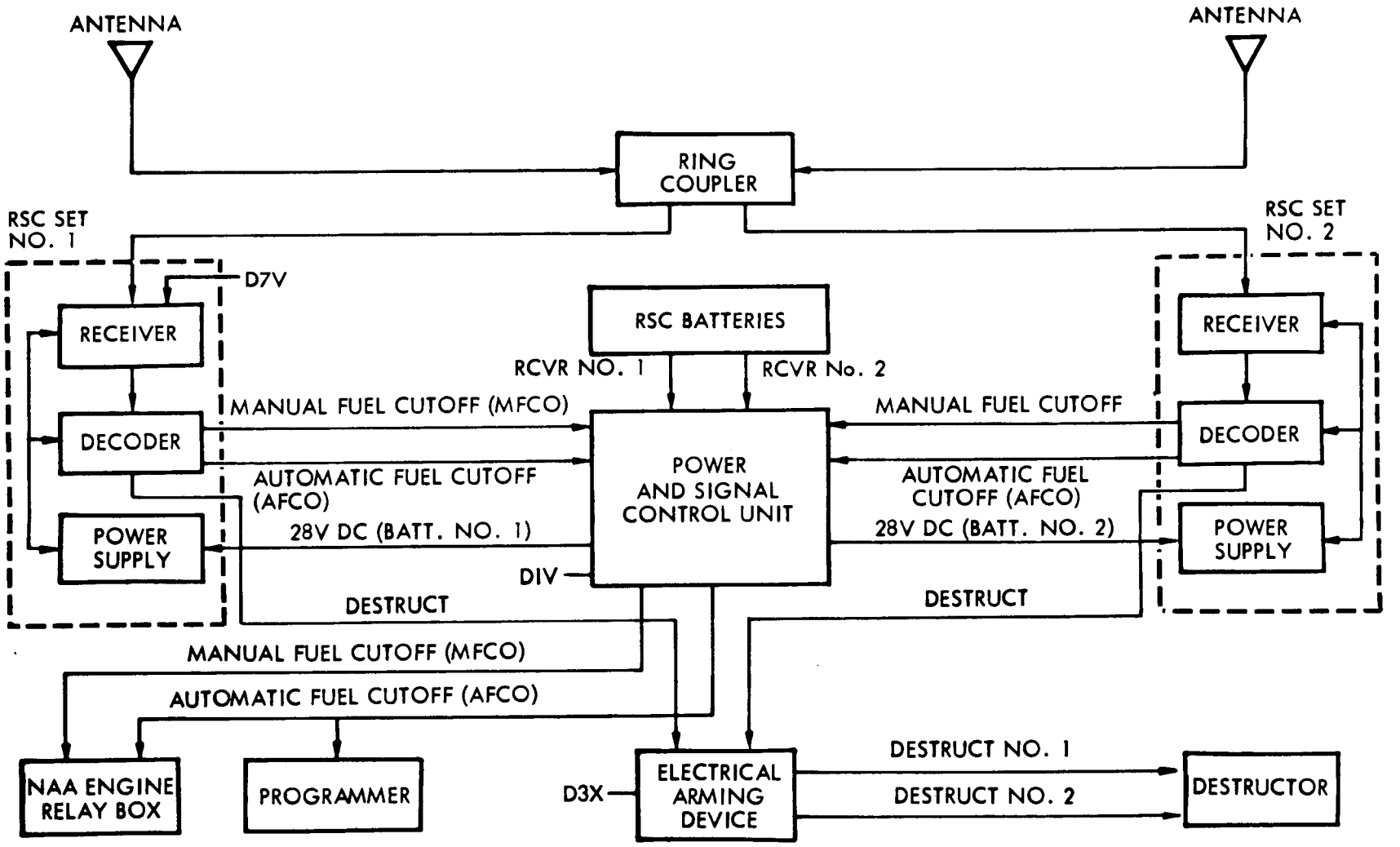

FIGURE 3.2-6: ATLAS RANGE SAFETY AND TERMINATION SYSTEM

Holddown and Release System

The holddown and release system operated satisfactorily in restraining the vehicle prior to release and in releasing the vehicle at liftoff. All values taken from the holddown-cylinder pressure-decay curves were within specifications.

Values obtained are shown in Table 4-7 of the Lunar Orbiter A Launch Report.

Landline Instrumentation

Performance of the landline instrumentation system was satisfactory.

Telemetry measurement P1326T, Sustainer Turbine Inlet Temperature, failed to provide valid data during the engine-start sequence. Failure of this measurement has been experienced on several other launches, from both WTR and ETR.

In an attempt to reduce the incidence of failure for this measurement, an engineering change has been incorporated on all SLV-3 vehicles launched from the ETR, as well as several vehicles launched from the WTR, starting with SLV-3 Serial Number 7114. This change provides for relocation of the transducer to a port farther downstream from the gas generator and removal of the temperature-sensing-element shield. This item is under continued study.

Propellant Tanking

Fuel was originally tanked for the simulated launch demonstration at T-2 launch on 4 August 1966. It was necessary to detank to permit replacement of the launcher Benbow valve. On 8 August, fuel was again tanked to a level 13 gallons above the 100% probe. At ignition, there were 76,788 pounds of fuel aboard at a density of 49.80 lb per cu ft. The American Petroleum Institute fuel rating was 43.8 degrees.

Liquid Oxygen (LO_2) Tanking

Liquid oxygen was tanked using the propellant loading control unit as the level monitoring system. Liquid oxygen was tanked during the countdown to the 100% probe and maintained near that level until securing. Liquid oxygen tank pressure and temperature at the break-away valve at securing were 5.8 psig and -295.5° F. Liquid oxygen density at ignition was 69.90 lb per cu ft. Calculated liquid oxygen weight at ignition was 173,119 pounds. Ground run time from sustainer flight lockin was 1.79 seconds.

3.2.2 AGENA PERFORMANCE

The Agena D used for the Lunar Orbiter I included a booster of basic cylindrical shape 60 inches in diameter and 279 inches long, booster adapter, and spacecraft adapter. The Agena configuration and profile are depicted in Figures 3.2-7 and 3.2-8.

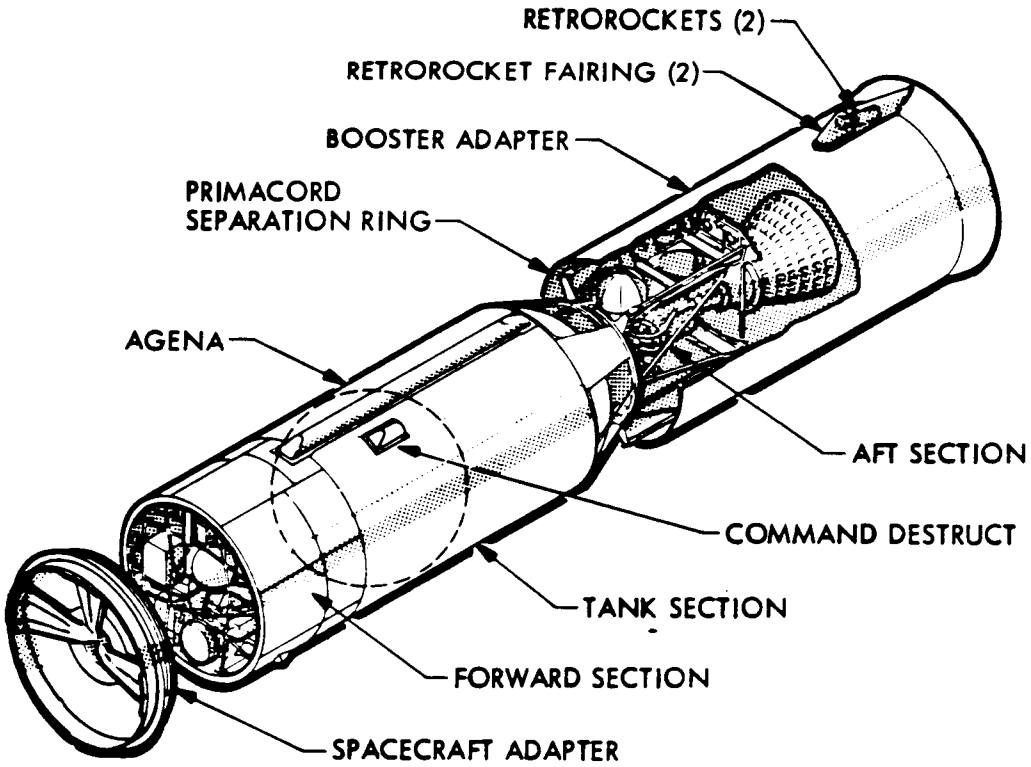

FIGURE 3.2-7: AGENA BASIC CONFIGURATION

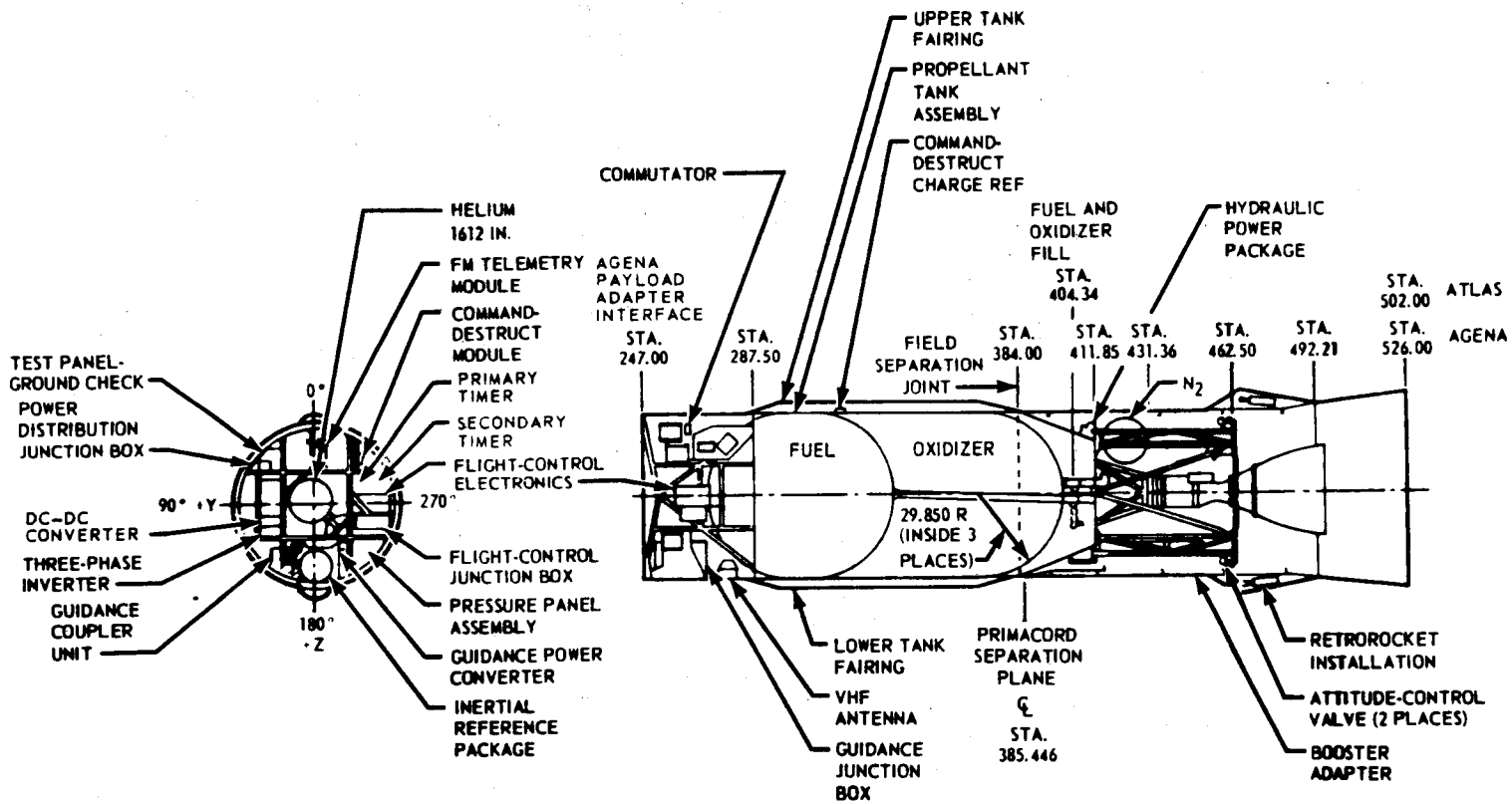

FIGURE 3.2-8: AGENA PROFILE

3.2.2.1 AIRFRAME

Configuration

The major airframe components were the booster adapter, basic airframe, and spacecraft adapter. The airframe was constructed primarily of magnesium and was of monocoque and semimonocoque design.

The adapter enclosed the Agena aft section and secured the Agena to the Atlas booster until Atlas-Agena separation. Most of the adapter remained with the booster. This adapter also housed two retrorockets used for separation.

The Agena airframe consisted of a forward equipment rack, propellant tank section, and an equipment mounting structure attached to the aft end of the propellant tank. The forward section was a welded truss-type tubular aluminum frame to which were bolted external rings, longerons, beryllium skin assemblies, and access doors. The forward equipment rack housed electrical, guidance, tracking, telemetry, and propellant-tank pressurization components; it also provided attach points for the spacecraft adapter.

The propellant tank section was a cylindrical vessel with an intermediate bulkhead separating the fuel and oxidizer compartments. The tank assembly was constructed of aluminum and was an integral part of the space frame, providing the skin for the center portion of the Agena. The forward chamber of the tank section was for fuel; the aft chamber was for the oxidizer. The chambers were separated by a common hemispherical bulkhead, and each chamber had a sump to provide scavaging and passive propellant orientation. These sumps inhibited reverse flow of propellants during coast phase. The net volume of the fuel tank with bottles was 75.9 cubic feet (553 gallons) and that of the oxidizer tank was 98.4 cubic feet (738 gallons). Two external fairings were attached to the clips external to the tanks to provide interconnecting tunnels between the forward and aft sections for plumbing, wiring, and for conditioned air during ground handling.

The aft structure provided attachment points for the rocket engine, a nitrogen-freon pressure sphere, attitude-control gas valves, and separation rollers. It also housed the detonator and mild detonating fuse (MDF) used for separation.

The booster adapter was 142 inches long and included two retrorocket fairings, space for two retrorockets, various access doors, fuel and oxidizer fill doors, and four separation rails. This adapter remains with the Atlas booster at Atlas-Agena separation, which is accomplished by a mild detonating fuse (MDF) separation device.

The spacecraft shroud provided environmental protection during prelaunch and flight until jettisoned just prior to the Atlas-Agena separation. The shroud was constructed of magnesium with a beryllium nose cap and an aluminum thermal liner. A V-band held the shroud to a mating lip on the spacecraft adapter until explosive bolts in the V-band were fired. The shroud was then ejected by spring-loaded ejectors.

Performance

Data presently available at AFETR indicates structural integrity of the Agena-Lunar Orbiter I spacecraft combination was maintained through loss of signal at Station 13 (T+2285 seconds). Nose-shroud separation occurred at T+314.2 seconds. SLV-3/Agena separation occurred satisfactorily at approximately T+316 seconds. Major forces experienced by the accelerometers during the ascent phase of the flight are shown in Figure 5-1 of the Lunar Orbiter A Launch Report, LMSC-273964. Agena-spacecraft separation occurred at T+2447.3 seconds.

3.2.2.2 PROPULSION

Configuration

The propulsion subsystem included the Bell Aero Systems Model 8096 rocket engine, propellant pressurization system, and pyrotechnics. A propulsion system schematic is shown in Figure 3.2-9. The regeneratively cooled, liquid-propellant engine used inhibited red fuming nitric acid (IRFNA) as the oxidizer and unsymmetrical dimethylhydrazine (UDMH) as the fuel. Rated thrust of the engine was 16,000 pounds in vacuum for a burn duration of approximately 240 seconds. The hypergolic propellants were fed to the single thrust chamber by a turbine pump assembly, which also supplied power to the hydraulic pump motor. Operation of the turbine pump was initiated by a solid-propellant starter assembly and maintained by combustion of propellants in a gas generator.

The engine electrical control comprised relays, valves, and squibs, which sequenced start, shutdown, and restart in accordance with signals from the Agena guidance and control subsystem.

A turbine pump assembly supplied fuel and oxidizer to the engine thrust chamber and to a gas generator. The thrust chamber assembly was an integral unit consisting of the combustion chamber, nozzle throat section, diversion nozzle section, and radiation-cooled titanium nozzle extension. The expansion ratio was 45:1. The thrust chamber and nozzle were regeneratively cooled by the oxidizer. The pressure-operated oxidizer and fuel valves controlled the flow of propellants from the pump to the engine thrust chamber.

Propellant tank pressurization was accomplished by helium stored in a pressurized spherical tank, a squib-operated control valve, and associated plumbing as shown in Figure 3.2-10. This system maintained desired pressures at the pump inlets from propellant loading through the end of Agena-engine second burn.

Pyrotechnics comprised pin pulleys, pin pushers, explosive bolts, and fixed-impulse rockets. Signals from the guidance and control sequence timers for the booster activated these devices.

Performance

Propulsion-system performance was satisfactory through loss of signal. Since the primary sequence timer was started approximately 3.6 seconds later than the published nominal, all timer-controlled propulsion functions were correspondingly late. First-burn engine ignition

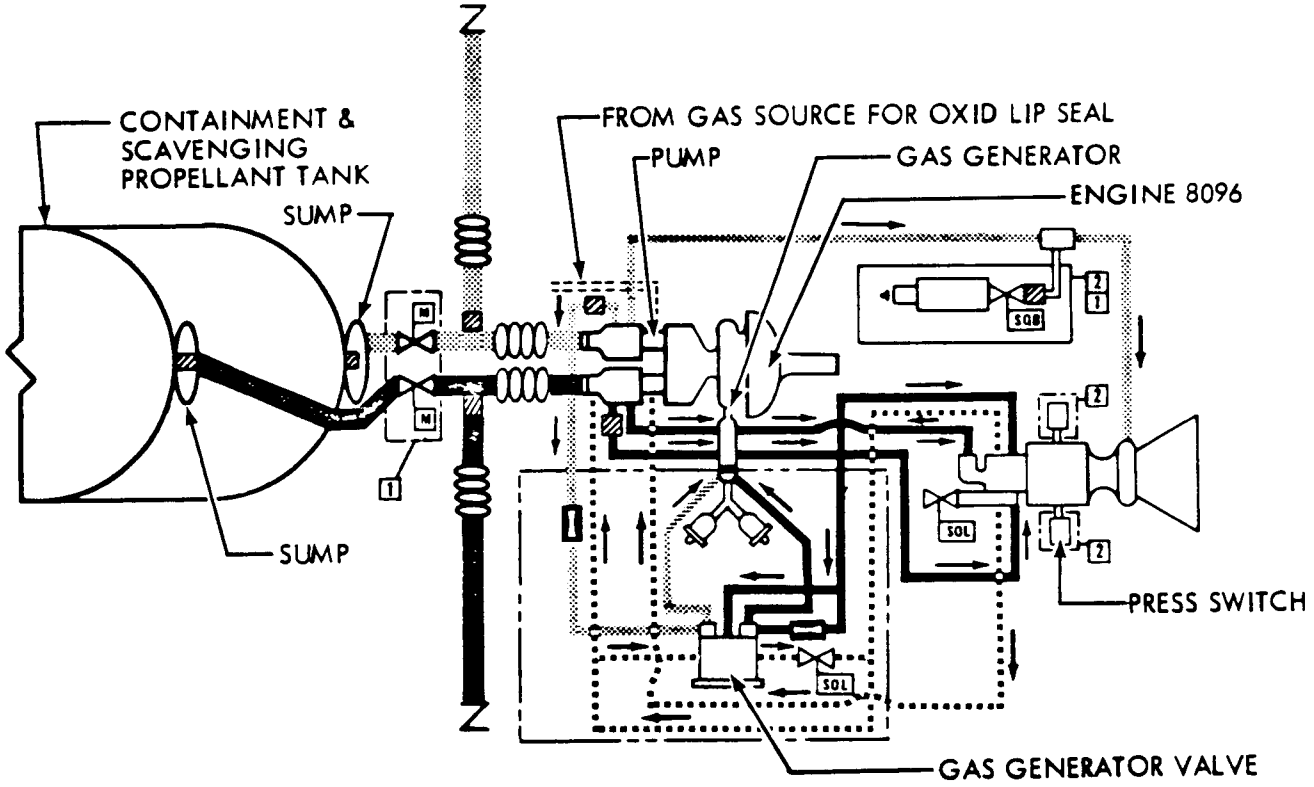

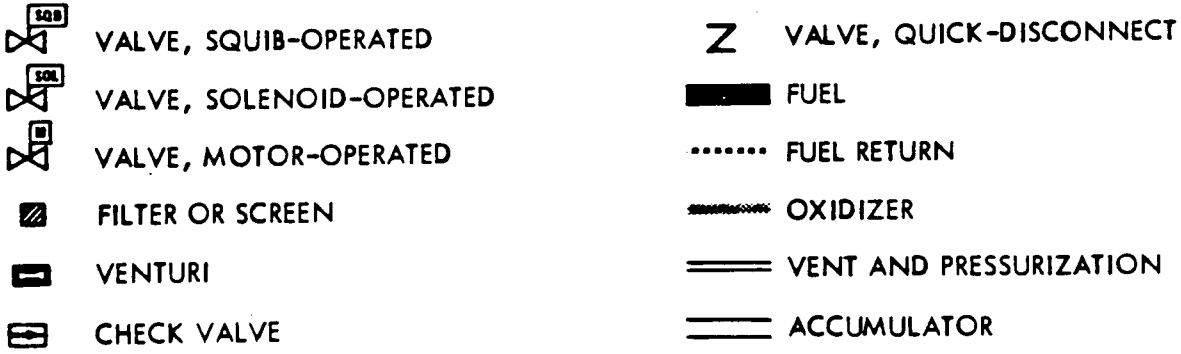

FIGURE 3.2-9: AGENA PROPULSION SYSTEM SCHEMATIC

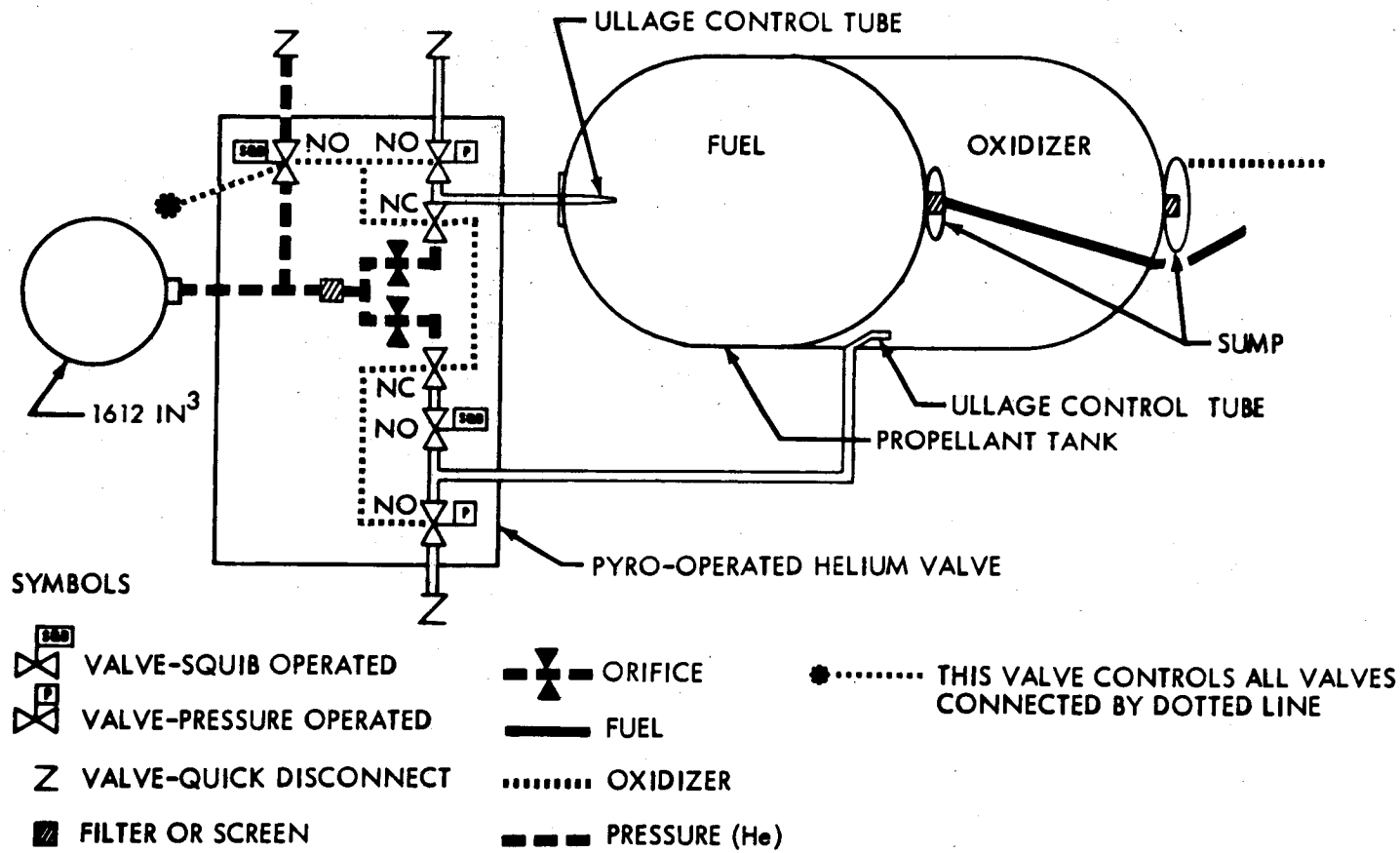

FIGURE 3.2-10: AGENA PRESSURIZATION SYSTEM SCHEMATIC

was properly initiated by the primary sequence timer, and the switch-group voltage levels were correct and occurred in proper sequence.

The average main-combustion-chamber pressure during first burn was 507.5 psia, which results in a calculated thrust of 16,072 pounds. The average turbine speed was measured at 24,920 rpm. The total propellant flow rate was computed at 55.22 pounds per second, and the specific impulse of the engine was calculated at 291.0 lb-sec/lb. First-burn duration (from 90% chamber pressure to engine shutdown) was 153.8 seconds, 2.1 seconds longer than predicted. Telemetered propulsion data is presented in Table 3-1 of the Lunar Orbiter A Launch Report, LMSC 273964. Propulsion parameters and computed propulsion data are displayed in Figures 5-2 and 5-3 of the same reference.

Quick-look analysis of Station 13 data indicates that propulsion-system performance was satisfactory during the second burn period. The average main-combustion-chamber pressure was 506 psia. The burn duration (from 90% chamber pressure to engine shutdown) was 87.8 seconds, which was 0.9 second longer than predicted.

3.2.2.3 ELECTRICAL POWER

Configuration

The electrical power subsystem was composed of power sources, conversion equipment, control units, and a distribution system. The power sources consisted of two Type IV-A batteries that supplied all vehicle power except for the command-destruct module, which was powered by two Type V secondary batteries. The primary battery had a nominal capacity rating of 340 watt-hours.

Power conversion equipment consisted of a 3-phase a.c. inverter and a d.c. to d.c. converter. The 3-phase inverter provided 115 v.a.c. (rms) 400-Hz, 3-phase power with Phase AB used for single-phase power source. The 3-phase inverter supplied a.c. power to the inertial reference package, velocity meter system, horizon sensor system, primary and secondary timers, and flight control electronics. The d.c. to d.c. converter supplied 28.3 v.d.c. regulated power to the inertial reference package, flight control system, velocity meter, and horizon sensor. The power distribution junction box was the principal distribution point for unregulated d.c. power, pyrotechnic power, 3-phase a.c. power, and single-phase a.c. power. Figure 3.2-11 is a schematic of the Agena power distribution system.

Performance

Electrical subsystem performance was satisfactory during both engine burn periods. All measurements remained within specified tolerances as shown in Figures 5-4 through 5-7 of the Lunar Orbiter A Launch Report, LMSC 273964.

The +28 v.d.c. unregulated current cycled between 14 and 20 amperes during first-burn period. At first-burn shutdown, the unregulated current rose briefly to 27 amperes and then returned to a normal cycle of 14 to 18 amperes. Pyro bus voltage dropped from 27.8 to 25.6 volts momentarily at cutoff. Structure current was 2.5 amperes during the first-burn period.

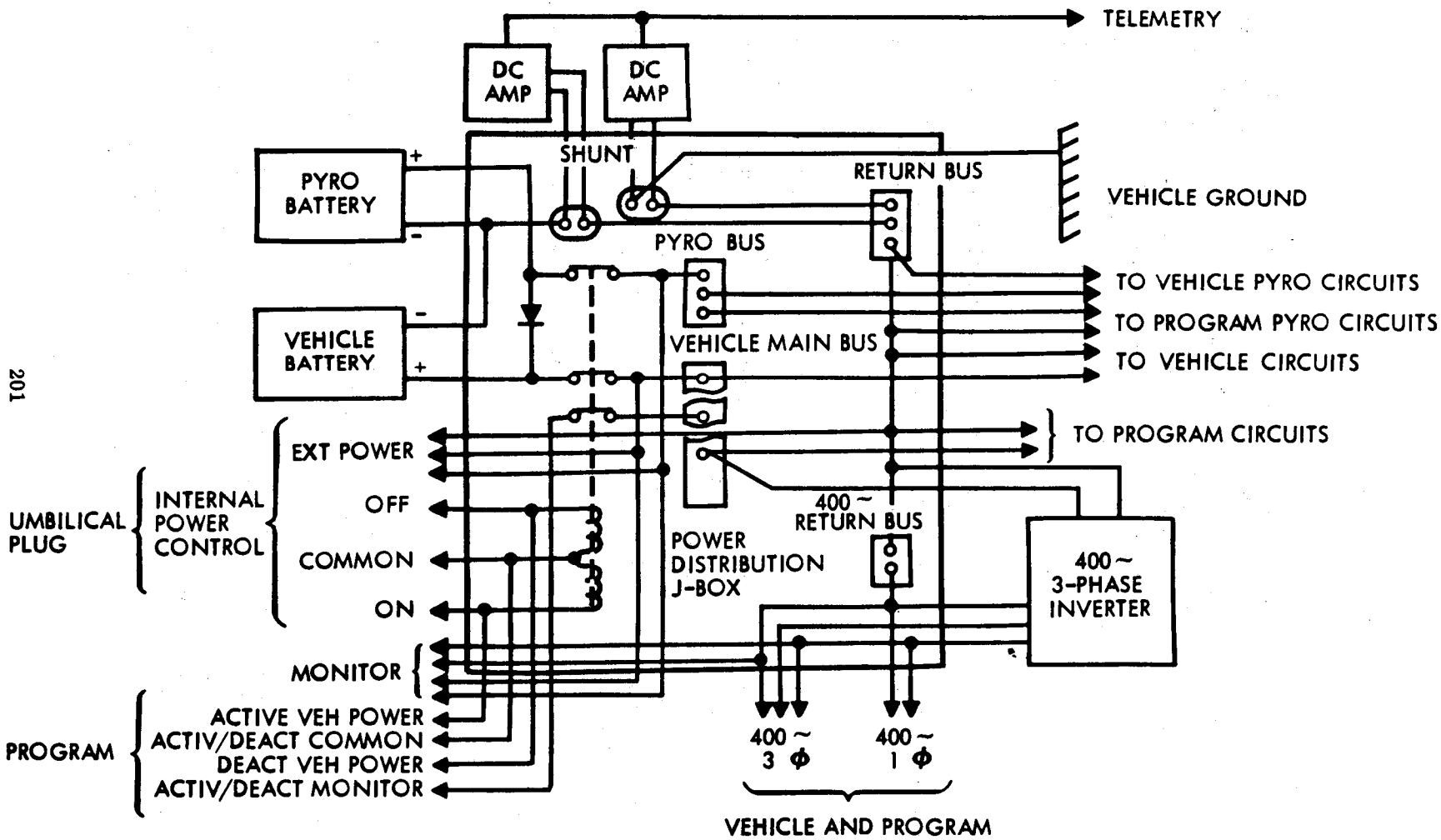

FIGURE 3.2-11: AGENA POWER DISTRIBUTION SYSTEM

3.2.2.4 COMMUNICATIONS AND CONTROL

Configuration

The major parts of the communications and control subsystem were the FM-FM telemetry package with commutated channels, the C-band tracking and the command destruct system. The telemetry package consisted of a Type V FM-FM telemetry unit and associated solid-state Type V 10-watt (VHF) FM transmitter, sensing devices, and a power controller harness and attached hardware. Vehicle state information was transmitted to ground receivers on IRIG Channels 5 through 18 and F. Channels 15 and 16 convey 60-point, no-return-to-zero, commutated data, a non-IRIG configuration. Main components were in the forward equipment section; sensing devices were located as needed throughout the vehicle. An F-slot cavity-type antenna was provided for telemetry purposes. Figure 3.2-12 is a block diagram of the telemetry system.

The SHF-band beacon transponder received 5690-MHz signals from the ground radar and transmitted 5765-MHz replies to facilitate radar tracking of the vehicle. A quarter-wave, recessed-stub antenna was provided for the beacon. The telemetry and beacon antennas were flush-mounted to the vehicle skin and designed for use with 50-ohm transmission lines.

Performance

Overall performance of the telemetry system was satisfactory, with no system malfunction indicated. Beacon performance was satisfactory with continuous interrogation throughout the observed period. The command destruct system operated satisfactorily during the activated period with signal strengths above 40 microvolts. At T+552 seconds (firing of horizon-sensor squibs), as the vehicle pitch attitude changed, the signal strength of the receivers varied between 2.4 and 40 microvolts. The command carrier was turned off at T+594 seconds. Figure 5-14 of the Lunar Orbiter A Launch Report, LMSC 273964, illustrates selected system parameters.

Telemetry power supply levels were nominal and the required inflight telemetry calibrations were performed.

3.2.2.5 GUIDANCE AND CONTROL

Configuration

The Agena guidance and control subsystem shown in Figure 3.2-13 performed the vehicle guidance, control, and flight programming functions necessary to accomplish the Lunar Orbiter I mission.

The guidance system included an inertial reference package (IRP), a horizon-sensor system, flight-control electronics unit, hydraulic and pneumatic attitude-control systems, velocity meter system, and two electromechanical sequence timers. All components were mounted in the forward equipment rack. The inertial reference package contained two hermetically sealed integrating gyroscopes to sense Agena pitch and yaw attitude and one miniature integrating gyroscope to sense the Agena roll attitude. Each gyro had a single degree of

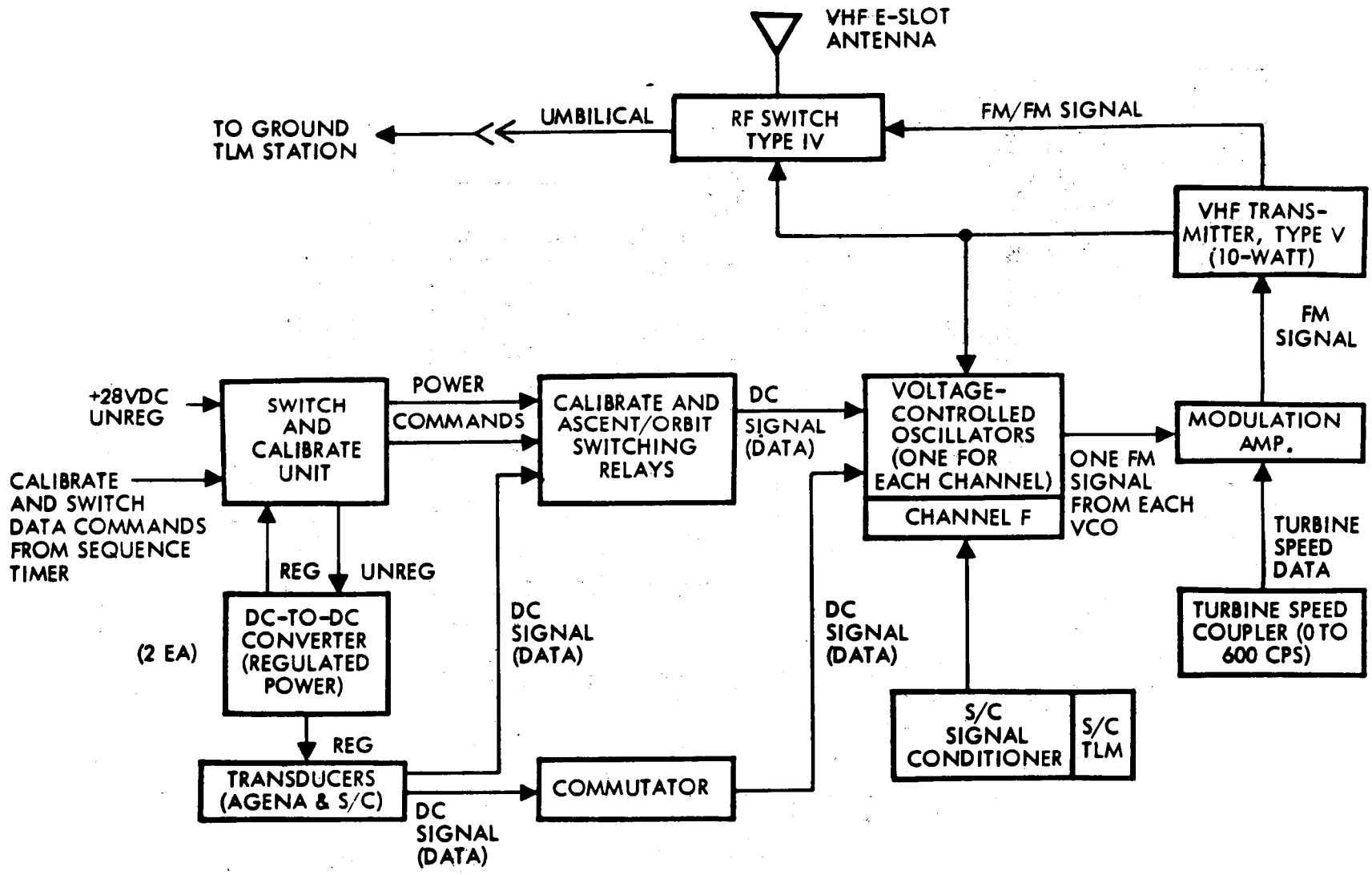

FIGURE 3.2-12: AGENA TELEMETRY SYSTEM BLOCK DIAGRAM

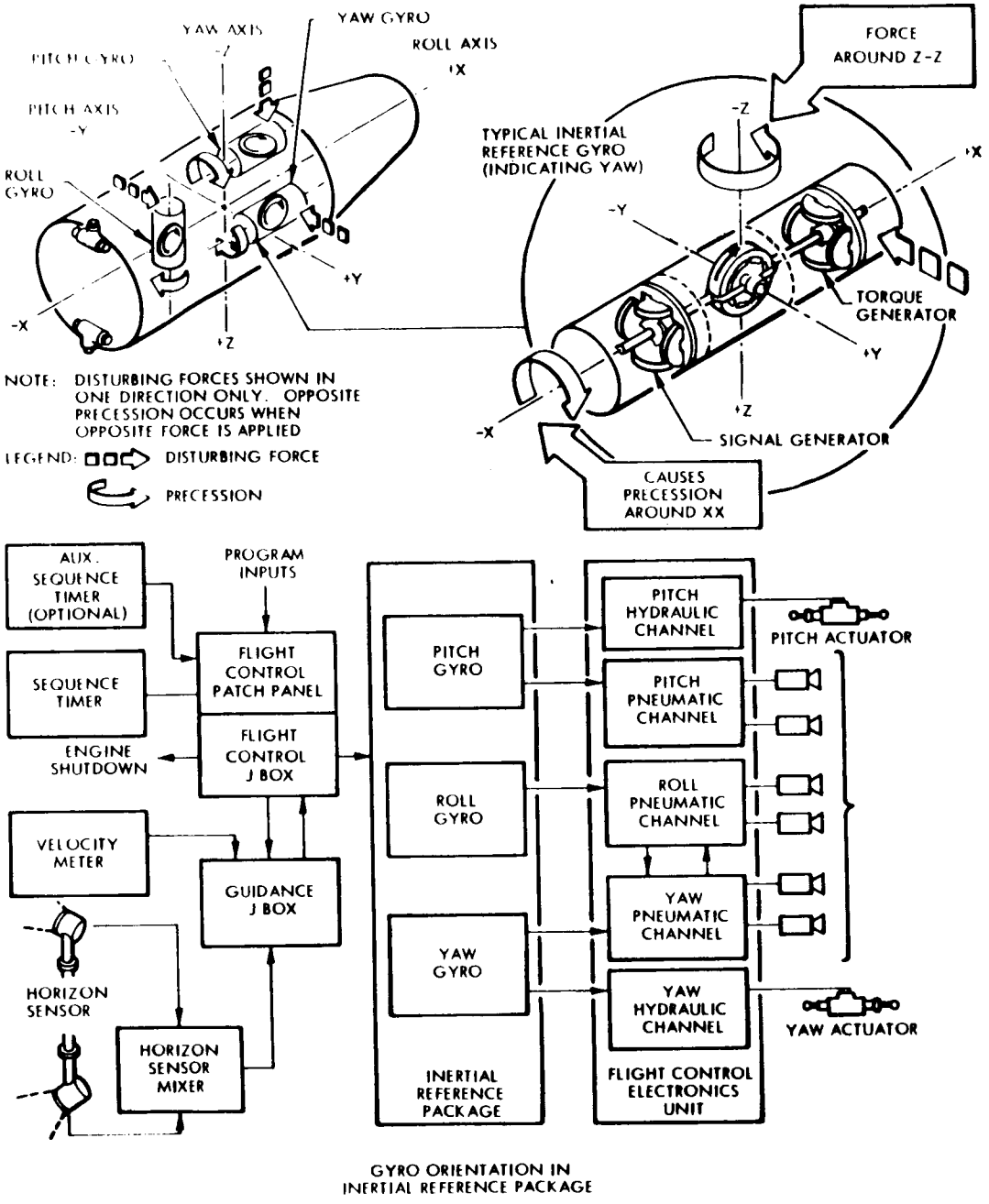

FIGURE 3.2-13: AGENA GUIDANCE AND CONTROL

freedom, was rate-integrating, and was temperature-controlled by internal heaters. The IRP was complemented by a horizon-sensor system consisting of two Barnes Model II-C infrared sensors, a single mixer, and a mounting fixture that can rotate (reposition) the sensor. This monitors vehicle pitch and roll relative to Earth (provides a local vertical reference) and corrects gyro references. The velocity meter system comprises a counter, accelerometer, and an accelerometer electronic unit. This system determined the vehicle velocity gain during each engine-burn period and terminated engine thrust when the correct velocity increase was gained.

The flight-control equipment comprised a nitrogen pneumatic control system, which (through six pneumatic thrust valves) provided three-axis corrective torques during coast periods and roll control while the rocket engine was operating; a hydraulic power package and servo actuators that altered engine thrust vector during powered flight; and an electronics system made up of an inertial-reference-package outputs and provided commands to the hydraulic actuators and thrust valves.

Performance

Guidance and flight control subsystem performance was normal during both engine-burn periods. Figures 5-8 through 5-13 of the Lunar Orbiter A Launch Report, LMSC 273964, illustrate selected Agena guidance and control parameters.

Inertial Reference Package

SLV-3 pitch and roll maneuvers were sensed by the caged Agena gyros during the boost phase. Small disturbances were also noted at BECO, while SLV-3/Agena separation produced almost none. The postseparation pitch-down maneuver was performed properly, and Telemetry Measurement D73, Pitch Torque, indicated close to the nominal -4 deg/min pitch rate for first burn.

Gyro disturbances at first-burn engine ignition were small: 0 degree in pitch, +2.8 degrees in roll, +1.89 degrees in yaw. Gas-valve action and hydraulic-actuator motion reduced the yaw error to +0.57 degree and the roll error to -1.2 degrees, and these biases were held constant throughout first-burn period. Pitch position moved slowly to -0.13 degree at T+380 seconds and then slowly returned to zero at first-burn cutoff. Actuator positions were +0.14 degree pitch, -0.25 degree yaw, and steady during first burn.

At first-burn cutoff, roll position moved to -2.0 degrees and pitch to +0.8 degree. Pitch error was reduced to zero by the gas valves within 7 seconds, but some roll error was noted for 30 seconds after cutoff. From T+536 to T+550 seconds, roll-gyro output and roll horizon-sensor output indicated a small sinusoidal motion of ±0.6 degree with a 1.6 second period. This motion was completely damped at T+550 seconds.

The vehicle then remained stable in the gyrocompassing mode, with zero pitch and roll errors through loss of signal at Station 91 (Antigua).

Gyro disturbances at second-burn ignition were small and were quickly damped out by hydraulic-actuator motion. Pitch-actuator offset during the second-burn period was +0.18 degree and yaw was -0.48 degree. Corresponding vehicle biases were -1.40 degrees in roll and +0.38 degree in yaw.

Horizon sensors—Horizon-sensor performance was satisfactory. At T+121 seconds, the pitch output began to move to a saturated negative conditon followed by the roll output to a saturated positive condition at T+138 seconds. The fairings were still attached at this time and aerodynamic heating of the fairings was the probable cause of saturation.

At fairing ejection (VECO) normal outputs were observed and appropriate gyro torquing signals produced. Vehicle disturbances noted above on the pitch and roll gyros were also present on the horizon-sensor outputs.

Reduction of the bias angle from 5.01 to 0.23 degree was noted at T+547.9 seconds, as well as the initiation of gyrocompassing at T+535.9 seconds.

Velocity meter—Agena first-burn cutoff was initiated by the velocity meter at T+523.0 seconds. The velocity meter telemetry remained connected to the accelerometer pendulum output throughout the cutoff and coast phases of flight, thus providing continuous data on vehicle longitudinal acceleration between burn periods. After first-burn cutoff, a normal string of output pulses of decreasing frequency was generated; at T+548 seconds, a pulse appeared that lasted 51.6 seconds, compared with 4.5 seconds for the immediately preceding pulse and 12.0 seconds for the following pulse. Because initiation of this long pulse occurred within 0.5 second of removal of the +5-degree horizon sensor bias angle and subsequent vehicle motion in the pitch plane, it is possible that a net zero or negative longitudinal acceleration was imposed on the velocity meter accelerometer during the 5-degree pitch adjustment, thus resulting in the long pulse. Pulses continued through loss of signal at Station 91, the last complete pulse having a 39-second duration.

During the coast phase between burn periods, the velocity meter output continued to pulse. Data from Station 12 (Goldstone) indicated pulses of 73-second duration, while Station 13 (Pretoria) data indicated pulses of 76-second duration.

The accelerometer output was disabled just prior to second-burn ignition, at which time telemetry was switched to the counter output to transfer the second-burn number from the storage register. Telemetry was then switched back to the velocity meter accelerometer output, and the velocity meter was enabled, as scheduled. Second-burn velocity-meter cutoff occurred at T+2282.2 seconds.

Sequence Timers

The primary sequence timer was started by an SLV-3 discrete command at T+294.9 seconds: timer brake release was verified by the appropriate step on D-14, the guidance and control monitor point. This start time was slightly later than the nominal of T+291.3 seconds. All timer-initiated events occurred within 0.1 second of the appropriate plus time from timer start.

Secondary timer start was not monitored directly on Agena telemetry; however, SLV-3 telemetry verified that the start discrete was transmitted at T+271.2 seconds. Correlating the time of second-burn ignition with the timer parameters for Launch Plan 10H indicates that the secondary timer functioned properly.

Table 5-4 of the Lunar Orbiter A Launch Report, LMSC 273964, presents the sequence of events through the first burn. This data is also included in Appendix C, "Sequence of Events."

Flight Controls

Hydraulic pressure (D60) was stable at 40 psig from liftoff to first-burn ignition. At ignition, pressure rose smoothly to 2960 psig within 1.5 seconds, then dropped to 2800 psig 2 seconds later. Pressure then rose gradually during first burn to about 2880 psig at cutoff. Cutoff caused a drop to 720 psig within 1 second, then a slower decrease to 80 psig at loss of signal at Station 91 (Antigua).

Hydraulic oil pressure rose smoothly to a peak of 2980 psig at second-burn ignition, then dropped to 2840 psig and remained steady for the duration of the burn period.

Both actuators performed properly. The pitch actuator moved from +0.73 degree at first ignition to -0.29 degree and back to +0.14 degree in 3 seconds, damping out the turbine runup transients. Position during first burn was steady at +0.14 degree. Yaw moved from +0.57 degree at first ignition to -0.66 degree and back to -0.25 degree in 3 seconds during runup transients. First-burn position was constant at -0.25 degree.

Gas-valve activity was initiated normally at SLV-3/Agena separation and continued through loss of signal. The following control-gas supply pressures were noted:

Liftoff	3680 psi
First ignition	3280 psi
First cutoff	3000 psi
Second ignition	2600 psi
Second cutoff	2400 psi

Selected guidance subsystem temperatures are tabulated in Table 5-3 of the Lunar Orbiter A Launch Report, LMSC 273964.

3.3 LAUNCH OPERATIONS

3.3.1 LAUNCH OPERATION PLAN

The Lunar Orbiter Launch Operation Plan, Lockheed Missiles and Space Company Document A751901, provided the overall planning information used by the organizations that participated in the Lunar Orbiter launch. Referenced in the document were the procedures to implement preflight tests, checkout, and launch of the space vehicle.

3.3.1.1 PRELAUNCH OPERATION ORGANIZATION

Launch operations required the efforts of many participating organizations: NASA, Langley Research Center (LRC); NASA, Lewis Research Center (LeRC); Jet Propulsion Laboratory (JPL); Kennedy Space Center/Unmanned Launch Operations (KSC/ULO); The Boeing Company (TBC); General Dynamics/Convair (GD/C); Lockheed Missiles and Space Company (LMSC); General Electric (GE); Burroughs Corporation (BC); and Air Force Eastern Test Range (AFETR).

The working relationships of these organizations are diagrammed in Figure 3.3-1. The responsibilities and authority for each of the participating agencies are briefly described in this section.

Langley Research Center (LRC)

Langley Research Center was responsible for all Lunar Orbiter program activities at AFETR. A deputy for AFETR operations was assigned by LRC to ensure complete integration and maximum usage of resources, procedures, and personnel. Langley Research Center was also responsible for spacecraft assembly and checkout.

Lewis Research Center (LeRC)

Lewis Research Center supported the Lunar Orbiter program by providing the Atlas-Agena launch vehicle and associated services necessary to launch and boost the spacecraft into the proper cislunar trajectory.

Jet Propulsion Laboratory (JPL)

Jet Propulsion Laboratory was responsible for operating DSIF Station 71, Hangar AO Control Center, and associated communication channels in support of spacecraft checkout activities and launch operations.

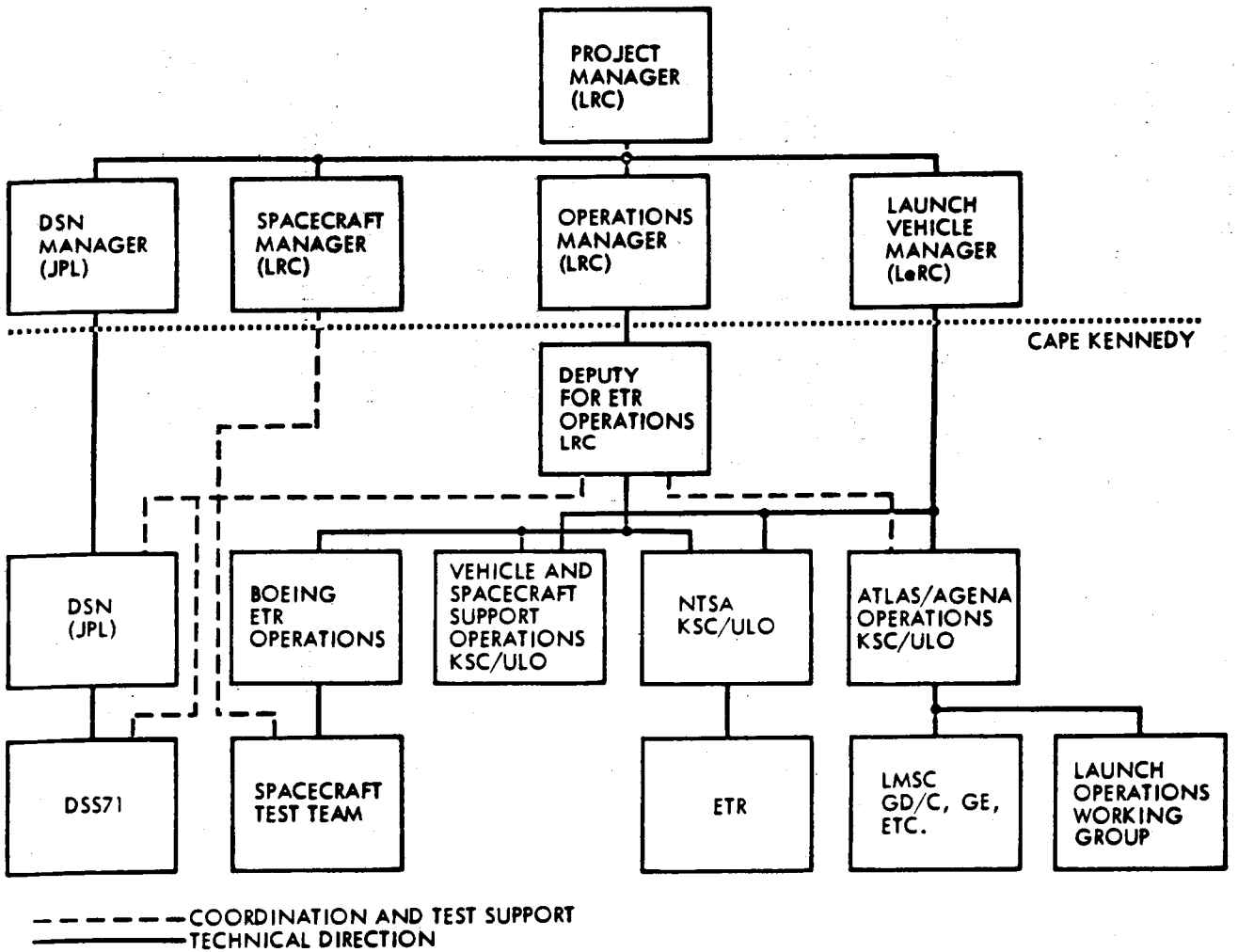

FIGURE 3.3-1: PRELAUNCH OPERATIONS ORGANIZATION

Kennedy Space Center (KSC/ULO)

The Unmanned Launch Operations Division had three areas of responsibility for supporting the Lunar Orbiter program:

1) Atlas-Agena Operations was responsible for all activities associated with launch-vehicle assembly and checkout and space-vehicle operations consistent with KSC/ULO and LeRC agreements. These responsibilities included:

   a) Technical direction of participating contractors,

   b) Integrated test planning and scheduling,

   c) Integration and coordination of space vehicle support requirements levied on AFETR,

   d) Conduct of launch operations at Complex 13,

   e) Chairmanship of Launch Operations Working Group (LOWG).

   (The LOWG participated in mission, spacecraft, launch vehicle, and range-readiness meetings and was the primary coordinating agency for flight preparations at the ETR).

2) Vehicle and Spacecraft Support Operations was responsible for providing spacecraft assembly and checkout facilities, coordinating spacecraft operations with launch-vehicle and AFETR personnel, obtaining minor range support, ensuring that operations were conducted in accordance with NASA and AFETR regulations, and serving in a monitoring and consulting capacity to the deputy of AFETR operations.

3) NASA Test Support Agena (NTSA) was responsible for officially representing the Lunar Orbiter program to the AFETR; submitting all range documentation and requirements; negotiating with the AFETR such matters as operations support and safety requirements; and ensuring that all support was obtained in a timely manner.

The Boeing Company (TBC)

The Boeing Company was responsible to LRC for receiving, inspection, assembly, and test of the Lunar Orbiter spacecraft through the launch phase. Boeing was also responsible for providing mission integration support to the Lunar Orbiter deputy for AFETR operations.

General Dynamics/Convair (GD/C)

General Dynamics was responsible for receiving, processing, testing, and launching the Atlas booster. Technical direction, as required, was provided by KSC/ULO representatives.

Lockheed Missiles and Space Company (LMSC)

Lockheed Missiles and Space Company was responsible for receiving, checkout, and launching the Agena. In addition, LMSC, under the direction of the Atlas-Agena LOWG, was responsible for the preparation of integrated launch operations test procedures, test directives, and milestone schedules for each flight; these were submitted to KSC/ULO for coordination and approval.

General Electric Company (GE)

General Electric Company was responsible to KSC/ULO for maintenance, checkout, and operation of the Mod III-G guidance facility at AFETR. The Mod III-G equipment provided the tracking data required for guidance of the Atlas during the boost phase of flight.

Burroughs Corporation (BC)

Burroughs Corporation was responsible to KSC/ULO for maintenance, prelaunch checkout, and operation of the Mod III-G guidance computer facility at AFETR. The computer used tracking data for trajectory computation to determine guidance commands.

Air Force Eastern Test Range (AFETR)

AFETR, a part of the National Range network, operated and maintained ETR and its support facilities. It also acquired, processed, and evaluated flight data as requested. Pan American World Airways (PAA) and Radio Corporation of America (RCA) under contract to the AFETR were responsible for the operation and management of its support facilities. The AFETR range representative served as the superintendent of range operations (SRO) during launch countdowns.

3.3.1.2 LAUNCH OPERATION ORGANIZATION

The operation organization for the countdown and launch was as shown in Figure 3.3-2. The Lunar Orbiter project manager as mission director (LRC) had overall authority, control, and responsibility for all mission operations. Three program systems managers assisted the mission director in interpreting special problems associated with launch operations and the launch phase of the mission.

1) The launch-vehicle system manager (LeRC) was in the launch vehicle control center and monitored launch vehicle operations. He was the final authority for determining that the launch vehicle was ready to launch.

2) The DSN system manager (JPL) was in the Space Flight Operations Facility (SFOF) at Pasadena, California during launch. He was available for telephone consultation with the mission director in matters pertaining to DSN readiness and operations.

3) The spacecraft system manager (LRC) witnessed the spacecraft countdown from DSS-71 and served as advisor to the mission director on technical problems encountered with the spacecraft.

Blockhouse Personnel

Launch Director

The launch director (KSC/ULO) had operational and technical direction over prelaunch operations of the launch vehicle and over launch operations of the launch vehicle and spacecraft combination. He supervised the launch countdown in compliance with previously established procedures.

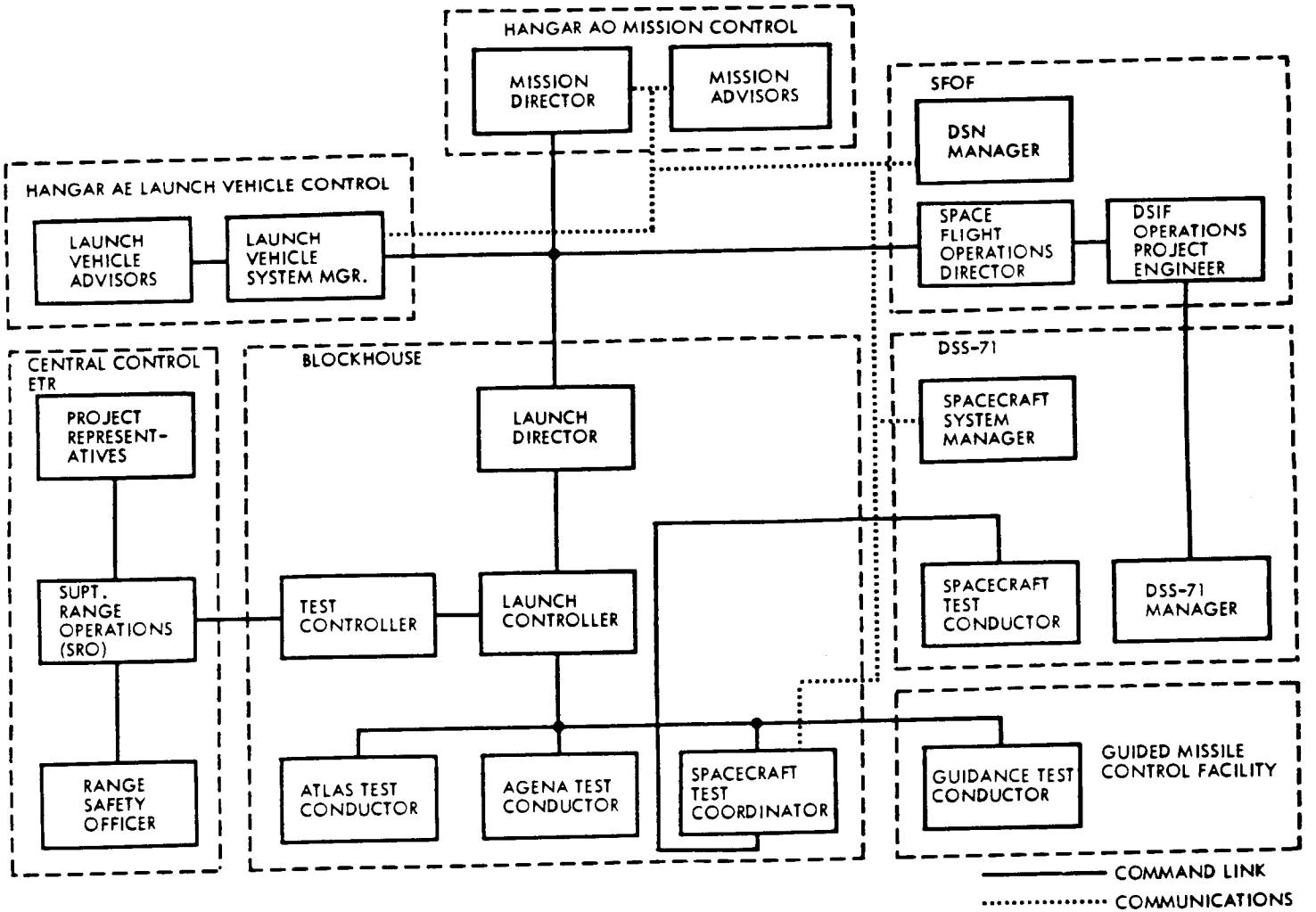

FIGURE 3.3-2: LAUNCH OPERATIONS ORGANIZATION

Launch Conductor

The launch conductor (GD/C) was responsible to the launch director for the launch countdown of the combined launch vehicle and spacecraft.

Atlas Test Conductor

The Atlas test conductor (GD/C) was responsible for maintaining readiness of the Atlas booster in accordance with the countdown. He reported Atlas status to the launch conductor.

Agena Test Conductor

The Agena test conductor (LMSC) was responsible for maintaining the readiness of the Agena in accordance with the countdown. He reported Agena status to the launch conductor.

Spacecraft Test Coordinator

The spacecraft test coordinator (KSC/ULO) was responsible for coordinating and integrating the spacecraft system into the overall countdown. He acted as the point of contact between the spacecraft and the launch conductor during the countdown.

Test Controller

The test controller (KSC/ULO) was the official contact with AFETR in matters concerning scheduling, project-readiness, range support, test termination, and related items.

DSS-71 Personnel

Spacecraft Test Conductor

The spacecraft test conductor (TBC) was responsible for maintaining spacecraft readiness in accordance with the countdown. He reported spacecraft status to the spacecraft test coordinator.

Spacecraft Test Team

The spacecraft test team (TBC) was responsible to the spacecraft test conductor for conducting spacecraft tests and ensuring spacecraft readiness in accordance with the countdown.

DSS-71 Manager

The DSS-71 manager (JPL) was responsible to the DSIF operations project engineer for station operations. He coordinated and controlled the personnel and equipment at DSS-71 during the preparation and execution of the flight.

Central Control Personnel

Superintendent Range Operations

The superintendent of range operations (PAA) was resonsible for range command. He was responsible for committing range resources to support the launch operations as described in applicable operations directives.

Range Safety Officer

The range safety officer (AFETR) monitored the flight path of the space vehicle. He was responsible for destroying the vehicle if required.

Project Representatives

The project representatives (LRC/KSU/ULO) monitored overall operations and served as technical consultants to the superintendent of range operations (SRO) on all project matters.

Guided Missile Control Facility 1

Guidance Test Conductor

The guidance test conductor (GE) was responsible for operating and maintaining readiness of GMCF-1 and the Mod III guidance system. He reported status to the launch conductor.

Space Flight Operations Facility (SFOF)

Space Flight Operations Director (SFOD)

The space flight operations director (LRC) was responsible for ensuring that flight operations personnel and DSN equipment were in the proper state of readiness for mission support and control of the mission following spacecraft acquisition by the DSIF. All command transmissions had to be approved by him, as were flight-operation decisions made during both standard and nonstandard modes of operation. He was responsible to the mission director for the conduct of flight operations.

DSIF Operations Project Engineer

The DSIF operations project engineer (JPL) was responsible for planning and coordinating the interface engineering and for DSN operational planning in support of the Lunar Orbiter project. He matched the requirements of the flight project with the capabilities of the DSN. During operations, he acted as an assistant to the SFOD for the DSN. He was assisted by the DSN system project engineers as necessary to achieve system integration and compatibility.

3.3.2 LAUNCH BASE FACILITIES (GENERAL)

The AFETR provided facilities for receiving, inspection, assembly, checkout, and launch of the space vehicle. Vehicle final assembly and checkout was conducted in the areas designated below:

User	Vehicle	Area
GD/C	Atlas	Hangar J
LMSC	Agena	Hangar E
TBC	Spacecraft	Hangar S

An explosive-safe area near the east edge of Area 5/6 was used for final preparation of the completed spacecraft, which included connection of pyrotechnic devices, and mating to the shroud and adapter. Launch Complex 13 was used to launch the space vehicle (Figure 3.3-3). The two major portions of the launch complex were the blockhouse and the test stand. The blockhouse contained the consoles and equipment for control and monitoring of all launch-vehicle systems (Figure 3.3-4). The spacecraft console was used to control and monitor limited spacecraft critical functions during prelaunch checkout and operations prior to liftoff; DSS-71, however, was the primary location for monitoring spacecraft functions during launch.

The major facilities comprising the test stand area were the launch service building, service tower (gantry), umbilical mast with boom, propellant storage and transfer equipment, gas storage and loading equipment, work shops, and general storage areas (Figure 3.3-5).

A spacecraft checkout van was located near the test stand and provided a backup capability for spacecraft checkout during on-pad operations. It was removed during the final countdown at T-285 minutes.

3.3.2.1 ETR INSTRUMENTATION AND COMMUNICATION FACILITIES

Data acquisition and tracking from space vehicle liftoff through the Agena yaw-around and retromaneuver were provided by AFETR instrumentation facilities. A summary of ETR stations, instrumentation available at each, and general use category is compiled in Table 3.3-1. Station coordinates for land-based stations, referenced to the Kaula Radar Coordinate System, are shown in Table 3.3-2.

Radar tracking data provided trajectory information for determining spacecraft maneuvers as well as space position. This data was gathered by the various tracking stations (Figure 3.3-6), transmitted to AFETR (Figure 3.3-7), and fed into computers that calculated trajectories and velocity.

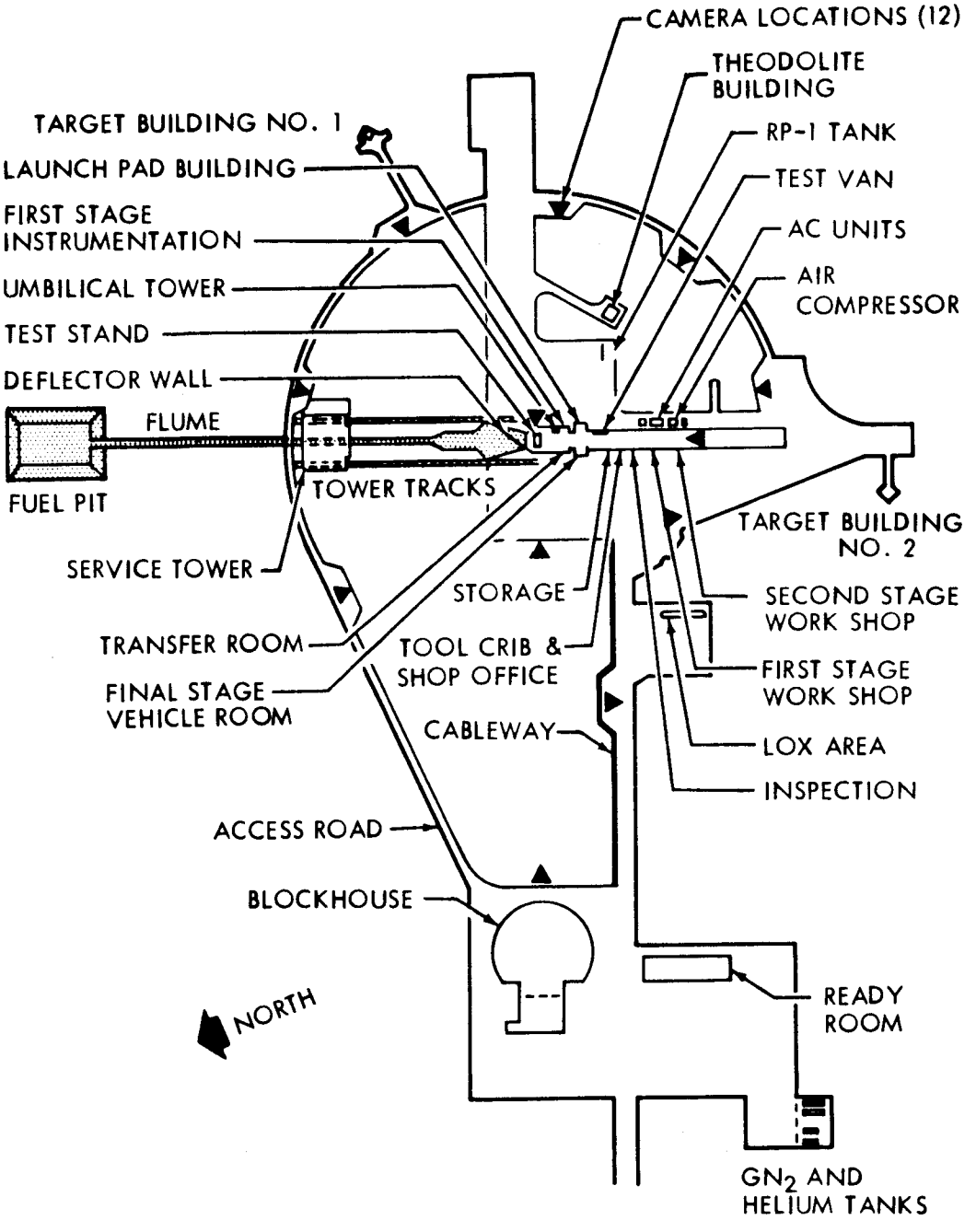

FIGURE 3.3-3: ETR LAUNCH COMPLEX 13 PLANVIEW

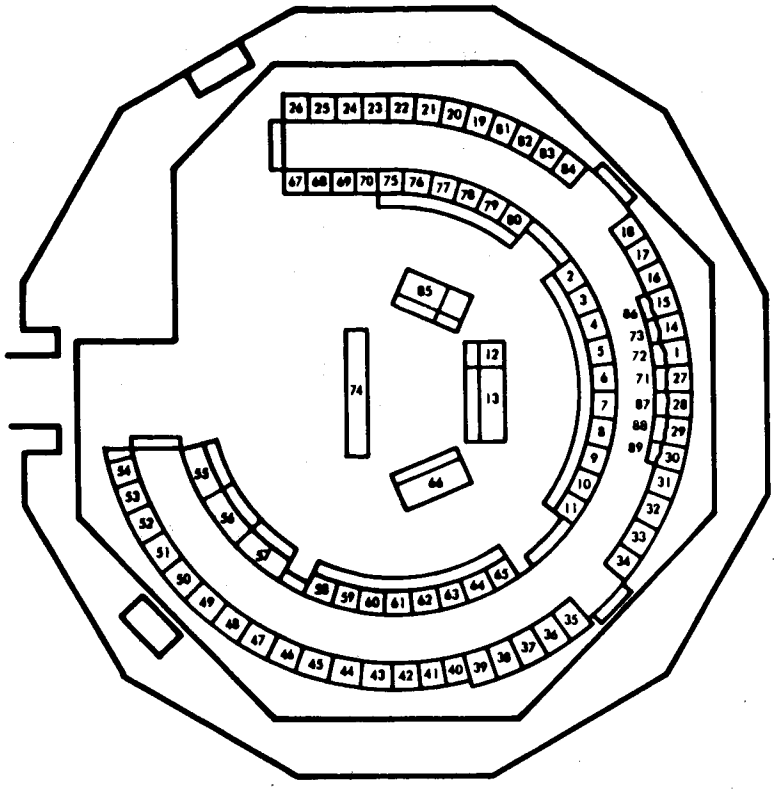

LEGEND

LOCATION NO.	EQUIPMENT	LOCATION NO.	EQUIPMENT
1	AUXILIARY, MSL, AND FACILITY POWER	35 - 36	AGENA SANBORN RECORDER RACK
2	AUTOPILOT CONSOLE NO. 1	37	AGENA SEQUENCER RECORDER
3	AUTOPILOT CONSOLE NO. 2	38 - 40	CEC TAPE SYSTEM
4	GUIDANCE CONSOLE	41	EQUIPMENT STORAGE RACK
5	HOLDDOWN/RELEASE AND HYDRAULIC CONSOLE	42	ANALOG PATCH PANEL
6	FUEL CONSOLE	43 - 50	BROWN GRAPHIC RECORDER RACK
7	LO_2 TANKING CONSOLE	51	SPARE RACK
8	PNEUMATIC CONSOLE	52 - 54	OSCILLOGRAPH RECORDER RACK
9	TELEMETRY AND RANGE SAFETY CONSOLE	55	SPACE
10	WATER SYSTEM CONSOLE	56	TV CONTROL CONSOLE
11	MISSILE POWER CONSOLE	57	INSTRUMENTATION CONTROL CONSOLE
12	BLOCKHOUSE MONITOR CONSOLE	58	AGENA COMMUNICATIONS CONSOLE
13	TEST CONDUCTOR'S CONSOLE	59 - 61	AGENA ELECTRICAL & GUIDANCE CONSOLE
14	SPARE RACK	62 - 63	AGENA PNEUMATIC & PROPULSION CONSOLE
15 - 17	SANBORN RECORDER RACK	64	AGENA POWER SUPPLY
18	AUTOPILOT RACK NO. 1	65	AGENA INTERCONNECT BOX
19 - 20	SPACE	66	AGENA LAUNCH CONDUCTOR'S CONSOLE
21 - 25	BROWN GRAPHIC RECORDER RACK	67 - 70	SPACES
26	SPARE RACK	71 - 73	TV MONITORS
27	RACK ASSEMBLY ENGINE TEST, AND PURGE	74	COMMUNICATIONS AND OPERATIONS TABLE
28	RANGE SAFETY COMMAND CHECKOUT SET	75 - 78	SPACE
29 - 30	SPARE RACK	79 - 80	SANBORN RECORDER RACKS
31	EQUIPMENT STORAGE RACK	81 - 84	SPACE
32	SEQUENCE RECORDER & PATCH PANEL	85	S/C MASTER LCC
33	SEQUENCE RECORDER RACK	86	PROVISIONS FOR TV MONITOR
34	SOUND RECORDER RACK	87 - 89	COUNTDOWN CLOCKS

FIGURE 3.3-4: ETR LAUNCH COMPLEX 13 BLOCKHOUSE EQUIPMENT LOCATION

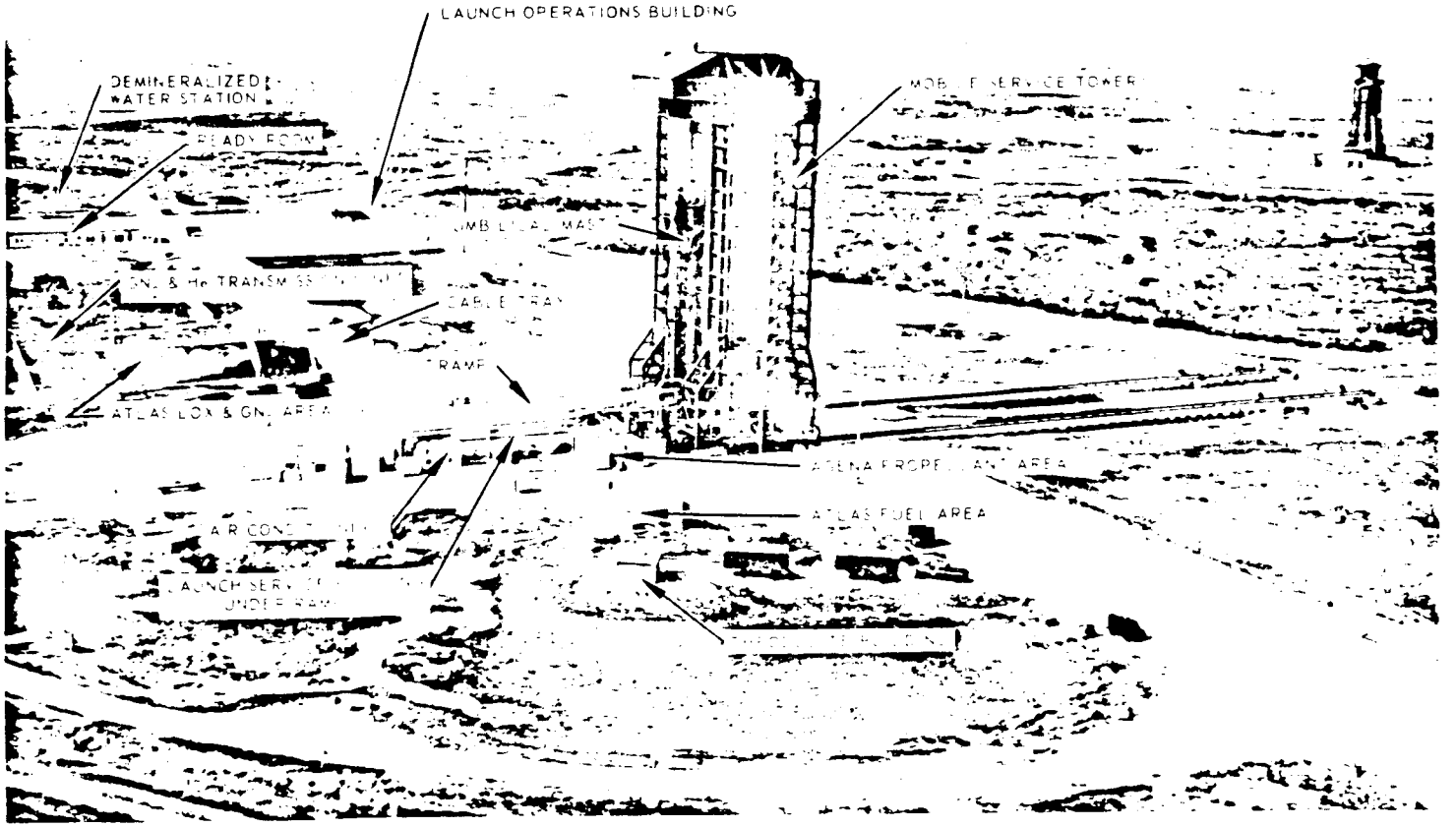

FIGURE 3.3-5: ETR LAUNCH COMPLEX 13

Table 3.3-1: ETR Instrumentation Summary

Station	Instrumentation	Use
Cape Kennedy Station 1	Ballistic Cameras (BC-4)	Metric Data
	Cinetheodolites	Metric Data
	C-Band Radar (FPS-16)	Metric Data, Range Safety
	Fixed Camera System (CZR and RC-5)	Metric Data
	Pad Cameras (16, 35, and 70 mm)	Engineering Sequential
	Telemetry PAM/FM/FM (VHF) 2 links FM/PM (S-Band) 1 link	Internal Data
	Command Destruct	Range Safety
	Wire Sky Screen	Range Safety
	TV Sky Screen	Range Safety
	Telemetry ELSSE	Range Safety
	L-Band Radar (AN/FPS-8)	Range Safety
	High-Resolution Radar Tracker (Mod IV)	Range Safety
	IBM 7094 Computer	Range Safety
	Igor (35- and 70-mm cameras)	Engineering Sequential
Williams Point	Igor (35- and 70-mm cameras)	Engineering Sequential
Cocoa Beach	Cinetheodolite	Metric Data
	Roti (70-mm cameras)	Engineering Sequential
Patrick AFB Station 0	Cinetheodolites	Metric Data
	C-Band Radar (AN/FPQ-6)	Metric Data, Range Safety
	Igor (35- and 70-mm cameras)	Engineering Sequential
Melbourne Beach	Roti (70-mm cameras)	Engineering Sequential

Table 3.3-1: (Cont'd.)

Station	Instrumentation	Use
Vero Beach	Roti (70-mm cameras)	Engineering Sequential
Grand Bahama Island Station 3	C-Band Radar (FPS-16) Ballistic Cameras (BC-4) Telemetry PAM/FM/FM (VHF) 2 links FM/PM (S-Band) 1 link Command Destruct	Metric Data Metric Data Internal Data Range Safety
Merritt Island Station 19	C-Band Radar (FPQ-6)	Metric Data
Grand Turk Station 7	Command Destruct C-Band Radar (TPQ-18)	Range Safety Metric Data
Antigua Station 91	C-Band Radar (AN/FPQ-6) Telemetry PAM/FM/FM (VHF) 2 links FM/PM (S-Band) 1 link Command Destruct	Metric Data, Range Safety Internal Data Range Safety
Ascension Station 12	C-Band Radar (AN/FPS-16 or AN/TPQ-18) Telemetry FM/FM (VHF) 1 link FM/PM (S-Band) 1 link	Metric Data Internal Data
Bermuda	C-Band Radar (FPS-16)	Contingent on Commitment by NASA

Table 3.3-1: (Cont'd.)

Station	Instrumentation	Use
Pretoria Station 13	C-Band Radar (AN/MPS-25) Telemetry FM/FM (VHF) 1 link FM/PM (S-Band) 1 link	Metric Data Internal Data
Ship* (VC2-S-AP3) Twin Falls, Victory (C4-S-A1) ARIS	C-Band Radar (FPS-16) Telemetry FM/FM (VHF) 1 link FM/PM (S-Band) 1 link	Metric Data Internal Data
Ship* (2 required) (C1-M-AV1)	Telemetry FM/PM (S-Band) 1 link Range User Equipment	Internal Data GE Guidance System Calibration
Aircraft	TM Data Receiving Equipment	Return of Data

* Use and position depends upon trajectory.

Table 3.3-2: ETR Station Coordinates

Station	Latitude	Longitude
Cape Kennedy, Sta. 1	28° 28' 54.06" N	80° 34' 36.2" W
Patrick AFB, Sta. 0	28° 13' 35.3" N	80° 35' 58.2" W
Grand Bahama Is., Sta. 3	26° 36' 56.5" N	78° 20' 52.94" W
Merritt Island, Sta. 19	28° 25' 29.212" N	80° 39' 52.612" W
Grand Turk, Sta. 7	21° 27' 46.03" N	71° 07' 55.86" W
Antigua, Sta. 91	17° 08' 37.14" N	61° 47' 33.93" W
Ascension, Sta. 12	7° 57' 05.83" S	14° 24' 44.71" W
Pretoria, Sta 13	25° 56' 36.09" S	28° 21' 40.73" E

Note: Coordinates referenced to the Kaula Radar Coordinate System.

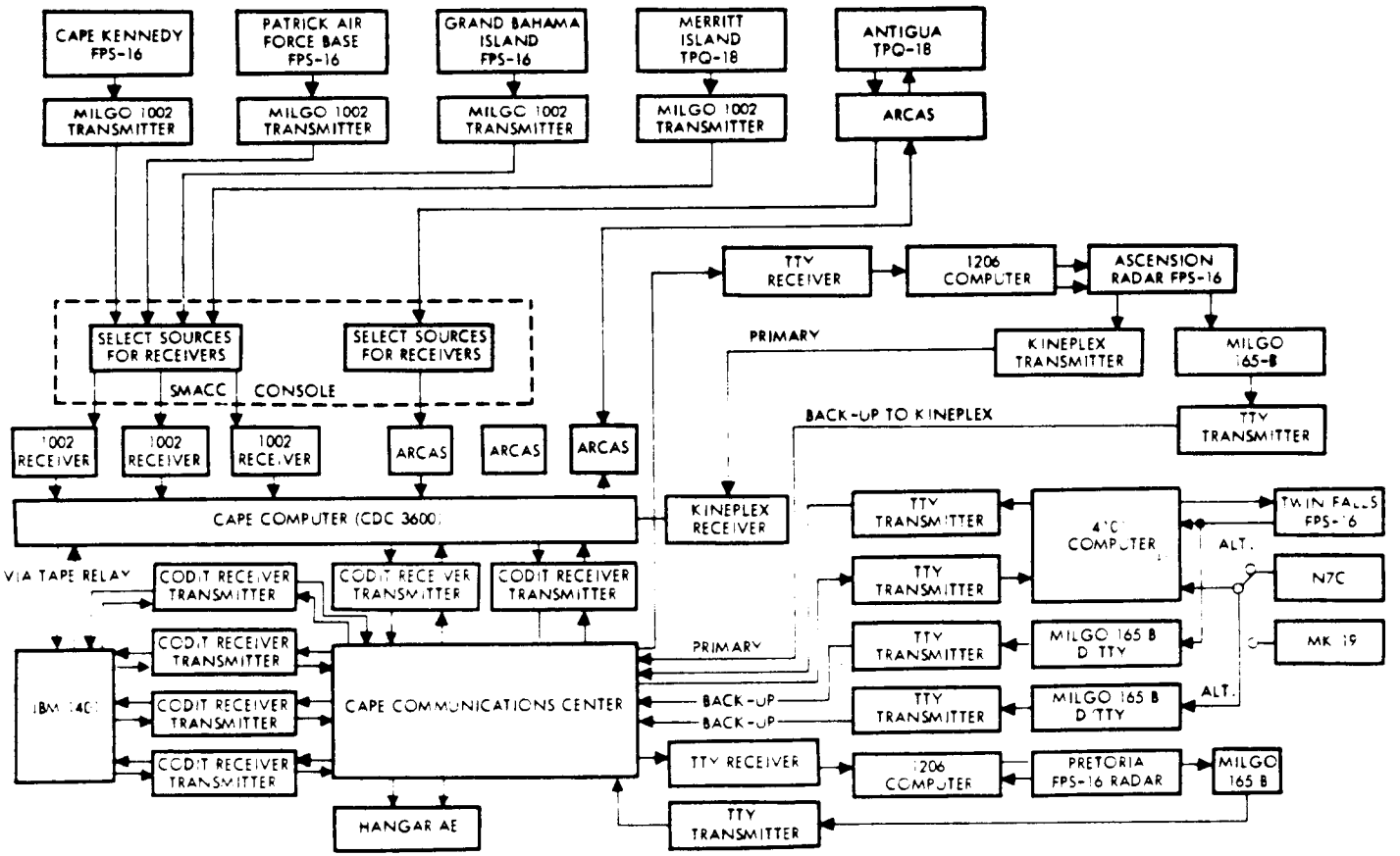

FIGURE 3.3-6: ETR TRACKING DATA HANDLING SYSTEM

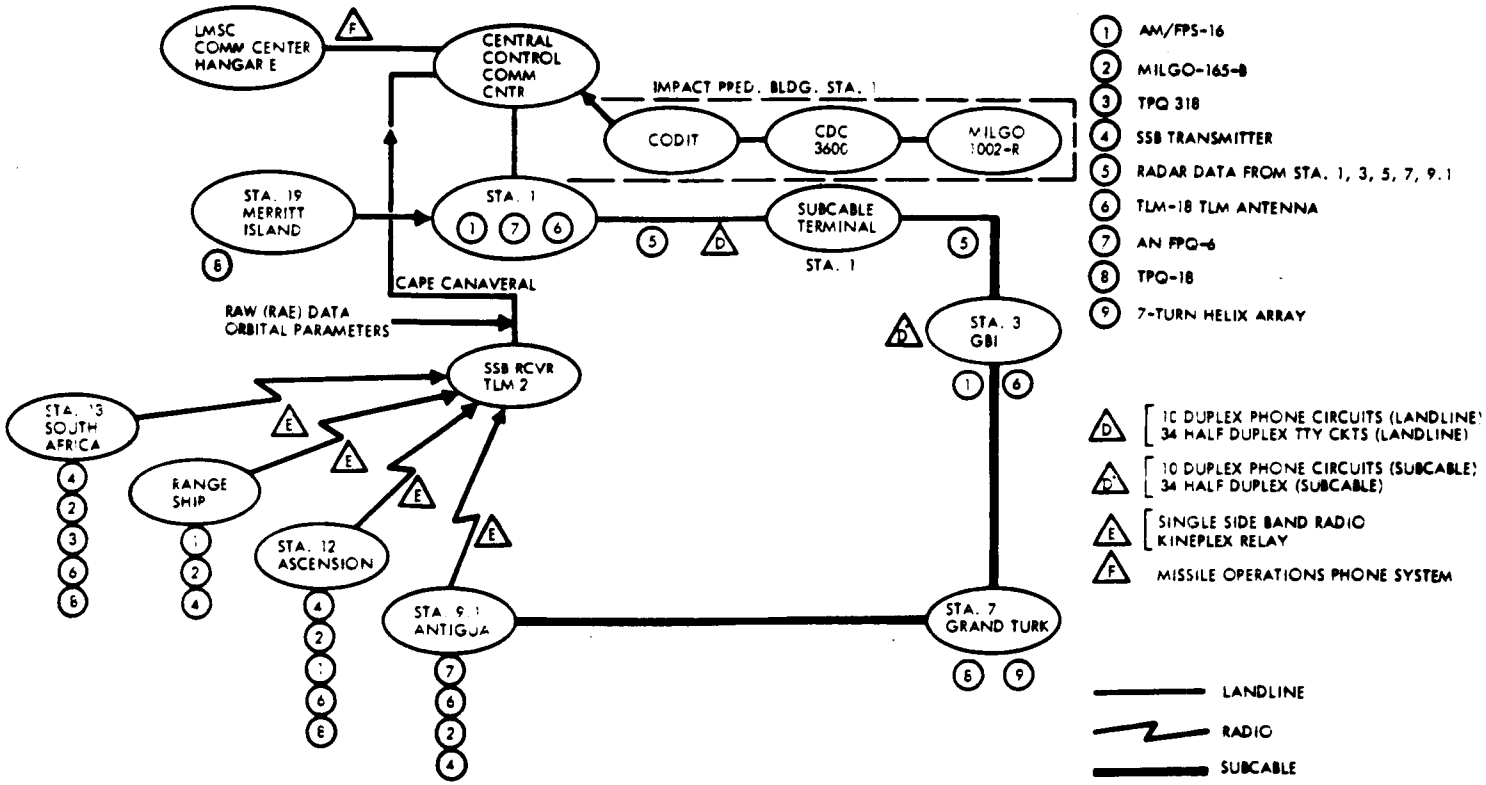

FIGURE 3.3-7: ETR LAUNCH DATA TRANSMISSION NETWORK

3.3.2.2 ATLAS GUIDANCE-GROUND EQUIPMENT

Two ground systems, the Mod III radio guidance and tracking and the Mod III guidance computer, provided guidance signals to the Mod III airborne equipment in the Atlas during portions of the Atlas-powered flight. (The airborne equipment is discussed in Section 3.2.1).

The Mod III radio guidance and tracking subsystem included position and rate measuring as well as flight-data recording equipment. An X-band tracking radar in conjunction with the airborne pulse beacon provided space-vehicle position data to the ground computer. This position data consisted of azimuth and elevation angles in digital form and slant range as a time delay between a ranging pulse and a reference pulse. Radial and lateral velocity vectors of the space vehicle were provided to the computer by the X-band rate-measuring radar and the airborne rate beacon. The flight-data recording equipment recorded performance of the ground-based Mod III radio guidance and tracking equipment.

The Mod III guidance computer was a Burroughs A-1 computer. It accepted space-vehicle position and velocity data from the X-band position and rate radars and, in accordance with guidance equations and target coordinates, computed steering and discrete commands that were transmitted to the Atlas via the X-band radar.

3.3.3 SPACECRAFT PROCESSING

The final spacecraft processing was conducted at Cape Kennedy, Florida, in three facilities: Hangar "S", Explosive-Safe Area 5/6, and Launch Complex 13.

3.3.3.1 HANGAR "S" (INDUSTRIAL AREA)

This facility housed the spacecraft test area, which was an enclosed room having approximately 2400 square feet of floor space. The environment in the room was maintained as a class 100,000 clean room as defined by Federal Standard 209. The room was provided with equipment and personnel air locks to maintain the cleanliness. All personnel within the room wore clean-room uniforms.

Adjacent to the spacecraft test area in Hangar "S" was a test directors room, camera loading room, ground reconstruction equipment area, darkrooms, and the spacecraft checkout van parking area. The layout of the Hangar "S" area is shown in Figures 3.3-8 and 3.3-9.

The flight spacecraft was processed at Hangar "S" to verify, by repeat of subsystem functional testing, that the spacecraft still complied with its design, construction, and performance requirements after shipment to ETR.

The Hangar "S" processing consisted of four test catagories: (1) equipment alignment, (2) functional checkout, (3) weight and balance, and (4) special tests. Equipment alignment was conducted on the optical alignment fixture, which was capable of measuring the alignment of critical components to a high degree of accuracy. The functional checkout was conducted with standard test equipment and some special equipment designed for the Lunar Orbiter. One of the major components was the three-axis test stand (see Figure 3.3-10).

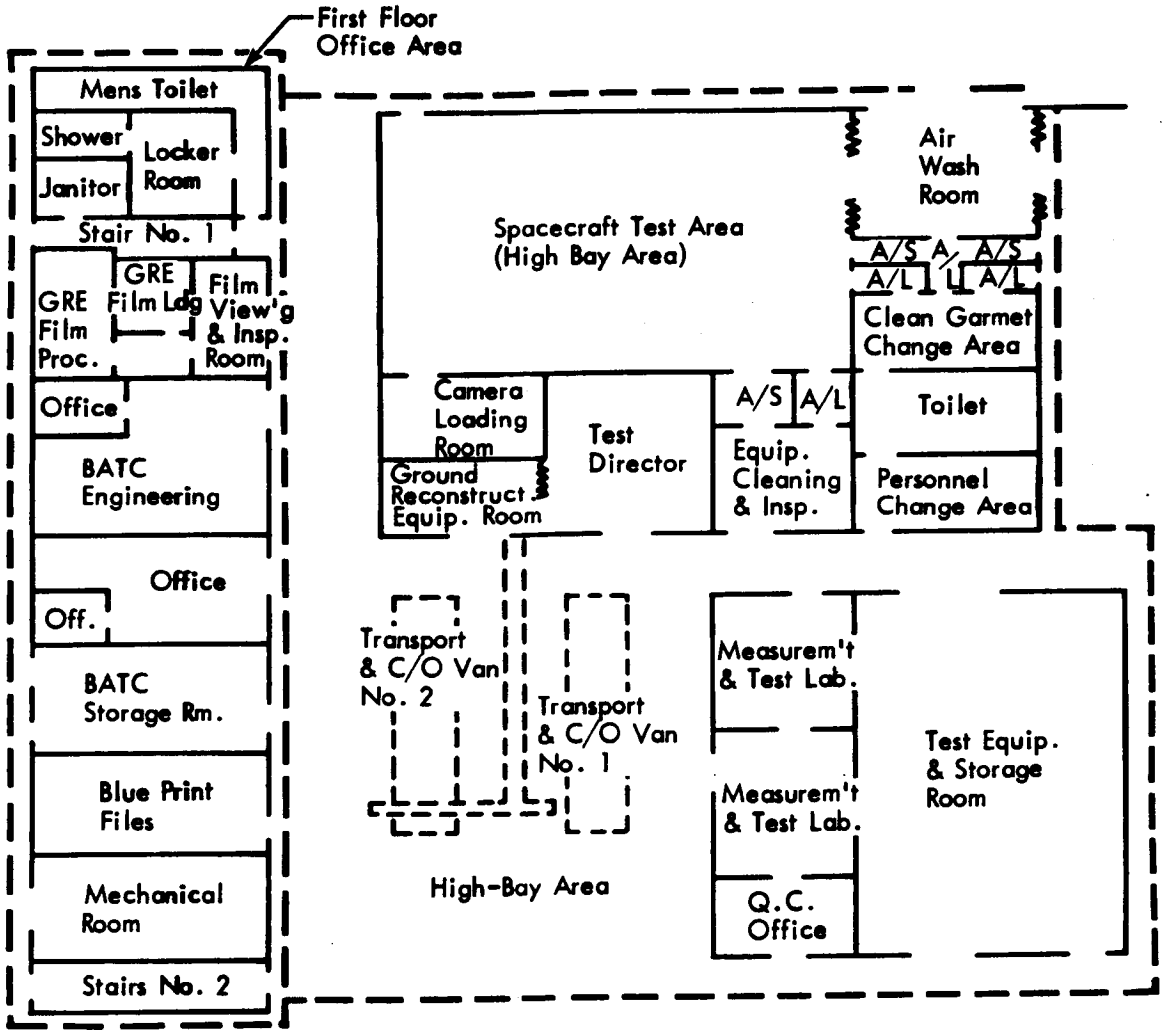

FIGURE 3.3-8: HANGAR "S" (INDUSTRIAL AREA) LAYOUT

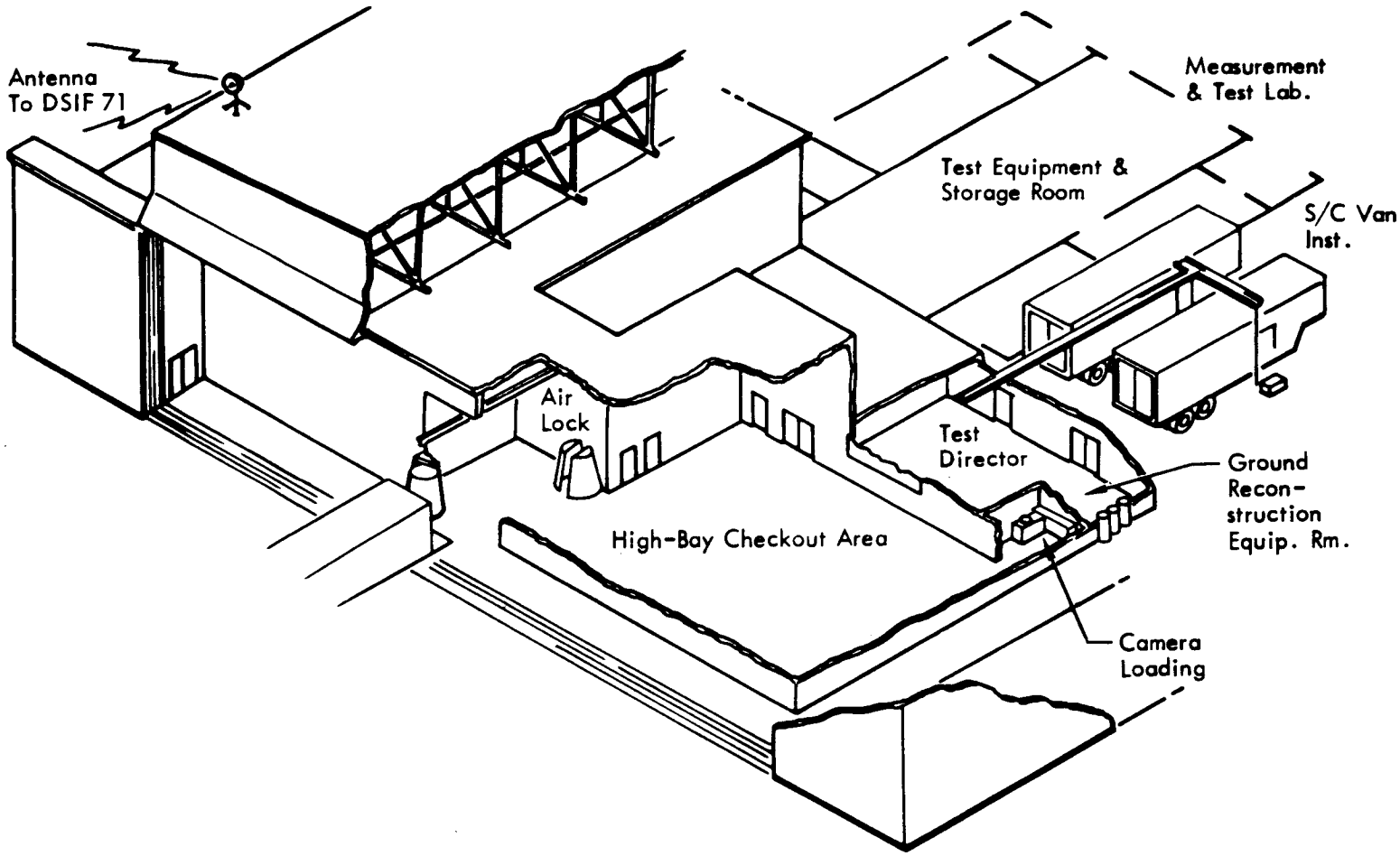

FIGURE 3.3-9: HANGAR "S" (INDUSTRIAL AREA)

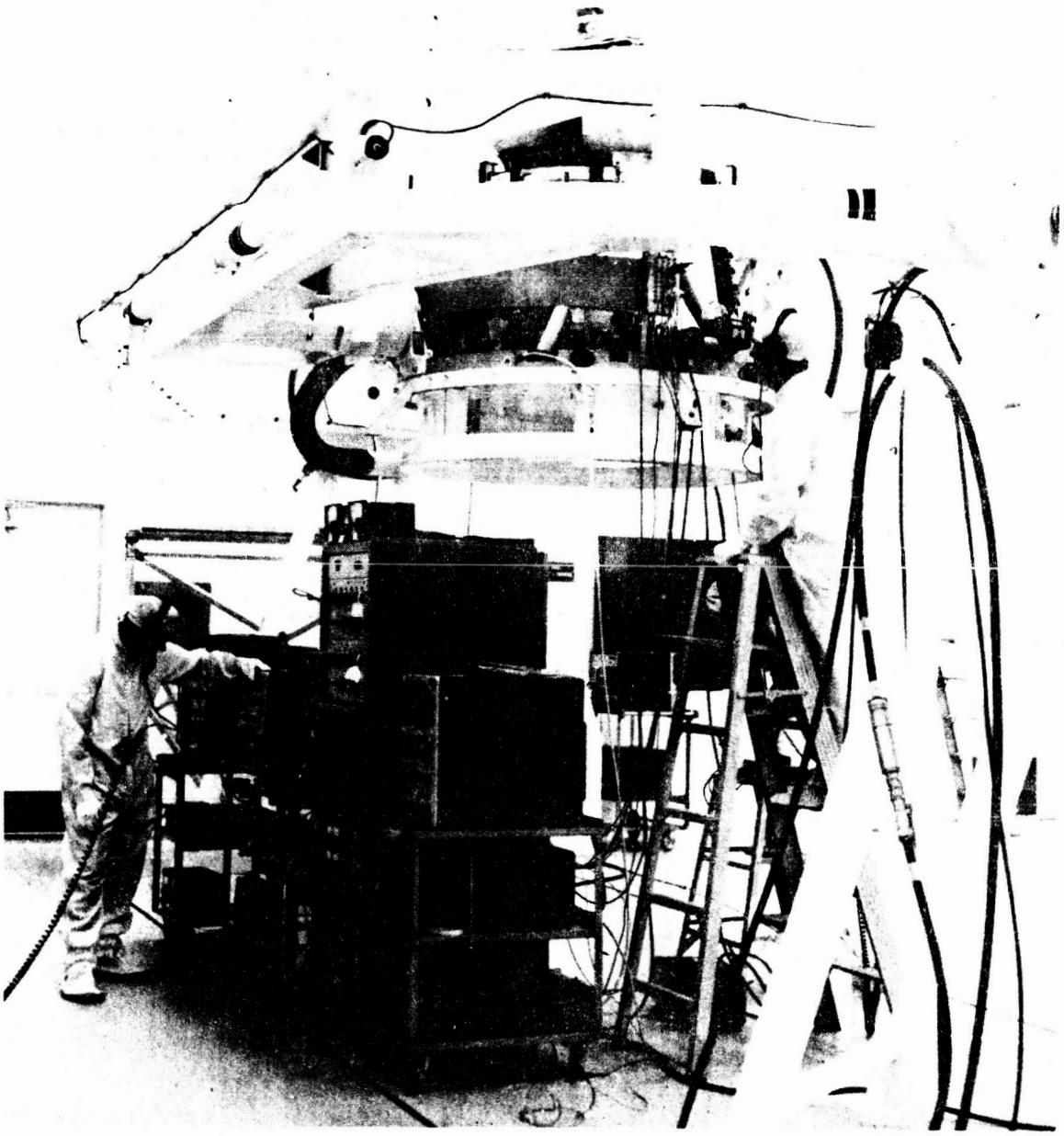

FIGURE 3.3-10: THREE-AXIS TEST STAND

This stand was capable of positioning the spacecraft with three axes of movement and was used primarily in the functional checkout of the attitude control subsystem. Functional checkout performance was compared with previous test results to establish that the various subsystems met their respective design and performance requirements.

Weight and balance tests were conducted with precision beam scales to establish a precise spacecraft center of gravity and weight for use in flight calculations and predictions.

The following is a list of the tests conducted in Hangar "S".

1) Weight and balance (dry);
2) Spacecraft alignment verification;
3) Prepower-on check;
4) Initial setup;
5) Initial systems status verification;
6) Communications performance test;
7) Radiation dosage scintillation counter FCO;
8) Attitude control subsystem functional test;
9) Velocity control subsystem functional test;
10) Power subsystem functional test;
11) High-gain antenna position control, camera thermal door operation, and antenna deployment test;
12) Solar panel test and low-gain antanna alignment;
13) Sun sensor alignment;
14) Equipment mount deck reflectance test;
15) Photo subsystem functional checkout;
16) Hangar "S"/DSIF/spacecraft compatibility test;
17) Transponder acquisition test;
18) Ranging acquisition and command threshold.

All tests were conducted to the satisfaction of NASA and Boeing. The above tests constituted the planned testing on the spacecraft and its components as specified in the Boeing Document D2-100404-2, Spacecraft #4 Test Procedures—ETR—Lunar Orbiter, Volume II. A series of special tests was also conducted to investigate anomalies that were encountered during normal testing or as a result of modifications that were incorporated. A list of these tests plus the results are listed in Boeing Document D2-100389-4 Volume VI*. Personnel training and operating techniques were also developed as a part of the ETR testing. Three

* Contract Compliance Review Summary Report, Spacecraft 4.

mission simulation countdown tests were performed while Lunar Orbiter I was in Hangar "S". The first one on June 15, 1966, was aborted approximately halfway through the count because of commercial power problems at AFETR. The second one on June 17, 1966, was the first complete countdown using the spacecraft, SFOF, and the DSN. The initial version of the countdown procedures Boeing Document D2-100626-1 Lunar Orbiter Spacecraft Countdown, was used from T-510 through T-0.

DSN training followed for 17 hours using Paragraph B1, Appendix B of Boeing Document D2-100475-3, DSN Mission Operations Training Procedures—Lunar Orbiter. The third practice countdown was conducted on July 23, 1966, using Boeing Document D2-100626-1 and Paragraph C1, Appendix C of Boeing Document D2-100475-3.

Hangar "S" testing was completed and the spacecraft was moved to the ESA on July 24. Lunar Orbiter I delivery review was conducted at ETR on July 26, 1966. The spacecraft was accepted by NASA subject to completion of postdelivery activities. Results of the Hangar "S" testing and condition of the spacecraft at time of delivery was documented in Boeing Document D2-100389-4, Volume VI, Contract Compliance Review Summary Report, Spacecraft 4.

Lunar Orbiter Spacecraft No. 5 arrived at ETR on June 10, 1966. Hangar "S" testing was completed, without a photo subsystem, by July 25 and it was available as a backup spacecraft.

3.3.3.2 EXPLOSIVE-SAFE AREA (ESA 5/6)

The ESA consisted of a spacecraft test building and three support buildings. The spacecraft test area was an enclosed room with approximately 550 square feet of floor space. The environment within the spacecraft test area was maintained as a Class 100,000 clean room. The temperature and relative humidity of this room was also closely controlled for the various tests and servicing conducted there. All of the hazardous operations on the spacecraft were conducted in this area and monitored from an adjacent test conductor area from which the spacecraft was visible through an explosion-proof window. Figure 3.3-11 shows fueling operations on Lunar Orbiter I. The support buildings in the area were used for propellant handling and storage, checkout van parking, equipment storage, and office area. The layout of the ESA is shown in Figures 3.3-12 and 3.3-13.

Spacecraft processing in the ESA was to complete all assembly, testing, and servicing prior to encapsulation into the launch configuration.

The spacecraft assembly operations accomplished were:

1) Flight battery installation;
2) Flight-ready photo subsystem installation;
3) Ordnance connection;
4) Camera thermal door installation;
5) Thermal barrier installation.

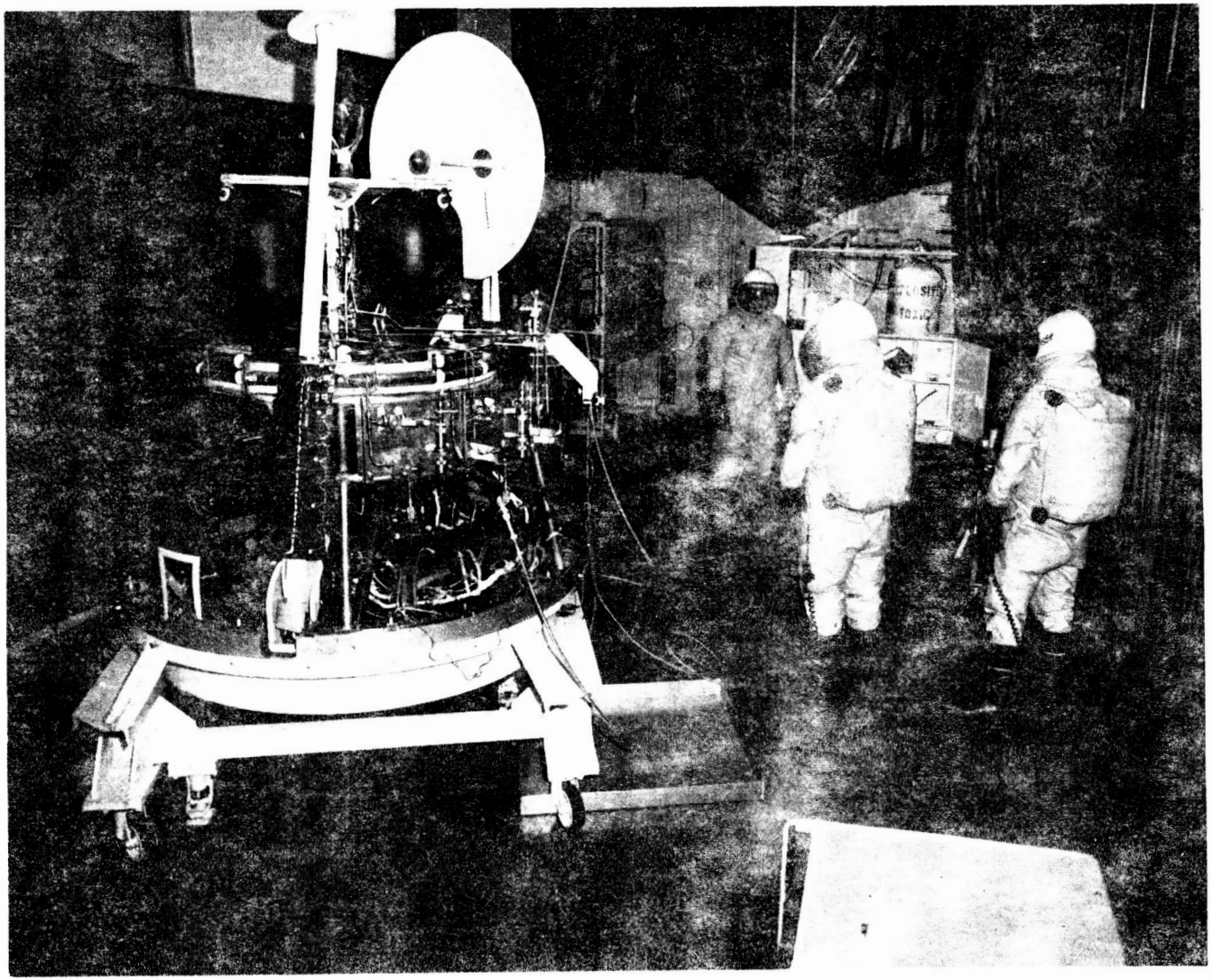

FIGURE 3.3-11: FUELING OPERATIONS AT ESA

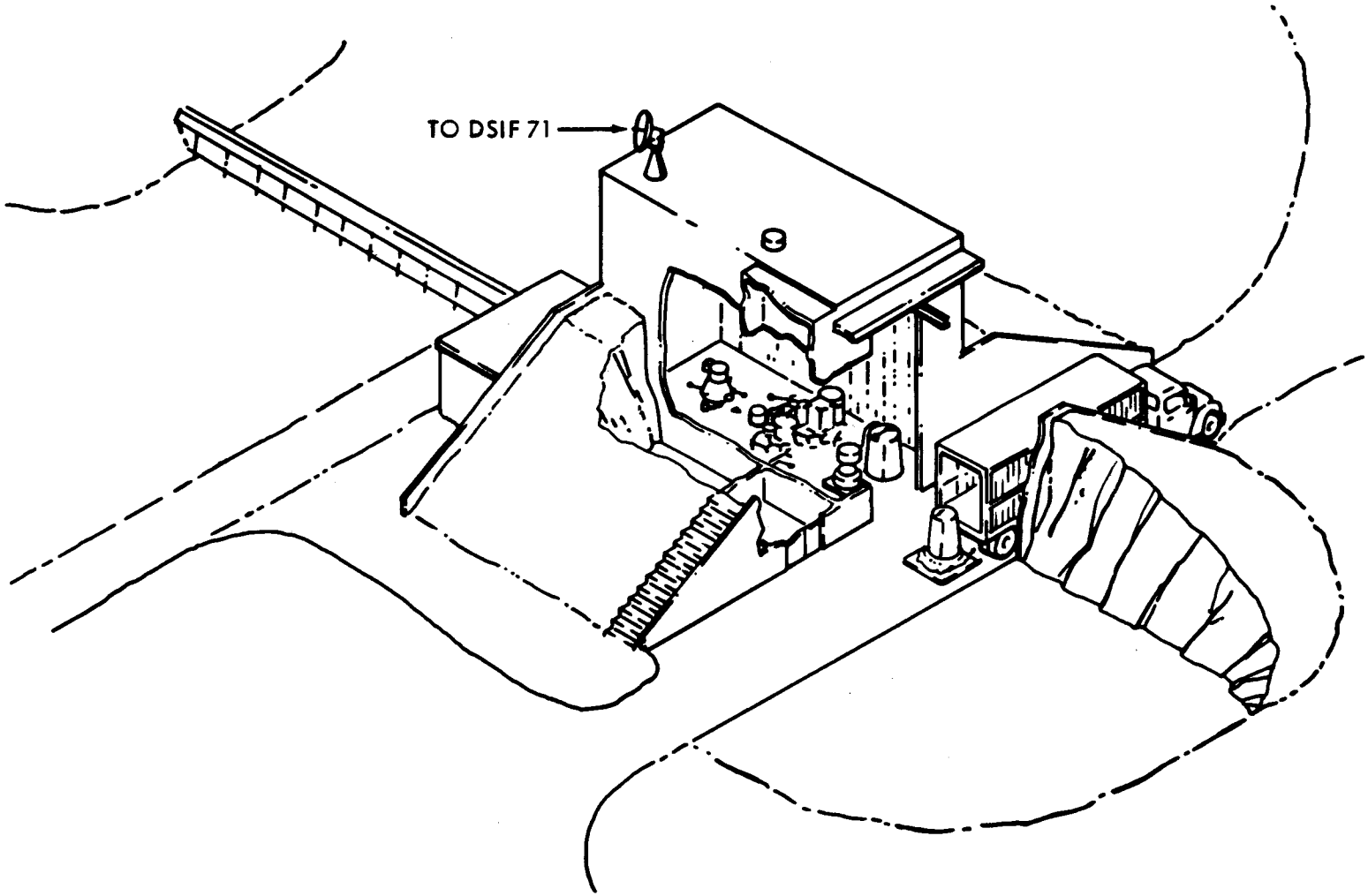

FIGURE 3.3-12: EXPLOSIVE SAFE AREA (ESA 5/6)

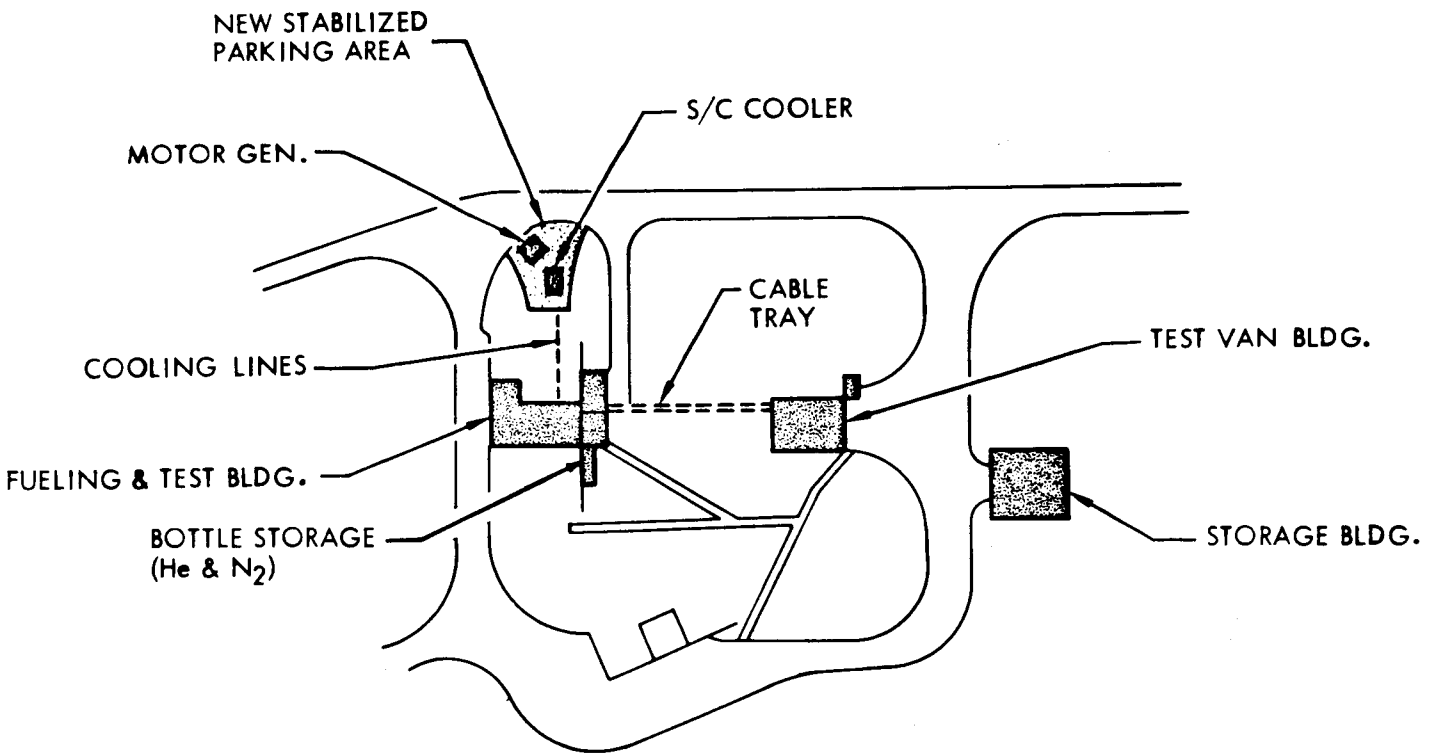

FIGURE 3.3-13: SITE PLAN (EXPLOSIVE SAFE AREA ESA 5/6)

2R
UNCLASSIFIED

The test operations conducted were:

1) Spacecraft nitrogen system regulator lockup and leak test;
2) Spacecraft velocity and reaction control subsystem leak test;
3) Photo subsystem alignment test;
4) Weight and balance flight load;
5) Battery connection verification;
6) Camera thermal door verification;
7) Ordnance check and hookup;
8) Propellant system bladder leak test;
9) Spacecraft - DSIF-71 compatibility test (without shroud).

The servicing operations performed were:

1) Fuel loading;
2) Oxidizer loading;
3) Nitrogen system pressurization.

These operations were all completed satisfactorily. The complete spacecraft assembly then was mated to the Agena vehicle adapter and the separation devices installed. The spacecraft was encapsulated with the nose shroud and the shroud separation device installed. An rf compatibility test between the spacecraft and DSIF-71 was performed again after encapsulation. This test included system checks to verify operability of the photo and communication subsystems.

At the conclusion of the ESA operations, the encapsulated spacecraft was shrouded with a thermal insulating blanket and transported to the launch complex on the spacecraft transporter as shown in Figure 3.3-14. During the transport period the spacecraft environment was maintained by an air conditioning unit on the transporter.

3.3.3.3 LAUNCH COMPLEX 13

There were no spacecraft-peculiar facilities at the launch complex. The spacecraft console was located in the blockhouse and the spacecraft power supply was located in the final-stage vehicle room. The wiring and on-pad cooling air were supplied by LMSC. A 10-foot-diameter repeater antenna was located on the umbilical tower to relay signals between the spacecraft and DSS-71.

Spacecraft processing at the launch pad was to ensure spacecraft and launch vehicle compatibility, spacecraft/DSIF/SFOF compatibility, and spacecraft readiness for launch.

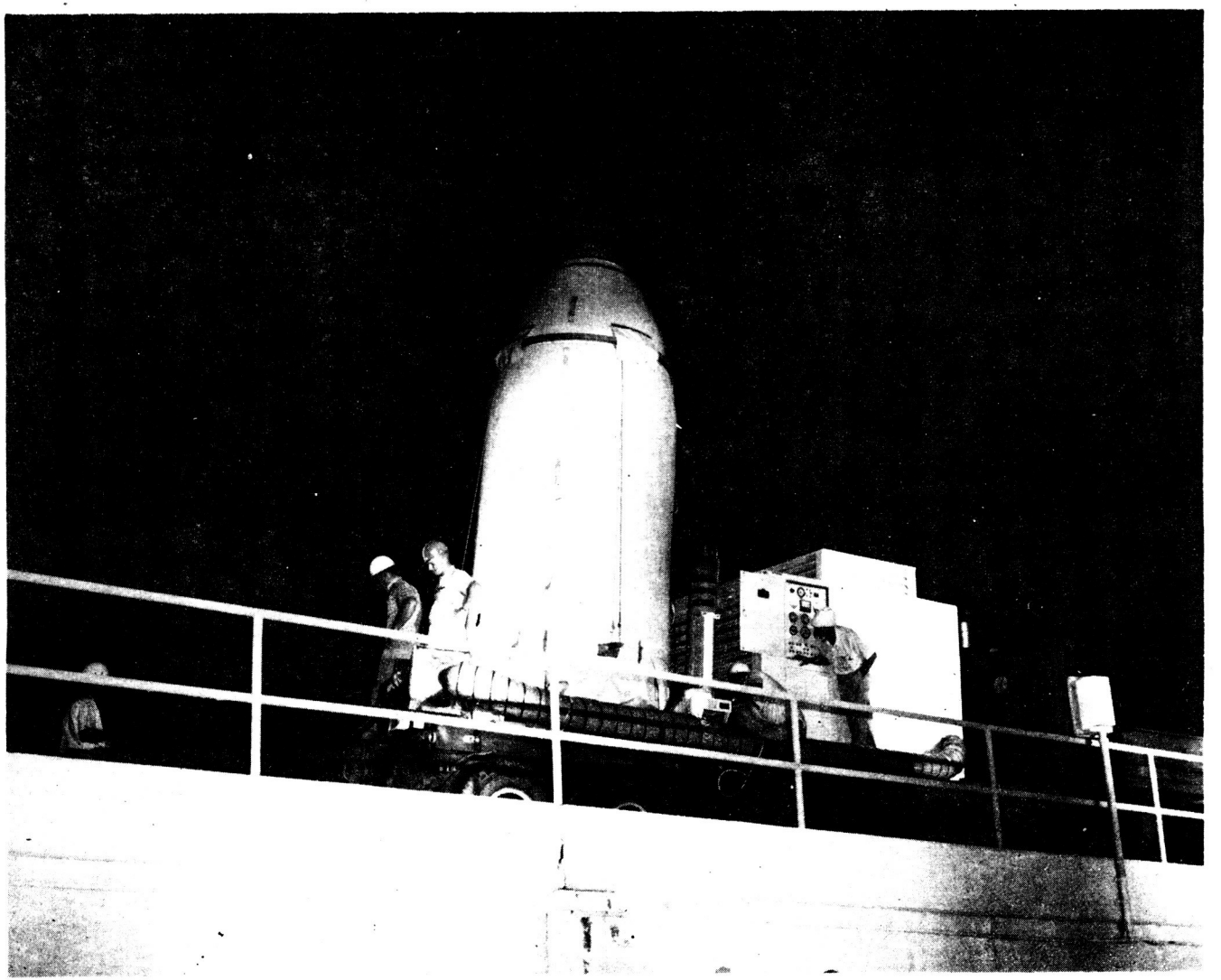

FIGURE 3.3-14: SPACECRAFT TRANSPORTER

Upon arrival of the spacecraft at the launch pad, it was hoisted to a position over the interface of the Agena and the matchmate was performed by LMSC (see Figure 3.3-15). After mating, the spacecraft environment was controlled by cooling air furnished by LMSC through the Agena adapter. After the mating was complete, the following compatibility and operational readiness tests were satisfactorily performed:

1) Checkout van, blockhouse, and spacecraft interface verification;

2) Spacecraft and DSIF operational verification;

3) Spacecraft and launch vehicle RFI compatibility test;

4) Joint flight acceptance test was conducted to verify completeness of the launch vehicle and the spacecraft as a flight-ready system;

5) Simulated launch (operational readiness test).

This testing concluded the spacecraft processing, which was conducted with minor anomalies that did not cause a launch delay or in any way cause degradation of the flight readiness of the spacecraft.

3.3.4 COUNTDOWN AND LAUNCH

After satisfactory completion of ETR processing and integration tests, the Lunar Orbiter and launch vehicle were considered ready for launch. The launch period covered a 5-day span from August 9 through August 13.

3.3.4.1 LAUNCH CRITERIA AND CONSTRAINTS

Specific launch criteria and constraints were generated for the spacecraft and launch vehicle, which aided the countdown personnel in determining the countdown status and launch readiness of the overall space vehicle system. The criteria and constraints covered the following major categories:

1) Operational limits (at launch) of subsystems;

2) Mandatory telemetry channels for launch;

3) Hold capabilities and redline criteria;

4) Ground equipment operation;

5) Tracking and telemetry coverage;

6) Weather restrictions;

7) Launch period and launch windows.

Details of the launch criteria and constraints were listed in the Lunar Orbiter Launch Operations Plan LMSC-A751901A and the Spacecraft Countdown Document (Boeing Document D2-100626-1).

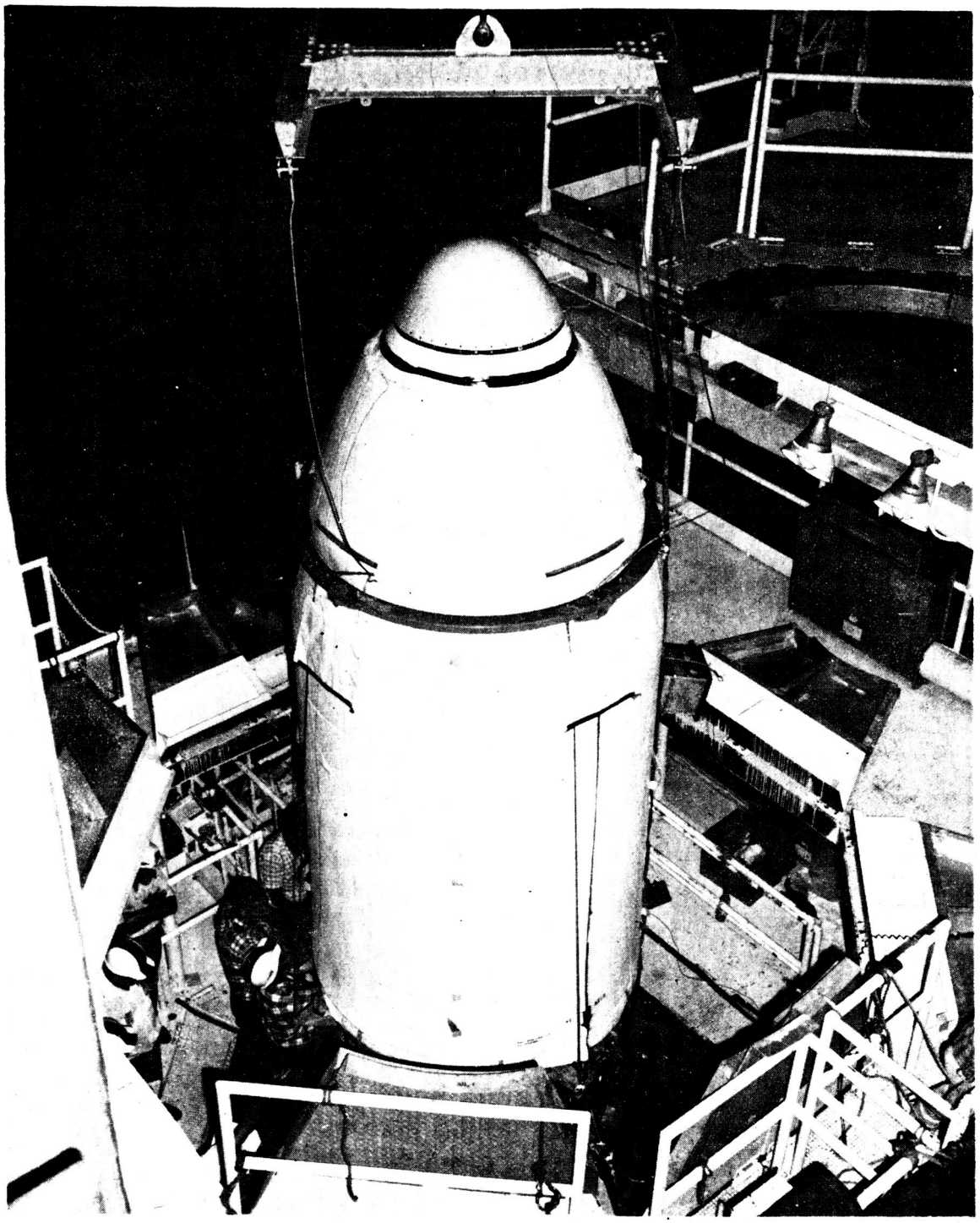

FIGURE 3.3-15: MATCHMATE

3.3.4.2 COUNTDOWN

Lunar Orbiter Master Countdown, LMSC Procedure ETR-133433, provided integrated instructions for launch complex activities required to launch the space vehicle consisting of the Atlas booster, the Agena second stage, and the Lunar Orbiter spacecraft. Subordinate procedures associated with this master countdown were provided in Boeing Document D2-100626-1, Lunar Orbiter Spacecraft Countdown, General Dynamics/Convair Document 69-42803-2, Atlas Countdown, Lockheed Document FCP-C60753, Agena, Countdown, and General Electric Document 66A121238 Guidance System Countdown.

During the countdown, spacecraft performance was verified by telemetry readings at DSIF-71, film readout on the GRE (ground reconstruction equipment), and status indicators on the spacecraft console in the blockhouse. Electrical measurements at the console were obtained through the electrical umbilical connection in the Agena. Telemetry readout at DSIF-71 was via an S-band rf link or via a UHF (Agena) link.

The countdown started at liftoff minus 500 minutes (T-500) and proceeded concurrently for all activities supporting the launch. Figure 3.3-16 indicates some of the major events that occurred during the countdown. The countdown of August 10, 1966, resulted in the actual launch of Lunar Orbiter I. However, this was preceded by a number of simulated countdowns and one aborted launch attempt prior to the actual launch. A summary of these countdowns follows.

3.3.4.2.1 August 4, 1966

The first simulated countdown, also known as an operational readiness test (ORT-1), included a prelaunch countdown plus a simulated launch phase. The countdown proceeded without major problems; however, the spacecraft EMD temperature rose above desirable levels because of air conditioning difficulties. ACS/VCS tests were completed satisfactorily, programmer memory was loaded correctly, GRE film evaluation was satisfactory, two-way lock was achieved, and communications checks were "GO." Arming of the spacecraft squibs was omitted. After simulated liftoff the teletype circuits were inoperative for about 10 minutes, but the remainder of the flight phase was satisfactory. The major concern during this countdown was the erratic operation of launch-pad air conditioning.

3.3.4.2.2 August 6, 1966

This simulated launch countdown was the final planned launch-pad activity prior to actual launch day. This test included all elements of the Lunar Orbiter I—launch vehicle, spacecraft, ETR, DSN, and operations teams. The countdown commenced at 10:17 GMT (T-425 minutes) and proceeded normally until T-204 minutes, when the air conditioning unit supplying the spacecraft ceased operating. Spacecraft EMD temperatures approached redline values. Approximately 10 minutes were required to change a module in the system while the countdown proceeded.

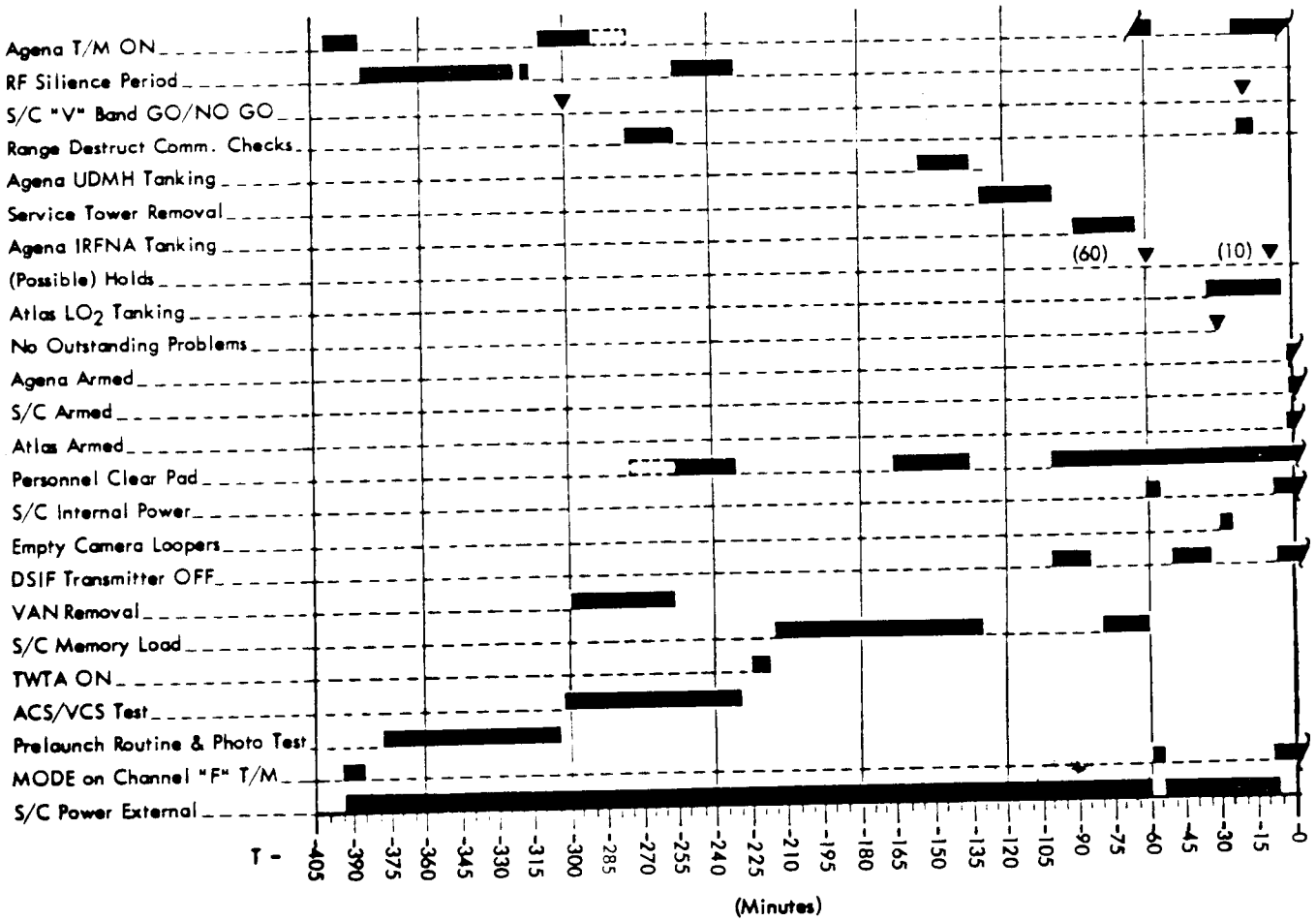

FIGURE 3.3-16: SPACECRAFT COUNTDOWN

A rerun of the Atlas guidance command test was necessary because of a guidance transmitter failure. The Atlas was tanked to approximately 10% of the oxidizer level and was detanked, after proper LOX system operation was verified, because of the threat of impending severe weather. At T-21 minutes a problem with the computer string at Pasadena (SFOF) developed, resulting in a NO-GO spacecraft condition. The computer was again in service at T-18 minutes and the spacecraft was ready at T-16 minutes. The computer problem reoccurred at T-11 minutes and an additional 30 seconds of the built-in 10-minute "hold" at T-7 were used before a GO was given for the computer.

The count resumed at T-7 and proceeded normally until T-3 minutes when a low-pressure redline on the Atlas east-side holddown release cylinder was announced. The countdown was recycled to T-7 minutes and investigation revealed the cylinder pressure was satisfactory for the test. The T-7 minute terminal count was held for a spacecraft readiness report; during this time the service tower was moved back around the vehicle because of the threat of impending severe weather. The count (T-7) resumed at 18:55 GMT and proceeded as planned until termination at T-10 seconds.

3.3.4.2.3 August 9, 1966

The countdown for the first launch attempt on 9 August 1966 began with a communications check at T-450 minutes (09:20 GMT). The count proceeded through a planned 50-minute hold at T-60 minutes (16:03 GMT) to the planned 10-minute hold at T-7 minutes (17:46 GMT). Some of the minor problems that arose but were resolved satisfactorily included:

1) The "X" and "Y" computer strings were down;

2) EMD temperature rose to 50.5°F at T-388 and to 53°F at T-241;

3) There was a TWTA power data problem;

4) The SLV-3 booster gas generator igniter panel light was intermittent;

5) The Agena boom enable light in the LOB went out.

The T-7 10-minute hold was increased by four additional holds. Finally the launch was scrubbed at 18:28 GMT due to Atlas anomalies. The problem was with the Atlas Acoustica propellant utilization valve system and the impending thunderstorm weather endangering the launch vehicle, requiring the gantry to be brought back to the pad.

3.3.4.2.4 August 10, 1966

The second Lunar Orbiter Mission I launch countdown was initiated at T-455 at 10:36 GMT on August 10, 1966. The launch window for this day was a total of 171 minutes from the planned start time of 19:11 GMT for launch plan 1OG. A brief resume' of the countdown follows:

1) At T-423 the spacecraft began sending telemetry data by Agena Channel F to DSS-71 for retransmission to SFOF, Pasadena, California.

2) At T-413 the weather report predicted improved conditions for the launch period. A major shift in upper wind direction was predicted to produce SE winds and high probability of no thunderstorms.

3) At T-390 all spacecraft systems checked GO and batteries were placed on charge.

4) At T-346 the EMD temperature was 47.6°F and rising slowly.

5) At T-293 the spacecraft EMD temperature reached 52°F as a result of LMSC air conditioner difficulties. At T-291 the temperature was 53°F.

6) At T-280 the EMD peaked at 53.2° F and began receding to 49° F at T-278.

7) At T-231 the Atlas had trouble obtaining sufficient booster hydraulic pressurization action but the problem was not considered major and was resolved in time to prevent an Atlas hold.

8) At T-200 the Atlas hydraulics were GO. A relay was found inoperative and was replaced.

9) At T-186 the spacecraft EMD was 48.7°F and gradually decreasing.

10) At T-168 the Sword Knot ship voice and teletype were RED but went GREEN at T-161.

11) At T-165 all spacecraft systems were GO.

12) At T-162 the air conditioner failed again, causing the temperature at the EMD to rise suddenly. Nitrogen purge was used while a backup unit was placed in operation. By T-159 the EMD was 55.5°F and creeping upward.

13) At T-149 the EMD was at 59°F.

14) At T-144 the EMD was 54.3°F and gradually dropping.

15) At T-126 the EMD was still at 54.5°F.

16) At T-101, LMSC requested premission to change back to the original air conditioning unit, which was now repaired, to achieve a greater cooling potential. A 10-minute delay would be required in tower removal. Permission was granted to obtain the desired lower EMD temperatures between 42° to 45°F at launch.

17) At T-90 the reworked air conditioning system was operational. Tower removal, normally at T-125, was delayed.

18) At T-71 the mission director authorized the spacecraft telemetry to be routed through DSIF-71 with the tower in place to keep the tower removal from detaining the spacecraft/SPAC countdown checkoff.

19) At T-65 the EMD reached 49.2°F and tower removal began.

20) At T-60 the scheduled 50-minute hold for Agena oxidizer tanking began at 17:11 GMT.

21) At 19 minutes into the hold the Woomera DSS-41 TTY went RED. It was learned that the cable between Hawaii and San Francisco was inoperative.

22) At 28 minutes into the hold the EMD reached 52°F and was fluctuating.

23) At 32 minutes into the hold the EMD reached a peak of 53.5°F.

24) At 42 minutes into the hold Woomera DSS-41 TTY was GREEN.

25) At 18:01 GMT the T-60 count resumed.

26) At 18:27 GMT a 12-minute 59-second hold was called to complete the required tower and launch vehicle count activities caused by the previous 60-minute delay for cooling the spacecraft EMD.

27) At 18:33 GMT and T-28 the launch plan was moved from 1OG to 1OH. The change in launch plan moved the launch beginning from 19:11 to 19:26 GMT; the launch end from 19:28 to 19:42 GMT; begin the launch azimuth changed from 98.6 to 99.9 degrees; and the end launch azimuth changed from 100.1 to 101.3 degrees.

28) At 19:09 GMT, the T-7 scheduled 10-minute hold started.

29) No further problems occurred during the remainder of the count to liftoff.

30) Liftoff was successfully accomplished on August 10, 1966, at 19:26:00.716 GMT with 159.58 minutes of the launch window remaining.

31) Figure 3.3-17 shows the EMD and some strategic component temperatures that were recorded during the August 10, 1966 countdown.

3.3.4.3 WEATHER

The chief weather concern of the Lunar Orbiter I space vehicle was surface and upper air winds, visibility, and the threat of weather-caused power outage. Surface winds were measured by an anemometer attached to the gantry (90 feet above the ground) while upper air balloon soundings were made at close intervals beginning 10 hours prior to launch.

The August launch data subjected the spacecraft to the threat of daily thunder storms. The summer temperatures and humidity heightened the seriousness of launch-pad air conditioning module outage. During the August 9 countdown, severe thunderstorms were predicted for 14:00 EST, but no damage was incurred. Weather during the launch operation of August 10 was good. Upper wind shears were within acceptable limits. At liftoff the following weather parameters were recorded:

Temperature	86°F
Relative Humidity	69%
Visibility	10 miles
Dew Point	75°F
Surface Winds	10 knots at 165 degrees
Clouds	Partly cloudy
Sea Level Atmospheric Pressure	1018.6 mb (30.079 " Hg)

3.3.4.4 TRACKING COVERAGE

The AFETR, DSN, and MSFN are the elements of the tracking and data system (TDS) that together support the tracking and telemetry requirements for the launch. Tracking stations and ships are described in Section 3.3.2.

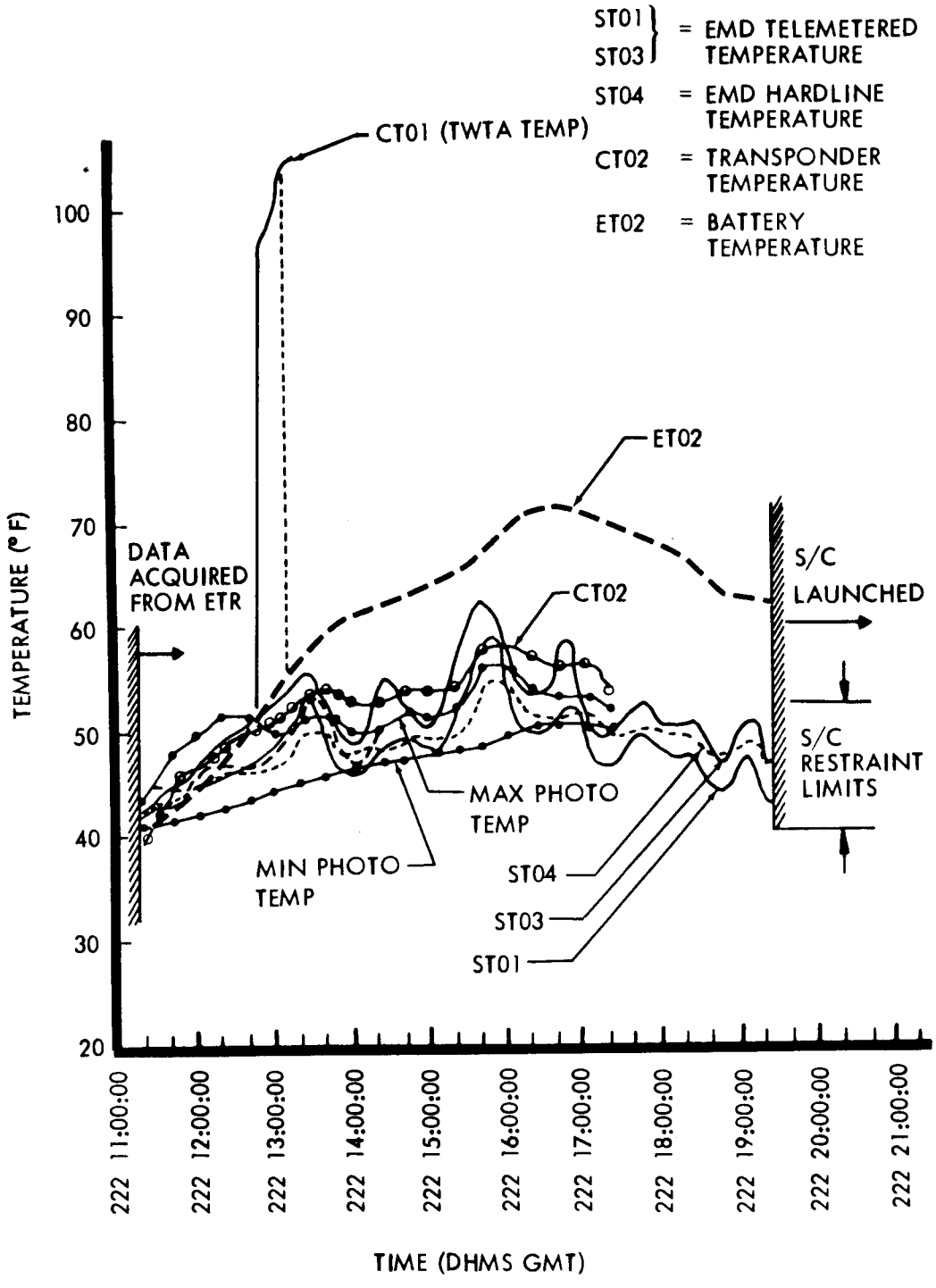

FIGURE 3.3-17: LUNAR ORBITER I COUNTDOWN 8/10/66 — SECOND LAUNCH OPPORTUNITY

Tracking during the launch phase consisted of C-band tracking of the launch vehicle and reception of VHF and S-band telemetry from the launch vehicle and spacecraft respectively.

Tracking data provided during the launch phase established the orbit and the normalcy of spacecraft cislunar injection in real time and for launch vehicle evaluation. This was done by tracking the Agena stage since, until Agena-spacecraft separation, the orbits of the spacecraft and Agena were the same. Even after separation, the relative velocity was only 2 ft per sec until Agena retro. Since this separation velocity was small, tracking of the Agena stage both prior to and subsequent to separation was very valuable in determining an early spacecraft orbit.

Other elements of the TDS also received tracking data to prepare acquisition and prediction data for their tracking stations. Prediction data based upon nominal launch vehicle performance were furnished to all stations prior to launch. However, prediction data based upon actual launch vehicle performance were used during initial acquisition by all stations, particularly if the trajectory was substantially different from nominal. The tracking data supplied by the uprange AFETR and Manned Space Flight Network (MSFN) radars were processed by the real-time computer system (RTCS) at the AFETR and station predictions were generated in real time for the AFETR, MSFN, and DSIF stations farther down range. In addition, the AFETR forwarded the tracking data directly to Goddard Space Flight Center (GSFC) so that GSFC would generate prediction data for the MSFN stations. These data were also relayed to the Space Flight Operations Facility (SFOF) for use with DSIF data in calculating the spacecraft orbit. The MSFN transmitted Bermuda and Carnarvon tracking data to the AFETR. The AFETR retransmitted their raw tracking data and that of the MSFN stations to Pasadena in near-real time.

Tracking coverage for various portions of the near-Earth phase of the launch trajectory is shown in Figure 3.3-18.

The ability to satisfy the near-Earth phase tracking and telemetry requirements was strongly dependent upon trajectory characteristics and TDS facilities during that phase. The dominant trajectory characteristic was the variable location of the transfer orbit injection. With the injection taking place far downrange, i.e., in the Indian Ocean, the support problems were quite different than for an injection uprange in the mid-Atlantic. An Earth map with injection loci for the August launch period is presented in Figure 3.3-19. It will be noticed that the injection point for the launch of August 10, 1966, on azimuth 99.9° was off the southern tip of Africa in the Indian Ocean.

The ability of a particular station to support near-Earth requirements was strongly dependent upon the transfer orbit injection location. In meeting requirements associated with the parking orbit injection, however, the coverage capability of those stations affected did not change since the parking orbit injection locus was invariant with respect to launch day and period. Figure 3.3-20 shows AFETR and MSFN uprange station coverage for any launch day. Figure 3.3-21 shows telemetry radar coverage during the injection phase.

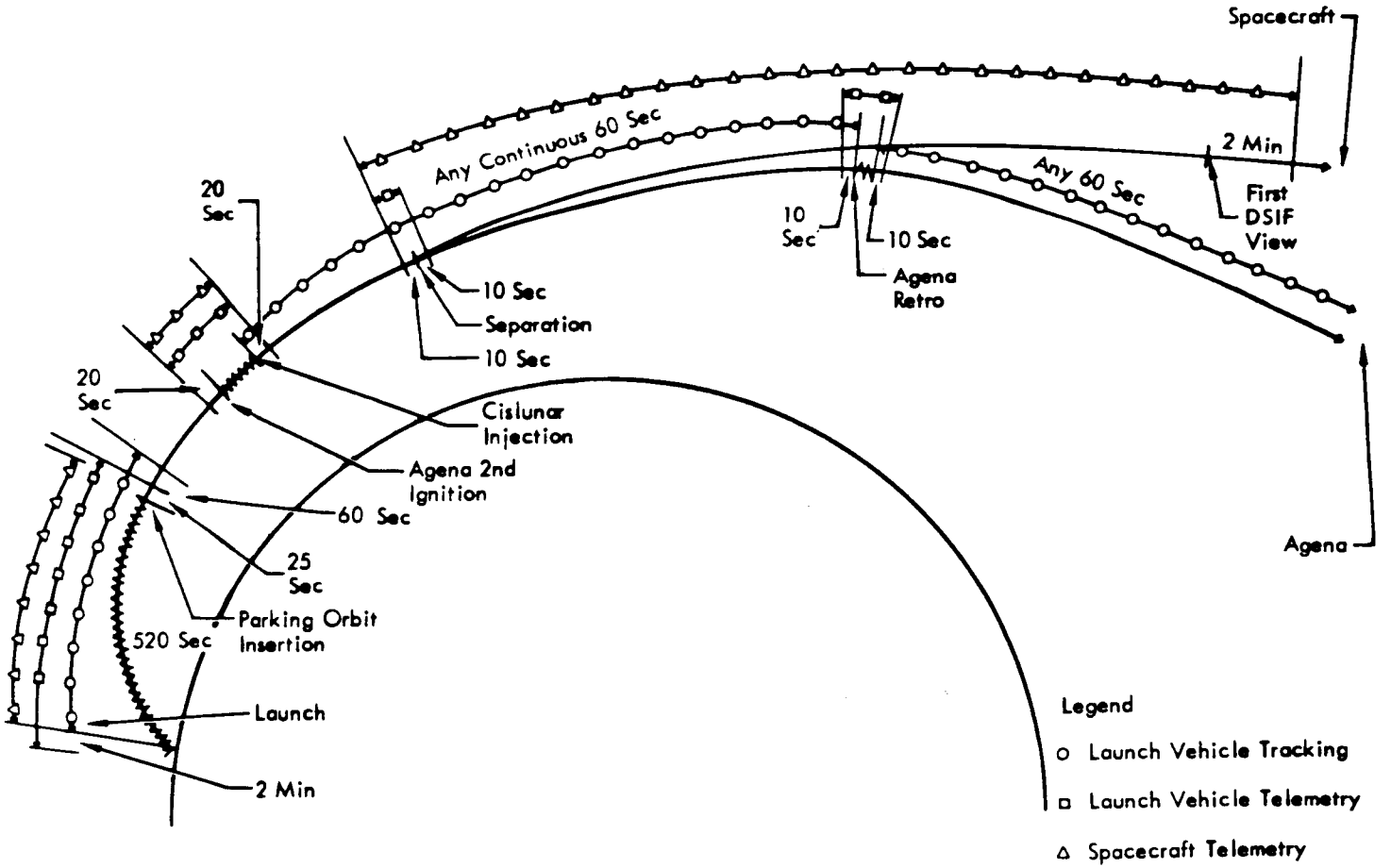

FIGURE 3.3-18: LUNAR ORBITER NEAR-EARTH CLASS I TRACKING AND DATA ACQUISITION

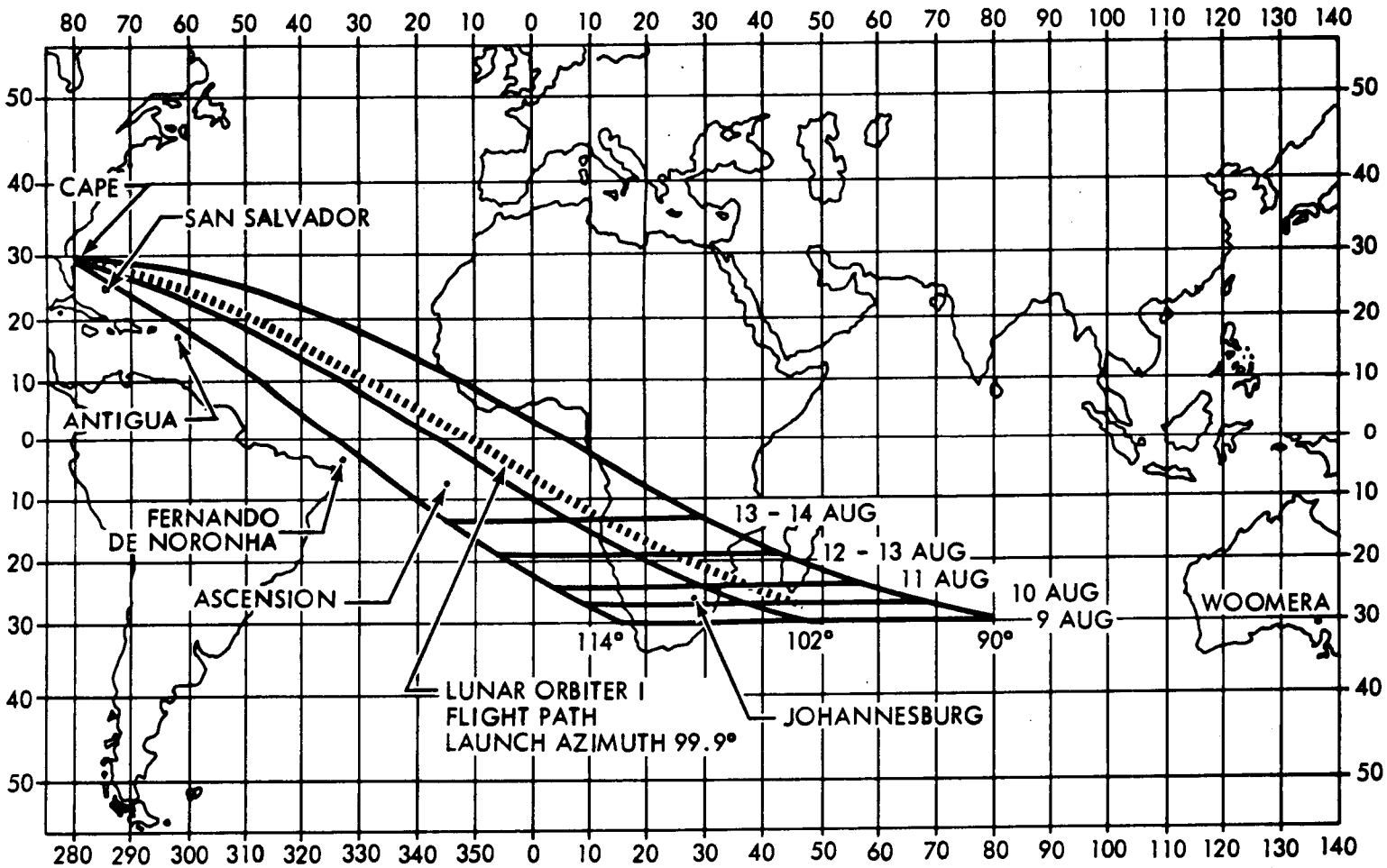

FIGURE 3.3-19: LUNAR ORBITER INJECTION LOCI FOR AUGUST 1966 LAUNCH PERIOD

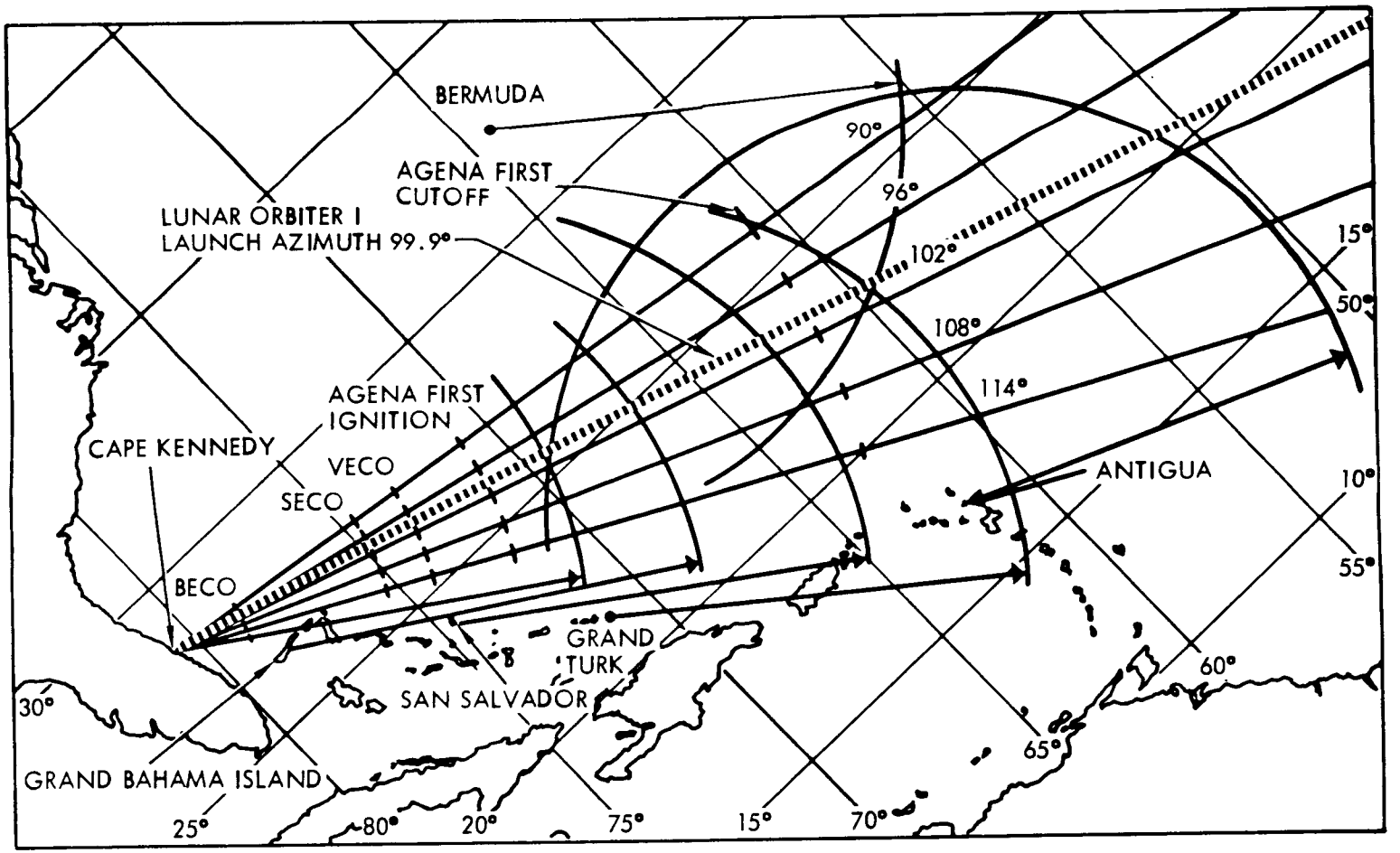

FIGURE 3.3-20: LUNAR ORBITER UPRANGE RADAR COVERAGE

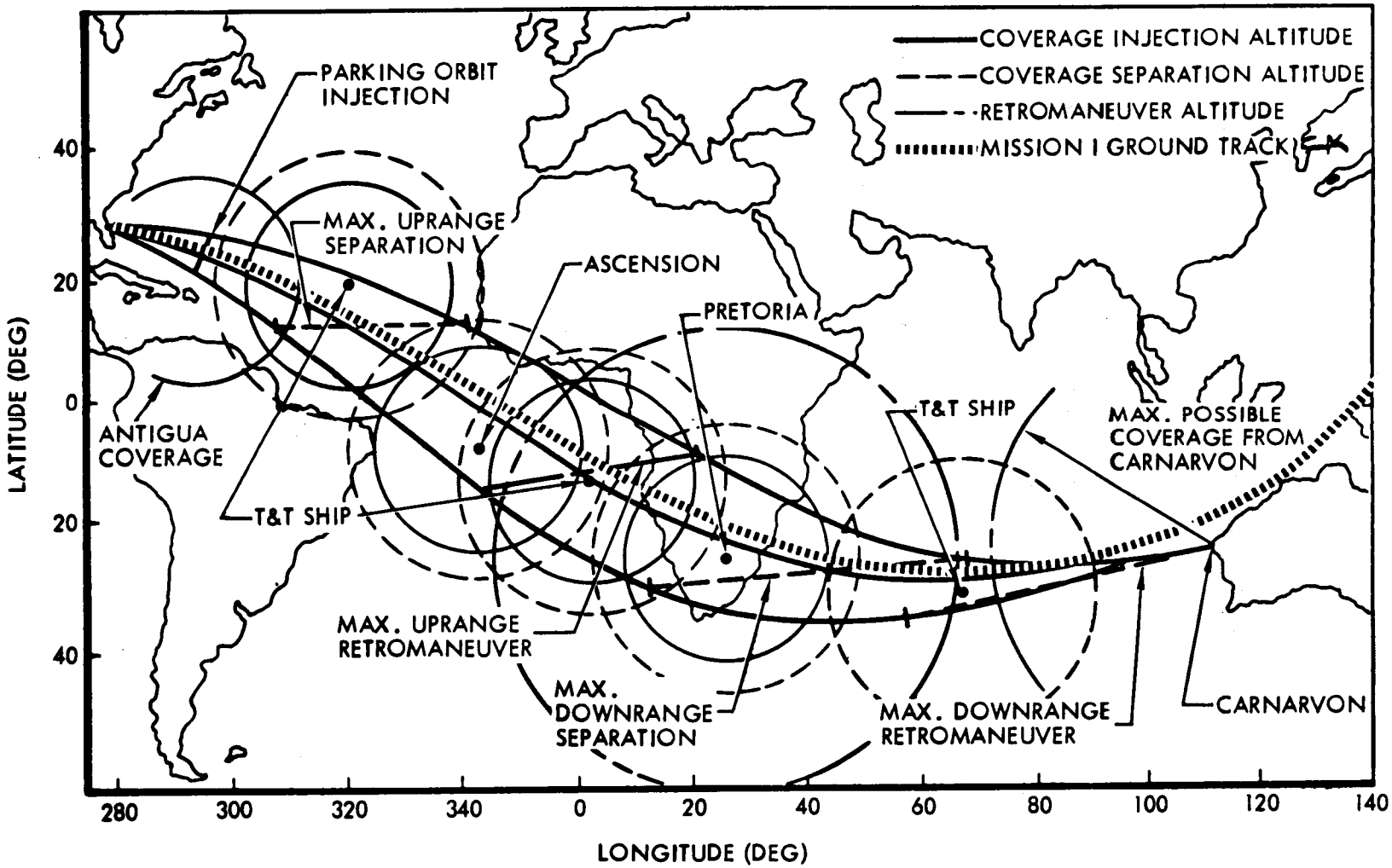

FIGURE 3.3-21: AFETR T/M AND RADAR COVERAGE, SPACECRAFT INJECTION PHASE

Actual Tracking coverage for Mission I follows:

RANGE RADAR

MAINLAND RADAR COVERAGE (Cape Kennedy)

RADAR	COVERAGE
Mod IV Radar 1.1	0 to 2 on TV
	+2 to +107 on infrared tracker
	+107 to +128 on automatic skin tracker
Mod IV Radar 1.2	+0 to +4 on TV
	+4 to +105 on infrared tracker
	+105 to +128 on automatic skin tracker
Mod II Radar 1.16	+10 to +95 on automatic skin tracker
	+95 to +240 on automatic beacon
PAFB Radar 0.18	+3 to +287, +356 to +473 on automatic beacon
	+287 to +356 on automatic skin tracker
Tel Elsse (Electronic Skyscreen Equipment) 14-110P Skyscreen program radar	+13 to +419
KSC Radar 19.18	+16 to +85, +280 to +360 on automatic skin tracker
	+85 to +280 on automatic beacon
Tel Elsse (Electronic Skyscreen Equipment) 12-110F Skyscreen flight line radar	+13 to +455

The range safety carrier was on from 13:52:29 to 19:27:42 GMT with no commands being sent.

STATION 3 RADAR COVERAGE (Grand Bahama)

RADAR	COVERAGE
Radar 3.16	+70 to +475 on automatic beacon
Radar 3.18	+83 to +459 on automatic beacon

The range safety carrier was on from 19:27:42 to 19:30:35Z with no commands being sent.

STATION 7 RADAR COVERAGE (Grand Turk)

Station 7 coverage for radar 7.18 was from +192 to +633 seconds on automatic beacon. The range safety carrier was on from 19:30:24 to 19:34:18Z with no commands being sent.

STATION 12 RADAR COVERAGE (Ascension)

RADAR	COVERAGE
12.16	+1205 to +1520 on automatic beacon
12.18	+1196 to +1572 on automatic beacon

STATION 13 RADAR COVERAGE (Pretoria, Africa)

RADAR	COVERAGE
13.16	+1924 to +2320 on automatic beacon

STATION 91 RADAR COVERAGE (Antigua)

RADAR	COVERAGE
91.18	+389 to +757 on automatic beacon

The range safety carrier was on from 19:34:16 to 19:35:12Z with no commands being sent.

The launch was supported by 13 metric cameras, 26 engineering sequential cameras, and 24 documentation cameras located at Cape Kennedy.

3.3.4.5 TELEMETRY COVERAGE

Various elements of the TDS received and recorded spacecraft and launch vehicle telemetry during the near-Earth phase of the mission. Spacecraft telemetry was received and recorded at both S-band and VHF via the Agena link.

Launch vehicle telemetry received by downrange AFETR stations was retransmitted to the Cape in real time except for channels 17 and 18, which were subsequently retransmitted during a playback of the tape. All vehicle telemetry from all stations and ships was retransmitted to Cape Kennedy within 1 hour of reception.

Spacecraft telemetry was received at the land stations and ships via the Agena link and was retransmitted to DSS-71 and the SFOF in real time. S-band telemetry received directly from the spacecraft was also transmitted in real time.

Telemetry coverage during the near-Earth part of the mission is tabulated below:

MAINLAND TELEMETRY COVERAGE (Cape Kennedy)

TELEMETRY (Mc)	COVERAGE
244.3 (Agena)	-7 to +497
249.9 (Atlas)	-7 to +497
S-Band	-7 to +55, +85 to +156

STATION 3 TELEMETRY COVERAGE (Grand Bahama)

TELEMETRY (Mc)	COVERAGE
244.3 (Agena)	+37 to +518
249.9 (Atlas)	+45 to +518
2298.3 (Spacecraft)	+130 to +518

STATION 12 TELEMETRY COVERAGE (Ascension)

TELEMETRY (Mc)	COVERAGE
244.3 (Agena)	+1179 to +1539
2298.3 (Spacecraft)	+1202 to +1539

STATION 13 TELEMETRY COVERAGE (Pretoria, Africa)

TELEMETRY (Mc)	COVERAGE
244.3 (Agena)	+1845 to +2300
2298.3 (Spacecraft)	

3.4 FLIGHT OPERATIONS

The successful accomplishment of the Lunar Orbiter I mission required teamwork from a select group of highly trained engineers, scientists, and technicians. The team was comprised of the engineers who designed and developed the launch vehicle, including the spacecraft and its subsystems, the technicians who built and launched it, the mission director with his staff of mission advisors from all cooperating agencies, and engineering and scientific specialists: FPAC, SPAC, and DSN.

The task of welding the bits and pieces of hardware into functioning systems that performed the photographic mission and obtained selenodetic data was huge. The problems involved with flight operations procedures were overcome without jeopardizing the mission, thus proving the operational flexibility philosophy under which the system was designed. Also overcome were the scheduling problems involved with use of AF Eastern Test Range facilities and Deep Space Network complexes which were required to support other programs simultaneously.

3.4.1 MISSION CONTROL

The flexibility of both the Lunar Orbiter spacecraft and the operational control personnel were well demonstrated during the conduct of Mission I. The preflight plan contained detailed sequences of events for all activities associated with the planned mission (see Figure 3.4-1). Included in the plan were all of the flight programmer core maps required to conduct the mission. Until the time of the initial attempt to acquire Canopus the mission proceeded precisely by the plan. Canopus acquisition difficulties were the first indication that the preflight plan would have to be modified extensively during the mission objectives.

The primary reasons for changes to the planned flight plan were:

1) Canopus star tracker's inability to function normally except in the Moon's shadow;

2) Degradation of the thermal paint on the equipment mounting deck, necessitated maneuvers off the Sun line to maintain satisfactory spacecraft temperatures;

3) Spurious activation of the high-resolution camera shutter and subsequent trouble shooting activities;

4) Late definition of photo targets for the "film set" photographs.

The effect on the planned mission may be illustrated by the following comparison of planned and actual spacecraft maneuvers during the mission.

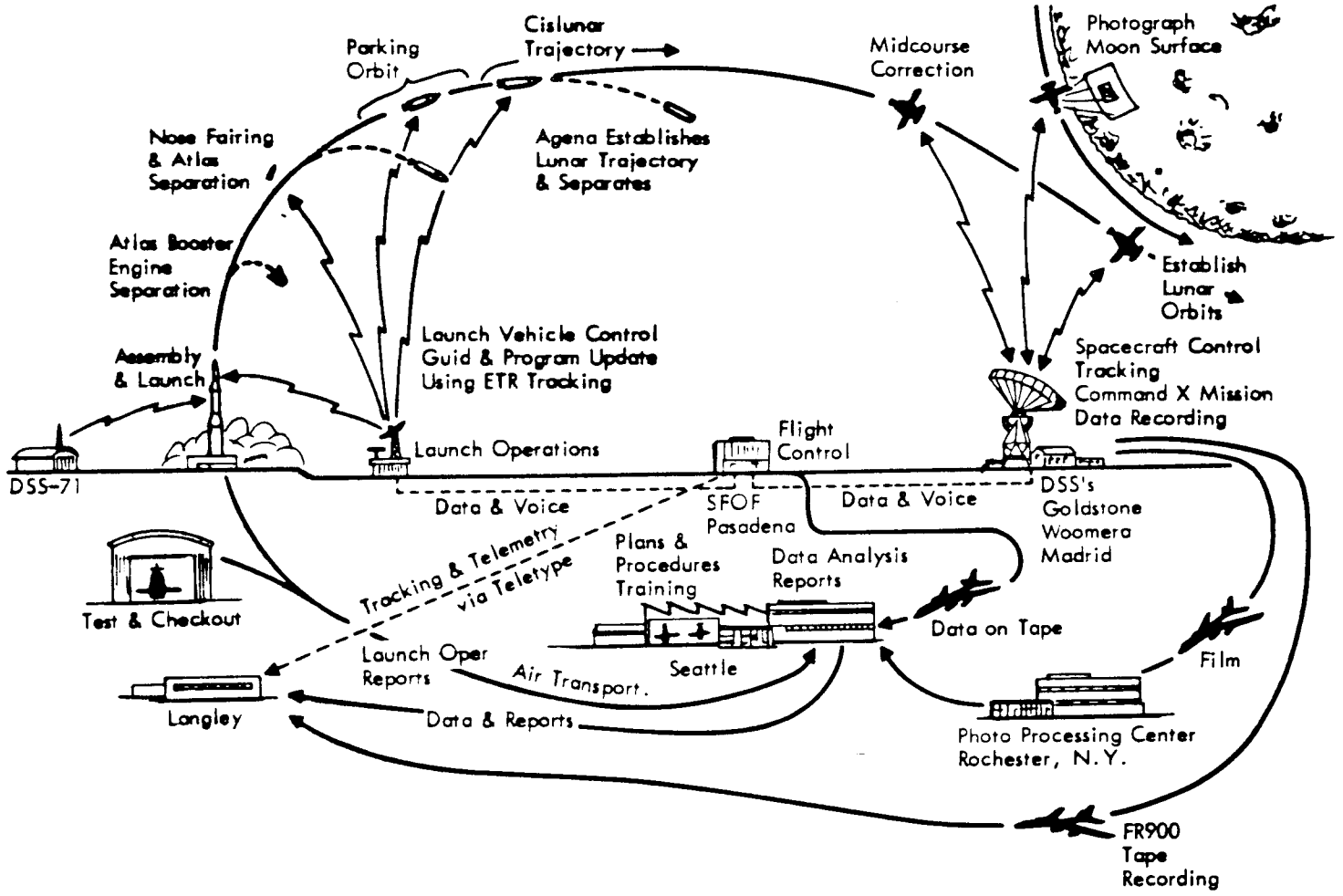

FIGURE 3.4-1: TYPICAL MISSION OPERATIONS

Maneuver	Actual	Planned
Star Map, Canopus Acquisition, and other	45	2
Thermal Pitch-Off	77	10
Attitude Up-date (Tracker, Antenna Pointing, and Thermal Effects)	144	0
Photo	92	66
Velocity Change	16	16
	374	94

It was possible to accomplish the additional maneuvers because no automatic Sun or Canopus reaquisitions were done during the time when manual updating techniques were being used.

Incorporation of the above activities required extensive revisions to the preplanned flight programmer core maps. The number of revisions made it impossible to project the programmer loading plan as far in advance as desirable.

Lunar Orbiter missions were to be controlled in a centralized control mode at all times, except when a communications failure precluded its use. In the centralized control mode, mission control was exercised by the space flight operations director (SFOD) from the SFOF, where the full support of assigned personnel, display facilities, hardware, and software were available. If a ground communications failure had occurred, mission control would have reverted to the decentralized mode until communications were restored. In the decentralized mode, responsibility for mission control functions and spacecraft performance analysis would have been assumed by the senior Lunar Orbiter engineer (SLOE) at the prime DSS. Use of the decentralized mode was unnecessary, since no communications failure occurred.

3.4.2 OPERATIONAL ORGANIZATION

Figure 3.4-2 illustrates the operational organization used to conduct Lunar Orbiter I mission flight operations.

A resume of operational organization major section functions follows.

3.4.2.1 SFOF PERSONNEL

Mission Director

The mission director had the overall responsibility for mission conduct, including all flight operations activities.

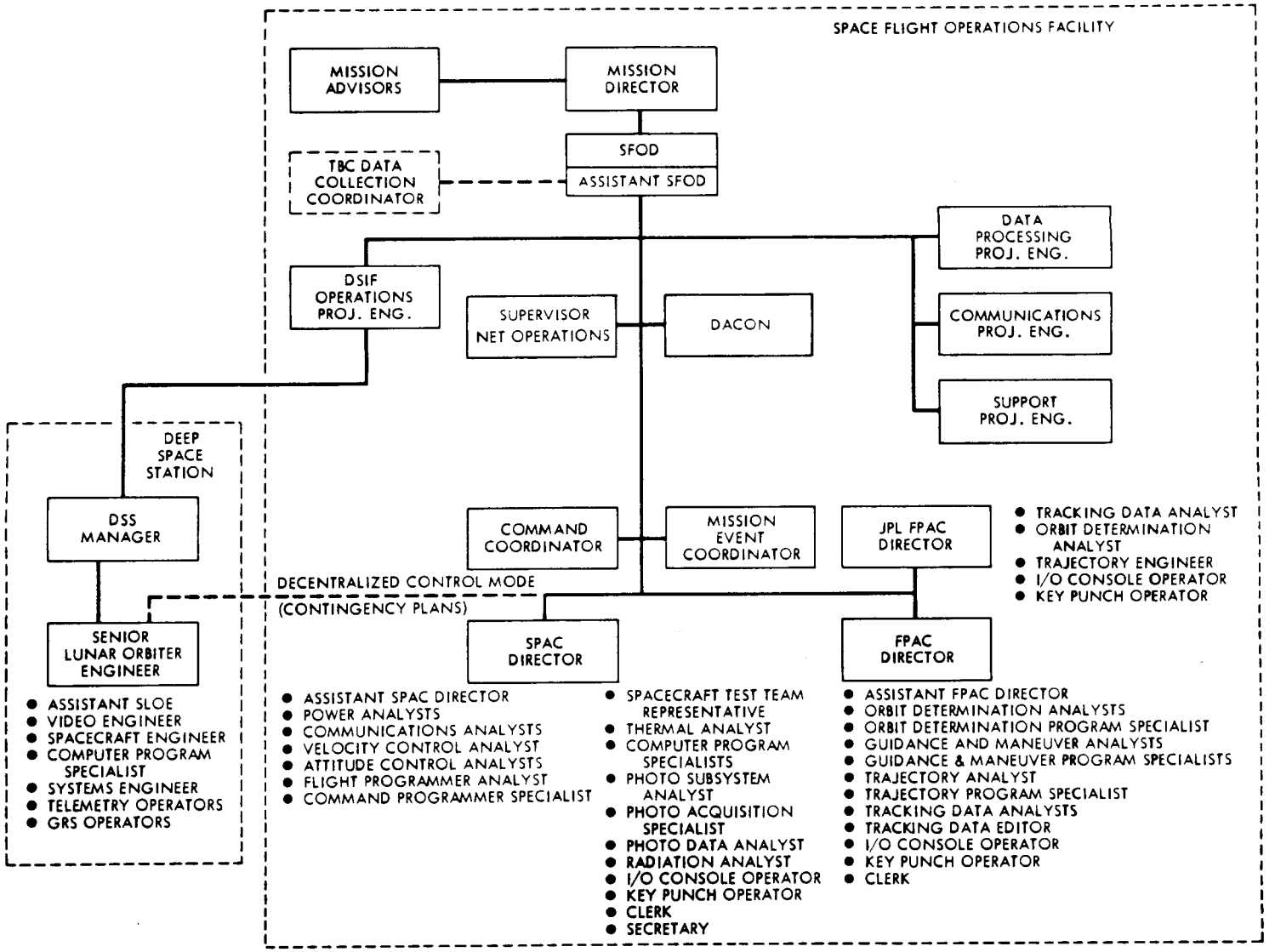

FIGURE 3.4-2: OPERATIONAL ORGANIZATION

Mission Advisors

NASA mission advisors assisted the mission director in the evaluation of mission and flight operations, and in monitoring the conduct of FPAC and SPAC activities. Their function included the selection of an alternate mission when the changes to the planned primary mission were considered.

Space Flight Operations Director (SFOD)

The SFOD was responsible for ensuring that flight operations personnel and DSN equipment were in the proper state of readiness for mission support and for control of the entire mission following spacecraft acquisition by the DSIF. He approved all command transmissions and made the flight operations decisions required during both standard and non-standard modes of operations. He was responsible to the mission director for the conduct of flight operations, including certain prelaunch responsibilities.

During critical aspects of mission progress, the SFOD was present in the mission control room and normally directed operations via the assistant SFODs (call names ACE 2 and DEUCE 2). Unassigned to an operational position, as such, he was relatively free, at his discretion, to investigate any non-nominal situations without affecting the full manning of the mission control function. The SFOD was present during all propulsion maneuvers and attended all critical command conferences.

The assistant SFODs acted interchangeably as ACE 2, DEUCE 2, and, to some extent, as PRIME 2 (assistant SFOD during launch function only). In fulfilling their assigned functions, the ASFODs acted with the authority of the SFOD.

Supervisor of Net Operations (SNOMAN)

The supervisor of net operations (call name SNOMAN) was responsible for the overall operation of the DSN as directed by the SFOD. Operationally, SNOMAN responded to requests from the SFOD for DSN configuration control, changes, and status reports. He was responsible for monitoring DSN performance, effecting and coordinating troubleshooting and repairs, and keeping the SFOD informed of anomalies as they were detected. SNOMAN was responsible for the preparation of the DSN for Lunar Orbiter use.

DSIF Operations Project Engineer (Track Chief)

During operations, the DSIF operations project engineer assisted the project in the use of the DSIF by serving as the principal interface between the SFOD and the DSS managers. In this capacity, he acted as the direct line of contact with the Net Control of the Deep Space Stations, supplying them with operational requirements and status information, and keeping the SFOD informed of DSN status.

Command Coordinator

The command coordinator was responsible to the SFOD for coordination of all commands to the spacecraft with all related activities. The command coordinator maintained close contact with the command programmer specialist in SPAC during generation and encoding of

command sequences. He directed command transmission operations and ensured that the proper command was received by the spacecraft and, when applicable, at the DSIF.

Mission Event Coordinator

The mission event coordinator was responsible to the SFOD for updating the mission event sequence to reflect all anticipated activities during at least the next 48 hours of the mission. He maintained close contact with the SPAC and FPAC directors, and the command coordinator. He coordinated event schedules to avoid activity conflicts and to facilitate mission conduct in an orderly and efficient manner.

Spacecraft Performance Analysis and Command (SPAC) Director

The SPAC director was responsible to the SFOD for spacecraft functioning during all phases of flight operations. He was responsible for preparation of spacecraft commands and analysis of spacecraft subsystems and components performance and reporting this information to the other interested persons and organizations. He was supported by a team of spacecraft subsystem and computer software specialists.

Flight Path Analysis and Command (FPAC) Director

During the 4 to 6 hours following launch and prior to confirmed acquisition of the spacecraft by the DSIF, the JPL FPAC director was responsible to the SFOD for orbit determination. The Boeing flight path analysis and command (FPAC) director was responsible to the SFOD after the first 4 to 6 hours of a Lunar Orbiter mission for spacecraft trajectory matters and camera pointing. The Boeing FPAC director's responsibilities included appropriate use of the DSN tracking services and computers for determining flight path corrections, attitude changes, and photo event timing to best fulfill the mission objectives. Also, he was responsible to the JPL FPAC director for the backup orbit determination computations during this period. Acquisition predictions to hasten DSIF contact with the spacecraft were the primary output of this early trajectory activity.

3.4.2.2 DSIF PERSONNEL

Tasks and responsibilities outlined herein are applicable to the three prime DSS's and to DSS-71 during prelaunch operation and early in the mission.

DSS Manager

Each DSS manager was responsible to the DSIF operations project engineer for directing the operations of his station. He coordinated and controlled the functions of the personnel and equipment at his station during the preparation and execution of each flight operation. He was supported by a regular, permanent complement of personnel.

Senior Lunar Orbiter Engineer (SLOE)

The SLOE's primary function was to assist the SFOD as required and directed in the role of mission control. Under SFOF direction, he was responsible for determining the commands to be transmitted to the spacecraft in emergency situations such as communication failures between the SFOF and the DSIF. He was also responsible for the coordination and direction of all Boeing personnel at the DSIF to ensure mission success.

3.4.3 DEEP SPACE NETWORK (DSN)

The DSN provided all facilities necessary to sustain the flight operations requirements of Lunar Orbiter Mission I. This was accomplished through a complex consisting of several Deep Space Instrumentation Facilities (DSIF's) strung around the globe and Space Flight Operations Facility (SFOF) located in Pasadena, California at the Jet Propulsion Laboratory. The DSIF's and the SFOF were interconnected by the Ground Communications Systems (GCS) voice and teletype circuits. In addition, the SFOF and DSIF-12, Goldstone-Echo, were connected by a microwave link.

3.4.3.1 SPACE FLIGHT OPERATIONS FACILITY (SFOF)

Command control of all Lunar Orbiter flight operations during Mission I was accomplished in the SFOF. In addition, the SFOF provided the data processing, communications, display, and support capabilities necessary to perform analysis and evaluation of spacecraft status and position as required for mission support and execution.

The SFOF maintained external communications with the Deep Space Instrumentation Facilties via the Ground Communications Systems teletype, voice, and high-speed data links.

The SFOF contains separate areas for mission control, spacecraft performance analysis and command (SPAC), flight path analysis and command (FPAC), and computer control. Communications between these areas is via an operational voice control system (OVCS), closed-circuit television, intercom and telephone. Computer systems, teletype, displays, bulk printers, administrative-printers, and plotting boards are provided for analysis of spacecraft status and performance.

SFOF Engineering and Operations

Data Processing System

The telemetry processing system (TPS) and the central computing complex (CCC) sections of the data processing system provided the Lunar Orbiter project with the telemetry data processing, tracking data processing, command generation transmission and verification. and prediction generation and transmission. The input/output (I/O) section provided the user areas (FPAA. MSA, MAA, DFCA) with I/O and data display equipment to analyze and evaluate spacecraft telemetry data.

Equipment Performance

In general, the hardware performance of the associated computers in the data processing system was excellent. Some intermittent problems were encountered with the Model 1301 disk files consisting primarily of format and parity errors due primarily to project software. Since these errors occurred during noncritical times, they did not seriously affect the mission. Some down time was recorded for the Stromberg Carlson off-line recorder due to a transistor failure. This problem caused some delay in data delivery.

A facility power failure occurred on September 1. All systems were back in service after a loss of approximately 3 hours processing time.

Operational Performance

Overall operational performance was good. The majority of problems were of a procedural type and quickly resolved.

DSN Intracommunications System (DSN/ICS)

Troubles experienced with this system were limited to one reported loss of video on a TV monitor in the FPAA. The monitor was replaced with an operational spare within 10 minutes.

There are a number of inherent hardware design restraints which severely limit the capability to provide multimission support. Extensive patching is required to fulfill user requests. This increased the possibility of human error, especially when nonstandard requests for special configurations were required. There were relatively few of these occurrences, however, and overall operational performance and operational procedures were quite satisfactory.

Tracking Data Quality Determination (TDQD)

This section discusses the activities, problems and plans for future data quality determination for Lunar Orbiter. The activities cover the launch phase of the mission (where the DSN was responsible for both orbit determination and tracking data quality determination) and the history of data quality and analysis throughout the mission. Some items covered have performance values and show how well the tracking station data met committed specifications. The future plans are a list of suggestions for correction of present problems and for making a smoother data quality determination.

Activities—During the first 6 hours from launch, orbit determination (OD) was a JPL DSN responsibility. Two JPL men assisted by two Boeing men handled the initial orbit determination. The orbits were determined within the allowable time given in the sequence of events and showed a nominal injection which was subsequently verified. The one anomaly that showed up in this phase was the X2 counter at Woomera. Several attempts to fix it failed, and it was recommended in the TDQD that this data be deleted from OD computations. There were enough X1 data blocks between the bad X2 to give a sufficiently stable orbit computation.

All data used for the midcourse maneuver OD calculation had been evaluated in the TDQD and assessed as good. There was a low-amplitude (0.03 Hz) 30-minute periodic error in the three-way doppler data from Madrid (which has yet to be explained), but this data was not used in the caluclations.

Data from the post-midcourse trajectory was plagued with perturbations resulting from spacecraft pitch and yaw maneuvers every few hours. These maneuvers added small accelerations to the spacecraft (all in approximately the same direction so there was no cancellation effect). The maneuvers were made to keep the temperature of the spacecraft

down and to evaluate a problem with the Canopus sensor. These maneuvers were clearly visible in the doppler data residuals and were of concern to the orbit determination personnel. Their effect on the prediction of position at deboost was estimated to be less than 10 km, but a better analysis should be made if this condition of maneuvers throughout the cislunar phase will exist on future missions. There was another anomaly in the Madrid data on Day 225 from 04:43 to 07:40 GMT caused by a bad counter, and this data was deleted from the orbit calculation. All other doppler data (obtained from midcourse to deboost) that had a good data condition code was indeed good. The accuracy of this data was well below 0.01 Hz for the 1-minute sample rate and, therefore, met the commitment specification of 0.2 Hz. Three frequency input errors were easily corrected and, thus, a good evaluation of the three-way doppler bias was possible prior to deboost.

After deboost and during initial orbit, excellent tracking data was obtained. Data quality determination showed consistency from the three stations. Where some systematic errors appeared, they always appeared at all stations at the same time in the orbit (i.e., near pericenter passage) and it was concluded that they were unknown lunar gravitational effects and not any tracking station phenomena.

This was further seen in the final or picture-taking orbits where these effects lasted much longer since the spacecraft altitude was lower. During this phase quite an extensive effort was made by DSN TDQD to resolve these effects, which caused predictions of doppler data to be off by 500 Hz in 2 days. Investigation was made with changes in sampling rates; integration step size; fitting with Chebishev polynominals; inserting low-thrust forces in a solar pressure mode; re-evaluating Earth gravitational constant (GM), Moon gravitational constant (GM), station location, and timing effects; trying J. Lorell's special harmonic coefficient set; and contacting Langley (R. Tolson) about any solutions they may have had. Hypotheses involving multipath effect, temperature variations, and a loose low-gain antenna were considered but were ruled out one by one as more data accumulated. The present postulates include: (1) a higher order harmonic not considered in the potential model, or (2) an error in the higher derivatives of range used in the orbit determination program to calculate doppler. These should be investigated prior to the next mission and will require some allocation of computer time. The poor prediction capability is a direct reflection of the poor fit to the data, which made it almost impossible to do a legitimate TDQD.

There was an anomaly in Woomera data from 08:40 to 09:40 GMT on Day 238 due to a 1-second timing error, as later verified by tracking data analysts. At this time, low-orbit tracking coverage was rather poor—almost all three-way doppler was deleted and the two-way doppler was bad due to picture taking or photo readout. The small amount obtained, however, seemed to be consistent and orbits calculated from this data followed a smooth evaluation of the spacecraft altitude over the last few weeks.

Problems—The following areas are commented upon and some problems are pointed out.

1) Scheduling—During prelaunch checkout and the mission itself, when DSN wanted computer time, there was always a question of priority between project and DSN.

2) Management Control—Good overlap data coverage during the orbit phase must be provided so both two-way and three-way doppler can be obtained and time synchronization can be maintained. The ranging system proved it could do this when checks made by the transported clocks gave the same results.

3) Hardware—The Model 047 card punch machines were used several times because the data system had failed and data was not on the disk. This happened during the transfer maneuver into final orbit, and cards were used to establish the first orbit.

4) Software—Postflight analysis may show errors that could be attributed in part to the program. The program is being continuously updated and make it more operationally efficient.

5) Data Coverage—It is very important after deboost or any transfer maneuver that the three-way doppler data be obtained. Only a few minutes of this data in conjunction with the two-way data will re-establish the orbit very accurately, whereas if it is not obtained it will take several hours to determine the orbit. If a station is about to set or rise and occultation cuts its final or initial view to only a few minutes and there is a maneuver occurring during this time, three-way doppler data becomes a must for rapid orbit determination. There should be more ranging data and time synchronization.

Flight Path Analysis and Command (FPAC) Problems

The Lunar Orbiter DSN FPAC team was responsible for the countdown, launch, and acquisition phases of Lunar Orbiter I's flight path analysis.

Software checkout and demonstration tests were started in February and completed by April 3 prior to start of simulation training tests. Simulation training tests uncovered a number of deficiencies in the Lunar Orbiter software system; these were quickly corrected. However, the second series of simulation training tests started without allowing sufficient time to redemonstrate the Lunar Orbiter software system and, consequently, some of these tests had problems. The most dramatic of these problems occurred on June 23 when the FPAC user programs caused a 2-hour hold in the first test involving the MSFN and AFETR. Subsequent software demonstration tests corrected all outstanding deficiencies; the tracking and data system test on July 28, and the countdown and launch phase ORT's on August 4 and 6 indicated satisfactory performance of the Lunar Orbiter software.

Other problems that adversely affected the performance of the DSN FPAC team during the latter part of July and early August were the failure of the SFOF data processing (including the card reader problems in FPAA 2) and the lack of DACON and mission control personnel (ACE 2's and DEUCE 2's) who were familiar with the FPAC team operations.

In anticipation of software, hardware, and personnel problems, a series of prelaunch countdown checkout cases was developed to be run from T-5 hours to T-70 minutes. These checkout cases were run on all the countdown, launch, and acquisition phase tests involving the DSN FPAC team (countdown and launch phase test on July 23, the tracking and data system test on July 28, the two countdown and launch operational readiness tests on August 4 and 6, the first launch attempt on August 9, and the actual launch countdown on August 10).

Due to the difficulties uncovered by the DSN FPAC team in getting through the prelaunch checkout cases successfully, the project FPAC team ran a series of prelaunch checkout cases between T-11 hours and T-5 hours.

For further data on FPAC operations, refer to Section 3.4.4.2.

Software Program

Program Development

Lunar Orbiter software design provided the tools necessary to monitor, predict, and control the spacecraft during its flight to and orbit around the Moon. Use of the resultant computer programs allowed mission analysts to make the decisions that controlled the spacecraft in successful accomplishment of the photo mission. Software design requirements were initially established in the Boeing proposal to NASA. Further definition of the engineering tasks required of the software was achieved by close coordination between Boeing and NASA engineers. The mission software framework was established upon submission of the Boeing engineers' requests for programming (RFP), containing program design parameters, to NASA for approval. Review, revision, and final acceptance of each RFP gave the go-ahead to the project to initiate a preliminary design specification (PDS). Paralleled preparation of the RFP and PDS was made possible by careful coordination of effort. The two documents, the RFP and the PDS, thus provided a formal means of communicating software engineering needs and design concepts between engineers, programmers, and project management.

The implementation of this complex and ambitious software program was made more difficult by the requirement that the Boeing-prepared software be compatible with existing NASA mission-independent facilities. A study of existing software and hardware facilities to establish needed interfaces before actual coding was undertaken and revealed that the Deep Space Network (DSN) was prepared for detailed assembly language programs but was not designed for compiler language programs. Since on-schedule accomplishment of the software program required almost exclusive use of compiler language, it was necessary to develop additional system interfaces. The use of high-powered compiler languages was not, however, universally applicable to the software program. Interfaces resulting from the study, and telemetry handling problems, necessitated that some of the work be done in technically weighty assembly computer languages.

Hardware Interface

The development of an extensive and complex software system for three different types of computers (see Figure 3.4-3) required access to real and/or simulated computer hardware. An IBM 1301 disk unit was added to the existing Boeing Aerospace IBM 7094 computer, making it possible to simulate an abbreviated SFOF computer system (Mode IV). An SDS 920 computer, with associated peripheral hardware and software, was leased and installed in Seattle. An IBM 7044 simulation package was provided to be used in conjunction with the IBM 7094. Thus, the hardware essential in developing the Lunar Orbiter software was made available in Seattle and checkout of the system was efficiently and economically accomplished.

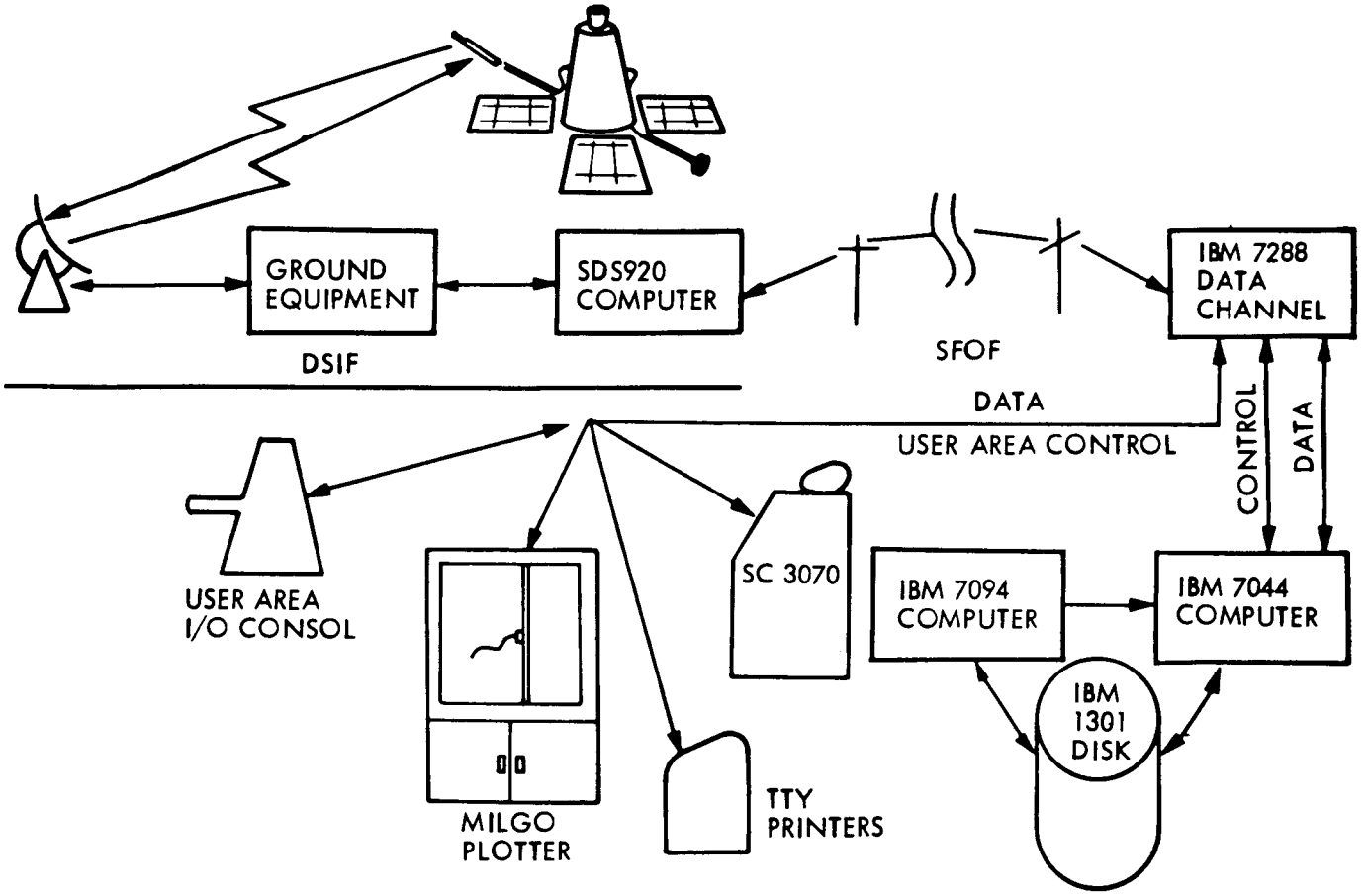

FIGURE 3.4-3: DSN COMPUTER CONFIGURATION

Software Structure

The Lunar Orbiter software system used with the JPL computers to support this mission was large and complex but proved to be most reliable. The structure of the software package is segmented into three areas: (1) command and telemetry data handling (CTDH); (2) spacecraft analysis and command (SPAC); and (3) flight path analysis and command (FPAC). The CTDH system collects spacecraft telemetry data used by engineering analysts and programs in the SPAC and FPAC areas (see Figure 3.4-4). The high-speed, two-way command and telemetry data (CTDH) program was developed to handle Lunar Orbiter telemetry and commands. The Deep Space Instrumentation Facilities (DSIF) computer program, written for the Scientific Data System 920 computer, provided transformation of the bit stream from a serial form—required by the receiving and transmitting equipment—to a word form compatible with teletype (TTY) and high-speed data line (HSDL) transmission techniques. Additional data handling and command transmission software was required within the Space Flight Operation Facility (SFOF): (1) A SFOF telemetry edit program was developed for the IBM 7044 and IBM 7094 computers to handle the spacecraft telemetry decommutation and command transmission format of Lunar Orbiter; (2) the unique nature of the Lunar Orbiter spacecraft also required extensive modification of the existing mission-independent SFOF data handling software. This modification was engineered jointly by Boeing and Jet Propulsion Laboratory software personnel.

The SPAC analysis programs use the spacecraft telemetry passed on by the CTDH system to monitor spacecraft conditions relating to temperatures, power and fuel consumption, attitude, environment, and photo subsystem status. Commands, prepared by the command generator program, enabled the analysts to operate the spacecraft with symbolic language based on the capabilities of the spacecraft. Telemetry from various spacecraft sensing devices provided the data foundation for SPAC analysis programs. Spacecraft position information, giving the location relative to Earth longitude and latitude, was also necessary for prediction purposes and was received from the FPAC area.

The primary duties of the FPAC group were to monitor and predict the spacecraft orbit, (or trajectory in the cislunar phase) and to supply maneuver angles and maps of the photo sites. The entire FPAC system was based on a modular function concept. Many of the pieces, or links, were prepared to be used in more than one flight path analysis program. Use of two or more analytic techniques, as parts of the user programs (i.e., trajectory integration by various numerical integration techniques), provided increased confidence in the calculated results.

The FPAC software used tracking data acquired by the DSN to determine spacecraft trajectory and orbital position. The orbit determination program (ODP), jointly developed by Boeing and JPL engineers, processed tracking data during lunar orbit to determine lunar gravitational parameters in conjunction with spacecraft position. The position and gravitational results calculated in the FPAC area, with spacecraft weight and propulsion capability calculated by the SPAC group, provided the computational data base for spacecraft orientation during photo exposure and readout. The FPAC software was designed to control the flight path of the spacecraft from launch through the final photo orbit.

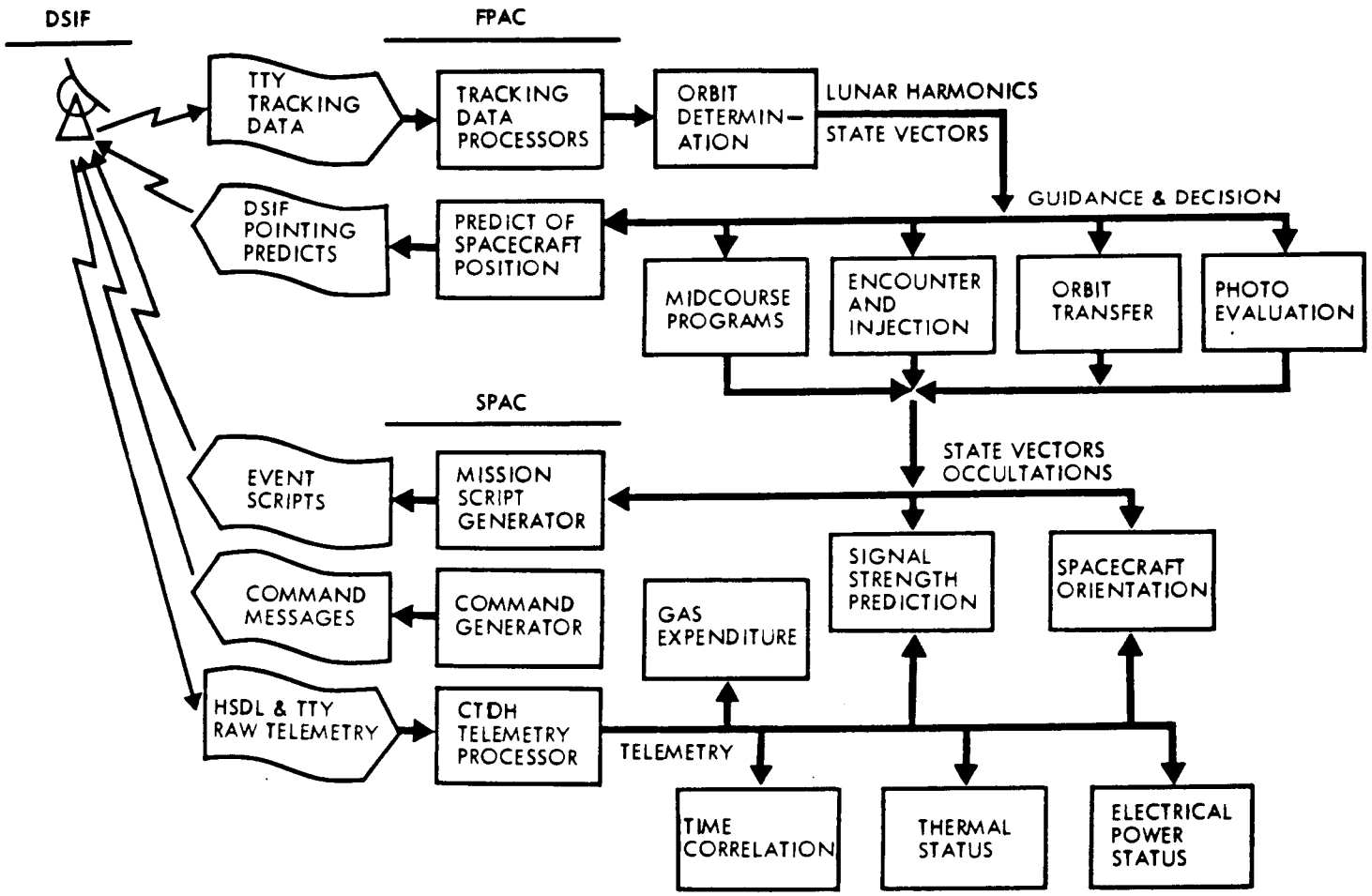

FIGURE 3.4-4: SIMPLIFIED SOFTWARE STRUCTURE

Delivery

Each program left Seattle only after successful demonstration of its capabilities on the Seattle-based computers. The programs were then delivered to NASA for integration into the SFOF computer system. The integration delivery package consisted of: (1) complete program symbolics; (2) a demonstration sequence described in a test plan with supporting test cases; and (3) preliminary drafts of the program document. The beginning of operational readiness tests awaited delivery of the last pieces of software and the program user guide documents. Exhaustive Seattle testing of Boeing programs provided a verification of the documented SFOF system capabilities and effectively reduced software personnel relocation during development of the analysis and data handling programs.

Training and Staffing

Operational training of the mission team commenced immediately following the integration tests. The training effort was the final step before the first mission. Extensive software support had to be provided during this period so that full software operational capabilities could be exploited. Operational analysts were chosen from the software and the engineering staff to provide complete technical coverage during the training phase.

The Dacon Position

Because of resource limitations, the DSN was unable to staff the data controller (DACON) position. The Boeing Company was directed to furnish the required support. The Boeing Company DACON's were accountable operationally to SNOMAN (supervisor of net operations). They received a hurried but complete classroom training session, lasting a week; later, they participated in mission simulations. By the arrival of the first operational readiness test, they were able to handle the DACON position. Using accumulated experience and the help of the Boeing "system monitors," they performed their job well throughout the flight.

Assessment

Conception, design, production, and final usage of the extensive Lunar Orbiter software program was completed within the original contracted schedule. Some problems with the software were encountered during the first mission. However, the software difficulties were minor and experience with the software peculiarities resulted in revised operation procedures.

Unplanned exercises in spacecraft orientation, such as the Earth-Moon photos taken on film-set frames, pointed the way toward software modifications to improve the capability of photo orbit maneuvers and evaluation calculations. It was necessary to correct minor anomalies in software during the first mission. Further problems will undoubtedly be encountered in later missions, but the first mission proved the Lunar Orbiter software program a success and explored the route to improved computer use in support of future space exploration.

3.4.3.2 DEEP SPACE INSTRUMENTATION FACILITY (DSIF)

The function of the DSIF during the Lunar Orbiter Mission I was to obtain and process telemetry and video data from the spacecraft, transmit commands to the spacecraft, and communicate and transmit both processed and raw data to other DSIF's when necessary and to higher user facilities.

Communications were effected through GCS. Physical material such as processed film, logs, and gross paperwork were shipped via air mail.

Three DSIF's were designated as prime DSIF's for the Lunar Orbiter: Goldstone-Echo, DSIF-12; Madrid, DSIF-61; and Woomera, DSIF-41. In addition, during the launch and cislunar phases of the mission, Johannesburg, DSIF-51, and Cape Kennedy, and ETR stations and ships were available to record spacecraft telemetry and provide the SFOF with real-time tracking data and to transmit commands to the spacecraft.

Each prime DSIF continually tracked the spacecraft from initial acquisition to the completion of the mission of Lunar Orbiter I, except during periods when the spacecraft was obscured by the Moon or was below the individual DSIF's Earth horizon.

Overall performance of the DSIF during Mission I was excellent. All commitments were met and the incidence of error was low. For the first 35 days of the mission, tracking totaled 1,003.53 hours, of which only 816 were committed.

In general all procedures worked well. In some areas improvements or expansion of procedures should be made to optimize them for future missions.

DSIF Data System

Tracking Data

The DSIF tracking data system was monitored and analyzed by the Systems Data Analysis (SDA) group of JPL DSIF Operations Section. The SDA function was staffed on a 24-hour-per-day basis until the end of the picture-taking portion of the mission on 29 August 1966. A total of eight men were available for this support, most of whom participated in all pre-mission simulation and ORT's. Further SDA support was provided by the SDA complement at the computing facility at DSIF-12, 24 hours per day for the same period using the Goldstone Tracking Data Monitor (TDM) program. The TDM program was manned with four persons during critical mission periods, two persons otherwise until the initial lunar orbit was well established, one person until the end of picture taking, and one person for one shift per day until the end of photo readout.

During the mission, the group provided rough-cut tracking data monitoring and quality assessment to OD, frequency inputs to OD, predictions to the DSIF, and advice to DSIF Operations Engineering in the track area.

The monitor function was performed using the Goldstone TDM program, which displays its output on TTY in the form of angle and doppler pseudoresiduals relative to an on-site trajectory program or to SFOF predicts, detrended doppler pseudoresiduals, and doppler standard deviation. In general this program functioned very well, within its limitations, which were rather severe in the Lunar Orbiter I case. It was of particular value in confirming propulsion maneuver accuracy.

DSIF predictions were generated in a timely manner, with a few exceptions. One of these occurred at approximately 4 hours after launch when the orbit determination group was processing early DSIF data and the decision to wait for a new state vector or use a previous one was made in favor of waiting briefly. A similar occurence took place during photo readout, predictions for the next orbit being sent during occultation. These events did not affect tracking performance. A malfunction in the occultation time computation was noted and has been corrected by the programmer.

Tracking data was generally well handled at the DSIF sites and within the GCS with relatively little loss to the users because of garbling in transmission, although data was lost fairly often within the SFOF because of computer problems. On some occasions, however, within overlap periods during photo readout when good data was at a premium, the stations tended to be somewhat indifferent to the importance of three-way data.

DSIF transmitter frequencies and data-type and data-monitor logging were kept up to very nearly real time to the end of picture taking by the TDA staff. It has been noted that occasionally frequency input errors—usually key-punch errors—delayed the tracking data quality determination function.

Data System Problem Areas

1) In the predict program (PRDL), the coding for occultation time computation was in error by amounts up to 4 minutes and has been corrected by a change in the source deck. However, it is highly desirable that the coding changes be incorporated into the Lunar Orbiter software system as soon as possible.

2) Because of the wide range of spacecraft temperature variation, the transponder best lock and auxiliary oscillator frequencies were usually out of date, causing some degree of alarm in DSIF net control and at the stations. Some means of evaluating these frequencies reliably and rapidly is necessary.

3) PRDL is characterized by very long running times and is often in competition with other FPAC programs, particularly ODP, on which it depends for initial conditions. During critical mission sequences, this conflict is quite serious.

4) Because of uncertainties in lunar potential and perhaps inadequacies in the trajectory computation in lunar orbit, PRDL tends to accumulate large errors in doppler prediction. Operationally this causes no great problems to the DSIF, but renders the TDM function inadequate for data noise evaluation.

5) In the early phases of the mission, tracking data was sent in batches, which adversely affected the TDM function. An agreement was reached with Operations Engineering to send data continuously for the remainder of the mission. This arrangement should be extended in the future to provide a line fully dedicated to tracking data. Concurrently, it is very desirable that a higher TDH sample rate (20 sec/sample) be maintained throughout the mission to enhance the value of TDM output analysis and input reliability.

6) Station overlap scheduling during lunar orbit was inadequate. To the degree that this data improves orbit determination it also improves prediction accuracy.

7) There exists a software incompatibility in the TDP/ODG between octal and decimal data in the TDH ranging field. It is desirable to record transmitter VCO frequency in this field for operational reliability when ranging is not being done. However, a conflict arises during ranging if all stations participating are not in ranging format simultaneously, and as a consequence, data is either rejected or must be laboriously processed. Two approaches are open to this problem: first, by ensuring concurrent format changes at the stations, which is being implemented; second, and very desirable, by changing software to accommodate format conflicts between stations.

Ranging and time synchronization—The first acquisition of range by the Mark I ranging system on an actual spacecraft was accomplished at 13:12:02 GMT on August 12, 1966. In addition, an attempt was made to measure the difference between the station master clocks by using the ranging system at each of the DSS sites involved in the Lunar Orbiter mission. The clock synchronization experiment was performed to support a project request for information on the deviation of station master clocks between sites with an uncertainty of 50 microseconds or less. This is not possible using the standard WWV synchronization techniques.

Ranging results—Data was obtained from DSIF-12 during the cislunar phase and from DSIF's 12, 41, and 61 during the orbital phase. Two correlations were made on the data; one against the predicted range from the orbit determination program based on integrated doppler, and a second for noise on the ranging data. The ranging system had an expected accuracy of 15 meters or better. The orbit determination program range prediction had an uncertainty of several hundred meters due in the most part to ephemeris errors. The residuals obtained by differencing the ranging data with the predicted range was less than the uncertainty in the predicted range. Over 1000 independent acquisitions have been accomplished.

Data noise was measured by a combination of looking at the noise on the orbit determination residuals and comparing the counted doppler between range points to the difference in range. Since the orbit program has a truncation error of 4 meters at this distance, its root mean square (RMS) error was about 4 meters during cislunar ranging. Actual data comparison gave an error of about 3 meters. During the first week of Lunar Orbiter ranging with DSIF's 12, 41, and 61, a noise level of 5 meters was indicated; however, when ranging was continued after photo readout, the noise level had increased to about 12 meters RMS and 30 meters peak to peak. Investigation is now under way to isolate the noise increase to the ground stations or to the spacecraft.

Recommendations

1) Ranging is a data type that might improve the cislunar orbit by a factor of two. The DSS Mark I system appears operational and is providing results close enough to its ±15-meter specification for the data to be of considerable value.

2) If possible, ranging data should be obtained as soon after launch as feasible, i.e., the first pass over DSS's 41, 61, and 12. This would aid in a quick early orbit determination and would provide an opportunity to evaluate the ranging while orbit determination range uncertainty was still low (25 to 50 meters).

Time synchronization results—Time synchronization was actually a measurement of the time difference between the station master clocks at the different sites by measuring the difference between the 1 pulse per second generated by the station clock and a commonly received pulse, which is the sync pulse for the range code. Setup and implementation of the test was relatively simple because the total equipment requirement beyond standard station equipment was one cable. Some problems have occurred due to operator error; however, the procedure is not difficult. As the operators become more familiar with the system, the problems will diminish. Because of several station clock failures during the Lunar Orbiter mission, it is strongly recommended that the measurement be carried out throughout the entire mission at least twice a week. The measurement should be made in microseconds or better. Results of the time synchronization experiment are shown in Table 3.4-1. Although more data was taken during the initial tests for evaluation purposes, it now appears that 10 points of data on 30-second centers are sufficient. Initial tests have shown that it is unlikely that more than 1 point out of the 10 will contain erroneous data and that the remaining points will all fall within a band of ±1 microsecond of the mean.

Table 3.4-1: Time Synchronization Experiment Results

DAY	TIME GMT	STATION	CLOCK WITH RESPECT TO DSS-12 MICROSECONDS
228	18:00	61	+ 7617.5
229	01:00	41	- 2091.9
257	06:30	61	+ 7075. *
257	22:30	41	- 1840. *

* Operator error at DSIF-61 made direct comparison with DSIF-12 impossible. Error obtained via DSIF-41-61 synchronization.

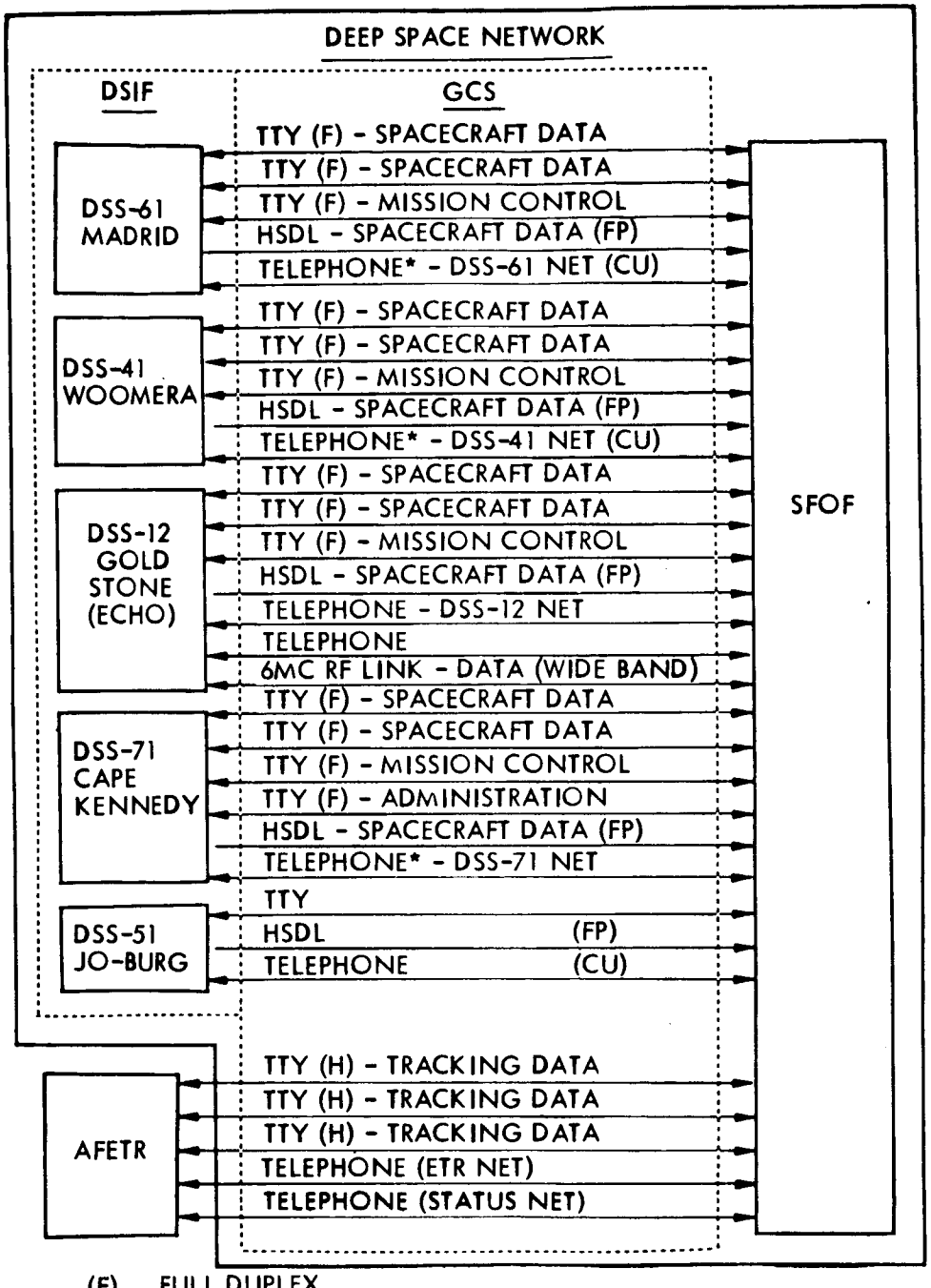

(F) FULL DUPLEX
(H) HALF DUPLEX
* SHARED LINE MISSION CONTR-LOP, DSIF CONTR-DSN
(CU) CALL UP 30 DAYS MAX. WITH 30 DAYS NOTICE
(FP) FULL PERIOD

FIGURE 3.4-5: GROUND COMMUNICATIONS NET CONFIGURATION

3.4.3.3 GROUND COMMUNICATIONS SYSTEM (GCS)

The DSN ground communications system consisted of: voice, normal-and high-data rate teletype circuits to provide a worldwide communications network between each overseas DSIF station and the SFOF; teletype and voice circuits between the SFOF, Goldstone stations, and Cape Kennedy; and a microwave link between the SFOF and Goldstone. The Ground Communications Net Configuration for Lunar Orbiter Mission I is shown in Figure 3.4-5.

GCS Operations

Minor circuit outages are normally experienced and expected during the routine operation of the DSN/GCS, the only major circuit outage occurred after launch when all three teletype and the high-speed data circuits were inoperative for 20 minutes between the SFOF and DSS-61. The outage was attributed to the commercial carrier at the Madrid facilities. It is believed that this problem is of a nonrepetitive nature and requires no action to prevent recurrence for subsequent missions.

Considerable difficulty was experienced in scheduling communications resources for the Lunar Orbiter project. This was primarily due to scheduling relationships with other user projects. Realignment of schedules and real-time modifications of previously scheduled activities became a daily task rather than an exception to routine operations. No solution to this problem is known; similar occurrences can be expected to occur for the next mission. Training of the communications operations personnel presented some problems but none of a serious nature. Additional personnel required for the Lunar Orbiter project were not provided but the work was accomplished by available people working overtime. The "comm man" position, which is the operational interface between the communications facilities and the project during critical mission phases, remains an unauthorized position in the contractor personnel manning allocation.

3.4.4 MISSION CONDUCT

3.4.4.1 OPERATIONAL CONTROL PROCEDURE

Centralized Control

Flight operations were conducted (primary mode) using a centralized control by the SFOD from the SFOF mission control room. In this room, personnel performed the following functions.

1) Continuously monitored progress to ensure that the mission was being conducted in accordance with the prearranged plan reflected in the current mission event sequence document.

2) Made decisions and issued directives as necessary to ensure mission success.

3) Conducted preliminary command and final command review conferences.

4) Periodically apprised the mission director of flight progress, reported when significant milestones had been passed, and alerted him to problems encountered.

5) Ensured that the following provisions were made to minimize the impact of a shifting to decentralized control:

   a) Critical stored program command (SPC) sequences were sent to a DSS for subsequent transmission to the spacecraft during the view period prior to that in which performance of the command sequence functions were to occur. This, for example, would require transmission of a command via the Madrid DSS, for performance of spacecraft functions during a Goldstone view period.

   b) A mission event sequence with at least a 12-hour look-ahead was normally available at the DSIF.

6) In the event of a nonstandard situation, implemented the applicable mission control fault isolation and correction procedures.

7) Approved each issue of the mission event sequence document or revision thereto.

8) Monitored the current capability of the DSN to support the Lunar Orbiter I mission.

9) Monitored status of the ground communications system and established appropriate traffic priorities.

Decentralized Control

Decentralized control was strictly a contingency measure to provide for appropriate action in the event of a complete communications failure between the SFOF and the active DSS. Once communications were restored after such a failure, mission control would be returned at once to the SFOD or his designated assistant.

Operations in a decentralized mode were expected to occur for a period of less than one DSS view period. During this time, certain key functions of SFOF personnel would have been performed by DSS personnel. These functions primarily involved continuing to assess spacecraft performance and monitoring events scheduled in the current sequence, and prompt implementation of fault isolation and correction procedures, including the timely transmission and verification of necessary spacecraft commands. In a decentralized control mode, the senior Lunar Orbiter engineer at the affected DSS would have assumed responsibility for mission control.

Since complete communication failure between SFOF and the DSIF's did not occur, use of this mode was unnecessary.

The flight operations group was divided into three equal teams (Red, White, and Blue) to provide 24-hour coverage of flight operations in the SFOF. Sufficient overlap was scheduled to allow detailed coordination between the shifts. Team changes were scheduled during periods of low spacecraft activity (e.g., Earth occultation periods) wherever possible. The lack of an off-line planning group to consider the effect of proposed spacecraft activities on the overall mission proved to be a problem throughout the mission. In some cases, during photo taking, decisions on the use of film-set frames allowed only minimum time for programming before the intended activity. Coordination between and within teams became difficult. On future missions, an off-line group for planning and coordination between teams is planned.

Command Procedures

Control of the various spacecraft subsystems was provided by inserting commands into the spacecraft flight programmer, which served as the primary center for storing, routing, and controlling spacecraft functions. The flight programmer interfaced with all spacecraft subsystems, providing control of the spacecraft in accordance with commands received from the command decoder and signals received from the spacecraft subsystems.

Simplification of spacecraft control and increased flexibility of operation during a mission were gained by holding to a minimum the flight sequences that were programmed into the spacecraft control system. The spacecraft was controlled, to a large extent, by commands transmitted from the ground. For this reason highly developed organizational and operational procedures were required for the preparation and transmission of commands to the spacecraft.

Two types of commands were used with the Lunar Orbiter spacecraft:

1) Real-Time Commands (RTC)—Each real-time command consisted of one 26-bit word and produced a spacecraft response within 500 milliseconds after receipt of the command-execute signal by the spacecraft command decoder.

2) Stored Program Commands (SPC)—Each stored program command consisted of two or more words, one of which was a time word. They were stored in a specified flight programmer memory location by a preceding RTC from the ground. They were stored automatically in sequence, unless otherwise commanded.

A command-execute signal was transmitted to the spacecraft after a command word had been retransmitted from the spacecraft and verified by comparison with the transmitted command. This signal caused real-time commands to be executed and stored program commands to be transferred from the spacecraft command decoder register to the flight programmer memory.

Command Preparations

As of 21:00 GMT on September 14, 4,510 commands had been executed; these included 2,522 commands stored in the programmer memory and 1,988 real-time commands. There was a small but indeterminate number of additional commands processed by the command decoder and programmer; these arose from aborted or retransmitted commands. Once, a command in the stored program sequence had an incorrect spacecraft address and was rejected. The sequence was reprocessed through the DSS SDS-920 computer, transmitted correctly, and accepted. One incorrect command was transmitted and executed (a small pitch command rather than a roll) but was of no consequence to the mission. The preparation of commands for transmittal to the spacecraft was initiated upon authorization by the SFOD. The original request for authorization could be originated by either the FPAC director or the SPAC director, depending on the purpose of the command. In general, the FPAC director initiated all requests for commands that were dictated by trajectory and mission considerations. The SPAC director generally initiated all requests associated with spacecraft functioning. The command coordinator performed the liaison and overall control

necessary to effect the timely processing of requests, authorization, command preparation, and transmission of commands to the spacecraft. Figure 3.4-6 depicts the activities and shows the flow of information associated with the preparation of commands by FPAC and SPAC personnel.

FPAC command activities—FPAC was responsible for providing the initial information required for guidance and photo commands and periodically supplied additional information to support the origination of certain commands in SPAC. Specific FPAC command preparation activities were as follows:

1) Based on the analysis of data from orbit determination, trajectory, and guidance and maneuver programs, FPAC notified the command coordinator when preliminary command information, or information indicating the need for a command, became available. The command coordinator arranged a preliminary command conference with the SFOD, the FPAC, and SPAC directors, and the mission event coordinator, to decide whether to proceed with the command.

2) Following a decision to proceed, FPAC prepared and provided SPAC with guidance and photo command parameters, based on data obtained from analysis of computer program outputs. Included were a preferred and several alternate maneuver sequences for achieving desired spacecraft attitudes.

3) In addition to the information provided for guidance and photo commands, FPAC periodically provided SPAC with spacecraft, Sun, and Earth occultation predictions, and Earth-spacecraft-Sun angles, in the form of computer program outputs.

SPAC command activities—In SPAC, certain commands were originated and all commands were prepared for transmission to the DSIF.

The SPAC command programmer specialist was responsible for command preparation. He was assisted by other SPAC analysts who ensured that the commands were compatible with spacecraft subsystems. Following is a description of the SPAC command preparation activities.

1) SPAC analysts were responsible for initiating requests for and preparing all real-time commands, high-gain antenna orientation commands, Sun occultation commands, and video data readout commands. SPAC also provided the information required in addition to that supplied by FPAC for photo-taking commands.

2) The command programmer specialist prepared a GMT-tagged subsystem event sequence from the FPAC and SPAC originated command information. The GMT-tagged sequence was used by SPAC analysts to provide inputs to the subsystem prediction programs that determine the impact of the command on the spacecraft subsystems. Alternate commands provided by FPAC would only be processed if the preferred guidance or photo command was determined to be unsuitable at any time during preparation.

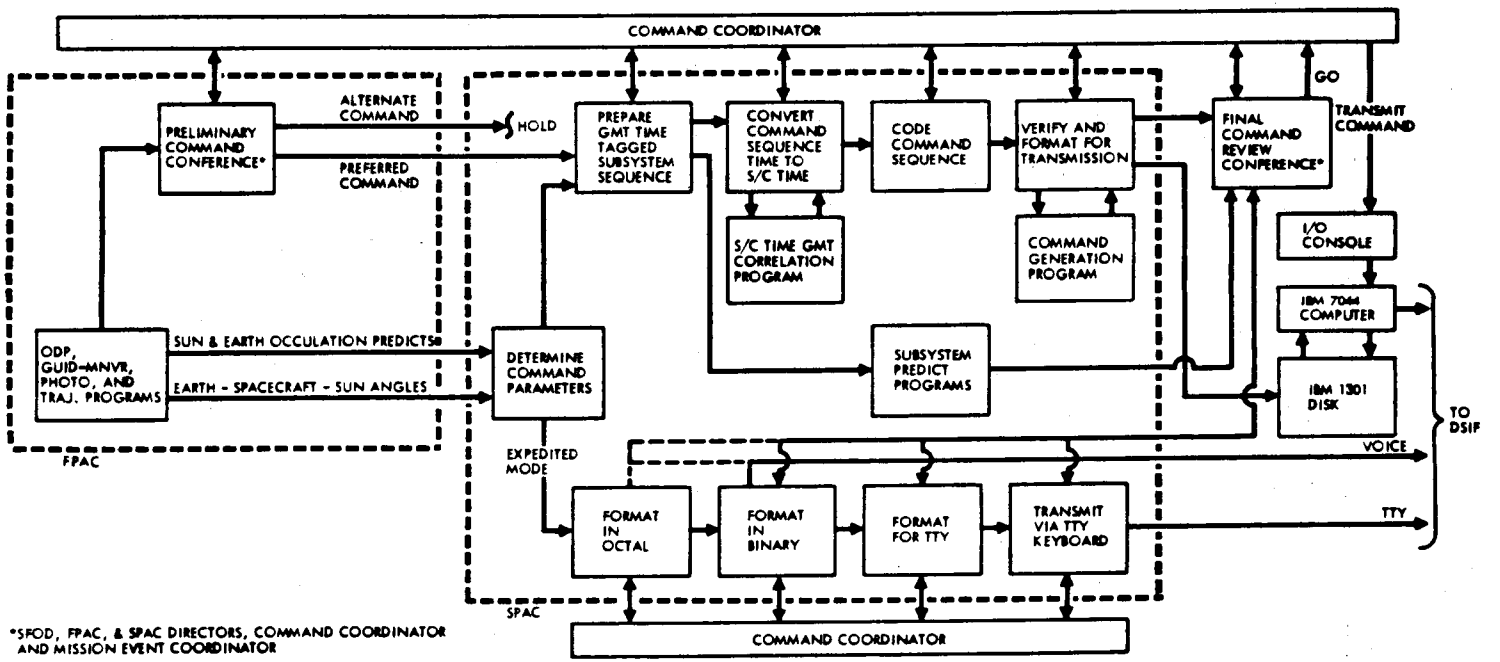

FIGURE 3.4-6: COMMAND PREPARATION SEQUENCE

3) The command programmer specialist used the spacecraft GMT correlation computer program to convert the command sequence to spacecraft time. He then coded the command sequence for input to the command generation program (COGL). This program verifies that the command is compatible with the flight programmer and stores it on the IBM 1301 disk, in a format suitable for transmission to the DSIF. The command programmer specialist was responsible for ensuring that the command generation program had been updated, prior to its use, to reflect the flight programmer memory status at the intended command transmission time. Using manual aids, the flight programmer analyst double checked that the command was compatible with the flight programmer.

4) Situations may arise where it is necessary to expedite the transmission of SPAC-originated commands. To accommodate commands requiring rapid execution, the command programmer specialist would format the command bit structure. The command coordinator would then transmit this command to a DSS by voice circuits for forwarding to the spacecraft by way of the command selector switches on the DSS command control equipment.

Command Approval

When a command sequence was stored on the disk ready for transmission, the command coordinator arranged a final command review conference with the SFOD, the FPAC, SPAC directors, and the mission event coordinator to obtain command approval and authorization for transmission of the sequence to a DSS. The SPAC director presented the command sequence and all pertinent information assembled during its preparation. He also provided information relative to the impact of the command on the spacecraft subsystems.

Command Transmission

Upon approval of a command sequence, the SFOD issued a command directive to the command coordinator. The command coordinator contacted the DSIF operations project engineer for a DSS readiness report and advised him of the transmission mode requirements and command transmission time. Upon receipt of the readiness report from the DSIF operations project engineer, and assurance that the proper functions had been performed at the DSS, the command coordinator initiated transmission of the command sequence.

The command transmission procedures used on Mission I were very adequate although in some instances unnecessarily redundant. The procedures required the transmission of commands from the command coordinator to the DSIF operations project engineer (Track Chief). then to the DSS manager, and finally to the senior Lunar Orbiter engineer (SLOE) at the site. In some occasions of peak spacecraft RTC activity, the time required for the command transmission did not allow for strict adherence to procedures, and the command coordinator contacted the SLOE directly. The procedures have been revised so that on future missions the command coordinator will coordinate most command activity directly with the SLOE.

Primary command transmission and verification modes—The primary modes of command transmission and verification were developed with considerations of communications reliability and the time available for the operation. The main reason for establishing modes is to facilitate the rapid relay of instructions from the SFOF to a DSS. The primary command modes are listed in Table 3.4-2, together with the significant transmission and verification functions performed at various locations throughout the system, to satisfy the mode requirements. Figure 3.4-7 shows a graphic presentation of command flow through the DDS system in each of the established modes.

Mode 1, delayed SPC mode, was used for storing commands in the flight programmer. The alternate modes were used as follows:

Mode 1A processed commands directly through the SDS-920 into the command equipment without use of delayed tape transmission. This mode was employed to correct nonstandard situations or to expedite transmission of Mode 1 sequences. Mode 2, delayed tape RTC mode, transmitted preprepared and stored taped RTC's at the prime DSS's were transmitted to the spacecraft directly from the MDE. Mode 2A, last taped RTC, was used to expedite transmission of the prepared and stored RTC's at the prime DSS's. Mode 3, verbal or teletyped SPC or RTC, transmitted commands by setting manual switches on the command equipment controlling the 26 bits of the command word. Mode 4, SDS-920 Workaround SPC/RTC, used DSS teletype punched tapes to enter commands into MDE (command) equipment. This mode was used when the SDS-920 computer at the DSS was off line for some reason.

Premission activity—Programmer core maps and a command generation software program (COGL) that simulated the entire mission were prepared prior to the mission. Commands for the countdown tests and for initial loading of the flight programmer memory were prepared and sent to DSS-71. In addition, Mode 2 commands (RTC's) were prepared prior to the mission and sent to DSS's 12, 41, and 61 for use during the mission. Soon after liftoff, prepared core maps and the COGL simulation became obsolete. On future missions, it is planned that the COGL simulation of the entire mission will not be attempted, but the core map activity will be retained.

Mission activity—Command preparation activity during the mission on occasion became a frantic process due to late definition of exact inputs or requirements, late changes, or requirements for programmer core storage in excess of an efficient level, necessitating programmer work-arounds. While all requirements were met, there were some cases of spacecraft core maps being stored at the last minute. Sometimes, the command programmers were unable to plan ahead for optimum flight programmer memory utilization. As a consequence, they could not take time to optimize the core maps and the number of commands in some sequences was increased.

Command preparation directives were issued in accordance with standard procedures for most photography and propulsion maneuvers. Once again the press of time in the preparation for some of the film-set photographs and in some of the spacecraft troubleshooting activities precluded use of the standard procedures. The established procedures and systems for verification of commands prior to their execution prevented the execution of incorrect commands in all but one (previously mentioned) case.

COMMAND MODE	COMMAND ORIGIN	COMMAND NAME	SFOF					DSS																				
			TRANSMISSION INITIATION		VERIFICATION			TTY EQUIP	SDS-920 COMPUTER			COMMAND CONTROL EQUIPMENT										VERIFICATION SELECTION				VERIFICATION		
					7040 OUTPUT	RECPT. AT SDS 920	RECPT AT S/C	COMMAND OUTPUT	COMMAND VERIFICATION		COMMAND INPUT		TAPE INPUT	TAPE SEARCH		DATA ENTRY/MODE SELECTOR											
			I/O TYPEWRITER	VERBAL OR ADMIN. TTY	ADMIN. PRINTER	KSR	100 WPM TELEPRINTER	TAPE PUNCH	TAPE PUNCH	TAPE READER VERIFICATION	TAPE READER (X MISSION)	SELECT APPROPRIATE ENABLE	TAPE READER	COMMAND SEARCH	SYNC SEARCH	SEARCH TAPE	MANUAL TAPE	AUTO. TAPE	MANUAL	COMPUTER	INPUT SWITCHES	GOOD	BAD	LOAD	TRANSMIT	VISUAL	PRINTER	EXECUTE
1	SFOF	DELAYED SPC	E		F	G	N		H	I	J	A								D		B 1	C 0	K		L	M	
1A	SFOF	FAST RTC/SPC	E		F	G	K					A								D		B 1	C 0	H		I	J	
2	DSS	DELAYED TAPED RTC					L					A	E		F	D	G					B 1	C 0	H	I	J	K	M
2A	DSS	FAST TAPED RTC					K					A	E		F	D		G				B 1	C 0	H		I	J	
3	SFOF	VERBAL OR TELEPRINTER SPC/RTC		A			K					B							C		F	D 1	E 0	G	H	I	J	L
4	SFOF	SDS-920 WORK AROUND	D		E			F				A	H	J	I	G		K				B 1	C 0	L		M	N	

LEGEND:

THE SEQUENCE IN WHICH TRANSMISSION AND VERIFICATION IS ACCOMPLISHED IS INDICATED IN ALPHABETICAL ORDER FOR EACH COMMAND MODE.

DECISION TO USE EITHER A OR B ENABLE WILL BE MADE PRIOR TO LAUNCH. UNLESS OTHERWISE DIRECTED THE SAME ENABLE WILL BE USED THROUGHOUT THE MISSION.

Table 3.4-2: PRIMARY COMMAND TRANSMISSION AND VERIFICATION MODES

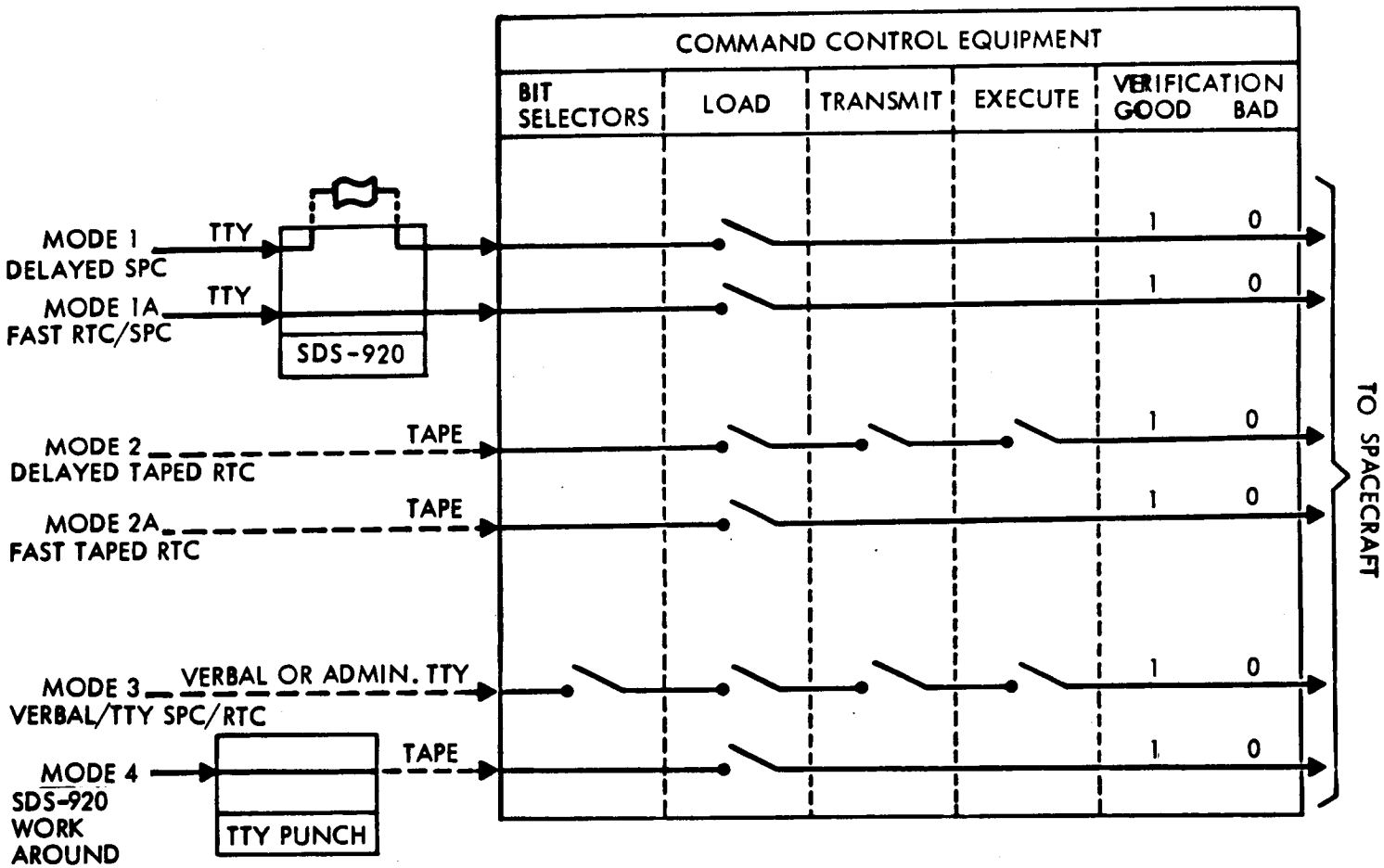

FIGURE 3.4-7: DSS COMMAND TRANSMISSION MODE REQUIREMENTS

Because of the increased activity for the command programmers in Mission I, it is planned that additional personnel will be assigned on future missions. The MATRIX functions will be divided into an off-line planning function and an on-line implementation function. The off-line programmer would plan memory maps to reflect changes in the mission plan that changed the order in which commands were to be executed.

Mission Event Sequence

Throughout Lunar Orbiter Mission I the mission event coordinator was reponsible to the SFOD for periodically updating the nominal mission event sequence prepared prior to the mission and presented in the applicable flight operations plan (reference Boeing Document D2-100106). He was also responsible for updating the sequence during the countdown, if holds had caused significant deviations from the nominal mission liftoff time. His prime task was to coordinate and schedule predicted events to avoid conflicts and to facilitate the conduct of a mission in an orderly and optimum manner.

The mission event coordinator used the IBM 7094 mission sequence of events program (designated as SEAL) to prepare the event sequence revisions. The program outputs, consisting of event lists and a bar chart depicting major activities, were distributed to operational personnel after checkout by the mission event coordinator and approval by the SFOD.

The mission event coordinator maintained close contact with the SFOD and other members of the operating team, particularly the FPAC and SPAC directors, the supervisor of net operation, and the DSIF operations project engineer, for the purpose of obtaining inputs to the event sequence.

To permit timely revisions to the mission event sequence, a computer program was designed to prestore the maximum amount of information that does not change from mission to mission. This information, consisting of standard inputs such as format data and fixed-time intervals between events, was placed in a master file (common environment) readily accessible to the program. Trajectory-dependent and other inputs of the type that change as the mission progresses were input to the program each time it was run. The result of a computer run is a printout of the event lists and bar charts using the standard format contained in the master file.

Copies of the sequence were distributed to all mission control personnel as revisions to the flight plan were determined. The computer program stored the activities to be performed during the view period of a particular DSS on a disk. These activities were transmitted to the station at the earliest possible time to provide them with maximum visibility of the planned flight. Early in the mission, the DSIF stations realized that complete data on the overall flight plan was required at each station, so for the latter part of the mission, planned activities were transmitted to all stations.

3.4.4.2 FLIGHT PATH CONTROL

Flight path control by the flight path analysis and command (FPAC) team entails execution of the following functions:

1) Tracking Data Analysis—The function of monitoring, passing judgement on the quality of the incoming radar tracking data (doppler and range), and provided assistance in keeping the tracking system locked to the spacecraft. Raw doppler tracking data was the sole link between the spacecraft and FPAC, and contained all information necessary to determine the position and velocity of the vehicle.

2) Orbit Determination—A process of finding a trajectory that "best" fits the doppler tracking data. Sometimes, as in first ellipse, this process is expanded to include solving for other physical parameters, such as terms representing the lunar gravity field. Thus, this process includes the tasks of editing the raw tracking data into a form acceptable to the orbit determination computer program (ODP), and subsequent operation of this program to obtain that trajectory best fitting the data—usually a lengthy task that consumes large blocks of computer time.

3) Flight Path Control—After the orbit determination process gives a trajectory, the flight path control function is to determine the need for a corrective maneuver or to specify the precise nature of a planned maneuver. Thus, this function is principally one of guidance, control, and flight path prediction.

The baseline plan of maneuvers and trajectory related events is furnished to FPAC by the mission design group in the form of a nominal flight plan. The FPAC plan of action is to control the vehicle so as to realize this nominal flight plan. To this end the nominal flight plan provides FPAC with criteria, ground rules, and constraints that must be observed in any maneuver design.

The principal tools used by FPAC in maneuver designs are the set of computer programs referred to as the FPAC software system. A brief summary of these programs is given in Table 3.4-3. A measure of the performance of these programs during Mission I is given in Table 3.4-4, where the overall success ratio of 90.92% is shown. From an FPAC standpoint, the number of unsuccessful runs was principally due to analyst input errors rather than equipment-related failures; this was in sharp contrast to premission simulations where the success ratio was about 60% and the majority of failures was due to equipment.

The organization of FPAC is unique in one respect: responsibility for the control of the mission from prelaunch checkout through about launch plus 6 hours belongs to the DSN, and they have a special team that mans the facility during this period. When the DSN has acquired the spacecraft and is returning good tracking data to the SFOF (about launch plus 6 hours), the DSN FPAC team is relieved by the Project FPAC team, which completes the mission with the tracking data analysis function carried out by a JPL analyst attached to the FPAC team. Table 3.4-5 illustrates the organization of these two teams.

Table 3.4-3: FPAC Software System

I. TRACKING DATA ANALYSIS PROGRAMS

1. PRDL - (Reference RFP 332-1, Feb. 26, 1965, JPL) - DSN program predicts spacecraft position relative to tracking stations. Has powered flight option for constant thrust.

2. POWL - (Reference TM 32-38, Sept. 23, 1960, JPL) - DSN program predicts spacecraft position relative to tracking stations for variable thrust vehicles near the Earth.

II. ORBIT DETERMINATION PROGRAMS

1. ODPL - (Reference D2-100538-2, March 18, 1966, TBC) - Orbit determination program determines spacecraft state vector at selected epochs. Has lunar harmonics determination and error prediction options.

2. TDPX - (Reference TM 312-653, JPL) - Tracking data processor edits raw tracking data formats.

3. ODGX - (Reference TM 312-653, JPL) - Orbit data generator program processes edited tracking data in a format acceptable to ODPL.

4. LFDL - (Reference D2-100430-2, unpublished, TBC) - Program determines orbital elements using doppler frequency data in the binary star technique. Backup for ODPL.

III. FLIGHT PATH CONTROL PROGRAMS

1. GENL - (Reference D2-100427-1, TBC) - Provides data communication between FPAC User Programs, and may be used to control inputs to all Flight Path Control Programs.

2. TJ1L - (Reference TM 33-198, Jan. 15, 1965, JPL) - Uses SPACE integrating trajectory program for cislunar trajectories with plot capability.

3. TJ2L - (Reference TM 33-198, Jan. 15, 1965, JPL) - Uses SPACE integrating trajectory program for cislunar trajectories.

4. TJ3L - (Reference TM 33-198, Jan. 15, 1965, JPL) - Uses SPACE integrating trajectory program for lunar orbits.

5. TRJL - (Reference TM 33-198, Jan. 15, 1965, JPL) - General purpose integrating trajectory program using SPACE.

Table 3.4-3: (Cont'd.)

6. MCSL - (Reference 2-1563-10-073, Aug. 6, 1966, TBC) - Computes state vector at input time on cislunar trajectory using Cowell integration method.

7. INTL - (Reference D2-100427-1, TBC) - Cowell method integrating trajectory program for cislunar trajectories with disk storage capability for data required by SPAC.

8. LIFL - (Reference D2-100427-1, TBC) - Mean elements trajectory program for lunar orbit lifetime studies with disk storage capability for data required by SPAC.

9. MDLL - (Reference D2-100427-1, TBC) - Programs used to determine if a midcourse maneuver is required.

10. MC1L - (Reference D2-100427-1, TBC) - Program used to determine impulsive midcourse maneuver data for study purposes.

11. MC2L - (Reference D2-100427-1, TBC) - An available program for second midcourse data when a second midcourse is contemplated while determining the first midcourse maneuver.

12. GCML - (Reference D2-100427-1, TBC) - Computes the guidance command data for an impulsive midcourse maneuver.

13. INML - (Reference D2-100427-1, TBC) - Computes optional impulsive injection maneuver from cislunar trajectory to first ellipse.

14. GCIL - (Reference D2-100427-1, TBC) - Computes guidance commands data for finite burn, constant thrust injection maneuver into first ellipse, based on selected impulsive injection maneuver data.

15. GCTL - (Reference D2-100427-1, TBC) - Computes guidance command data for impulsive transfer from first to second ellipse.

16. GCPL - (Reference D2-100427-1, TBC) - Computes guidance command data for lunar photographs with camera pointing options.

17. EVAL - (Reference D2-100427-1, TBC) - Program used for postphoto evaluation of photo data.

18. FAIL - (Reference D2-100427-1, TBC) - A program to provide attitude commands for a variety of maneuver situations.

IV. SPECIAL PROGRAM

1. PS1X - (Reference ED-199, Jan. 4, 1964, JPL) - SFOF program used to compile JPTRAJ source programs into machine level code and stores them on the disk.

Table 3.4-4: Performance of FPAC Software

PROGRAM	SUCCESSFUL RUNS	UNSUCCESSFUL RUNS	TOTAL RUNS	% SUCCESS
PRDL	76	15	91	83.52
POWL	9	0	9	100.00
ODPL	293	34	327	89.60
TDPX	497	43	540	92.04
ODGX	196	25	221	88.69
LFDL	15	3	18	83.33
GENL	465	57	522	89.08
TJ1L	2	1	3	66.67
TJ2L	2	1	3	66.67
TJ3L	7	1	8	87.50
TRJL	125	8	133	93.98
MCSL	20	0	20	100.00
INTL	60	1	61	98.36
LIFL	127	10	137	92.70
MDLL	14	2	16	87.50
MC1L	64	0	64	100.00
MC2L	8	1	9	88.89
GCML	24	0	24	100.00
INML	45	3	48	93.75
GCIL	30	3[c]) See	33	90.91
GCTL	55	2[c]) Note c	57	96.49
GCPL	78	12	90	86.67
EVAL	132	8	140	94.29
FAIL	25	1	26	96.15
PS1X	33	9	42	78.57
TOTAL	2402	240	2642	

OVERALL % SUCCESS = 90.92

NOTES:
a) Results compiled from Flight 2 log
b) Covers period 9 Aug to 2 Sept 1966, inclusive
c) Does not include runs of GCIL and GCTL, which were partially useful despite the timing errors in these programs.

DSN FPAC (countdown, launch, acquisition phase)

* FPC - Flight Path Control

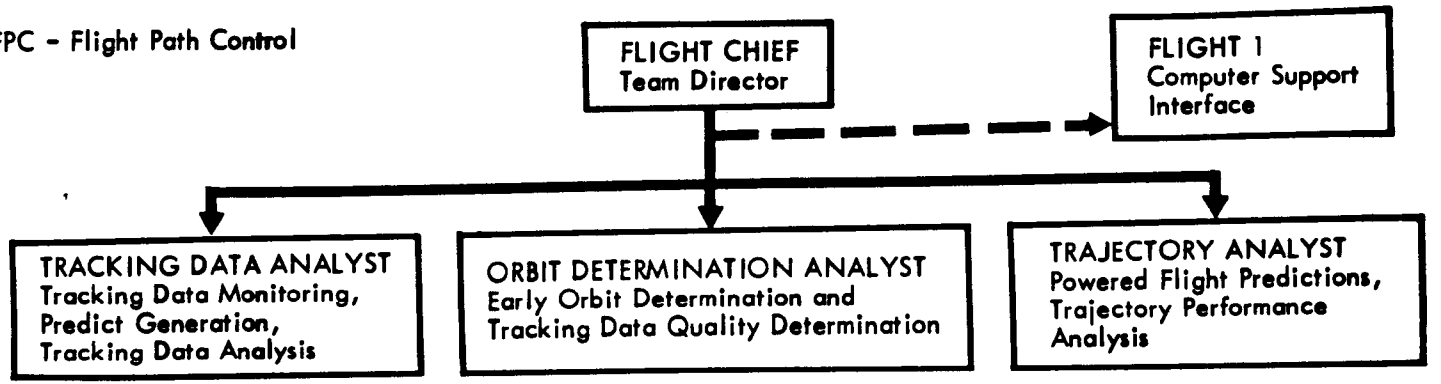

PROJECT FPAC (cislunar, lunar phase)

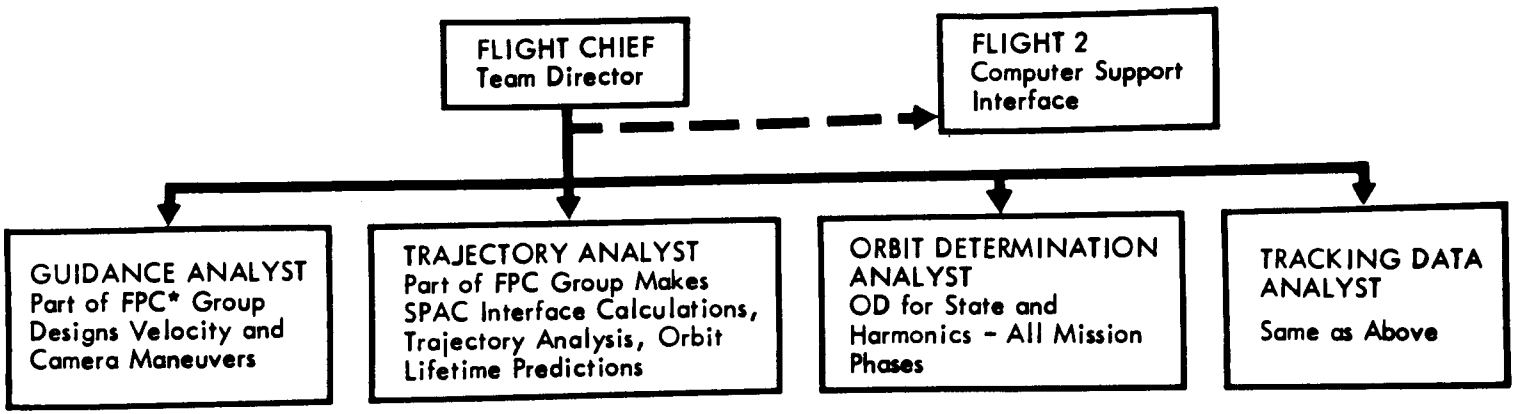

Table 3.4-5: FPAC ORGANIZATION

Trajectory Sequence of Events Summary

From a trajectory viewpoint, the mission can be subdivided into the following phases:

1) Countdown, Launch and Acquisition—Begins when FPAC enters the countdown, carries through DSN acquisition of the spacecraft, and ends at handover from DSN FPAC team to Project FPAC team.

2) Cislunar—From handover through injection into lunar orbit (also referred to as "deboost").

3) First Ellipse—From end of injection burn through first transfer maneuver. Includes Site I-0 photos.

4) Second Ellipse—From end of first transfer burn through second transfer maneuver. Site I-1 through I-5 photos.

5) Third Ellipse—From end of second transfer burn through end of photo readout activity. Site I-6 through I-9.2b photos.

Table 3.4-6 lists the principal FPAC events and their times of occurrence within these phases. Orbit determination and flight path control functions executed in these phases will be discussed in the following subsections; however, tracking data analysis will not be included since it is contained in other Lunar Orbiter project documentation.

Countdown, Launch, and Acquisition Phase*

This phase covers the period of FPAC mission participation from the time countdown is entered, through the launch and powered flight portion of the trajectory, to the time that FPAC responsibility is handed over from the DSN team to the project team. This handover occurred about launch plus 6 hours, and was predicated upon successful acquisition of the spacecraft by the DSN.

The normal entry of FPAC to the network countdown procedure was at about launch minus 5 hours when the DSN FPAC team—backed up by the project team—initiated a prescribed set of prelaunch checkout cases that were designed to exercise the major elements of the FPAC software system and demonstrate its launch readiness. However, because of the troubles experienced with these exercises due to both software and equipment during the operational readiness tests (ORT), the Project FPAC team entered the countdown at launch minus 11 hours and began "pre-prelaunch" check cases. These tests served the purpose of identifying software/equipment problems at a time early enough to institute corrective measures.

*For detailed records of events in this phase, consult the preliminary Lockheed Report, Lunar Orbiter A Launch Report, LMSC-273964, August 23, 1966. The DSN FPAC activities are summarized in the JPL Interoffice Memorandum, "DSN FPAC Team Operations in Support of Lunar Orbiter I," 312.1 - 150-JPB, 26 September 1966

Table 3.4-6: Trajectory Sequence of Events

Countdown, Launch, and Acquisition Phase

10 Aug, 08:30:	FPAC begins prelaunch checkout of software system.
10 Aug, 19:26:	Launch.
10 Aug, 19:35:	Agena first burn complete. Start 861.3-sec. coast.
10 Aug, 20:04:	Agena second burn complete. Cislunar injection.
10 Aug, 20:26:	First DSS (41) two-way doppler data.
11 Aug, 00:00:	Calculated midcourse for execution at 15 hrs: 23 m/sec (not used).
11 Aug, 01:30:	DSN FPAC completes Orbit determination 1103 and relinquishes control to Project FPAC.

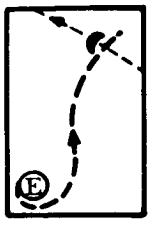

Cislunar Phase

12 Aug, 00:00:	Execute midcourse Start burn: 00:00:0.0; HROLL: 73.35°; ΔV: 37.83 m/sec PITCH: -25.24°; Δt: 32 sec
12 Aug, 17:00:	Concluded post-midcourse maneuver state determination.
12 Aug, 19:00:	Completed initial design of lunar injection maneuver.
14 Aug, 15:34:	Start burn for lunar injection maneuver. Start burn: 15:34:43.22; HROLL: 19.17°; ΔV: 790.0 m/sec PITCH: -108.73°; Δt: 579 sec

First-Ellipse Phase

14 Aug, 16:20:	OD converged using two-station data from end of burn to first occultation; confirmed expected postinjection state.
18 Aug, 14:42:	Site IO photos on Orbit 26 still using Goudas 2 harmonics
19 Aug, 14:00:	OD group presents gravity harmonics results; solutions from OD 4138 selected.
21 Aug, 09:50:	Transfer from first ellipse to second ellipse on Orbit 45. Start burn: 09:49:58.7; HROLL: 43.40°; ΔV: 40.15 m/sec PITCH: 25.31°; Δt: 22 sec

Second-Ellipse Phase

21 Aug, 11:30:	OD confirms success of first transfer maneuver.
22 Aug, 15:23:	Site I1 photos on Orbit 9.
22 Aug, 18:51:	Site I2 photos on Orbit 10.
23 Aug, 08:46:	Site I3 photos on Orbit 14.
24 Aug, 09:09:	Site I4 photos on Orbit 21.
25 Aug, 13:02:	Site I5 photos on Orbit 29.
23 Aug, 16:36:	First Earth-Moon photo on Orbit 16.
25 Aug, 16:01:	Transfer from 2nd ellipse to 3rd ellipse on Orbit 30. Start burn: 16:01:29.2; HROLL: 34.28°; ΔV: 5.43 m/sec PITCH: -129.76°; Δt: 3 sec

Third-Ellipse Phase

25 Aug, 20:00:	ODP confirms nominal execution second transfer maneuver.
26 Aug, 23:32:	Site I6 photos on Orbit 39.
28 Aug, 06:28:	Site I7 photos on Orbit 48.
29 Aug, 06:32:	Site I8.1 photos on Orbit 55.
29 Aug, 09:56:	Site I9.2a photos on Orbit 56.
29 Aug, 13:23:	Site I9.2b photos on Orbit 57.

At the start of the DSN FPAC team countdown for the first launch attempt on August 9, problems were encountered on both X and Y computer strings. An attempt was made to operate using the W string from the Surveyor FPAC area in the SFOF, but this proved impractical. As a result of these problems only a limited number of prelaunch checkout cases were run before T-70 minutes when the terminal countdown phase was started. The frequency reports and POWL cases were run successfully; however, the launch was scrubbed due to an anomaly in blockhouse measurement in the atlas propellant utilization system. Although the problem was suspected to be within ground instrumentation, the onboard system was replaced prior to countdown the following day.

On August 10, the actual launch date, the FPAC team ran through all the required prelaunch countdown checkout cases and many of the nonmandatory cases. The frequency reports were received from DSIF-71 on schedule, and frequency parameters were supplied to the RTCS for DSIF predicts. All the expected liftoff time POWL cases were run as required. The actual liftoff time POWL cases were cancelled since the expected liftoff time POWL cases provided adequate data. Launch occurred at 19:26:00.716 GMT with flight plan 10H and launch vehicle flight azimuth of 100.5 degrees. Table 3.4-7 lists some of the major powered flight events from liftoff through completion of the second Agena burn.

During the powered flight phase the DSN OD group used manned space flight net (MSFN) and eastern test range (ETR) tracking data to back up ETR-produced parking orbit and transfer orbit predictions. The required orbital elements and injection conditions, predictions for DSIF's 71, 51, and 41, and Mark Time and lunar encounter data were received from ETR and evaluated by the FPAC team. The DSN OD group received and processed DSIF-41 tracking data and ran four separate orbit determinations, (including one by the project personnel), prior to the time control of the FPAC team was relinquished to the project at launch plus 6 hours. Tracking predictions and trajectories were run based on these orbits and predictions were sent to the necessary Deep Space Stations. These early orbit determination results are shown in Figure 3.4-8, where the solution has been mapped forward to lunar encounter.

The raw tracking data supplied by the MSFN and ETR and the computations performed by the RTCS in support of Lunar Orbiter I were outstanding. The performance of the SFOF data processing system during the Lunar Orbiter mission was excellent. These two factors, plus the nominal performance of the launch vehicle and spacecraft and the early acquisition by the Woomera DSS-41, allowed the Lunar Orbiter FPAC team to operate very smoothly.

Cislunar Phase

The cislunar portion of the mission is the free-flight part of the trajectory from second Agena shutoff (cislunar injection) to the end of the burn that places the spacecraft in lunar orbit (lunar orbit injection or deboost). This phase included a single midcourse correction at about 28 hours after cislunar injection to null out the error imparted at cislunar injection. Orbit determination in this phase used doppler and angle tracking data from the three DSIF sites; in addition, a test was made with ranging data in support of DSIF clock synchronization.

Table 3.4-7: Powered Flight Trajectory Events

MARK	EVENT	ACTUAL TIME (GMT)
0	Liftoff	19:26:00.7
1	Atlas Booster Engine Cutoff (BECO)	19:28:09.5
2	Atlas Booster Engine Jettison	19:28:12.6
3	Start Agena Secondary Timer	19:30:32.0
4	Atlas Sustainer Cutoff (SECO)	19:30:51.6
5	Start Agena Primary Timer	19:30:55.6
6	Atlas Vernier Cutoff (VECO)	19:31:12.5
7	Shroud Separation	19:31:15.0
8	Atlas-Agena Separation	19:31:17.1
9	Agena First Ignition	19:32:9.9
10	Agena First Shutdown (Parking Orbit Injection)	19:34:43.7
11	Agena Second Ignition	20:02:35.1
12	Agena Second Shutdown (Cislunar Injection)	20:04:02.9
13	Agena-Spacecraft Separation	20:06:48
14	Begin Agena Yaw	Not Available
15	Stop Agena Yaw	Not Available
16	Agena Retro	Not Available

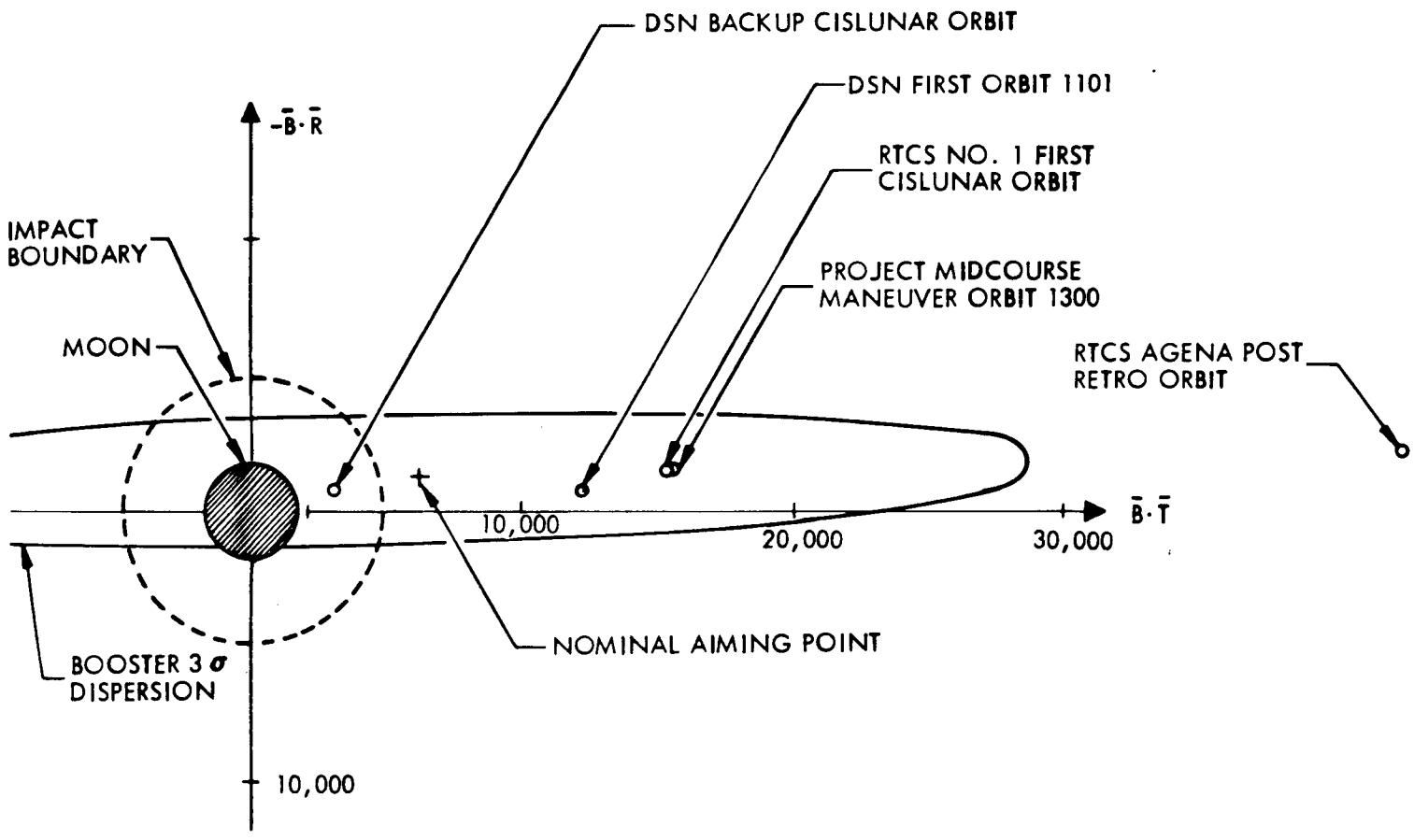

FIGURE 3.4-8: LUNAR ORBIT I EARLY ORBIT DETERMINATION RESULTS

Nonstandard procedures used by FPAC in this phase were:

1) Midcourse design using the Moon for roll reference;

2) Redesign of the lunar injection maneuver to overcome a software timing error;

3) Provision of alternate maneuver designs for midcourse and injection using high-gain antenna for roll reference;

4) First use of the ranging transponder to receive ranging tracking data.

Orbit Determination

Orbit determination in the cislunar phase consisted of three primary tasks.

1) Tracking Data Editing—The raw tracking data from the DSIF's were received at the SFOF; this was primarily the responsibility of the DSN tracking data analyst (TDA). The data were loaded into the 7094 computer through the 7044 computer, and then preliminarily edited with TDPX. As a backup, in case of a 7044 computer failure, the incoming data could be punched on cards by an 047 paper tape to card conversion machine. The cards would then be read into the 7094 system by means of TDPX. The data file to be used by the orbit determination program was then setup by ODGX. The data types received in the cislunar phase were:

   a) Two-way doppler (CC3) - Doppler shift measured by one station transmitting and receiving.

   b) Three-way doppler (C3) - Two-way doppler plus doppler shift measured by one station receiving but not transmitting.

   c) Hour angle (HA) - Angle in equatorial plane between object and station.

   d) Declination (DEC) - Angle from equatorial plane to object.

   e) Ranging (RU) - Two-way distance to spacecraft measured in range units (RU $\approx$ 1.0 meter).

   These data types were deleted or value adjusted in the editing process at the recommendations of the DSN data validation group.

2) Data Validation—The DSN data validation group periodically checked the tracking data to define data anomalies such as station transmitter frequency errors and timing bias between stations. The orbit determination program (ODPL) was used to process the data in special ways to discover anomalies.

3) Orbit Determination—Orbit determination consisted of defining a state vector at some time (epoch) by fitting tracking data in a weighted least-square sense. The solutions depended entirely on the data processed (i.e., no a priori knowledge was used); therefore, as much data as possible was considered in each fit. The method of holding the epoch constant and maintaining the end of the arc near real time was followed throughout this phase. Periods of free-flight only (no maneuvers) were considered for the cislunar phase and two epochs were used: post-injection and post-midcourse.

From injection into cislunar trajectory to handover, the DSN orbit determination group had prime responsibility. The objective was to define the orbit well enough to ensure continued tracking of the spacecraft by the tracking stations. The Project group (TBC) worked in parallel with DSN. The objective was to check the DSN group's results and determine the cislunar trajectory well enough to define approximate midcourse requirements. Also, early determinations provided a more accurate initial guess for later determinations.

Once acquisition had been accomplished and it was determined that the cislunar trajectory was near nominal, the DSN made periodic data validation runs and the Project continued making orbit determinations over longer data arcs.

After midcourse execution, unusually long data arcs were required to obtain reasonable results. The geometry of the trajectory was such that a "straight line" could just about fit the data for data arcs less than 20 hours long.

In addition to standard orbit determinations, the Project monitored predicted and actual doppler shifts during midcourse and deboost engine burns.

Appendix B contains a summary of all orbit determination runs made by the project during this mission phase.

Tracking data editing—This section discusses tracking data editing with the TDP/ODG programs to support orbit determination. Input deck listings, data file summaries, maneuvers, tracking data bar chart, and tracking data tape numbers are included in Appendix B for assistance in postmission evaluations.

Angle and doppler data were received at 10- and 60-second sample rates. The 10-second sample rate was employed for a short period after injection and during the midcourse maneuver. These data were received from stations:

Identity	External Number	TDPX-ODGX-ODPL Internal No.
Woomera	41	4
Johannesburg	51	5
Goldstone (ECHO)	12	12
Madrid	61	13

Tracking data received from Station 51 was rejected by TDPX because of bad data condition codes (the station was unable to attain suitable lock-up for the initial pass). Further commitments for Station 51 viewing were not made by the DSN, thereby eliminating any further acquisitions from this station. The prime stations for Lunar Orbiter (DSIF's 41, 12, and 61) provided all data used for orbit determination. Good data were obtained the majority of the time; however, data received during spacecraft maneuvers, primarily roll, caused a cycling of residuals, and pitch and yaw caused a slight trajectory alteration. For these reasons a list of spacecraft maneuvers is presented in Appendix B.

After midcourse, the ranging transponder was turned on and ranging unit (RU) data were received for the first time. This data type enabled the DSIF stations to determine time biases between stations. The values used were received from the DSN data validation orbit determination group and are contained in Appendix B in the input deck listings.

Two anomalies occurred during this mission phase.

1) When not receiving ranging unit data, the stations sent the receiver frequency in the range field of the tracking data message format. All ranging unit data types were in octal, but the frequency values were in decimal. Strict format fields are designated in TDPX so both types could not be processed simultaneously without rejection of certain data. This difficulty was overcome by making two passes through the tracking data whenever ranging units were received. The data were first processed using an octal format that allowed acceptance of data messages containing range units. The rejected data were then processed using a decimal format. This procedure allowed acceptance of all good data and still provided for proper handling of octal formatted ranging unit data.

2) Shortly before monitoring the deboost maneuver, it was realized that TDPX was approximately 30 minutes behind real time in obtaining the tracking data. This problem was later attributed to a malfunctioning editor (EDTX) program. To temporarily overcome this difficulty, the 047 card punch machines were used to record tracking data on IBM cards. These cards were read directly into TDPX for near real-time acquisition of the tracking data. Early acquisition of tracking data allowed for determination of the state vector 10 minutes sooner than the allotted time, thus enabling the station predictions to be generated and sent before the spacecraft emerged from occultation.

Two magnetic tapes are available with approximately identical tracking data files for the entire cislunar phase. B1 tape numbers and file summaries can be found in Appendix B.

The TDPX/ODGX source deck and data deck listings are in Appendix B. The tracking data bar chart in Appendix B gives station rise and set times, frequencies for ODGX input, and lists significant spacecraft attitude changes.

Orbit determination for midcourse and deboost maneuvers—The FPAC Orbit Determination Program ODPL was used for all OD work. In general, the following procedure was followed:

1) The new tracking data was processed with TDP and ODG to create an input file as discussed earlier.

2) Only the "state vector" X, Y, Z, $\dot{X}$, $\dot{Y}$, $\dot{Z}$ at a particular epoch was solved for.

3) No a priori covariance matrix was used.

4) All available doppler data, C3 and CC3, were processed. Frequency errors and "blunder points" in this data were corrected or deleted as they were discovered, through either the ODG or ODP. Premidcourse orbit determination used declination and hour angle data to obtain the first solution. All subsequent determinations used only C3 and CC3 data. Ranging data was never processed as a data type.

5) Convergence was considered complete when change in position and velocity from the previous iteration were about $\pm 1 \times 10^{-6}$ km and 1×10^{-9} km/sec respectively and the sum of squares of residuals (SOS) was small.

6) The converged state vector and covariance matrix were mapped to the midcourse time (for premidcourse OD only) and encounter time.

7) The above solutions were converted to the desired coordinate system for flight path control calculations.

The procedure described above was repeated five times for pre-midcourse phase and 15 times for post-midcourse phase. The orbit determination used to calculate the midcourse maneuver was obtained 11 hours before midcourse. The determination for deboost was obtained 26 hours before deboost. These long lead times were required for mission control, but subsequent orbit determinations were made to confirm validity.

The orbit determinations upon which the design for midcourse and deboost maneuvers were based are:

Midcourse: OD 1300

Deboost: OD 2104

The OD numbers are defined as follows:

First digit - (Mission Phase)

1 = Injection to 1st midcourse

2 = 1st midcourse to deboost

4 = Deboost to 1st transfer

5 = 1st transfer to 2nd transfer

6 = 2nd transfer to mission end

Second digit - (Team)

1 = Red team

2 = White team

3 = Blue team

Third and Fourth digit - (Run number for current phase)

Project used even numbers and DSN validation team used the odd numbers.

This numbering system was used throughout the mission and will be used in later discussions on orbit determinations.

A detailed description of the converged state vectors and physical constants used for the design of the midcourse and deboost maneuvers is given in Tables 3.4-8 and 3.4-9.

Other cislunar orbit determinations—Eighteen other determinations were made in the cislunar mission phase. These are reported in detail in Appendix B. Dispersion of the determinations in the $\bar{B}\cdot\bar{T}$ - $\bar{B}\cdot\bar{R}$ plane are shown in Tables 3.4-10 and 3.4-11 and Figures 3.4-9 and 3.4-10 for pre-midcourse and post-midcourse respectively. For the pre-midcourse phase, the lines connecting sequential determinations by the project group indicate the degree of compatability between them. DSN determination (odd-numbered cases) are also shown. It should be noted that the primary purpose of the DSN runs were: (1) Data validation; and (2) Supplying sufficient information to the tracking data analyst for ensuring continued tracking of the spacecraft.

Doppler data monitoring during midcourse and deboost maneuvers—As an early indication of the success of the midcourse and deboost maneuvers, the actual doppler data was compared with the predicted. Three schemes were used:

1) Tracking Data Monitoring Program (TDM) coupled with the MILGO plotter;

2) Manual plotting method;

3) TDPX-ODGX method.

The TDM program computed residuals between the observed doppler and doppler predicted from the latest orbit determination. These residuals were automatically plotted by the MILGO plotter about 2 minutes behind real time. The manual plotting method and TDPX-ODGX method are closely related.

For the manual method, doppler predictions were run using the latest orbit determination. About 1 hour before the maneuver, these predicts were plotted versus time through the maneuver. Actual doppler frequency over this time period (computed by hand from the cycle count displayed on teletype printout) was plotted by hand against the predicted points in near real time.

For the TDPX-ODGX method, editing programs were run shortly after the maneuver, when all burn data had been received, and doppler frequency obtained from ODGX. This data was plotted with the predicts.

This latter scheme fills in any missing points from the former and serves as a check. The manual method is close to real time (5 to 10 minutes), whereas the TDPX-ODGX lags real time by approximately 15 minutes.

Figure 3.4-11 shows the doppler plot for the midcourse maneuver. Although predicted and actual doppler curves do not coincide—due to a change in the station frequency from the predicted by 45 cps—the results indicate a nominal maneuver. Ignition occurred at 00:00 on Day 224, and the burn continued for 32.2 seconds. These times and the resulting doppler shift of 332 cps were as predicted.

Table 3.4-8: Midcourse Maneuver Orbit (OD 1300)

1) Epoch 66/08/10 20:15:47.9

2) State (Geocentric true of date coordinates)

	STATE		STANDARD DEVIATIONS	
X	7710.5550	km	0.317	km
Y	77.83328	km	2.54	km
Z	-3602.8491	km	2.48	km
DX	4.1860701	km/sec	0.19×10^{-2}	km/sec
DY	8.5659717	km/sec	0.32×10^{-3}	km/sec
DZ	0.23214645	km/sec	0.63×10^{-3}	km/sec

3) Encounter Conditions (Target Centered)

NOMINAL AIMPOINT		ACTUAL	STANDARD DEVIATIONS
B	6431 km	15,734.1 km	72.1 km
B · R	-1135 km	- 1,686.3 km	71.8 km
B · T	6330 km	15,643.4 km	7.3 km

4) Data Summary

STATION NUMBER	DATA TYPE	START	TIME	STOP	TIME	NUMBER OF POINTS	STANDARD DEVIATIONS
41	CC3	8/10	21:22	8/10	21:28	6	0.8×10^{-2}
	CC3	8/10	21:29	8/10	21:54	152	0.4×10^{-1}
	CC3	8/10	21:55	8/10	22:23	20	0.1×10^{-1}
	CC3	8/10	22:23	8/10	22:40	94	0.4×10^{-1}
	CC3	8/10	22:54	8/11	03:57	227	0.9×10^{-2}
51	C3	8/11	02:40	8/11	07:25	159	0.1×10^{-1}
61	CC3	8/11	05:10	8/11	10:15	214	0.2×10^{-1}

5) Summary

The above solution converged in three iterations; the resulting SOS was 11.1. No a priori covariance matrix was used and no other parameters were estimated in the solution. A standard data weight of 0.1 cps was applied for all stations; data during which S/C attitude maneuvers occurred was deleted. However, the trajectory remained slightly skewed because the maneuvers were uncoupled and perturbed the free-flight trajectory.

The data included 10-second data and used no time or frequency adjustments. However, it appeared that the C3 data from Station 51 had a bias of approximately -0.078 cycles. These data were not very abundant and did not perturb the solution. The solution was mapped to encounter, and 20, 30, 40, and 50 hours past injection for midcourse guidance studies. It was used to calculate the midcourse maneuver, which occurred at 00:00:0.0 on Day 224.

Table 3.4-9: Deboost Maneuver Orbit (OD 2104)

1) Epoch 66/08/12 00:00:0.0

2) State (Geocentric true of date coordinates)

	STATE		STANDARD DEVIATIONS	
X	- 61505.669	km	1.05	km
Y	188870.24	km	0.23	km
Z	81848.159	km	0.88	km
DX	- 0.65395354	km/sec	0.17×10^{-4}	km/sec
DY	0.90410928	km/sec	0.84×10^{-5}	km/sec
DZ	0.55029345	km/sec	0.13×10^{-4}	km/sec

3) Encounter Conditions (Target Centered)

	M/C AIMPOINT	ACTUAL	STANDARD DEVIATIONS
B	6508.7 km	6554.9 km	3.1 km
B · R	-1171.4 km	-1119.6 km	3.0 km
B · T	6402.4 km	6458.5 km	0.78 km

4) Data Summary

STATION NUMBER	DATA TYPE	START	TIME	STOP	TIME	NUMBER OF POINTS	STANDARD DEVIATIONS
41	CC3	8/12	00:28	8/12	04:13	201	0.0114
	CC3	8/12	04:14	8/13	03:04	226	0.0225
61	CC3	8/12	04:34	8/12	04:39	6	0.0051
	CC3	8/12	04:40	8/12	12:44	397	0.0146
12	CC3	8/12	12:48	8/12	23:08	1633	0.0232

5) Summary

This solution, OD 2104, was used to calculate the deboost maneuver. Although periodically discontinuous because of the many pitch and yaw maneuvers, the fit of the data was very good. As in the pre-midcourse solution, the data weight was 0.1 cps, and data during which the spacecraft was torqued was eliminated. No time or frequency adjustments were used.

Only the state was considered in the solution; no a priori covariance matrix was used. After convergence, achieved in seven iterations, the sum of squares was only 38.6. All subsequent orbit determinations substantiated this solution.

6) Residual plots are in Appendix B.

Table 3.4-10: Pre-Midcourse Encounter Dispersions

Nominal Encounter Aim Point $\bar{B} \cdot \bar{R} = -1135$ $\bar{B} \cdot \bar{T} = 6330$				
	PREDICTION		DIFFERENCE FROM NOMINAL	
OD SOLUTION NO.	$\bar{B} \cdot \bar{R}$	$\bar{B} \cdot \bar{T}$	$\Delta\bar{B} \cdot \bar{R}$	$\Delta\bar{B} \cdot \bar{T}$
ETR	- 836.5	3103	298.5	-3227
1100	-2228	15780	-1093	9450
1101	- 977	14095	158	7765
1200	-1924.4	15552	-789.4	9222
1103	-1724.8	15265	-589.8	8935
1103A	-1726.3	15260	-591.3	8930
1105	-1824.5	15574	-689.5	9244
1107	-1659.5	15644	-524.5	9314
1300	-1686.3	15643	-551.3	9313
1102	-1725.1	15650	-590.1	9320

Table 3.4-11: Post-Midcourse Encounter Dispersions

Midcourse Encounter Aim Point $\bar{B} \cdot \bar{R} = -1171.4$ $\bar{B} \cdot \bar{T} = 6402.4$				
	PREDICTION		DIFFERENCE FROM NOMINAL	
OD SOLUTION NO.	$\bar{B} \cdot \bar{R}$	$\bar{B} \cdot \bar{T}$	$\Delta\bar{B} \cdot \bar{R}$	$\Delta\bar{B} \cdot \bar{T}$
2300	-1136	6370.5	35.4	-31.9
2302	-1114.2	6456.5	57.2	54.1
2304	-1111.9	6454.9	59.5	52.5
2102	-1114.6	6457.3	56.8	54.9
2104	-1119.6	6458.5	51.8	56.1
2208	-1117.1	6457.5	54.3	55.1
2310	-1115.5	6459.2	55.9	56.8
2114	-1126.3	6465.2	45.1	62.8
2116	-1110.1	6465.0	61.3	62.6
2210	-1111.2	6458.0	60.2	55.6

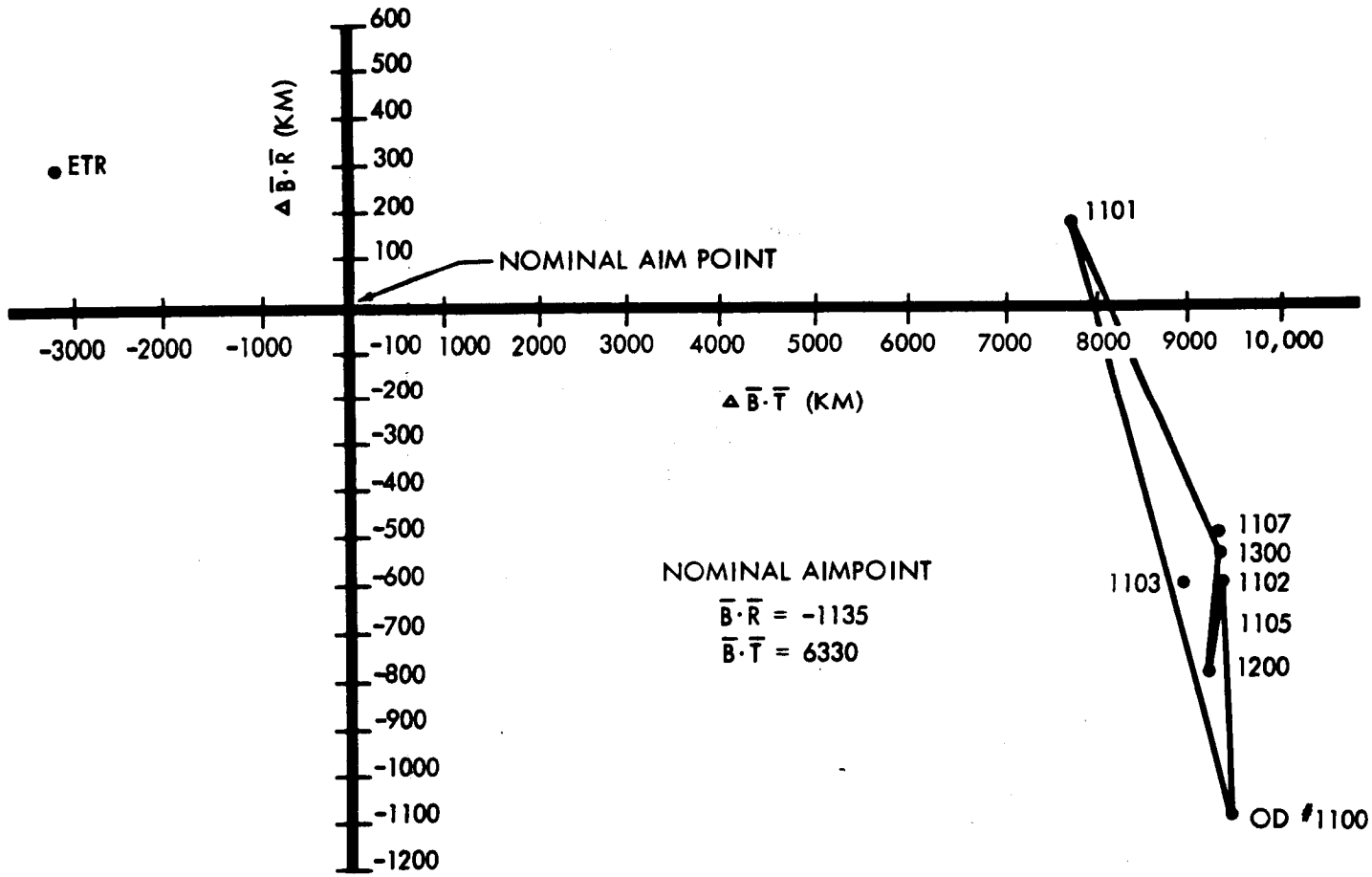

FIGURE 3.4-9: OD AIMING POINT DISPERSIONS — PRE-MIDCOURSE

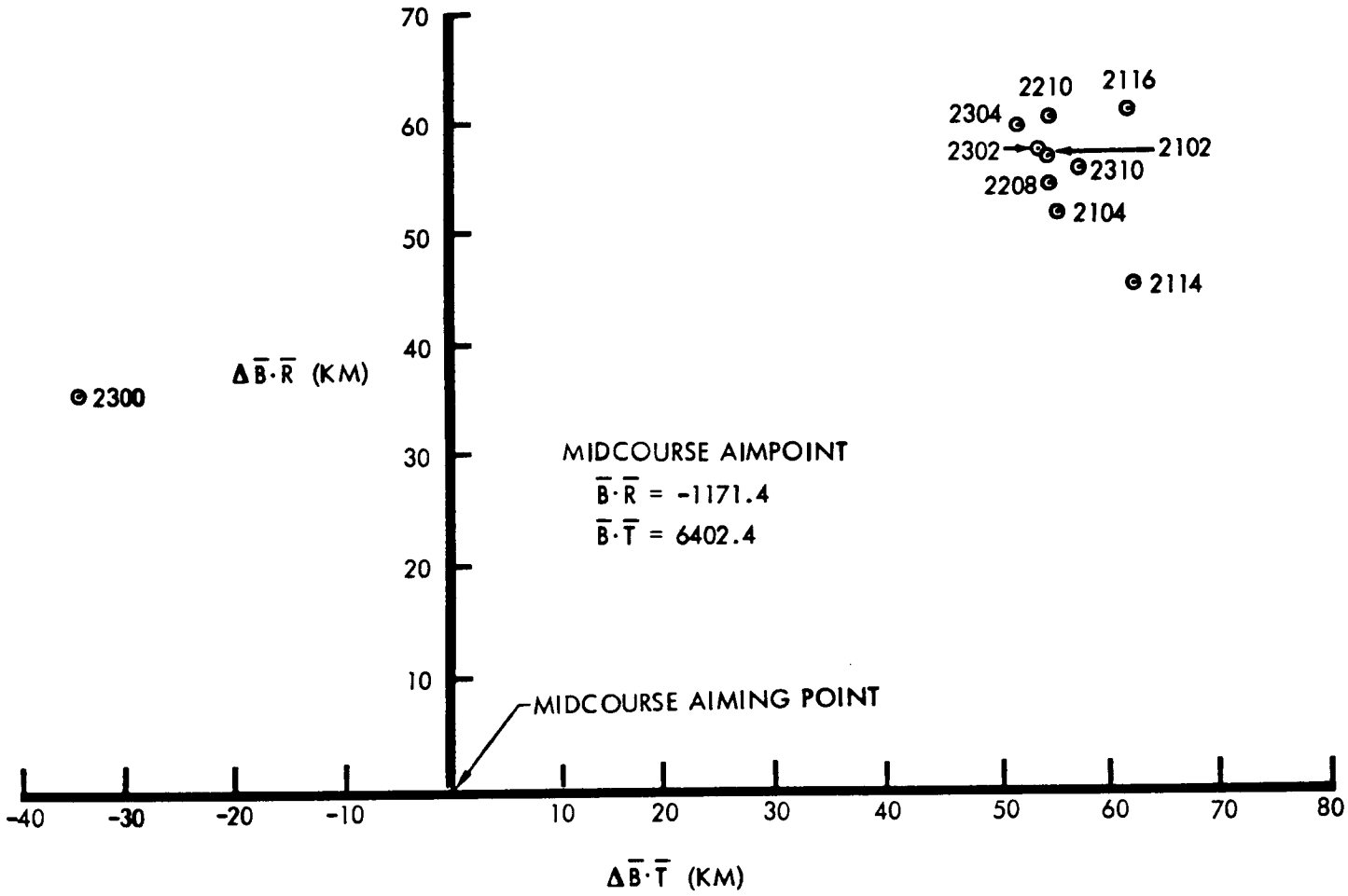

FIGURE 3.4-10: OUTSIDE AIMING POINT DISPERSIONS — POST-MIDCOURSE

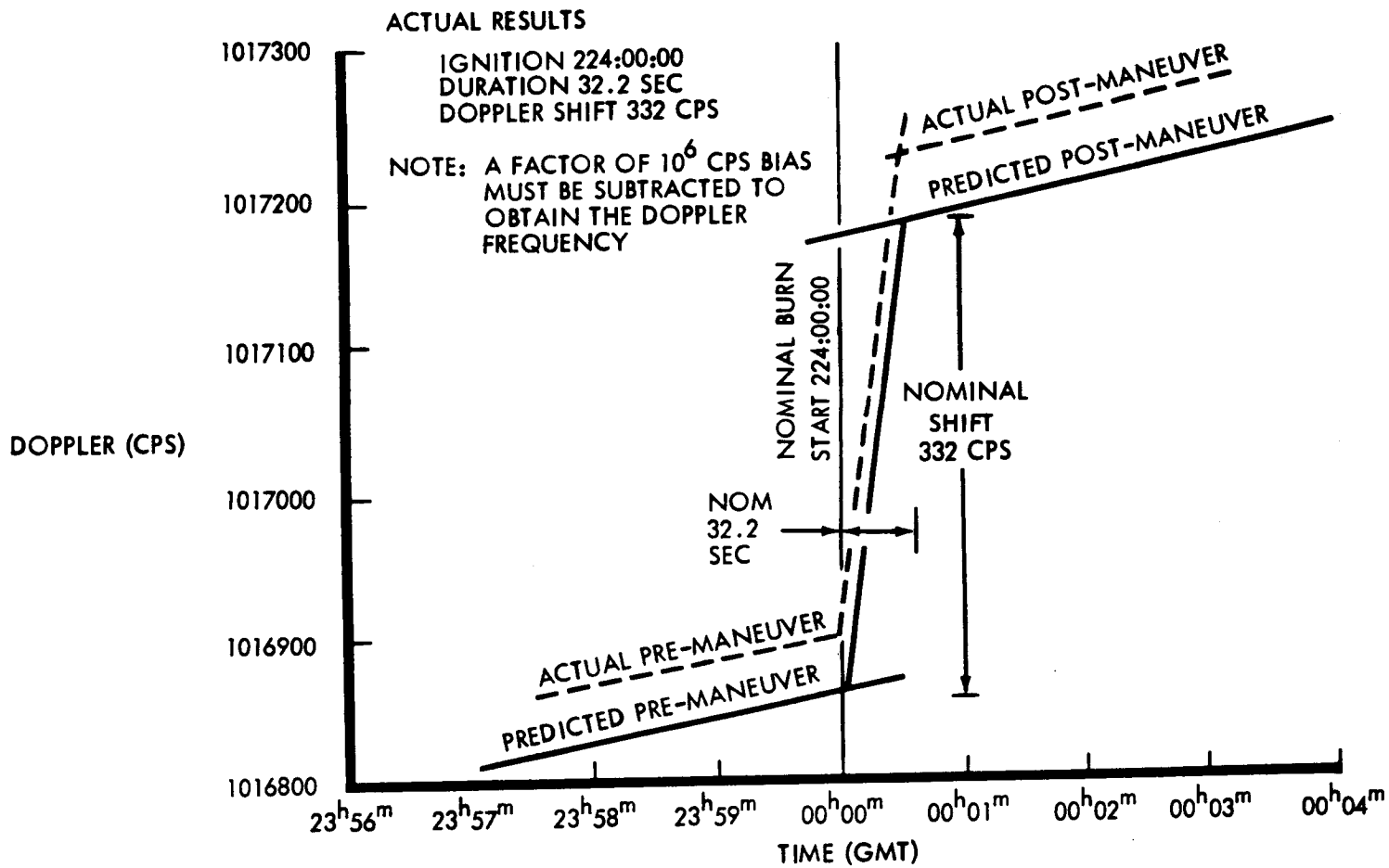

FIGURE 3.4-11: MIDCOURSE MANEUVER STATION 41, TWO-WAY DOPPLER, DAYS 233 AND 244, 1966

Figure 3.4-12 shows the doppler plot for the deboost maneuver. The actual pre- and post-maneuver data matched the predicted curve quite well. However, minor deviations were evident at the beginning and end of the engine burn. The magnitude of the maneuver necessitated a rather coarse scale on the doppler plot. Consequently, the accuracy in determining the actual results was rather limited. However, the approximate results were:

1) Ignition time: 15:34:04. , Day 226

2) Burn duration: 580 seconds

3) Doppler shift: 3910 cps

This was very close to the expected results. The significant result appeared in the post-maneuver portion of the curve. The predicted and actual doppler matched well and gave an indication that the maneuver was nominal.

Midcourse Design and Execution

Injection into the cislunar trajectory occurred on August 10, 20:15:47.9. Within 2 hours, orbit determination results established the necessity for a midcourse maneuver. The projected conditions on the lunar encounter hyperbola, without a midcourse maneuver, were:

	Pre-Midcourse*	Nominal±
Semi-major axis (km)	-6338.	-6048.
Eccentricity	2.677	1.458
Inclination (deg)	7.32	10.99
Longitude of Ascending Node (deg)	309.85	303.71
Argument of perilune (deg)	78.94	110.33
Time of closest approach, August 14	15:55:58.3	14:5:54.0

These values were based upon OD state number 1300 using 11 hours of tracking data. From the existing trajectory an acceptable lunar orbit could not be achieved; thus, a midcourse correction was required to reshape the approach trajectory.

A criterion used in designing the midcourse maneuver was to minimize fuel, or ΔV, not only for the midcourse, but also for subsequent lunar injection and transfer maneuvers. The constraint of acceptable first and second ellipse was also imposed upon the design.

Optimization of lunar injection (plus transfer) ΔV is done internally by the FPAC computer programs for fixed midcourse execution and flight times. Hence, it is possible to minimize the total ΔV (sum of all maneuvers) by varying flight and midcourse times.

* Selenographic coordinates at August 14, 15:50:0.0 GMT.

± Nominal values from Boeing Document D2-100388-2 in selenographic coordinates at August 14, 13:56:56.3.

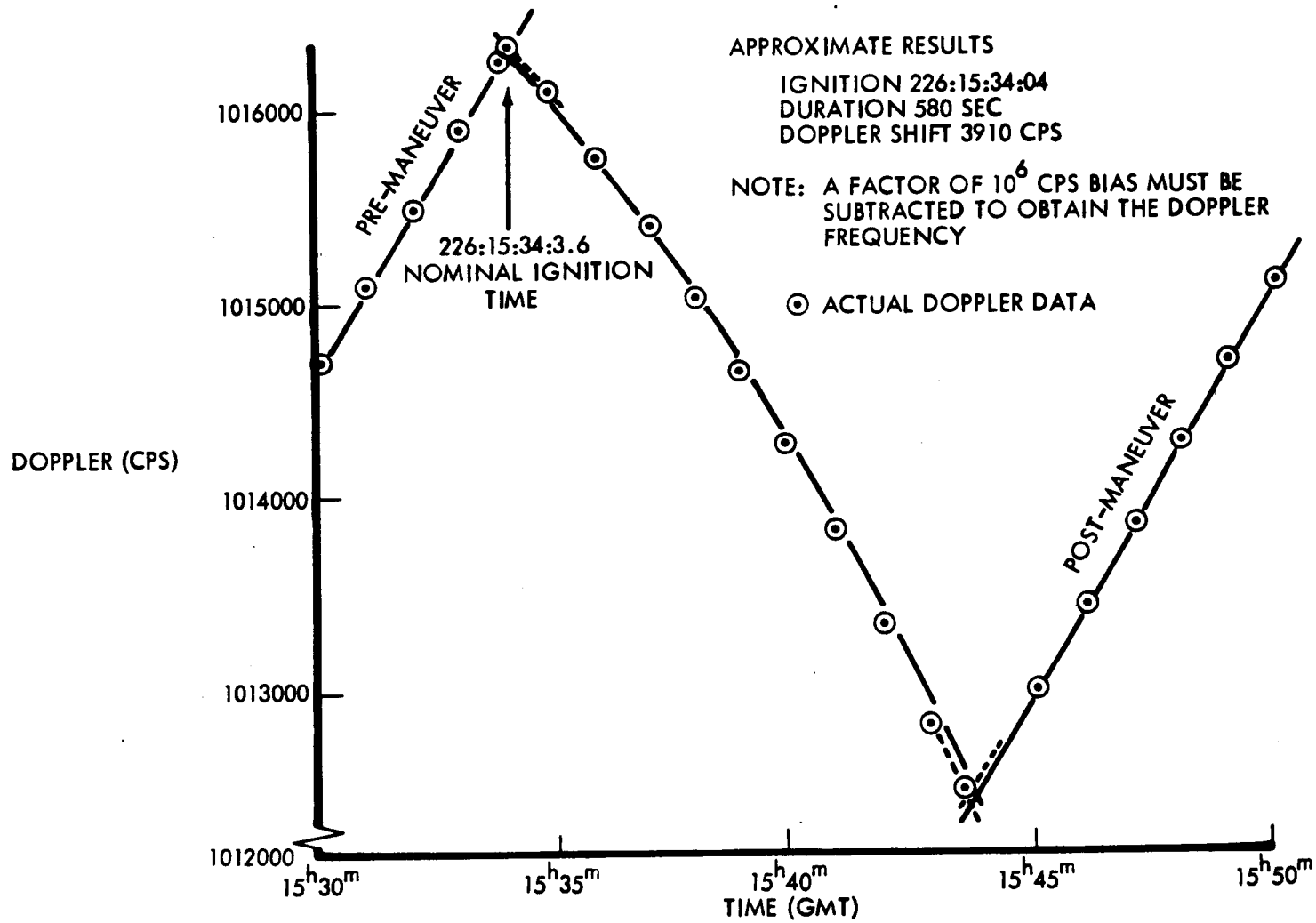

FIGURE 3.4-12: DEBOOST MANEUVER STATION 12, TWO-WAY DOPPLER, DAY 226, 1966

A study of midcourse execution time, Appendix B, with a constant flight time of 90 hours, showed that the midcourse maneuver could be delayed to at least 40 hours after translunar injection without exceeding 77 m/sec, the ΔV budgeted for first midcourse.

A study of arrival or flight time, Appendix B, with a constant midcourse execution time of 40 hours, showed that a flight time of 92 hours optimized the total impulsive ΔV. Two-station viewing was still available during lunar injection with the 92-hour flight time.

A problem arose with the Canopus tracker which overrode propellant usage as prime consideration for midcourse execution time. Loss of Canopus as a roll attitude reference required using either the Moon as a reference in place of Canopus, or maximum signal strength at the DSIF station, using the high-gain antenna, as a replacement for Canopus. It was decided to use the Moon as the prime roll reference, with the DSIF station as a back-up reference. FPAC software was adaptable to this nonstandard situation. Because the Moon was moving out of the Canopus tracker field of view, as shown in Figure 3.4-13, the midcourse maneuver was scheduled as early as possible. The selected time was August 12, 00:00:0.0. The flight time of 92 hours was used in the midcourse design to optimize the ΔV.

Conditions at lunar encounter after the designed midcourse were predicted to be (selenographic of date):

Semi-major axis	=	-6374. km
Eccentricity	=	1.429
Inclination	=	11.06 degrees
Longitude of Ascending Node	=	300.53 degrees
Argument of Perilune	=	113.72 degrees
Time of closest approach	=	August 14, 15:50:0.5

The predicted lunar injection resulted in a nominal first ellipse.

The variation in aimpoint is tabulated below and illustrated in Figure 3.4-14.

	Pre-Midcourse	Post-Midcourse (Design)	Std. Dev. Control Uncertainty	Std. Dev. Navigation Uncertainty	Nominal*
B·T (km)	15645	6402	33	7	6315
B·R (km)	- 1686	-1171	48	72	-1128
R_p (km)	10626	2736	10	-	2769
ΔV_{Inj} (km/sec)	0.8795	0.8770	0.0075	-	0.9003

* Again from Boeing Document D2-100388-2

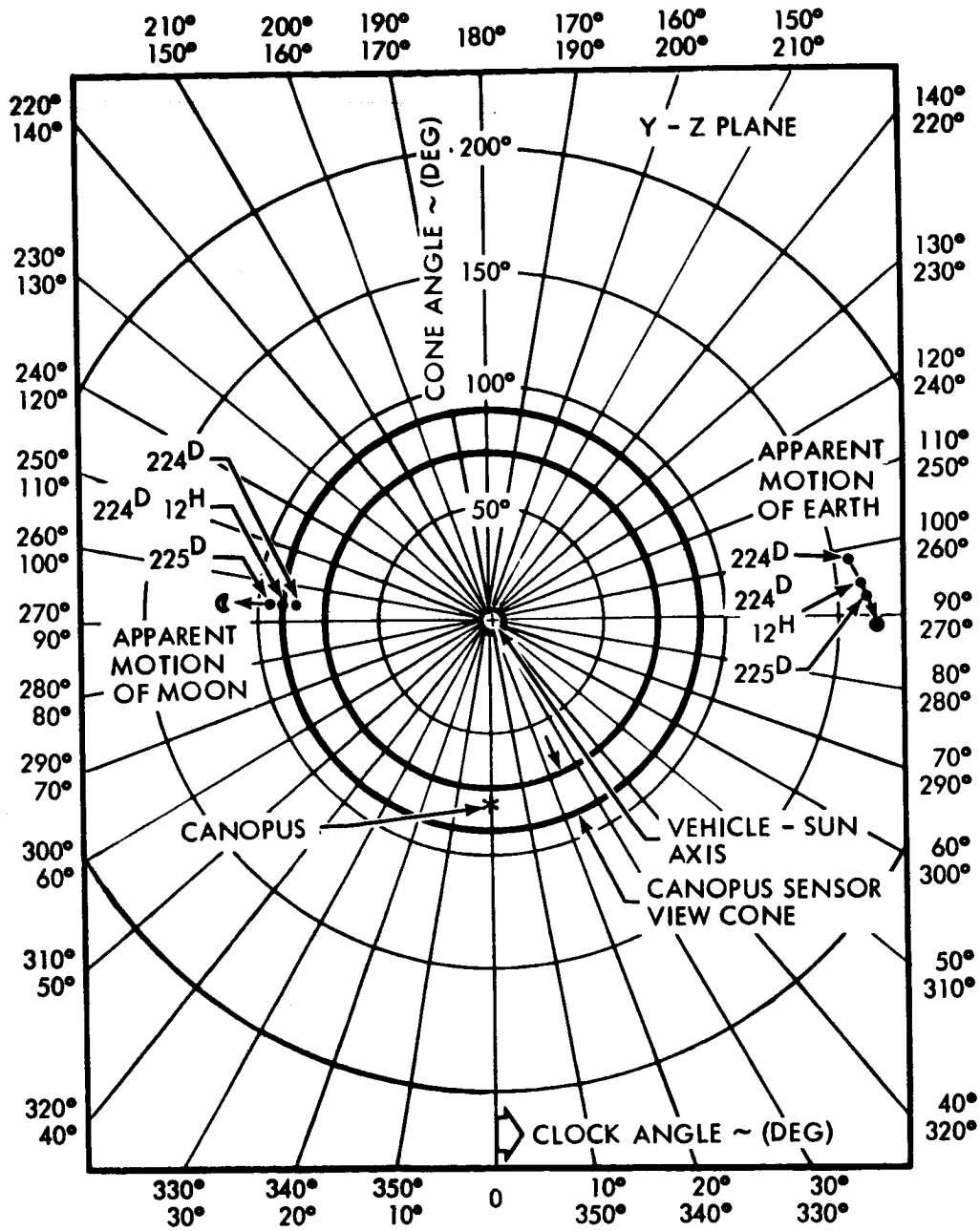

FIGURE 3.4-13: CELESTIAL REFERENCES — PRE-MIDCOURSE

The midcourse maneuver recommended by FPAC was

Sun roll	=	73.35 degrees	Moon as roll reference
Pitch	=	-25.24 degrees	
$\Delta V_{M/C}$	=	37.83 m/sec	
Execution time	=	August 12, 00:00:0.0	

The attitude maneuver was chosen from the 12 possible two-axis maneuvers on the basis of: (1) not passing near or through any antenna null regions, (2) minimizing total maneuver rotation, and (3) maintaining Sun lock as long as possible.

Two sources of error were recognized before midcourse execution, although error magnitudes were not known until after midcourse design. The first error was due to inaccuracy of the state (OD-1300) used for midcourse design. Subsequent states indicated a difference from OD-1300 of 7 km in $B \cdot T$ and -39 km in $B \cdot R$. The second error occurred because the center of the Moon at ignition time was input to the FPAC programs as a roll reference for computation of the attitude maneuvers, but the actual roll reference was established 8 hours before ignition time. Since the clock angle of the Moon changed about 0.25 degree during that time, a roll error of 0.25 degree existed when the attitude maneuver started.

Ignition occurred at exactly 00:00:0.0 on August 12. The burn continued for 32.2 seconds and the resulting doppler shift was 332 cps; all values as predicted. The predicted and actual doppler curves, Figure 3.4-11, did not coincide because of a change in station frequency from the predicted frequency. Allowing for this constant bias, the results indicated a nominal burn.

Lunar Orbit Injection Design and Execution

The design philosophy of the lunar orbit injection maneuver was to guide the spacecraft from its approach hyperbola into a desired ellipse with minimum propellant (ΔV) expenditure.

Approximately 33 hours of post-midcourse tracking data indicated a 2σ dispersion due to control errors between the actual and desired aim points (see Figure 3.4-14.) The desired, actual, and nominal* aim points were:

	Desired	Actual	Nominal*
$\bar{B} \cdot \bar{T}$ (km)	6402	6459	6315
$\bar{B} \cdot \bar{R}$ (km)	-1171	-1119	-1128

The penalty required to correct for these control errors at injection is a $\Delta V = 4.5$ m/sec.

* Nominal values from D2-100388-2, Lunar Orbiter Trajectory Data for P-5 Mission - Part II Tabulated Trajectory Data, in selenographic coordinates at August 14, 13:56:56.3

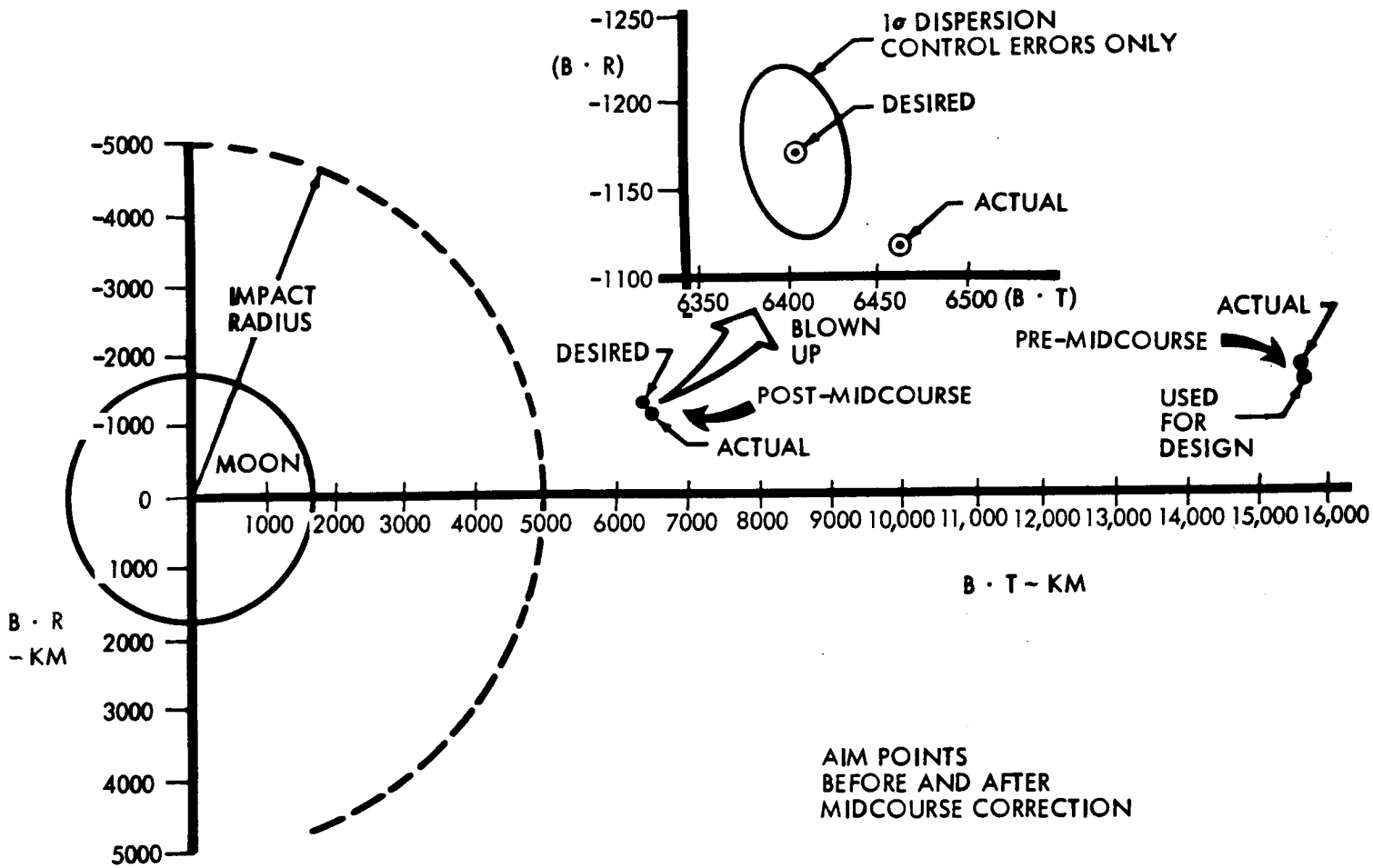

FIGURE 3.4-14: AIM POINTS BEFORE AND AFTER MIDCOURSE CORRECTION

Because of possible Canopus acquisition problems, two injection maneuvers were designed—one using the Canopus roll reference, the other based on DSIF maximum signal strength for spacecraft roll reference. Because the actual maneuver took place in the Moon's shadow, it was possible to use the Canopus reference.

Because arrival conditions were near design nominals, the injection design was based on a minimum ΔV search, and nominal values of first-ellipse parameters. An impulsive minimum ΔV solution was found that satisfied all constraints and resulted in a perilune radius very close to nominal.

Based on the impulsive ΔV solution, a finite burn solution was computed. The converged finite burn solution is compared in Table 3.4-12 with various preliminary design solutions. As can be seen, the finite burn solution predicted a first ellipse almost identical to the design nominal.

Table 3.4-12: Postinjection Conditions (Selenographic)

PARAMETER	MISSION DESIGN [1]	PREFLIGHT NOMINAL-SIMULATION [1]	PRE-MIDCOURSE DESIGN	FINITE BURN SOLUTION
Epoch	[2] 226:13:56:56.30	[2] 226:13:52:02.08	226:15:41:51.99	226:15:42:53.03
a (km)	2763.09	2761.12	2763.09	2762.71
e	0.298579	0.299522	0.298579	0.298714
i (deg)	12.04	12.04	12.04	12.04
Ω (deg)	326.08	326.87	325.33	325.71
ω (deg)	182.42	181.18	180.86	180.83
Apolune Alt (km)	1850.0	1850.0	1850.0	1849.9
Perilune Alt (km)	200.0	196.0	200.0	199.3

[1] Based on nominal 102-degree launch azimuth

[2] Based on impulsive injection

The FPAC maneuver recommended to guide the spacecraft into the designed first ellipse is compared with the nominal* below.

	FPAC	Nominal*
H Roll	19.17 degrees	17.00 degrees
Pitch	-108.72 degrees	-105.00 degrees
Ignition Time	8/14/66, 15:34:03.64 GMT	8/14/66, 13:57:00 GMT
ΔV	790.03 m/sec	797.10 m/sec

*Again from D2-100388-2

The spacecraft entered the Moon's shadow at 8/14/66, 15:23:00 GMT, 5 minutes before the attitude maneuvers started and 11 minutes before engine ignition. Since Sun lock could not be maintained, a slight error in the attitude commands occurred as indicated below:

Sun Reference	H Roll = 19.17 degrees	Pitch = -108.72 degrees
IRU Reference	Roll = 19.15 degrees	Pitch = -108.66 degrees
Error	+0.02 degree	- 0.06 degree

Ignition occurred while in the Moon's shadow, with engine shutdown occurring 578.7 seconds later, 18 minutes before emerging from the shadow. It reached first perilune 48 minutes later. The injection geometry is shown in Figure 3.4-15.

Postinjection tracking data indicated the injection maneuver was very near nominal and well within tolerance, as shown below.

PARAMETER	ACTUAL[1]	DESIGN	DEVIATION FROM DESIGN
Perilune Altitude (km)	189.3	199.3	-10
Apolune Altitude (km)	1865.9	1849.9	+16
Inclination (deg)	12.16	12.04	+ 0.12
Argument of Perilune (deg)	180.3	180.83	- 0.33

[1] Based on OD Solution 4138, integrated backwards to injection time.

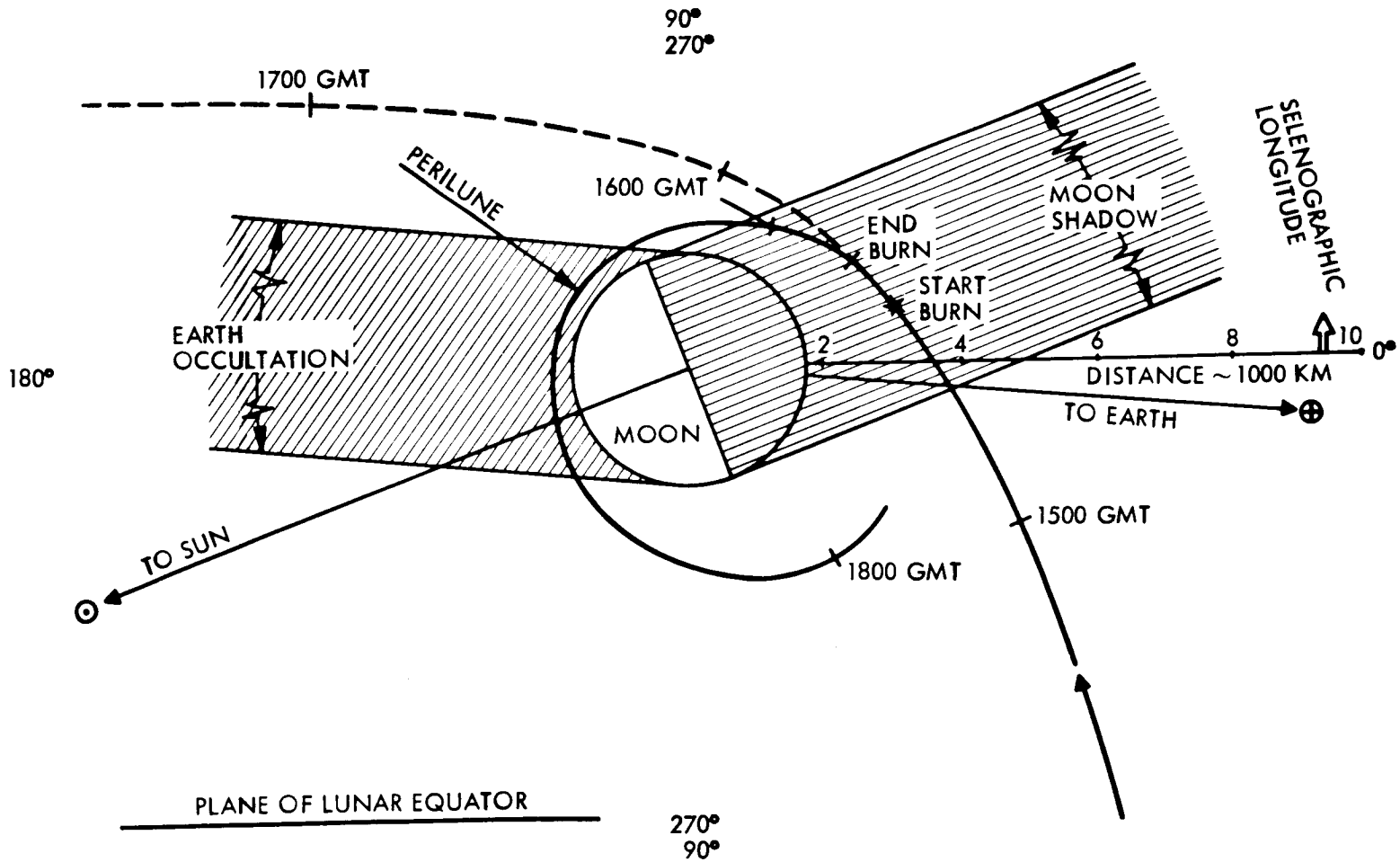

FIGURE 3.4-15: LUNAR INJECTION GEOMETRY — DAY 226

First Ellipse Phase

This phase began when the burn was completed for injection into lunar orbit and extended through the first transfer maneuver for orbit modification about 7 days later. During this interval, the principal FPAC tasks were to:

1) Solve for lunar gravity field harmonic coefficients;
2) Establish tracking data experience in an orbital flight phase;
3) Design the maneuvers for photographic coverage of Site I-O;
4) Design a transfer maneuver for a second ellipse that yields proper photo coverage of all Mission I sites.

During this phase FPAC responded to the following non-normal mission situations:

1) Designs for greatly expanded photo coverage for film-set frames; this included several farside photos.
2) A transfer redesign to overcome a last-minute timing error discovered in the transfer design program (GCTL);
3) A change in the editor program (ODGX);
4) A correction to the predicts program (PRDL) to improve accuracy of Earthrise/set calculations.

Orbit Determination in First Ellipse

Orbit determination in the first ellipse consisted of the following jobs:

1) Tracking Data Editing—Data editing was essentially the same for this phase as for the cislunar phase.
2) Orbit Determination—The prime objective of orbit determination during initial ellipse phase was to estimate coefficients of gravitational spherical harmonics. Coefficients of all terms up to the fourth order were estimated. The objective was to establish a preliminary Moon model adequate to predict orbit lifetime and motion of the spacecraft through subsequent photo activity.

   The second objective was to obtain accurate "state vectors" (position and velocity) for the spacecraft. These state vectors were used for short-range (less than 2 days) spacecraft predictions, determination of time for site IO photo, and for the first orbit transfer maneuver.

   These objectives were adequately achieved for mission control purposes. Computer programs ODPL and LHDL were used in parallel to determine the gravitational field with 6 days of continuous effort. How well this field approximates the actual is not yet known.

Tracking data editing—Angle and doppler data were the prime data types received during this mission phase. However, due to the small arc involved between observations, all angle data were ignored in ODGX. Range data were taken for the purpose of determining station time asynchronization (time bias). Range data were placed on the ODP file to compare the fit with the converged ODPL solution using doppler data only. Range data were weighted out in ODPL, i.e., range units were not used to obtain the fit.

Revised values for doppler bias between stations as well as new timing bias estimates were received from the DSN orbit determination group. These values were incorporated in the ODGX input deck.

A coding error in ODGX was found during this mission phase. Whenever a simultaneous time shift and a data adjustment were made on data for a station, the program would go into a buffer writing loop. This caused program run time to be exceedingly long. Bulk printer operation was also hampered because more than the number of available buffers were used, which caused recycling of the buffers. The problem was eliminated with a machine language instruction (octal patch) in the source deck which then required compilation of the ODGX source deck with PSIX after each computer string switch.

TDPX/ODGX input data deck listings may be found in Appendix B. This includes transmitter-on times, station frequencies, and DSIF tracking data editing control option. The B1 (master file) tape numbers, data file summaries, and spacecraft maneuver information can be found in Appendix B. Photo readout has deleterious effects on tracking data because it overpowers the carrier signal. Hence, these times are also listed in Appendix B.

Lunar potential model determination—The problem was to estimate the lunar gravitational field and state vector in the first ellipse with sufficient accuracy to predict orbit lifetime and design a transfer maneuver that resulted in proper photo coverage of all Mission I sites.

The lunar gravitational potential (μ) can be approximated with the associated Legendre polynominal P_{nm} ($\sin\phi$) through the fourth order.

$$\mu = \frac{\mu_{\mathbb{C}}}{r}\left[1 + \sum_{n,m=2,0}^{4,\eta} \left(\frac{a_m}{r}\right)^h P_{nm}(\sin\phi) \times \left|C_{nm}\cos m\lambda + S_{nm}\sin m\lambda\right|\right]$$

ϕ = latitude

λ = longitude

r = radius vector to point of interest

a_m = equatorial radius of Moon

The unknowns in the expansion for μ are the coefficients C_{nm} and S_{nm}. These are known as harmonics. When m = 0, they are called zonal harmonics; m = n sectoral harmonics;

$m \neq n$, $m \neq 0$ tesseral harmonics. The harmonics define humps, bumps, and depressions on the Moon (mass distribution) and thus mathematically define the lunar potential field. For a physical description of the harmonics see John D. Nicolaide's and Mark M. Macomber's paper, "Navigation and Geodetic Satellites".

Much was unknown about the lunar gravitational field before the flight. The gravitational constant of the Moon (KM) was known within $\pm .2$ km^3/sec^2 and the lunar harmonics J20 and C22 were known within about $\pm$ 10%. It was also felt that the magnitudes of C21 and S21 would be small. This conclusion follows from a dynamical symmetry argument concerning the observed librations of the Moon.

A maximum of 6 days were available to process 7 days worth of tracking data from the three DSIF stations, Goldstone, Madrid, and Woomera. Orbital geometry was as shown in Figure 3.4-16. The orbital elements at deboost were:

semi-major axis	2765.4 km
apolune radius	3603.7 km
perilune radius	1927.04 km
eccentricity	0.3031558
inclination	12.156 deg
argument of perilune	180.280 deg
longitude of node	325.933 deg

The orbit determination computer program ODPL was the primary tool available. This program minimizes the tracking data residuals in a least-squares sense and has the capability of solving for the state vector and 11 constants at one time. The constants which can be solved for include the 21 harmonics through fourth order.

A second orbit determination program LHDL was available in an off-line backup capacity. This special program based on ODPL was capable of solving for the state vector and 21 harmonics instead of only 11. LHDL was not operated by the regular OD FPAC people, but rather by a special team of TBC and LRC personnel.

Two complementary methods for defining the lunar model were employed: the direct method, and the element plotting method.

The direct method consisted of solving for the state vector and all lunar harmonics through fourth order except J20, C22, S21, and C21. Two "solve for" lists were used (Table 3.4-13) because ODPL is restricted to solving for only 11 constants at a time and there are 17 to be estimated. The lists were chosen so that the correlations between harmonics in each "solve for" list were minimum.

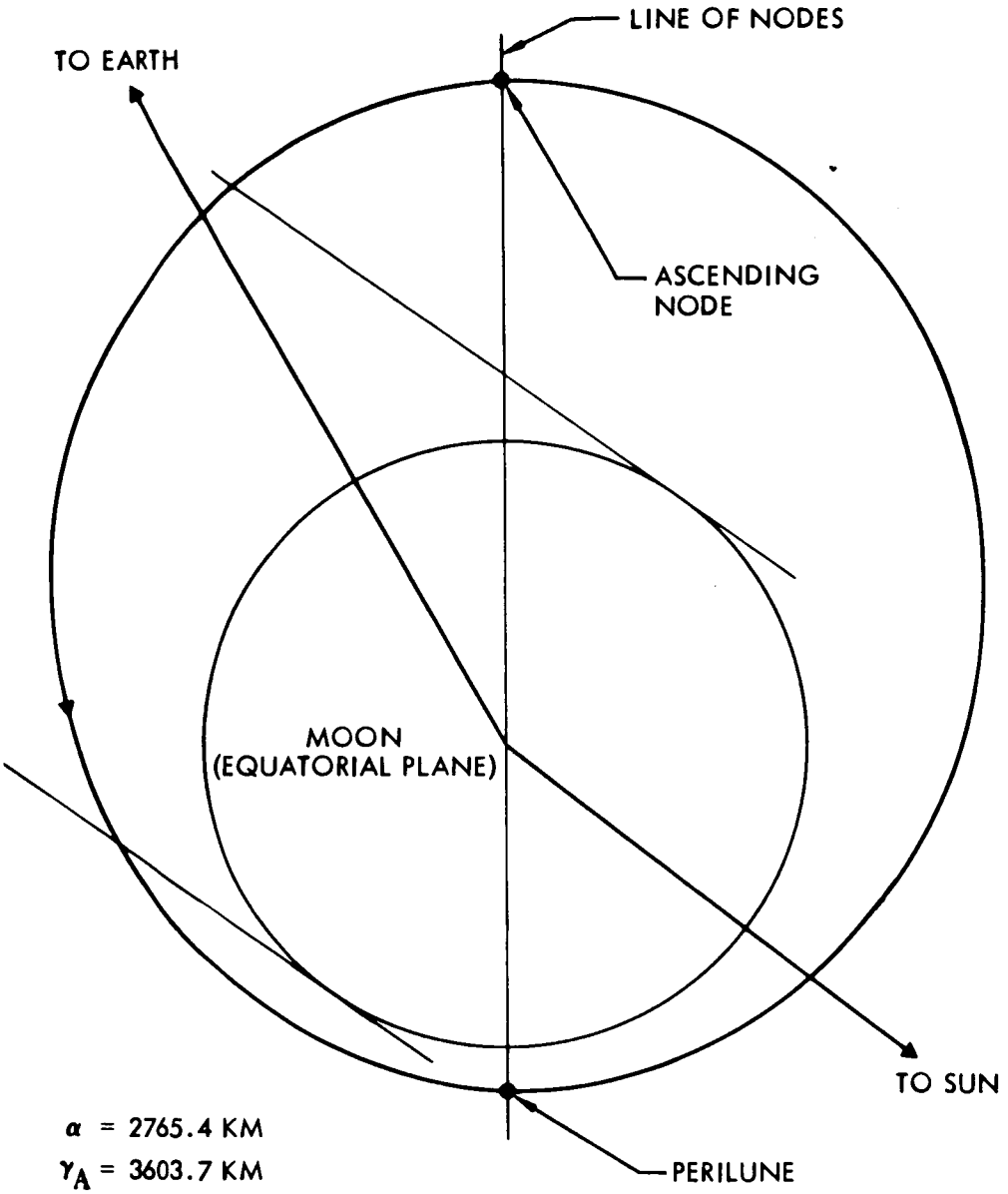

α = 2765.4 KM
r_A = 3603.7 KM
r_P = 1927.04 KM
e = 0.3031558
i = 12.156 DEG
ω = 180.3 DEG
Ω = 325.9 DEG

FIGURE 3.4-16: ORBIT GEOMETRY

Table 3.4-13: Solve-For Lists

Set A	Set B
x	x
y	y
z	z
$\dot{x}$	$\dot{x}$
$\dot{y}$	$\dot{y}$
$\dot{z}$	$\dot{z}$
J30	J40
C41	C31
C32	C42
C33	C33
C43	C43
C44	S31
S41	S22
S32	S42
S33	S33
S43	S43
S44	

Values for parameters not solved for were:

J20	2.048×10^{-4}
C22	0.230×10^{-4}
C21	0
S21	0
KM	4902.58 km^3/sec^2

Any errors in these assigned values would be absorbed in the constants solved for, but this effect was not considered significant for mission control purposes.

The two "solve for" lists were used in alternate ODPL runs. That is, set A was solved for first; on the next run set B was solved for. Both runs process the same tracking data. Each run used the results of the preceding run, implying a quasirelaxation technique. Several iterations were made over the same data arc until a converged solution was reached; that is, when the tracking data residuals were small, sum of the squares (SOS) was minimum, first and second moments of the residuals were small. The data arc was then increased by approximately one orbit revolution and the above procedure repeated.

The procedure described above was followed through the first 4 days. Converged solutions for each of the data arcs beginning with the 1300-minute arc are shown in Tables 3.4-14 and 3.4-15.

As the data arcs increased in length up to 2430 minutes, a converged solution became harder to obtain. An indication of this was the trend of the SOS for the converged solutions. The SOS approximately doubled with each increase of the data arc. In an attempt to obtain a better solution, the state vector was deleted from the solve-for lists starting with the 1735-minute data arc. This did not improve the solution but did cut down the number of iterations required to converge.

Concurrently with the ODPL work on the 2430-minute arc, the LHDL team had acquired a solution for a 2400-minute data arc that looked better than the ODPL solution. That is, the LHDL solution fit the tracking data better as indicated by the SOS (1400 vs. 260 - Table 3.4-16). In addition, the element plotting method indicated a negative sign for J30 (see below). LHDL agreed with this, but the ODPL solution indicated a positive sign. At this point, the best LHDL solution was adopted by the ODPL team as a starting point. By the time this decision was made, LHDL had a solution for a 2600-minute data arc (Table 3.4-17). This solution was then input to the ODPL and the following events took place:

1) Only the state vector was solved for over a 2600-minute data arc for two iterations (Table 3.4-18). Note how the small changes in the "state" produced a large change in the SOS.

2) Solve-for lists A and B were solved for over the 2600-minute data arc (Table 3.4-19).

3) Solve-for lists A and B were solved for over a 2800-minute data arc (Table 3.4-20). Comparatively large changes in the state vector resulted but a good fit was noted in the first iteration on set A. List A was solved for again and the results were interpreted as indicative of a divergent situation. This diverging situation was similar to that experienced when shorter data arcs were processed.

   It was then decided to solve for only the state vector starting with the most recent set of harmonics and state vector that produced a good fit. Table 3.4-21 shows the harmonics and state chosen. They are the conditions that resulted in the best fit as shown in Table 3.4-20, Iteration 1.

Table 3.4-14: ODPL Solutions From 1300 Through 1735 Minute Data Arcs

DATA ARC	1300 MIN.	1520 MIN.	1735 MIN.
*X (km)	2251.64	2251.67	2251.67
Y (km)	179.594	179.666	179.666
Z (km)	646.747	646.629	646.629
DX (km/sec)	- 0.647074	- 0.647086	- 0.647086
DY (km/sec)	1.35622	1.35622	1.35622
DZ (km/sec)	0.377311	0.377300	0.377300
$J20 \times 10^{-4}$	2.048×10^{-4}		
$J30 \times 10^{-4}$	0.0575×10^{-4}	0.0282×10^{-4}	0.0357×10^{-4}
$J40 \times 10^{-4}$	0.7274	0.6280	0.5832
$C21 \times 10^{-4}$	0	0	0
$C31 \times 10^{-4}$	0.9852	0.9483	0.9340
$C41 \times 10^{-4}$	- 0.3256	- 0.3139	- 0.3029
$C22 \times 10^{-4}$	0.23	0.23	0.23
$C32 \times 10^{-4}$	0.0541	0.0371	0.0220
$C42 \times 10^{-4}$	- 0.1412	- 0.1468	- 0.1566
$C33 \times 10^{-4}$	0.0516	0.0528	0.0552
$C43 \times 10^{-4}$	0.0263	0.0241	0.0206
$C44 \times 10^{-4}$	- 0.0051	- 0.0044	- 0.0040
$S21 \times 10^{-4}$	0	0	0
$S31 \times 10^{-4}$	0.2339	0.2513	0.2511
$S41 \times 10^{-4}$	- 0.1637	- 0.1638	- 0.1510
$S22 \times 10^{-4}$	0.0026	- 0.0018	- 0.0054
$S32 \times 10^{-4}$	0.5603	0.5657	0.5648
$S42 \times 10^{-4}$	- 0.1978	- 0.1972	- 0.2002
$S33 \times 10^{-4}$	- 0.0344	- 0.346	- 0.0331
$S43 \times 10^{-4}$	- 0.0542	- 0.0501	- 0.0500
$S44 \times 10^{-4}$	- 0.0003	- 0.0002	- 0.00003
SOS	66	116	348

*The state vector is in a selenocentric of date coordinate system at post-deboost (August 14, 1966, 16:03:52.013)

Table 3.4-15: ODPL Solutions From 1995 Through 2430 Minute Data Arcs

DATA ARC	1995 MIN.	2210 MIN.	2430 MIN.
*X (km)	2251.67	2251.67	2251.67
Y (km)	179.666	179.666	179.666
Z (km)	646.629	646.629	646.629
DX (km/sec)	0.647086	0.647086	0.647086
DY (km/sec)	1.35622	1.35622	1.35622
DZ (km/sec)	0.377300	0.377300	0.377300
$J20 \times 10^{-4}$	2.048	2.048	2.048
$J30 \times 10^{-4}$	0.06604	0.1249	0.2026
$J40 \times 10^{-4}$	0.4333	0.4595	0.3100
$C21 \times 10^{-4}$	0	0	0
$C31 \times 10^{-4}$	0.8777	0.8948	0.8317
$C41 \times 10^{-4}$	- 0.2779	- 0.2843	- 0.2984
$C22 \times 10^{-4}$	0.2300	0.2300	0.2300
$C32 \times 10^{-4}$	- 0.0340	- 0.0346	- 0.0323
$C42 \times 10^{-4}$	- 0.1743	- 0.1803	- 0.1862
$C33 \times 10^{-4}$	0.0630	0.0620	0.0607
$C43 \times 10^{-4}$	0.0026	0.0029	0.0044
$C44 \times 10^{-4}$	- 0.0027	- 0.0022	- 0.0019
$S21 \times 10^{-4}$	0	0	0
$S31 \times 10^{-4}$	0.2742	0.2443	0.3114
$S41 \times 10^{-4}$	- 0.1270	- 0.1101	- 0.0893
$S22 \times 10^{-4}$	- 0.0057	- 0.0167	- 0.0050
$S32 \times 10^{-4}$	0.5459	0.5418	0.5445
$S42 \times 10^{-4}$	- 0.1965	- 0.2049	- 0.1848
$S33 \times 10^{-4}$	- 0.0286	- 0.0289	- 0.0300
$S43 \times 10^{-4}$	- 0.0442	- 0.0423	- 0.0426
$S44 \times 10^{-4}$	0.0016	0.0013	0.0012
SOS	797	1388	2184

*The state vector is in a selenocentric of date coordinate system at post-deboost (August 14, 1966, 16:03:52.013).

Table 3.4-16: Lunar Models Determined by ODPL and LHDL From 2400 Minute Data Arc

	ODPL SOLUTION	LHDL SOLUTION
X (km)	2251.6738	2251.8013
Y (km)	179.66630	180.23209
Z (km)	646.62957	645.68219
DX (km/sec)	- 0.64708620	- 0.64710364
DY (km/sec)	1.3562200	1.3563038
DZ (km/sec)	0.37729964	0.37712672
$J20 \times 10^{-4}$	2.048	2.048
$J30 \times 10^{-4}$	0.203	- 1.2780
$J40 \times 10^{-4}$	0.310	- 1.1461
$C21 \times 10^{-4}$	0	0
$C31 \times 10^{-4}$	0.832	- 0.2076
$C41 \times 10^{-4}$	- 0.298	0.0242
$C22 \times 10^{-4}$	0.2300	0.2300
$C32 \times 10^{-4}$	- 0.0323	- 0.1763
$C42 \times 10^{-4}$	- 0.186	0.0351
$C33 \times 10^{-4}$	0.0607	0.0329
$C43 \times 10^{-4}$	0.00443	0.0112
$C44 \times 10^{-4}$	- 0.00191	- 0.0004
$S21 \times 10^{-4}$	0	0
$S31 \times 10^{-4}$	0.311	0.4279
$S41 \times 10^{-4}$	- 0.0893	- 0.0657
$S22 \times 10^{-4}$	- 0.00504	- 0.0209
$S32 \times 10^{-4}$	0.545	0.0893
$S42 \times 10^{-4}$	- 0.185	0.0021
$S33 \times 10^{-4}$	- 0.0230	0.0151
$S43 \times 10^{-4}$	- 0.0426	0.0041
$S44 \times 10^{-4}$	0.00120	- 0.0029
SOS	1388	260

NOTE: State Vector is in a selenocentric of date coordinate system at post-deboost (August 14, 1966, 16:03:52.013).

Table 3.4-17: Lunar Model Determined by LHDL Over 2600 Minute Data Arc

X (km)	2251.8013
Y (km)	180.23209
Z (km)	645.68219
DX (km/sec)	- 0.64710364
DY (km/sec)	1.3563038
DZ (km/sec)	0.37712672
J20 x 10^{-4}	2.048
J30 x 10^{-4}	- 1.225
J40 x 10^{-4}	- 1.118
C21 x 10^{-4}	0
C31 x 10^{-4}	- 0.183
C41 x 10^{-4}	0.0157
C22 x 10^{-4}	0.230
C32 x 10^{-4}	- 0.177
C42 x 10^{-4}	0.0370
C33 x 10^{-4}	0.0330
C43 x 10^{-4}	0.0118
C44 x 10^{-4}	- 0.000437
S21 x 10^{-4}	0
S31 x 10^{-4}	0.427
S41 x 10^{-4}	- 0.0664
S22 x 10^{-4}	- 0.0259
S32 x 10^{-4}	0.0916
S42 x 10^{-4}	- 0.00530
S33 x 10^{-4}	0.0158
S43 x 10^{-4}	0.00380
S44 x 10^{-4}	- 0.00294
S0S	292

NOTE: State vector is in a selenocentric of date coordinate system at post-deboost (August 14, 1966, 16:03:52.013).

Table 3.4-18: ODPL Solution Over 2600 Minute Data Arc
(Solving for Only State Vector)

	INPUT STATE VECTOR (OBTAINED FROM LHDL SOLUTION)	SOLUTION FROM 1ST ITERATION	SOLUTION FROM 2ND ITERATION
X (km)	2251.8013	2251.8033	2251.8017
Y (km)	180.23209	180.25524	180.24326
Z (km)	645.68219	645.65855	645.67298
DX (km/sec)	- 0.64710364	- 0.64711145	- 0.64710805
DY (km/sec)	1.3563038	1.3563037	1.3563034
DZ (km/sec)	0.37712672	0.37712067	0.37712417
SOS	2610	290	680

NOTE: 1. Harmonics from LHDL 2600-minute data arc used.
2. Only state vector solved for.
3. The state vector is in a selenocentric of data coordinate system at post-deboost (August 14, 1966, 16:03:52.013).

4) Only the state vector was solved for over the 2800-minute data arc using the initial state and harmonics of Table 3.4-21. The input conditions provided an adequate fit and the data arc was increased to 3000 minutes. The fit of the first iteration again was good. The data arc was increased to 3200 minutes and three iterations were made with favorable results. Again the data arc was expanded, this time to 3500 minutes. After two iterations over this data arc, the fit appeared to be diverging. Results of this last sequence of runs are shown in Table 3.4-22.

5) At this time, the 11 harmonics with the largest absolute magnitude were chosen to be solved for along with the state vector over a 4000-minute data arc. The rest of the harmonics, small in magnitude, were frozen to the values shown in Table 3.4-21. Values for the harmonics shown in this table and the last state vector found from processing the 3200-minute data arc were used as the intial guesses, Iteration O, Table 3.4-23. To prevent the state from oscillating, a tight a priori covariance matrix was assigned. It consisted of diagonal elements having 1σ values as follows:

Position - 1.0×10^{-3} km

Velocity - 1.0×10^{-3} km/sec

Furthermore, to limit the rapid change of the harmonic coefficients, a diagonal a priori having 1σ values of $1. \times 10^{-5}$ was used. This allowed the coefficients to stabilize gradually and prevented a divergent situation.

Table 3.4-19: ODPL Solution Over 2600 Minute Data Arc
(Solving For State Vector and Harmonics)

NOMENCLATURE	ITERATION		
	0	1	2
X (km)	2251.8017	2251.8114	2251.8042
Y (km)	180.24326	180.25682	180.22014
Z (km)	645.67298	645.64541	645.69207
DX (km/sec)	- 0.64710805	- 0.64710825	- 0.64709884
DY (km/sec)	1.3563034	1.3563009	1.3563015
DZ (km/sec)	0.37712417	0.37712608	0.37713124
J20 x 10^{-4}	2.048	2.048	2.048
J30 x 10^{-4}	- 1.2250	- 1.2250	- 1.3127
J40 x 10^{-4}	- 1.1183	- 1.1208	- 1.1208
C21 x 10^{-4}	0	0	0
C31 x 10^{-4}	- 0.1830	- 0.1837	- 0.1837
C41 x 10^{-4}	0.0157	0.0157	0.0330
C22 x 10^{-4}	0.2300	0.2300	0.2300
C32 x 10^{-4}	- 0.1770	- 0.1770	- 0.1743
C42 x 10^{-4}	0.0370	0.0386	0.0386
C33 x 10^{-4}	0.0330	0.0335	0.0343
C43 x 10^{-4}	0.0118	0.0123	0.0155
C44 x 10^{-4}	- 0.0004	- 0.0004	- 0.0003
S21 x 10^{-4}	0	0	0
S31 x 10^{-4}	0.4274	0.4311	0.4311
S41 x 10^{-4}	- 0.0664	- 0.0664	- 0.0855
S22 x 10^{-4}	- 0.0259	- 0.0235	- 0.0235
S32 x 10^{-4}	0.0916	- 0.0916	0.1127
S42 x 10^{-4}	- 0.0053	- 0.0045	- 0.0045
S33 x 10^{-4}	0.0158	0.0146	0.0127
S43 x 10^{-4}	0.0038	0.0039	0.0057
S44 x 10^{-4}	- 0.0029	- 0.0029	- 0.0032
SOS	681	488	—
SOLVED FOR	LIST B	LIST A	LIST B

NOTE: State vector is in a selenocentric of date coordinate system at post-deboost (August 14, 1966, 16:03:52.013).

Table 3.4-20: ODPL Solution Over 2800-Minute Data Arc
(Solving For State Vector and Harmonics)

NOMENCLATURE	ITERATION			
	0	1	2	3
X (km)	2251.8042	2251.7938	2251.8124	2251.7935
Y (km)	180.22014	180.17988	180.28080	180.15091
Z (km)	645.69207	645.75208	645.63094	645.77868
DX (km/sec)	- 0.64709884	- 0.64708752	- 0.64711400	- 0.64707875
DY (km/sec)	1.3563015	1.3563041	1.3563006	1.3562996
DZ (km/sec)	0.37713124	0.37713504	0.37712044	0.37713837
$J20 \times 10^{-4}$	2.048	2.048	2.048	2.048
$J30 \times 10^{-4}$	- 1.3127	- 1.3127	- 1.1400	- 1.568
$J40 \times 10^{-4}$	- 1.1208	- 1.1277	- 1.1277	- 1.1277
$C21 \times 10^{-4}$	0	0	0	0
$C31 \times 10^{-4}$	- 0.1837	- 0.1942	- 0.1942	- 0.1942
$C41 \times 10^{-4}$	0.0330	0.0330	0.0050	0.0791
$C22 \times 10^{-4}$	0.2300	0.2300	0.2300	0.2300
$C32 \times 10^{-4}$	- 0.1743	- 0.1743	- 0.1924	- 0.1582
$C42 \times 10^{-4}$	0.0386	0.0417	0.0417	0.0417
$C33 \times 10^{-4}$	0.0343	0.0346	0.0346	0.0363
$C43 \times 10^{-4}$	0.0155	0.0146	0.0062	0.0296
$C44 \times 10^{-4}$	- 0.0003	- 0.0003	0.00004	0.0001
$S21 \times 10^{-4}$	0	0	0	0
$S31 \times 10^{-4}$	0.4311	0.4485	0.4485	0.4485
$S41 \times 10^{-4}$	- 0.0855	- 0.0855	- 0.0444	- 0.1370
$S22 \times 10^{-4}$	- 0.0235	- 0.0176	- 0.0176	- 0.0176
$S32 \times 10^{-4}$	0.1127	0.1127	0.0729	0.1855
$S42 \times 10^{-4}$	- 0.0045	0.0060	0.0060	0.0060
$S33 \times 10^{-4}$	0.0127	0.0073	0.0141	0.0046
$S43 \times 10^{-4}$	0.0057	0.0075	0.0072	0.0135
$S44 \times 10^{-4}$	- 0.0032	- 0.0032	- 0.0024	- 0.0043
SOS	2403	777	1314	-
SOLVED FOR	LIST B	LIST A	LIST A	-

NOTE: State vector is in a selenocentric of date coordinate system at post-deboost (August 14, 1966, 16:03:52.013).

Table 3.4-21: Converged 2800-Minute State and Harmonics

X (km)	2251.7938
Y (km)	180.17988
Z (km)	645.75208
DX (km/sec)	-0.64708752
DY (km/sec)	1.3563041
DZ (km/sec)	0.37713504
J20 x 10^{-4}	2.048
J30 x 10^{-4}	-1.3126709
J40 x 10^{-4}	-1.1277127
C21 x 10^{-4}	0
C31 x 10^{-4}	-0.19419583
C41 x 10^{-4}	0.0329946
C22 x 10^{-4}	0.23000
C32 x 10^{-4}	-0.17429462
C42 x 10^{-4}	0.041699422
C33 x 10^{-4}	0.0346414
C43 x 10^{-4}	0.0146381
C44 x 10^{-4}	-0.0003388
S21 x 10^{-4}	0
S31 x 10^{-4}	0.448494
S41 x 10^{-4}	-0.0855243
S22 x 10^{-4}	-0.0176414
S32 x 10^{-4}	0.11272561
S42 x 10^{-4}	0.006001
S33 x 10^{-4}	0.009253
S43 x 10^{-4}	-0.007489
S44 x 10^{-4}	-0.00321272

Note: State vector is in a selenocentric of date coordinate system at post-deboost (August 14, 1966, 16:03:52.013).

Every fifth data point was processed from the 4000-minute data arc. Only CC3 data was included; therefore, no frequency adjustments were necessary. However, to account for asynchronizations in the station clocks, data from Station 41 was shifted by +2.095 milliseconds, and data from Station 61 by -7.620 milliseconds; Station 12 was used as the reference standard. A data weight of 0.1 cps was used throughout.

Table 3.4-22: ODPL Solutions Over 2800 Through 3500-Minute Data Arcs
(Only State Vector Solved For)

NOMENCLATURE	DATA ARC (MIN)							
	2800	3000	3200			3500		
X	2251.7938	2251.7946	2251.7972	2251.7974	2251.7977	2251.7978	2251.7937	2251.7929
Y	180.17988	180.17074	180.17779	180.17048	180.17608	180.18227	180.17166	180.14826
Z	645.75207	645.75556	645.74470	645.75110	645.74493	645.73927	645.74821	645.78284
DX	-0.64708751	-0.64708370	-0.64708479	-0.64708228	-0.64708411	-0.64708631	-0.64708504	-0.64707704
DY	1.3563041	1.3563043	1.3563043	1.3563038	1.3563041	1.3563042	1.3563031	1.3563016
DZ	0.37713504	0.37713802	0.37713623	0.37713921	0.37713732	0.37713533	0.37714073	0.37714973
ITERATION	1	1	1	2	3	1	2	3
SOS	478	438	746	628	637	829	2608	-

NOTE: State vector is in a selenocentric of date coordinate system at post-deboost (August 14, 1966, 16:03:52.013).

A summary of the data used appears below:

Station Number	Data Type	Start Time	Stop Time	Number of Points	Standard Dev.
41	CC3	8/15 0023	8/15 0516	51	0.041
	CC3	8/15 2340	8/16 0638	66	0.044
	CC3	8/17 0116	8/17 0750	62	0.085
12	CC3	8/14 1604	8/14 2335	68	0.065
	CC3	8/15 1452	8/15 2326	81	0.043
	CC3	8/16 1736	8/17 0052	65	0.081
61	CC3	8/15 0537	8/15 1408	72	0.045
	CC3	8/16 0652	8/16 1533	74	0.039
	CC3	8/17 0807	8/17 1043	22	0.070

Changes in the harmonics and state vector from the initial guesses to the converged set were small (Table 3.4-23). Since the lunar model had not been solved for between the 2800- to 4000-minute data arc solutions and the state from 3200- to 4000-minute solutions, it was concluded that a reasonable state vector and lunar model had been determined. This model is known as the 4138 solution and is summarized in Table 3.4-24. Residual plots for the 4138 solution are presented in Appendix B.

Element plotting was a method used to define "effective" values for the main unknown zonal harmonics, J30 and J40. It was expected that two purposes would be served by this method:

1) If the direct method failed, the element plotting solution would provide a basis for predicting a possible impact with the lunar surface so that a safe transfer maneuver could be designed.

2) The element plotting solution would act as a check on the signs and magnitudes of J30 and J40 from the direct solutions.

The element plotting method consisted of the following steps:

1) A state vector was determined at several points along the trajectory.

2) A trajectory program run (TJ3L) was made where:

   a) The first state vector found in (1) above was used.

   b) The lunar model consisted of KM = 4902.58 km^3/sec^2, J20 = 2.048×10^{-4}, and C22 = 0.23×10^{-2}. All other harmonics were zero.

   c) Earth perterbations were included.

3) The effect of harmonics other than J20, C22 on radius of perilune and argument of perilune (r_p and ω respectively) was determined by plotting time histories of the differences in these parameters between the trajectories computed in (1) and (2) above. (i.e., Δr_p versus time and $\Delta\omega$ versus time).

Table 3.4-23: ODPL Solutions Over 4000-Minute Data Arc

NOMENCLATURE	ITERATION				
	0	1	2	3	4
X (km)	2251.7978	2251.7954	2251.7951	2251.7952	2251.7951
Y (km)	180.18227	180.18401	180.18411	180.18422	180.18420
Z (km)	645.73926	645.73998	645.73947	645.73976	645.73968
DX (km/sec)	-0.64708631	-0.64708573	-0.64708309	-0.64708424	-0.64708391
DY (km/sec)	1.3563042	1.3562999	1.3563014	1.3563010	1.3563011
DZ (km/sec)	0.37713533	0.37713733	0.37713743	0.37713746	0.37713746
$J30 \times 10^{-4}$	-1.3127	-1.2155	-1.2561	-1.2313	-1.24129
$J40 \times 10^{-4}$	-1.1277	-0.91095	-0.928512	-0.92112	-0.92255
$C31 \times 10^{-4}$	-0.19420	-0.08285	-0.09720	-0.09004	-0.09217
$C41 \times 10^{-4}$	0.03299	0.02501	0.03268	0.02832	0.03022
$C32 \times 10^{-4}$	-0.17429	-0.12407	-0.12668	-0.12613	-0.126124
$C33 \times 10^{-4}$	0.03464	0.03296	0.03297	0.03280	0.03276
$S31 \times 10^{-4}$	0.44849	0.37133	0.06376	0.36885	0.36634
$S41 \times 10^{-4}$	-0.08552	-0.07785	-0.07944	-0.07014	-0.07865
$S22 \times 10^{-4}$	-0.01764	-0.02228	-0.02268	-0.02286	-0.02315
$S32 \times 10^{-4}$	0.11273	0.11237	0.10725	0.10979	0.10894
$S33 \times 10^{-4}$	0.00925	0.00394	0.00404	0.00376	0.00386
SOS	2805	2050	1312	950	-

NOTE: State vector is in a selenocentric of date coordinate system at post-deboost (August 14, 1966, 16:03:52.013).

Table 3.4-24: ODPL 4138 Lunar Model

X (km)	2251.7951
Y (km)	180.18420
Z (km)	645.73968
DX (km/sec)	-0.64708391
DY (km/sec)	1.3563011
DZ (km/sec)	0.37713746
KM (km^3/sec^2)	4902.5801
J20 x 10^{-4}	2.048
J30 x 10^{-4}	-1.2412
J40 x 10^{-4}	-0.9225
C21 x 10^{-4}	0
C31 x 10^{-4}	-0.0921
C41 x 10^{-4}	0.0302
C22 x 10^{-4}	0.23
C32 x 10^{-4}	-0.1261
C42 x 10^{-4}	0.0417
C33 x 10^{-4}	0.0327
C43 x 10^{-4}	0.0146
C44 x 10^{-4}	-0.00034
S21 x 10^{-4}	0
S31 x 10^{-4}	0.3663
S41 x 10^{-4}	-0.0786
S22 x 10^{-4}	-0.0231
S32 x 10^{-4}	0.1089
S42 x 10^{-4}	0.0060
S33 x 10^{-4}	0.0038
S43 x 10^{-4}	0.0075
S44 x 10^{-4}	-0.0032

NOTE: The state vector is in a selenocentric of date coordinate system at post-deboost (August 14, 1966, 16:03:52.013).

4) J30 and J40 were then estimated in the following way:

   a) The best linear curves through the Δr_p and $\Delta\omega$ data were drawn and their slopes computed.

   b) The first-order perturbations in the elements r_p and ω due to unit values of J30 and J40 were calculated.

   c) J30 and J40 were calculated assuming that the changes in r_p and ω found in (3) could be attributed entirely to J30 and J40. Since harmonics other than J30 and J40 were perturbing the orbit, the values computed for J30 and J40 absorbed these effects, hence the term "effective values".

Two estimates of J30 and J40 were made using element plotting:

1st estimate:	J30	=	-1.35×10^{-4}
	J40	$\simeq$	0
2nd estimate:	J30	=	-1.10×10^{-4}
	J40	=	$+0.28 \times 10^{-4}$

The first estimate was based on data obtained from a direct method solution over a 20-hour data arc (4118) extrapolated out to 33 hours. Figures 3.4-17 and 3.4-18 show the Δr_p and $\Delta\omega$ plots. The Δr_p plot accommodated the linear curve nicely. However, the $\Delta\omega$ plot was extremely nonlinear and the absolute magnitudes of the data small. Therefore, J40 was assumed to be zero.

State vector determinations obtained from processing short data arcs with ODPL defined the data points for the second element plotting solution. Data arcs equal to or greater than one orbit in length were processed where two stations were viewing and the state vector was solved for.

These orbit determinations are summarized in Appendix B. The Δr_p data confirmed data from the first solution. The $\Delta\omega$ data showed a linear trend that permitted a better estimation for J40. For details of the calculations, see Appendix B.

To obtain a parallel solution for lunar gravitational harmonics with LHDL, a state vector was obtained from an ODPL solution for an epoch soon after injection. Using a relatively short data arc (about 60 minutes) and Goudas 2 values for the lunar gravitational harmonic coefficients, the state vector was refined by solving for the state vector plus lower-order harmonics. The data arc length was then increased one orbit revolution and higher-order harmonics were introduced into the solution vector. A number of iterations were prformed until the sum of squares of the residuals was acceptably low. The data arc was again expanded by an orbit revolution and the procedure was repeated. More harmonics were introduced into the solution vector as the data arc increased in length.

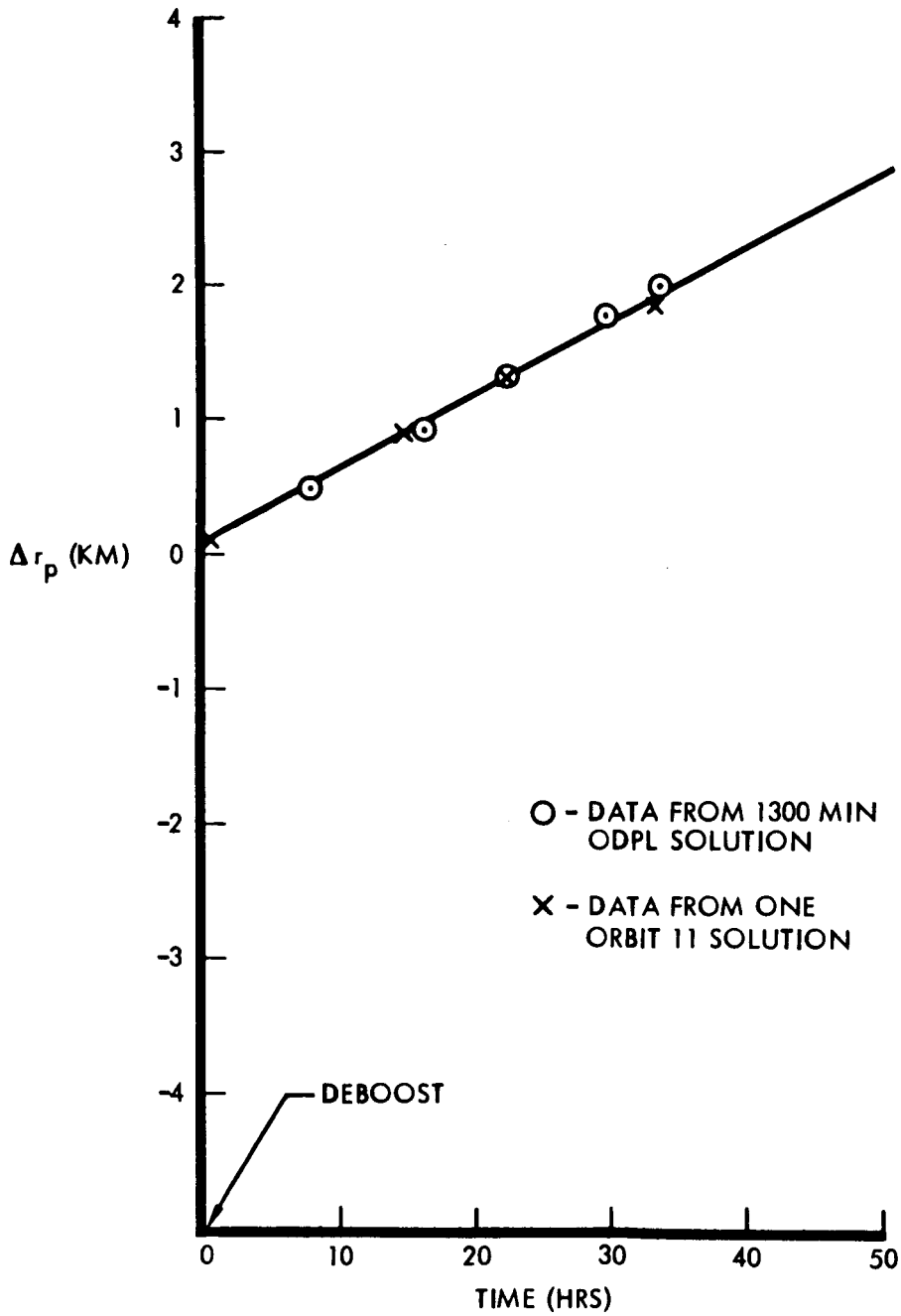

FIGURE 3.4-17: REAL-TIME PLOT TO ESTIMATE J30

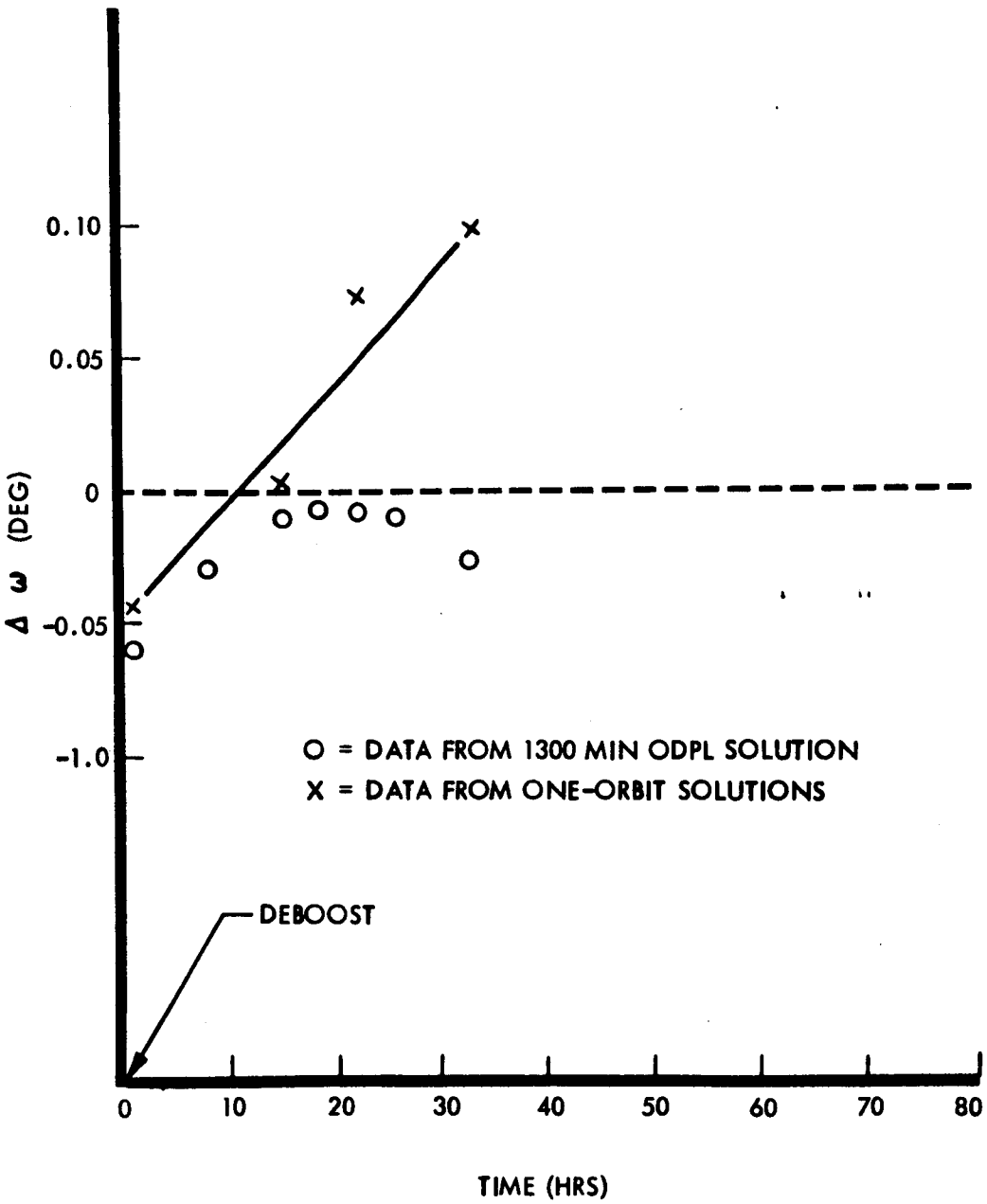

FIGURE 3.4-18: REAL-TIME PLOT TO ESTIMATE J40

The original intent had been to operate LHDL independently from ODPL, with the exception of an initial state vector solution from ODPL. This independence could not be maintained for long. By 36 hours after deboost, LHDL had logged only 2 or 3 hours on the computer and had fallen far behind ODPL in the length of data arc processed. At this time, a new state vector from ODPL was input to LHDL. At deboost plus 51 hours, marginal progress on LHDL again required adoption of a newer ODPL solution vector. At deboost plus 4 days, the situation was reversed when ODPL adopted the 2600-minute LHDL solution (Table 3.4-17). Using the LHDL solution at 2600 minutes, ODPL was able to rapidly extend the data arc to 4000 minutes, by solving for the state vector only. Meanwhile, LHDL convergence beyond 2600 minutes was marginal, so to save time LHDL adopted the ODPL solution at 4000 minutes and obtained convergence (Table 3.4-23). This solution was later verified over a 6000-minute arc shortly before transfer. Thus the role played by LHDL was one of parallel operation prepared to administer a "transfusion" when necessary. Appendix B gives a chronological summary of the LHDL operational sequence.

Choice of the lunar model—Approximately 2 days before the first transfer maneuver was scheduled, a meeting was held to discuss selection of a lunar model upon which to base the transfer maneuver to the lower orbit. There were three models under consideration:

1) The ODPL 4138 solution

2) The LHDL 66-2/3 hours solution

3) Langley Research Center's LUNGFISH Program Solution 6.

These models are listed with the Goudas 2 model in Table 3.4-25.

The ODPL 4138 solution was chosen as the Moon model to use for the transfer maneuver from a consideration of Figure 3.4-19. This figure shows lifetime projections made with all three models and indicated that the ODPL prediction lay between the two other predictions. For this reason, ODPL Solution 4138 was chosen for the transfer maneuver.

Orbit determination used for first transfer—The orbit determination used for the first transfer was the state vector from OD 4150 (Table 3.4-26) and the lunar model from OD 4138 (see "Lunar Potential Model Determination").

The FPAC ODPL was used to process doppler data as close to the scheduled transfer time as possible. Two-way doppler data (CC3) from a 500-minute data arc beginning 2 days before transfer was processed. The state vector and harmonics J30, J40, C31, C32, C33, S31, S41, S22, S32, and S33 were solved for. All other constants were fixed to their 4138 values. Only the state vector from this solution was used to calculate the transfer maneuver. The harmonics were included in the solution only to aid data fit. Using only three iterations, convergence was obtained. The resulting SOS of 19.7 indicated a good fit of the data. A diagonal a priori covariance matrix having 1σ values as follows was used to direct the solution:

Position - 0.5 km
Velocity - 1.0×10^{-3} km/sec
Harmonics - 1.0×10^{-4}

Table 3.4-25: Moon Model Summary

	GOUDAS TWO	LHDL	ODPL	LUNGFISH
DATA ARC		66-2/3/100 hours checked out o.k.	4138 66-2/3 hours	Soln. 6 9 Passes (3 days) 84 hours
EPOCH				
DAY		226	226	226
HOUR		16	16	15
MIN		03	03	43
SEC		52.013	52.013	52.013
STATE				
X		2251.7957	2253.4648	2484.1804
Y		180.18522	171.95486	-1387.4610
Z		645.74239	642.14879	80.1653
DX		-0.64708910	-0.64151248	0.18998669
DY		1.3563036	1.3586709	1.1707229
DZ		0.37713482	0.37812428	0.51512804
KM		4902.5800	4902.5801	4902.78
HARMONICS				
$J20 \times 10^{-4}$	2.048	2.0477	*2.048	2.048
$J30 \times 10^{-4}$	-0.98	-1.3123	-1.2412	-0.9989
$J40 \times 10^{-4}$	-0.48	-1.1271	-0.9225	-0.6221
$C21 \times 10^{-4}$	0	0.0007	*0	-0.06852
$C31 \times 10^{-4}$	0	-0.1946	-0.0921	0.02679
$C41 \times 10^{-4}$	0	0.0328	0.0302	-0.03369
$C22 \times 10^{-4}$	0.23	0.2281	*0.23	0.2664
$C32 \times 10^{-4}$	-0.15	-0.1749	-0.1261	0.03123
$C42 \times 10^{-4}$	-0.14	0.0423	0.0417	0.01609
$C33 \times 10^{-4}$	0	0.0342	0.0327	0.01143
$C43 \times 10^{-4}$	0	0.0145	0.0146	0.001308
$C44 \times 10^{-4}$	0.17	-0.0001	-0.00034	0.0006442
$S21 \times 10^{-4}$	0	0.0008	*0	0.1232
$S31 \times 10^{-4}$	0.21	0.4494	0.3663	0.1862
$S41 \times 10^{-4}$	0.54	-0.0857	-0.0786	0.1212
$S22 \times 10^{-4}$	0	-0.0177	-0.0231	0.01527
$S32 \times 10^{-4}$	0	0.1124	0.1089	0.09153
$S42 \times 10^{-4}$	0	0.0069	0.0060	0.08136
$S33 \times 10^{-4}$	0.18	0.0087	0.0038	-0.005946
$S43 \times 10^{-4}$	0.032	0.0082	0.0075	0.0006801
$S44 \times 10^{-4}$	0	-0.0030	-0.0032	-0.002506

*Fixed in solution

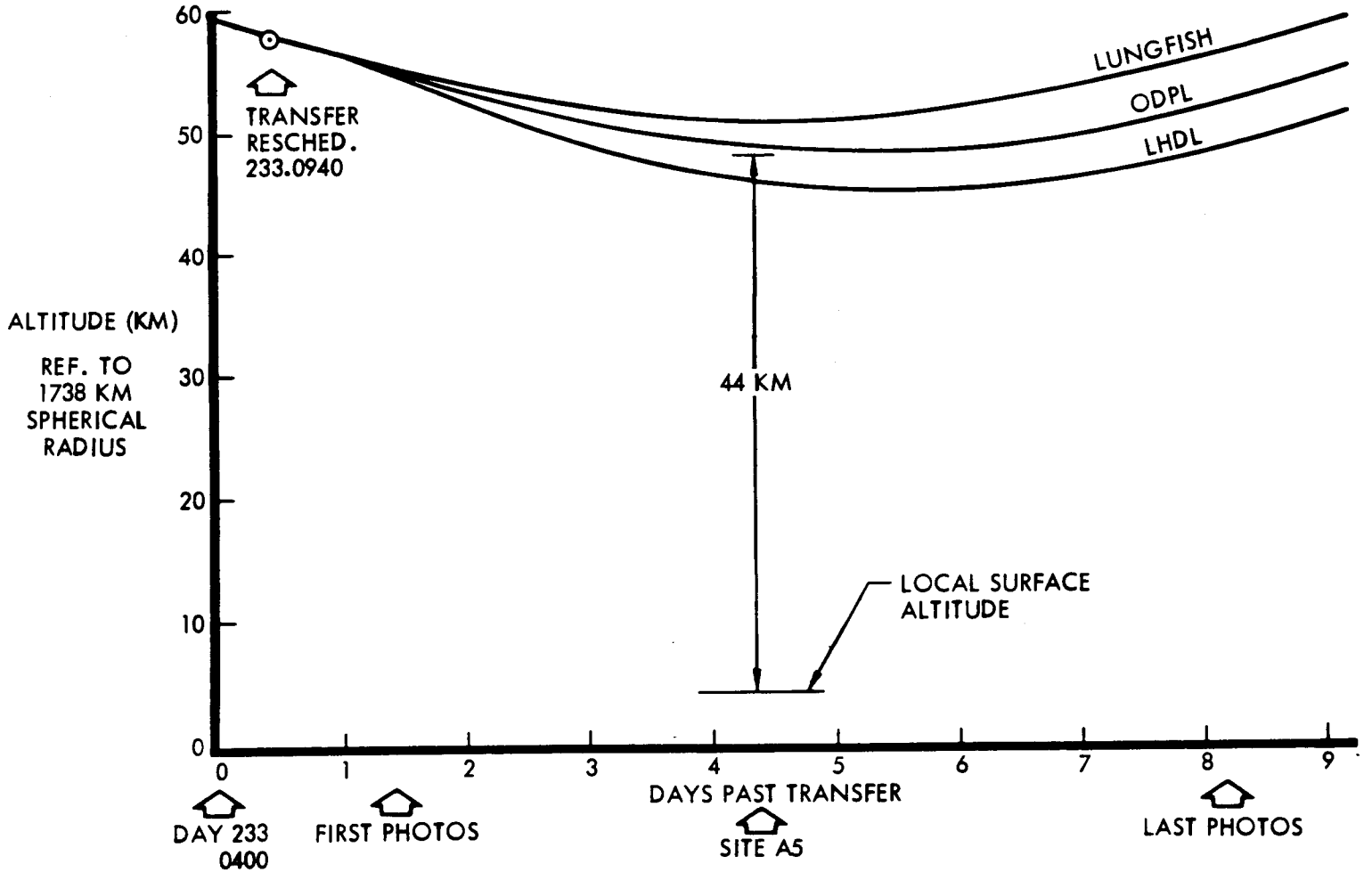

FIGURE 3.4-19: EFFECT OF MOON MODEL ON FINAL ELLIPSE PERILUNE FOR TRANSFER BASED ON ODPL MOON MODEL

Table 3.4-26: Transfer Maneuver Orbit (OD 4150)

1) Epoch 66/08/19 09:13:52.012^s

2) State (Selenocentric true of date coordinates)

	STATE		STANDARD DEVIATIONS	
X	-1793.6721	km	0.132	km
Y	1254.8997	km	0.104	km
Z	37.669022	km	0.474	km
DX	- 1.1341323	km/sec	0.399×10^{-4}	km/sec
DY	- 0.98394287	km/sec	0.216×10^{-3}	km/sec
DZ	- 0.67219859	km/sec	0.299×10^{-3}	km/sec

3) Lunar Harmonic Coefficients (OD No. 4138)

J30	$= -1.2412896 \times 10^{-4}$	KM	$= 4902.5801$ km^3/sec^2
J40	$= -0.92254632 \times 10^{-4}$	J20	$= 2.048 \times 10^{-4}$
C31	$= -0.92166451 \times 10^{-5}$	C21	$= 0.0$
C41	$= 0.30222376 \times 10^{-5}$	C22	$= 0.23 \times 10^{-4}$
C32	$= -0.12612434 \times 10^{-4}$	C42	$= 0.41699421 \times 10^{-5}$
C33	$= 0.32764172 \times 10^{-5}$	C43	$= 0.14638130 \times 10^{-5}$
S31	$= 0.36633914 \times 10^{-4}$	C44	$= -0.33877178 \times 10^{-7}$
S41	$= -0.78655566 \times 10^{-5}$	S21	$= 0.0$
S22	$= -0.23146328 \times 10^{-5}$	S42	$= 0.60008693 \times 10^{-6}$
S32	$= 0.10894609 \times 10^{-4}$	S43	$= 0.74887457 \times 10^{-6}$
S33	$= 0.38634092 \times 10^{-6}$	S44	$= -0.32127172 \times 10^{-6}$

4) Data Summary for OD No. 4150

STATION NUMBER	DATA TYPE	START	TIME	STOP	TIME	NUMBER OF POINTS	STANDARD DEVIATIONS
61	CC3	8/19	11:03	8/19	17:33	126	0.040

No frequency adjustments were used because the only CC3 data used came from Station 61. However, to correct timing asynchronization, a time shift of -7.620 milliseconds was applied. The data weight was 0.1 cps as in the translunar phase of the mission. The fit of the data was fairly good, having but small oscillations in the residuals. Detailed results are tabulated in Table 3.4-26.

Orbit determinations for photographic Site I-0—Orbit determination 4320 was used for Site I-0 photo commands. This was the "direct" solution obtained over a 1520-minute data arc. (See "Lunar Potential Model Determination"). The results are shown in Table 3.4-27. The first five iterations were used to solve only for lunar harmonic coefficients. The last two iterations considered both state and harmonics in the solution vector. Data fit was fairly good. The state vector from this solution was used in calculating Site I-0 photo commands. Goudas 2 harmonics were substituted for those determined in this solution, because the results were still preliminary and unconfirmed.

Orbital Characteristics

A prediction of orbital behavior after the maneuver execution is always included in the maneuver design. These predictions are based on the postmaneuver state vector and a set of lunar harmonics considered to be the most accurate representation of the real Moon. With a given state epoch, and set of lunar harmonics, the state and Kepler element variations are predicted with a mean element integrating computer program (LIFL). Each of the five Kepler elements are plotted versus time. A measure of the accuracy success of the actual maneuver can be judged by comparing the orbital elements of the post maneuver OD solutions with the predictions at the time of maneuver. Furthermore, an indication of the validity of the lunar harmonics can be made by noting any divergence from the predicted behavior of the orbit elements.

Orbit element variations for Lunar Orbiter Mission I are presented in Figures 3.4-20 through 3.4-24. These figures are histories of: perilune radius, apolune radius, orbit inclination, argument of perilune, and longitude of the ascending node. To clearly show what happened throughout the photo mission, the figures cover a period of 30 days from lunar injection (Days 226 to 256) and, thus, cover all three ellipses. The second and third ellipse predictions are based on the OD 4138 harmonics (see Table 3.4-24). The prediction for the first ellipse is based on the Goudas 2 harmonics (Table 3.4-25). The Goudas 2 harmonics were also the basis for preflight planning and design of the injection maneuver and Site I-0 photo. As the figures show, the OD 4138 harmonics predicted the actual orbit quite well during the photo-taking period. Bias between the design state prediction and the OD solutions was removed during photo design by using the latest OD state and the OD 4138 harmonics. The principal deviation became apparent 6 or 7 after the second transfer.

Before first transfer particular interest was shown in orbit lifetime predictions. An orbit lifetime prediction for three different sets of harmonics is shown in Figure 3.4-25. All three sets indicate an indefinite lifetime because the perilune minimums due to Earth effects show a rising trend.

Table 3.4-27: For Mission Phase First Ellipse

OD Identification Number 4320

Time of Run _____ Item Number _____

Epoch of Solution 66/08/14 16:03:52.013

Converged Solution and statistics (Selenocentric Mean 1950.0 Coord.)

	State Vector		Std. Dev.		A priori Std. Dev.	
X	2253.3272	km	0.021	km	10	km
Y	171.39710	km	0.055	km	10	km
Z	643.10718	km	0.084	km	10	km
DX	-0.64150812	km/sec	0.12×10^{-4}	km/sec	10×10^{-3}	km/sec
DY	1.3585897	km/sec	0.67×10^{-5}	km/sec	10×10^{-3}	km/sec
DZ	0.37829307	km/sec	0.58×10^{-5}	km/sec	10×10^{-3}	km/sec

Corresponding Orbital Parameters (Selenographic True of Date Coord.)

a	2765.4801	km	e	0.30319877		ω	180.19612	deg
Ω	326.02335	deg	i	12.176832	deg	T_p	-1637.7488	sec
r_p		km	r_a		km	P		min
h_p		km	h_a		km			

Other Parameters in the Solution Vector

J40	$0.62798471 \times 10^{-4}$	S33	$-0.34632684 \times 10^{-5}$	S32	$0.56570666 \times 10^{-4}$
C31	$0.94826143 \times 10^{-4}$	S43	$-0.50122844 \times 10^{-5}$		
C42	$-0.14677102 \times 10^{-4}$	J30	$0.28211320 \times 10^{-5}$		
C33	$0.52800733 \times 10^{-5}$	C41	$-0.31391684 \times 10^{-4}$		
C43	$0.24123290 \times 10^{-5}$	C32	$0.37144971 \times 10^{-5}$		
S31	$0.25128937 \times 10^{-4}$	C44	$-0.43602736 \times 10^{-6}$		
S22	$-0.17789742 \times 10^{-6}$	S41	$-0.16383835 \times 10^{-4}$		
S42	$-0.19723712 \times 10^{-4}$	S44	$-0.16815974 \times 10^{-7}$		

Number of Iterations 7 converges SOS 116

Data Summary:

STA. NO.	DATA TYPE	START	TIME	STOP	TIME	NUMBER OF POINTS	STD. DEV.	FIRST MOMENT	SECOND MOMENT
41	C3	8/14	21:30	8/14	22:23	52	0.019	0.031	0.0014
	C3	8/14	22:24	8/15	06:41	84	0.028	0.016	0.0011
	CC3	8/15	00:23	8/15	05:18	249	0.024	-0.012	0.0007
12	CC3	8/14	16:04	8/14	18:33	100	0.035	-0.00045	0.0012
	C3	8/15	13:09	8/15	14:08	58	0.033	0.024	0.0016
61	C3	8/14	16:04	8/15	17:23	199	0.053	-0.017	0.0031
	CC3	8/15	05:37	8/15	14:08	334	0.033	-0.0014	0.0011

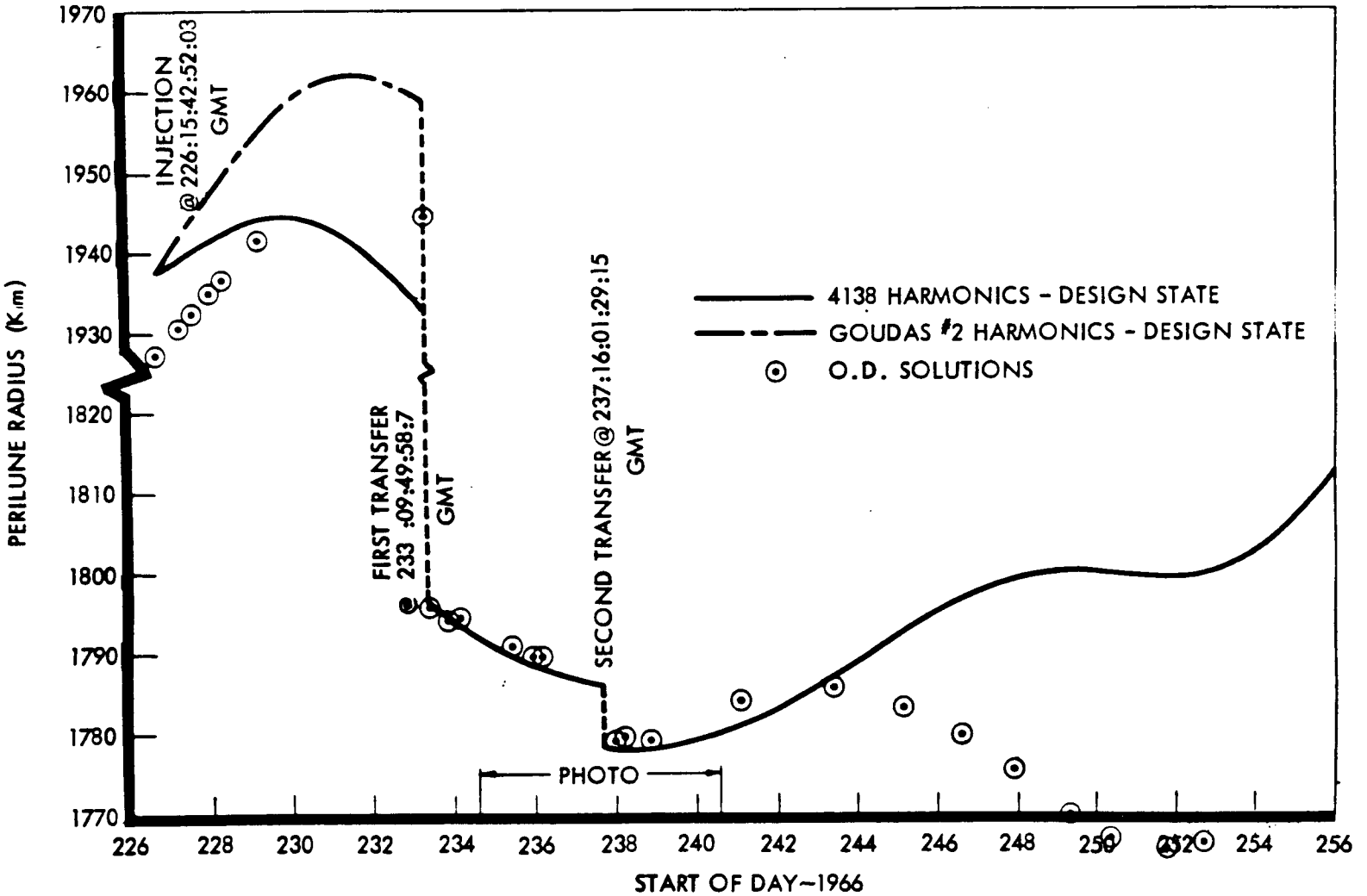

FIGURE 3.4-20: LUNAR ORBITER MISSION I PERILUNE RADIUS HISTORY

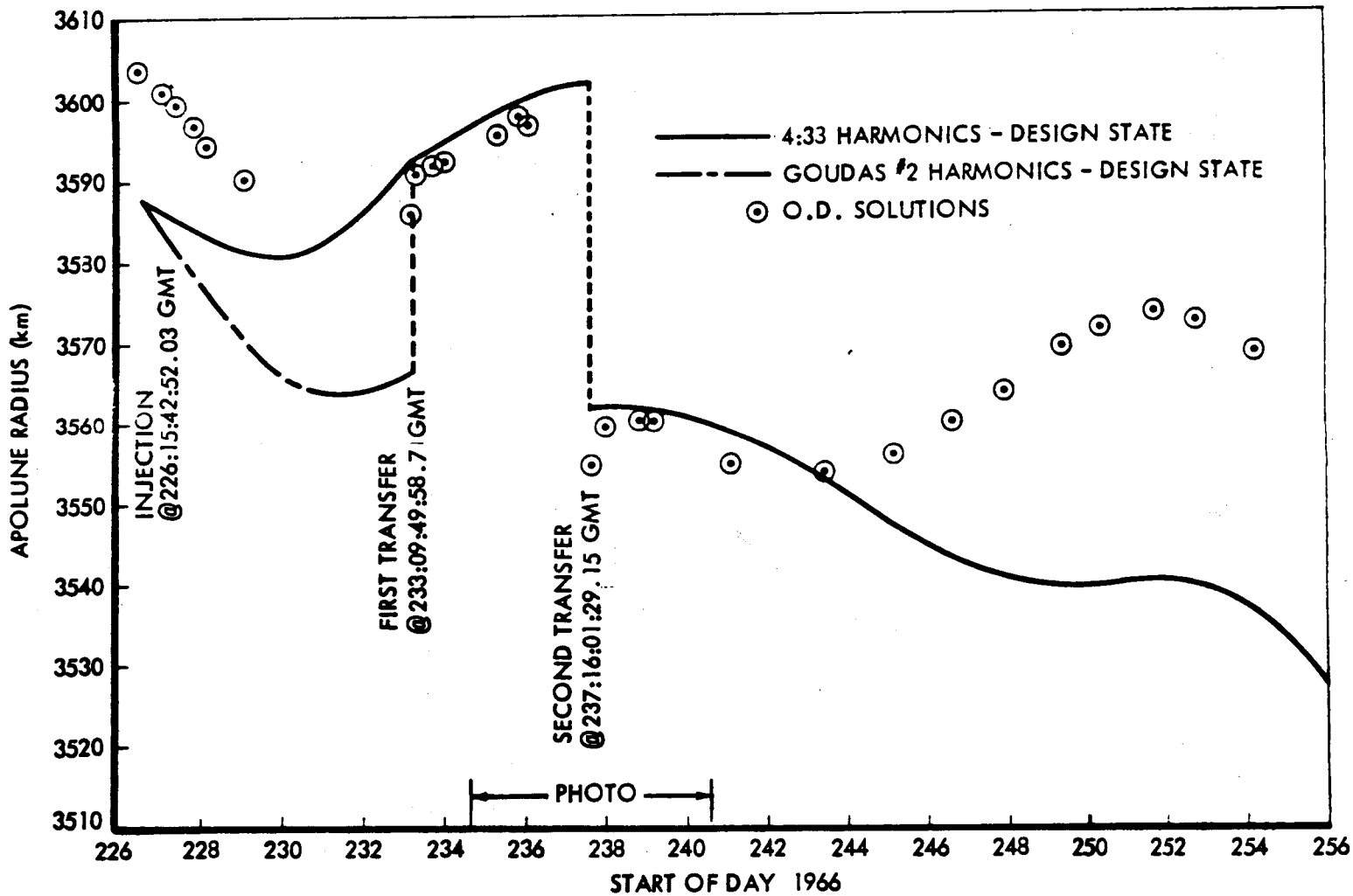

FIGURE 3.4-21: LUNAR ORBITER MISSION APOLENE RADIUS HISTORY

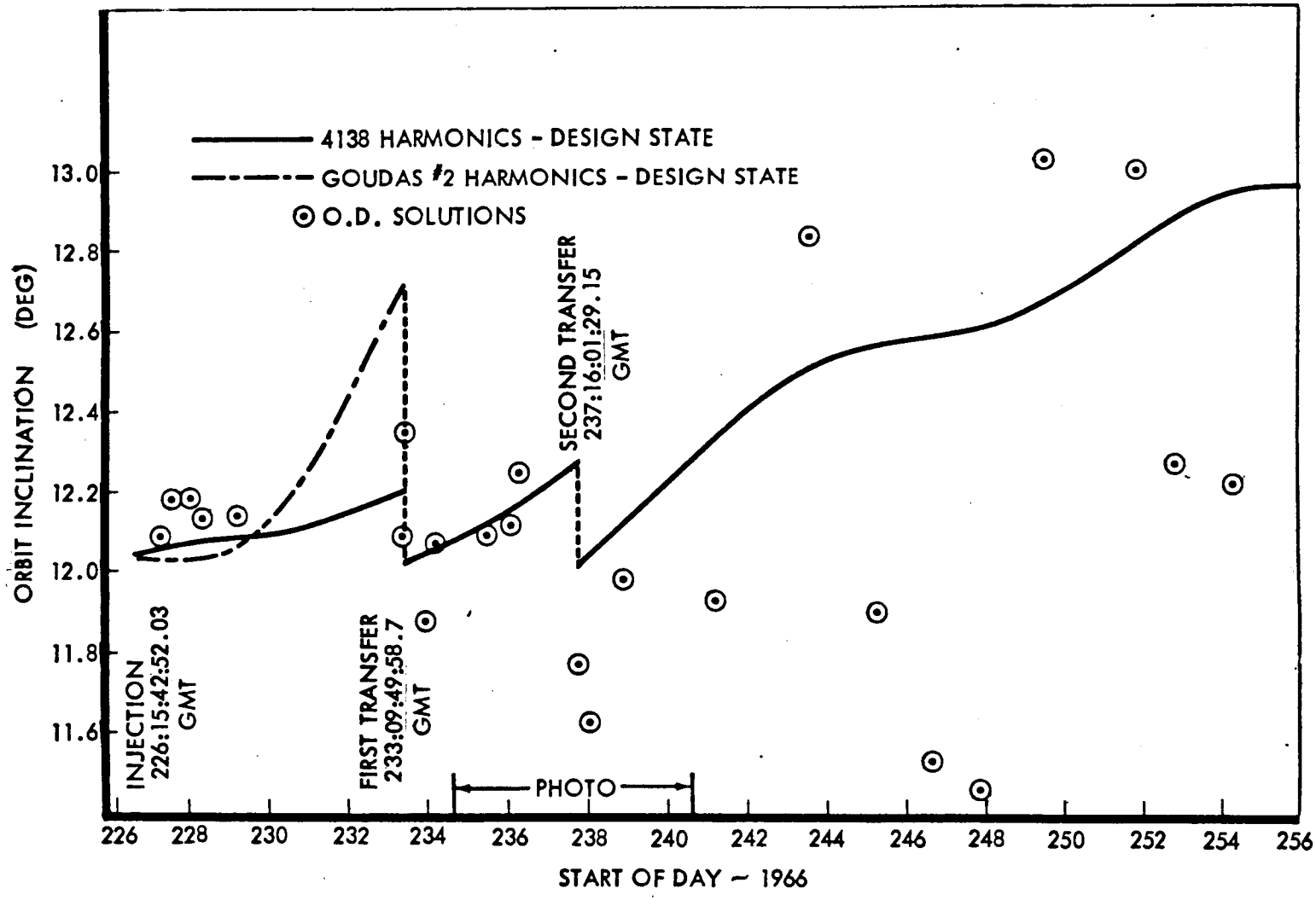

FIGURE 3.4-22: LUNAR ORBITER MISSION I ORBIT INCLINATION HISTORY

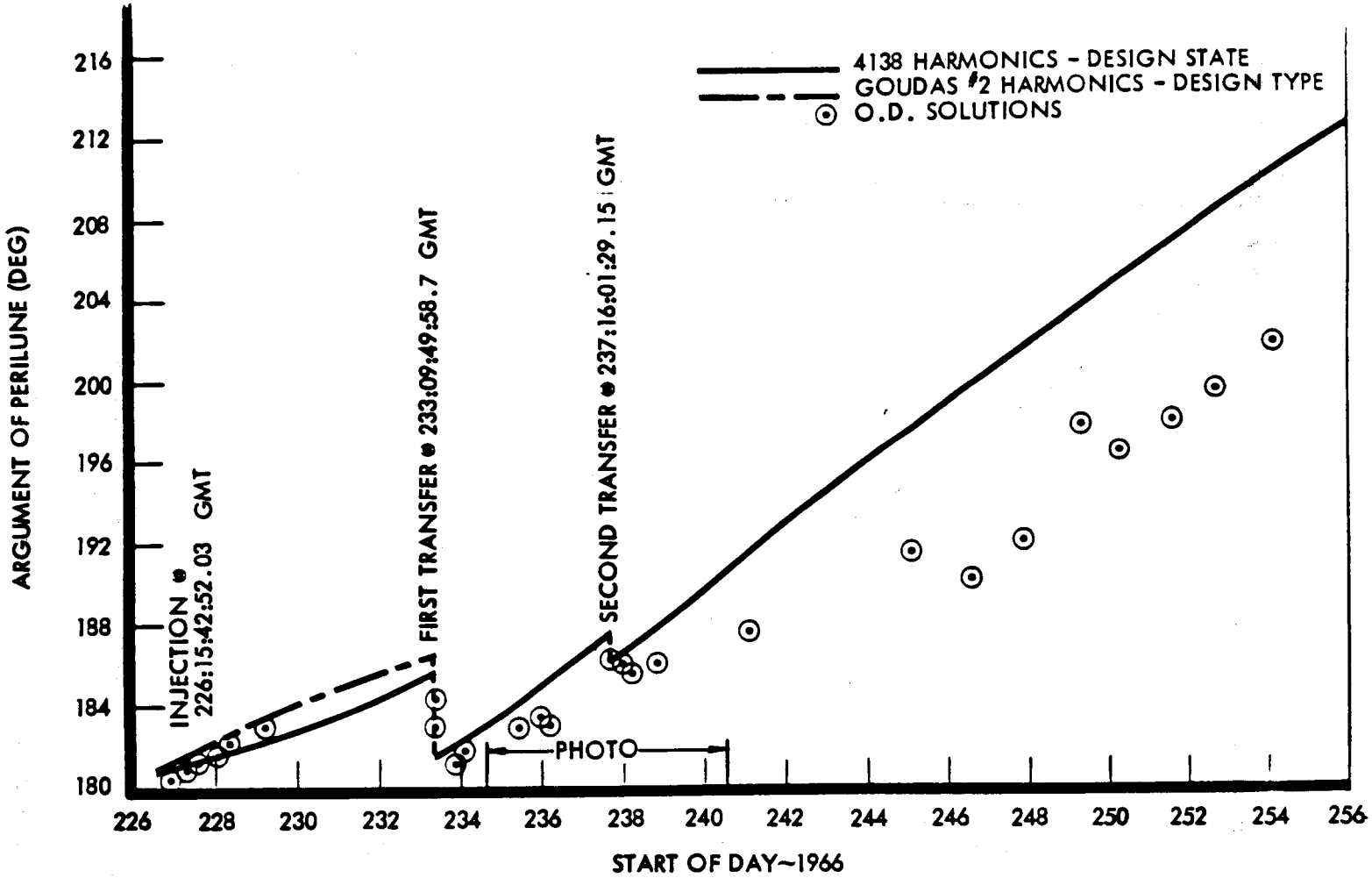

FIGURE 3.4-23: LUNAR ORBITER MISSION I ARGUMENT OF PERILUNE HISTORY

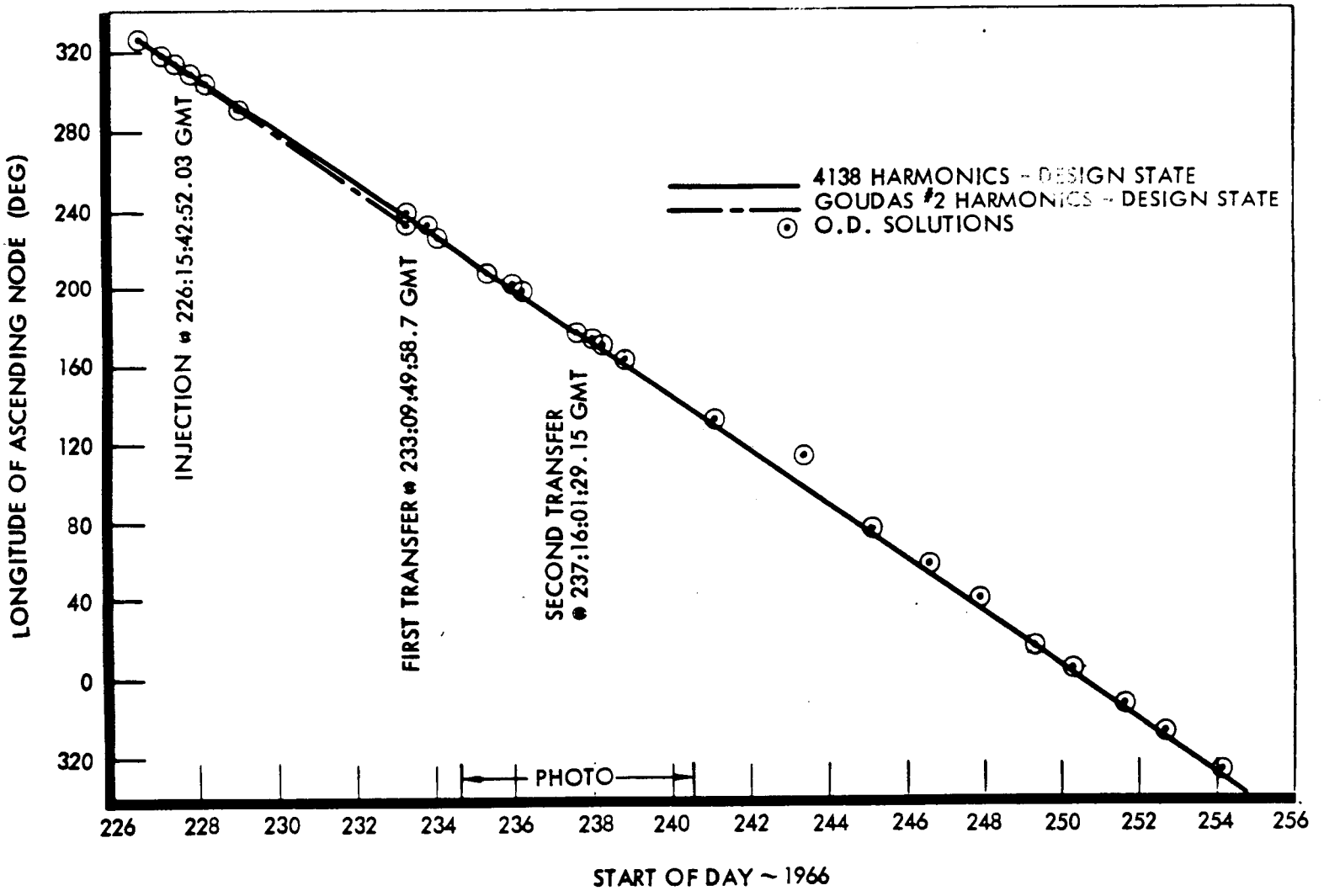

FIGURE 3.4-24: LUNAR ORBITER MISSION I LONGITUDE OF ASCENDING NODE HISTORY

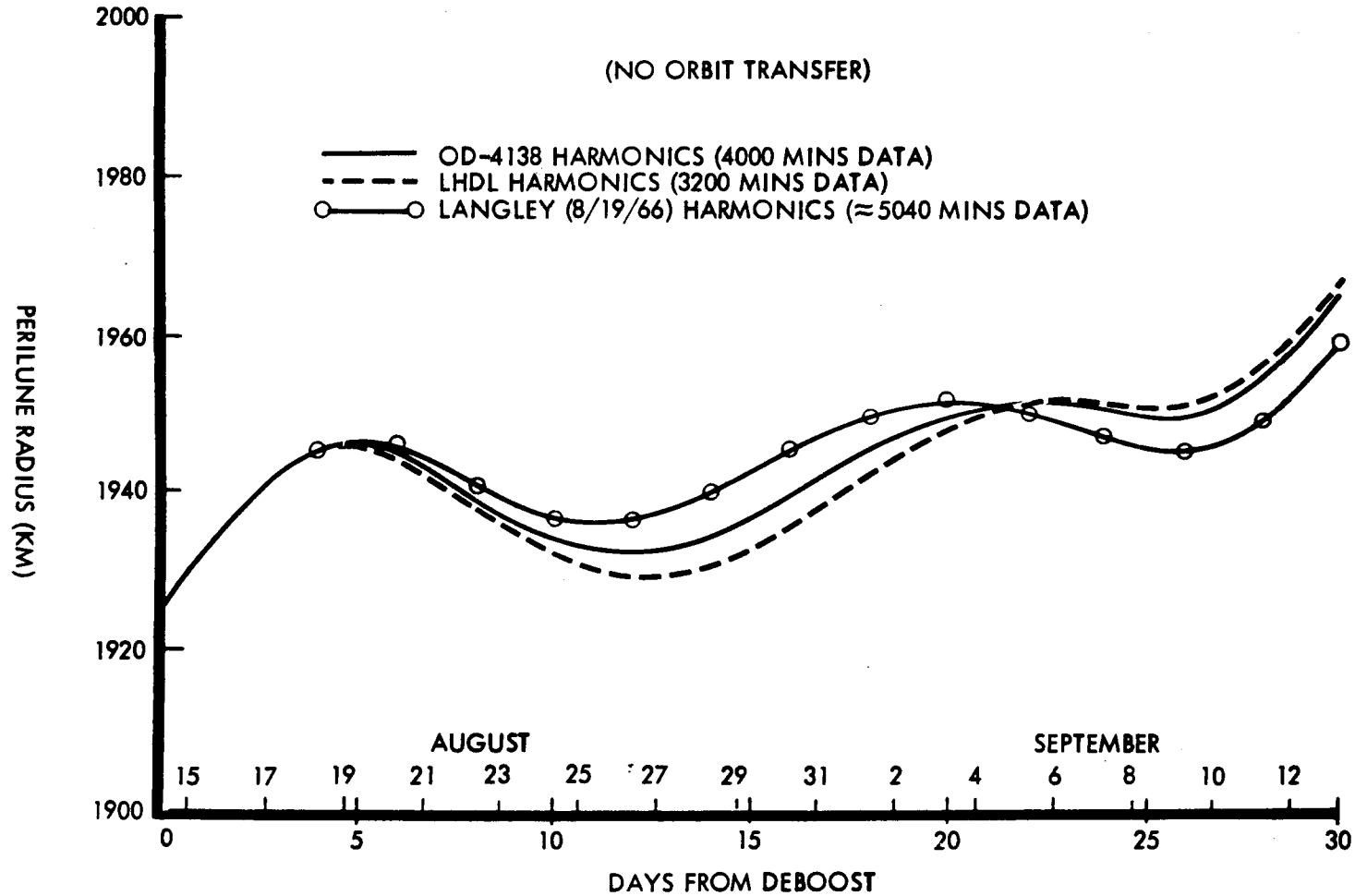

FIGURE 3.4-25: FIRST-ELLIPSE PERILUNE ALTITUDE PREDICTIONS

First-Ellipse Photography

The photographic portion of the mission was initiated with exposure of 20 frames of film over Site I-0 approximately 4 days after injection into the first ellipse. This began a sequence of 39 frames exposed during the first-ellipse portion of the mission. The following table lists the purpose of each of the frames exposed while in the first ellipse. A detailed tabulation of photo information is contained in Section 2.3.

FRAME NUMBERS	TYPE OF PHOTOS
5 through 20	Site I-0
21 through 24*	Additional Site I-0
25*, 26, 27*, 29*, 31* through 43*	Film set front side
28, 30	Film-set back side

*Denotes film-set frames where FPAC did not select the camera-on time.

The Goudas 2 lunar model was used to compute the trajectory for attitude maneuvers and camera-on times. All other primary site camera-on times and attitude maneuvers were generated using the OD 4138 lunar harmonics. The state vector used for Site I-0 was OD Solution 4320. A check was made of camera-on time and attitude maneuver for Site I-0 using OD lunar harmonics 4138 when they became available. The difference in camera-on time resulted in an error of less than one frame in the photo footprint. The difference in the attitude maneuver was negligible.

Following Site I-0, nine single-frame exposures were made for film-set purposes, along with two multiframe sequences of four and six frames. FPAC supported the selection of camera-on times for three of the nine single-frame exposures. Two of the three frames were backside photos in the PM lighting region which required a roll about the Sun line of 180 degrees to point the camera at the lunar surface. Figure 3.4-26 illustrates the geometry of PM photography using the 180-degree roll technique. For simplicity, the geometry shown is for an equatorial orbit. A description of PM photography is presented in Appendix B. See "Second-Ellipse Photography" for a discussion of film-set frame photography.

The LHDL lunar harmonics were used to generate trajectories for selecting the camera-on times for the three film-set frames.

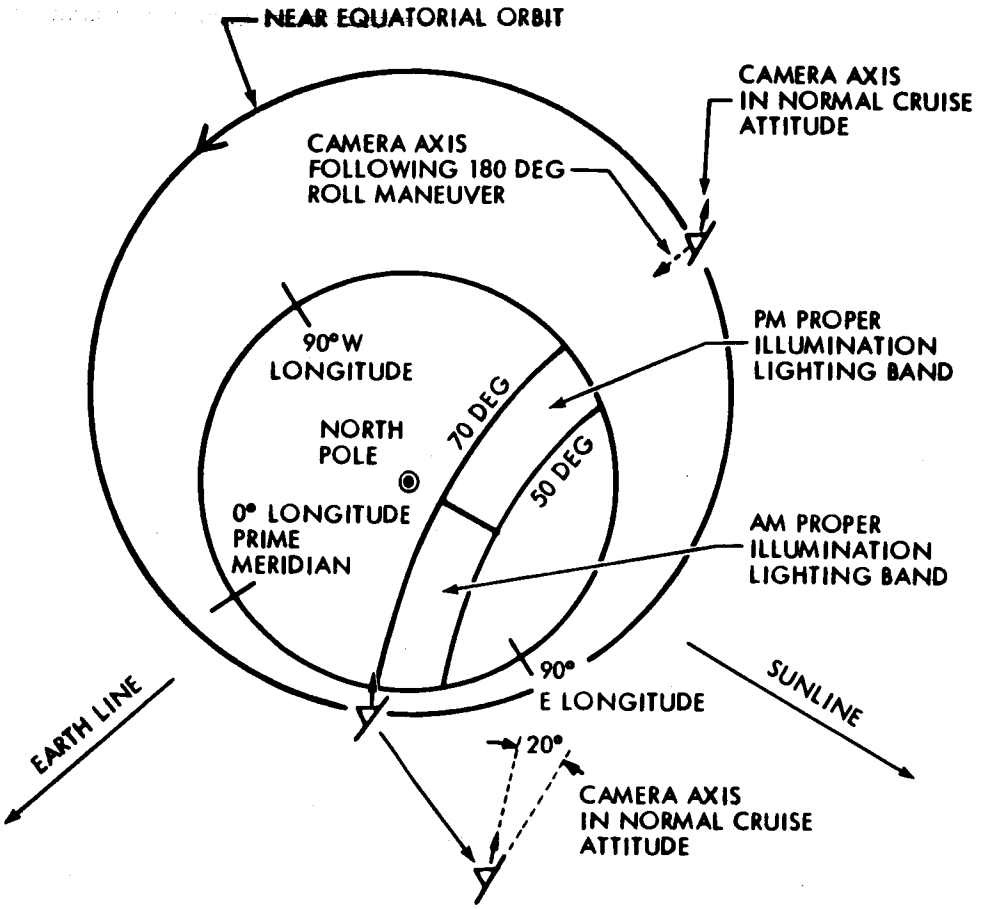

NOTE: THIS ILLUSTRATION REPRESENTS THE EARTH-MOON-SUN GEOMETRY PRIOR TO TRANSFER FROM THE FIRST ELLIPSE TO THE SECOND ELLIPSE

FIGURE 3.4-26: GEOMETRY PHOTOGRAPHY USING 180-DEGREE ROLL

Transfer Design and Execution

Transfer from the first to second ellipse was executed at Day 223, 09:50:58.1 GMT and resulted in a second ellipse almost identical to the designed ellipse. This event concluded approximately 7 days in the first ellipse.

Design of the transfer maneuver was based on the following ground rules:

1) Minimum perilune altitude of 48 km;

2) Minimum photo sidelap of 5%;

3) Illumination angles at primary targets of between 50 and 75 degrees;

4) Transfer at least 24 hours prior to first photo;

5) A minimum of 20 minutes tracking between end of earth occultation and start of engine burn.

The OD 4138 lunar harmonic coefficients were used during this analysis. The maneuver design was based on a state vector from OD Solution 4150.

Orbit 44 of the first ellipse was selected for transfer, allowing between seven and eight orbit revolutions from transfer to first photo. Because of camera subsystem difficulties, NASA mission advisors requested that FPAC design two transfer maneuvers for second ellipses with minimum perilune altitudes of both 100 km and 48 km. Only the transfer resulting in the 48-km minimum perilune is discussed here because the 100-km transfer was not used.

A trial second ellipse was designed based on an in-plane transfer maneuver at apolune, changing only perilune altitude. The resulting second ellipse with a minimum perilune altitude of 48 km provided an initial solution for the photo coverage geometry. It gave the perilune trace (locus of perilune passage points of successive orbits) with respect to the photo targets, and the illumination angle at each of the targets. Conic elements of the second ellipse obtained via this in-plane transfer were:

Semi-major axis	$\triangleq a = 2342.4$ km	
Eccentricity	$\triangleq e = 0.33201$	
Inclination	$\triangleq i = 12.2$ degrees	Selenographic of-date coordinates
Argument of perilune	$\triangleq \omega = 185.76$ degrees	
Longitude of ascending node	$\triangleq \Omega = 234.24$ degrees	

Figure 3.4-27 shows orientation of the perilune trace along with the inner and outer Sun band geometry obtained via the in-plane transfer. The lighting angle at all targets was acceptable, indicating that longitude of ascending node was satisfactory. Perilune trace however, was not centered with respect to the targets which would result in an undesirable variation in photo altitudes. A reduction in the argument of perilune to equalize photo altitudes at the targets was required.

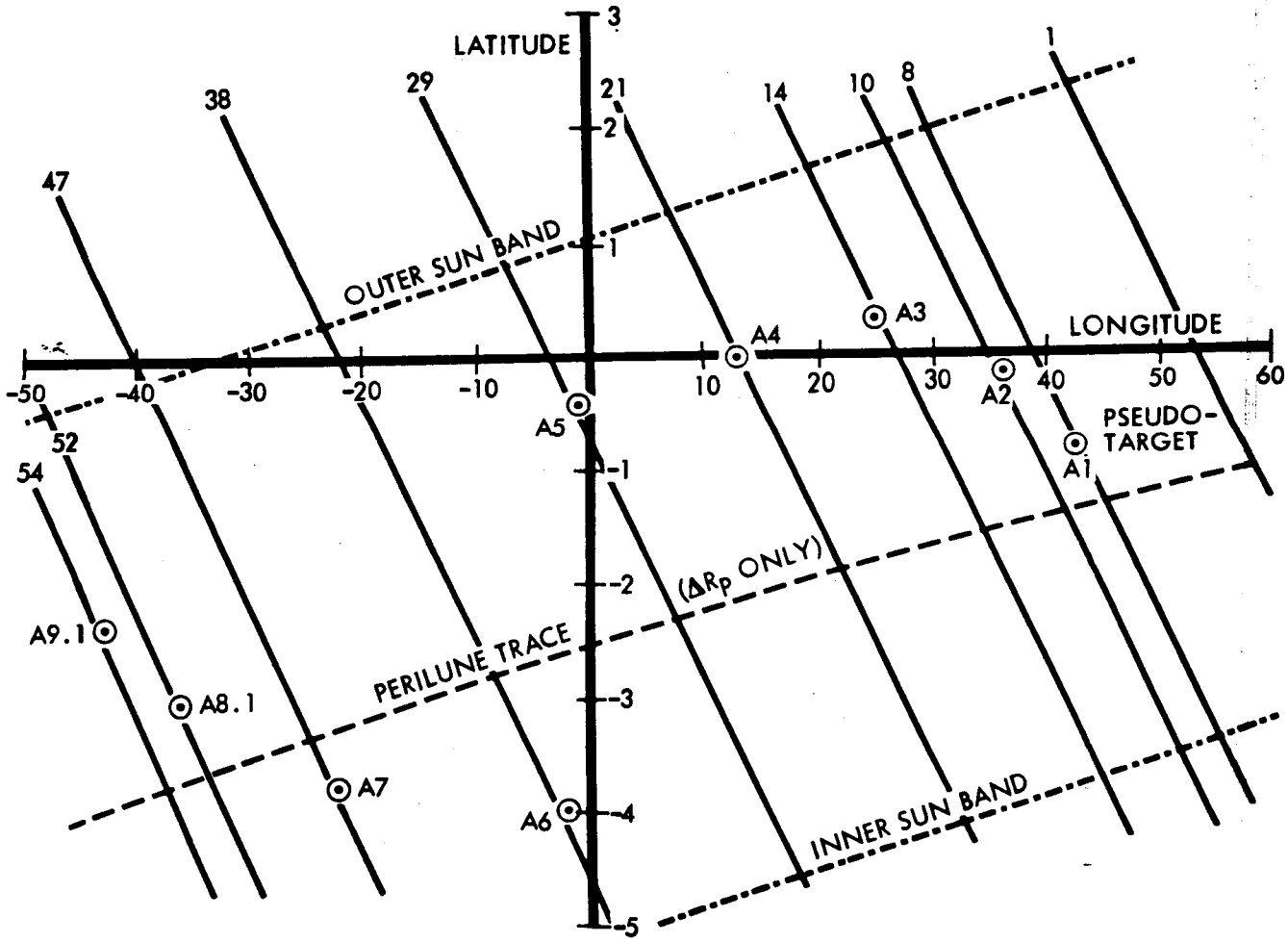

FIGURE 3.4-27: PERILUNE TRACE

The final transfer maneuver design was carried out by targeting to the three parameters, perilune altitude, inclination, and latitude of perilune passage. These parameters were specified for the first perilune after transfer and were defined on the basis of the foregoing analysis so that all requirements were satisfied. The first perilune altitude after transfer was 57.3 km, which resulted in a minimum perilune altitude of 48 km. Orbit inclination was 12.04 degrees to guarantee a photo sidelap greater than 5%. The third targeting parameter, latitude of perilune, was adjusted to minimize extremes in photo altitude variation. A perilune latitude of -0.33 degrees gave the "best" distribution of photo altitudes over the targets.

The ground rule for the 48 Δkm minimum-perilune-altitude is a conservative combination of the following components:

1) Minimum altitude of approximately 38 km for proper V/H sensor response;

2) Terrain elevation of approximately 4 km above spherical Moon near Site I-5;

3) Control errors of approximately 5 km in execution of transfer;

4) Uncertainty in lunar radius and terrain elevation of approximately 1 km.

The results of targeting to the three selected parameters are presented in Figures 3.4-28, 3.4-29, and 3.4-30. Figure 3.4-28 shows the perilune altitude as a function of longitude of descending node. Perilune trace and lighting angle geometry is shown in Figure 3.4-29. The photo altitude and lighting angle for each site are shown in Figure 3.4-30.

The minimum ΔV transfer maneuver would occur at a true anomaly of approximately 140 degrees. However, to provide at least 20 minutes of tracking before the start of burn, the transfer maneuver was scheduled at a true anomaly of 180 degrees. This resulted in a ΔV requirement of 40.15 meters per second. While this was greater than the minimum ΔV requirement (for transfer at 140 degrees true anomaly), it was well below the ΔV budget of 199.0 meters per second. Orbit geometry at the time of transfer is shown in Figure 3.4-31. The maneuver angles required for the transfer were:

HROLL	43.40 degrees
PITCH	25.31 degrees

Selection of this maneuver sequence was based on maintenance of Sun lock as long as possible and compliance with antenna constraints with a minimum spacecraft rotation. A lifetime prediction based on the computed posttransfer state and the OD 4138 lunar harmonics indicated an indefinite lifetime in the final ellipse as is shown in Figure 3.4-32.

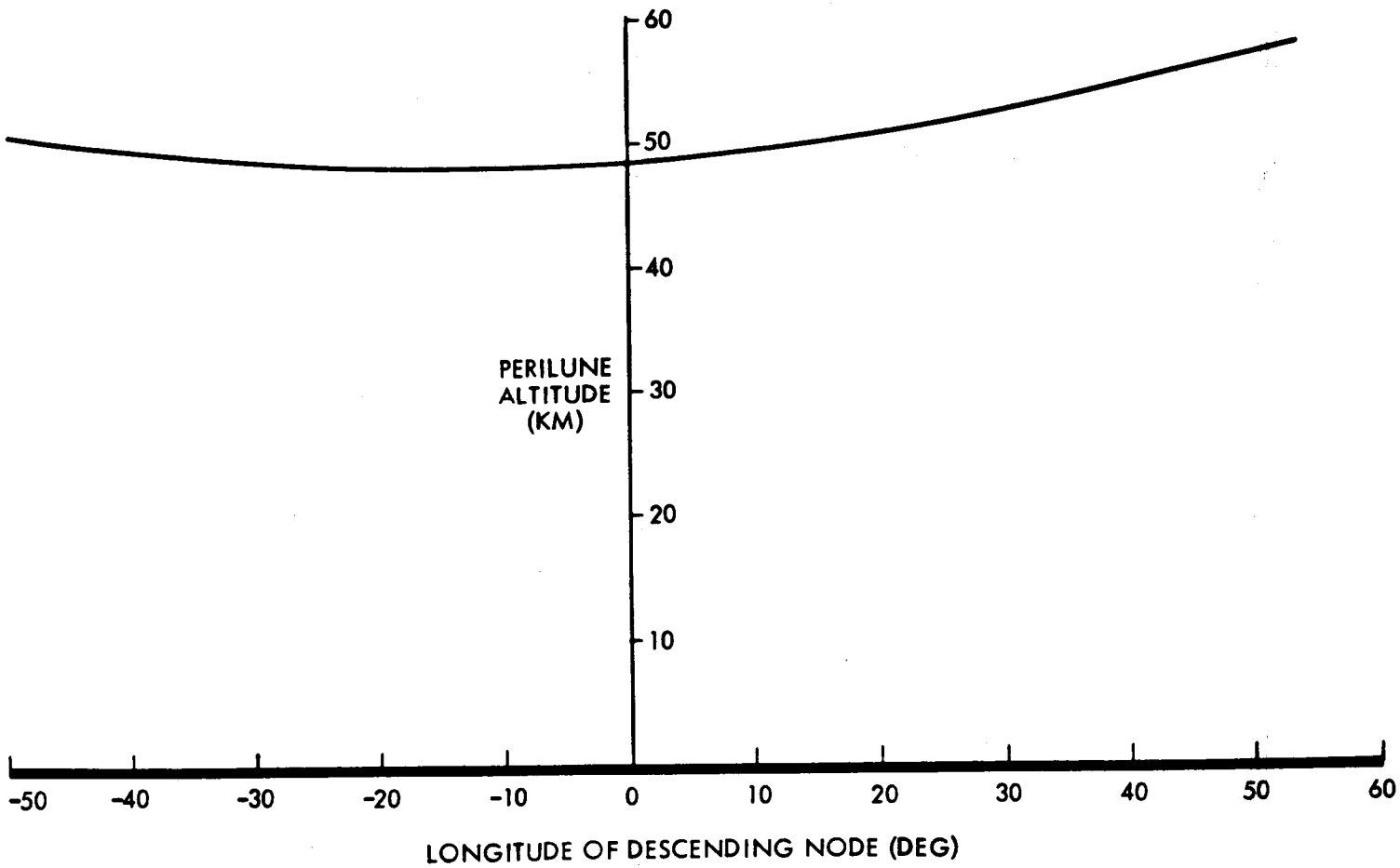

FIGURE 3.4-28: PERILUNE ALTITUDE VERSUS LONGITUDE OF DESCENDING NODE

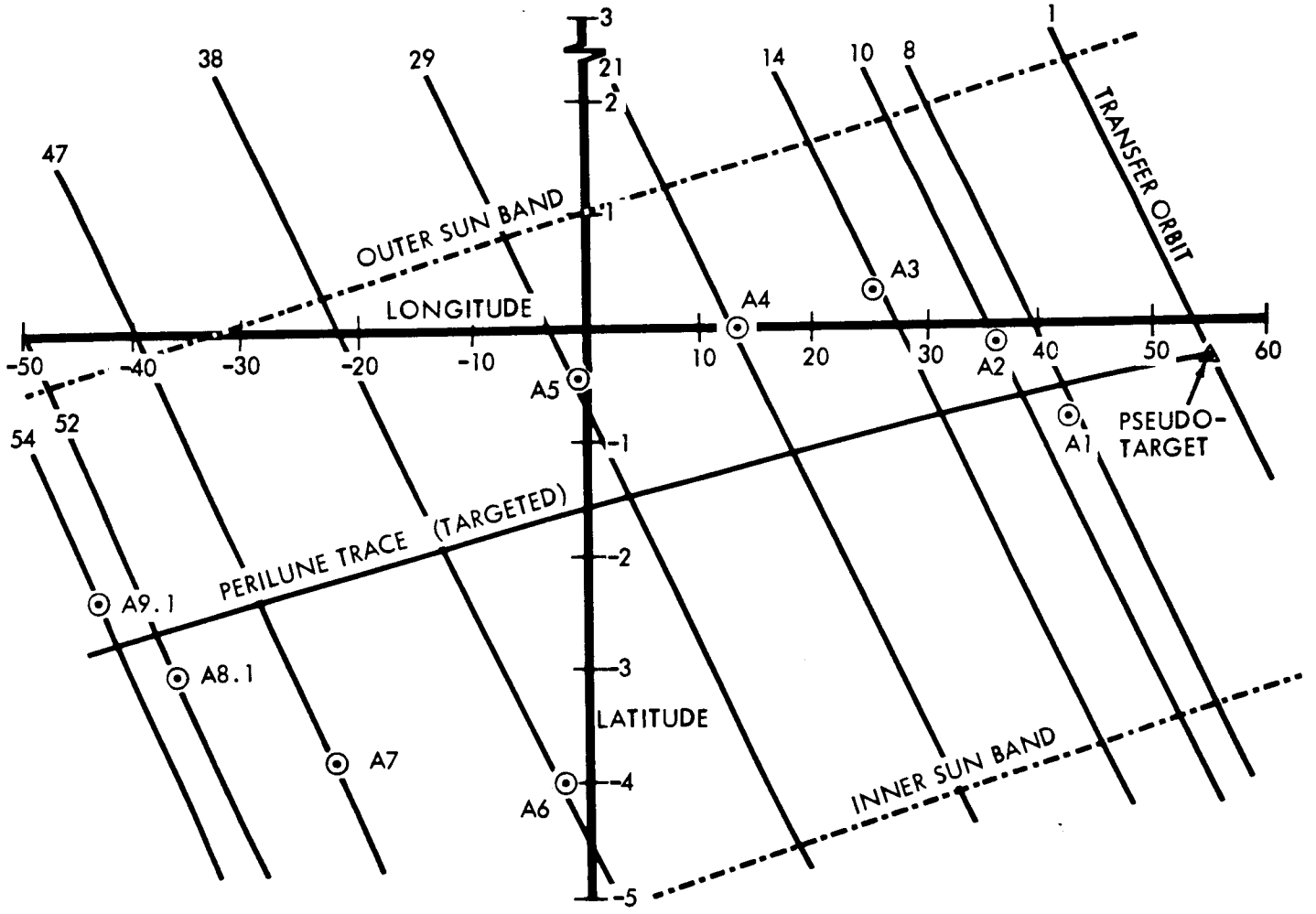

FIGURE 3.4-29: TARGETED PERILUNE TRACE

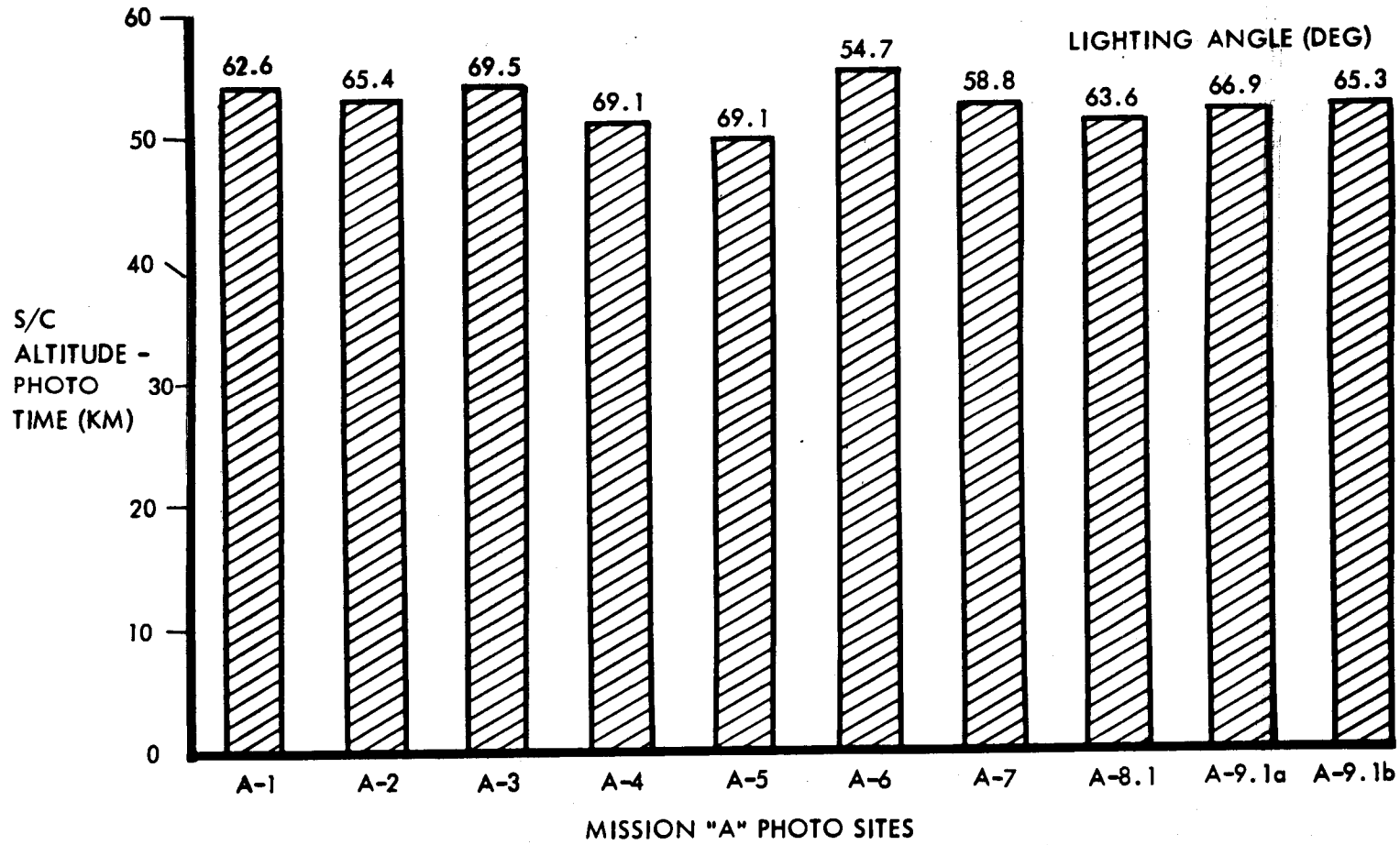

FIGURE 3.4-30: SITE PHOTO ALTITUDE AND LIGHTING ANGLES

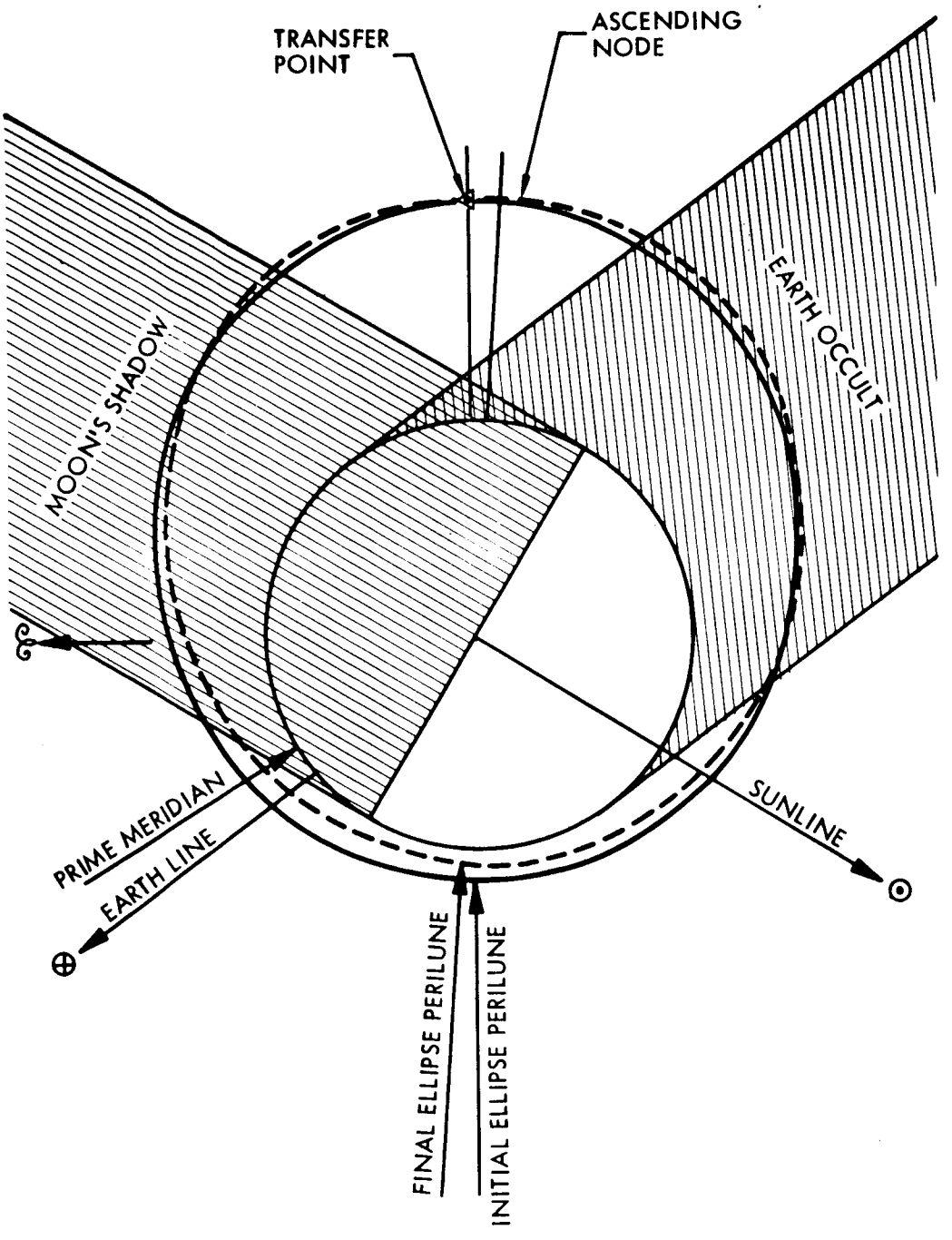

FIGURE 3.4-31: FLIGHT TRANSFER ORBIT GEOMETRY
INITIAL: ORBIT NO. 44
FINAL: ORBIT NO. 1
233:09:50:58.09

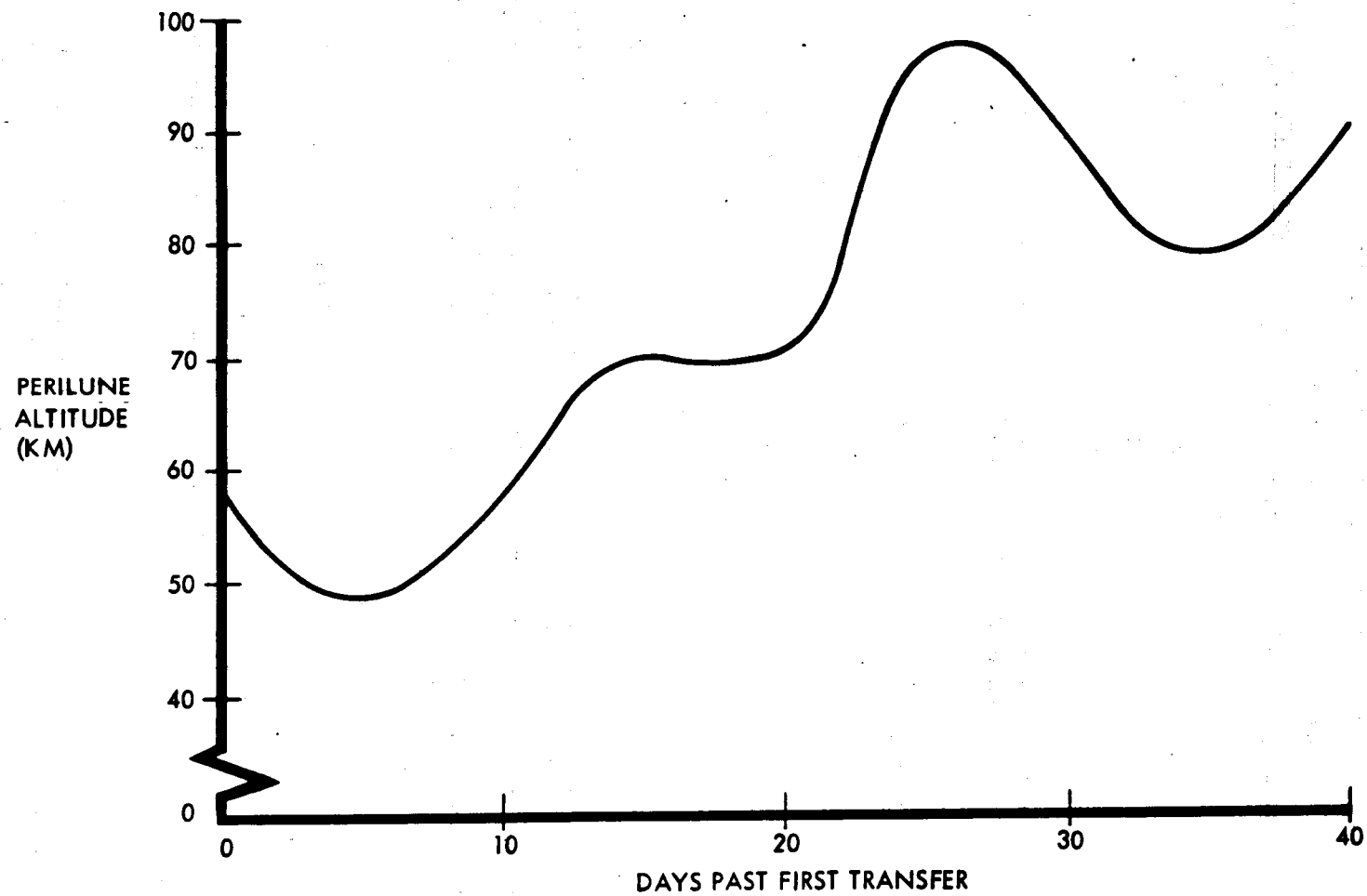

FIGURE 3.4-32: FINAL ORBIT LIFETIME

Predicted conic elements before and after the transfer maneuver were:

Element	Pretransfer	Post-Transfer
r_a	3588.7 km	3592.6 km
r_p	1943.9 km	1795.8 km
i	12.2 deg	12.04 deg
ω	185.19 deg	181.50 deg
Ω	234.16 deg	234.09 deg

Postmaneuver orbit determination results indicated the actual maneuver to be very close to designed conditions. A summary of the results follows:

Element	Actual	Difference (Actual - Design)
r_a	3592.0 km	-0.6 km
r_p	1795.5 km	-0.3 km
i	12.00 deg	-0.04 deg
ω	181.20 deg	-0.30 deg
Ω	234.00 deg	-0.09 deg

Second-Ellipse Phase

The second-ellipse phase extended from the end of first-transfer burn through the completion of a second-transfer burn. It was intended that all Mission I sites would be photographed from this second ellipse, and that no further velocity maneuvers would be performed. However, due to a difficulty in camera performance, only Sites I-1 through I-5 were photographed from the second ellipse and a second transfer to a third ellipse was made to complete coverage of Mission I sites.

Principal FPAC tasks in this phase included:

1) Orbit determination prior to each photo site, which formed the basis for final camera pointing commands;

2) Photo coverage studies leading to proper camera-on times for film set frames;

3) Design of a second transfer maneuver leading to a third ellipse having a minimum perilune altitude of 40 km;

4) General-purpose trajectory predictions.

A major deviation from the mission plan followed direction to design film-set photos for both backside and Earth-Moon limb targets. The second-transfer design was also a deviation from the mission plan, but this was essentially a repeat of the first-transfer design.

Orbit Determination of Second Ellipse

This section describes the second-ellipse orbit determinations performed for the purposes of camera pointing maneuvers, second-transfer maneuver, and perilune altitude monitoring. Included are:

1) Tracking data editing;

2) Technique used for orbit determinations;

3) Orbit determinations used for photo commands;

4) Orbit determination used for second-transfer maneuver;

5) Perilune altitude monitoring.

Tracking data editing—Angle and doppler tracking data were received during the second ellipse. Angle data were disregarded as before. No attempt was made to take ranging data. The timing and doppler bias corrections employed during the first ellipse were also applied in the second ellipse. There were no major anomalies in the tracking data editing in this phase. However, all tracking data received during photo readout activities were not usable because of the high modulation of the carrier frequency. Starting with this mission phase, the tracking data received during photo readout were given a "bad" data condition code. Such data are missing from B1 master file data tapes. The quality of some of the remaining data received was suspect because of changing spacecraft power levels associated with pitching off the Sun line to avoid overheating of the spacecraft.

Input deck listings, data file summaries, photo readout times, and B1 tape numbers are in Appendix B.

Orbit determination method—The orbit determination program (ODPL) was used to process DSIF tracking data to determine state vectors as close to the photo events and second-transfer time as possible. These state vectors were then used along with the lunar harmonic constants from OD 4138 to compute the desired trajectories for flight path analysis. The procedure used to determine the state vector was as follows:

1) Short data arcs including as much as possible of a two-station view period were processed. Tracking data received during photo readout was not processed. Data types C3 and CC3 were considered using 0.1 data weight.

2) The state vector was generally solved for by itself. However, some harmonics were included when the fit was thereby improved. This was the case for OD 5128.

3) An a priori matrix tight enough to prevent divergence but not so tight as to unnecessarily constrain the solution was used.

Orbit determinations for photo sites—The orbit determination runs used for the I-1 to I-5 photo sites are listed below.

PHOTO SITE	OD NO.	FIGURE
I-1 and I-2	5212	3.4-33
I-3	5118	3.4-34
I-4	5122	3.4-35
I-5	5128	3.4-36

Figures 3.4-33 through 3.4-36 are summaries of these four-orbit determinations.

Orbit determination used for the second-transfer maneuver—The state vector used in the design of the second transfer maneuver was from orbit determination run 5128, summarized in Figure 3.4-36. The lunar OD 4138 harmonic model was used.

Perilune altitude monitoring—Other determinations were made during the second ellipse phase. Among other things, these provided data for perilune altitude monitoring. These determinations are summarized in Appendix B. A plot of perilune altitude is shown in "Orbital Characteristics."

Cyclic doppler residuals near perilune—Large cyclic doppler residuals near perilune were first noticed in the second ellipse. Within 30 minutes of each perilune, the observed minus predicted doppler shift had a sinusoidal nature with amplitudes of 5 to 10 cycles per second (the general noise level was 0.5 cps) with periods of 10 to 30 minutes. This was an unexpected phenomenon and still unexplained. Among the hypotheses offered so far are:

1) Rf reflections from the surface of the Moon;

2) Program inaccuracy in ODPL (a series of truncation error);

3) Lunar surface lumps or highly localized irregularities in mass distribution.

4) Doppler count sample rate too coarse.

During the mission none of these hypotheses was eliminated from contention. Considerable postflight analysis work will probably be necessary to establish the cause of this phenomenon. These residual oscillations apparently occurred at every perilune passage although photo readout frequently caused the doppler data to be lost in the region of perilune.

Orbital Characteristics

After the first transfer, a lifetime prediction was again made using OD 5212 state and OD 4138 harmonics. Figure 3.4-37 shows the results. Again an indefinite lifetime is indicated. The minimum perilune altitude was 48 km on Day 237.

MISSION PHASE SECOND ELLIPSE WORK SHEET

OD ~~Identification Number~~ 5212

Time of Run _____ Item Number 2097 and 2098

Epoch of Solution 66/08/21 $20^h\ 30^m\ 8.094^s$

Converged Solution and Statistics (selenocentric mean 1950.0 coordinate.)

	State Vector		Std. Dev.		A priori Std. Dev.	
X	630.50555	km	0.13	km	None	km
Y	-3283.7847	km	0.49	km		km
Z	-1114.1220	km	1.43	km		km
DX	0.90765160	km/sec	0.11×10^{-3}	km/sec		km/sec
DY	0.21108215	km/sec	0.72×10^{-4}	km/sec		km/sec
DZ	0.30536918	km/sec	0.46×10^{-3}	km/sec		km/sec

Corresponding Orbital Parameters (selenographic true of date coordinate)

a	2693.1796	km	e	0.33373822		ω	181.05891	dec
Ω	228.62346	dec	i	11.879296	dec	T_p	-5239.1372	sec
r_p	1794.36	km	r_a		km	P		min
h_p	56.27	km	h_a		km			

Other Parameters in the Solution Vector

None

Number of Iterations 5 converged SOS 3.3

Data Summary:

STA. NO.	DATA TYPE	START	TIME	STOP	TIME	NUMBER OF POINTS	STD. DEV.	FIRST MOMENT	SECOND MOMENT
12	CC3	8/21	20:37	8/21	21:29	52	0.018	0.0032	0.00032
61	C3	8/21	20:37	8/21	21:29	50	0.021	-0.0020	0.00046

Comments: The converged state vector of this solution and the 4138 harmonics were used for photo sites I-1 and I-2. The fit of the data was very good.

Figure 3.4-33:

MISSION PHASE SECOND ELLIPSE WORK SHEET

OD Identification Number 5118

Time of Run _____ Item Number 2270

Epoch of Solution 66/08/22 $22^h\ 12^m\ 00^s$

Converged Solution and Statistics (selenocentric mean 1950.0 coordinate.)

	State Vector		Std. Dev.		A priori Std. Dev.	
X	1066.3612	km	0.07	km	5	km
Y	1314.8273	km	0.41	km	5	km
Z	766.26113	km	0.95	km	5	km
DX	-1.5934759	km/sec	0.15×10^{-3}	km/sec	100×10^{-3}	km/sec
DY	0.95764866	km/sec	0.21×10^{-3}	km/sec	100×10^{-3}	km/sec
DZ	-0.026644698	km/sec	0.72×10^{-3}	km/sec	100×10^{-3}	km/sec

Corresponding Orbital Parameters (selenographic true of date coordinate)

a	2694.2870	km	e	0.33517529		ω	182.27066	dec
Ω	213.65778	dec	i	11.924385	dec	T_p	-521.21996	sec
r_p		km	r_a		km	P		min
h_p		km	h_a		km			

Other parameters in the Solution Vector

None

Number of iterations 6 converged SOS 45.7

Data Summary:

STA. NO.	DATA TYPE	START	TIME	STOP	TIME	NUMBER OF POINTS	STD. DEV.	FIRST MOMENT	SECOND MOMENT
12	CC3	8/22	20:43	8/22	22:04	78	0.070	0.013	0.005
61	C3	8/22	20:42	8/22	22:01	73	0.057	-0.0028	0.0033

Comments: The cartesian and conic state vectors appearing in the above summary were obtained by mapping the converged state vector at 66/08/22 $20^h\ 27^m\ 00^s$ to the end of the data arc processed. The statistics are those obtained at the original epoch (66/08/22 $20^h\ 27^m\ 00^s$). The OD 4138 harmonics were used. This solution was used for Site I-3 photos.

Figure 3.4-34:

MISSION PHASE SECOND ELLIPSE WORK SHEET

OD Identification Number 5122

Time of Run _____ Item Number 2466

Epoch of Solution 66/08/23 $22^h\ 51^m\ 00^s$

Converged Solution and Statistics (selenocentric mean 1950.0 coordinate)

	State Vector		Std. Dev.		A priori Std. Dev.	
X	-632.84553	km	2.07	km	10	km
Y	1655.4904	km	3.09	km	10	km
Z	470.70587	km	8.01	km	10	km
DX	-1.7707500	km/sec	0.23×10^{-2}	km/sec	10×10^{-3}	km/sec
DY	-0.29231096	km/sec	0.34×10^{-2}	km/sec	10×10^{-3}	km/sec
DZ	-0.55323994	km/sec	0.90×10^{-2}	km/sec	10×10^{-3}	km/sec

Corresponding Orbital Parameters (selenographic true of date coordinate)

a	2693.8358	km	e	0.33564217		ω	183.29269	dec
Ω	199.59587	deg	i	12.102043	dec	T_p	419.45829	sec
r_p	1789.670906	km	r_a	3598.000	km	P		min
h_p	51.58	km	h_a	1859.91	km			

Other Parameters in the Solution Vector

None

Number of Iterations converged S0S

Data Summary:

STA. NO.	DATA TYPE	START	TIME	STOP	TIME	NUMBER OF POINTS	STD. DEV.	FIRST MOMENT	SECOND MOMENT
61	C3	8/23	21:43	8/23	22:13	90	0.038	-0.011	0.0016
	CC3	8/23	21:19	8/23	21:35	41	0.026	-0.0034	0.0007

Comments: The cartesian and conic state vectors appearing in the above summary were obtained by mapping the converged state vector at 66/08/23 $21^h\ 10^m\ 00^s$ to 66/08/23 $22^h\ 51^m\ 00^s$ (end of data arc processed.)

This OD was used for photo Site I-4.

This was considered a poor orbit determination. Data from Station 12 was not on the disk at the time this solution was obtained. OD 5124 (see Appendix B) reprocessed this data arc when station 12 data was available. The change in the state vector from OD 5122 to OD 5124 was $\Delta X = 2.6$ km; $\Delta Y = 3.4$ km; $\Delta Z = -9.2$ km; $\Delta X = 0.036$ K/S; $\Delta Y = 0.061$ K/S, $\Delta Z = -0.153$ K/S

Figure 3.4-35:

MISSION PHASE SECOND ELLIPSE WORK SHEET

OD Identification Number 5128

Time of Run _____ Item Number _____

Epoch of Solution 66/08/23 $21^h\ 13^m\ 00^s$

Converged Solution and Statistics (selenocentric true of date coordinate)

	State Vector		Std. Dev.		A priori Std. Dev.	
X	489.16750	km	0.13	km	10	km
Y	-3324.3888	km	0.21	km	10	km
Z	-1159.5957	km	0.53	km	10	km
DX	0.91488604	km/sec	0.54×10^{-4}	km/sec	10×10^{-3}	km/sec
DY	0.14636570	km/sec	0.81×10^{-4}	km/sec	10×10^{-3}	km/sec
DZ	0.28234544	km/sec	0.21×10^{-4}	km/sec	10×10^{-3}	km/sec

Corresponding Orbital Parameters (selenographic true of date coordinate)

a	Not presently	km	e			ω	dec
Ω	Available	deg	i		dec	T_p	sec
r_p		km	r_a		km	P	min
h_p		km	h_a		km		

Other Parameters in the Solution Vector

C33
S33
C43
S43
C44
S44

These parameters were included in the solution vector to aid the fit of the data. The values to which they converged were not used for the photo calculations.

Number of Iterations 3 converged SOS 235

Data Summary:

STA. NO.	DATA TYPE	START	TIME	STOP	TIME	NUMBER OF POINTS	STD. DEV.	FIRST MOMENT	SECOND MOMENT
41	C3	8/24	05:09	8/24	05:11	3	0.024	Not available	
	CC3	8/24	06:35	8/24	10:10	46	0.045		
12	C3	8/24	06:35	8/24	06:39	5	0.141		
	CC3	8/23	21:40	8/24	05:11	113	0.092		
61	C3	8/23	21:42	8/23	22:11	30	0.033		
	CC3	8/23	21:19	8/23	21:34	15	0.042		

Comments: The above solution was used for Site I-5 photos. The determination was not as refined as it might have been with several more iterations, but no time remained to do this. The results were needed immediately by the FPAC Guidance group to accomplish calculation of necessary commands for the photos. This OD was also used for designs of the second-transfer maneuver.

Figure 3.4-36:

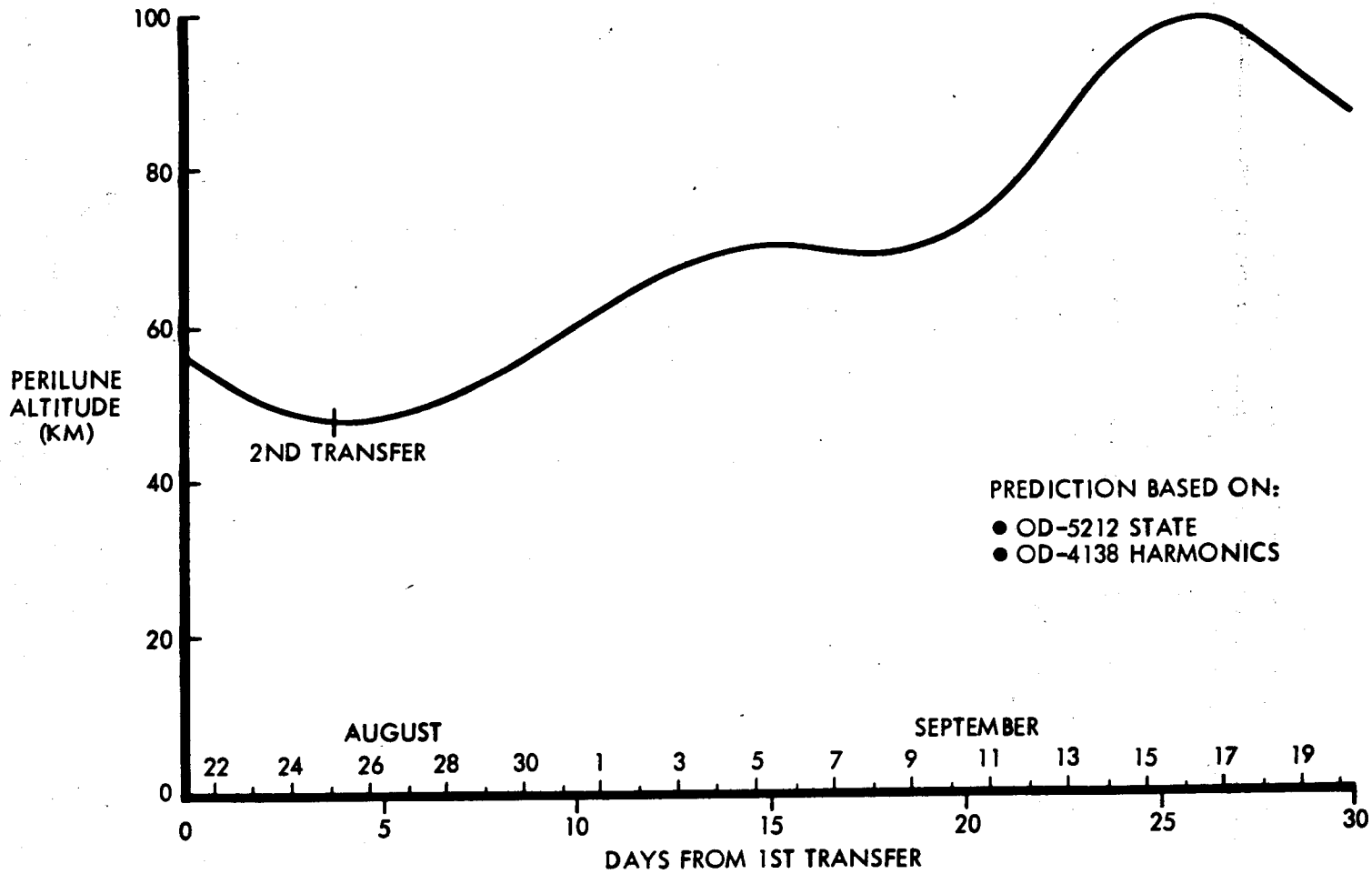

FIGURE 3.4-37: PERILUNE ALTITUDE PREDICTION (POST FIRST-TRANSFER ELLIPSE)

Second-Ellipse Photography

Second-ellipse photography included 18 frames of film-set photos and 72 frames of primary site photos. Section 2.3 contains a detailed listing of photo information, including actual camera-on times and attitude maneuvers. A summary of the frames exposed during second-ellipse is given in Table 3.4-28.

Table 3.4-28: Photos Exposed During Second Ellipse

FRAME NUMBERS	TYPE OF PHOTO
44*, 45*	Film-set farside
46*, 47*, 48*, 49*, 50, 51	Film-set frontside
52 through 67	Site I-1
68 through 83	Site I-2
84	Film-set frontside
85 through 100	Site I-3
101	Film exposed with thermal door closed
102	Film-set Earth photo
103	Film-set frontside
104	Film exposed with thermal door closed
105 through 112	Site I-4
113, 114	Film-set frontside
115, 116	Film-set farside
117	Film-set Earth photo
118 through 133	Site I-5
The asterisk denotes film-set frames where FPAC did not select the camera on time.	

The OD 4138 lunar harmonics were used in the calculation attitude maneuvers and camera-on times.

FPAC support for film set photography had not been planned. Because of this, camera-on times and attitude maneuvers for film-set frames were worked into the schedule on a non-interference basis. Originally film-set frames were to be taken without an attitude maneuver, i.e., from normal cruise attitude. Photos were to be taken near perilune where the lighting angle was approximately 70 degrees on the AM side (See Figure 3.4-26). Following site I-0

photos in the first ellipse, FPAC was directed to design a farside photo using a 180-degree roll to point the camera at the lunar surface. This was the first of several requests to deviate from the original plans for film-set frames. In the second ellipse, two additional backside photos requiring 180-degree roll maneuvers were designed as well as two film-set photos of the eastern limb of the Moon and the Earth. A detailed description of Earth-Moon photos is contained in Section 2.0.

Five primary sites were photographed during the second-ellipse phase of the flight. Listings of camera-on times and attitude maneuvers for the primary-site photos and information on film-set frames is presented in Section 2.3. Photo analysis using state vectors near the photo times, as determined by the OD group in postmission analysis, indicates that all primary site photos were within acceptable lighting angle bounds (see Figure 3.4-38). The accuracy in predicting primary-site photo coverage using the same postmission data in comparison with real-time predictions is shown in Figure 3.4-39. These errors resulted from small differences in state vector determinations and small timing errors from the mean element trajectory program used to compute the trajectory during the mission. Site I-3 is an example of a gross camera-on timing error of approximately 16 seconds. Following Site I-3 the timing error was reduced by forwarding state vectors to within one orbit of the photo site using an integrating trajectory program, thus limiting use of the mean element program to less than one orbit revolution. Accuracy of photo coverage will not be finally known until the pictures have all been located on a selenographic grid. Preliminary analysis of several of the pictures has already indicated deviations from the photo trajectory analysis estimates.

Second-Transfer Design and Execution

The unscheduled second-transfer maneuver was made with the hope that better quality high-resolution photographs might be obtained. It was hypothesized that a higher V/H (velocity to altitude) ratio would eliminate the high-resolution camera problem. There were also indications that the Moon had an average radius 2 to 4 km lower than the nominal 1738 km. . On the basis of these considerations it was decided to lower the perilune altitude by performing a second-transfer maneuver.

The requirements for the second transfer were:

1) Design an orbit-adjust maneuver for execution on SEAL Orbit 30.

2) Design the maneuver so that the maximum possible V/H is achieved at all targets without danger of exceeding the maximum allowable, 0.05 radian per second.

3) Account for the surface elevation at each of the sites as estimated by NASA and listed below.

4) Observe the minimum engine burn-time constraint, $\Delta V \geq 2.5$ meters per second.

5) Allow 10 minutes after earthrise before maneuver so that a real time thrust terminate command can be loaded and used if necessary.

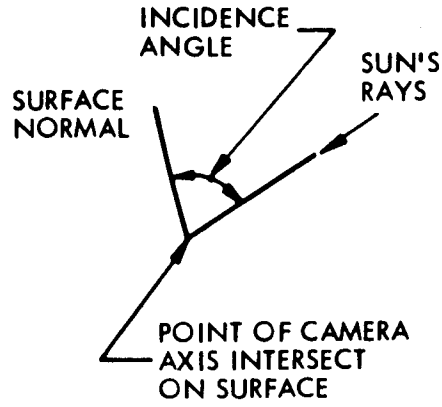

LIMITS: REFER TO D2-100388-3 FOR NOMINAL, ADD ±3.5 DEGREES

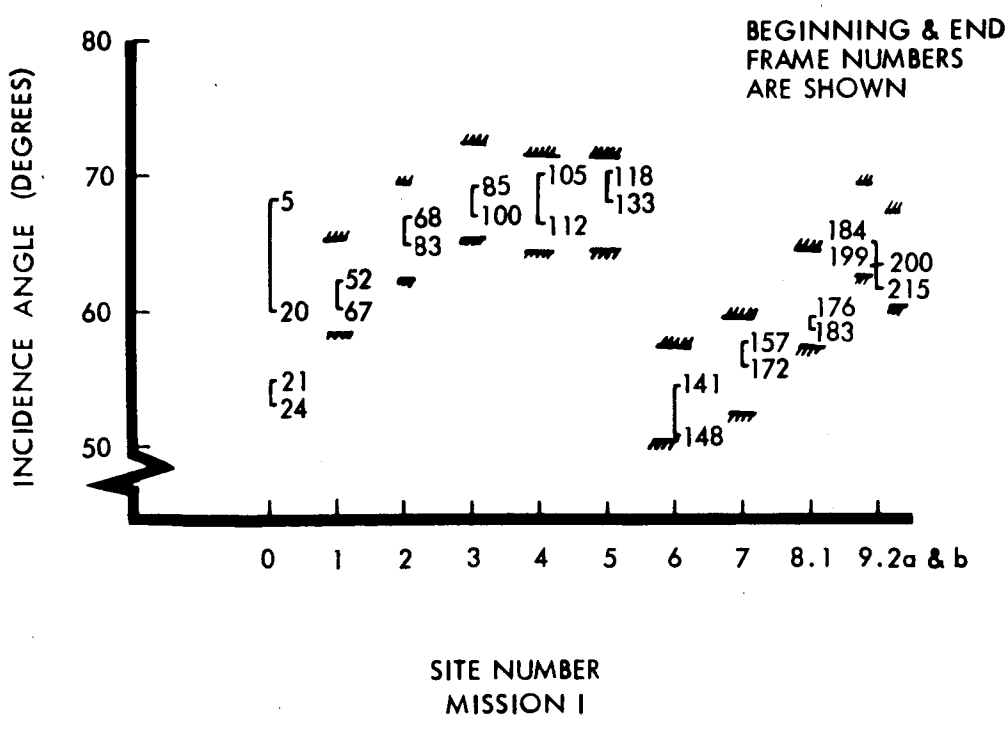

FIGURE 3.4-38: PHOTO QUALITY — INCIDENCE ANGLE

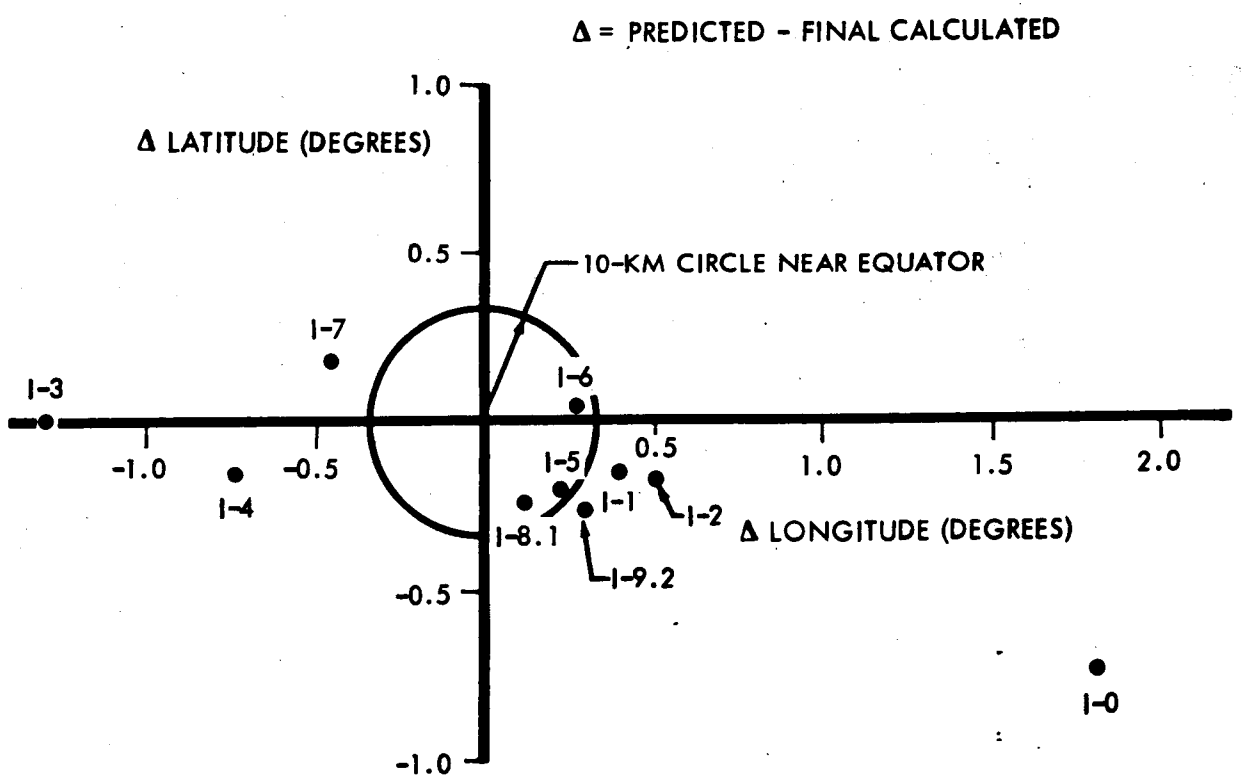

FIGURE 3.4-39: ACCURACY IN PREDICTING "I" SITE COVERAGE

The radii to the lunar surface given by NASA for each remaining site were:

Site I-6	1743.0 km
I-7	1740.5 km
I-8.1	1738.0 km
I-9.1	1739.5 km

The OD 4138 lunar harmonics were used for the design of the second transfer. The state vector used in the design was OD Solution 5128 (SEAL Orbit 22).

The second transfer maneuver could be described as an "orbit adjust" maneuver. It was found to be extremely sensitive to thrust misalignments at ignition. For this reason it was decided to perform the attitude maneuver while in the Sun shadow, to avoid any possible spacecraft reflections into the Canopus tracker. The attitude maneuver could then be initiated while the star Canopus was in the tracker field of view, and roll error would be minimized.

Sun-Earth-Moon geometry and orientation of the second ellipse during SEAL Orbit 30 are shown in Figure 3.4-40. To execute the maneuver in the Sun shadow and have at least 10 minutes of tracking beforehand the maneuver had to be performed between 226 to 303 degrees true anomaly.

For the first cut at designing the second transfer maneuver, perilune radius, inclination, and latitude were used as targeting parameters. This set of parameters had been successfully used in the design of the first transfer maneuver. However, after examining data over the true anomaly range of interest, it was observed that the apolune radius would vary in an undesirable manner. Targeting parameters were then changed to perilune radius, inclination, and semi-major axis to hold apolune radius to the desired value. This set of targeting parameters resulted in a transfer design for a third ellipse that closely maintained the perilune trace and lighting angles at the targets. In addition to reducing the perilune radius by 9.5 km, the transfer maneuver was designed to reduce the apolune radius by 37 km. This was done for two reasons:

1) To raise the maneuver ΔV well above the 2.5 meters per second minimum burn ΔV.

2) To decrease the ratio of time in Sun to time in shadow in third ellipse, and thus slightly alleviate excessive spacecraft temperature.

Final design of the second transfer was targeted to:

Perilune radius	1778.0 km
Semi-major axis	2670.0 km
Inclination	12.025 degrees
Transfer true anomaly	268.21 degrees

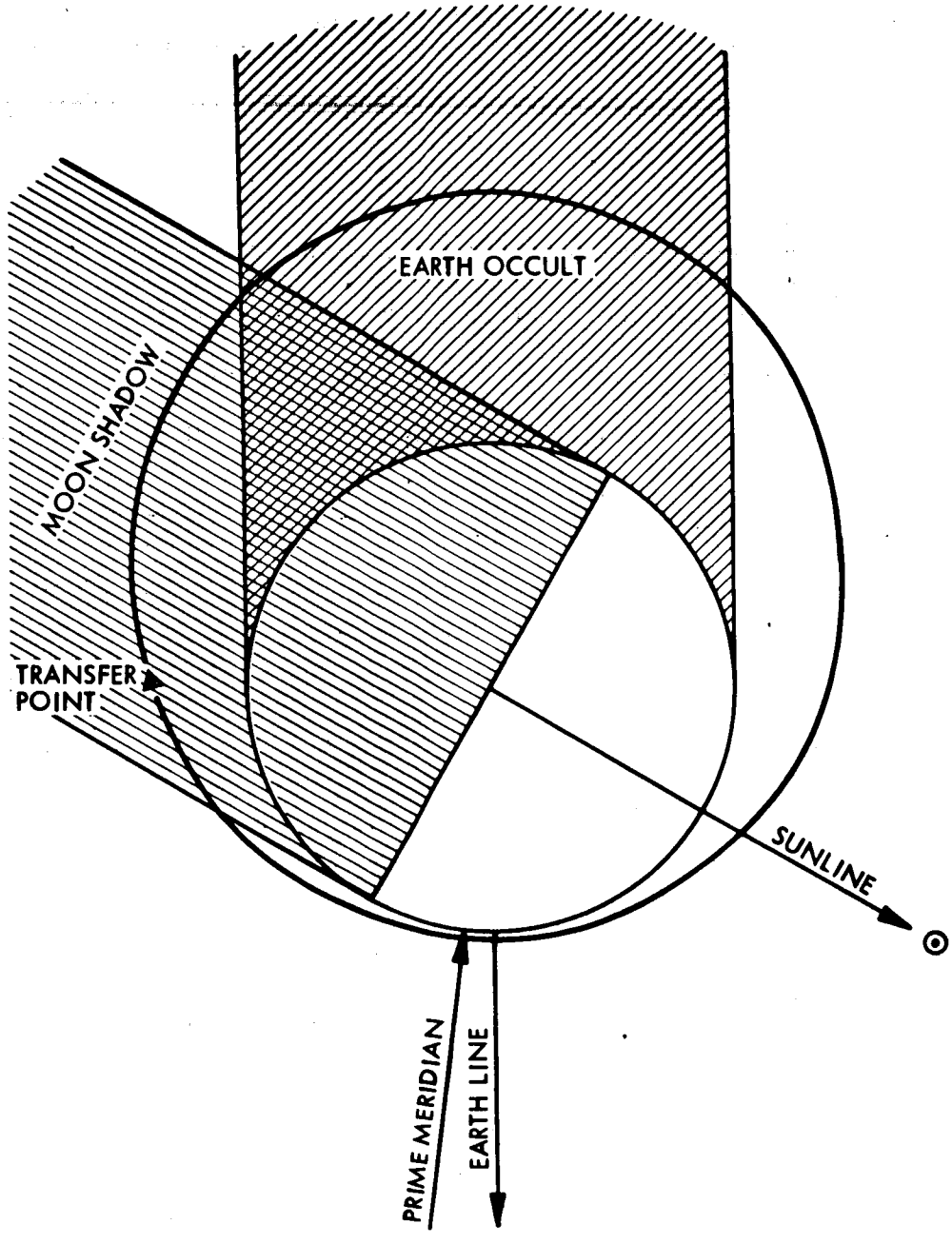

FIGURE 3.4-40: GEOMETRY AND ORIENTATION OF SECOND ELLIPSE — ORBIT 30

The resulting transfer maneuver required a ΔV of 5.43 meters/second and engine ignition at Day 237, 16:01:29.2 GMT. This time was 37 minutes after Earthrise and 14 minutes before Sunrise. The attitude maneuver to align the engine axis with the required ΔV direction was:

Roll	34.28 degrees
Pitch	-129.76 degrees

Because this maneuver was performed in the Sun shadow, the first maneuver was roll about the IRU roll axis rather than the usual sunline roll. The selected attitude maneuver represented a minimum total rotation angle with all antenna constraints satisfied.

Predicted conic elements before and after the second transfer engine burn were:

ELEMENT	PRE-TRANSFER	POST-TRANSFER
R_a	3599.0 km	3562.0 km
R_p	1787.5 km	1778.0 km
i	12.025 degrees	12.025 degrees
ω	185.00 degrees	186.03 degrees
Ω	176.18 degrees	176.72 degrees

Figures 3.4-41 and 3.4-42 illustrate the effects of the second transfer maneuver on the photo coverage of the remaining four sites (I-6, I-7, I-8.1, I-9.1). Figure 3.4-41 shows the perilune trace and inner and outer Sun band geometry. Figure 3.4-42 shows the effect of the transfer on lighting angle and photo altitudes.

Postmaneuver orbit determination results indicated the actual maneuver to be very close to the designed conditions. A summary of the results follows:

ELEMENT	ACTUAL	DIFFERENCE (ACTUAL - DESIGN)
R_a	3560.2 km	-1.8 km
R_p	1778.5 km	0.5 km
i	11.9 degrees	-0.125 degree
ω	185.3 degrees	-0.73 degree
Ω	177.0 degrees	0.28 degree

Third Ellipse Phase

The third ellipse phase begins at second-transfer and extends through completion of the prime mission, i.e., completion of photo readout.

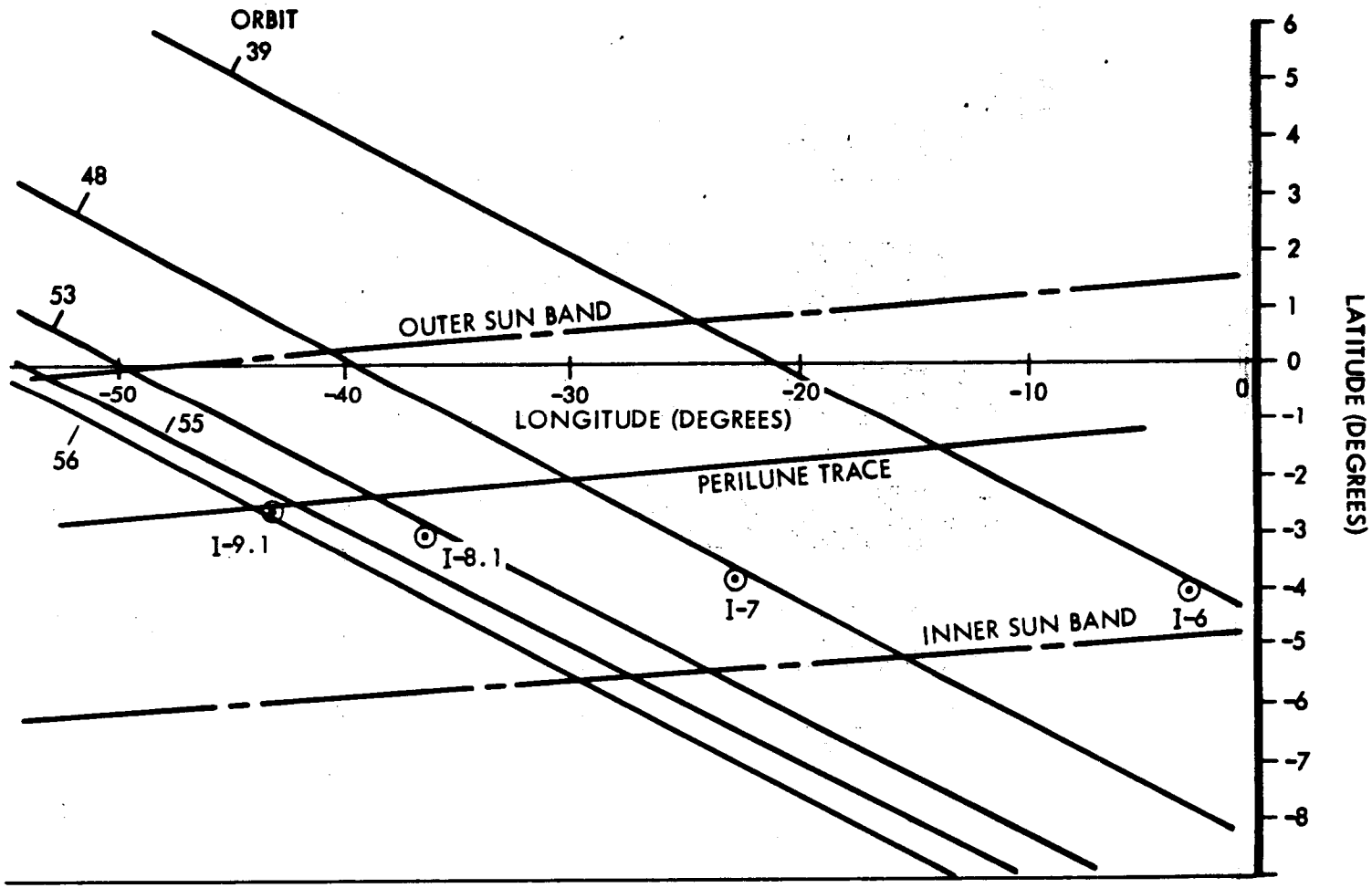

FIGURE 3.4-41: ORBIT GROUND TRACKS

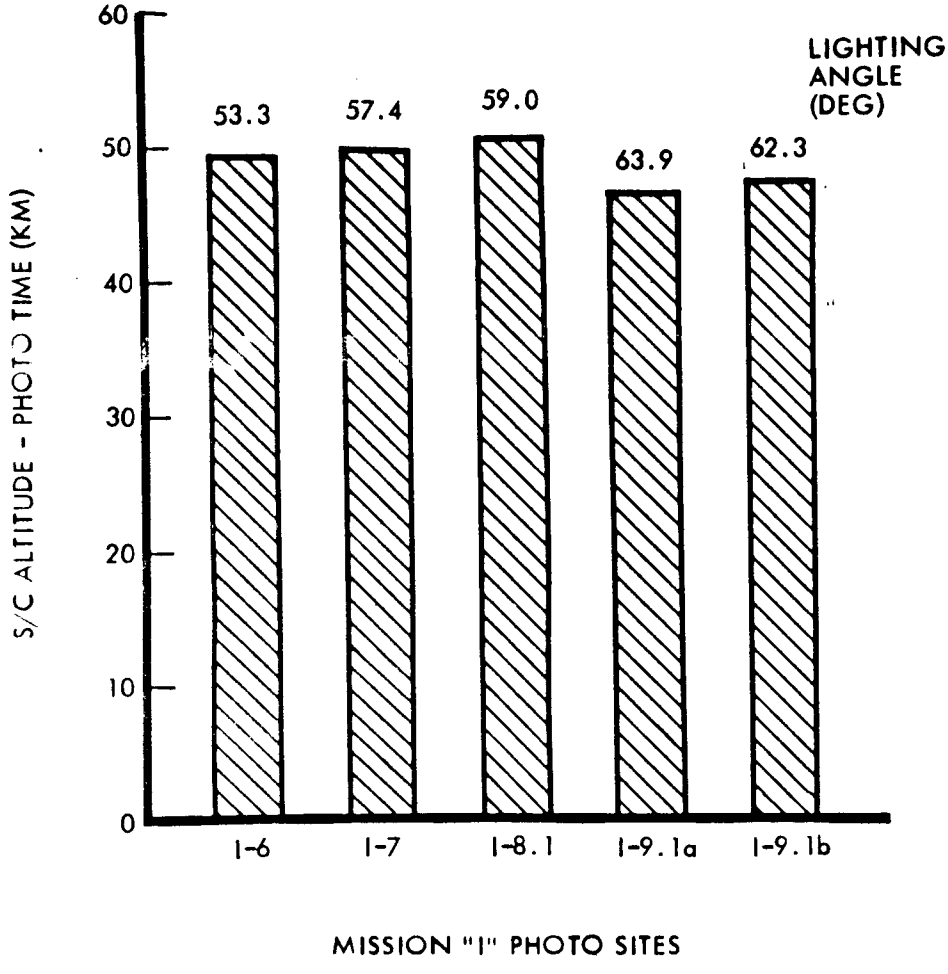

FIGURE 3.4-42: SITE PHOTO ALTITUDE AND LIGHTING ANGLE

FPAC tasks in this mission phase were:

Orbit determination prior to each photo site(I-6 through I-9.2a) to be used at the basis for ~~camera pointing commands.~~

Post photo orbit determinations for each photo site to be used for determining photo locations.

Confirmation of indefinite lifetime in this ellipse.

Once the actual photo commands were completed the high-activity portion of FPAC operations was over and the remaining tasks were routine tracking data monitoring and orbit determination. Routine orbit determination is required to keep a current trajectory file available for SPAC during the readout phase and to provide tracking predicts for the DSS.

Orbit Determination

This section includes:

1) Tracking Data Editing

2) Orbit Determinations for Photo Sites

3) Perilune Altitude Monitoring

Tracking data editing—Data types received during this mission phase were doppler and angles. The doppler data were handled as in the preceding phase with respect to the ODGX data deck adjustment values for doppler bias and station bias. In an attempt to eliminate oscillations in the residuals around perilune, data with sampling rates of 20, 30, and 60 seconds were requested and received. Data received during photo readout were flagged with a "bad data condition" code by the stations and rejected by TDPX.

After the final photo was taken--but before readout began--all tracking data used for orbit determination was obtained by processing a log tape. This resulted in short arcs of tracking data spaced considerable distances apart. Records of the input decks for the editing programs for each of these short-arc orbit determinations, or the file summaries associated with them, were not saved. (See below.)

During the extended-mission phase, the backlog of tracking data was processed and is presently contained on JPL Library tape number 9708 and LRC tape number L.T. 27, the data arc being from 16h 02m 00s 237d to 01h 00m 00s 260d. Spacecraft maneuvers and photo readout periods are listed in Appendix B.

Orbit determination for photo sites—The orbit determination program was used to process DSIF tracking data. The objective was to define state vectors as close to the photo sites as possible to minimize errors due to extrapolating these state vectors with the lunar model.

The general procedure used for this OD work follows:

1) Two orbits including C3 and CC3 data were processed of a two-station view period (if possible). The data within 30 minutes of perilune were excluded, resulting in a 1-hour data gap in addition to the photo readout and occultation data gaps. A data weight of 0.1 cps was used for both C3 and CC3.

2) Parameters solved for were:

   a) State vector;

   b) Harmonics, if the fit was improved by their inclusion.

3) An a priori covariance matrix tight enough to insure convergence but loose enough to avoid unnecessary constraint on the solution was used.

4) Lunar potential model defined by OD 4138 was used.

The orbit determination runs used to design spacecraft maneuvers for third-ellipse photos are shown below. Figure 3.4-43 and 3.4-44 are summaries of the data processed and final results.

PHOTO SITE	OD NO.	FIGURE
I-6	6106	3.4-43
I-7	6114	3.4-44
I-8.1	6114	3.4-44
I-9.2a	6114	3.4-44
I-9.2b	6114	3.4-44

Perilune altitude monitoring—In addition to the orbit determination discussed above, other orbit determinations were made for routine purposes. These determinations are summarized in Appendix B; a plot of perilune altitude is shown under "Orbital Characteristics."

Cyclic doppler residuals near perilune—The phenomenon of large cyclic doppler residuals near perilune mentioned earlier continued during this mission phase.

An experiment to evaluate the theory that the doppler count sample rate was too short was performed early in this mission phase by the DSN tracking data quality evaluation team. Results were negative.

MISSION PHASE THIRD ELLIPSE WORK SHEET

OD Identification Number 6106

Time of Run _____ Item Number _____

Epoch of Solution 66/08/26 $04^h\ 19^m\ 00^s$

Converged Solution and Statistics (selenocentric mean 1950.0 coordinate)

	State Vector		Std. Dev.		A Priori Std. Dev.	
X	-1004.0889	km	0.23	km	1.0	km
Y	-3037.6601	km	0.51	km	1.0	km
Z	-1421.7333	km	0.86	km	1.0	km
DX	0.86848350	km/sec	0.90×10^{-4}	km/sec	10×10^{-3}	km/sec
DY	-0.45507082	km/sec	0.10×10^{-3}	km/sec	10×10^{-3}	km/sec
DZ	0.054948420	km/sec	0.20×10^{-3}	km/sec	10×10^{-3}	km/sec

Corresponding Orbital Parameters (selenographic true of date coordinate)

a	2669.7949	km	e	0.33346385		ω	184.80566	deg
Ω	170.99043	km	i	12.735644	deg	T_p	+5232.2797	sec
r_p	1779.51	km	r_a	3560.08	km	P		min
h_p	41.42	km	h_a	1821.99	km			

Other Parameters in the Solution Vector

C33
C43
C44
S33
S43
S44
DS(12)
DS(13)

These parameters were included in the solution vector only to aid data fit. Therefore, the values to which they converged are not summarized here, since the data arc was too short for the values to be significant in themselves.

Number of Iterations 1 after a restart Converged SOS 1.5

Data Summary:

STA. NO.	DATA TYPE	START	TIME	STOP	TIME	NUMBER OF POINTS	STD. DEV.	FIRST MOMENT	SECOND MOMENT
12	CC3	8/25	23:59	8/26	04:12	119	0.016	-0.79×10^{-3}	0.25×10^{-3}
61	C3	8/25	23:59	8/26	00:12	27	0.027	-0.18×10^{-2}	0.71×10^{-3}

Comments: The state vectors (cartesian and conic) resulted from mapping the converged conditions at 66/08/25 $23^h\ 59^m\ 00^s$ forward with the 4138 harmonics. The statistics, however, apply at the original epoch. This solution fits the data very well and was used for calculation of Site I-4 photos.

Figure 3.4-43:

MISSION PHASE THIRD ELLIPSE WORK SHEET

OD Identification Number 6114

Time of Run _____ Item Number _____

Epoch of Solution 66/08/26 $20^h\ 30^m\ 00^s$

Converged Solution and Statistics (selenocentric mean 1950.0 coordinate)

	State Vector		Std. Dev.		A priori Std. Dev.	
X	-2189.1881	km	0.21	km	1.0	km
Y	319.41015	km	0.45	km	1.0	km
Z	-345.12110	km	0.72	km	1.0	km
DX	-0.69027104	km/sec	0.26×10^{-4}	km/sec	10×10^{-4}	km
DY	1.2552936	km/sec	0.21×10^{-3}	km/sec	10×10^{-4}	km/sec
DZ	-0.64734511	km/sec	0.39×10^{-3}	km/sec	10×10^{-4}	km/sec

Corresponding Orbital Parameters (selenographic true of date coordinate)

a	2669.8872	km	e	0.33356190		ω	186.00848	deg
Ω	161.27963	deg	i	11.979195	deg	T_p	1603.3628	sec
r_p	1779.314	km	r_a	3560.46	km	P		min
h_p	41.22	km	h_a	1822.37	km			

Other Parameters in the Solution Vector

C42 DS (13)
C33
C43
C44
S42
S33
S43
S44

Number of Iterations _____ Converged SOS 171

Data Summary:

STA. NO.	DATA TYPE	START	TIME	STOP	TIME	NUMBER OF POINTS	STD. DEV.	FIRST MOMENT	SECOND MOMENT
61	C3	8/27	00:34	8/27	00:44	21	0.014	0.0025	0.0002
	CC3	8/26	20:31	8/27	00:24	255	0.12	-0.011	0.014
12	C3	8/27	00:15	8/27	00:25	12	0.007	0.22	0.048
	CC3	8/27	00:32	8/27	01:04	58	0.035	0.11	0.014

Comments: A 300-minute data arc was processed for this solution. The state vector was solved, alone, over a 60-minute arc to convergence. The data arc was then increased to 240 minutes and the parameters noted above solved for. Data within ±20 minutes from perilune was eliminated to obtain the converged solution. This solution was believed to be fair because of the short data arc and meager amount of two-station view time. Along with the 4138 harmonic coefficients, this state was used for Site I-7, I-8.1, I-9.2a, and I-9.2b photos.

Figure 3.4-44:

At the end of the mission (September 15) an experiment was performed with the orientation of high- and low-gain antennas to evaluate the theory that reflections from the lunar surface were causing the perilune residuals. Preliminary results were negative. A full report on the tests is given in Boeing Document D2-100719-1, Early Post-Photo Mission Tests with Lunar Orbiter I.

Orbital Characteristics

A summary of the perilune altitude variation as determined by OD solutions at epochs after the second transfer is shown in Figure 3.4-45. This is a curve of the actual perilune altitude, as closely as can be determined to Day 279. An indefinite lifetime is again predicted.

Third-Ellipse Photography

The photographic portion of Mission I was concluded during the third-ellipse phase of the flight with the exposure of 70 frames of film. Actual camera-on times and attitude maneuvers are contained in Volume II of this document. A summary of the photography during the third ellipse follows:

FRAME NUMBERS	TYPE OF PHOTO
134, 135	Film Set Nearside
136	Film Set Farside
137, 138, 139, 140	Film Set Nearside
141 thru 148	Site I-6
149, 150, 151, 152, 153 thru 156	Film Set Nearside
157 thru 172	Site I-7
173, 174, 175	Film Set Nearside
176 thru 183	Site I-8.1
184 thru 199	Site I-9.2a
200 thru 215	Site I-9.2b

After transfer to the third ellipse, film-set Frames 134, 135, 136, 137, and 138 were exposed before a post-transfer state vector was available. In designing the camera-on time for these film-set frames, the predicted post-transfer state vector was used along with OD 4138 lunar harmonics. These harmonics were used for all photo analysis in the third ellipse.

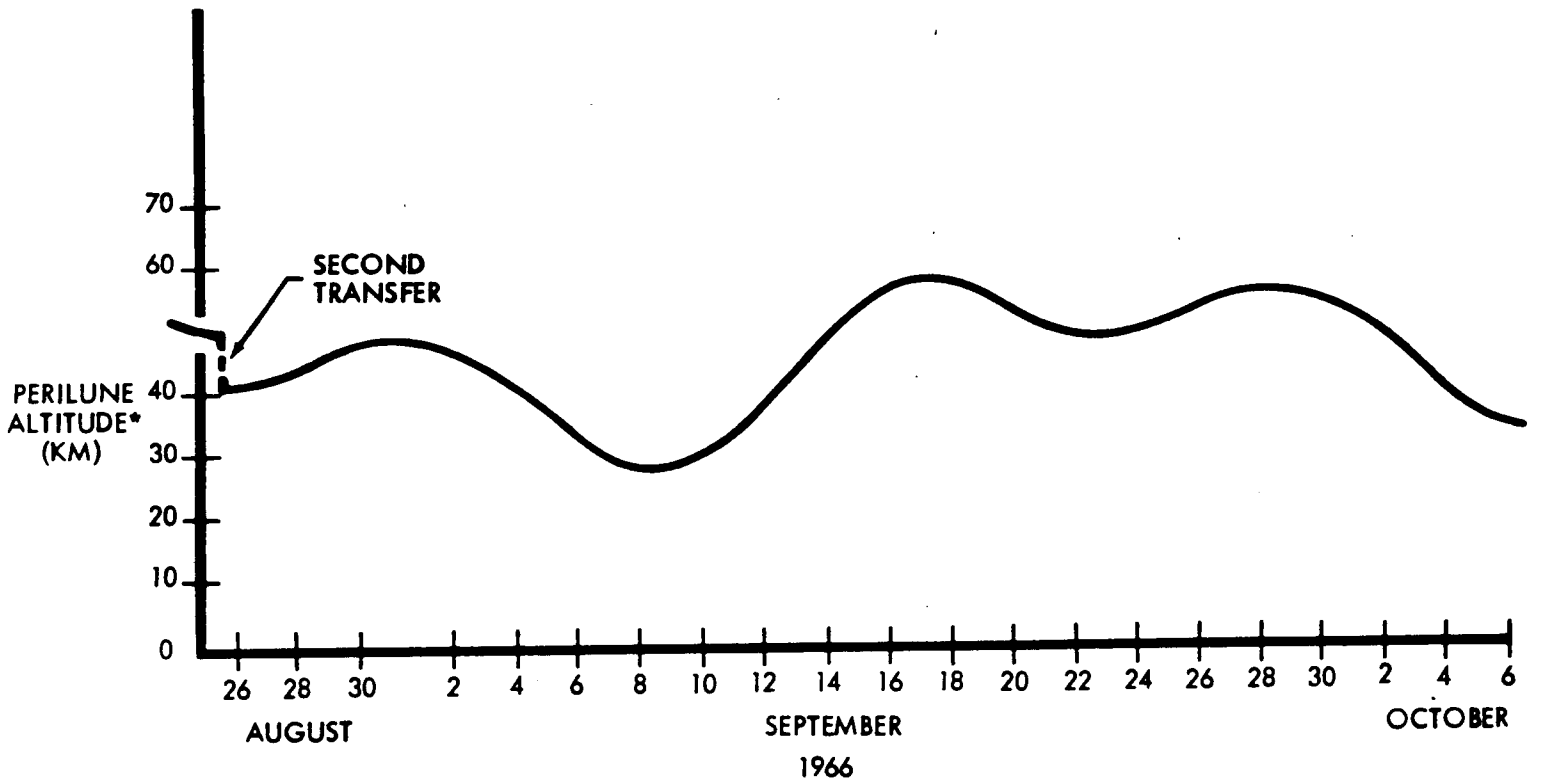

*WRT 1738 KM RADIUS SURFACE

FIGURE 3.4-45 : THIRD-ELLIPSE PERILUNE HISTORY

Film-set Frame 136 was a farside photo requiring a 180-degree roll maneuver. Frames 149 and 152 were designed to photograph the same lunar area (Site II-9) with 100% side lap for a stereo effect. Frame 152 required a 28-degree roll maneuver to obtain the desired sidelap. Frame 151 was exposed while pitched 16 degrees off the Sun for temperature control purposes. All other film-set photos during this phase were near perilune and required no attitude maneuver.

The final four primary photo sites were photographed in the third ellipse with the last site (I-9.2) being photographed on two successive orbit passes. The point target for Site I-9.2 was modified from the premission point target upon direction from the mission advisors prior to designing the camera-on time and attitude maneuvers for the Site I-9.2 photos. Volume II of this document contains detailed information on the camera-on times and attitude maneuvers for all photos taken during third-ellipse.

The discussion of the accuracy of primary site photography preceding includes the primary sites covered in the third ellipse.

Spacecraft Control

Spacecraft control was maintained by the Spacecraft Performance Analysis and Command (SPAC) Organization which was located at the SFOF. Its function was to monitor spacecraft performance throughout the mission, and using telemetry data and information from FPAC, prepare and encode command sequences to fulfill a specified set of spacecraft functions and analyze the effects of these commands on the spacecraft performance and capability.

Several identifiable mission activities imposed unique tasks on the SPAC organization, as follows.

Prelaunch

The duties performed during the prelaunch phase consisted mainly of computer initialization at the SFOF, checkout of communications facilities and telemetry displays, and preparation of stored program commands to be loaded into the spacecraft via DSS-71 before launch. Initialization of the computers involved inputting all calibration coefficients in the IBM 7094 and 7044 computers for the current spacecraft configuration and other inputs for the user programs that were fixed at that time. User programs, displays, and data handling were checked using simulated data to verify the operational readiness of the facility.

Analysts monitored spacecraft telemetry data as it became available from DSIF-71 and, via the SPAC director, maintained liaison with DSIF-71 to ensure that the data was being received, processed, and displayed satisfactorily. Following launch, the GMT at liftoff and any bias between the spacecraft clock and liftoff time were entered into the user programs.

Cruise

Functions performed during that portion of cislunar cruise, which is characterized by no programmed events taking place in the spacecraft, were primarily those of monitoring telemetry data, making periodic status reports, and performing analyses, as required, to maintain spacecraft status. The analyses consisted primarily of periodic evaluation of gas consumption, limit-cycle operation of the attitude control subsystem, thermal performance, and updating the analysis program inputs from the telemetered data.

During the cruise phases in lunar orbit, the functions were similar to those during the cislunar phase, except that analysis programs to update the battery charge status and thermal status were run at more frequent intervals because of the Sun occultation periods, which produce wider variations. During Earth occultation, no telemetry data was received and user programs for updating the battery charge and thermal status programs were run without interfering with operations. In addition to these functions, periodic reporting of spacecraft status and preparation of commands for Sun occultation and antenna orientation comprised the major activities during this phase.

Maneuvers

The activity in the SPAC area during maneuvers consisted of review and analysis of the command sequences for the maneuver, monitoring of real-time data during the maneuver, and analysis of the spacecraft performance after the maneuver was completed. The analysis of the command sequence was performed substantially before execution of the maneuver.

The maneuver requirements were generated in FPAC and included the magnitude of the angles, the ΔV required, and the time to start engine burn. From these data a maneuver command sequence was generated by the SPAC command programmer specialist. During this operation, a subsystem event sequence was prepared for use with analysis programs. The analysis and review of the maneuver consisted of: (1) a prediction of the battery charge and power subsystem status throughout the maneuver; (2) a prediction of the thermal status at key points in the spacecraft during the maneuver; (3) a plot of the spacecraft/DSIF vector on the low-gain antenna pattern to identify points of passage through nulls; and (4) a general review by the subsystem analysts and SPAC director to verify the capability of the spacecraft to perform the maneuver. As a result of the review, a maneuver sequence acceptable to the FPAC and SPAC directors and the SFOD was selected for encoding and transmission to the spacecraft.

Prior to the time of a maneuver, the appropriate telemetry display formats were selected and the plotters were energized. A spacecraft status report by the subsystem analysts was made to the SPAC director, who certified to the SFOD that the spacecraft was ready for the maneuver. During the maneuver, the flight programmer analyst and the attitude control analyst called off the events as they occurred. The maneuvers were observed via the plotters and teleprinters to verify the spacecraft maneuver. System analysts closely observed the data for abnormal conditions. During the engine burn a 60-wpm printer in FPAA No. 2 was used to display tracking data from the DSIF, to verify engine firing. In addition, near-real-time plots of the tracking data were prepared manually by FPAC analysts for comparison with computer-generated predictions.

Upon completion of the maneuver, the spacecraft telemetry was monitored and a spacecraft status report was made, including an estimate of the maneuver performance. Data formats for the cruise mode were selected, the programmer memory record was updated by the command programmer specialist, and analyses of the maneuver were performed. These included the maneuver error analysis, the ΔV capability remaining, and a comparison of the measured versus predicted values for the communications, power, and thermal subsystem. The time of significant events and the results of the analyses were logged as part of the daily summary report.

Command Preparation and Loading

One of the primary activities of SPAC was command encoding in spacecraft programmer language, command approval, and command transmission to the spacecraft. The command was assembled in a GMT sequence, which was then converted to spacecraft time and coded in programmer symbolic language for insertion into the command generation program. The time conversion operation was accomplished using the spacecraft time/GMT correlation program. The primary functions of the command generation program were to assemble the command sequence, verify that it was compatible with the flight programmer, and place it on disk in a format compatible for teletype transmission to a DSS. The command programmer specialist prepared the inputs to and analyzed the outputs from the above programs. All pertinent information was presented at a command approval conference to obtain SFOD authorization to transmit the command.

The transmission of commands was initiated by the command coordinator upon direction of the SFOD. Outgoing commands were displayed on an administrative printer and the SC 3070 in an octal format whereby the command coordinator and command programmer specialist could compare the transmitted sequence with the original command. A punched paper tape on the teletype line was also available in Mission Support Area Number 2 for a bit-by-bit comparison of the data actually sent over the teletype line.

The command programmer specialist supported the command coordinator during command transmission by monitoring the telemetered verification of the command, using selected display formats on a 100-wpm teleprinter. The command programmer specialist also updated the manually maintained core map as each command was inserted in the flight programmer. Upon completion of the command loading, a programmer simulation was run to update the computer core map. The updated core map then became the current map from which all future programming was done.

A flight programmer breadboard was located in the SPAC area to "follow" the mission in real time from launch countdown through the end of photo readout. As each command sequence was sent to the appropriate DSS, a paper tape was being punched in the MSA No. 2 area. When the command sequence was transmitted to the spacecraft, the tape was inserted into the programmer breadboard. During Earth occultations, the operation of the flight programmer was followed at the SFOF by observing breadboard performance.

Before the mission, when the countdown commands and Mode 2 commands were sent to the DSIF, these commands were punched on paper tape as they were being sent and were then checked on the programmer breadboard. During one of the prelaunch countdown exercises with the spacecraft, the storage of an extra command in the programmer following the issuance of a Ranging ON or OFF command was discovered. The breadboard was following the exercise at the time; since it did not exhibit this extra storage, the search was shifted from the command sequence to some other spacecraft subsystem. The cause of this problem was determined to be a momentary loss of the uplink lock due to a power transient initiated by the issuing of RF ON, RF OFF, Ranging ON or Ranging OFF. This loss interrupted the ENABLE and EXECUTE tones. After the momentary lock loss, these tones were reestablished but the command had been shifted out of the command decoder leaving all zeros. The return of the EXECUTE tone caused the programmer to store the "all zero" command in the memory.

Photo sequence—The SPAC functions during this phase were similar to the maneuver phase except that a photo sequence was executed instead of a velocity change. In addition to monitoring the maneuver, the execution of the photo function was observed and recorded. The status of the camera looper, take-up reel, platten operations, and shutter counts and setting were recorded in the photo log to aid in correlation of the readout with the frame numbers and to keep track of where specific photos were located in the film roll. The photo subsystem was monitored by the photo subsystem analyst and the photo data analyst to maintain close cognizance of camera operations and environmental conditions. The V/H ratio was also recorded and supplied to FPAC for correlation with trajectory data. Following the photo sequence, an error analysis of the photo maneuver was performed to supply camera pointing error data to FPAC for determination, at a later date, of the location of the photographs relative to the lunar coordinates. The photo acquisition specialist in the SPAC area was responsible for recording all pertinent data in the photo status log, to serve as supporting information for mission control and subsequent photo evaluation.

Photo Readout—This phase required close liaison with the DSIF and extensive use of real-time commands to control the photo readout. Prior to photo readout, a series of commands was stored in the flight programmer to prepare for, and terminate, each photo readout period. Initiation of photo readout and adjustment of readout functions were done by a series of real-time commands to the spacecraft. Readout was terminated by commands stored in the flight programmer.

Before readout initiation, the status of the spacecraft subsystems were monitored and reported to the SPAC director. The high-gain-antenna position was checked by telemetry data and the signal margin prediction program was run to establish the optimum antenna position, the antenna pointing error, and the signal margin expected. Real-time commands were sent to the spacecraft, as necessary, to adjust the high gain antenna orientation to correct for differences between the telemetered position and the desired position. All commands were handled in the manner previously described except that these commands did not require preparatory analysis, as in the case of a maneuver sequence.

Following execution of readout preparation stored program commands by the spacecraft flight programmer, the SPAC director and the photo data analyst provided support as necessary to the senior Lunar Orbiter engineer at the applicable DSS, relative to interpretation of video data and the origination of adjustment and readout initiation commands. During readout operations, direct voice contact between the photo data analyst and the DSS video engineer was maintained. Periodically the video engineer provided SPAC with framelet numbers and exposure times obtained from processed film to facilitate data correlation activities.

Subsystem performance was closely monitored during readout, particularly in the area of communications, electrical, thermal, and photo subsystems to detect any abnormal condition that would result in damage or degradation to any part of the spacecraft. Display formats for readout were selected prior to entering this mode.

Photo data readout between photo passes was limited by subsystem constraints to one photo frame per orbit. After all photography was completed, photo data readout was between 2.00 and 2.37 frames per orbit. The turn-on and turn-off times of the GRE camera were logged and transmitted to the SFOF, where the photo acquisition specialist recorded and correlated the information with telemetered film footage data to determine the film frames which were read out.

ASSESSMENT SUMMARY OF LUNAR ORBITER I ANOMALIES

SEPTEMBER 7, 1966

MATERIAL PRESENTED BY THE BOEING COMPANY

Revision "A" Updated and Incorporated Final Action for Second Flight Readiness Review on October 17, 18, and 19, 1966

PRECEDING PAGE BLANK NOT FILMED.

CONTENTS

	Page
Thermal Control	3
Pressure Transducer	8
Velocity Control Regulator	10
Canopus Star Tracker	11
Relief Valve	24
Modulation Index	24
Transponder Double Execute Problem	26
Transponder Telemetry Power Change	27
Power Transistor Failure	29
Photo System	33
RF Signal Level Drop	34

PRECEDING PAGE BLANK NOT FILMED.

THERMAL CONTROL

STATEMENT OF PROBLEM

During the Lunar Orbiter I flight, EMD temperatures were rising at a faster rate than anticipated on the basis of the B-1056 white thermal control coating UV-irradiation tests. It is believed that the B-1056 coating is degrading at a higher rate than predicted.

HISTORY OF PROBLEM

Some of the Boeing and JPL test data, and the Pegasus and OSOS flight data indicates that the paint degradation after 150 sun hours degrades at a faster rate than the predicted values presently used for analysis of Lunar Orbiter I flight data. At present, there is no explanation for the observed variations from the predicted values.

STATUS OF ACTION

Three courses of action were initiated as follows:

1) Peak temperatures were taken from the TWX data for the three deck locations (ST01, ST02, and ST03) and plotted to verify the SPAC findings.

2) A computer run was made for Orbit 36 using the α/ϵ data received from SPAC, the present orbital trajectory, and readout mode to get temperature data for comparison.

3) A discussion was held with Materials and Processes (M & P) Research, Kent to determine the state of the art at TBC regarding the use of second surface mirrors to lower temperatures on future spacecraft (per request from G. W. Hettrick).

The results of the Item (1), above, are shown in the attached graphs. Superimposed on these peak data are plots of anticipated temperature rise resulting from B-1056 degradation as determined from the first in situ development tests. Examination of these graphs indicates that the temperature rise appears to be in excess of that anticipated.

The results of Item (2), above, indicated that the ST01 (TWTA) temperature was 3.6°F cooler, the ST02 (transponder) temperature was 9.6°F warmer, and the ST03 (IRU-Canopus-Programmer) temperature was 7.7°F warmer than predicted by the computer run.

Discussion with M & P Research, Kent (Item 3 above), involved both second surface mirrors and an overlay of a modified B-1056 paint. In regard to second surface mirrors, these can be purchased from Optical Coating Lab, Santa Rosa, California, to a LMSC specification. They are about 1 x 1 x 0.008 inch with silver

deposited on the fused silica, and Inconel deposited over the silver. They are attached to a prepared metal substrate with LTV-615 silicone. They could be attached to the EMD after removal and cleaning of the B-1056, but a more practical approach would be to attach them right over the B-1056 where desired. This, however, involves the problem of catalyst interaction, the LTV-615 catalyst being sensitive to the SRC-05 catalyst used in the B-1056 silicone vehicle (RTV-602). The reason the LTV-615 is used for an adhesive to attach the mirrors rather than the RTV-602 is because the latter tarnishes the silver.

In regard to the modified B-1056, a new coating has been under development using RTV-602 with a TMG catalyst. Using this coating (0.002 in.) over our present B-1056 (0.008 in.) results in about a 0.02 improvement in α_s degradation in 850 ESH. However, this has not been verified by α_s measurements in vacuum; i.e., after irradiation the specimens have always been withdrawn from vacuum and measured in air because of TBC equipment limitations.

RECOMMENDED ACTION

1. Evaluation of the Lunar Orbiter I temperature data versus predicted temperature data should be continued.

2. Additional computer runs should be made to determine temperature differences between actuals and calculated.

3. First, develop a method to use the second surface mirrors over the B-1056 white coating. Experiment with glass slides to work out the LTV-615 adhesive system. Purchase some second surface mirrors. Prepare a panel with the mirrors and run vibration tests.

   Second, prepare a standard B-1056 specimen and overcoat it with 0.002 in. of B-1056 using TMG catalyst. Arrange to have it tested in situ at Hughes Aircraft Company to determine its degradation under UV in vacuum.

4. Until such time as permanent corrective action can be ascertained to correct for paint degradation, plan to fly the Lunar Orbiter II mission "off-Sun" when required to provide temperature control for equipment mounted on the EMD.

FINAL ACTION

Evaluation to date has shown the degradation of the EMD paint is above normal. Testing of two other paints, namely B-1059 (Boeing) and S-13G (Illinois Institute of Technology), overcoated on the EMD paint indicate a reduction in degradation. Only the S-13G paint has adequate time in situ testing to establish an improvement in spacecraft temperatures. The absorptance (α_s) values of the paints are shown on the attached graph.

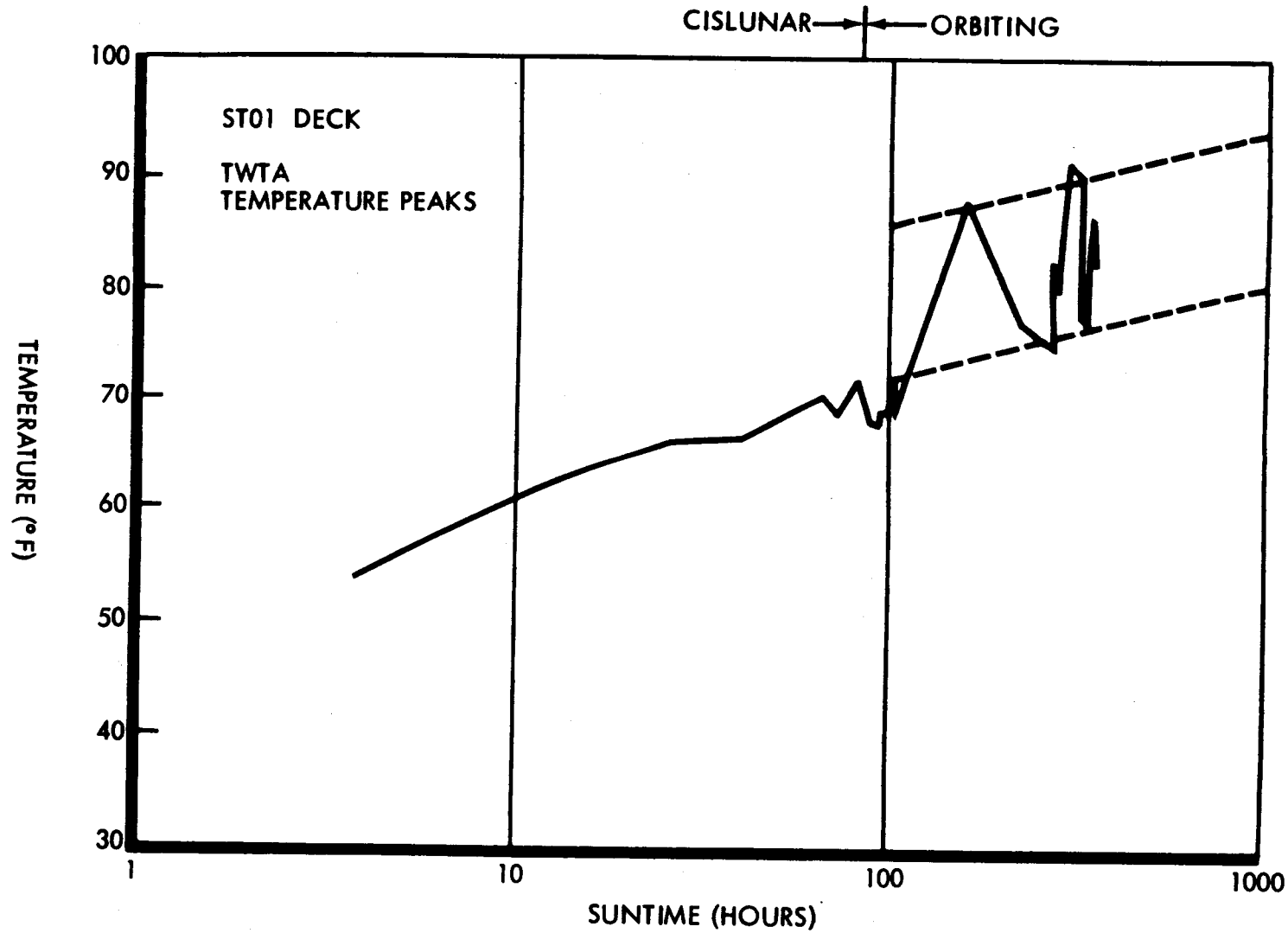
CISLUNAR
ORBITING
ST01 DECK
TWTA
TEMPERATURE PEAKS
TEMPERATURE (°F)
100
90
80
70
60
50
40
30
1
10
100
1000
SUNTIME (HOURS)

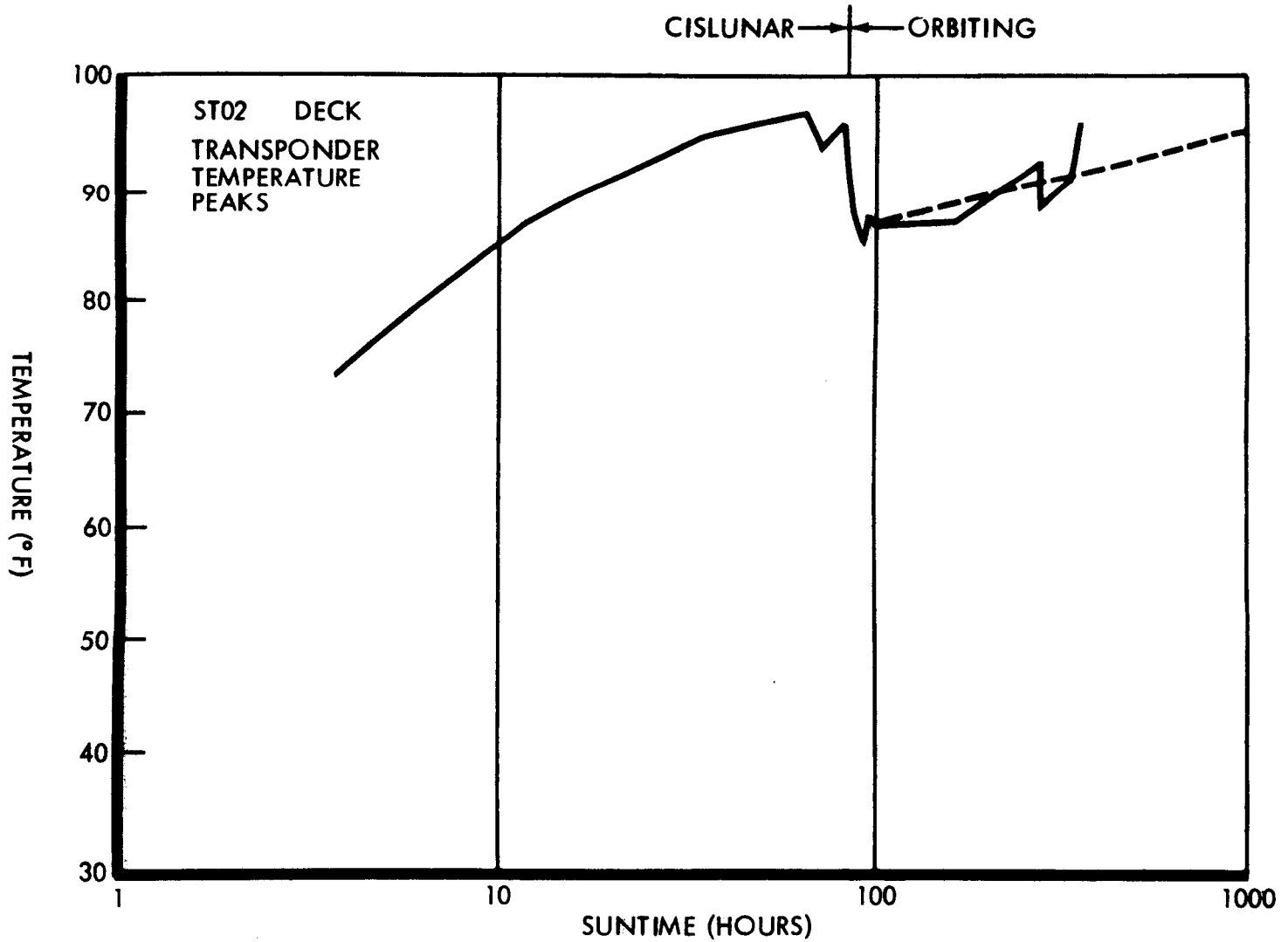
CISLUNAR
ORBITING
ST02 DECK
TRANSPONDER
TEMPERATURE
PEAKS
TEMPERATURE (°F)
100
90
80
70
60
50
40
30
1
10
100
1000
SUNTIME (HOURS)

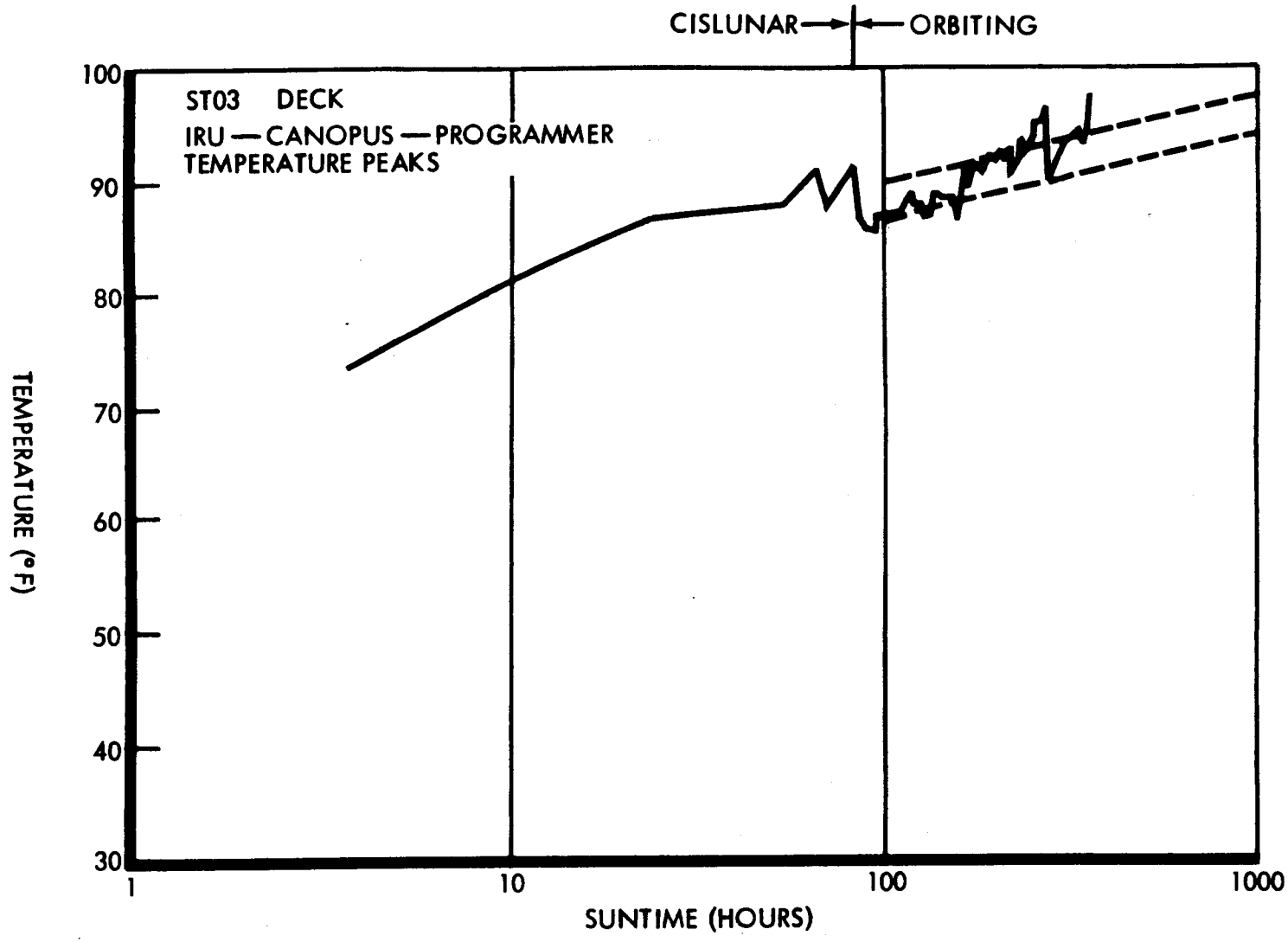
CISLUNAR
ORBITING
ST03 DECK
IRU — CANOPUS — PROGRAMMER
TEMPERATURE PEAKS
100
90
80
70
60
50
40
30
TEMPERATURE (°F)
1
10
100
1000
SUNTIME (HOURS)

An improvement of approximately 12 degrees in temperature can be expected with the use of S-13G overcoating and preparations are underway to spray overcoat the Lunar Orbiter B and C equipment mount deck white paint. Incorporation of the overcoating is subject to peel and quick pumpdown tests to confirm adequate adhesion of the paint. The painting will be done by Illinois Institute Technology personnel at E.T.R.

In addition, four flight-tests coupons will be mounted below the E.M.D. on Lunar Orbiter B to determine absorptance degradation in flight for B-1056 (current spacecraft paint), S-13G, B-1059, and second surface mirrors. Thermistors are mounted on the coupons to provide temperature data during the flight.

PRESSURE TRANSDUCER 10-72004-3

STATEMENT OF PROBLEM

During the simulated countdowns on Lunar Orbiter I, it was found that the high-pressure transducer (10-72004-3) provided an incorrect indication of the pressure in the N_2 tank when the spacecraft was on battery power (bus voltage less than 28 v.d.c.) . The transducer provided correct pressure readings when the spacecraft was returned to ground power (bus voltage approximately 30.5 v.d.c.). At the time the tanks were filled and the spacecraft was on ground power, there was good correlation between the transducer indication and the ground equipment pressure gage. This peculiar performance, where the transducer output becomes erratic when the bus voltage drops below about 28 v.d.c., has continued throughout the flight of Lunar Orbiter I.

HISTORY OF THE COMPONENT

This particular transducer (SN 3681) has had no previous failures. However, four pressure transducers have failed during the first acceptance test vibration testing of the N_2 panels (Ref: Problem Packages 840 and 1259). In each case, the failure was caused by broken lead wires on resistors mounted on the compensation board. These failures are not related to subject problem since the transducer output was either at zero or saturated.

STATUS OF ACTION

The transducer supplier is investigating the problem currently to isolate the exact component that could cause these symptoms. The problem appears to be caused by the erratic behavior of a component in the voltage regulation circuit of the transducer. Meaningful pressure data is being obtained from Lunar Orbiter I by using only the data obtained when the solar panels are illuminated, and the bus voltage is at 30.56 v.d.c.

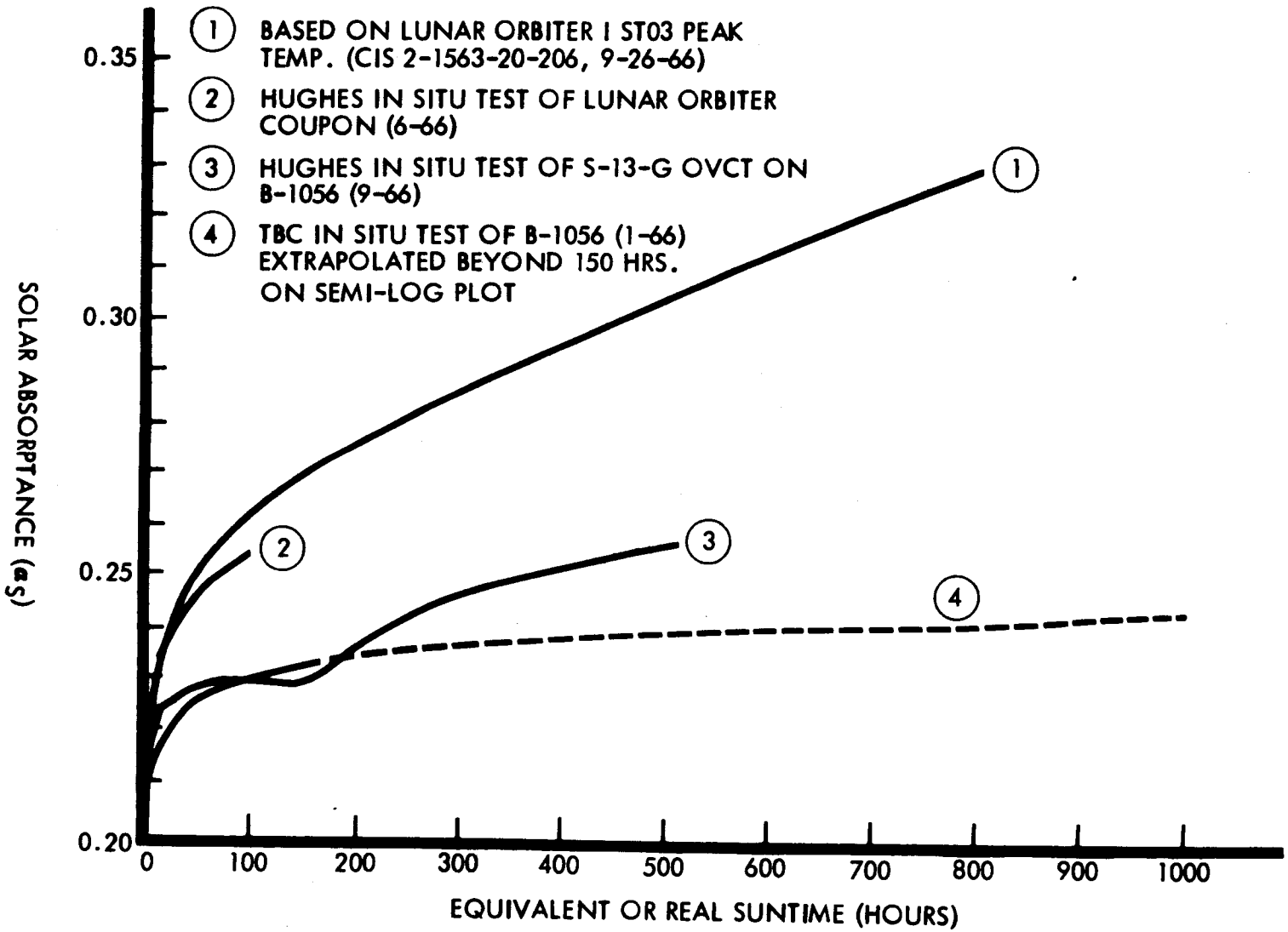

SOLAR ABSORPTANCE VERSUS EXPOSURE TIME

RECOMMENDED DISPOSTION

This is the first transducer failure that has occurred subsequent to N_2 panel vibration, and it is believed to be a random failure of unknown source at this time. No changes in the transducers for future flights are anticipated at this time. However, particular attention will be paid to the performance of these transducers during spacecraft testing and during N_2 loading prior to flight.

FINAL ACTION

No change is being incorporated.

INTERNAL LEAKAGE NOTED IN THE VELOCITY CONTROL PRESSURE REGULATOR OPERATION — LUNAR ORBITER I FLIGHT

STATEMENT OF PROBLEM

Following injection into lunar orbit, excessive "lock-up" (internal) leakage of the velocity control regulator was observed. The leakage caused the pressure in the propellant tanks to rise at a rate of 6 psi per day, which is equivalent to approximately 0.1 pound of nitrogen per day.

BRIEF HISTORY OF COMPONENT

The regulator went through qualification tests with no anomalies and met the leakage requirements. The qualification tests included regulation over a range of 3820 to 650 psig over flow rates of 1 to 6 scfm. A reliability demonstration test (RDT) of the regulator was conducted as a part of Set C tests. During the 2-month RDT-Set C test, the regulator did not allow the pressure to build up over 220 psia. Pressure was kept on the tanks at all times except when we refueled for the second mission. During Spacecraft B mission simulation testing (MST) the N_2 squib was fired on June 23, 1966, and pressure was maintained until August 3, 1966. During this time period, the propellant tank pressure slowly increased from 194 to 230 psi on August 3, 1966. Accordingly, a leakage of 0.88 psi/day.

The incoming acceptance test (IAT) of the regulators and final acceptance testing (FAT) have not revealed any regulators with excessive leakage.

STATUS OF ACTION

Action complete.

RECOMMENDED DISPOSITION

In view of the foregoing, it is concluded that the excessive leakage exhibited by the pressure regulator is an isolated case attributed to a foreign particle under the seat of the regulator, thus preventing it from closing completely.

A design change is not recommended, since a leak even of the magnitude observed in flight is not serious enough to affect the mission since the squib valve (nitrogen shutoff) can be fired after completion of orbit transfer and prevent further leakage to space. Further testing is not recommended since regulator leakage tests are currently being performed in all possible test areas.

FINAL ACTION

No change is being incorporated.

CANOPUS STAR TRACKER ON LUNAR ORBITER I — DEGRADATION DUE TO STRAY LIGHT

PROBLEM STATEMENT

At all times when the tracker on Lunar Orbiter I is operated in the periods from orbital Sunrise to orbital Sunset, the star map voltage is unexpectedly high, as if stray light were entering the tracker's optical field of view. This has made it difficult to locate the star Canopus. When the tracker is operated from orbital Sunset to orbital Sunrise, however, the star Canopus is readily located and tracked. The phenomenon associated with the problem appears to be Sunlight "glint," which is seen by the tracker at almost all attitudes. The source of the glint is not yet known, but tests are in progress to locate the cause and initiate any necessary modifications.

PREFLIGHT HISTORY

The star tracker on Lunar Orbiter I is International Telephone and Telegraph — Federal Laboratories (ITTFL) S/N 7-G2. This tracker completed FAT at the vendor's plant on March 14, 1966, at which time the star map output at one times Canopus was approximately 2.5 volts. During spacecraft FAT in Seattle, the tracker was exposed to excess light. The source of this light was traced to ionization gages in the thermal-vacuum chamber. The light from the gages was bounced off a post in the chamber into the tracker's optics. As a result, the star map voltage dropped to about 1.8 volts, when measured by ITTFL on May 5, 1966. The vendor retailored the star map voltage upwards to about 3 volts on May 6, 1966, and the tracker was then calibration-mated to Star Tracker Test Set Number 4. Subsequent tests of the star tracker at TBC-Seattle, using STTS Number 4, resulted in questionable readings, so the tracker and STTS were again returned to the vendor on May 26, 1966 for recheck. At that time, the vendor found the star tracker star map output voltage for one times Canopus to be correct at approximately 2.9 volts. The test set was modified by adding mylar around each of five lamps and soldering them in place. Calibration of the STTS lamp output was then made at ITTFL using the Spectra Pritchard photometer. On May 28, 1966, at ETR, when the tracker was routinely checked using this STTS, the "plus edge" and "center" lamps gave questionable readings. When checked using the photometer, the suspect lamps in the STTS were found to have

shifted in intensity, and the two lamps were recalibrated using the photometer. No other tests of the star tracker's performance were made before launch. On the basis of the foregoing, the star map voltage at one times Canopus was expected to be about 2.9 volts when the tracker was locked on Canopus in space.

FLIGHT HISTORY

Canopus Star Tracker S/N 7-G2, installed in Lunar Orbiter I, was turned "on" about 6 hours 45 minutes after liftoff from Cape Kennedy on August 10, 1966. At the time of tracker power turn-on, it was noted that the star map output for most spacecraft attitudes was unexpectedly high (over 4 volts at times). A number of attempts at star mapping were made to locate the Canopus star, but without success. In order to provide a roll attitude reference, necessary for the midcourse maneuver, the Canopus tracker was commanded to track the Moon, which it did (with the star map output at 5 volts when locked on the Moon).

A number of attempts were again made to locate the star Canopus by means of star mapping, but the results were ambiguous due to the high star map voltages experienced.

It is a characteristic of the Canopus star tracker that acquisition of the star in the presence of high background light is more readily accomplished if the tracker is pointed at the star and the tracker power is turned from "off" to "on." This technique was employed, and about 66 hours after liftoff the Canopus star was acquired by the tracker and used to successfully track that star (but with star map output of about 1.4 to 1.5 volts).

Since the star tracker performance continued to be adversely affected by stray light, the technique was adopted of keeping the tracker "off" most of the time. However, when a fix on the star Canopus was desired it was readily accomplished after orbital Sunset and before orbital Sunrise, when stray light did not present a problem.

ACTION STATUS

Since the source of the stray light phenomenon is as yet unexplained, an analysis and test program has been authorized by NASA, and TBC has proceeded with setting it up and accomplishing it as "new work."

The end result of this test program may be modifications to flight spacecraft and ground test spacecraft equipment, which also will be considered as new work under Contract NAS1-3800.

The schedule for accomplishing these tests is as follows:

1) Released ECM Work Sheet 8/30/66

2) Make tracker S/N 4B from Spacecraft -1 available for Phase I tests (off-axis Canopus tracker sensitivity test — on bench 8/31/66

3)	Start Phase I tests	8/31/66
4)	Make solar simulator available to MPC air bearing simulator room for Phase II tests (L.O. stray light measurements — in dark room with solar simulator shining on spacecraft)	9/2/66
5)	Make Spacecraft 1 available in MPC air bearing simulator room for Phase II tests	9/6/66
6)	Short Phase II tests	9/6/66
7)	Complete Phase I and II tests	9/23/66
8)	Provide interim report on Phase I and II tests	10/1/66
9)	Provide final report on Phase I and II tests	10/10/66

a) (Include availability of calibrated Tracker for Phase III Tests) — Canopus Tracker Star Map Calibration Check

b) (Include recommendations on Phase IV Tests) — L.O. Spacecraft Illumination Test

RECOMMENDATIONS FOR LUNAR ORBITER II

The results of the tracker stray light tests now in progress must be reviewed before recommendations regarding Lunar Orbiter B can be made. Regarding Tracker S/N 8-G2 on Lunar Orbiter B, however, all available data indicate it is a good, flightworthy tracker.

CANOPUS TRACKER UPDATED STATUS CHARTS

On the following pages appear the results of various tests on all delivered trackers. The list includes the component qualification and RDT trackers.

TEST RESULTS

Star tracker interference is defined as the condition that exists when the tracker switches from the search mode to the track mode because of the stray light environment. The light level seen by the tracker at that time will be called the interference level. The following tabulation lists the individual contributions to the stray light environment made by individual solar illuminated portions of the spacecraft. The contributions are given in terms of fractions of the interference level.

Before Fix		Interference Level
1.	Low-gain antenna, painted white	1.09
2.	Solar Panel 2, edge not painted	0.068
3.	Solar Panel 4, edge not painted	0.021
4.	High-gain antenna (multiple reflection)	0.035
5.	EMD (multiple reflection), solar panel top flat black, edge not painted	0.46
	TOTAL	1.674

After Fix		
1.	Low-gain antenna, boom gloss black, disks flat black	0.027
2.	Solar Panels 2 and 4, edges taped black, below noise level	-
3.	High-gain antenna, below noise level	-
4.	EMD (multiple reflections) solar panel top flat black, edge taped black	0.27
	TOTAL	0.297

FINAL ACTION

Paint the low-gain antenna and those portions of the solar panels contributing to stray light.

STAR TRACKER TEST DATA

Tracker	S/C No.	Date	Type of Test	Location	Test Equipment	Times Canopus	*Star Map T/M Output	**Roll Error Output at 0-deg. Yaw, 0-deg. Roll	Comments
S/N 4 (Original Nonrigid Design)	S/C #1	11/12/65	FAT	ITT	SSS #1	1.0	2.45 v	+50 mv	Primary standard
	S/C #1	11/18/65	STTS #4 Calibration	ITT	SSS #1	1.0	2.30 v	+34	Primary standard
	S/C #1	1/23/66	S/C Qual	TBC	STTS #4	1.0	2.1 v	---	Pre-FAT T-V
	S/C #1	3/14/66	S/C Qual	TBC	STTS #4	1.0	2.1 v	---	Post-FAT T-V
	S/C #1	3/18/66	S/C Qual	TBC	STTS #4	1.0	2.1 v	---	Post-FAT T-V
	S/C #1	3/23/66	S/C Qual	TBC	STTS #4	1.0	2.1 v	---	Return to vendor
	S/C #1	3/30/66	Recheck	ITT	SSS #1	1.1	1.4 v	+7	Primary standard. Star map degraded due to exposure to light at TBC
	S/C #1	3/31/66	Recheck after tailoring	ITT	SSS #1	1.1	3.34 v	---	Primary standard. Star map output needed retailoring. Output too high after conformal coating cure
	S/C #1	4/1/66	Recheck after tailoring	ITT	SSS #1	1.1	2.72 v	+16	Primary standard. Acceptable after star map retailoring

REQMT: *2.3 to 3.7 v at 1.1 times Canopus; nominal is 2.7 v at 1.1 times Canopus

**0 ±200 mv

STAR TRACKER TEST DATA

Tracker	S/C No.	Date	Type of Test	Location	Test Equipment	Times Canopus	*Star Map T/M Output	**Roll Error Output at 0-deg. Yaw, 0-deg. Roll	Comments
S/N 4B (Added Rear Support Snubber)	S/C #1	4/7/66	S/C Qual.	TBC	STTS #2	1.1	4.4 v	---	Return to vendor
	S/C #1	5/5/66	Recheck	ITT	SSS #1	1.1	3.15	-6 mv	Primary standard. Prior to degaussing
	S/C #1	5/5/66	Recheck	ITT	SSS #1	1.1	3.13	-16	Primary standard. After degaussing
	S/C #1	5/6/66	Mate to STTS #5	ITT	STTS #5	1.1	3.02	-14	New concept: mate tracker to STTS #5
	S/C #1	5/17/66	Previbration S/C #1 Qual.	TBC	STTS #5	1.1	(In Spec)	+179 to +182	-----
	S/C #1	5/18/66	Postvibration #1 and previbration #2 S/C Qual.	TBC	STTS #5	1.1	(In Spec)	+177	-----
	S/C #1	5/24/66	Postvibration #2 S/C Qual.	TBC	STTS #5	1.1	(In Spec)	+88 to +64	-----
	S/C #1	6/3/66	Postrotational Vibration S/C Qual.	TBC	STTS #5	1.1	(In Spec)	+70 mv	-----
	S/C #1	6/27/66	Postenvironmental system. Verification test—S/C Qual.	TBC	STTS #5	1.0	2.0	-29	-----

REQMT: * 2.3 to 3.7 v at 1.1 times Canopus; nominal is 2.7 v at 1.1 times Canopus

** 0 ±200 mv

STAR TRACKER TEST DATA

Tracker	S/C No.	Date	Type of Test	Location	Test Equipment	Times Canopus	*Star Map T/M Output	**Roll Error Output at 0-deg. Yaw, 0-deg. Roll	Comments
S/N 4B (Cont.)	S/C #1	7/6/66	Post-Qual. Test	TBC	STTS #5	1.0	2.0	-12	At plus edge, the roll error output was +62 mv; at minus edge, the roll error output was -175 mv. Compared to FAT vendor data, tracker experienced rotational null shift as the result of TBC S/C Qual using this nonrigidized version of tracker.
S/N 5B-G2	S/C #2	2/18/66	FAT	ITT	SSS #1	1.0	2.56 v	-32 mv	Primary standard. Out of tolerance from ±30 mv (old reqm't). Required post-FAT stress cycling
	S/C #2	2/21/66	Post-FAT stress	ITT	SSS #1	1.0	(In Spec)	-22	Primary standard. Stress consisted of 3 hrs. at +85°F; 3 hrs. at -35°F; and return to ambient
	S/C #2	2/21/66	Post-FAT stress	ITT	SSS #1	1.0	(In Spec)	-23	Primary standard. Stress consisted of 4 hrs. at 10^{-5} mm Hg. and return to atmospheric
	S/C #2	4/22/66	S/C Post-environment	ITT	STTS #5	1.1	2.5	-330	Tracker not mated to STTS #5
	S/C #2	4/22/66	S/C Post-environment	ITT	STTS #2	1.1	2.5	-122	Tracker not mated to STTS #2
	S/C #2	6/1/66	Pre-MST recheck	TBC	SSS #2	1.0	2.4	-105	Primary standard. Tracker in spec.

REQMT: * 2.3 to 3.7 v at 1.1 times Canopus; nominal is 2.7 v at 1.1 times Canopus

** 0 ±200 mv

STAR TRACKER TEST DATA

Tracker	S/C No.	Date	Type of Test	Location	Test Equipment	Times Canopus	*Star Map T/M Output	**Roll Error Output at 0-deg. Yaw, 0-deg. Roll	Comments
S/N 5B-G2 (Cont.)	S/C #2	6/1/66	Mate to STTS #5	TBC	SSS #2	1.1	2.4 v	-105 mv	Primary standard
	S/C #2	6/27/66	S/C MST	TBC	Van T/M	(No star present)	(Out of spec. Should be 0.7 ±0.2 v with no star)	0	(After inadvertent turn-on of tracker in starting S/C MST vacuum, roll error and star map signals noted to be out of tolerance)
	S/C #2	7/14/66	Recheck tracker	ITT	SSS	1.1	2.69 v	-30	Tracker required rework and retailoring of star map after failure in S/C MST. Primary standard
6B-G2	--- (Component Qual.)	5/12/66	FAT	ITT	SSS #1	1.1	2.34	-16 mv	Primary standard, (Component used for star tracker qual. test)
	--- (Component Qual.)	7/27/66	QUAL	ITT	SSS #1	1.1	2.50	-165	Qual. test completed. -149 mv roll error shift attributable to random vibration
7-G2	S/C #4	3/14/66	FAT	ITT	SSS #1	1.1	2.68 v	+30 mv	Primary standard
	S/C #4	3/21/66	IAT	TBC	STTS #2	1.0	2.32 v	+17 mv	Incoming acceptance
	S/C #4	4/18/66	S/C Test	TBC	STTS #2	1.0	2.3 v	-2 mv	
	S/C #4	5/3/66	S/C Test	TBC	STTS #2	1.0	1.75	---	Star map output appeared to be degraded
	S/C #4	5/3/66	Bench	TBC	STTS #2	1.0	1.4	---	Degradation of star map output confirmed
	S/C #4	5/4/66	Recheck	TBC	SSS #2	1.0	1.23	0 mv	SSS #2 calibration not certified. Return tracker to vendor

REQMT: * 2.3 to 3.7 v at 1.1 times Canopus; nominal is 2.7 v at 1.1 times Canopus
** 0 ±200 mv

STAR TRACKER TEST DATA

Tracker	S/C No.	Date	Type of Test	Location	Test Equipment	Times Canopus	*Star Map T/M Output	**Roll Error Output at 0-deg. Yaw, 0-deg. Roll	Comments
7-G2 (Cont.)	S/C #4	5/5/66	Recheck	ITT	SSS #1	1.1	1.86	-9 mv	Primary standard. After degauss, before tailoring
	S/C #4	5/6/66	Recheck	ITT	SSS #1	1.1	3.09	-13 mv	Primary standard. After retailoring
	S/C #4	5/7/66	Mate to STTS #4	ITT	SSS #1	1.1	3.12	-13 mv	Primary standard
	S/C #4	5/26/66	Remate to STTS #4	ITT	SSS #1	1.1	3.15	+12 mv	Primary standard. STTS #4 midway and center bulbs bad; STTS modified to add mylar around lamps and to solder lamps into place
	S/C #4	5/28/66	S/C check	TBC ETR	STTS #4	1.1	1.64	-10 mv	Suspected + edge and center columns data interchanged
	S/C #4	6/16/66	S/C check	TBC ETR	STTS #4	1.1	3.15	-10 mv	Recalibrated STTS #4 star map to tracker data package
	S/C #4	6/23/66	S/C check	TBC ETR	Pritchard Photometer Model 1960-PR	---	---	---	Recalibrated suspect lamps on STTS #4 using photometer. Thereby proved that STTS #4 center lamp had shifted back to same intensity as existed on 5/26/66 when star map data vs times Canopus was taken for STTS #4 data package. This test, using photometer, also showed that the + edge lamp now remains at the new intensity level to which it had shifted, as measured at ETR.

REQMT: * 2.3 to 3.7 v at 1.1 times Canopus; nominal is 2.7 v at 1.1 times Canopus

** 0 ±200 mv

STAR TRACKER TEST DATA

Tracker	S/C No.	Date	Type of Test	Location	Test Equipment	Times Canopus	*Star Map T/M Output	**Roll Error Output at 0-deg. Yaw, 0-deg. Roll	Comments
7-G2 (Cont.)									Conclusion: Tracker is good. STTS lamp intensity output has shifted as described above
	S/C #4	8/14/66	Actual Flight	Space	Telemetry	1.0	1.46 (Later to 1.5 volts)	--- (Tracks OK)	Star map output may have been degraded not only by excess stray light but also by tracking on Moon prior to midcourse correction
S/N 8-G2	S/C #5	3/28/66	FAT	ITT	SSS #1	1.1	2.66 v	0 mv	Primary standard
	S/C #5	4/1/66	Check	ITT	SSS #1	1.1	2.80 v	+9 mv	Primary standard (when checking out STTS #4)
	S/C #5	4/14/66	IAT	TBC	STTS #2	1.0	3.0 v	+40 mv	
	S/C #5	4/15/66	S/C check	TBC	STTS #2	1.0	3.0 v	-5 mv	
	S/C #5	5/4/66	S/C post-vibration	TBC	STTS #2	1.0	2.84 v	-205 mv	Suspect STTS has shifted
	S/C #5	5/18/66	Tracker check	TBC	SSS #2	1.02	1.95	-126 mv	Primary standard (before calibration of TBC SSS #2 was completed and certified Return to vendor
	S/C #5	5/19/66	Check	ITT	SSS #1	1.1	2.74	-97 mv	Primary standard. Prior to degaussing

REQMT: * 2.3 to 3.7 v at 1.1 times Canopus; nominal is 2.7 v at 1.1 times Canopus

** 0 ±200 mv

STAR TRACKER TEST DATA

Tracker	S/C No.	Date	Type of Test	Location	Test Equipment	Times Canopus	*Star Map T/M Output	**Roll Error Output at 0-deg. Yaw, 0-deg. Roll	Comments
S/N 8-G2 (Cont.)	S/C #5	5/19/66	Check	ITT	SSS #1	1.1	2.74	+24 mv	Primary standard. After degaussing
	S/C #5	5/19/66	Recheck	ITT	SSS #1	1.1	2.81	+36 mv	Primary standard. Field-of-view tests
	S/C #5	5/23/66	Mate with STTS #1	ITT	SSS #1	1.1	2.92	+34 mv	Primary standard
	S/C #5	6/17/66	S/C check	TBC ETR	STTS #1	1.0	2.9 v	+38 mv	Four lamps (but not center lamp) on STTS #1 were suspected of having shifted
	S/C #5	6/23/66	Check	ITT ETR	SSS #3	1.1	2.91	+47 mv	Primary standard. (Tracker checked on ITT's SSS #3 at ETR) Conclusion: Tracker is good. STTS has shifted
S/N 11-G2	S/C #6	5/16/66	FAT	ITT	SSS #1	1.1	2.79	-58 mv	Primary standard
	S/C #6	5/17/66	FAT	ITT	SSS #1	1.1	2.47	-58mv	Primary standard. Field-of-view check
	S/C #6	5/21/66	Mate to STTS #3	ITT	SSS #1	1.1	2.70	+66mv	Primary standard
	S/C #6	5/25/66	IAT	TBC	STTS #3	1.0	3.3	+48mv	TBC incoming acceptance test
	S/C #6	6/14/66	S/C test	TBC	STTS #3	1.1	2.7	+57mv	Tracker repeats 5/21/66 data
	S/C #6	8/16/66	S/C test	TBC	STTS #3	1.1	4.3	+30mv	STTS suspected defective

REQMT: * 2.3 to 3.7 v at 1.1 times Canopus; nominal is 2.7 v at 1.1 times Canopus

** 0 ±200 mv

STAR TRACKER TEST DATA

Tracker	S/C No.	Date	Type of Test	Location	Test Equipment	Times Canopus	*Star Map T/M Output	**Roll Error Output at 0-deg. Yaw, 0-deg. Roll	Comments
S/N 11-G2 (Cont.)	S/C #6	8/19/66	Recheck	TBC	SSS #2	1.0	2.38	+138	Primary standard. High roll error output indicated that recheck by ITT was advisable
	S/C #6	8/20/66	Recheck	ITT	SSS #1	1.1	3.20	+57	Primary standard. Before degaussing. Results indicate faulty STTS
	S/C #6	8/20/66	Recheck	ITT	SSS #1	1.1	3.19	+46	Primary standard. After degaussing. Results indicate negligible residual magnetism effects
	S/C #6	8/20/66	Mate to STTS #2	ITT	SSS #1	1.1	3.38	+65	Tracker and test set now mated and shipped to ETR for reinstallation of tracker in S/C #6
S/N 12-G2	--- (Component RDT)	6/21/66	FAT	ITT	SSS #1	1.1	3.06	-48 mv	Primary standard
	--- (Component RDT)	8/4/66	RDT start	ITT	SSS #1	1.1	1.65	-34	Primary standard. Star map voltage dropped so low as to prevent acquisition at start of second 15-day RDT cycle. Star map voltage was then retailored upward

REQMT:

* 2.3 to 3.7 v at 1.1 times Canopus; nominal is 2.7 v at 1.1 times Canopus

** 0 ±200 mv

STAR TRACKER TEST DATA

Tracker	S/C No.	Date	Type of Test	Location	Test Equipment	Times Canopus	*Star Map T/M Output	**Roll Error Output at 0-deg. Yaw, 0-deg. Roll	Comments
S/N 12-G2 (Cont.)	--- (Component RDT)	8/5/66	RDT mid-point	ITT	SSS #1	1.1	3.32	-34	Primary standard. After retailoring of star map. Solar impingements then deleted from remainder of RDT until very last day.
	--- (Component (RDT)	8/22/66	RDT conclusion	ITT	SSS #1	1.1	2.05	-34	Primary standard. ITT concludes that constantly looking at star Canopus during RDT resulted in star map voltage degradation
	--- (Component RDT)	8/23/66	Post-RDT	ITT	SSS #1	1.1	2.5	-34	Primary standard. A recovery trend has appeared in star map output
	--- (Component RDT)	8/23/66	Post-RDT	ITT	SSS #1	1.1	3.49	-34	Primary standard. This test was run later in the afternoon of the same day as the above test, indicating continual recovery of star map voltage
	--- (Component RDT)	8/25/66	Post-RDT	ITT	SSS #1	1.1	3.70	-34	Primary standard. Continued recovery exhibited
S/N 10A-G2	S/C #7	8/28/66	FAT	ITT	SSS #1	1.1	3.14 v	+84 mv	Primary standard
	S/C #7	9/1/66	IAT	TBC	STTS #3	1.0	2.9	+95 mv	Incoming acceptance test

REQMT:

* 2.3 to 3.7 v at 1.1 times Canopus; nominal is 2.7 v at 1.1 times Canopus

LUNAR ORBITER I VELOCITY CONTROL RELIEF VALVE PERFORMANCE ANALYSIS

This discussion on the Lunar Orbiter I relief valve performance is presented to explain the operating characteristics observed as indicated by telemetry data of the propellant tank pressures.

The condition observed shows that the relief valves maintain essentially a constant upstream pressure under flow conditions and close shortly after the flow ceases to hold the pressure at the cracking level. The pressure then gradually leaked down until a firm reseat was accomplished as would be expected because of the large ullage volume of nitrogen in the propellant tanks at that time. The oxidizer relief valve appeared to reseat within 1 to 2 psi of cracking pressure. The fuel tank pressure dropped at a rate indicating a leakage rate of approximately 125 scc per hour until a firm reseat was established approximately 6 psi below cracking pressure.

Qualification testing of the relief valve has shown that after thousands of cycles of each of two units that the valves immediately reseated after flow ceased and the internal leakage across the relief valve seat dropped below 50 scc per hour between 2 and 6 psi below the cracking pressure.

The propellant tank pressures have not exceeded the relief valve cracking pressure tolerance; operation of the relief valves following cessation of flow has indicated that their lock-up leakage rates are well within specification tolerances. The operation of the relief valves on Lunar Orbiter I is therefore considered to be satisfactory in all respects.

FINAL ACTION

No change is being incorporated.

MODULATION INDEX

STATEMENT OF PROBLEM

A high modulation index was noted on Lunar Orbiter B at ETR during spacecraft testing and was also evident on Spacecraft 2 during MST. An investigation of the problem disclosed that with certain combinations of mod selector and transponder, an rf mismatch existed which resulted in the high modulation index. On Lunar Orbiter I the rf match is good, and the modulation index is within tolerance. On Lunar Orbiter C, the transponder was replaced to improve the match, and the modulation index came into tolerance.

HISTORY OF COMPONENT

There is no known previous occurrence of this problem prior to Lunar Orbiter B.

STATUS OF ACTION

An investigation of the problem has been conducted that included consultations with the transponder and mod selector suppliers.

As a result it was confirmed that the problem was caused by an rf mismatch between the transponder and mod selector. It was also concluded that test equipment and cabling both have an effect on the measured mod index.

Major concern has been with the stability of the mod index to remain constant once the proper index has been established. A limited review of Lunar Orbiter I data has indicated that the mod index is stable and has not changed from that observed prior to launch.

RECOMMENDED DISPOSITION

The following action is recommended:

1) Special tests will be incorporated into spacecraft testing to measure the mod index and confirm that it is within tolerance.

2) If the mod index is out of tolerance, the transponder and/or mod selector will be changed to optimize the match and bring the mod index into tolerance.

3) The mod index will be monitored during spacecraft testing to confirm that it is stable.

4) Continue monitoring Lunar Orbiter I and conduct a special modulation sensitivity test on Lunar Orbiter I after completion of photo readout.

FINAL ACTION

Special tests have been incorporated into the spacecraft test procedures to measure the mod index at both Seattle and the Cape. The results of these tests follow.

Lunar Orbiter B (Cape Kennedy)

Mode 3 mod index	= 1.58 radians	(30 kc)
Mode 2 mod index	= 3.70 radians	(310 kc)
	= 2.92 radians	(140 kc)
	= 0.19 radian	(30 kc)
	= 0.45 radian	(38.75 kc)

$$m = \frac{3.92 - 3.70}{3.92} = 5.6\% \text{ (6\% allowable)}$$

Lunar Orbiter C (Cape Kennedy)

Mode 3 mod index	= 1.37 radians	(30 kc)
Mode 2 mod index	= 3.34 radians	(310 kc)
	= 3.52 radians	(140 kc)
	= 0.21 radian	(30 kc)
	= 0.43 radian	(38.75 kc)

$$m = \frac{3.52 - 3.34}{3.52} = 5.1\% \text{ (6\% allowable)}$$

Lunar Orbiter D* (Seattle)

Mode 3 mod index	= 1.48 radians	(30 kc)
Mode 2 mod index	= 3.54 radians	(310 kc)
	= 3.64 radians	(140 kc)
	= 0.17 radian	(30 kc)
	= 0.41 radian	(38.75 kc)

$$m = \frac{3.64 - 3.54}{3.64} = 2.75\% \text{ (5\% allowable)}$$

* Required transponder change from S/N 08 to S/N 10

Per tests conducted at Woomera, mod index on Lunar Orbiter I was 1.43 radians for Mode 3. Spectrum and sidebands had equal amplitude (TWTA on). Prior to launch this measured 1.45 radians.

The above spacecraft test procedure change has solved the modulation index problem. No change will be made in hardware.

TRANSPONDER DOUBLE-EXECUTE PROBLEM

STATEMENT OF PROBLEM

During Lunar Orbiter I testing and data review at ETR, it was noted that the programmer advanced one stored program address (SPA) when a ranging-on command was sent in real time.

Concurrent testing on Lunar Orbiter I and B at ETR and on the test vehicle at Seattle has shown that the switching of the ranging circuit causes a transient on the plus 15-volt supply in the transponder. This transient causes the transponder to lose lock momentarily. While lock is lost, the command decoder is not receiving the execute tone, and its output to the programmer is removed. When the transponder regains lock, the command decoder again receives the execute tone and reapplies its output to the programmer. With the first execute signal, the programmer destructively samples the command decoder register. With the second execute signal, the programmer again samples the command decoder register (now all zeros), stores this information in the stored program address at which it is located, and steps to the next address.

HISTORY OF COMPONENT

There was no known history of this problem prior to its occurrence on Lunar Orbiter I, as noted above.

STATUS OF ACTION

An investigation has been conducted and the following conclusions drawn:

1) The double-execute problem is caused by momentary loss of transponder phase lock resulting from transients on the transponder plus-15-volt supply.

2) The transients on the plus-15-volt line are caused by momentarily loading and unloading the circuit with the isolation amplifier in the ranging loop.

3) At present, switching of the ranging function is the only known source of transients that will cause a double execute.

4) The double execute will never cause a spurious real-time command.

5) The double execute will always fill the SPA with zeros.

6) The double-execute problem can be circumvented operationally by:

   a) Commanding ranging on/off by stored program command preceded by a programmed delay.

   b) Locating the programmer on a SPA with a vacant or a noncritical command refilling the location if double execute occurs.

RECOMMENDED DISPOSITION

Item 6 above will be incorporated into all future spacecraft operations.

FINAL ACTION

After completion of photo readout on Lunar Orbiter I, ranging was commanded off and on in real time and operated as predicted in the statement of problem.

Ranging mode will be commanded on or off by a SPC or, if RTC is to be used, the SPA will be chosen such that the information lost from memory is of no consequence.

TRANSPONDER TELEMETRY POWER CHANGE

STATEMENT OF PROBLEM

The transponder rf power output telemetry (CE10) has experienced numerous shifts of up to about 10% (0.41 db) during the flight.

HISTORY OF COMPONENT

These same shifts occurred during Lunar Orbiter I thermal vacuum and were analyzed as temperature-VSWR effects caused by the hardwire rf coupling between the spacecraft and van.

STATUS OF ACTION

Lunar Orbiter I test data has been reviewed for changes in CE10 resulting from vibration. No changes noted.

A review of Lunar Orbiter I thermal vacuum test data discloses similar variations in the transponder RFPO T/M, particularly during certain portions of the orbits where the transponder passed through specific temperature ranges.

Flight data has been reviewed for correlation between CE10 changes and other activities in the spacecraft, and the following has been noted:

1) The CI10 changes are often coincident with antenna position changes.

2) CE10 changes are occasionally coincident with spacecraft roll maneuvers.

3) No correlation has been made between C-10 changes and received power at the ground stations.

4) On Friday, August 26, 1966 (Day 238), CE10 shifted five times — once during antenna rotation, twice with no known accompanying activity, and twice accompanied by activities as yet undetermined. Spacecraft load current had a 1.0-amp step function, and the gyros (AG05 and AG06) gave a transient output similar to those experienced during antenna rotation.

It was believed that the changes were caused by transients on the transponder plus-15-volt supply; however, the temperature signal conditioning amplifier is identical to the rf power signal conditioning amplifier and both are connected to the plus-15-volt supply. The temperature telemetry did not experience variations similar to those of the rf power telemetry.

The thermal vacuum data for Lunar Orbiter B and Lunar Orbiter C has been reviewed. Lunar Orbiter B appears not to have this problem whereas Lunar Orbiter C exhibits the same to a lesser degree. Subsequent change of transponder in Lunar Orbiter B may have altered the above.

RECOMMENDED DISPOSITION

Continue to review Lunar Orbiter I data to determine with what spacecraft functions or activities this anomaly is coincident; attempt to determine by ground station observations whether the anomaly is in the measurement or the power output.

Since the variations are within the measurement accuracy limitations, and the indicated rf power output has been well over the minimum specified output, it is believed that this anomaly in no way jeopardizes completion of this mission or of future missions.

FINAL ACTION

Review of Lunar Orbiter I data has not disclosed any new insight with respect to this anomaly.

From data received, it appears that:

1) The power output has not changed other than that due to temperature effects;

2) CE10 (T/M rf power) remains well within specification tolerance and is repeatable with respect to temperature changes;

3) Coincidence of CE10 change with changes in station received power has not been detected to date.

No change being incorporated. Continue routine data observations.

POWER TRANSISTOR FAILURE

PROBLEM

In Orbit 20 of Lunar Orbiter I, it became evident that approximately 1.257 amperes in excess of predicted normal loads were being drawn from the spacecraft battery during the lunar night. Analysis of the facts leads to the conclusion that probably a shunt power transistor shorted from collector to emitter in a manner similar to that reported in Failure Report LO 1270 for Spacecraft 1. The flight spacecraft is continuing to operate according to plan with this additional lunar night load.

BRIEF HISTORY OF COMPONENT

Transistors of two different internal configurations were built into the power transistor assemblies. The change in configuration was precipitated by a high dropout rate due primarily to solder ball contamination at the transistor manufacturer's facility. The earlier, solder ball prone, transistor was used on Spacecraft 1, for qualifications tests and on Lunar Orbiter I. The improved design transistor successfully completed component qualification and spacecraft MST-1 with no solder ball shorts. Total test time in transistor hours on the improved transistor by the time of the next planned launch is expected to represent:

18,000 hours of part burn-in
4,232 hours of component FAT
27,400 hours of component Qual.
17,350 hours of spacecraft FAT
5,568 hours of spacecraft testing at ETR

A problem on Spacecraft 2 during MST-1 was experienced with the shunt regulator and power dissipation components. This problem, which affected spacecraft voltage regulation, was not related to the transistor solder ball problem. A complete report of the Spacecraft 2 voltage regulation problem is contained in Failure Report LO-1326. It concludes that the failure mode was unique to Spacecraft 2, because it was a collector-to-ground short and therefore external to the transistor. Other types of failures not experienced to date are:

Base-to-Emitter Short

A base-to-emitter short will cause that leg of the circuit to turn off and not pull any current through the power dissipation resistors. It would also cause a loss of voltage regulation by causing the base of the eight transistors to be clamped to ground through the 2.5-ohm emitter resistor. However, this would occur at some value of shunt regulator current above the 2.8-ampere limit seen on Spacecraft 2.

Base-to-Collector Short

A base-to-collector short will look the same as a collector-to-emitter short (16.5 ohms + 2.5 ohms = 19 ohms). The resulting current through the 2.5-ohm resistor would present a higher voltage than the shunt regulator is applying to the base of the remaining transistors. Therefore no voltage regulation would be lost.

Although a base-to-emitter short would be catastrophic, the gap to be bridged is 0.075 inch and it is very unlikely that a solder ball of this dimension would escape visual and X-ray inspection.

STATUS OF ACTION

Change LO-I-0542 was initiated to effect the action necessary to ensure the flightworthiness of the remaining flight spacecraft. This action includes replacing transistor assemblies on Lunar Orbiters B and C. The transistor assemblies that were removed contained the solder ball prone transistors. The spare assemblies replacing these units contain the improved style transistors. Change LO-I-0542 also resulted in a transistor X-ray program to (1) verify the accuracy of lot-date-code identification of transistors used in the transistor assemblies and (2) verify that the improved configuration is in fact solder-ball free. In both cases verification was achieved.

RECOMMENDED DISPOSITION WITH RESPECT TO NEXT FLIGHT

Completion of the action specified by Change LO-I-0542 ensures the flight readiness of the remaining flight spacecraft with respect to the shunt regulator and power dissipation components.

FINAL ACTION

Change LO-I-0542, which eliminates all solder-ball-prone transistors, has been incorporated on all remaining flight spacecraft.

MISSION I ANOMALIES — PHOTO SYSTEM

SHUTTER

Shutter analysis is now being conducted. The preliminary fix has been determined. Shutter pulse circuitry is being redesigned to reduce susceptibility of shutter to EMI. Tests are to be completed September 6. Parts are available. Shutters for PS 5 and PS 6 will be modified and tested within 8 days after fix is confirmed.

The planned test program is:

1) Engineering test on breadboard and development shutter;
2) In-process test of new board;
3) Camera-level tests of shutter timing, input parameter variation, EMI test on V/H test stand, and dynamic photo test;
4) Payload-level tests on V/H test stand;
5) Engineering tests on PS 3.

Eastman Kodak will submit a complete resume of findings of their investigation and description of the test program that is to be used to verify the fix. All tests will simulate flight conditions as closely as possible.

The shutter acceptance tests will be reviewed to ensure that all future units are tested for in-sequence operation and susceptance to extraneous pulse.

FLARE

The flare problem in the GRE's is associated with a particular configuration of CRT. A tentative fix, by masking, has been accomplished on the GRE's at the Goldstone site. Latest film from Goldstone demonstrated satisfactory performance. The GRE's at Woomera are operating properly. The mask fix has been applied at Madrid. The permanent fix requires new CRT's to replace the particular configuration of CRT in service at Madrid and Goldstone. Eastman Kodak is looking for replacements for these tubes.

Any optical system including the CRT recording system, exhibits flare to some degree. Tests indicated that flare in the photo subsystem is within specification.

An examination of the edge print on flight film indicates that the process of exposure of this edge print on the film is according to specification and fully meets

the requirements of the Lunar Orbiter program. Eastman Kodak Quality Control has records to confirm to the satisfactory condition of the PS 4 flight film in this respect. Also, the sample that was processed at ETR confirms the adequacy of the edge print.

The GRE kinetube specification and acceptance test will be adjusted to ensure that future CRT's perform properly with respect to minimum flare.

GRE FRAMELET INTENSITY

Nonuniformity of GRE film can be attributed to nonuniformity of the LST. This lack of uniformity has been accepted by Boeing and NASA, who have participated in several briefings with Eastman Kodak on the cause and cure. The cure involves dynamic focus of the LST with its associated delay of probably as much as a year.

BIMAT

Eastman Kodak indicates that the bimat cut and clear anomalous operation detected in PS 1 and PS 5 has been corrected and that further problems in this area are not anticipated. Two successful cuts have been made on PS 1 since incorporation of fixes, which consisted of: increasing tension on the readout looper and bracket on two dryer, rollers, and a slight increase in the width of a diffusion channel in the processer-dryer.

Film and bimat data sheets that are originated at Eastman Kodak will be continued through ETR tests and forwarded to Pasadena after the launch to assist in maintaining a precise accounting of the quantity and use of film and bimat throughout the test, launch, and flight operation.

PHOTOS FOR DESIGN ANOMALIES

Arrangements will be made to expedite copies of flight photos to Eastman Kodak when any future PS flight anomalies occur. Kodak has indicated that they do not require copies of the photos for design analysis unless some problem arises.

PS DELIVERY SCHEDULE

Eastman Kodak is not in a position to provide a firm delivery schedule on PS 5 and PS 6 as of this date. Dr. Feldman and Mr. Elle indicated on September 6 that they are confident of delivering in time for the November launch. Specific dates should be available later this week.

FLIGHT PHOTO REASSEMBLY

Reassembled flight photos are now being shipped in accordance with predicted schedules. Large shipments were accomplished last week and as of 4:00 p.m. Friday, September 2, no backlog existed at Eastman Kodak.

UPDATED STATUS — MISSION I ANOMALIES — PHOTO SYSTEM

SHUTTER

Analysis of the problem has been completed and a fix determined and verified by breadboard test. The fix involved redesign of a portion of the shutter pulse circuitry to reduce susceptibility to PS-generated transients, plus addition of a resistor capacitance filter between 28-volt and 6-volt return lines to reduce the level of the transients. The circuit changes were implemented by modifying one of the shutter circuit boards and by incorporating the filter in a cap on the test connector. The change is being incorporated in PS 1 and all remaining flight units.

A test program has been developed for verification of shutter circuitry redesign and for demonstration of adequacy of the total change at both photo subsystem and spacecraft level. The test program includes:

1) Engineering tests on breadboard and development shutter (complete);

2) Engineering tests on PS 3 (complete);

3) In-process test of each redesigned shutter circuit board (complete for PS-5 and PS-6);

4) Engineering tests at camera level to verify no degradation of normal operation (complete);

5) Photo subsystem FAT tests on all flight PS on V/H test stand to give a direct measurement of proper IMC (complete for PS-5 and PS-6);

6) Photo subsystem and spacecraft-level tests of PS-1 to verify IMC (as in Item 5 above) (complete);

7) Spacecraft-level test of PS-5 in spacecraft to verify proper IMC (as in Item 5 above) (to be conducted at ETR).

Final Action: See "Bimat" below.

FLARE

The CRT has been removed from GRE 4 at Goldstone and returned to Eastman Kodak, who indicated that tube characteristics had changed with use. It has been returned to RCA for evaluation.

Final Action

Masking will be applied to GRE's at Goldstone and Madrid. GRE's at Woomera are operating properly. Eastman Kodak is continuing their analysis and is looking for possible tube replacement.

GRE FRAMELET INTENSITY

Final Action

No hardware change is being incorporated. Procedures and techniques for achieving better and more uniform adjustment of photo subsystem readout, communications, and GRE are being studied by NASA and Boeing.

BIMAT

The bimat cut and clear anomalous operation detected in PS-1 and PS-5 has been corrected. No problems of this nature have occurred in PS-1, PS-5, and PS-6 since incorporation of the fixes which consisted of: increasing tension on the readout looper, bracket on two dryer rollers, and a slight increase in the width of a diffusion channel in the processer-dryer.

Film and bimat data sheets that are originated at Eastman Kodak will be continued through ETR tests and forwarded to Pasadena after the launch to assist in maintaining a precise accounting of the quantity and use of film and bimat throughout the test, launch, and flight operation.

Final Action

Incorporate redesigned shutter pulse circuitry, filter, and bimat fixes. Conduct photo subsystem and spacecraft-level tests outlined in "Shutter" above.

PHOTO FOR DESIGN ANOMALIES

Final Action

Kodak engineers at Pasadena will have access to the data from the GRE located at the SFOF. Eastman Kodak will be provided copies of data on an expedited basis should any flight anomalies occur.

RF SIGNAL LEVEL DROP

From Day 230 (August 18) at 15:30 GMT until Day 231 (August 19) at 16:00 GMT, the ground-received power dropped from about -135 dbm to about -147 dbm. During this drop the transponder AGC indicated a drop of about 4 db in the spacecraft received power. Again, from Day 234 (August 22) until Day 237 (August 25), the ground received power dropped from -135 dbm to -142 dbm while the spacecraft received power dropped about 2 db. In neither case was a change in TWTA or transponder RF Power output telemetry noted.

There is no known previous occurrence of this problem.

2-1553-30-386
Code 0402, 0500

To: National Aeronautics and Space Administration
Langley Research Center
Lunar Orbiter Project Office
Attn: T. H. Elder, Technical Representative
Building 1192B
Langley Station
Hampton, Virginia 23365

Subject: Contract NAS1-3800, Lunar Orbiter Project, Velocity Control Relief Valve Performance

Reference: Boeing Presentation Meeting at Langley dated Sept. 7, 1966, on the Assessment Summary of S/C 4 Anomalies

1. As a result of the reference meeting, the Contractor was requested to provide substantiating data for the performance analysis presented for the velocity control relief valve, SCD 10-72023, and to conduct a thermal analysis of the solar panel backside heat reflectance to the equipment mounting deck.

2. The Contractor believes that the attached analysis and data sheets, supplementing the assessment summary analysis, shows that the relief valves on S/C 4 operated satisfactorily. Analysis of the thermal effects of the solar arrays and the solar array mount configuration was made approximately one year ago. The results of this analysis indicated the net effect of the solar arrays to be thermally negligible upon the spacecraft. The flight data obtained from S/C #4, though indicative of the EMD thermal characteristics, does not isolate any effect of the solar arrays to support revision of the original analysis. Any additional analysis, therefore, would necessitate assumptions as made originally and would lead to the same answer.

3. This constitutes closing action by the Contractor on the above two action items resulting from the reference meeting.

THE BOEING COMPANY
Space Division

G. H. Hage
Engineering Manager

Attachment

cc: E. J. Janota
AFPR (CMRSD)
R. D. Eisenhart
K. L. Wadlin

LUNAR ORBITER I VELOCITY CONTROL RELIEF VALVE PERFORMANCE ANALYSIS*

In support of the reference discussion regarding the qualification test results, the attached data sheets, taken from the qualification test report for the Apollo counterpart to the Lunar Orbiter relief valve, illustrate the performance with respect to cracking pressure, reseat, full flow, and leakage. It should be noted that the cracking and reseat pressures are determined at the point where leakage is 20 scc per hour, as required by the qualification test procedures. Thus, the relief valve may effectively reseat at some higher pressure but with a leakage rate greater than 20 scc per hour, yet not provide an observable decrease in pressure over a short period of time (minutes).

The inlet pressure required for full flow is slightly above or slightly below the cracking pressure, indicating that the relief valve operates similar to a pressure regulator maintaining essentially a constant inlet pressure from cracking to full-flow conditions.

Also attached is a current plot of propellant tank pressures, from telemetry data, illustrating relief valve operation following actuation (actuation resulted from a temperature-induced pressure rise with the tank heaters on). It can be seen, therefore, that the reduction in pressure to achieve a firm reseat is approximately 6 psi, which is consistent with the qualification test data.

*Reference: Assessment Summary of Lunar Orbiter I Anomalies, dated September 7, 1966, Pg. 25

2-1553-30-399
Code 0402, 0500

To: National Aeronautics and Space Administration
Langley Research Center
Lunar Orbiter Project Office
Attn: T. H. Elder, Technical Representative
Building 1192B
Langley Station
Hampton, Virginia 23365

Subject: NASA Contract NAS1-3800, Lunar Orbiter Project, Velocity Control Relief Valve Performance on S/C 4

Reference:
(a) NASA Letter BD-1902-RDA, dated Oct. 3, 1966, same subject
(b) Boeing Letter 2-1553-30-386, dated Sept. 19, 1966, same subject
(c) Boeing Presentation Meeting at Langley dated Sept. 7, 1966, Assessment Summary of S/C 4 Anomalies

1. The reference (a) letter requested the Contractor to provide data, in addition to references (b) and (c), substantiating that the stabilization of propellant tank pressure at the relief valve cracking pressure is a "normal mode of operation" for the relief valves, as observed from S/C 4 flight data. This specific condition existed from August 23, 1966, until August 29, 1966.

During this time period the two relief valves were relieving nitrogen at a flow rate equivalent to the regulator leakage rate which was established to be 0.1 pound of nitrogen per day (820 standard cubic centimeters per hour for each relief valve) while maintaining the system at a pressure of 230 to 233 psi.

2. No specific tests have been documented to establish the system pressure under relief valve flow conditions of 820 scc/hr. The qualification data transmitted by reference (b) does, however, provide the following information which is pertinent for minimum and maximum flow conditions.

2. (Continued)

a. The system pressure stablized at 223 to 231 psi at flow rates of 20 scc/hour.

b. The system pressure stablized at 229.5 to 239.8 psi at full flow conditions (15 SCFM).

c. The cracking pressure ranged from 228 to 234 psi.

3. On the basis of the foregoing information the Contractor can only conclude that the condition discussed in paragraph 1. is normal and plans no further action on this item. NASA concurrence that this action item is closed is assumed unless the Contractor is advised to the contrary.

THE BOEING COMPANY
Space Division

G. H. Hage
Engineering Manager

cc: E. J. Janota, LRC
AFPR (CMRSD)
R. D. Eisenhart
K. L. Wadlin

Since available information is not adequate to conclusively establish the cause of the anomaly, several possible problems are discussed in terms of available data.

CHANGE IN MODULATION INDEX

A change in the transponder modulation index would not cause the observed change in the transponder AGC indication.

During the lower signal conditions, sideband and carrier power levels were checked, and these were compared with data taken under normal conditions. The power ratios were nearly unchanged, indicating no significant change in modulation index.

GROUND STATION EQUIPMENT MALFUNCTION

There are no reports of equipment repairs at the ends of the low signal periods. However, at a latter date, Station 12 had maser problems and reported a 0.5°F maser temperature rise resulting in a 7-db loss in maser output.

The probability of simultaneous identical malfunctions and clearing of the malfunctions at three sites is extremely remote.

SPACECRAFT ATTITUDE — OPERATION IN LOW-GAIN ANTENNA NULL

Since the antenna nulls are very close for transmit and receive, little difference is expected for signal loss for up and down links during operation near a null.

The spacecraft was rolled during the reduced signal period with no evidence that it had been operating near a null.

The spacecraft was in inertial hold on Canopus, as it had been previous to, and was after the problem.

TRANSPONDER MALFUNCTION

A drop in transponder rf power output (from the X30 module to the rf package) would have been reflected in transponder and TWTA rf power telemetry, as well as at the ground station and would not have caused a reduction in transponder AGC.

The only portions of the transponder common to the up and down link rf are the low pass filter and the circulator in the rf package. A failure in the filter would probably affect up and down links nearly the same and would probably not be self-healing. A failure in the circulator which would cause a 12-db reduction in rf power output would probably result in reflected power causing significant changes in TWTA drive and/or rf power output telemetry. Again, self-healing is not probable.

LOW-GAIN ANTENNA OR CABLE FAILURE

A break in the inner or outer conductors would probably result in a high, unstable loss which would not be self-healing. A connector failure would have similar results.

A change in the antenna pattern due to reflections from a loose or torn thermal barrier would probably be small (0.2 db) and would be sensitive to spacecraft position and movement. Self-healing (in terms of radiated pattern) is not probable.

Changes in VSWR sufficient to cause a 12-db loss would result only from extensive damage which would probably not be self-healing.

Changes in ellipticity are not considered of adequate magnitude, since complete loss of one vector would result in only 3 db loss in up or down link power.

MULTIPATH

Multipath from the lunar surface would not be so sharply defined in terms of time, would be extremely unstable, and could only reach 12 db for extremely short periods, due to lunar surface irregularities and relative spacecraft to lunar surface motion.

Multipath from parts of the spacecraft would be sensitive to spacecraft position. The signal level problem was unaffected by a spacecraft roll maneuver.

GROUND STATION ANTENNA POINTING

JPL Engineering Document 256 (referenced in TIM, EDP 331, Volume I) provides beamwidth specs of 0.36 receive and 0.45 transmit. Using a parabola approximation for the lobe pattern at the -12-db point on receive, the calculated transmit pattern is approximately -7.7 db, which is reasonably close to the telemetered transponder AGC drop.

It is logical to assume that if errors were made in establishing the tracking predictions for this period of time, these errors would be reflected in the predictions for all three stations.

Shifts occurred between Earthset and Earthrise, when changes in the predictions would probably be made.

It appears trom the limited information available that the ground-received power during TWTA operation also experienced a drop during this period.

The tracking reports indicate that the antenna was pointed off of the predictions in the declination angle (in one direction only) in an attempt to improve the signal level. No indication of a search in hour angle was indicated, nor in the other direction in declination angle.

The following action is recommended:

1) A review of ground antenna pointing predictions should be accomplished to establish accuracy.

2) If problem reappears on Spacecraft 4, accomplish antenna pointing and other tests to further investigate the problem.

3) Continue review of data for additional clues.

No change is being incorporated.

VELOCITY CONTROL SUBSYSTEM PERFORMANCE

OVERALL PERFORMANCE

The velocity control subsystem was successfully restarted after a time period of 79 days, 17 hours following spacecraft launch. A period of 64 days, 20 hours had elapsed since the previous operation. The subsystem was allowed to operate to propellant depletion without difficulty. The prelaunch performance prediction for Lunar Orbiter I was a velocity increment capability of 1027 ±43 mps; during normal operation, the VCS imparted a total velocity of 1042.25 mps, with an additional velocity of 9.17 mps being imparted in a nonstandard mode consisting predominantly of fuel expulsion.

There was no degradation of the VCS during the entire Mission I; propellant tank pressures actually increased slightly as a result of the gradually increasing thermal environment. During final engine operation, there was no indication of combustion instability.

LUNAR IMPACT ENGINE-BURN SUMMARY

VELOCITY CHANGES

During the fifth engine operating cycle which initiated the lunar impact trajectory at the end of the extended mission, a velocity change of 168.8 mps was imparted to the spacecraft in 94 seconds of normal engine operation; an additional 6.4 mps were imparted resulting from the expulsion and vaporization of fuel. Subsequently, the engine valves were opened for an additional 3 minutes, and an additional 2.77 mps were supplied in this sixth burn. During the normal phase of the fifth burn, the average delivered thrust was approximately 109 pounds (due to elevated tank pressures) at a specific impulse of 276 seconds; during the tail-off phase, the thrust level is estimated to be on the order of 15 pounds at a specific impulse of approximately 100 seconds.

NITROGEN USAGE

During the extended mission, nitrogen consumption for the purpose of attitude control amounted to approximately 0.014 pound per day. Periodic larger consumptions were observed during times of experimental activity. In the hours prior to spacecraft impact, the amount of on-board nitrogen was estimated to have been 0.8 pound.

GIMBAL OPERATION

Gimbal actuators cycled normally during the fifth engine burn. During the last burn, actuator motion was extremely radical because of a nonexistent control torque: the actuators were moving between the plus and minus limits of motion.

OXIDIZER EXHAUSTION

Telemetry data indicates that an oxidizer exhaustion condition existed at the conclusion of the fifth operational cycle. Analysis indicates that an oxidizer expulsion efficiency of 99.1% was achieved.

TIME HISTORY DATA

Figures E-1 and E-2 present subsystem parameter time histories covering the duration of the extended mission; Figure E-1 shows propellant tank and nitrogen supply pressure data, and Figure E-2 presents temperature data and the amount of on-board nitrogen. From Figure E-1 it will be observed that the subsystem remained in a leak-tight condition. There was, in fact, a slight rise in propellant tank pressures resulting from the gradually increasing thermal environment. A comparison of the temperature data plotted in Figure E-2 with comparable data contained in the reference indicates that temperatures continued to increase even though the spacecraft was predominantly pitched off the sunline by approximately 30 to 40 degrees. The thermal transient noted on the 66th day of the mission (and the corresponding pressure increase shown in Figure E-1) are the result of maintaining Sun acquisition for longer than normal, which, in turn, resulted from a command preparation anomaly.

The consumption of nitrogen gas for spacecraft maneuvers and normal attitude control (Figure E-2) is worthy of special mention. In the extended-mission mode of operation, attitude control consumption of nitrogen was on the order of 0.014 pound per day, approximately 1/10 that observed during final readout of the primary mission. The rate was minimal to the degree that any maneuvers for experimental purposes (i.e., the Stanford experiment for reflecting the high-gain-antenna beam off the lunar surface) is clearly reflected as a discontinuity in the data presentation. The effects of the aforementioned command anomaly are markedly apparent in that approximately 0.5 pound of gas was consumed. A high consumption rate during the final 3 days resulted from the increased level of experimental activity (star mapping, antenna mapping and rotations, attitude maneuver, etc.). In the hours preceding impact, the amount of nitrogen on board the spacecraft was estimated to be on the order of 0.8 pound. The validity of this value is directly related to the accuracy of supply pressure telemetry, which is very questionable in this low regime. The aforementioned 0.014 pound per day consumption is slightly less than premission analytical predictions, which had been predicated on maintaining Sun acquisition.

MANEUVER PERFORMANCE FOR LUNAR IMPACT

On October 29, at GMT 12:25:25, a velocity-change maneuver was initiated to place Lunar Orbiter I on a trajectory that would impact the lunar surface. The purpose of the maneuver was to avoid even the remotest possibility of rf interference between Lunar Orbiter I and the forthcoming Mission II. While only a minimal velocity change was required to achieve impact, the maneuver was programmed to allow the VCS engine to operate to propellant exhausting, thereby

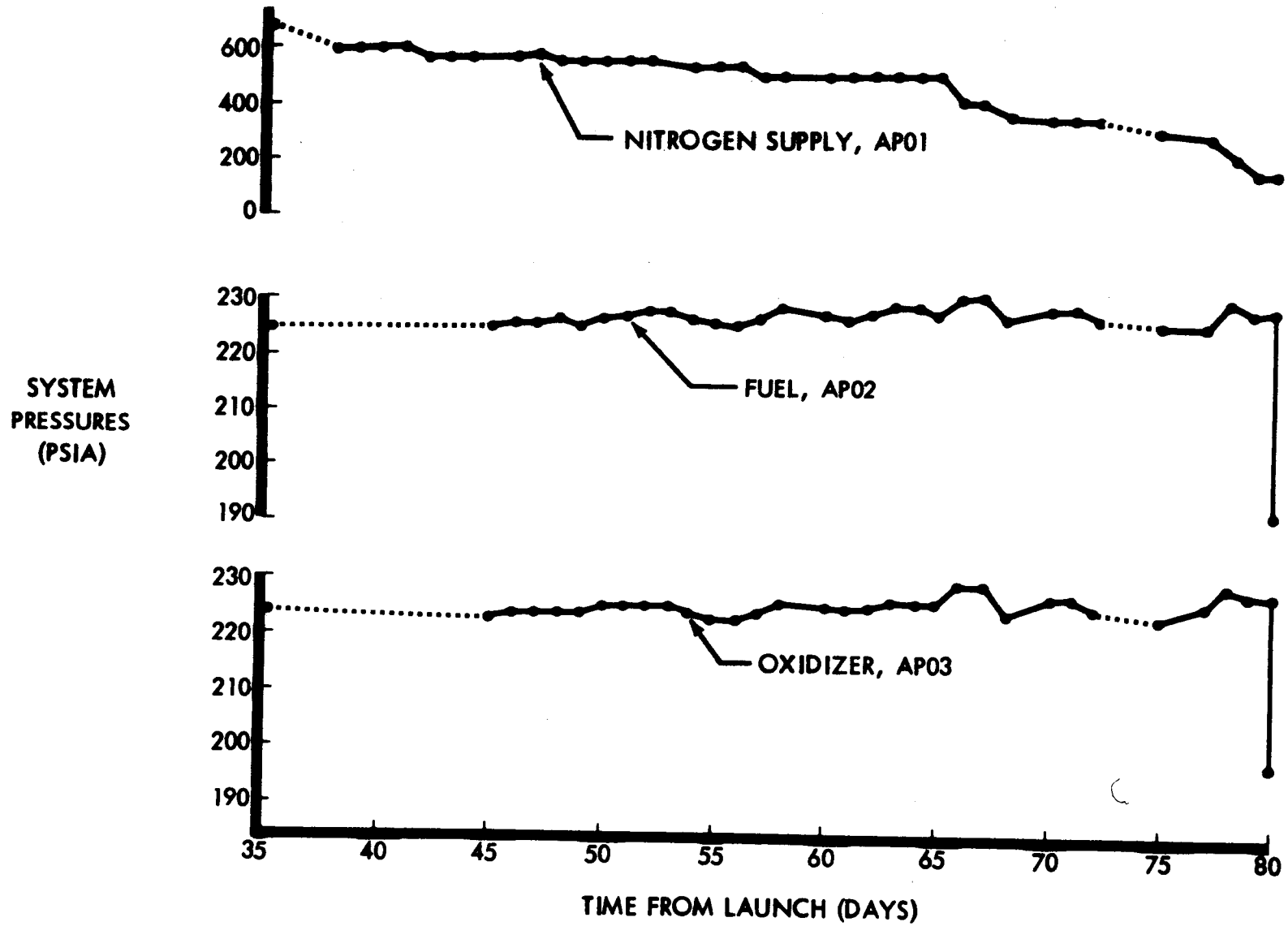
SYSTEM PRESSURES (PSIA)
600
400
200
0
NITROGEN SUPPLY, AP01
230
220
210
200
190
FUEL, AP02
230
220
210
200
190
OXIDIZER, AP03
35
40
45
50
55
60
65
70
75
80
TIME FROM LAUNCH (DAYS)

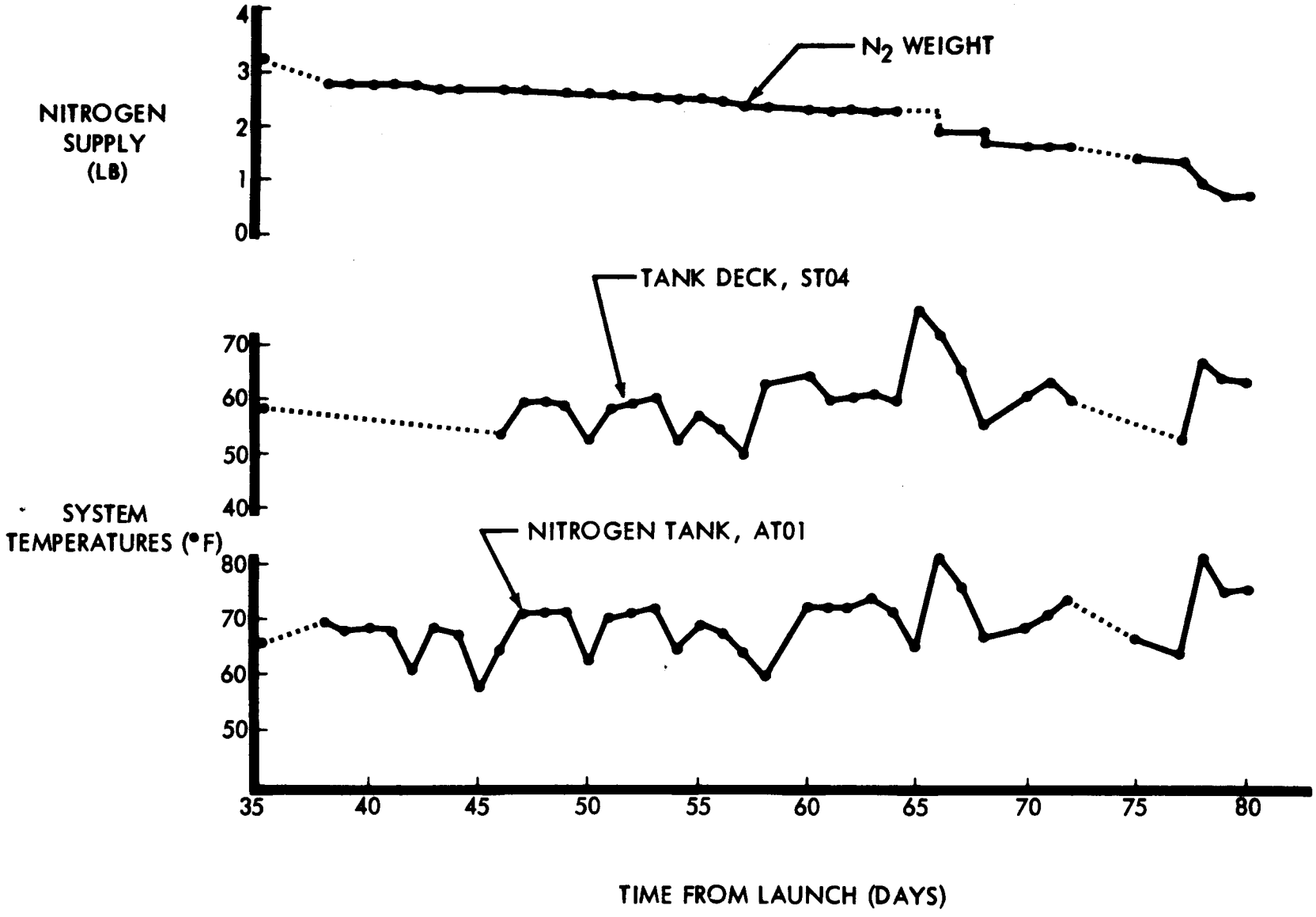
NITROGEN SUPPLY (LB)
4
3
2
1
0
N_2 WEIGHT
TANK DECK, ST04
70
60
50
40
SYSTEM TEMPERATURES (°F)
NITROGEN TANK, AT01
80
70
60
50
35
40
45
50
55
60
65
70
75
80
TIME FROM LAUNCH (DAYS)

achieving a data point to compare with prelaunch performance predictions, and to ascertain subsystem operating characteristics when subjected to propellant exhaustion.

The orbit transfer maneuver was arranged in such a manner as to be conducted at apolune with the spacecraft "locked" on the Sun reference; i.e., no attitude maneuvers were performed. Subsequent to the programmed maneuver, the engine valves were reopened for 3 minutes to ascertain if any further velocity change could be achieved.

The maneuver was successfully conducted. At the time of engine ignition, a time interval of 79 days, 17 hours had elapsed since spacecraft launch, and 64 days, 20.3 hours had transpired since the previous engine operation. This is the longest known operational cycle to which a bipropellant propulsion system has been subjected in a deep-space environment.

Spacecraft velocity change is plotted in Figure E-3 as a function of the indicated telemetry frame time. Observe that the velocity change incremented in a normal manner for 94 seconds, imparting a velocity of 168.8 mps (a slight reduction in the slope of the curve is noted after about 79 seconds of operation, indicative of increasing pressure loss across the expulsion bladders and lower chamber pressure; i.e., lower thrust). At that point, the effects of propellant exhaustion become apparent, and spacecraft acceleration is markedly reduced, the engine providing impulse in a "dribble" manner until the engine valves were closed by RTC after a total "On" time of 117.5 seconds. Table E-1 tabulates an approximation of engine performance during the initial 94 seconds of operation.

Table E-1: FINAL MANEUVER PERFORMANCE — LUNAR ORBITER I

	Predict	Actual
Velocity Increment, mps	163 ± 5	168.85
Thrust, lb		
Initial		114
Average	109	109
Final		104
Specific Impulse, sec	276	276
Operating Time, sec	89.5 ± 4.5	94

Note: Does not include "dribble mode" operational characteristics.

The final 23.5 seconds of operation contributed an additional 6.4 mps of velocity incrementation. This impulse was provided predominantly by the expulsion and vaporization of residual fuel (there may also have been some low-level combustion with oxidizer droplets). During this phase of engine operation, the delivered thrust is estimated to have been on the order of 15 pounds at a specific impulse of approximately 100 seconds.

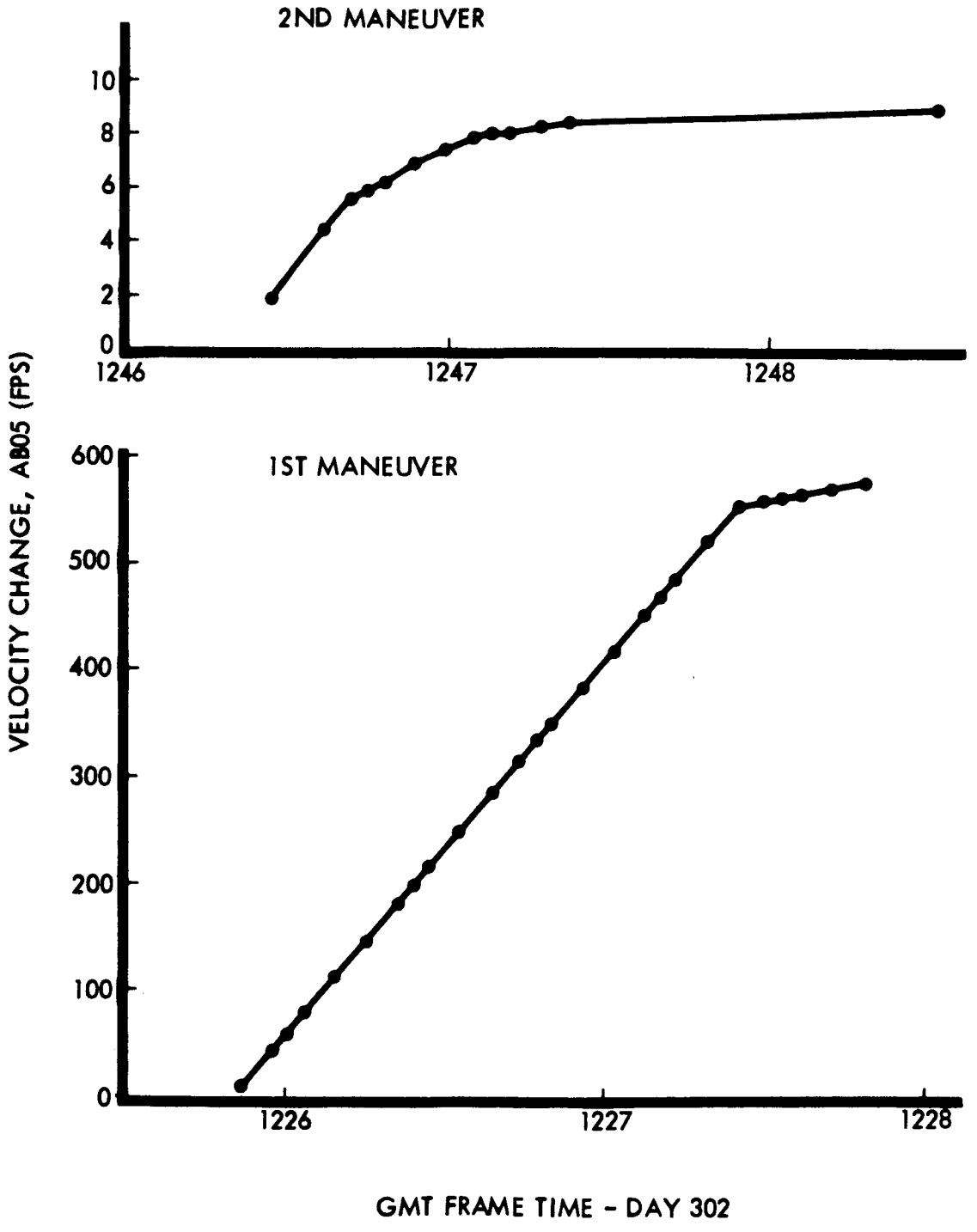
2ND MANEUVER
10
8
6
4
2
0
1246
1247
1248
1ST MANEUVER
600
500
400
300
200
100
0
1226
1227
1228
VELOCITY CHANGE, ΔB05 (FPS)
GMT FRAME TIME - DAY 302

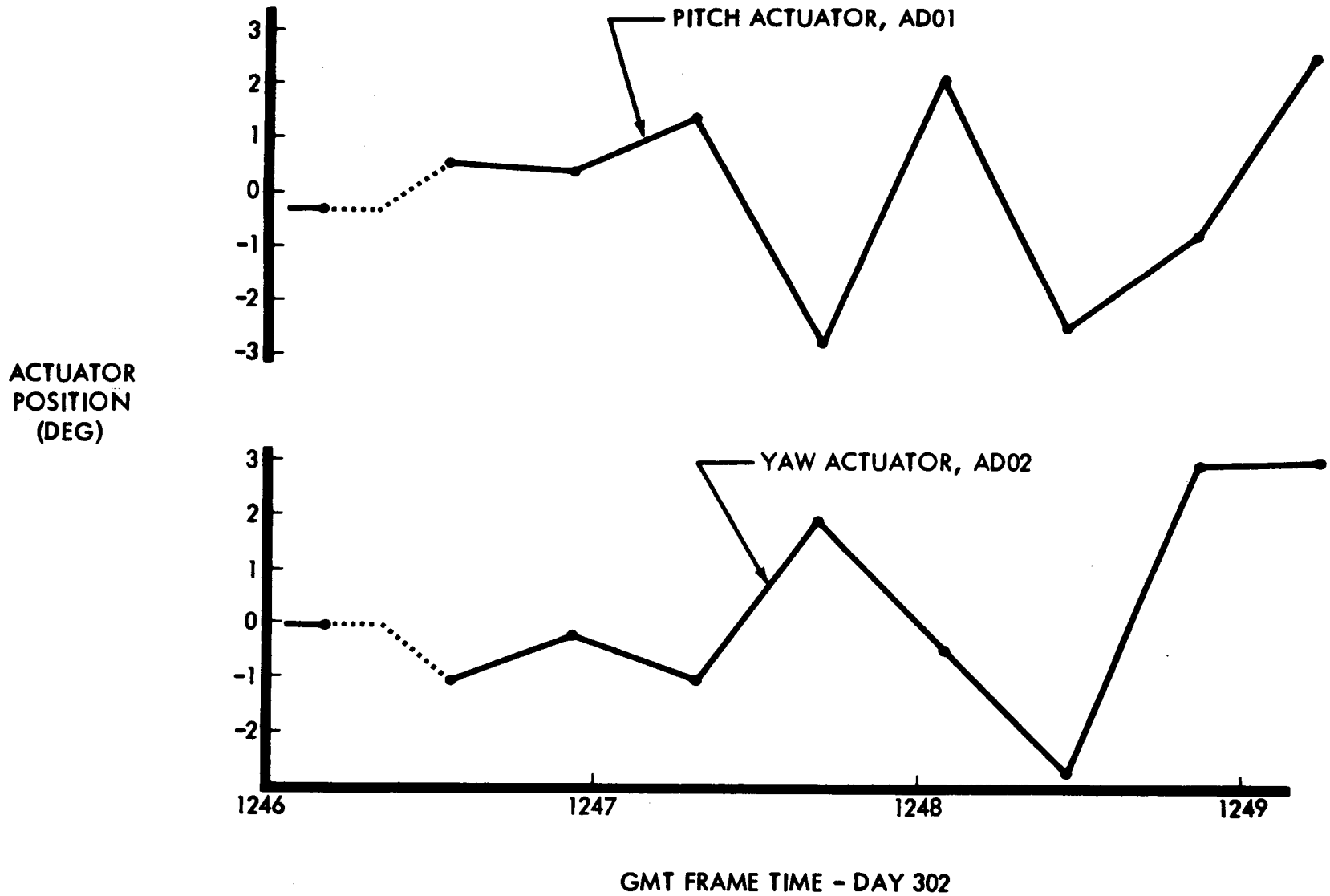
PITCH ACTUATOR, AD01
YAW ACTUATOR, AD02
ACTUATOR POSITION (DEG)
3
2
1
0
-1
-2
-3
1246
1247
1248
1249
GMT FRAME TIME - DAY 302

It was subsequently decided to repeat the maneuver to ascertain if any further velocity change could be achieved from the system. The flight programmer was "jumped" back to the maneuver sequence at 12:46:20 GMT; the engine valves were closed by RTC 3 minutes later. A velocity increment of 2.77 mps was achieved as a result of further fuel expulsion. The velocity, ABO5, is shown at the top of Figure E-3; note that the majority of the achieved velocity was accomplished within the first 50 seconds of the maneuver. A factor affecting the rate is that the engine had cooled and no longer heated the fuel to as great a degree; hence, a lower exhaust velocity.

Figure E-4 presents propellant tank pressure and gimbal actuator response during the maneuver (data are plotted as a function of indicated telemetry frame time and are not adjusted in terms of their respective time within the frame). As the nitrogen shutoff squib had been actuated during the primary mission, there was no change in nitrogen supply pressure during the maneuver; the value remained constant at 175 psia. Observe that the oxidizer tank pressure (APO3) stabilized before engine cutoff; this characteristic implies oxidizer exhaustion and occurs at approximately the same time as the discontinuity in velocity change (Figure E-3). Gimbal actuator excursions were as expected, and are essentially identical to those observed during previous Mission I maneuvers.

Gimbal actuator positions during the second burn are plotted in Figure E-5. Excursions are greater than normal, but not excessive, during the 50-second period in which the aforementioned velocity change was imparted. Following this, however, the actuators assumed a characteristic of cycling to the plus and minus extremes. In the absence of a thrust vector, reaction control thrusters would have generated a control torque that the actuators would attempt to correct. The combination of the engine valves being on and the actuators in a "stall" position (together with other spacecraft loads), at times produced a current demand of 13.5 amps. With a premaneuver "base" of 3.25 amps, the engine and actuators were, at times, producing a demand of 10.25 amps, a value to be expected for the specific conditions.

Maximum engine valve temperature (ATO3) during these exercises was observed to be 97.9°F following the second maneuver; the maximum was 89.4°F following the first maneuver when the valves were reopened, the small amount of residual fuel momentarily reducing the temperature to 87.4°F.

As an experimental test, the accelerometer power was cycled "Off" and "On" following the propulsive maneuvers. Accelerometer power was turned off at 13:11 GMT, and then successfully turned on again at 13:15 GMT.

CONCLUSION

Operating the velocity control subsystem to propellant exhaustion provided a significant performance data point that would not otherwise be available. Prior to Lunar Orbiter I launch, the velocity increment capability was predicted to be

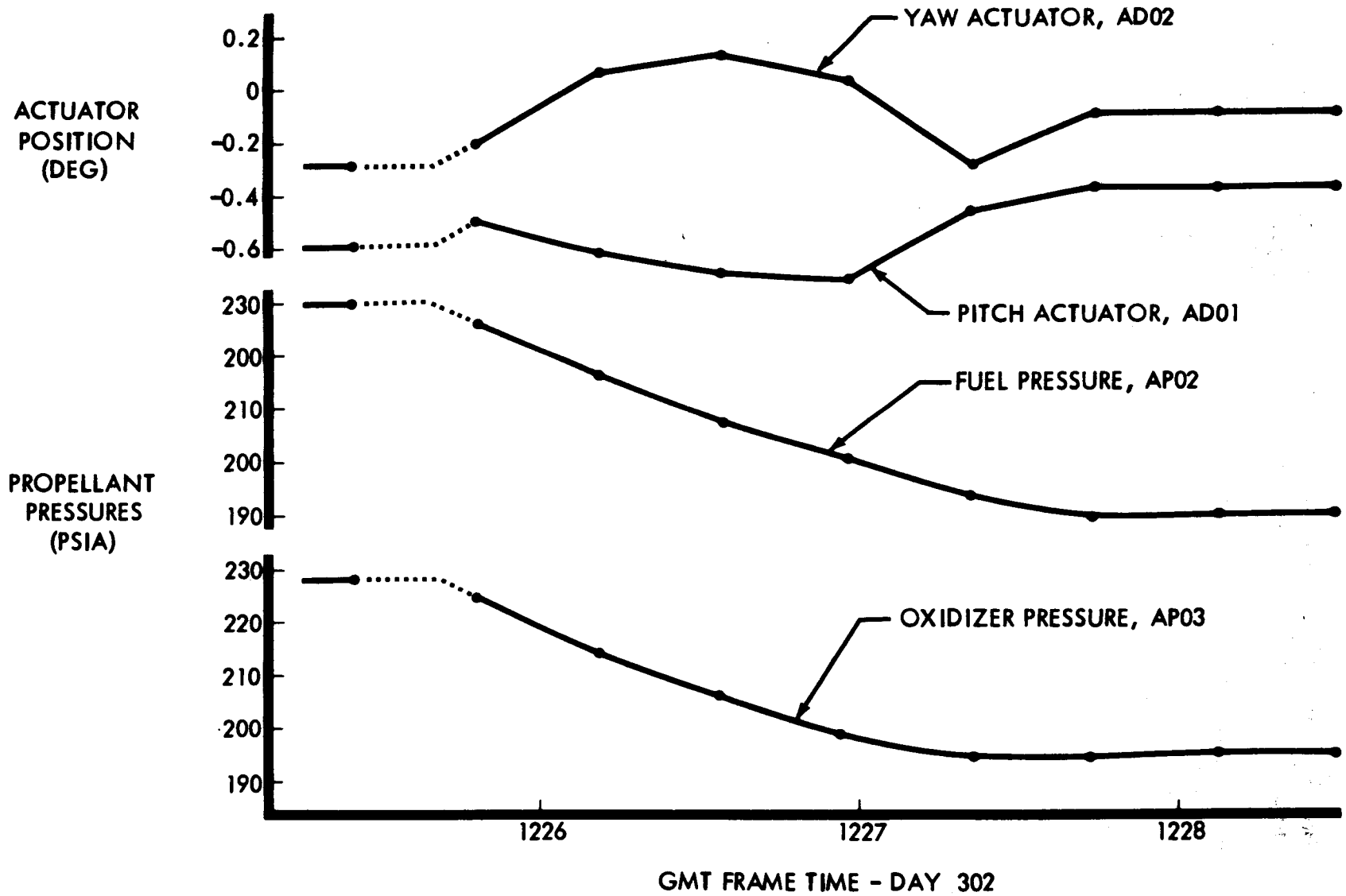
ACTUATOR POSITION (DEG)
0.2
0
-0.2
-0.4
-0.6
YAW ACTUATOR, AD02
PITCH ACTUATOR, AD01
PROPELLANT PRESSURES (PSIA)
230
200
210
200
190
FUEL PRESSURE, AP02
230
220
210
200
190
OXIDIZER PRESSURE, AP03
1226
1227
1228
GMT FRAME TIME - DAY 302

1027 ± 43 mps (3-sigma tolerance). The summation of five normal maneuvers yields an achieved velocity of 1042.25 mps, a prediction error of 1.5% due predominatly to a 99% expulsion efficiency rather than the design point of 98%. The expenditure of residual fuel permits evaluation of the system's operating mixture ratio; analysis yields a value of 1.99 ± 0.02 as compared to a prelaunch estimate of 1.98. Total engine operating time (normal) was 730 seconds in five cycles during Mission I, thereby providing a total impulse of 75,015 lb-sec as compared to a prelaunch prediction of 74,000 lb-sec and a minimum requirement of 70,850 lb-sec.

N67-27419

ERRATA

NASA CONTRACTOR REPORT-66324

LUNAR ORBITER I FINAL REPORT
MISSION OPERATIONAL PERFORMANCE
VOLUME III
Boeing Document D2-100727-3

The Boeing Company
February 3, 1967

On page v of the Contents, the following items should be added after the item 3.4.4.2:

ADDENDA: (to follow page 381)

ASSESSMENT SUMMARY OF LUNAR ORBITER I ANOMALIES 1
VELOCITY CONTROL SUBSYSTEM PERFORMANCE 43